frontiers | Research Topics

Anatomical and functional neural networks changes in cognitive impairment and healthy aging

Edited by
Fermín Segovia and Cosimo Urgesi

Published in
Frontiers in Aging Neuroscience

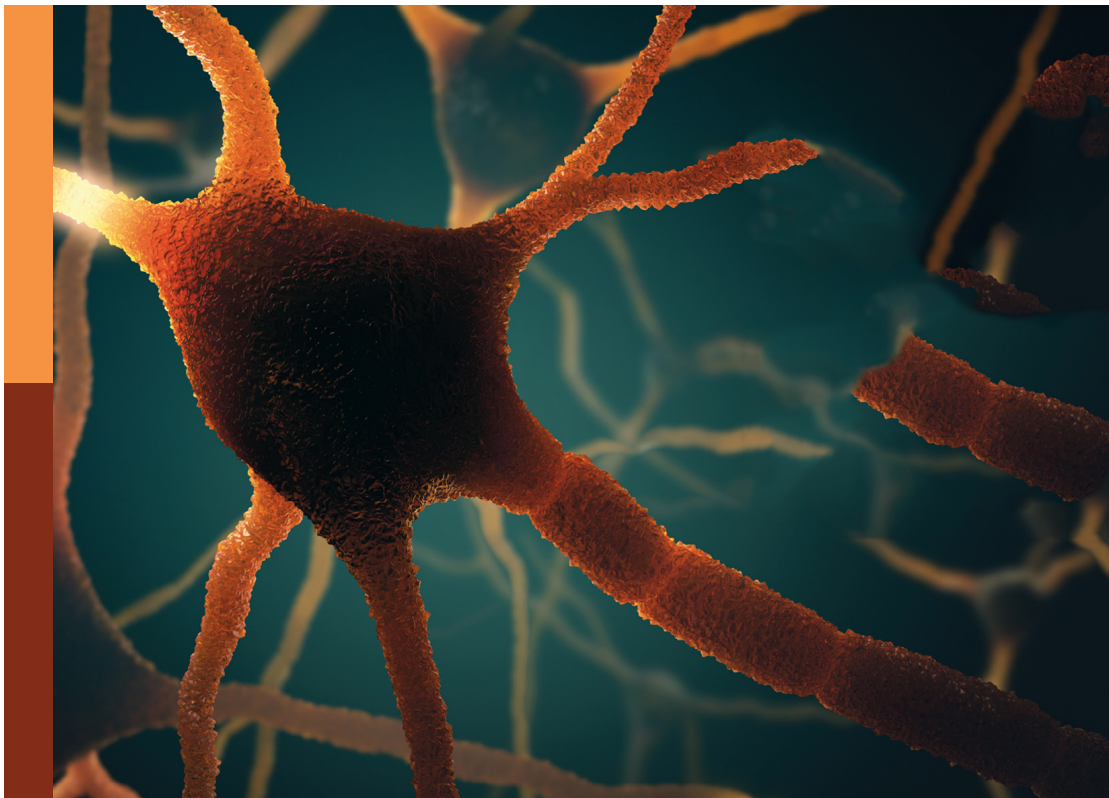

ISSN 1664-8714
ISBN 978-2-83252-075-8
DOI 10.3389/978-2-83252-075-8

About Frontiers

Frontiers is more than just an open access publisher of scholarly articles: it is a pioneering approach to the world of academia, radically improving the way scholarly research is managed. The grand vision of Frontiers is a world where all people have an equal opportunity to seek, share and generate knowledge. Frontiers provides immediate and permanent online open access to all its publications, but this alone is not enough to realize our grand goals.

Frontiers journal series

The Frontiers journal series is a multi-tier and interdisciplinary set of open-access, online journals, promising a paradigm shift from the current review, selection and dissemination processes in academic publishing. All Frontiers journals are driven by researchers for researchers; therefore, they constitute a service to the scholarly community. At the same time, the *Frontiers journal series* operates on a revolutionary invention, the tiered publishing system, initially addressing specific communities of scholars, and gradually climbing up to broader public understanding, thus serving the interests of the lay society, too.

Dedication to quality

Each Frontiers article is a landmark of the highest quality, thanks to genuinely collaborative interactions between authors and review editors, who include some of the world's best academicians. Research must be certified by peers before entering a stream of knowledge that may eventually reach the public - and shape society; therefore, Frontiers only applies the most rigorous and unbiased reviews. Frontiers revolutionizes research publishing by freely delivering the most outstanding research, evaluated with no bias from both the academic and social point of view. By applying the most advanced information technologies, Frontiers is catapulting scholarly publishing into a new generation.

What are Frontiers Research Topics?

Frontiers Research Topics are very popular trademarks of the *Frontiers journals series*: they are collections of at least ten articles, all centered on a particular subject. With their unique mix of varied contributions from Original Research to Review Articles, Frontiers Research Topics unify the most influential researchers, the latest key findings and historical advances in a hot research area.

Find out more on how to host your own Frontiers Research Topic or contribute to one as an author by contacting the Frontiers editorial office: frontiersin.org/about/contact

Anatomical and functional neural networks changes in cognitive impairment and healthy aging

Topic editors

Fermín Segovia — University of Granada, Spain

Cosimo Urgesi — University of Udine, Italy

Citation

Segovia, F., Urgesi, C., eds. (2023). *Anatomical and functional neural networks changes in cognitive impairment and healthy aging.* Lausanne: Frontiers Media SA. doi: 10.3389/978-2-83252-075-8

Table of contents

frontiers in Aging Neuroscience

ORIGINAL RESEARCH
published: 29 January 2020
doi: 10.3389/fnagi.2020.00006

Disrupted Brain Structural Connectivity Network in Subcortical Ischemic Vascular Cognitive Impairment With No Dementia

Linqiong Sang[1†], Chen Liu[2†], Li Wang[1], Jingna Zhang[1], Ye Zhang[1], Pengyue Li[1], Liang Qiao[1], Chuanming Li[3] and Mingguo Qiu[1]**

[1] Department of Medical Imaging, School of Biomedical Engineering, Third Military Medical University, Chongqing, China, [2] Department of Radiology, Southwest Hospital, Third Military Medical University, Chongqing, China, [3] Department of Radiology, The Second Affiliated Hospital of Chongqing Medical University, Chongqing, China

OPEN ACCESS

Edited by:
Philip P. Foster,
The University of Texas Health Science Center at Houston, United States

Reviewed by:
Boon-Seng Wong,
Singapore Institute of Technology, Singapore
Xiao-Xin Yan,
Central South University, China

***Correspondence:**
Chuanming Li
li_chuanming@yeah.net
Mingguo Qiu
qiumg_2002@sina.com

[†] These authors have contributed equally to this work

Received: 10 September 2019
Accepted: 10 January 2020
Published: 29 January 2020

Citation:
Sang L, Liu C, Wang L, Zhang J, Zhang Y, Li P, Qiao L, Li C and Qiu M (2020) Disrupted Brain Structural Connectivity Network in Subcortical Ischemic Vascular Cognitive Impairment With No Dementia. Front. Aging Neurosci. 12:6. doi: 10.3389/fnagi.2020.00006

The alteration of the functional topological organization in subcortical ischemic vascular cognitive impairment with no dementia (SIVCIND) patients has been illuminated by previous neuroimaging studies. However, in regard to the changes in the structural connectivity of brain networks, little has been reported. In this study, a total of 27 subjects, consisting of 13 SIVCIND patients, and 14 normal controls, were recruited. Each of the structural connectivity networks was constructed by diffusion tensor tractography. Subsequently, graph theory, and network-based statistics (NBS) were employed to analyze the whole-brain mean factional anisotropy matrix. After removing the factor of age, gender, and duration of formal education, the clustering coefficients (C_p) and global efficiency (E_{glob}) were significantly decreased and the mean path length (L_p) was significantly increased in SIVCIND patients compared with normal controls. Using the combination of four network topological parameters as the classification feature, a classification accuracy of 78% was obtained by leave-one-out cross-validation for all subjects with a sensitivity of 69% and a specificity of 86%. Moreover, we also found decreased structural connections in the SIVCIND patients, which mainly concerned fronto-occipital, fronto-subcortical, and tempo-occipital connections (NBS corrected, $p < 0.01$). Additionally, significantly altered nodal centralities were found in several brain regions of the SIVCIND patients, mainly located in the prefrontal, subcortical, and temporal cortices. These results suggest that cognitive impairment in SIVCIND patients is associated with disrupted topological organization and provide structural evidence for developing reliable biomarkers related to cognitive decline in SIVCIND.

Keywords: subcortical ischemic vascular cognitive impairment with no dementia, graph theoretical analysis, brain structural network, network-based statistic, topological organization

INTRODUCTION

Cognitive impairment is frequently induced by the subcortical ischemic vascular disease (SIVD), and it is marked by lacunar infarcts and deep white matter changes (Erkinjuntti, 2003; O'Brien and Thomas, 2015). Subcortical ischemic vascular cognitive impairment with no dementia (SIVCIND) has been considered a "disconnection syndrome" due to the extensive damage to the white matter tracts or U-fibers, which connect cortical and subcortical regions. Early identification of SIVCIND is of great importance since managing these risk factors in a timely manner may prevent disease development and reduce disease progression. However, the definite etiology and pathogenesis of cognitive decline induced by SIVD remains poorly understood.

Some studies have shown that changes in white matter of brain were existed in patients with cognitive impairment induced by SIVD. For instance, decreased fractional anisotropy (FA) was found in several projection fibers and association fibers in SIVCIND patients, including the posterior thalamic radiations, cingulum, and fronto-occipital fasciculus (Lin et al., 2015). Zhou et al. (2011) found decreased FA in several brain regions located in the bilateral frontal, occipital, and temporal cortices in SIVCIND patients compared with normal controls. Another research (Xu et al., 2010) recruited patients with SIVD, who were subdivided into three groups: normal cognition, cognitive impairment with no dementia, and dementia. Significant differences were found in the FA values in whole-brain white matter between normal cognition group and cognitive impairment group; the FA values were also significantly correlated with attention, executive, and memory performance. Although it is incremental in the knowledge of the structural abnormalities in specific regions of the brain, the definite biomarkers which may identify the cognitive decline induced by SIVD remain unclear.

Recently, the increasing studies have shown that many of the important topological organizations of brain networks could be revealed by graph theoretical approaches (Bullmore and Sporns, 2009; He and Evans, 2010; Lopes et al., 2017). Moreover, the topological organization of whole-brain functional and structural networks could be employed to characterize some neurological and psychiatric disorders (Zhang et al., 2011; Shu et al., 2012; Zhu et al., 2016). Notably, one study recruited 127 small vessel disease patients which were comprised of 76 mild cognitive impairment patients and 51 normal cognitive patients; the results showed that global network efficiency was significantly correlated with cognitive state ($p < 0.01$) (Du et al., 2019). Another study (Heinen et al., 2018) considered the relationship between total small vessel disease burden score, global network efficiency and cognition; the results showed that global network efficiency was relevant to the performance on the information processing speed, attention and executive functioning. However, it remains unclear regarding the changes in the structural connectivity network in SIVCIND patients and the power of network parameters identifying SIVCIND patients from controls.

In this study, we aimed to observe alterations in the whole-brain structural connectivity networks in SIVCIND patients and explore the relationship between changes in brain structural organization and cognitive deficits. Here, we hypothesized that the organization of the structural connectivity network would be disrupted and that the changes would be related to cognitive decline. More specifically, we expected that the cognitive impairment caused by SIVD would be associated with altered global parameters of the whiter matter network. In other words, the topological properties of the white matter network may be related to cognitive state. Finally, the study was carried out to estimate whether the feature of topological organization of the brain white matter network could be biomarkers of the cognitive decline induced by SIVD.

MATERIALS AND METHODS

Participants

Twenty-seven Right-handed participants were recruited in the study, including 13 SIVCIND patients and 14 normal controls. Written informed consent was obtained from all subjects. This study was approved by the local Medical Ethics Committee at Third Military Medical University (Chongqing, China) on Human Studies.

According to the criteria suggested by Galluzz, only the SIVCIND patients who had a subcortical WM hyperintensity on T2-weighted imaging and had at least two lacunar infarcts were enrolled in this study (Galluzzi et al., 2005). Moreover, the special inclusion criteria for SIVCIND was insufficient cognitive impairment to meet the DSM-V criteria for dementia, and the Hachinski Ischemic Score (HIS) $\geq$7 (Sachdev et al., 2014; Yu et al., 2017). For detailed description of inclusion criteria and exclusion criteria for SIVCIND, please see Sang et al. (2018). All patients received baseline evaluations, including complete sociodemographic, and clinical data collection. The performance on cognitive functioning was assessed by several neuropsychological tests including the Mini Mental State Examination (MMSE), the Clinical Dementia Rating (CDR), the Global Deterioration Scale (GDS), the Montreal Cognitive Assessment (MoCA) (Folstein et al., 1975; Hachinski et al., 1975; Reisberg et al., 1982; Warren et al., 1989; Moris, 1993; Cummings et al., 1994; Nasreddine et al., 2005).

Each of the normal controls had well-documented normal cognitive performance and none have any nervous system diseases. The conventional MRI and neuropsychological tests was implemented for each normal control. None had vascular risk factors that could induce cognitive impairment or current or a history of psychiatric illness. Moreover, none of them had brain trauma, brain tumors, systemic disease or other MRI contraindications, such as claustrophobia.

Data Acquisition

All subjects underwent MRI scanning using a Siemens 3.0 T Trio MRI scanner (Siemens, Erlangen, Germany) at Southwest hospital, chongqing, china. The T1-weighted anatomical images (repetition time = 1900 ms; echo time = 2.52 ms; flip angle = 9°; voxel size = 1 × 1 × 1 mm^3; slice thickness = 1 mm with no gap; 176 slices; field of view = 260 mm; matrix = 256 × 256)

were acquired. Then, the diffusion tensor images [repetition time = 5500 ms; echo time = 93 ms; flip angle = 90°; voxel size = 1.8 × 1.8 × 3 mm^3; slice thickness = 3 mm with no gap, 40 slices; field of view = 230 mm; matrix = 128 × 128; 64 non-collinear diffusion-weighted gradient direction (b = 1000 s/mm^2) and one additional unweighted image b0 ($b = 0$ s/mm^2)] were acquired.

Network Construction

Data Preprocessing

First, we used FSL software[1] to correct head motion and eddy currents by registering each diffusion-weighted image to the first unweighted b0 image, and the FSL-BET program was applied to remove skull and other non-brain tissue. Subsequently, a deterministic streamline fiber tractography algorithm was performed to obtain each subject's whole-brain tractography in the native diffusion space (Fiber Assignment by Continuous Tracking algorithm, FACT) implemented in the Diffusion Toolkit software[2]. If the FA value was less than 0.2 and the curvature of path tracing was greater than 45°, the tracking would be terminated.

Node Definition

Nodes and edges are two components of a network. The node definition in the structural connectivity network was made according to the AAL template (45 for each hemisphere). In this study, the AAL template was mapped from the standard MNI space to the individual's native DTI space by inverse transformations from spatial normalization and registration. Detailed information on each brain region in the AAL template is presented in **Supplementary Table S1**.

Edge Definition

An edge in the structural connectivity network was defined when the number of fibers between two regions was equal to or greater than three. If at least three fibers were present, the two regions were considered linked through an edge, and the value of the edge was set to 1. The final value of the edge was obtained by multiplying the mean FA values along the fiber bundles connecting a pair of regions; in this way, the edges revealed the white matter structure. Therefore, the weighted structural connectivity network was constructed for each subject.

Finally, the factors of age, gender and formal education duration were removed from each weighted connectivity matrix by regression. The resultant structural network of each subject is a sparse matrix, and the sparsity of each network, ranging from 20 to 28%, is shown in **Figure 1**.

Network Analysis

To ensure that all resultant networks had the same number of nodes and edges, the weighted network was thresholded at different levels of sparsity ranging from 5 to 20% in increments of 1%. At each threshold, the network metrics were calculated. Specifically, the global metrics of each structural network were

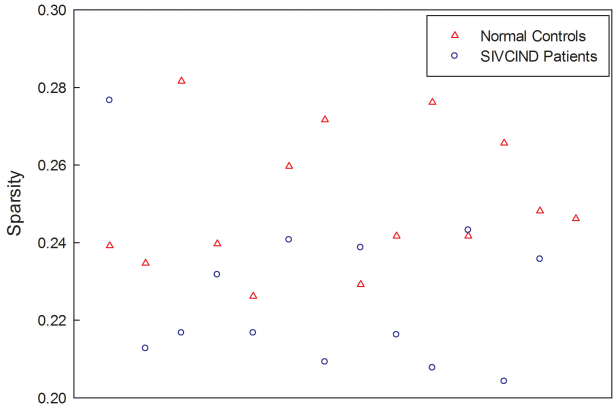

FIGURE 1 | The sparsity of each subject's brain structural connectivity network.

constant and ranged from 14 to 20% (**Supplementary Figure S1**); hence, the threshold at different levels of sparsity, ranging from 5 to 14%, was employed in this study.

Moreover, we calculated several global network parameters of the weighted brain structural network: the clustering coefficient (C_p), the mean path length (L_p), the global efficiency (E_{glob}), and the local efficiency (E_{loc}). Definitions of these metrics are as follows.

The C_p of a network G describes the connectedness of direct neighbors around individual nodes (Watts and Strogatz, 1998). It is expressed as follows (Onnela et al., 2005):

$$C_p(G) = \underset{i \in node}{mean} \frac{2}{k_i(k_i-1)} \sum_{j,k} (\overline{w_{ij} w_{jk} w_{ki}})^{1/3}$$

where w_{ij} is the weight value of the edges between node i and node j in the network, and k_i is the strength of node i.

The L_p of G quantifies the ability for information transfer in parallel. It is expressed as follows:

$$L_p(G) = \frac{1}{N(N-1)} \sum_{i \neq j \in G} L_{ij}$$

where N is the number of nodes, and L_{ij} is the shortest path length between nodes i and j in the network.

The value E_g of G quantifies the E_{glob} of the parallel information transfer in the network. It is expressed as follows:

$$E_g(G) = \frac{1}{N(N-1)} \sum_{i \neq j \in G} \frac{1}{L_{ij}}$$

where N is the number of nodes, and L_{ij} is the shortest path length between nodes i and j in the network.

The E_{loc} of G quantifies the fault tolerance of a network (Achard and Bullmore, 2007). It is expressed as follows:

$$E_{loc}(G) = \frac{1}{N(N-1)} \sum_{i \neq j \in G} E_g(G_i)$$

[1]http://www.fmrib.ox.ac.uk/fsl

[2]http://trackvis.org/dtk/

where N is the number of nodes, and G_i represents the subgraph which is comprised of the direct neighbors around node i.

Moreover, we calculated the nodal global efficiency E_{nodal_glob} and nodal local efficiency E_{nodal_loc} to quantify the ability of information transfer between a node and all other nodes and its direct neighbors in the network. They are expressed as follows:

$$E_{nodal\_glob}(i) = \frac{1}{N-1} \sum_{i \neq j \in G} \frac{1}{L_{ij}}$$

$$E_{nodal\_loc}(i) = E_g(G_i)$$

where N is the number of nodes, L_{ij} is the shortest path length between nodes i and j, and G_i represents the subgraph which is comprised of the direct neighbors around node i.

The topological parameters of the brain networks were computed using GRETNA toolbox[3]. Furthermore, the area under the curve (AUC) for each network metric (C_p, L_p, E_g, E_{bloc}, E_{nodal_glob}, and E_{nodal_loc}) was calculated to characterize the topological organization of the brain structural network according to previous studies (He et al., 2009).

An SVM was applied to build classification models with a radial basis function as the kernel function, which determines the power of a combination of global topological parameters to predict the subject groups. In this classification model, the predictors were the combination of the four global network metrics (C_p, L_p, E_g, and E_{bloc}), and the response was the subject's group. Furthermore, we performed leave-one-out cross-validation to evaluate the classification accuracy, which guarantees a relatively unbiased estimate of the generalization power of the classifiers to new subjects. Subsequently, the sensitivity and specificity were calculated.

Moreover, the network-based statistics (NBS) approach, a validated non-parametric statistical approach for controlling familywise error in connectome analyses (Zalesky et al., 2010), was applied to identify the altered structural connections in patients. First, the strength of each edge weight in the structural connectivity matrix was compared between the patient group and the control group by using a one-tailed *t*-test. Second, the network components involving the surviving connected edges with an uncorrected *p*-value of 0.005 were retained. Third, the size of the largest network component was computed. Then, the groups were randomly shuffled (10,000 permutations), and the largest network component size was calculated by repeating steps 1, 2, and 3. In this way, an empirical null distribution was generated to evaluate the statistical significance of the network component sizes. Moreover, the corrected *p*-value for a network component with size M, which was found in the correct grouping of controls and patients, was determined by calculating the proportion of the maximal network component that was larger than M in the 10,000 permutations.

In this study, we used circos software[4] to show significant connections between patients and controls by circular graphical representations (Irimia et al., 2012). In a circular graph, links between pairwise regions are colored by connection type, such as blue representing left intrahemispheric connections, green representing right intrahemispheric connections, and red representing interhemispheric connections. ROIs were grouped into frontal, temporal, parietal, medial temporal, occipital, and subcortical according to Salvador et al. (2005). According to a previous study, the ROIs with a high degree of significant connections ($k > 1$ SD above the mean) were deemed "network hubs" (Lopes et al., 2017).

[3]https://www.nitrc.org/projects/gretna/

[4]http://www.circos.ca

Statistical Analysis

The non-parametric permutation test was performed on the AUC of each network metric to identify between-group differences based on a null permutation distribution, which was generated by randomly assigning two groups with the same sizes as the original groups of patients and normal controls. This randomization procedure was repeated for 10,000 permutations, and the between-group differences of each graph metric were calculated to generate a null permutation distribution. The *p*-value was obtained by computing the proportion of differences exceeding the value in the correct grouping of patients and normal controls in the null distribution. A *p*-value lower than 0.05 was deemed to manifest statistical significance. Specially, the effects of age, gender and formal education duration were removed using multiple linear regression before the permutation test.

Furthermore, to identify the relationship between the topological properties of the structural connectivity network and cognitive performance, we performed Person's correlation between the global topological metrics (C_p, L_p, E_g, and E_{bloc}) and the cognitive scores (MMSE and MoCA) in SIVCIND patients. Additionally, we computed the *Z*-scores of each cognitive scores, and the statistical significance level of *p*-value is lower than 0.05.

RESULTS

Clinical Statistics

Subject demographics are listed in **Table 1**. A two-sample *t*-test revealed that the SIVCIND patients showed lower MMSE ($T = 5.729$, $p < 0.001$) and MoCA scores ($T = 10.294$, $p < 0.001$)

TABLE 1 | Demographics and clinical characteristics of the subjects.

	NC (*n* = 14)	SIVCIND (*n* = 13)	*p*-Value
Gender (male/female)	8/6	7/6	0.564[a]
Age (years)	58–76 (65.1 ± 5.0)	47–83 (68.3 ± 9.8)	0.285[b]
Education (years)	0–16 (10.4 ± 4.1)	1–16 (8.5 ± 4.1)	0.246[b]
MMSE	22–30 (28.4 ± 2.2)	18–26 (23.5 ± 2.3)	<0.001[b]
MoCA	21–30 (27.1 ± 2.3)	8–22 (14.7 ± 3.8)	<0.001[b]
HIS	–	7–14 (8.7 ± 1.4)	
GDS	–	3–5 (3.7 ± 0.5)	
CDR	–	0.5–1 (0.6 ± 0.1)	

Data are expressed as the min–max (mean ± SD). MMSE, Mini-Mental State Examination; MoCA, Montreal Cognitive Assessment; HIS, Hachinski Ischemic Score; GDS, Global Deterioration Scale; CDR, Clinical Dementia Rating. [a]p-value obtained using Pearson's Chi-squared test. [b]p-value obtained using a two-sample t-test.

compared to the normal controls. No significant difference was found between the two groups in terms of gender ($\chi^2 = 0.333$, $p = 0.564$), age ($T = -1.092$, $p = 0.285$) and duration of formal education ($T = 1.188$, $p = 0.246$).

Altered Global Topological Properties

The SIVCIND patients showed a significantly decreased C_p ($p = 0.003$, FDR corrected) and global efficiency E_g ($p < 0.001$, FDR corrected) and a significantly increased L_p ($p < 0.001$, FDR corrected) compared to the normal controls as determined by the non-parametric permutation test (**Figure 2**). Moreover, there was no significant difference in E_{bloc} between the SIVCIND patients and the normal controls (**Figure 2**).

Between-Group Differences in Nodal Efficiency

The non-parametric permutation test revealed that the SIVCIND patients showed remarkably decreased E_{nodal_glob} compared with the normal controls, and only several brain regions exhibited altered nodal local efficiency ($p < 0.05$, FDR corrected) (**Figure 3**, and **Table 2**). Compared with the NCs, the SIVCIND patients showed decreased E_{nodal_glob} in prefrontal, parietal, temporal, mediotemporal and subcortical regions, such as the bilateral thalamus; the left middle frontal gyrus, inferior frontal gyrus, supplementary motor area, parahippocampal gyrus, insula, caudate nucleus, putamen, and pallidum; and the right superior frontal gyrus (orbital medial part), hippocampal gyrus, fusiform gyrus, inferior parietal gyrus, and precuneus. Moreover, the SIVCIND patients exhibited increased E_{nodal_glob} in the left olfactory cortex (**Figure 3A** and **Table 2**).

Compared with the NCs, the SIVCIND patients exhibited lower nodal local efficiency in the bilateral angular gyrus and middle temporal gyrus, the right inferior parietal gyrus, and the left superior temporal gyrus (**Figure 3B** and **Table 2**).

Altered Structural Connectivity

Compared with the NCs, the SIVCIND patients showed 46 significantly decreased structural connections (NBS corrected, $p < 0.01$) (**Figure 4**). There was an approximately 30% decrease in the structural connectivity between cortical regions and subcortical regions. Notably, most of the decreased structural connectivity in the SIVCIND patients was involved in the default mode network.

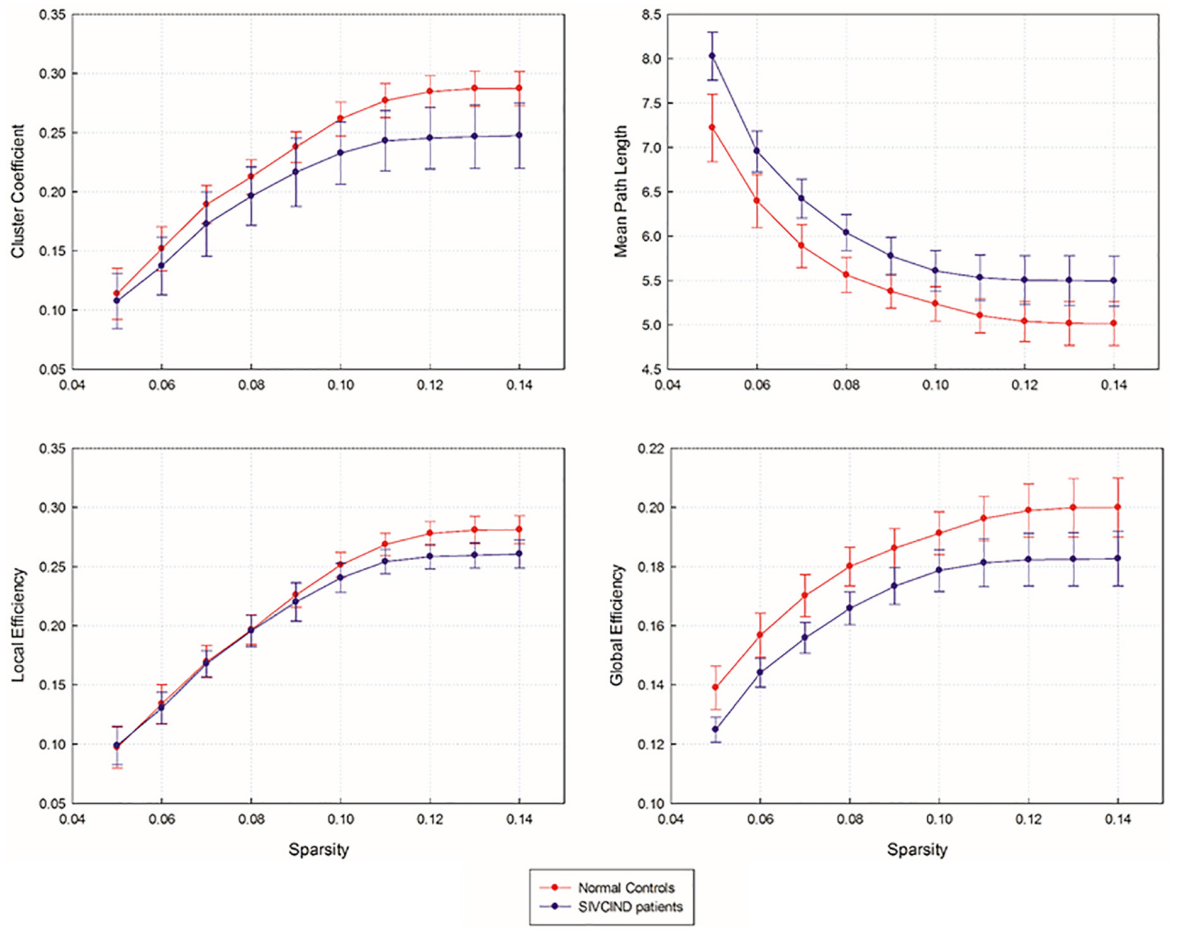

FIGURE 2 | Network topological parameters of structural brain network as a function of sparsity ranging from 5 to 14%. Error bars denote standard deviations.

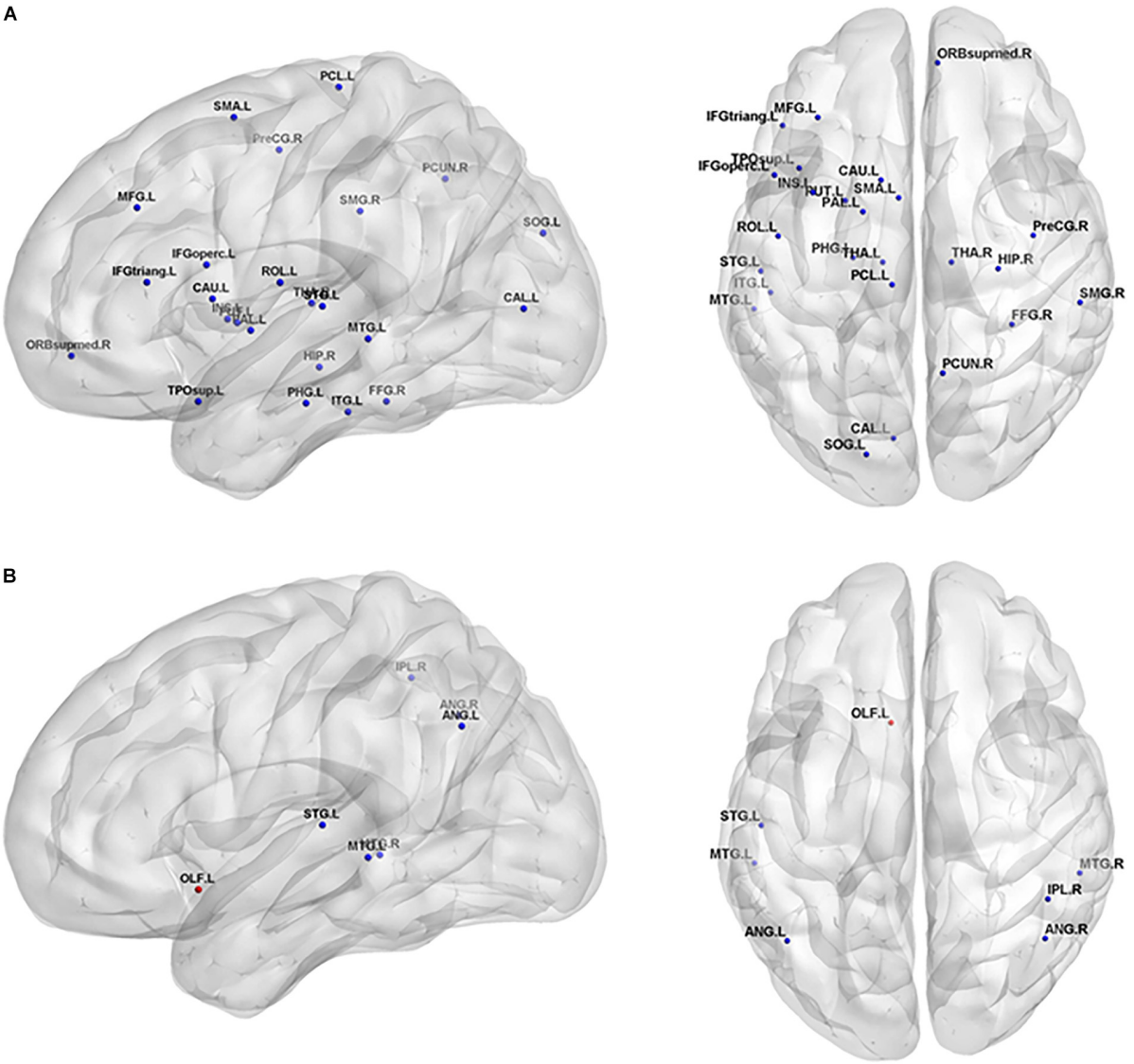

FIGURE 3 | Brain regions show significant alterations of nodal efficiency in SIVCIND patients compared with normal controls ($p < 0.05$, FDR-corrected). The results were visualized using BrainNet Viewer (NKLCNL, Beijing Normal University). Three-dimensional maps show the significant differences in nodal global efficiency **(A)** and nodal local efficiency **(B)** between the SIVCIND patients and normal controls. Red/blue spheres denote regions where nodal efficiency are increased/decreased in SIVCIND patients. Detailed brain region information corresponding to the anatomical labels can be found in AAL.

In addition, compared with the NCs, the SIVCIND patients had weaker hub connections in the bilateral precuneus; the right hippocampal gyrus and the calcarine cortices; and the left inferior frontal gyrus (triangular part), superior frontal gyrus (orbital media part), insula, lingual gyrus, middle occipital gyrus, paracentral lobule, caudate nucleus, putamen, thalamus, and middle temporal gyrus.

Relationships Between Topological Properties and Cognitive Test Scores

There was a positively significant correlation between C_p values and the MMSE scores, and an approximately negative correlation between L_p values and the MMSE scores (**Figure 5**).

Sensitivity and Specificity of Network Properties in Differentiating Patients From Normal Controls

Using the combination of the four network metrics (Cp, Lp, Eg, and Eloc) as predictors, a classification accuracy of 78% was obtained with a sensitivity of 69% and a specificity of 86%.

DISCUSSION

In this study, we investigated the altered topological properties of the structural network in SIVCIND patients. The results revealed

TABLE 2 | Brain regions showing abnormal nodal efficiency in SIVCIND patients compared with normal controls (FDR-corrected $p < 0.05$ shown in bold font).

Regions	Nodal global efficiency	Nodal local efficiency
SIVCIND patients < Normal controls		
Right precentral gyrus	**0.02**	0.231
Left middle frontal gyrus	**0.017**	0.874
Left inferior frontal gyrus, operculum part	**0.001**	0.197
Left inferior frontal gyrus, triangular part	**<0.001**	0.413
Left Rolandic operculum	**0.001**	0.316
Left supplementary motor area	**0.005**	0.183
Right superior frontal gyrus, orbital media part	**0.024**	0.363
Left insula	**0.003**	0.075
Right hippocampal gyrus	**0.045**	0.334
Left parahippocampal gyrus	**0.033**	0.789
Left calcarine cortices	**0.011**	0.553
Left superior occipital gyrus	**0.034**	0.795
Right fusiform gyrus	**0.007**	0.481
Right inferior parietal gyrus	**0.047**	**0.038**
Right supramarginal gyrus	**0.009**	0.591
Left angular gyrus	0.1	**0.018**
Right angular gyrus	0.227	**0.009**
Right precuneus	**0.002**	0.569
Left paracentral lobule	**<0.001**	0.849
Left caudate nucleus	**0.034**	0.512
Left putamen	**0.012**	0.056
Left pallidum	**0.007**	0.227
Left thalamus	**0.025**	0.337
Right thalamus	**0.022**	0.654
Left superior temporal gyrus	**0.013**	**0.006**
Left superior temporal gyrus, pole part	**0.004**	0.271
Left middle temporal gyrus	**0.009**	**0.002**
Right middle temporal gyrus	0.282	**0.004**
Left inferior temporal gyrus	**0.02**	0.283
SIVCIND patients > Normal controls		
Left olfactory cortex	0.775	**0.007**

that the C_p and E_{glob} decreased and the L_p increased in SIVCIND patients. More specifically, using the four network global parameters as features to discriminate SIVCIND patients from normal controls, a classification accuracy of 78% was obtained for all subjects, with a sensitivity of 69% and a specificity of 86%. These results implied a disturbance in information exchange in the structural brain network of SIVCIND patients. Moreover, the significantly decreased structural connectivity mainly concerned the prefrontal, temporal, parietal and subcortical cortices. Additionally, we observed several brain regions showing decreased E_{nodal_glob} in the SIVCIND patients, mostly located in the prefrontal, subcortical, and media temporal cortices. More specifically, we found significantly increased nodal local efficiency in the left olfactory cortex in the SIVCIND patients. These results provide insights into the relationship between altered structural networks and cognitive deficits in SIVCIND patients.

Altered Global Topological Properties in SIVCIND Patients Compared With Normal Controls

As shown by the significant decrease in the values of the C_p and E_{glob} and significant increase in the values of the L_p in the SIVCIND patients, there was a disruption in the organization of the brain structural network in this cohort (**Figure 2**). The changes in these global network metrics could be attributable to decreased long-distance structural connections and the density of connections involved in specialized networks such as the default mode network in SIVCIND patients (**Figure 4**). Specifically, the MMSE scores were positively correlated with the C_p and had a tendency of negative correlation with L_p (**Figure 5**). Hence, the deterioration of the cognitive functioning in the SIVCIND patients was associated with less-extended local clustering and a reduced ability to transmit information from distributed brain regions. Our results were in keeping with previous studies. For instance, Du et al. (2019) found that the global network efficiency of the brain structural network was significantly related to the cognitive state in patients with mild cognitive impairment caused by small vessel disease. Moreover, Heinen et al. (2018) also found that global network efficiency of the brain structural network was related to cognitive functioning such as information processing speed, attention, and executive functioning in patients with mild cognitive impairment caused by small vessel disease.

Our results are also in accord with some previous studies regarding functional organization in SIVCIND. For example, one study found that there was decreased C_p and E_{glob} in several brain regions located in parietal and temporal cortices, and these changes were related to the performance on cognitive test (Yu et al., 2015). Moreover, our recent work (Sang et al., 2018) also found that SIVCIND patients showed significantly decreased E_{glob} and C_p in the brain functional connectivity network, and these changes were correlated with cognitive deficits.

Decreased Nodal Efficiency in SIVCIND Compared With Normal Controls

The local (global) efficiency at the nodal level was also studied, which describes the capacity for information exchange between one node and the direct neighbors (and all other nodes in the networks). Notably, twenty-six brain regions exhibited significantly decreased E_{nodal_glob} and no brain region exhibited significantly increased E_{nodal_glob}, suggesting that the capacity of information transfer was reduced between one node and the remaining nodes in the network in SIVCIND patients (**Figure 3** and **Table 2**).

Several regions of decreased E_{nodal_glob} were found in SIVCIND patients compared with normal controls, including the prefrontal and subcortical cortex, which are the primary components of the prefrontal/subcortical circuit. Previous studies verified that the interruption of this circuit was associated with executive dysfunction, which is a specific symptom of cognitive dysfunction seen in SIVCIND patients (Román et al., 2002; Erkinjuntti, 2003). Moreover, SIVCIND has been considered to be a syndrome of extensive damage to the white

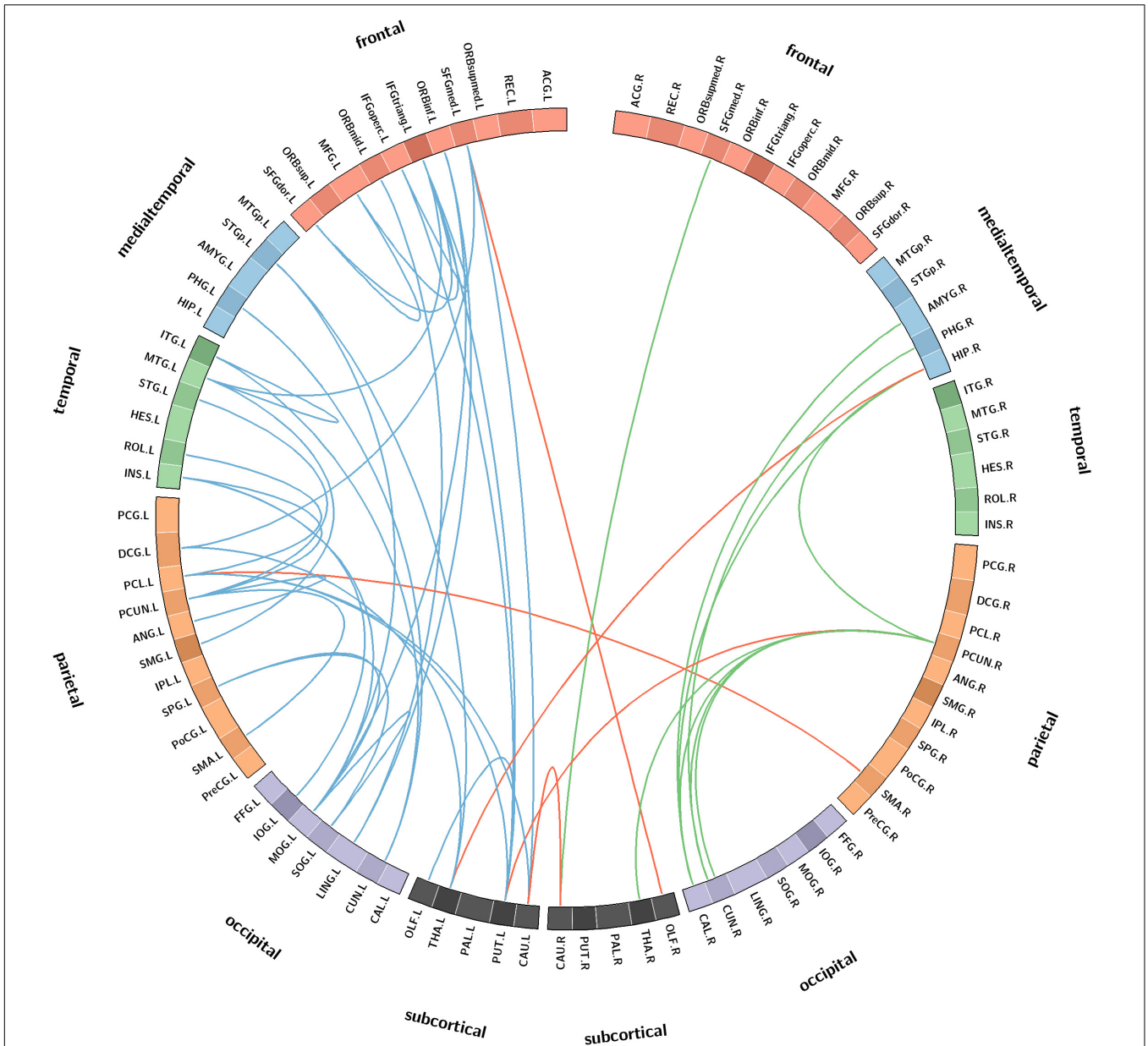

FIGURE 4 | Connectograms show the decreased structural connections in SIVCIND patients compared to NCs (NBS corrected, $p < 0.01$). Links are colored by connection type as follows: left intrahemispheric (blue), interhemispheric (red) and right intrahemispheric (green). ROIs were grouped according to Salvador (Salvador et al., 2005) (i.e., frontal, temporal, parietal, medial temporal, occipital, and subcortical).

matter tracts or U-fibers, which connect cortical and subcortical regions. Thus, our results are in line with previous studies.

Specifically, we found that the SIVCIND patients showed significantly increased nodal local efficiency in the left olfactory cortex (**Figure 3** and **Table 2**). The olfactory cortex is the area responsible for receiving and processing smell-related stimuli and includes the prepyriform area and the entorhinal cortex (EC). Specifically, the EC is an important memory center in the brain. The EC forms the main input to the hippocampus and is responsible for the preprocessing of the input signals (Buzsaki and Moser, 2013), and the EC-hippocampus system plays an important role in memory consolidation and optimization in sleep. Increased nodal local efficiency of the olfactory gyrus may act as a compensation mechanism for memory deficits in SIVCIND patients.

Compared with the NCs, the SIVCIND patients had lower nodal global and local efficiency in several temporal and parietal brain areas, including the inferior parietal gyrus, superior and middle temporal gyrus. Moreover, Thong et al. (2014) found that the parietal and temporal cortices thin as cognitive impairment worsens in patients with cognitive impairment caused by SIVD, showing evidence of structural alterations in

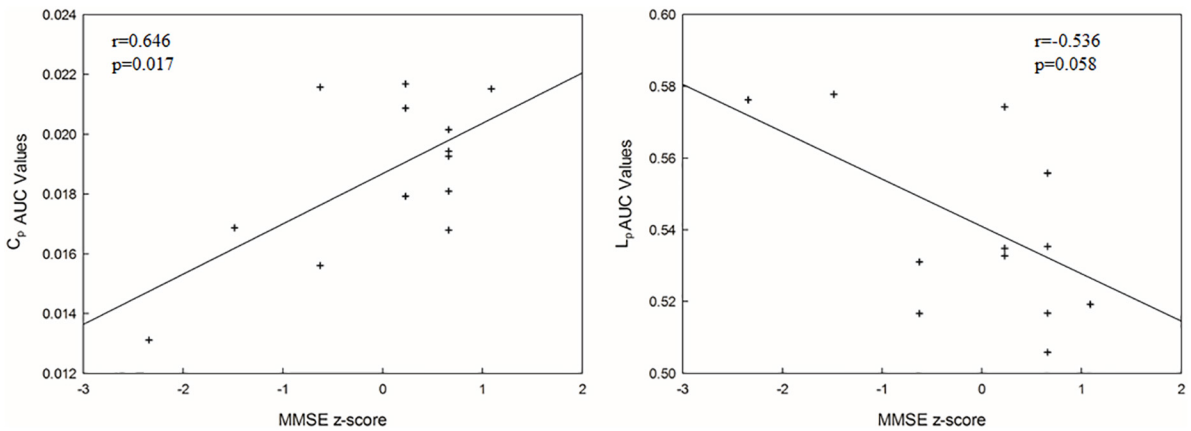

FIGURE 5 | The correlations between each AUC network metric value and MMSE score ($p < 0.05$). C_p, clustering coefficient; L_p, mean path length.

SIVCIND patients. Additionally, decreased nodal efficiency in the parietal/temporal areas suggests that their lower capacity for information exchange in the structural connectivity network is presumably associated with non-cognitive symptoms such as apathy and decreased motor function in SIVCIND patients (Gupta and Dasgupta, 2014).

Decreased Structural Connectivity in SIVCIND

The NBS analyses found decreased structural connections in the SIVCIND patients compared with the normal controls (**Figure 4**). A previous structural study found cortical thinning in SIVCIND patients, and the extent and severity of the cortical thinning were in accordance with those seen in cognitive impairment (Meyer et al., 2007; Seo et al., 2010). An examination of the connectogram shows that the weakened alterations in the SIVCIND patients mainly concerned fronto-occipital, fronto-subcortical and temporo-occipital connections. Some previous DTI studies found alterations in the brain white matter between SIVCIND patients and normal controls. For instance, decreased FA value was found in several projection fibers and association fibers in SIVCIND patients, including the posterior thalamic radiations, cingulum, and fronto-occipital fasciculus (Lin et al., 2015). Moreover, Zhou et al. (2011) found decreased FA value in the bilateral frontal lobes, occipital lobes, temporal lobes, and insula in SIVCIND patients compared with normal controls. Therefore, the results from this study are in line with those previous studies, and these alterations may be responsible for cognitive impairment in SIVCIND patients. Additionally, significantly decreased connections were observed in the mediotemporal cortices in the SIVCIND patients, which is thought to be involved in encoding declarative memory (Squire et al., 2004), and decreased connections in this area can lead to forgetfulness, a clinical manifestation of cognitive impairment caused by SIVD (Román et al., 2002).

Furthermore, almost all the network hubs were components of the default mode network (DMN) (**Table 3**). The DMN is considered a critical resting-state functional network of the brain. Previous studies have suggested that the DMN is associated with cognitive and emotional processing (Mantini and Vanduffel, 2013). Decreased functional connections in the DMN were found in our recent study (Sang et al., 2018). Moreover, Jiang et al. (2018) also found decreased functional connections in the DMN in ischemic stroke patients. The significantly decreased structural connectivity in these brain regions may lead to functional disruption in the DMN in the functional network and may provide new insight to investigate the relationship between structural alterations and functional degeneration.

Several limitations in our study need to be further addressed. First, although the patients enrolled in the study were been strictly checked to ensure the homogeneity of vascular lesions as far as possible, the severity degree of the lesions was not absolutely uniform across the patients. In future studies, we should recruit more patients to ensure the homogeneity of vascular lesions.

TABLE 3 | Significant structural connectivity differences between SIVCIND patients and normal controls ($p < 0.01$, NBS corrected).

Contrast	Side	Brain regions
NC vs. SIVCIND		
	Right	Hippocampal gyrus
		Precuneus
		Calcarine cortices
	Left	Inferior frontal gyrus, triangular part
		Superior frontal gyrus, orbital media part
		Insula
		Lingual gyrus
		Precuneus
		Middle occipital gyrus
		Paracentral lobule
		Caudate nucleus
		Putamen
		Thalamus
		Middle temporal gyrus

Only cortical and subcortical regions with a high degree of significant connections (k > 1 SD above the mean) are reported.

Second, the sample size in this study was not large which may lead to insufficient statistical power identifying the group difference between SIVCIND patients and normal controls. Third, the study employed deterministic tractography methods to construct a brain white matter connectivity network. However, the tracking procedure would terminate when it arrived at a voxel with fiber crossings or spreading, which always reduces the tracking of existing fibers. In future studies, to obtain a more accurate assessment of white matter connectivity, we should apply more advanced diffusion acquisition techniques and diffusion models, such as probabilistic tractography (Behrens et al., 2007).

CONCLUSION

Our results revealed that cognitive impairment in SIVCIND patients is associated with alterations in the structural connectivity network. The topological organization of the network in SIVCIND was disrupted, with significantly decreased C_p and E_{glob} and a significantly increased L_p. Moreover, a significantly decreased E_{nodal_glob} was found in some areas that are mainly involved in the prefrontal, parietal, mediotemporal and subcortical cortices in the SIVCIND patients. Decreased structural connections were found in SIVCIND mainly concerning cortical-subcortical connectivity. These results suggest a disrupted organization in the brain structural connectivity network in SIVCIND patients; these results may be helpful to develop reliable biomarkers of structural network changes related to cognitive decline in SIVD.

DATA AVAILABILITY STATEMENT

The datasets generated for this study are available on request to the corresponding author.

ETHICS STATEMENT

The studies involving human participants were reviewed and approved by the local Medical Ethics Committee at Third Military Medical University (Chongqing, China). The patients/participants provided their written informed consent to participate in this study.

AUTHOR CONTRIBUTIONS

LS, CLi, and MQ conceived and designed the experiments. LS, CLiu, LW, JZ, YZ, and PL performed the experiments. LS, JZ, and LQ analyzed the data. JZ and YZ contributed the reagents, materials, and analysis tools. LS wrote the manuscript and performed figure processing.

FUNDING

This work was supported by the 2018 Youth Development Program of the Third Military Medical University to LS (2018XQN04), the Chongqing Science and Health Joint Medical Research Project to CLi (2018ZDXM005), the Technological Innovation and Application Demonstration of Chongqing CSTC of China to LQ (cstc2018jscx-msybX0073), the 2016 Youth Development Program of Third Military Medical University to LW (2016XPY05), the National Natural Science Foundation of China to JZ (81601970), and National Natural Science Foundation of China to YZ (81802253).

SUPPLEMENTARY MATERIAL

The Supplementary Material for this article can be found online at: https://www.frontiersin.org/articles/10.3389/fnagi.2020.00006/full#supplementary-material

REFERENCES

Achard, S., and Bullmore, E. (2007). Efficiency and Sparsity of economical brain functional networks. *PLoS Comput. Biol.* 3:e17. doi: 10.1371/journal.pcbi.0030017

Behrens, T. E. J., Berg, H. J., Jbabdi, S., Rushworth, M. F. S., and Woolrich, M. W. (2007). Probabilistic diffusion tractography with multiple fibre orientations: what can we gain? *Neuroimage* 1, 144–155. doi: 10.1016/j.neuroimage.2006.09.018

Bullmore, E., and Sporns, O. (2009). Complex brain networks: graph theoretical analysis of structural and functional systems. *Nat. Rev.* 10, 186–198. doi: 10.1038/nrn2575

Buzsaki, G., and Moser, E. I. (2013). Memory, navigation and theta rhythm in the hippocampal-entorhinal system. *Nat. Neurosci.* 2, 130–138. doi: 10.1038/nn.3304

Cummings, J., Mega, M., Gray, K., Rosenberg-Thompson, S., Carusi, D., and Gornbein, J. (1994). The Neuropsychiatric inventory: comprehensive assessment of psychopathol-ogy in dementia. *Neurology* 44, 2308–2314.

Du, J., Wang, Y., Zhia, N., Genga, J., Cao, W., Yua, L., et al. (2019). Structural brain network measures are superior to vascular burden scores in predicting early cognitive impairment in post stroke patients with small vessel disease. *Neuroimage* 22:101712. doi: 10.1016/j.nicl.2019.101712

Erkinjuntti, T. (2003). Subcortical ischemic vascular disease and dementia. *Int. Psychogeriatr.* 15(Suppl. 1), 23–26. doi: 10.1017/s1041610203008925

Folstein, M., Folstein, S., and McHugh, P. (1975). "Mini-mental state": a practical method for grading the cognitive state of patients for the clinician. *J. Psychiatr. Res.* 3, 189–198.

Galluzzi, S., Sheu, C., Zanetti, O., and Frisoni, G. B. (2005). Distinctive clinical features of mild cognitive impairment with subcortical cerebrovascular disease. *Dement. Geriatr. Cogn. Disord.* 4, 196–203. doi: 10.1159/000083499

Gupta, M., and Dasgupta, A. (2014). Behavioural and psychological symptoms in poststroke vascular cognitive impairment. *Behav. Neurol.* 2014:430128. doi: 10.1155/2014/430128

Hachinski, V., Iliff, L., Zilhka, E., Du Boulay, G., McAllister, V., and Marshall, J. (1975). Cerebralblood flow in dementia. *Arch. Neurol.* 32, 632–637.

He, Y., and Evans, A. (2010). Graph theoretical modeling of brain connectivity. *Curr. Opin. Neurol.* 4, 341–350.

He, Y., Wang, J., Wang, L., Chen, Z. J., Yan, C., Yang, H., et al. (2009). Uncovering intrinsic modular organization of spontaneous brain activity in humans. *PLoS One* 4:e5226. doi: 10.1371/journal.pone.0005226

Heinen, R., Vlegels, N., de Bresser, J., Leemans, A., Biessels, G. J., and Reijmer, Y. D. (2018). The cumulative effect of small vessel disease lesions is reflected in structural brain networks of memory clinic patients. *Neuroimage* 19, 963–969. doi: 10.1016/j.nicl.2018.06.025

Irimia, A., Chambers, M. C., Torgerson, C. M., and Van Horn, J. D. (2012). Circular representation of human cortical networks for subject and population-level connectomic visualization. *Neuroimage* 2, 1340–1351. doi: 10.1016/j.neuroimage.2012.01.107

Jiang, L., Geng, W., Chen, Y., Chen, H., Zhang, H., Bo, F., et al. (2018). Decreased functional connectivity within the default-mode network in acute brainstem ischemic stroke. *Eur. J. Radiol.* 105, 221–226. doi: 10.1016/j.ejrad.2018.06.018

Lin, L., Xue, Y., Duan, Q., Sun, B., Lin, H., Chen, X., et al. (2015). Microstructural white matter abnormalities and cognitive dysfunction in subcortical ischemic vascular disease: an atlas-based diffusion tensor analysis study. *J. Mol. Neurosci.* 2, 363–370. doi: 10.1007/s12031-015-0550-5

Lopes, R., Delmaire, C., Defebvre, L., Moonen, A. J., Duits, A. A., Hofman, P., et al. (2017). Cognitive phenotypes in parkinson's disease differ in terms of brain-network organization and connectivity. *Hum. Brain Mapp.* 3, 1604–1621. doi: 10.1002/hbm.23474

Mantini, D., and Vanduffel, W. (2013). Emerging roles of the brain's default network. *Neuroscientist* 1, 76–87. doi: 10.1177/1073858412446202

Meyer, J., Huang, J., and Chowdhury, M. (2007). MRI confirms mild cognitive impairments prodromal for Alzheimer's, vascular and Parkinson–Lewy body dementias. *J. Neurol. Sci.* 257, 97–104. doi: 10.1016/j.jns.2007.01.016

Moris, J. C. (1993). The Clinical Dementia Rating (CDR): current version and scoringrules. *Neurology* 43, 2412–2414.

Nasreddine, Z., Phillips, N., Bedirian, V., Charbonneau, S., Whitehead, V., and CollinI. (2005). The montreal cognitive assessment, MoCA: a brief screening tool for mildcognitive impairment. *J. Am. Geriatr. Soc.* 53, 695–699. doi: 10.1111/j.1532-5415.2005.53221.x

O'Brien, J. T., and Thomas, A. (2015). Vascular dementia. *Lancet* 386, 1698–1706. doi: 10.1016/S0140-6736(15)00463-8

Onnela, J. P., Saramaki, J., Kertesz, J., and Kaski, K. (2005). Intensity and coherence of motifs in weighted complex networks. *Phys. Rev. E Stat. Nonlin. Soft. Matter Phys.* 6(Pt 2):65103.

Reisberg, B., Ferris, S., de Leon, M., and Crook, T. (1982). The global deteriorationscale for assessment of primary degenerative dementia. *Am. J. Psychiatry* 139, 1136–1139. doi: 10.1176/ajp.139.9.1136

Román, G. C., Erkinjuntti, T., Wallin, A., Pantoni, L., and Chui, H. C. (2002). Subcortical ischaemic vascular dementia. *Lancet Neurol.* 1, 426–436. doi: 10.1016/s1474-4422(02)00190-4

Sachdev, P., Kalaria, R., O'Brien, J., Skoog, I., Alladi, S., Black, S. E., et al. (2014). Diagnostic criteria for vascular cognitive disorders. *Alzheimer Dis. Assoc. Disord.* 3, 206–218.

Salvador, R., Suckling, J., Coleman, M. R., Pickard, J. D., Menon, D., and Bullmore, E. (2005). Neurophysiological architecture of functional magnetic resonance images of human brain. *Cereb. Cortex* 9, 1332–1342. doi: 10.1093/cercor/bhi016

Sang, L., Chen, L., Wang, L., Zhang, J., Zhang, Y., Li, P., et al. (2018). Progressively disrupted brain functional connectivity network in subcortical ischemic vascular cognitive impairment patients. *Front. Neurol.* 9:94. doi: 10.3389/fneur.2018.00094

Seo, S. W., Ahn, J., Yoon, U., Im, K., Lee, J., Sung, T. K., et al. (2010). Cortical thinning in vascular mild cognitive impairment and vascular dementia of subcortical type. *J. Neuroimaging* 20, 37–45. doi: 10.1111/j.1552-6569.2008.00293.x

Shu, N., Liang, Y., Li, H., Zhang, J., Li, X., Wang, L., et al. (2012). Disrupted topological organization in white matter structural networks in amnestic mild cognitive impairment: relationship to subtype1. *Radiology* 2, 518–527. doi: 10.1148/radiol.12112361

Squire, L. R., Stark, C. E. L., and Clark, R. E. (2004). The medial temporal lobe. *Annu. Rev. Neurosci.* 1, 279–306.

Thong, J. Y. J., Du, J., Ratnarajah, N., Dong, Y., Soon, H. W., Saini, M., et al. (2014). Abnormalities of cortical thickness, subcortical shapes, and white matter integrity in subcortical vascular cognitive impairment. *Hum. Brain Mapp.* 5, 2320–2332. doi: 10.1002/hbm.22330

Warren, E., Grek, A., Conn, D., Herrmann, N., Icyk, E., Kohl, J., et al. (1989). A correlationbetween cognitive performance and daily functioning in elderly people. *J. Geri-atr. Psychiatry Neurol.* 2, 96–100. doi: 10.1177/089198878900200209

Watts, D. J., and Strogatz, S. H. (1998). Collective dynamics of 'small-world' networks. *Nature* 393, 440–442. doi: 10.1038/30918

Xu, Q., Zhou, Y., Li, Y. S., Cao, W. W., Lin, Y., Pan, Y. M., et al. (2010). Diffusion tensor imaging changes correlate with cognition better than conventional MRI findings in patients with subcortical ischemic vascular disease. *Dement. Geriatr. Cogn. Disord.* 4, 317–326. doi: 10.1159/000320491

Yu, Y., Liang, X., Yu, H., Zhao, W., Lu, Y., Huang, Y., et al. (2017). How does white matter microstructure differ between the vascular and amnestic mild cognitive impairment? *Oncotarget* 1, 42–50. doi: 10.18632/oncotarget.13960

Yu, Y., Zhou, X., Wang, H., Hu, X., Zhu, X., Xu, L., et al. (2015). Small-world brain network and dynamic functional distribution in patients with subcortical vascular cognitive impairment. *PLoS One* 7:e131893. doi: 10.1371/journal.pone.0131893

Zalesky, A., Fornito, A., and Bullmore, E. T. (2010). Network-based statistic: identifying differences in brain networks. *Neuroimage* 4, 1197–1207. doi: 10.1016/j.neuroimage.2010.06.041

Zhang, J., Wang, J., Wu, Q., Kuang, W., Huang, X., He, Y., et al. (2011). Disrupted brain connectivity networks in drug-naive, first-episode major depressive disorder. *Biol. Psychiatry* 70, 334–342. doi: 10.1016/j.biopsych.2011.05.018

Zhou, Y., Qun, X., Qin, L., Qian, L., Cao, W., and Xu, J. (2011). A primary study of diffusion tensor imaging-based histogram analysis in vascular cognitive impairment with no dementia. *Clin. Neurol. Neurosurg.* 113, 92–97. doi: 10.1016/j.clineuro.2010.09.007

Zhu, Y., Bai, L., Liang, P., Kang, S., Gao, H., and Yang, H. (2016). Disrupted brain connectivity networks in acute ischemic stroke patients. *Brain Imaging Behav.* 11, 444–453. doi: 10.1007/s11682-016-9525-6

Conflict of Interest: The authors declare that the research was conducted in the absence of any commercial or financial relationships that could be construed as a potential conflict of interest.

frontiers in Aging Neuroscience

ORIGINAL RESEARCH
published: 12 June 2020
doi: 10.3389/fnagi.2020.00177

The Role of Resting-State Network Functional Connectivity in Cognitive Aging

*Hanna K. Hausman[1], Andrew O'Shea[1], Jessica N. Kraft[1], Emanuel M. Boutzoukas[1], Nicole D. Evangelista[1], Emily J. Van Etten[2], Pradyumna K. Bharadwaj[2], Samantha G. Smith[2], Eric Porges[1], Georg A. Hishaw[3], Samuel Wu[4], Steven DeKosky[5], Gene E. Alexander[2,6], Michael Marsiske[1], Ronald Cohen[1] and Adam J. Woods[1]**

[1]*Department of Clinical and Health Psychology, Center for Cognitive Aging and Memory, College of Public Health and Health Professions, McKnight Brain Institute, University of Florida, Gainesville, FL, United States,* [2]*Department of Psychology, McKnight Brain Institute, University of Arizona, Tucson, AZ, United States,* [3]*Department of Psychiatry and Neurology, College of Medicine, University of Arizona, Tucson, AZ, United States,* [4]*Department of Biostatistics, College of Public Health and Health Professions, College of Medicine, University of Florida, Gainesville, FL, United States,* [5]*Department of Neurology, College of Medicine, Center for Cognitive Aging and Memory, McKnight Brain Institute, University of Florida, Gainesville, FL, United States,* [6]*Department of Psychiatry, Neuroscience and Physiological Sciences Graduate Interdisciplinary Programs, and BIO5 Institute, University of Arizona and Arizona Alzheimer's Disease Consortium, Tucson, AZ, United States*

OPEN ACCESS

Edited by:
P. Hemachandra Reddy, Texas Tech University Health Sciences Center, United States

Reviewed by:
Boon-Seng Wong, Singapore Institute of Technology, Singapore
Ben Nephew, Worcester Polytechnic Institute, United States

***Correspondence:**
Adam J. Woods
ajwoods@phhp.ufl.edu

Received: *31 January 2020*
Accepted: *22 May 2020*
Published: *12 June 2020*

Citation:
Hausman HK, O'Shea A, Kraft JN, Boutzoukas EM, Evangelista ND, Van Etten EJ, Bharadwaj PK, Smith SG, Porges E, Hishaw GA, Wu S, DeKosky S, Alexander GE, Marsiske M, Cohen R and Woods AJ (2020) The Role of Resting-State Network Functional Connectivity in Cognitive Aging. Front. Aging Neurosci. 12:177. doi: 10.3389/fnagi.2020.00177

Aging is associated with disruptions in the resting-state functional architecture of the brain. Previous studies have primarily focused on age-related declines in the default mode network (DMN) and its implications in Alzheimer's disease. However, due to mixed findings, it is unclear if changes in resting-state network functional connectivity are linked to cognitive decline in healthy older adults. In the present study, we evaluated the influence of intra-network coherence for four higher-order cognitive resting-state networks on a sensitive measure of cognitive aging (i.e., NIH Toolbox Fluid Cognition Battery) in 154 healthy older adults with a mean age of 71 and education ranging between 12 years and 21 years (mean = 16). Only coherence within the cingulo-opercular network (CON) was significantly related to Fluid Cognition Composite scores, explaining more variance in scores than age and education. Furthermore, we mapped CON connectivity onto fluid cognitive subdomains that typically decline in advanced age. Greater CON connectivity was associated with better performance on episodic memory, attention, and executive function tasks. Overall, the present study provides evidence to propose CON coherence as a potential novel neural marker for nonpathological cognitive aging.

Keywords: cingulo-opercular, cognitive aging, functional connectivity, resting-state, networks

INTRODUCTION

By the year 2050, the number of adults over the age of 65 in the United States population is expected to double, signifying one of the fastest-growing age cohorts. With advanced age, crystallized cognitive abilities, such as accumulated knowledge and vocabulary, are maintained and can even improve over time. Conversely, even in the absence of pathology, older adults experience declines in fluid cognitive abilities such as thinking abstractly, reasoning, and decision-making

(Salthouse, 2010; Murman, 2015). Declines in these capacities are linked to underlying age-related deficits in processing speed, attention, memory, and executive function (i.e., cognitive aging; Salthouse, 1994, 2000, 2010; Glisky, 2007). Cognitive aging in later life is associated with functional impairments in managing new information, manipulating the environment, and solving problems (Salthouse, 1994, 2000, 2010; Buckner, 2004; Wecker et al., 2005; Harada et al., 2013). These impairments can affect older adults' ability to function independently within society and the home. Also, extensive evidence reveals that cognitive decline and associated functional decline in older adults has been related to changes in the structure and function of the brain (Salat et al., 1999; Raz, 2000; Reuter-Lorenz et al., 2000; Cabeza, 2002; Raz et al., 2005; Andrews-Hanna et al., 2007; Kennedy and Raz, 2009). Therefore, it is imperative to identify what brain-based factors significantly contribute to cognitive aging. A more comprehensive understanding of age-related neural alterations within cognitive aging may facilitate better differentiation of nonpathological aging from disease states and the identification of target brain areas for intervention.

One of the increasingly popular methods used to study age and pathology-related changes in the brain is resting-state functional magnetic resonance imaging (rs-fMRI). rs-fMRI is used to identify coherent fluctuations in brain activity when a person is not actively engaging in a cognitive task (i.e., at rest; Biswal et al., 2010; Biswal, 2012). rs-fMRI is particularly advantageous when studying aging populations because it allows for the examination of functional connectivity while removing the demand of a task that may be confounded by potential cognitive or motor impairments. Additionally, scan times are relatively short (5–15 min), benefitting older adults that may have difficulties lying on one's back for long periods or those with psychological concerns regarding a novel scanning environment.

Across the lifespan, rs-fMRI has identified low-frequency resting-state networks that depict the functional architecture of the brain. Resting-state networks have been characterized for aspects of attention (Fox et al., 2006), memory (Vincent et al., 2006), cognitive control (Dosenbach et al., 2007; Vincent et al., 2008; Cole et al., 2010), default mode (Raichle et al., 2001; Buckner et al., 2008), motor (Biswal et al., 1995), and sensory systems (De Luca et al., 2005; Damoiseaux et al., 2006). Yeo et al. (2011) published a parcellation of the brain into seven major resting-state networks: the default mode network (DMN), the dorsal attention network (DAN), the frontoparietal control network (FPCN), the cingulo-opercular network (CON) [commonly referred to as the salience (Seeley et al., 2007) or ventral attention network (Fox et al., 2006)], the limbic network, the visual network, and the somatomotor network.

Investigators have used rs-fMRI techniques to examine how patterns of resting-state network functional connectivity change with age (Andrews-Hanna et al., 2007; Chan et al., 2014; Damoiseaux, 2017; Siman-Tov et al., 2017; Spreng and Turner, 2019). While previous studies have primarily focused on age-related declines in the connectivity of the DMN (Andrews-Hanna et al., 2007; Damoiseaux et al., 2007; Ferreira and Busatto, 2013), recent research has uncovered several additional "higher-order cognitive" networks vulnerable to the aging process (e.g., FPCN, CON, DAN; Geerligs et al., 2015a; Siman-Tov et al., 2017). While it is clear that resting-state network connectivity is disrupted in healthy older adults, it is unclear whether these age-related changes in resting-state functional connectivity contribute to the cognitive aging process. Studies examining the relationship between network connectivity and cognition in older adults have used a variety of cognitive tasks and resting-state methods, producing inconsistent results (see Ferreira and Busatto, 2013 for review). For example, some studies have shown DMN, FPCN, and CON connectivity in older adults to be associated with performance on specific executive functioning, memory, and processing speed tasks (Andrews-Hanna et al., 2007; Damoiseaux et al., 2007; Shaw et al., 2015). However, Onoda et al. (2012) only found an association between CON connectivity and executive functioning (i.e., the Frontal Assessment Battery and Kohs' Block Design) and did not replicate a relationship between the other higher-order cognitive networks and cognitive performance in older adults. Lastly, Geerligs et al. (2015a) did not find a significant relationship between any of the seven major resting-state networks and cognitive performance in older adults. These inconsistent findings are surprising given the emphasis in the literature on DMN connectivity in aging (Ferreira and Busatto, 2013), suggesting future research should include other networks in analyses and incorporate sensitive cognitive measures that model the cognitive aging process. Importantly, a majority of previous studies compared resting-state connectivity patterns and cognitive performance between younger and older adults. This type of experimental design can be problematic for characterizing connectivity, as it is confounded by cohort effects and age differences in head motion, heart rate variability, and cerebrovascular function (D'Esposito et al., 1999; Geerligs et al., 2015b, 2017; Prins and Scheltens, 2015). Additionally, a majority of these studies had small sample sizes, potentially contributing to null findings. Consequently, there is a need for a study with a large sample of older adults to evaluate the association between sensitive measures of cognitive aging and inter-individual differences in resting-state network functional connectivity.

To comprehensively assess cognitive aging, we used the NIH Toolbox Cognition Battery (Weintraub et al., 2013)[1]. The NIH Toolbox yields a Fluid Cognition Composite, which consists of measures categorized as skills that decline as a function of advanced age: the Dimensional Change Card Sort (executive function), Flanker (executive function and attention), Picture Sequence Memory (episodic memory), List Sorting (working memory), and Pattern Comparison tasks (processing speed). The primary aim was to identify a relationship between resting-state network connectivity and the overall cognitive aging process. As such, this study analyzed the contribution of the four higher-order cognitive networks (DMN, DAN, FPCN, CON) on Fluid Cognition Composite scores in a large sample of healthy older adults. Although the prior literature has been highly variable regarding which networks relate to cognition in older adults, the DMN, FPCN, and CON networks are the most common networks implicated (Andrews-Hanna et al., 2007; Onoda et al.,

[1] www.nihtoolbox.org

2012; Shaw et al., 2015) with little evidence for the DAN, which may be less sensitive to the effects of age compared to the other higher-order cognitive networks (Chan et al., 2014; Grady et al., 2016). Therefore, we predicted that older adults with greater within-network resting-state functional connectivity of the DMN, FPCN, and CON networks would have higher Fluid Cognition Composite scores. In secondary analyses, we mapped networks significantly related to the Fluid Cognition Composite onto the subtests to identify which specific domains characterized the relationship between network connectivity and cognitive aging. Our results provide important new insights into age-related cognitive declines and inter-individual variability in resting-state network connectivity, identifying a potential neural marker for nonpathological cognitive aging.

TABLE 1 | Participant demographics and NIH toolbox scores.

Demographics	**Mean/SD**
Age	71.4 ± 5.1
Education (Number of years)	16.2 ± 2.4
Gender	**N**
Males	65
Females	94
NIH toolbox	**Mean/SD**
Fluid cognition composite	93.1 ± 8.6
List sorting	98.2 ± 8.9
Pattern comparison	90.6 ± 14.0
Picture sequence memory	95.7 ± 10.2
Flanker	93.9 ± 6.7
Dimensional change card sort	100.9 ± 7.3

Notes: NIH toolbox scores are unadjusted standard scores.

MATERIALS AND METHODS

Participants

Data were collected at baseline from participants recruited for the Stimulated Brain (K01AG050707) and the Augmenting Cognitive Training in Older Adults (ACT, R01AG054077) studies (Woods et al., 2018). Our sample included 159 healthy older adults ranging from 65 to 87 years old (mean age = 71.4 ± 5.1; 92 females; mean education = 16.2 ± 2.4, education range = 12–21 years; **Table 1**) recruited at the University of Florida (n = 110) and the University of Arizona (n = 49). Woods et al. (2018) detail the inclusion and exclusion criteria. In brief, participants were between the ages of 65–89, had no history of major psychiatric illness, no history of brain or head injury resulting in loss of consciousness greater than 20 min, and no formal diagnosis or evidence of mild cognitive impairment (MCI), dementia, or neurological brain disease. The Unified Data Set (UDS) of the National Alzheimer's Coordinating Center (NACC) was used to screen for individuals with possible MCI or dementia (Weintraub et al., 2009). Possible MCI was defined by 1.5 standard deviations below the mean in any of the following domains: general cognition, memory, visuospatial, executive functioning/working memory, or language. All participants were right-handed and had no contraindications for MRI scanning. Before beginning all study procedures, participants signed a consent form approved by the Institutional Review Boards at the University of Florida and the University of Arizona. At the baseline visit, participants completed a variety of cognitive assessments, medical history and mood questionnaires, and an MRI scan. In this study, we used the NIH Toolbox Cognition battery and the rs-fMRI data for our analyses. Three participants were excluded due to incomplete or extreme scores (greater than three standard deviations from the mean) on the NIH toolbox. Additionally, two participants were excluded as outliers due to extreme network connectivity values resulting in a total sample size of 154 older adults.

NIH Toolbox

The NIH Toolbox Cognition Battery is a brief set of sensitive measures used to assess a range of cognitive domains (Weintraub et al., 2013). In the present study, we used the unadjusted standard scores for the Fluid Cognition Composite and its five subtests that measure cognitive abilities shown to decline with advanced age. These subtests measure components of executive function, attention, episodic memory, working memory, and processing speed. For instance, the Dimensional Change Card Sort task assesses the set-shifting component of executive function (i.e., the ability to switch among multiple task strategies and rules). Here, a participant must match a target stimulus to a choice stimulus according to the shifting criterion of either shape or color. The Flanker task is a visuospatial attention task that also requires inhibitory control over automatic responses. The goal of this task is to determine the direction of a central target arrow that is flanked by similar stimuli on the left and right. The Picture Sequence Memory task targets episodic memory, a cognitive process involved in the retrieval of learned information. In this task, thematically related pictures are displayed in a sequence, and participants must remember and move the pictures into the sequence demonstrated. The List Sorting task is a measure of working memory, the ability to temporarily hold and manipulate a limited capacity of information. This requires participants to sequence and sort a list of visual and auditory stimuli from smallest to largest increasing in the number of categories and items. Lastly, the Pattern Comparison task is a measure of processing speed, where participants quickly identify whether or not two visual patterns are the same.

Imaging Acquisition

rs-fMRI data were collected using a 3-Tesla Siemens Magnetom Prisma scanner with a 64-channel head coil at the Center for Cognitive Aging and Memory at the University of Florida and using a 3-Tesla Siemens Magnetom Skyra scanner with a 32-channel head coil at the University of Arizona. Scanner type was included as a covariate in our statistical analyses to control for potential differences in the quality and acquisition of MRI data. Both study sites followed the same scanning procedures and used identical sequences. Participant head motion was constrained by foam padding, and participants were provided with earplugs to reduce the adverse effects of scanner noise. For acquiring resting-state data, participants were asked to rest for about 6 min while keeping their eyes open, as a blood-oxygen-level-dependent (BOLD) scan was acquired with an echo-planar functional protocol [number of volumes = 120,

repetition time (TR) = 3,000 ms, echo time (TE) = 30 ms; flip angle = 70°, 3.0 × 3.0 × 3.0 mm^3 voxels; 44 slices, field of view (FOV) = 240 × 240 mm]. To assist the normalization of the resting-state functional images in the preprocessing stage, high-resolution T1-weighted 3D magnetization prepared rapid acquisition gradient echo (MPRAGE) images were collected (TR = 1,800 ms; TE = 2.26 ms; 1.0 × 1.0 × 1.0 mm^3 voxels; 176 slices; FOV = 256 × 256 mm; FA = 8°; time = 3 min and 3 s).

rs-fMRI Preprocessing

Structural and functional images were preprocessed and analyzed using the MATLAB R2016b based functional connectivity toolbox "Conn toolbox" version 18b and SPM 12 (Penny et al., 2007; Whitfield-Gabrieli and Nieto-Castanon, 2012). We followed a preprocessing pipeline which included the functional realignment and unwarping, functional centering of the image to (0, 0, 0) coordinates, slice-timing correction, structural centering to (0, 0, 0) coordinates, structural segmentation and normalization to MNI space, functional normalization to MNI space, and spatial smoothing with a smoothing kernel of 8 mm FWHM. During preprocessing, the Conn toolbox implements an anatomical, component-based, noise correction strategy (*aCompCor*) for spatial and temporal processing to remove physiological noise factors from the data (Behzadi et al., 2007). The implementation of *aCompCor* combined with the quantification of participant motion and the identification of outlier scans through the Artifact Rejection Toolbox (ART)[2] allows for better interpretation of functional connectivity results (Behzadi et al., 2007; Whitfield-Gabrieli and Nieto-Castanon, 2012; Shirer et al., 2015). The ART was set to the 97th percentile setting with the mean global-signal deviation threshold set at $z = \pm 5$ and the participant-motion threshold set at 0.9 mm. Due to potential confounding effects, the resulting motion information and frame-wise outliers were included as covariates in our first-level analyses (Behzadi et al., 2007; Power et al., 2012; van Dijk et al., 2012). Applying linear regression and using a band-pass filter of 0.008–0.09 Hz, data were denoised to exclude signal frequencies outside of the range of expected BOLD signals (such as low-frequency scanner drift), minimize participant motion, extract white matter and cerebral spinal fluid noise components, and control for within-participant realignment and scrubbing covariates.

Within-Network Connectivity and Cognitive Performance Analyses

For the rs-fMRI analyses, we used a publicly available network parcellation of the brain defined by Yeo et al. (2011) that has been commonly used in the resting-state literature (Betzel et al., 2014; Fjell et al., 2017; Khasawinah et al., 2017; Dixon et al., 2018; Dubois et al., 2018; Ruiz-Rizzo et al., 2019). The resting-state networks were projected into MNI152 space, and we specifically defined four of the networks (DMN, DAN, FPCN, and CON) as regions of interests (ROIs) for ROI-ROI functional connectivity analyses. ROI-ROI analyses are Fisher z-transformed bivariate correlations between brain regions' BOLD time-series that quantify associations in the activation at rest and serve as a proxy for connectivity. Using the CONN toolbox, every participant's average within-network connectivity was calculated by computing the mean of the pairwise correlations between the specified (Yeo et al., 2011) ROIs that comprised each of the four higher-order cognitive networks (**Figure 1**).

First, to assess how the four networks contribute to the general domain of cognitive aging, we ran a multiple linear regression evaluating the unique effect of within-network connectivity on Fluid Cognition Composite scores. For secondary analyses, linear regressions were conducted to characterize the resting-state networks' domain-specific influence in cognitive aging by regressing within-network connectivity onto the cognitive subtests: Dimensional Change Card Sort, Flanker, Picture Sequence Memory, List Sorting, and Pattern Comparison. In the secondary analyses, we only evaluated networks that significantly contributed to Fluid Cognition Composite scores, since our primary question concerns identifying important resting-state networks in the cognitive aging process overall. We controlled for age, education, sex, and scanner type in all of our models. All statistical analyses were performed using SPSS version 25.

RESULTS

Primary Analyses: Within-Network Connectivity and Composite Scores

First, we regressed within-network connectivity values for DMN, DAN, FPCN, and CON simultaneously on Fluid Cognition Composite scores to evaluate which network has the greatest influence in the general cognitive aging process. In these primary analyses, age and education were significantly associated with Fluid Cognition Composite scores (p-values < 0.01), such that older age was associated with lower composite scores and more years of education was associated with higher composite scores. Conversely, sex and scanner type were not significantly associated with Fluid Cognition Composite scores. Out of the four high-order cognitive networks, only CON within-network connectivity had a significant relationship with Fluid Cognition Composite scores, such that greater CON connectivity was associated with better performance ($R^2 = 0.20$, $\beta = 0.33$, $p < 0.001$). The overall model explained 20% of the variance in Fluid Cognition Composite scores, and notably, CON connectivity explained 7.4% of the variance, while age and education explained 3.8% and 5.7%, respectively (**Table 2**; **Figures 2**, **3**).

Within-Network Connectivity and NIH Toolbox Subtests

To better characterize the relationship between CON connectivity and cognitive aging, we ran secondary analyses to identify which specific fluid cognitive subtests were associated with the CON network. The distribution of scores on the Flanker subtest was positively skewed; therefore, we performed a square root transformation to meet normality assumptions before analyses. Notably, CON within-network connectivity was related to better performance across three of the five fluid

[2]www.nitrc.org/projects/artifact_detect

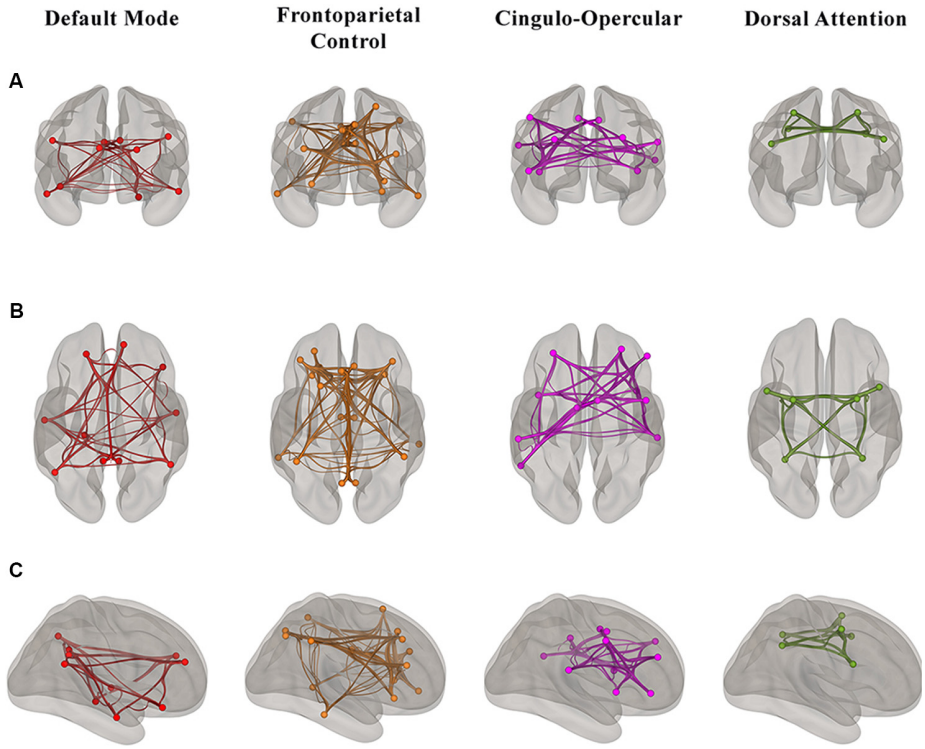

FIGURE 1 | Visualization of the regions of interest (ROI)-ROI connections in each of four higher-order cognitive networks (Yeo et al., 2011) in our sample of healthy older adults from **(A)** anterior **(B)** superior and **(C)** right hemisphere views. Each network is color-coded; however, the colors do not depict different levels of correlation strength.

TABLE 2 | Within-network connectivity and fluid composite score results.

Predictors	*β*	*t*	*p*	*Model R^2*
Age	−0.21	−2.64	0.01*	0.20
Education	0.25	3.22	0.002*	
Sex	0.05	0.70	0.49	
Scanner	−0.001	−0.02	0.98	
CON	0.33	3.66	<0.001*	
FPCN	−0.01	−0.06	0.96	
DMN	−0.06	0.78	0.61	
DAN	−0.03	0.36	0.78	

*Notes: CON, cingulo-opercular network; FPCN, frontoparietal control network; DMN, default mode network; DAN, dorsal attention network. *Significant result $p < 0.01$.*

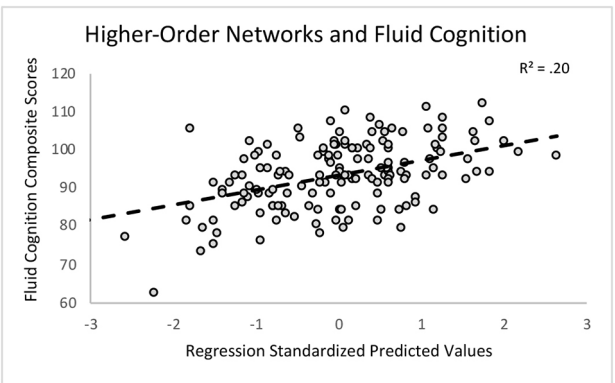

FIGURE 2 | A scatterplot depicting the primary regression analysis with the standardized predicted values (X-axis) resulting from regressing age, sex, education, scanner, and within-network connectivity values of the cingulo-opercular network (CON), frontoparietal control network (FPCN), default mode network (DMN), and dorsal attention network (DAN) on the Fluid Cognition Composite unadjusted standard scores (Y-axis).

cognition subtests, suggesting the network has a relatively broad relationship with cognitive aging rather than a relationship-driven by a specific domain. Greater CON within-network connectivity was associated with higher scores on Dimensional Change Card Sort (R^2 = 0.15, β = 0.26, p = 0.001), Flanker (R^2 = 0.17, β = 0.29, $p < 0.001$), and Picture Sequence Memory tasks (R^2 = 0.17, β = 0.25, p = 0.001). CON connectivity was not significantly related to performance on List Sorting (R^2 = 0.07, β = 0.10, p = 0.20) or Pattern Comparison (R^2 = 0.09, β = 0.12, p = 0.13; **Table 3**; **Figure 4**).

In these subtest analyses, age was significantly related to performance on the Pattern Comparison task, such that older age was associated with worse performance (β = −0.22, p = 0.008). Sex was significantly related to performance on Picture Sequence Memory, such that females performed better than males (β = 0.28, $p < 0.001$). Lastly, those with higher education performed significantly better on the List Sorting (β = 0.21, p = 0.01), Pattern Comparison (β = 0.15, p = 0.05),

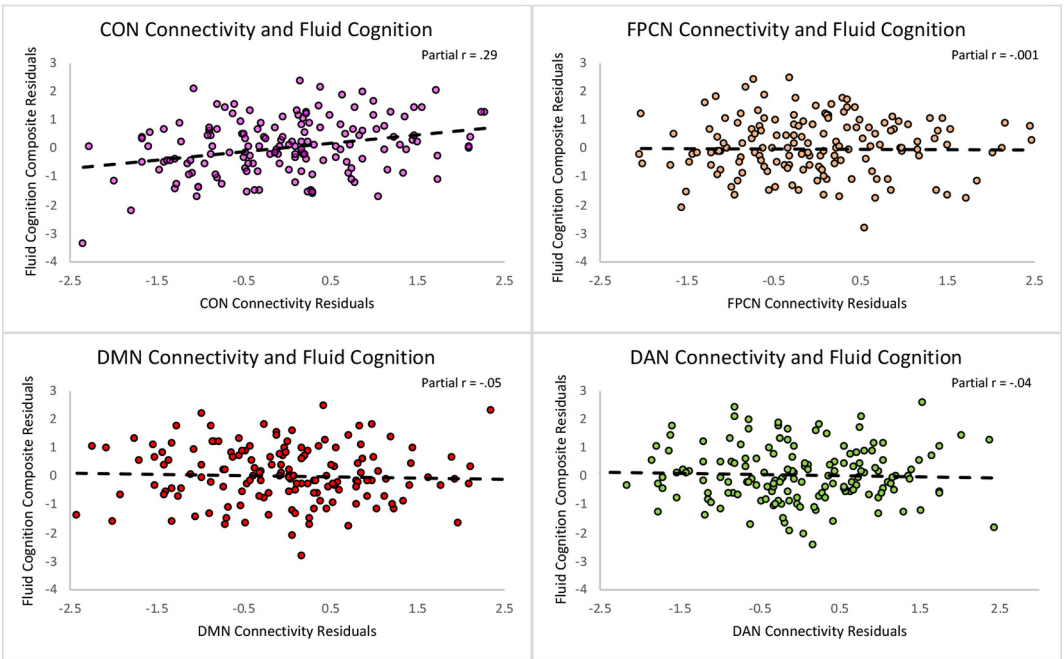

FIGURE 3 | Scatterplots depicting the unique relationships between each network and the Fluid Cognition Composite controlling for the rest of the predictors in the regression. The X and Y axes represent the standardized residuals for the independent and dependent variables, partialling out the effects of the remaining predictors. As such, the slopes reflect partial correlations.

TABLE 3 | CON within-network connectivity and NIH toolbox subtest results.

Fluid tasks	*Model R^2*	*β*	*t*	*p*	*sr^2*
Flanker	0.17	0.29	3.74	<0.001*	0.08
Picture sequence	0.17	0.25	3.27	0.001*	0.06
DCCS	0.15	0.26	3.33	0.001*	0.06
List sorting	0.07	0.10	1.28	0.20	0.01
Pattern comparison	0.09	0.12	1.54	0.13	0.01

*Notes: CON, cingulo-opercular network; DCCS, Dimensional Change Card Sort. *Significant result $p < 0.01$.*

Flanker ($\beta = 0.23$, $p = 0.004$), and Dimensional Change Card Sort ($\beta = 0.26$, $p = 0.001$) tasks.

DISCUSSION

Aging is associated with disruptions in the functional architecture of the brain. However, due to previously mixed findings, it is unclear if age-related changes in resting-state network functional connectivity are linked to the cognitive aging process. The present study offers important new insights by uncovering a specific relationship between resting-state network functional connectivity and cognitive performance in a large sample of healthy older adults. Here, we identified a resting-state network involved in general fluid cognition. Additionally, we outlined the cognitive scope of this network by mapping connectivity onto processing speed, episodic memory, working memory, attention, and executive function subdomains. By linking resting-state network connectivity to various aspects of the cognitive aging process, we hope to create a foundation for future targeted intervention strategies. While the literature has focused on the DMN and its implications in Alzheimer's disease (Buckner et al., 2008; Ferreira and Busatto, 2013; Sullivan et al., 2019), our findings suggest further examination of the CON in the context of nonpathological cognitive aging (Onoda et al., 2012; Geerligs et al., 2015a; Siman-Tov et al., 2017).

Cognitive Control in Cognitive Aging: Cingulo-Opercular Network

The CON is commonly referred to as one of the cognitive control networks (Cole and Schneider, 2007; Dosenbach et al., 2008). Cognitive control is necessary for flexibly allocating mental resources to produce goal-directed behavior. Examples of control processes include attending to stimuli, preparing and initiating a response, and adapting to feedback (Cole and Schneider, 2007). These components of cognition are necessary for the successful completion of a variety of tasks in daily life. In the present study, CON was the only network that was significantly associated with the NIH Toolbox Fluid Cognition Composite. Beyond the matter of significance, CON intra-network coherence explained more of the variance in composite scores than both age and education. These results suggest that CON connectivity is an important factor that influences fluid cognition and may be a compelling target for novel interventions (e.g., transcranial direct current stimulation) to enhance overall cognitive function in older adults. Additionally,

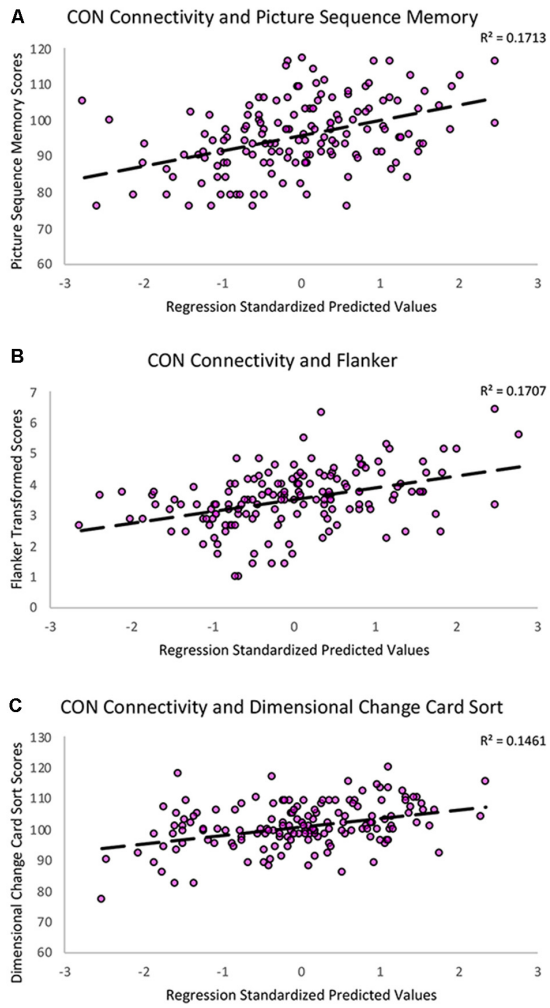

FIGURE 4 | Scatterplots showing the significant relationships between **(A)** Picture Sequence Memory **(B)** Flanker and **(C)** Dimensional Change Card Sort subtest scores and CON within-network resting-state connectivity controlling for age, education, sex, and scanner covariates. The Y-axes reflect the unadjusted standard scores for Picture Sequence Memory and Dimensional Change Card Sort and the square root transformed scores for the Flanker task.

CON within-network connectivity was positively associated with performance on three out of the five subtest domains typically vulnerable to the aging process: episodic memory, attention, and executive function. This pattern of findings suggests the CON network has a relatively global relationship with the cognitive aging process rather than a relationship driven by a specific domain. These results support the notion of the general widespread involvement of the CON network in cognitive control (Dosenbach et al., 2007; Sestieri et al., 2014). Broadly, CON is involved in the implementation and maintenance of the perceptual and attentional information in a task (Dosenbach et al., 2006, 2007, 2008). This is evident through CON's sustained activation during trial initiation, target detection, task maintenance, and response (Dosenbach et al., 2007, 2008; Sestieri et al., 2014; Han et al., 2018). CON's expansive functional responsibility is necessary for the brain's moment-to-moment information processing, a general proficiency greatly affected by age (Salthouse, 2000, 2010). Therefore, our findings suggest that greater functional connectivity within CON at rest may reflect a better ability to properly activate this important network during the execution of fluid cognitive tasks in older adults.

Additionally, CON consists of brain regions important for fluid cognitive abilities like decision-making, planning, target and error detection, updating, and switching (i.e., frontal operculum, medial superior frontal cortex, dorsal anterior cingulate cortex, and anterior insula; Gehring and Knight, 2000; Jung and Haier, 2007; Han et al., 2018). These regions are susceptible to gray matter atrophy and white matter disruptions with age, which contribute to functional activation alterations and declines in cognitive performance (Salat et al., 1999; Raz, 2000; Reuter-Lorenz et al., 2000; Cabeza, 2002; Raz et al., 2005; Andrews-Hanna et al., 2007; Kennedy and Raz, 2009). He et al. (2014) showed that gray matter volume of the insular cortices and the dorsal anterior cingulate, major hubs in the CON network, as well as the functional connectivity of the left insula cortex were associated with scores on the Mini-Mental Status Examination in their sample of older adults. The resting-state functional connectivity of the left insula specifically has also been shown to mediate the association between age and visual processing speed in healthy older adults (Ruiz-Rizzo et al., 2019). Greater CON resting-state connectivity may signify greater maintenance of structural integrity in these regions involved in fluid cognition. Future research should utilize multimodal imaging to further assess the relationship between age-related structural changes and resting-state network functional connectivity.

Higher-Order Cognitive Networks in Cognitive Aging: Default Mode, Dorsal Attention, Frontoparietal Control, Cingulo-Opercular

CON is a part of a larger group of networks referred to as the higher-order cognitive networks (i.e., CON, FPCN, DMN, DAN). Functional connectivity within these networks typically decreases with age along the same trajectory of age-related structural deterioration and cognitive decline (Park and Reuter-Lorenz, 2009; Giorgio et al., 2010; Geerligs et al., 2015a; Siman-Tov et al., 2017). Conversely, connectivity within sensory and motor resting-state networks remains relatively stable in advanced age. Together, these patterns of age-related alterations in connectivity support the "last in, first out" hypothesis which suggests that brain regions that are the last to develop are the first to be affected by the aging process (Raz, 2000). In addition to CON, we also expected to find a relationship with DMN and FPCN connectivity and cognitive performance in our sample of healthy older adults.

In the present study, functional connectivity within DMN, FPCN, and DAN were not significantly related to the Fluid Cognition Composite. These results are surprising given the historic focus on the DMN as an individual network and its interactions with DAN and FPCN (Fox et al., 2005;

Buckner et al., 2008; Ferreira and Busatto, 2013; Spreng et al., 2013). The most common finding in the resting-state and aging literature is that there are disruptions in resting-state functional connectivity within the DMN present in nonpathological aging and Alzheimer's disease (Greicius et al., 2004; Buckner et al., 2008; Ferreira and Busatto, 2013; Ferreira et al., 2016). However, relating resting-state characteristics of the DMN and other networks to actual cognitive performance in older adults has resulted in mixed findings (Andrews-Hanna et al., 2007; Damoiseaux et al., 2007; Geerligs et al., 2015a; Ferreira et al., 2016). While disruptions in DMN resting-state connectivity may be a marker for memory deficits and Alzheimer's disease pathology (Buckner, 2004; Buckner et al., 2008), our findings suggest that CON resting-state connectivity is a more robust marker for declines in attention-demanding cognitive domains present in nonpathological cognitive aging. This distinction between the roles of DMN and CON in the cognitive aging process may help facilitate better differentiation of nonpathological aging from disease states.

Limitations and Future Directions

The present study is not without limitations regarding cohort characteristics and methodology. First, the age range of our older adult sample is relatively restricted (65–87). Therefore, we may only be representing connectivity and cognition relationships for a specific subset of older adults. Additionally, while our sample of older adults had an education range of 12–21 years, 67.5% of the sample obtained a bachelor's degree or higher. Future work should examine this research question with a wider age range and a higher representation of older adults with education below 16 years to broaden the generalizability of these results. We conducted an ROI-ROI analysis to mitigate multiple comparisons and to limit our analyses to regions involved in established resting-state networks. Future studies should also examine voxel-wise approaches and whole-brain metrics to further explore the relationships found in the current study. Finally, we associated resting-state functional connectivity and cognitive performance in healthy older adults at one point in time. Therefore, we cannot make any conclusions about within-participant changes in connectivity and cognitive performance over time. In the course of neurodegenerative diseases, disrupted connectivity is apparent long before the presence of cognitive decline (Chen et al., 2016). As such, our findings may offer specific networks central to the early stages of cognitive aging. Future work should longitudinally assess changes in CON connectivity to see if disruptions in these networks are associated with the progression to MCI and Alzheimer's disease.

CONCLUSION

This study provides important new insights on inter-individual differences in resting-state network connectivity and the cognitive aging process. Notably, we provide evidence to suggest CON coherence as a potential new marker for fluid cognitive performance capacity in nonpathological aging. Out of the four higher-order cognitive networks, connectivity within the CON network exhibited the strongest relationship with a sensitive measure of general fluid cognitive ability in our large sample of healthy older adults. Furthermore, CON connectivity explained a greater percentage of the variance in fluid cognitive performance than both age and education. CON connectivity mapped onto three out of the five fluid cognitive subtests, reflecting a global rather than domain-specific influence on the cognitive aging process. Collectively, these results suggest that CON connectivity may be a central facet of the cognitive aging process and deserves increased focus in future research investigating the neural substrates of age-related cognitive decline.

DATA AVAILABILITY STATEMENT

Data are managed under the data-sharing agreement established with NIA and the parent R01 clinical trial Data Safety and Monitoring Board in the context of an ongoing Phase III clinical trial (ACT study, R01AG054077). All trial data will be made publicly available 2 years after completion of the parent clinical trial, per NIA and DSMB agreement. Requests for baseline data can be submitted to the ACT Publication and Presentation (P&P) Committee and will require submission of data use, authorship, and analytic plan for review by the P&P committee (ajwoods@phhp.ufl.edu).

ETHICS STATEMENT

The studies involving human participants were reviewed and approved by Institutional Review Boards at the University of Florida and the University of Arizona. The patients/participants provided their written informed consent to participate in this study.

AUTHOR CONTRIBUTIONS

HH and AW contributed to the conception and design of the study. HH extracted the data, performed the statistical analyses, and wrote the first draft of the manuscript. AW, AO'S, JK, EB, and NE helped organize data and provide resources. EV, PB, and SS collected data. EP, GH, SW, SD, GA, MM, RC, and AW were involved in project administration. All authors contributed to manuscript revision, read, and approved the submitted version.

FUNDING

We would like to acknowledge support from the National Institute on Aging (NIA R01AG054077, NIA K01AG050707, NIA P30AG019610), the State of Arizona and Arizona Department of Health Services (ADHS), and the McKnight Brain Research Foundation.

REFERENCES

Andrews-Hanna, J. R., Snyder, A. Z., Vincent, J. L., Lustig, C., Head, D., Raichle, M. E., et al. (2007). Disruption of large-scale brain systems in advanced aging. *Neuron* 56, 924–935. doi: 10.1016/j.neuron.2007.10.038

Behzadi, Y., Restom, K., Liau, J., and Liu, T. T. (2007). A component based noise correction method (CompCor) for BOLD and perfusion based fMRI. *NeuroImage* 37, 90–101. doi: 10.1016/j.neuroimage.2007.04.042

Betzel, R. F., Byrge, L., He, Y., Goñi, J., Zuo, X.-N. N., Sporns, O., et al. (2014). Changes in structural and functional connectivity among resting-state networks across the human lifespan. *NeuroImage* 102, 345–357. doi: 10.1016/j.neuroimage.2014.07.067

Biswal, B. B. (2012). Resting state fMRI: a personal history. *NeuroImage* 62, 938–944. doi: 10.1016/j.neuroimage.2012.01.090

Biswal, B. B., Mennes, M., Zuo, X.-N., Gohel, S., Kelly, C., Smith, S. M., et al. (2010). Toward discovery science of human brain function. *Proc. Natl. Acad. Sci. U S A* 107, 4734–4739. doi: 10.1073/pnas.0911855107

Biswal, B. B., Yetkin, F. Z., Haughton, V. M., and Hyde, J. S. (1995). Functional connectivity in the motor cortex of resting human brain using echo-planar mri. *Magn. Reson. Med.* 34, 537–541. doi: 10.1002/mrm.1910340409

Buckner, R. L. (2004). Memory and executive function in aging and ad: multiple factors that cause decline and reserve factors that compensate. *Neuron* 44, 195–208. doi: 10.1016/j.neuron.2004.09.006

Buckner, R. L., Andrews-Hanna, J. R., and Schacter, D. L. (2008). The brain's default network: anatomy, function, and relevance to disease. *Ann. N Y Acad. Sci.* 1124, 1–38. doi: 10.1196/annals.1440.011

Cabeza, R. (2002). Hemispheric asymmetry reduction in older adults: the HAROLD model. *Psychol. Aging* 17, 85–100. doi: 10.1037/0882-7974.17.1.85

Chan, M. Y., Park, D. C., Savalia, N. K., Petersen, S. E., and Wig, G. S. (2014). Decreased segregation of brain systems across the healthy adult lifespan. *Proc. Natl. Acad. Sci. U S A* 111, E4997–E5006. doi: 10.1073/pnas.1415122111

Chen, G. G., Shu, H., Chen, G. G., Ward, B. D., Antuono, P. G., Zhang, Z., et al. (2016). Staging Alzheimer's disease risk by sequencing brain function and structure, cerebrospinal fluid, and cognition biomarkers. *J. Alzheimers Dis.* 54, 983–993. doi: 10.3233/JAD-160537

Cole, M. W., Pathak, S., and Schneider, W. (2010). Identifying the brain's most globally connected regions. *NeuroImage* 49, 3132–3148. doi: 10.1016/j.neuroimage.2009.11.001

Cole, M. W., and Schneider, W. (2007). The cognitive control network: integrated cortical regions with dissociable functions. *NeuroImage* 37, 343–360. doi: 10.1016/j.neuroimage.2007.03.071

D'Esposito, M., Zarahn, E., Aguirre, G. K., and Rypma, B. (1999). The effect of normal aging on the coupling of neural activity to the bold hemodynamic response. *NeuroImage* 10, 6–14. doi: 10.1006/nimg.1999.0444

Damoiseaux, J. S. (2017). Effects of aging on functional and structural brain connectivity. *NeuroImage* 160, 32–40. doi: 10.1016/j.neuroimage.2017.01.077

Damoiseaux, J. S., Beckmann, C. F., Arigita, E. J. S., Barkhof, F., Scheltens, P., Stam, C. J., et al. (2007). Reduced resting-state brain activity in the "default network" in normal aging. *Cereb. Cortex* 18, 1856–1864. doi: 10.1093/cercor/bhm207

Damoiseaux, J. S., Rombouts, S. A. R. B., Barkhof, F., Scheltens, P., Stam, C. J., Smith, S. M., et al. (2006). Consistent resting-state networks across healthy subjects. *Proc. Natl. Acad. Sci. U S A* 103, 13848–13853. doi: 10.1073/pnas.0601417103

De Luca, M., Smith, S., De Stefano, N., Federico, A., and Matthews, P. M. (2005). Blood oxygenation level dependent contrast resting state networks are relevant to functional activity in the neocortical sensorimotor system. *Exp. Brain Res.* 167, 587–594. doi: 10.1007/s00221-005-0059-1

Dixon, M. L., La Vega, A. D., Mills, C., Andrews-Hanna, J., Spreng, R. N., Cole, M. W., et al. (2018). Heterogeneity within the frontoparietal control network and its relationship to the default and dorsal attention networks. *Proc. Natl. Acad. Sci. U S A* 115, E1598–E1607. doi: 10.1073/pnas.1715766115

Dosenbach, N. U. F., Fair, D. A., Cohen, A. L., Schlaggar, B. L., and Petersen, S. E. (2008). A dual-networks architecture of top-down control. *Trends Cogn. Sci.* 12, 99–105. doi: 10.1016/j.tics.2008.01.001

Dosenbach, N. U. F., Fair, D. A., Miezin, F. M., Cohen, A. L., Wenger, K. K., Dosenbach, R. A. T., et al. (2007). Distinct brain networks for adaptive and stable task control in humans. *Proc. Natl. Acad. Sci. U S A* 104, 11073–11078. doi: 10.1073/pnas.0704320104

Dosenbach, N. U. F., Visscher, K. M., Palmer, E. D., Miezin, F. M., Wenger, K. K., Kang, H. C., et al. (2006). A core system for the implementation of task sets. *Neuron* 50, 799–812. doi: 10.1016/j.neuron.2006.04.031

Dubois, J., Galdi, P., Paul, L. K., and Adolphs, R. (2018). A distributed brain network predicts general intelligence from resting-state human neuroimaging data. *Philos. Trans. R. Soc. B Biol. Sci.* 373:20170284. doi: 10.1098/rstb.2017.0284

Ferreira, L. K., and Busatto, G. F. (2013). Resting-state functional connectivity in normal brain aging. *Neurosci. Biobehav. Rev.* 37, 384–400. doi: 10.1016/j.neubiorev.2013.01.017

Ferreira, L. K., Regina, A. C. B., Kovacevic, N., da Martin, M. G. M., Santos, P. P., de Carneiro, C. G., et al. (2016). Aging effects on whole-brain functional connectivity in adults free of cognitive and psychiatric disorders. *Cereb. Cortex* 26, 3851–3865. doi: 10.1093/cercor/bhv190

Fjell, A. M., Sneve, M. H., Grydeland, H., Storsve, A. B., and Walhovd, K. B. (2017). The disconnected brain and executive function decline in aging. *Cereb. Cortex* 27, 2303–2317. doi: 10.1093/cercor/bhw082

Fox, M. D., Corbetta, M., Snyder, A., Vincent, J. L., and Raichle, M. E. (2006). Spontaneous neuronal activity distinguishes human dorsal and ventral attention systems. *Proc. Natl. Acad. Sci. U S A* 103, 10046–10051. doi: 10.1073/pnas.0604187103

Fox, M. D., Snyder, A. Z., Vincent, J. L., Corbetta, M., and Van Essen, D. C. (2005). The human brain is intrinsically organized into dynamic, anticorrelated functional networks. *Proc. Natl. Acad. Sci. U S A* 102, 9673–9678. doi: 10.1073/pnas.0504136102

Geerligs, L., Renken, R. J., Saliasi, E., Maurits, N. M., and Lorist, M. M. (2015a). A brain-wide study of age-related changes in functional connectivity. *Cereb. Cortex* 25, 1987–1999. doi: 10.1093/cercor/bhu012

Geerligs, L., Rubinov, M., Cam-Can, and Henson, R. N. (2015b). State and trait components of functional connectivity: individual differences vary with mental state. *J. Neurosci.* 35, 13949–13961. doi: 10.1523/JNEUROSCI.1324-15.2015

Geerligs, L., Tsvetanov, K. A., Cam-Can, and Henson, R. N. (2017). Challenges in measuring individual differences in functional connectivity using fMRI: the case of healthy aging. *Hum. Brain Mapp.* 38, 4125–4156. doi: 10.1002/hbm.23653

Gehring, W. J., and Knight, R. T. (2000). Prefrontal-cingulate interactions in action monitoring. *Nat. Neurosci.* 3, 516–520. doi: 10.1038/74899

Giorgio, A., Santelli, L., Tomassini, V., Bosnell, R., Smith, S., De Stefano, N., et al. (2010). Age-related changes in grey and white matter structure throughout adulthood. *NeuroImage* 51, 943–951. doi: 10.1016/j.neuroimage.2010.03.004

Glisky, E. L. (2007). "Changes in cognitive function in human aging," in *Brain Aging: Models, Methods, and Mechanisms.*, ed. D. R. Riddle (Boca Raton, FL: CRC Press/Taylor & Francis), 3–20.

Grady, C., Sarraf, S., Saverino, C., and Campbell, K. (2016). Age differences in the functional interactions among the default, frontoparietal control and dorsal attention networks. *Neurobiol. Aging* 41, 159–172. doi: 10.1016/j.neurobiolaging.2016.02.020

Greicius, M. D., Srivastava, G., Reiss, A. L., and Menon, V. (2004). Default-mode network activity distinguishes Alzheimer's disease from healthy aging: evidence from functional MRI. *Proc. Natl. Acad. Sci. U S A* 101, 4637–4642. doi: 10.1073/pnas.0308627101

Han, S. W., Eaton, H. P., and Marois, R. (2018). Functional fractionation of the cingulo-opercular network: alerting insula and updating cingulate. *Cereb. Cortex* 29, 2624–2638. doi: 10.1093/cercor/bhy130

Harada, C. N., Natelson Love, M. C., and Triebel, K. L. (2013). Normal cognitive aging. *Clin. Geriatr. Med.* 29, 737–752. doi: 10.1016/j.cger.2013.07.002

He, X., Qin, W., Liu, Y., Zhang, X., Duan, Y., Song, J., et al. (2014). Abnormal salience network in normal aging and in amnestic mild cognitive impairment and Alzheimer's disease. *Hum. Brain Mapp.* 35, 3446–3464. doi: 10.1002/hbm.22414

Jung, R. E., and Haier, R. J. (2007). The Parieto-Frontal Integration Theory (P-FIT) of intelligence: converging neuroimaging evidence. *Behav. Brain Sci.* 30, 135–154. doi: 10.1017/S0140525X07001185

Kennedy, K. M., and Raz, N. (2009). Aging white matter and cognition: differential effects of regional variations in diffusion properties on memory,

executive functions and speed. *Neuropsychologia* 47, 916–927. doi: 10.1016/j.neuropsychologia.2009.01.001

Khasawinah, S., Chuang, Y.-F., Caffo, B., Erickson, K. I., Kramer, A. F., and Carlson, C. M. (2017). The association between functional connectivity and cognition in older adults. *J. Syst. Integr. Neurosci.* 3:3. doi: 10.15761/jsin.1000164

Murman, D. L. (2015). The impact of age on cognition. *Semin. Hear.* 36, 111–121. doi: 10.1055/s-0035-1555115

Onoda, K., Ishihara, M., and Yamaguchi, S. (2012). Decreased functional connectivity by aging is associated with cognitive decline. *J. Cogn. Neurosci.* 24, 2186–2198. doi: 10.1162/jocn_a_00269

Park, D. C., and Reuter-Lorenz, P. (2009). The adaptive brain: aging and neurocognitive scaffolding. *Annu. Rev. Psychol.* 60, 173–196. doi: 10.1146/annurev.psych.59.103006.093656

Penny, W., Friston, K., Ashburner, J., Kiebel, S., and Nichols, T. (2007). *Statistical Parametric Mapping: The Analysis of Functional Brain Images.* Amsterdam; Boston: Elsevier/Academic Press.

Power, J. D., Barnes, K. A., Snyder, A. Z., Schlaggar, B. L., and Petersen, S. E. (2012). Spurious but systematic correlations in functional connectivity MRI networks arise from subject motion. *NeuroImage* 59, 2142–2154. doi: 10.1016/j.neuroimage.2011.10.018

Prins, N. D., and Scheltens, P. (2015). White matter hyperintensities, cognitive impairment and dementia: an update. *Nat. Rev. Neurol.* 11, 157–165. doi: 10.1038/nrneurol.2015.10

Raichle, M. E., MacLeod, A. M., Snyder, A. Z., Powers, W. J., Gusnard, D. A., and Shulman, G. L. (2001). A default mode of brain function. *Proc. Natl. Acad. Sci. U S A* 98, 676–682. doi: 10.1073/pnas.98.2.676

Raz, N. (2000). ''Aging of the brain and its impact on cognitive performance: integration of structural and functional findings,'' in *Handbook of Aging and Cognition, 2nd Edn*, eds F. I. M. Craik and T. A. Salthouse (Mahwah, NJ: Erlbaum), 1–90.

Raz, N., Lindenberger, U., Rodrigue, K. M., Kennedy, K. M., Head, D., Williamson, A., et al. (2005). Regional brain changes in aging healthy adults: general trends, individual differences and modifiers. *Cereb. Cortex* 15, 1676–1689. doi: 10.1093/cercor/bhi044

Reuter-Lorenz, P. A., Jonides, J., Smith, E. E., Hartley, A., Miller, A., Marshuetz, C., et al. (2000). Age differences in the frontal lateralization of verbal and spatial working memory revealed by PET. *J. Cogn. Neurosci.* 12, 174–187. doi: 10.1162/089892900561814

Ruiz-Rizzo, A. L., Sorg, C., Napiórkowski, N., Neitzel, J., Menegaux, A., Müller, H. J., et al. (2019). Decreased cingulo-opercular network functional connectivity mediates the impact of aging on visual processing speed. *Neurobiol. Aging* 73, 50–60. doi: 10.1016/j.neurobiolaging.2018.09.014

Salat, D. H., Kaye, J. A., and Janowsky, J. S. (1999). Prefrontal gray and white matter volumes in healthy aging and Alzheimer disease. *Arch. Neurol.* 56, 338–344. doi: 10.1001/archneur.56.3.338

Salthouse, T. A. (1994). The aging of working memory. *Neuropsychology* 8, 535–543. doi: 10.1037/0894-4105.8.4.535

Salthouse, T. A. (2000). Aging and measures of processing speed. *Biol. Psychol.* 54, 35–54. doi: 10.1016/s0301-0511(00)00052-1

Salthouse, T. A. (2010). Selective review of cognitive aging. *J. Int. Neuropsychol. Soc.* 16, 754–760. doi: 10.1017/S1355617710000706

Seeley, W. W., Menon, V., Schatzberg, A. F., Keller, J., Glover, G. H., Kenna, H., et al. (2007). Dissociable intrinsic connectivity networks for salience processing and executive control. *J. Neurosci.* 27, 2349–2356. doi: 10.1523/JNEUROSCI.5587-06.2007

Sestieri, C., Corbetta, M., Spadone, S., Romani, G. L., and Shulman, G. L. (2014). Domain-general signals in the cingulo-opercular network for visuospatial attention and episodic memory. *J. Cogn. Neurosci.* 26, 551–568. doi: 10.1162/jocn_a_00504

Shaw, E. E., Schultz, A. P., Sperling, R. A., and Hedden, T. (2015). Functional connectivity in multiple cortical networks is associated with performance across cognitive domains in older adults. *Brain Connect.* 5, 505–516. doi: 10.1089/brain.2014.0327

Shirer, W. R., Jiang, H., Price, C. M., Ng, B., and Greicius, M. D. (2015). Optimization of rs-fMRI pre-processing for enhanced signal-noise separation, test-retest reliability and group discrimination. *NeuroImage* 117, 67–79. doi: 10.1016/j.neuroimage.2015.05.015

Siman-Tov, T., Bosak, N., Sprecher, E., Paz, R., Eran, A., Aharon-Peretz, J., et al. (2017). Early age-related functional connectivity decline in high-order cognitive networks. *Front. Aging Neurosci.* 8:330. doi: 10.3389/fnagi.2016.00330

Spreng, R. N., Sepulcre, J., Turner, G. R., Stevens, W. D., and Schacter, D. L. (2013). Intrinsic architecture underlying the relations among the default, dorsal attention, and frontoparietal control networks of the human brain. *J. Cogn. Neurosci.* 25, 74–86. doi: 10.1162/jocn_a_00281

Spreng, R. N., and Turner, G. R. (2019). The shifting architecture of cognition and brain function in older adulthood. *Perspect. Psychol. Sci.* 14, 523–542. doi: 10.1177/1745691619827511

Sullivan, M. D., Anderson, J. A. E., Turner, G. R., and Spreng, R. N. (2019). Intrinsic neurocognitive network connectivity differences between normal aging and mild cognitive impairment are associated with cognitive status and age. *Neurobiol. Aging* 73, 219–228. doi: 10.1016/j.neurobiolaging.2018.10.001

van Dijk, K. R. A., Sabuncu, M. R., and Buckner, R. L. (2012). The influence of head motion on intrinsic functional connectivity MRI. *NeuroImage* 59, 431–438. doi: 10.1016/j.neuroimage.2011.07.044

Vincent, J. L., Kahn, I., Snyder, A. Z., Raichle, M. E., Buckner, R. L., Snyder, A. Z., et al. (2008). Evidence for a frontoparietal control system revealed by intrinsic functional connectivity. *J. Neurophysiol.* 100, 3328–3342. doi: 10.1152/jn.90355.2008

Vincent, J. L., Snyder, A. Z., Fox, M. D., Shannon, B. J., Andrews, J. R., Raichle, M. E., et al. (2006). Coherent spontaneous activity identifies a hippocampal-parietal memory network. *J. Neurophysiol.* 96, 3517–3531. doi: 10.1152/jn.00048.2006

Wecker, N. S., Kramer, J. H., Hallam, B. J., and Delis, D. C. (2005). Mental flexibility: age effects on switching. *Neuropsychology* 19, 345–352. doi: 10.1037/0894-4105.19.3.345

Weintraub, S., Dikmen, S. S., Heaton, R. K., Tulsky, D. S., Zelazo, P. D., Bauer, P. J., et al. (2013). Cognition assessment using the NIH toolbox. *Neurology* 80, S54–S64. doi: 10.1212/WNL.0b013e3182872ded

Weintraub, S., Salmon, D., Mercaldo, N., Ferris, S., Graff-Radford, N. R., Chui, H., et al. (2009). The Alzheimer's disease centers' uniform data set (UDS): the neuropsychologic test battery. *Alzheimer Dis. Assoc. Disord.* 23, 91–101. doi: 10.1097/WAD.0b013e318191c7dd

Whitfield-Gabrieli, S., and Nieto-Castanon, A. (2012). Conn: a functional connectivity toolbox for correlated and anticorrelated brain networks. *Brain Connect.* 2, 125–141. doi: 10.1089/brain.2012.0073

Woods, A. J., Cohen, R., Marsiske, M., Alexander, G. E., Czaja, S. J., and Wu, S. (2018). Augmenting cognitive training in older adults (The ACT Study): design and Methods of a Phase III tDCS and cognitive training trial. *Contemp. Clin. Trials* 65, 19–32. doi: 10.1016/j.cct.2017.11.017

Yeo, B. T. T., Krienen, F. M., Sepulcre, J., Sabuncu, M. R., Lashkari, D., Hollinshead, M., et al. (2011). The organization of the human cerebral cortex estimated by intrinsic functional connectivity. *J. Neurophysiol.* 106, 1125–1165. doi: 10.1152/jn.00338.2011

Conflict of Interest: The authors declare that the research was conducted in the absence of any commercial or financial relationships that could be construed as a potential conflict of interest.

frontiers in Aging Neuroscience

ORIGINAL RESEARCH
published: 11 June 2021
doi: 10.3389/fnagi.2021.482447

Correlation Between Gait and Near-Infrared Brain Functional Connectivity Under Cognitive Tasks in Elderly Subjects With Mild Cognitive Impairment

Ying Liu[1,2,3], Congcong Huo[1,2], Kuan Lu[4], Qianying Liu[5], Gongcheng Xu[1,2], Run Ji[1,2], Tengyu Zhang[1,2], Pan Shang[1,2], Zeping Lv[2] and Zengyong Li[1,2,3]**

[1] Beijing Key Laboratory of Rehabilitation Technical Aids for Old-Age Disability, National Research Center for Rehabilitation Technical Aids, Beijing, China, [2] Rehabilitation Hospital, National Research Center for Rehabilitation Technical Aids, Beijing, China, [3] Key Laboratory of Neuro-functional Information and Rehabilitation Engineering of The Ministry of Civil Affairs, Beijing, China, [4] China Academy of Information and Communications Technology, Beijing, China, [5] China Electronics Standardization Institute, Beijing, China

OPEN ACCESS

Edited by:
Philip P. Foster,
Baylor College of Medicine,
United States

Reviewed by:
Ramesh Kandimalla,
Indian Institute of Chemical Technology (CSIR), India
Martin J. McKeown,
University of British Columbia, Canada

***Correspondence:**
Zengyong Li
lizengyong@nrcrta.cn
Zeping Lv
lvzeping@163.com

Received: 25 July 2019
Accepted: 06 May 2021
Published: 11 June 2021

Citation:
Liu Y, Huo C, Lu K, Liu Q, Xu G, Ji R, Zhang T, Shang P, Lv Z and Li Z (2021) Correlation Between Gait and Near-Infrared Brain Functional Connectivity Under Cognitive Tasks in Elderly Subjects With Mild Cognitive Impairment. Front. Aging Neurosci. 13:482447. doi: 10.3389/fnagi.2021.482447

Older adults with mild cognitive impairment (MCI) have a high risk of developing Alzheimer's disease. Gait performance is a potential clinical marker for the progression of MCI into dementia. However, the relationship between gait and brain functional connectivity (FC) in older adults with MCI remains unclear. Forty-five subjects [MCI group, n = 23; healthy control (HC) group, n = 22] were recruited. Each subject performed a walking task (Task 01), counting backward–walking task (Task 02), naming animals–walking task (Task 03), and calculating–walking task (Task 04). The gait parameters and cerebral oxygenation signals from the left prefrontal cortex (LPFC), right prefrontal cortex (RPFC), left motor cortex (LMC), right motor cortex (RMC), left occipital leaf cortex (LOL), and right occipital leaf cortex (ROL) were obtained simultaneously. Wavelet phase coherence was calculated in two frequency intervals: low frequency (interval I, 0.052–0.145 Hz) and very low frequency (interval II, 0.021–0.052 Hz). Results showed that the FC of RPFC–RMC is significantly lower in interval I in Task 03 compared with that in Task 02 in the MCI group (p = 0.001). Also, the right relative symmetry index (IDpsR) is significantly lower in Task 03 compared with that in Task 02 (p = 0.000). The IDpsR is positively correlated with the FC of RPFC–RMC in interval I in the MCI group (R = 0.205, p = 0.041). The gait symmetry such as left relative symmetry index (IDpsL) and IDpsR is significantly lower in the dual-task (DT) situation compared with the single task in the two groups ($p < 0.05$). The results suggested that the IDpsR might reflect abnormal change in FC of RPFC–RMC in interval I in the MCI population during Task 03. The gait symmetry is affected by DTs in both groups. The findings of this study may have a pivotal role in the early monitoring and intervention of brain dysfunction among older adults with MCI.

Keywords: mild cognitive impairment, functional connectivity, wavelet phase coherence, gait symmetry, dual-tasks

INTRODUCTION

Mild cognitive impairment (MCI) is a transitional state between normal aging and early dementia. The annual conversion rate of MCI into Alzheimer's disease is 8–15%, and MCI is the appropriate stage for preventive intervention (Prince et al., 2016). However, the population base is large, the community lacks doctors with diagnostic capabilities, the examination methods are cumbersome, and the patient compliance requirements are high. The early screening and diagnosis of MCI are important (Barry and Serge, 2008), but early objective evaluation indicators for MCI are lacking.

Gait refers to the postural and behavioral characteristics of the human body while walking. Gait parameters are commonly used to assess the risk for MCI in a population. These parameters assess the process of moving the body in a certain direction by measuring a series of continuous activities of the hip, knee, ankle, and toe (Montero-Odasso et al., 2012). Gait analysis is used to reveal the gait abnormalities based on biomechanics and kinematics in subjects with MCI during walking (Crockett et al., 2017). Abnormal gait is a prevalent feature among older adults with cognitive impairment (Ganz et al., 2007). Abnormal gait in the elderly can be attributed to neurologic diseases, arthritis, and acquired foot deformities (Alexander, 1996; Verghese et al., 2002; Wilson et al., 2002).

Dual-task (DT) gait testing is used to assess the interaction among cognition, gait, and fall risk. The DT paradigm refers to the observation of people walking while performing a second task that needs attention and reflects the relationship between cognition and gait (Tian et al., 2017). Gait variability is correlated with fall risk, disease duration and severity, and motor and cognitive functions. Increased gait variability and decreased walking speed are demonstrated in subjects with MCI during the DT test with increasing DT complexity (Tian et al., 2017). It has been demonstrated that abnormal brain regions were related to motor function in subjects with Parkinson's disease under resting state (Canu et al., 2016).

More challenging mobility performance tasks, such as DT walking, may better capture early brain abnormalities (Beauchet et al., 2013). For example, the hippocampus (H) has a functional connection with the prefrontal cortex (PFC) through the entorhinal cortex (E) and the substantia nigra striatum (NS) system (Jordan et al., 2004). The degradation of the hippocampus leads to the decomposition of visual, vestibular, and proprioceptive sensory and contextual information into spatial maps, leading to gait disorders. Damage to the PFC may lead to executive dysfunction, leading to gait disturbance (Jordan et al., 2004).

Functional near-infrared spectroscopy (fNIRS) is non-invasive, secure, and cheap, and it exhibits good mobility and high time resolution (Bernjak et al., 2012; Ferrari and Quaresima, 2012). fNIRS maps human brain functions by measuring local changes in the hemoglobin concentrations in the brain (Boas et al., 2014; Scholkmann et al., 2014). Functional connectivity (FC) can be derived from fNIRS signals. FC reflects the important connections among different spatial regions of the cerebral cortex. The FC network can reveal the intrinsic characteristics of the brain network (Biswal et al., 1995; Fox and Raichle, 2007). Studies on FC based on fNIRS have been popular in recent years (Fox and Raichle, 2007). Some studies have used fNIRS to evaluate the prefrontal brain activation of healthy young people in the walking environment of working memory tasks. These studies found that in young people, the neural related factors of executive function and dynamic posture control tend to be concurrent with the walking environment and process. The cognitive load changes with different tasks (Lin and Lin, 2016). However, the specific relationship between gait and FC in older adults with MCI while performing tasks remains unclear.

The hypothesis of this study is that gait abnormalities are related to brain function in subjects with MCI. This study aims to (1) analyze the brain FC of older adults with MCI during the single task and DTs and (2) examine the correlation between brain FC and gait symmetry indices during the single task and DTs based on the gait and cerebral oxygen parameters recorded simultaneously using the Vicon three-dimensional (3D) dynamic capture system and portable fNIRS device.

MATERIALS AND METHODS

Subjects

In this study, 45 elderly subjects were recruited from a local community. The inclusion criteria for patients were as follows: (a) no abnormal brain structure, such as contusions caused by tumors and head trauma, which may impair cognitive function; (b) objective evidence of impairment in the cognitive domain: memory, executive function/attention, language, or vision spatial skills; (c) normal functional activities; (d) no dementia (Park et al., 2011). After screening, the MCI and healthy control (HC) groups were formed with 20 and 17 members, respectively. The experimental procedure was approved by the Ethics Committee of the National Research Center for Rehabilitation Technical Aids. Informed consent was obtained from each participant before the experiment. **Table 1** shows the information regarding the age, body mass index, blood pressure, and Mini-Mental State Examination (MMSE) and Montreal Cognitive Assessment (MoCA) scores of the subjects before the experiment.

TABLE 1 | Basic information of the subjects.

Parameters	MCI group (standard deviations)	HC group (standard deviations)	*t*	*p*
			Independent sample *T*-test	
Age (years)	62.41 (5.03)	64.38 (5.46)	0.914	0.389
Body mass index (BMI)	24.27 (2.51)	25.23 (2.43)	0.639	0.533
Systolic blood pressure (mmHg)	69.10 (4.38)	74.81 (4.68)	−2.571	0.039
Diastolic blood pressure (mmHg)	128.26 (3.54)	112.83 (5.34)	−1.064	0.316
Mini-Mental State Examination (MMSE)	27.64(1.76)	29.09 (1.15)	−1.738	0.122
Montreal Cognitive Assessment (MoCA)	22.64 (2.54)	27.05(1.29)	−5.522	0.000

Gait Test

The subjects wore the same tight shorts and sneakers. Sixteen marks were pasted strictly in accordance with Plug-in Gait requirements (Kadaba et al., 1990). The motion capture system using 12 cameras (Vicon, Oxford Metrics Limited, United Kingdom) was used to collect kinematic data at a sampling frequency of 100 Hz. Two force platforms (OR-65, AMTI, United States) were used to record ground reaction force (GRF) data at a sampling frequency of 1.5 kHz. At the beginning of the experiment, the subjects walked back and forth on a fixed path.

Mental Tasks

During the test, the MMSE and MoCA scales were used to assess the cognitive level of the subjects. The evaluation and diagnosis of MCI and HC groups were completed by doctors from the Affiliated Hospital of the National Rehabilitation Aid Research Center. The assessment scale was combined with the main complaints and clinical history information and recognition provided by patients and their families in the evaluation process to determine the sample grouping. Patients or families of MCI subjects had subjective cognitive decline complaints. The MMSE scores were between 24 and 29 (Stokholm et al., 2006), and the MoCA scores of all subjects were between 22 and 26 (Freitas et al., 2012). All subjects had lower memory and computational performance in MMSE and MoCA scales. The scores of the MMSE and MoCA scales of the HC group must be greater than the prescribed normal scores.

Functional Near-Infrared Spectroscopy Measurements

A 14-channel fNIRS device (Danyang Huichuang Medical Equipment Co., Ltd.) was used to collect cerebral blood oxygen signals, and the brain region position used for the measurements was based on the internationally used 10/10 electrode position (Oostenveld and Praamstra, 2001). Light sources and detectors were placed in the following cortical areas: left prefrontal cortex (LPFC), right prefrontal cortex (RPFC), left motor cortex (LMC), right motor cortex (RMC), left occipital leaf cortex (LOL), and right occipital leaf cortex (ROL). The distance between the source and detector was 30 mm. The sampling frequency was set at 10 Hz. **Figure 1A** shows the arrangement of the probe for the measurement and typical examples of the diagram of brain FC. A light source and a detector formed the channel.

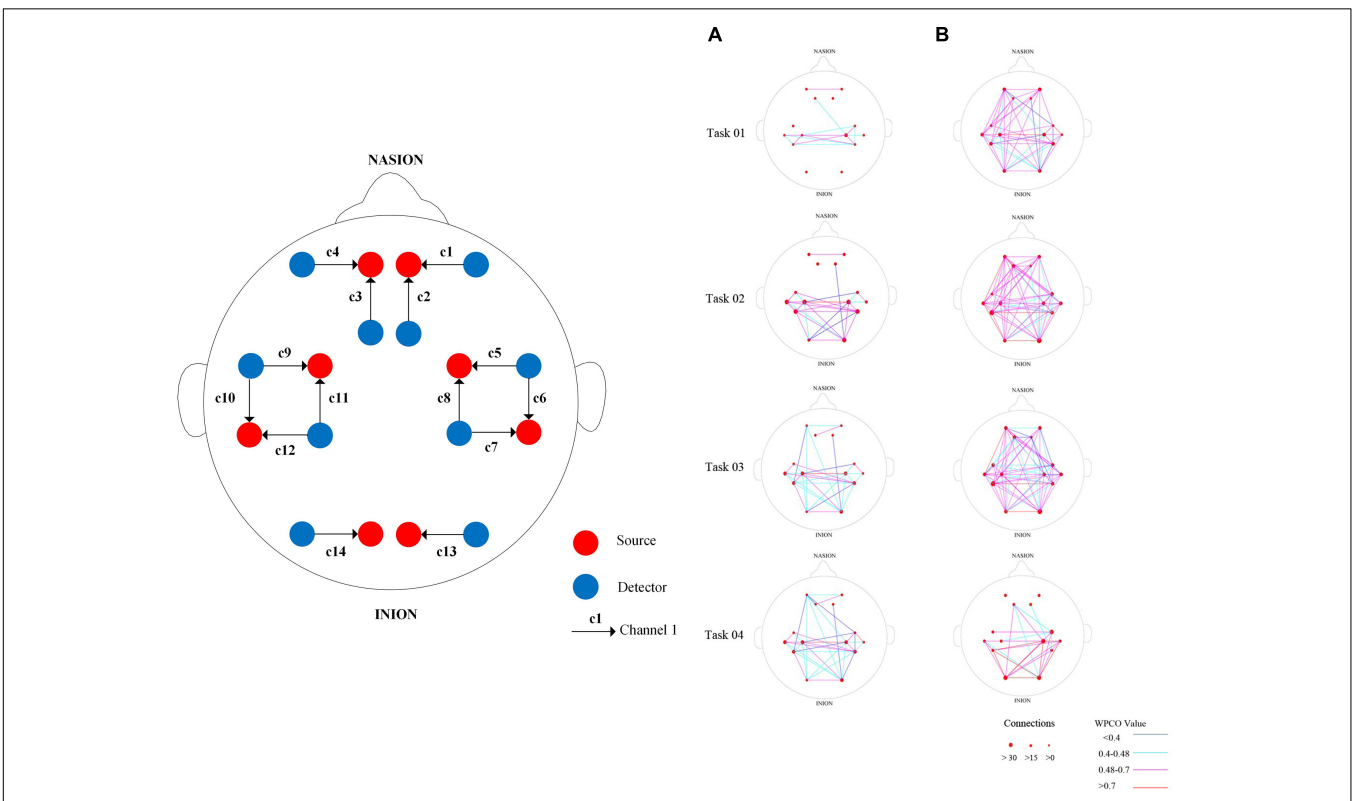

FIGURE 1 | Near-infrared channel probe layout **(A)** and typical examples of diagram of brain functional connectivity (FC) in interval I from the two groups. Arrangement of source optodes (red dots, S), detector optodes (blue dots, D), and measurement channels (black arrow, C) in the prefrontal cortex, motor cortex, and occipital leaf cortical areas based on the international 10/10 system. **(B)** Comparisons of wavelet phase coherence (WPCO) in the 15 connectivity types among the groups. (a) WPCO of MCI group in four states of interval I. (b) WPCO of control group in four states of interval I. Red lines represent WPCO values greater than 0.7. Pink lines represent WPCO values between 0.48 and 0.7. Light green lines represent WPCO values between 0.4 and 0.48. Blue lines represent WPCO values under 0.4. The size of the red dot at channel position represents the density of connection on this channel. The largest red dot means the number of connections on this channel is greater than 30; medium red dot, the number is between 0 and 15; smallest red dot, the number is 0–14. a, MCI group; b, healthy control (HC) group.

Areas Tested by Functional Near-Infrared Spectroscopy

Prefrontal Cortex (PFC)

It is generally considered to be the human cognitive cortical area (Yang et al., 2001; Wang et al., 2005). This cortical area participates in the execution process, including working memory, attention resource allocation, and plot information processing, especially working memory in a DT context (Gouwanda, 2014). Therefore, PFC is a suitable research object to investigate changes in brain activity related to distraction.

Motor Cortex (MC)

It participates in feeling the posture and movement of the human body and controls the contralateral limb. Movement plays an important role in people's feelings and movement control.

Occipital Leaf (OL)

It is mainly used for visual information processing and is also associated with functions such as memory and motor perception (Wu and Pan, 2014). **Figure 1B** shows the arrangement of the probe for the measurement and typical examples of the diagram of brain FC. A light source and a detector formed the channel.

Experimental Procedure

Three-dimensional gait analysis was performed in a gait laboratory. The cerebral blood oxygen signals were obtained using a portable fNIRS instrument (Danyang Huichuang Medical Equipment Co., Ltd.). Each subject performed four different tasks: walking task (Task 01), counting backward–walking task (Task 02), naming animals–walking task (Task 03), and calculating–walking task (Task 04) (Hittmair-Delazer et al., 1994; Weiss et al., 2003). Task 01 was a single task, whereas Task 02, Task 03, and Task 04 were DTs. The subjects were asked to walk for 10 min in a comfortable manner on a 3-m walkway in each task. A 5-min break was provided between experiments to prevent fatigue. Each task was demonstrated to each participant to ensure that he or she was familiar with the experimental process before the experiment began. The laboratory provided the subjects' experimental clothes with uniform lower body and disposable shorts to facilitate labeling. The research idea and scheme of this study are shown in **Figure 2**.

Gait Analysis

3D Motion

Before each gait test, the system should be calibrated. Marks were pasted on the subjects (according to Plug-in Gait requirements) to collect gait actions. A new database on Vicon Nexus was created, and then a static model was established to collect gait actions.

Data Processing

The start and end time of the video were set for analysis, and the marked points were identified and checked. The processed image data could be viewed and output through the software. Finally, the output processing data were imported into the Matlab software gait parameter script to run to complete the calculation of gait symmetry parameters, including gait speed, step length, step length change, DT speed consumption, and other parameters. **Figure 3** shows the processing gait data in VICON. A prominent feature of the normal gait of the human body is the symmetry of motion. The effects of special or abnormal conditions (e.g., crossing obstacles and walking dysfunction) on the overall characteristics of gait hinder the symmetry of walking. Therefore, the symmetry of gait is important for the comprehensive evaluation of gait movement and walking function (Wu and Pan, 2014). See the **Appendix** for the calculation formula of gait symmetry indices. **Figure 4** shows the definitions of lower limb gait features in polar coordinates.

Wavelet Phase Coherence

Wavelet phase coherence (WPCO) is a brain FC analysis method for illustrating the phase relationship of brain function adjustment (Bernjak et al., 2012). A large WPCO value indicates a high phase synchronism and strong FC. In this study, the phase synchronization value was calculated using the WPCO method and used in the analysis of the FC of each brain region. The WPCO was calculated in two frequency intervals: interval I was at 0.052–0.145 Hz, and interval II was at 0.021–0.052 Hz. See the **Appendix** for the formula of WPCO.

Amplitude-adjusted Fourier transform (AAFT) was used to analyze the phase synchronization between cerebral blood oxygen signals to test its true level. A total of 100 AAFT replacement signals were calculated for each blood oxygen signal, and the 100 phase coherence values between the corresponding substitute signals of each of the two blood oxygen signals were calculated. The WPCO value between the two blood oxygen signals was considered significant if the measured WPCO value was greater than the mean of the corresponding 100 substitute signal WPCO values plus twice the standard deviation (Gao et al., 2015). Otherwise, the WPCO value was not significant, and no FC existed between the corresponding channels (Theiler et al., 1992).

The WPCO between every two channels was calculated using the WPCO analysis method. The trapezoidal integral was divided by the band range to obtain the WPCO mean between the two channels. Fifteen functional zone pairs, namely, LPFC–RPFC, LPFC–LMC, LPFC–RMC, LPFC–LOL, LPFC–ROL, RPFC–LMC, RPFC–RMC, RPFC–LOL, RPFC–ROL, LMC–RMC, LMC–LOL, LMC–ROL, RMC–LOL, RMC–ROL, and LOL–ROL, were formed from the six cortical regions.

STATISTICAL ANALYSIS

The Shapiro–Wilk's test and Levene's test were used to test the normal distribution and homogeneity of variance of the two groups (Wu and Pan, 2014). For the data with non-normal distribution or uneven variance, the non-parametric method Mann–Whitney U test was used to compare the two sets of data. For the normal distribution and homogeneity of variance, the parametric method T-test was used. The effects of different conditions on FC and gait were performed using the repeated ANOVA. Correction for multiple comparisons was performed with Bonferroni method. The Pearson correlation coefficient was

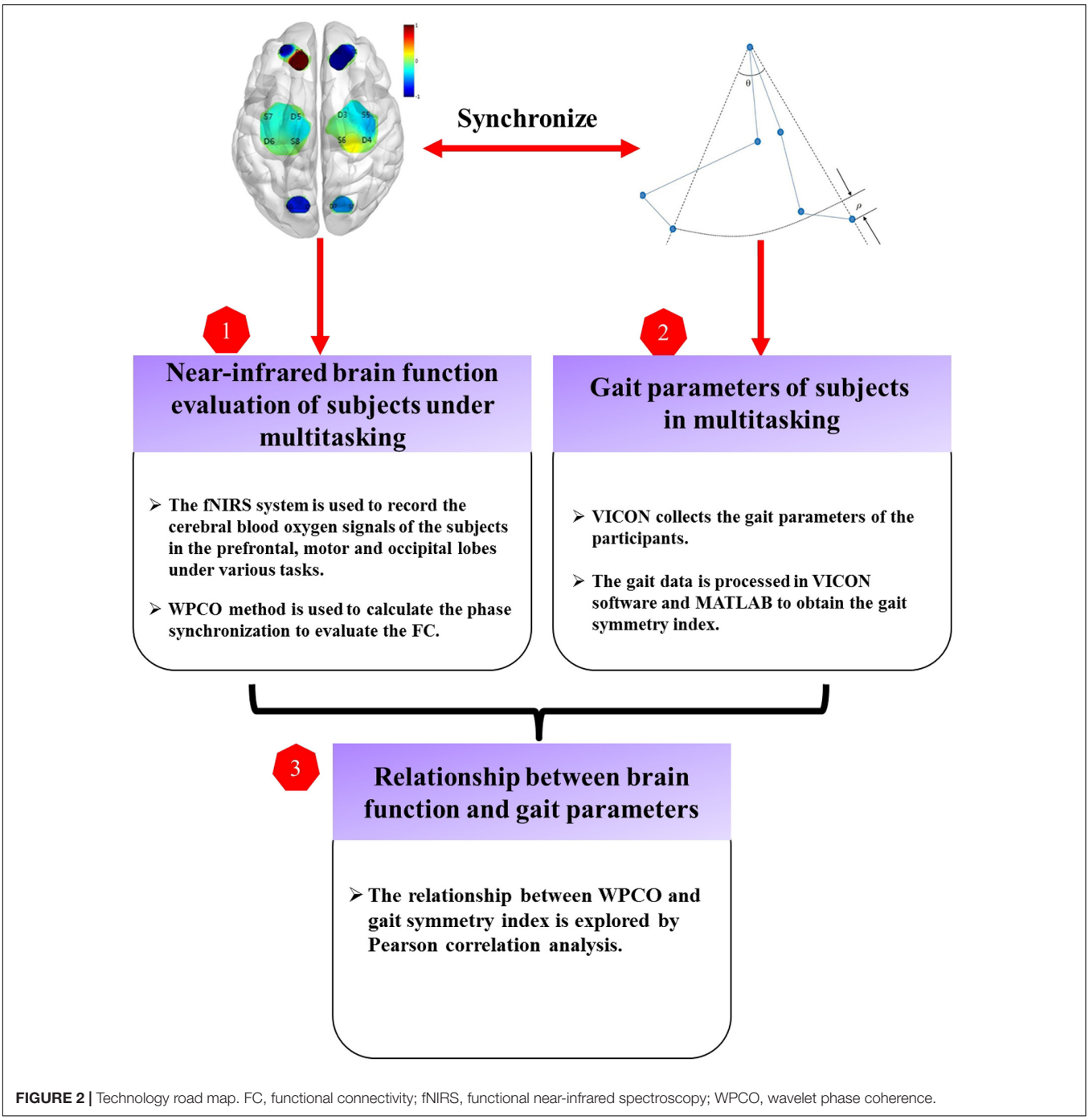

FIGURE 2 | Technology road map. FC, functional connectivity; fNIRS, functional near-infrared spectroscopy; WPCO, wavelet phase coherence.

used to analyze the correlation between the WPCO value and the gait symmetry index, and the *p*-value of Pearson's correlation coefficient was less than 0.05 (Wu and Pan, 2014).

RESULTS

Comparison in FC Among the Four Tasks

Figure 5 shows the comparisons in WPCO in interval I and interval II. The results show that the FC of RPFC–RMC in the MCI group is significantly lower in interval I in Task 03 compared with in Task 02 ($p = 0.001$). The FC in interval I is significantly higher in the MCI group than that in the HC group ($p = 0.008$) in Task 03. The FC in interval II is significantly higher in MCI group than that in HC group ($p = 0.017$) in Task 02.

The repeated ANOVA showed that the FCs of LPFC–ROL were significantly different in interval II in the HC group among the four tasks ($p < 0.05$). The FC of LPFC–ROL in interval II is significantly higher in Task 03 compared with that in Task 02 ($p = 0.000$).

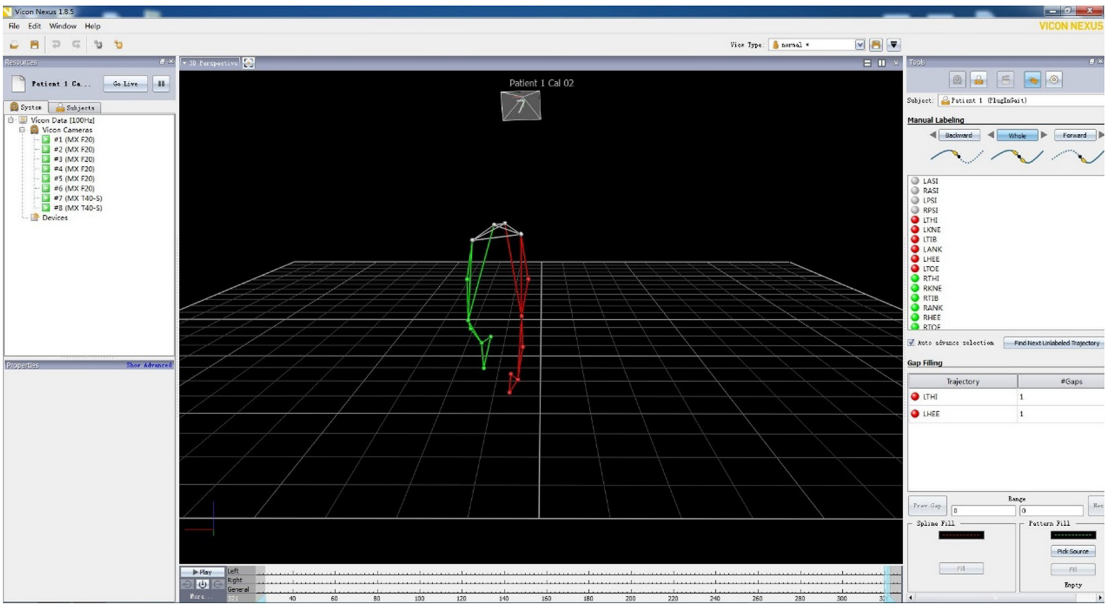

FIGURE 3 | Processing gait data in VICON.

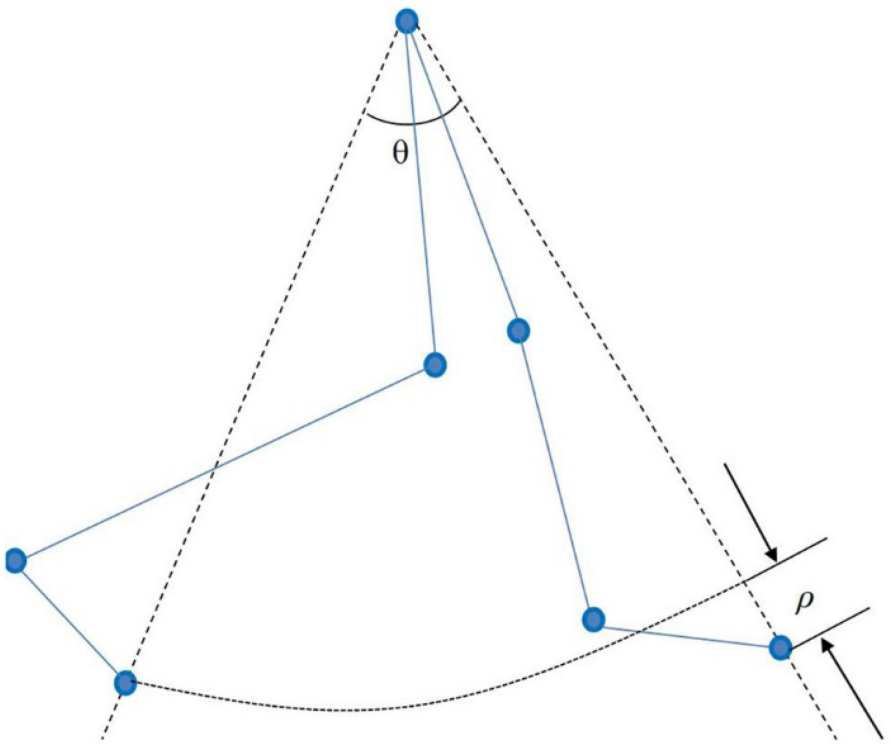

FIGURE 4 | Definition of lower limb gait characteristics in polar coordinates.

Comparison in Gait Parameters Among the Four Tasks

As shown in **Figure 6**, the right relative symmetry index (IDpsR) was significantly lower in Task 03 compared with Task 02 in the MCI group ($p = 0.000$). The asymmetry index (ASI) values were significantly higher in Task 03 ($p = 0.000$) and Task 04 ($p = 0.037$) compared with those in Task 01. Compared with that of Task 02, the ASI value was significantly higher in Task 03 ($p = 0.009$).

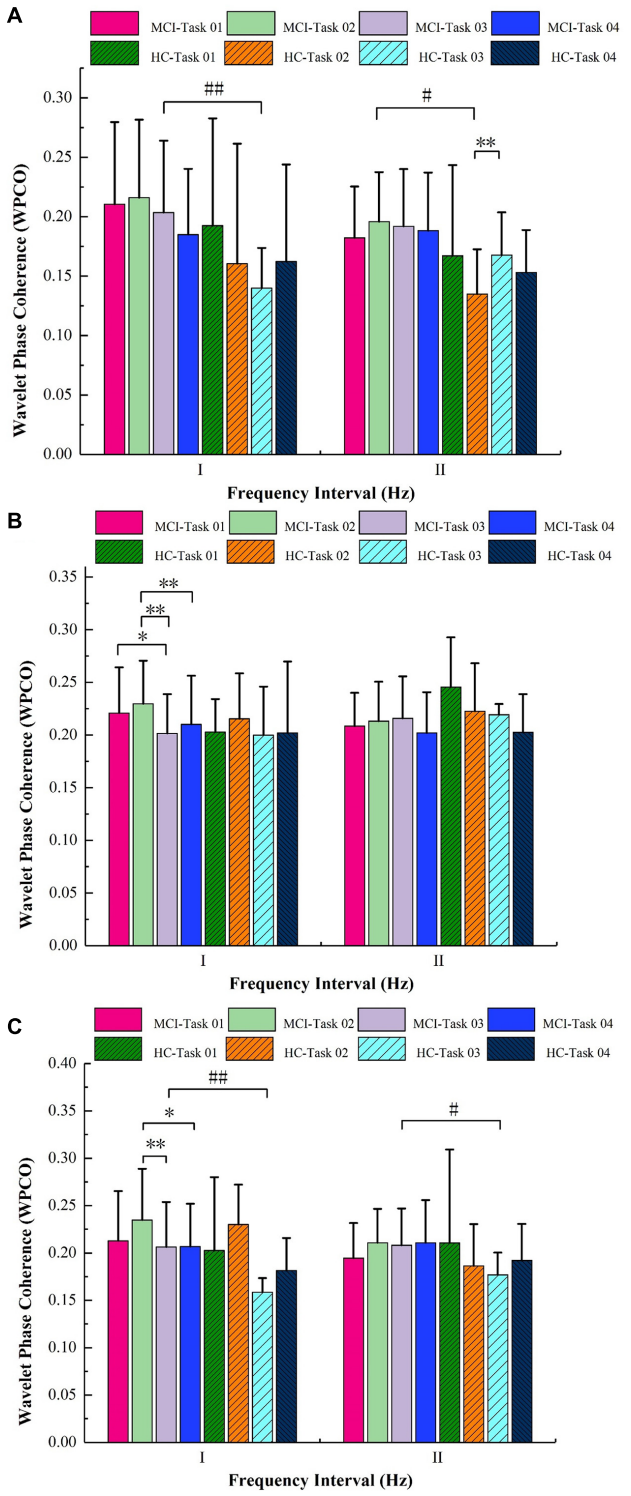

FIGURE 5 | Results of wavelet phase coherence (WPCO) in different brain regions among the groups under the four tasks. **(A)** WPCO of left prefrontal cortex–right occipital leaf cortex (LPFC–ROL), **(B)** WPCO of right prefrontal cortex–right motor cortex (RPFC–RMC), **(C)** WPCO of left prefrontal cortex–left motor cortex (LPFC–LMC). Significant levels are marked with $^{\#}p < 0.05$, $^{\#\#}p < 0.01$, $^{*}p < 0.05$, $^{**}p < 0.01$. HC, healthy control; MCI, mild cognitive impairment.

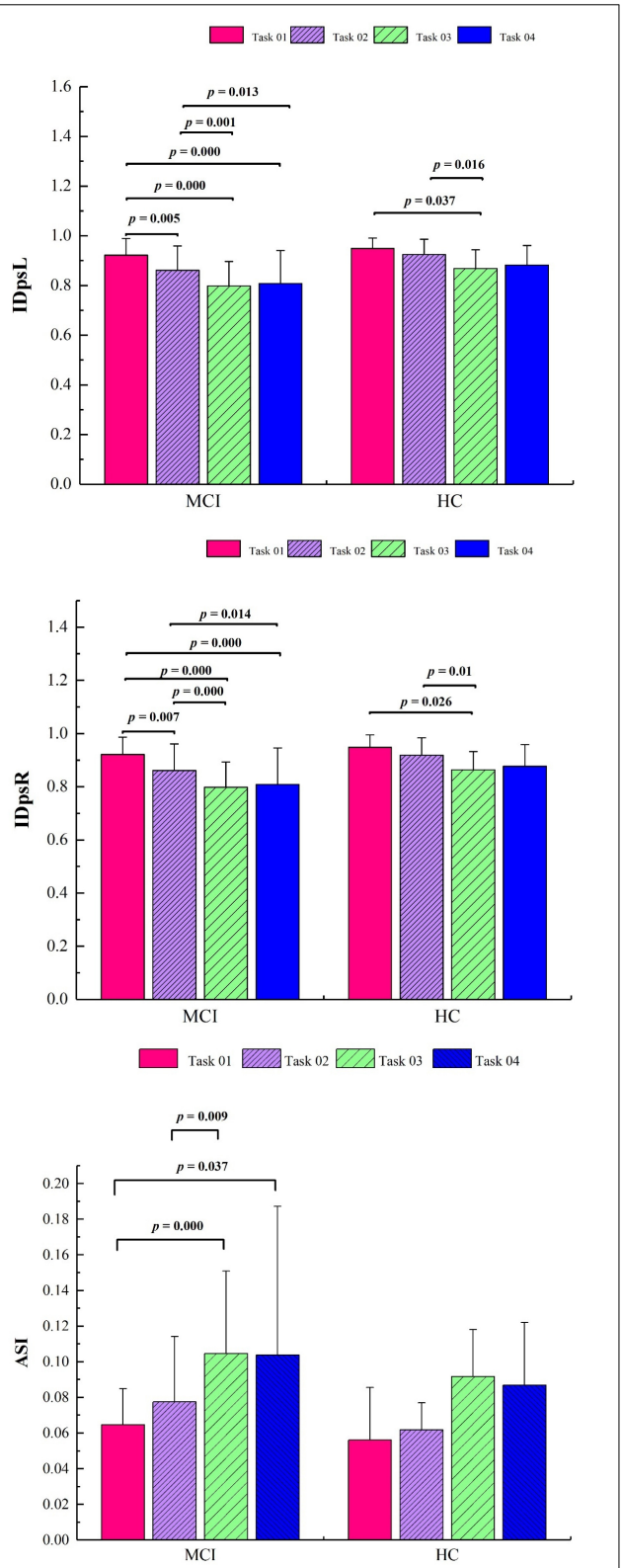

FIGURE 6 | Significant results of gait symmetry indices for four tasks in the two groups. IDpsL, left relative symmetry index; IDpsR, right relative symmetry index; ASI, asymmetry index; HC, healthy control; MCI, mild cognitive impairment.

Calculated using repeated measurements of ANOVA, the ASI was significantly different in the MCI group ($p < 0.05$).

Correlation Between Functional Connectivity and Gait Parameters

Figures 7A–E show the results of the Pearson correlation analysis between FC and gait parameters. In the MCI group, the IDpsR is positively correlated with the FC of RPFC–RMC in interval I (R = 0.205, p = 0.041). However, the relative symmetry index (IDpsL and IDpsR) is negatively correlated with the FC of LPFC–LMC in interval II group (R = -0.234, p = 0.019; R = -0.225, p = 0.024). In the HC group, the ASI is positively correlated with the FC of LPFC–LMC in interval II (R = 0.472, p = 0.035). Also, the step size symmetry index in polar coordinates (IDpsθ) is positively correlated with the FC of LPFC–ROL in the HC group (R = 0.457, p = 0.043).

DISCUSSION

The purpose of this study is to analyze the brain FC of older adults with MCI during the single task and DTs and examine the correlation between brain FC and gait symmetry indices during the single task and DTs. The main findings are as follows: (1) The gait symmetry indices show a remarkable decrease during DT compared with those during the single task in both groups. (2) The IDpsR could reflect the abnormal change in FC of RPFC–RMC in interval I in the MCI group during naming animals–walking task.

Prior studies have been demonstrated that more challenging mobility performance tasks, such as DT walking, may better capture early brain abnormalities (Camicioli et al., 1997; Beauchet et al., 2013). During the execution of DTs, the neural network of each single task does not operate independently or in parallel but integrates with other brain regions to form a neural network to further improve executive function (Dove et al., 2000). Walking and counting backward (Task 02) examines working memory and attention. Walking and naming animals (Task 03) are about verbal fluency and relies on semantic memory. Walking while calculating (Task 04) examines working memory and attention. Working memory, attention, episodic recall, and conscious perception extensively activate the frontal and parietal cortex. However, there are difficulties in locating the executive function brain areas in the DT processing and exploring their specific functions, and the functional neuroanatomy of the processing has not reached consensus (Dove et al., 2000).

In the present study, the FC of LPFC–ROL in interval II is significantly higher in the MCI group than that in the HC group in counting backward–walking task (Task 02). The hemodynamic parameters in interval II are closely regulated through tight neurovascular coupling and partial autonomic control within the brain (Zhang et al., 2002). The PFC is widely recognized as the cognitive cortical region of humans (Dove et al., 2000; Morgan et al., 2011; Schättin et al., 2016). The cortical area participates in the execution process, including working memory, attention resource allocation, and plot information processing, especially in the context of DTs (Pashler et al., 2001). The OL is mainly used for visual information processing and is also associated with functions such as memory and motor perception (Wu and Pan, 2014). The counting backward–walking task examines working memory and attention. Thus, the higher FC of LPFC–ROL in interval II might suggest that the MCI group needs more visual information processing to regulate the counting backward cognitive task than the HC group under the regulation of neural activity.

The frequency interval I is associated with changes in the peripheral sympathetic nerve activities that reflect sympathetically mediated and local myogenic mechanisms (Zhang et al., 2002). In the present study, the FC of RPFC–RMC in interval I is significantly lower in naming animals–walking task compared with that in counting backward–walking task in the MCI group. Counting backward–walking task examines working memory and attention. Naming animals–walking task is about verbal fluency and relies on semantic memory. The lower FC of RPFC–RMC suggests that naming animals–walking task relies less on executive function.

The PFC is considered an essential part of working memory. The PFC has a functional connection with the hippocampus (H) through the entorhinal cortex (E) and the substantia nigra striatum (NS) system. The degradation of the hippocampus leads to the decomposition of visual, vestibular, and proprioceptive sensory and contextual information into spatial maps and thus leading to gait disorders. Therefore, damage to the PFC may lead to executive dysfunction, leading to gait disturbance (Jordan et al., 2004; Tan et al., 2016).

Gait symmetry is an important aspect of the comprehensive evaluation of gait movement and walking function (Jin and Zhang, 2011). The values of IDpsL and IDpsR are between 0 and 1. A value closer to 1 indicates a better gait symmetry (Scholkmann et al., 2014). In the present study, the gait symmetry is reduced in the DT situation compared with the single task in the two groups. The results further confirm that gait symmetry is affected by cognitive tasks (Dove et al., 2000).

The IDpsθ exhibits a positive correlation with the FC of LPFC–ROL in interval II in the HC group in Task 02. However, there was no significant correlation between FC and gait parameters in the MCI group. The results suggest that compared with the MCI group, the HC group has a stronger ability to adapt to cognitive tasks under the regulation of neural activity.

IDpsR is positively correlated with the FC of RPFC-RMC in the MCI group. At the same time, compared with counting backward–walking task, the IDpsR of naming animals–walking task decreased significantly in the MCI group. Therefore, the IDpsR might reflect abnormal change in FC of RPFC-RMC in interval I in the MCI population during naming animals–walking task under myogenic activities.

The hemodynamic parameters are closely regulated through tight neurovascular coupling and partial autonomic control in interval II within the brain (Zhang et al., 2002). In interval II, the FC of LPFC–LMC under naming animals–walking

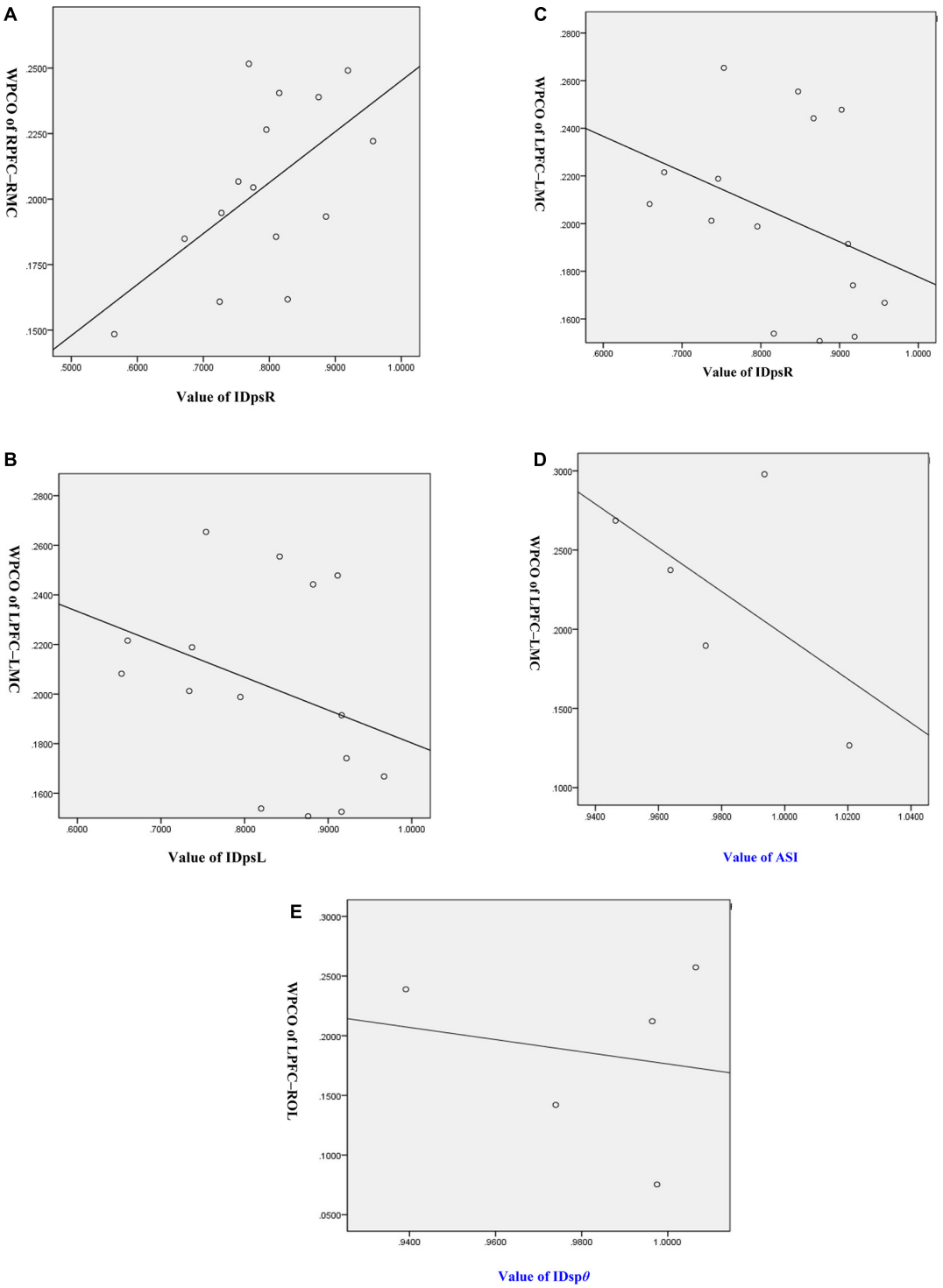

FIGURE 7 | Correlation analysis of wavelet phase coherence (WPCO) values and gait symmetry values. **(A)** Correlation analysis between WPCO values of RPFC-RMC and values of IDpsR. **(B)** Correlation analysis between WPCO values of LPFC-LMC and values of IDpsL. **(C)** Correlation analysis between WPCO values of LPFC-LMC and values of IDpsR. **(D)** Correlation analysis between WPCO values of LPFC-LMC and values of ASI. **(E)** Correlation analysis between WPCO values of LPFC-ROL and values of IDspθ. IDpsL, left relative symmetry index; IDpsR, right relative symmetry index; ASI, asymmetry index; IDspθ, the step size symmetry index in polar coordinates; RPFC, right prefrontal cortex; LPFC, left prefrontal cortex; RMC, right motor cortex; LMC, left motor cortex; ROL, right occipital leaf cortex.

task of the MCI group is significantly higher than that of the HC group. At the same time, the FC of the MCI group at this connectivity is negatively correlated with IDpsL and IDpsR. However, the FC of the HC group at this connectivity is positively correlated with ASI. Therefore, naming animals–walking task, the FC was adjusted with different gait parameters to complete the task under tight neurovascular coupling and partial autonomic control.

Limitations

The consideration of the results must further address the system activity interference within the set interval. In this study, interval I ranges from 0.052 to 0.145 Hz. The interference caused by heart rate and blood pressure fluctuations cannot be completely ruled out. The frequency interval I (0.06–0.15 Hz) is associated with changes in the peripheral sympathetic nerve activities that reflect sympathetically mediated and local myogenic mechanisms (Zhang et al., 2002). In one study, systemic signals contribute only 35% of hemodynamic changes when oxyhemoglobin is carried out in the frequency interval of 0.04–0.15 Hz (Katura et al., 2006). Therefore, these system activity disturbances may affect the results of FC, and the Meyer wave disturbances should be considered in future research.

CONCLUSION

The IDpsR might reflect the abnormal change in FC of RPFC–RMC in interval I in the MCI group during the naming animals–walking task. The gait symmetry is affected by DTs in both groups. The findings of this study may have a pivotal role in the early monitoring and intervention of brain dysfunction among older adults with MCI.

DATA AVAILABILITY STATEMENT

The raw data supporting the conclusions of this manuscript will be made available by the authors, without undue reservation, to any qualified researcher.

ETHICS STATEMENT

The studies involving human participants were reviewed and approved by the Ethics Committee of the National Rehabilitation Aids Research Center. The patients/participants provided their written informed consent to participate in this study.

AUTHOR CONTRIBUTIONS

ZLi designed the study and edited the manuscript. YL did the experiment, analyzed the data, and drafted the manuscript. KL and QL did the experiment. GX analyzed the data. CH performed the statistical analysis. RJ, TZ, and PS contributed to the physiological interpretation of the results. ZLv edited the manuscript. All authors contributed to the article and approved the submitted version.

FUNDING

The project was supported by the National Key R&D Program of China (Grant No. 2018YFC2001700), the National Natural Science Foundation of China (NSFC Nos. 31771071, 61761166007, and 11732015), and the Fundamental Research Funds for Central Public Welfare Research Institutes (118009001000160001).

REFERENCES

Alexander, N. B. (1996). Differential diagnosis of gait disorders in older adults. *Clin. Geriatr. Med.* 12, 689–703. doi: 10.1016/s0749-0690(18)30196-4

Barry, R., and Serge, G. (2008). Current evidence for subjective cognitive impairment (SCI) as the pre-mild cognitive impairment (MCI) stage of subsequently manifest Alzheimer's disease. *Int. Psychogeriatr.* 20, 1–16. doi: 10.1017/s1041610207006412

Beauchet, O., Allali, G., Launay, C., Herrmann, F. R., and Annweiler, C. (2013). Gait variability at fast-pace walking speed: a biomarker of mild cognitive impairment? *J. Nutr. Health Aging* 17, 235–239. doi: 10.1007/s12603-012-0394-4

Bernjak, A., Stefanovska, A., McClintock, P. V. E., Owen-Lynch, P. J., and Clarkson, P. (2012). Coherence between fluctuations in blood flow and oxygen saturation. *Fluctuation Noise Lett.* 11:1240013. doi: 10.1142/s0219477512400135

Biswal, B., Zerrin Yetkin, F., Haughton, V. M., and Hyde, J. S. (1995). Functional connectivity in the motor cortex of resting human brain using echo-planar mri. *Magn. Reson. Med.* 34, 537–541. doi: 10.1002/mrm.1910340409

Boas, D. A., Elwell, C. E., Ferrari, M., and Taga, G. (2014). Twenty years of functional near-infrared spectroscopy: introduction for the special issue. *NeuroImage* 85, 1–5. doi: 10.1016/j.neuroimage.2013.11.033

Camicioli, R., Howieson, D., Lehman, S., and Kaye, J. (1997). Talking while walking: the effect of a dual task in aging and Alzheimer's disease. *Neurology* 48, 955–958. doi: 10.1212/wnl.48.4.955

Canu, E., Agosta, F., Sarasso, E., Volontè, M. A., Basaia, S., Stojkovic, T., et al. (2016). Brain structural and functional connectivity in parkinson's disease with freezing of gait. *Hum. Brain Mapp.* 36, 5064–5078. doi: 10.1002/hbm.22994

Crockett, R. A., Hsu, C. L., Best, J. R., and Liu-Ambrose, T. (2017). Resting State default Mode network connectivity, dual task performance, gait speed, and postural sway in older adults with mild cognitive impairment. *Front. Aging Neurosci.* 9:423. doi: 10.3389/fnagi.2017.00423

Dove, A., Pollmann, S., Schubert, T., Wiggins, C. J., and von Cramon, D. Y. (2000). Prefrontal cortex activation in task switching: an event-related fMRI study. *Cogn. Brain Res.* 9, 103–109. doi: 10.1016/s0926-6410(99)00029-4

Ferrari, M., and Quaresima, V. (2012). A brief review on the history of human functional near-infrared spectroscopy (fNIRS) development and fields of application. *Neuroimage* 63, 921–935. doi: 10.1016/j.neuroimage.2012.03.049

Fox, M. D., and Raichle, M. E. (2007). Spontaneous fluctuations in brain activity observed with functional magnetic resonance imaging. *Nat. Rev. Neurosci.* 8, 700–711. doi: 10.1038/nrn2201

Freitas, S., Simoes, M. R., Maroco, J., Alves, L., and Santana, I. (2012). Construct validity of the montreal cognitive assessment (MoCA). *J. Int. Neuropsychol. Soc.* 18, 242–250. doi: 10.1017/s1355617711001573

Ganz, D. A., Bao, Y., Shekelle, P. G., and Rubenstein, L. Z. (2007). Will my patient fall? *JAMA* 297, 77–86. doi: 10.1001/jama.297.1.77

Gao, Y., Zhang, M., Han, Q., Li, W., Xin, Q., Wang, Y., et al. (2015). Cerebral autoregulation in response to posture change in elderly subjects-assessment

by wavelet phase coherence analysis of cerebral tissue oxyhemoglobin concentrations and arterial blood pressure signals. *Behav. Brain Res.* 278, 330–336. doi: 10.1016/j.bbr.2014.10.019

Gouwanda, D. (2014). Comparison of gait symmetry indicators in overground walking and treadmill walking using wireless gyroscopes. *J. Mech. Med. Biol.* 14, 241–253.

Hittmair-Delazer, M., Semenza, C., and Denes, G. (1994). Concepts and facts in calculation. *Brain* 117(Pt 4), 715–728. doi: 10.1093/brain/117.4.715

Jin, D., and Zhang, J. (2011). *Bio-Mechanology in Rehabilitation Engineering*. Beijing: Tsinghua University Press, 88–89.

Jordan, K., Schadow, J., Wuestenberg, T., Heinze, H.-J., and Ja¨ncke, L. (2004). Different cortical activations for subjects using allocentric or egocentric strategies in a virtual navigation task. *Neuroreport* 15, 135–140. doi: 10.1097/00001756-200401190-00026

Kadaba, M. P., Ramakrishnan, H. K., and Wootten, M. E. (1990). Measurement of lower extremity kinematics during level walking. *J. Orthop. Res.* 8, 383–392. doi: 10.1002/jor.1100080310

Katura, T., Tanaka, N., Obata, A., Sato, H., and Maki, A. (2006). Quantitative evaluation of interrelations between spontaneous low-frequency oscillations in cerebral hemodynamics and systemic cardiovascular dynamics. *Neuroimage* 31, 1592–1600. doi: 10.1016/j.neuroimage.2006.02.010

Kutilek, P., Viteckova, S., Svoboda, Z., Socha, V., and Smrcka, P. (2014). Kinematic quantification of gait asymmetry based on characteristics of angle-angle diagrams. *Acta Polytechn. Hung.* 11, 25–38.

Lin, M. I. B., and Lin, K. H. (2016). Department of Industrial and Information Management, National Cheng Kung University. Walking while performing working memory tasks changes the prefrontal cortex hemodynamic activations and gait kinematics. *Front. Behav. Neurosci.* 10:92. doi: 10.3389/fnbeh.2016.00092

Montero-Odasso, M., Verghese, J., Beauchet, O., and Hausdorff, J. M. (2012). Gait and cognition: a complementary approach to understanding brain function and the risk of falling. *J. Am. Geriatr. Soc.* 60, 2127–2136. doi: 10.1111/j.1532-5415.2012.04209.x

Morgan, H. M., Muthukumaraswamy, S. D., Hibbs, C. S., Shapiro, K. L., Bracewell, R. M., Singh, K. D., et al. (2011). Feature integration in visual working memory: parietal gamma activity is related cognitive coordination. *J. Neurophysiol.* 106, 3185–3194. doi: 10.1152/jn.00246.2011

Oostenveld, R., and Praamstra, P. (2001). The five percent electrode system for high-resolution EEG and ERP measurements. *Clin. Neurophysiol.* 112, 713–719. doi: 10.1016/s1388-2457(00)00527-7

Park, C.-H., Chang, W.-H., Ohn, S.-H., Kim, S.-T., Bang, O.-Y., Pascual-Leone, A., et al. (2011). Longitudinal changes of resting-state functional connectivity during motor recovery after stroke. *Stroke* 42, 1357–1362. doi: 10.1161/strokeaha.110.596155

Pashler, H., Johnston, J. C., and Ruthruff, E. (2001). Attention and performance. *Annu. Rev. Psychol.* 52, 629–651.

Prince, M., Comas-Herrera, A., Knapp, M., Guerchet, M., and Karagiannidou, M. (2016). *World Alzheimer Report 2016: Improving Healthcare for people Living with Dementia: Coverage, Quality and Costs Now and in the Future*. London: Alzheimer's Disease International.

Schättin, A., Arner, R., Gennaro, F., and de Bruin, E. D. (2016). Adaptations of prefrontal brain activity, executive functions, and gait in healthy elderly following exergame and balance training: a randomized-controlled study. *Front. Aging Neurosci.* 8:278. doi: 10.3389/fnagi.2016.00278

Scholkmann, F., Kleiser, S., Metz, A. J., Zimmermann, R., Mata, P. J., Wolf, U., et al. (2014). A review on continuous wave functional near-infrared spectroscopy and imaging instrumentation and methodology. *Neuroimage* 85(Pt 1), 6–27. doi: 10.1016/j.neuroimage.2013.05.004

Stokholm, J., Vogel, A., Gade, A., and Waldemar, G. (2006). Heterogeneity in executive impairment in patients with very mild Alzheimer's disease. *Dement. Geriatr. Cogn. Disord.* 22, 54–59. doi: 10.1159/000093262

Tan, Q., Zhang, M., Wang, Y., Zhang, M., Wang, B., Xin, Q., et al. (2016). Age-related alterations in phase synchronization of oxyhemoglobin concentration changes in prefrontal tissues as measured by near-infrared spectroscopy signals. *Microvasc. Res.* 103, 19–25. doi: 10.1016/j.mvr.2015.10.002

Theiler, J., Eubank, S., Longtin, A., Galdrikian, B., and Farmer, J. D. (1992). Testing for nonlinearity in time series: the method of surrogate data. *Physica D* 58, 77–94. doi: 10.1016/0167-2789(92)90102-s

Tian, Q., Chastan, N., Bair, W. N., Resnick, S. M., Ferrucci, L., and Studenski, S. A. (2017). The brain map of gait variability in aging, cognitive impairment and dementia—a systematic review. *Neurosci. Biobehav. Rev.* 74, 149–162. doi: 10.1016/j.neubiorev.2017.01.020

Verghese, J., Lipton, R. B., Hall, C. B., Kuslansky, G., Katz, M. J., and Buschke, H. (2002). Abnormality of gait as a predictor of non-Alzheimer's dementia. *N. Engl. J. Med.* 347, 1761–1768. doi: 10.1056/nejmoa020441

Wang, R., Zhang, M., Hua, C., Deng, X., Yang, N., and Jin, D. (2005). Evaluation indices for gait symmetry based on Fitts's law. *J. Tsinghua Univ. (Sci. Tech.)* 45, 191–192.

Weiss, E. M., Siedentopf, C., Hofer, A., Deisenhammer, E., and Delazer, M. (2003). Brain activation pattern during a verbal fluency test in healthy male and female volunteers: a functional magnetic resonance imaging study. *Neurosci. Lett.* 352, 191–194. doi: 10.1016/j.neulet.2003.08.071

Wilson, R. S., Schneider, J. A., Beckett, L. A., Evans, D. A., and Bennett, D. A. (2002). Progression of gait disorder and rigidity and risk of death in older persons. *Neurology* 58, 1815–1819. doi: 10.1212/wnl.58.12.1815

Wu, S., and Pan, F. (2014). *SPSS Statistical Analysis Daquan*. Beijing: Tsinghua University Press, 218.

Yang, N. F., Wang, R. C., Jin, D. W., Dong, H., Huang, C. H., and Zhang, M. (2001). Evaluation method of human upper limb movement function based on Fitts' law. *Chin. J. Rehabil. Med.* 16:336339.

Zhang, R., Zuckerman, J. H., Iwasaki, K., Wilson, T. E., Crandall, C. G., and Levine, B. D. (2002). Autonomic neural control of dynamic cerebral autoregulation in humans. *Circulation* 106, 1814–1820. doi: 10.1161/01.cir.0000031798.07790.fe

Conflict of Interest: The authors declare that the research was conducted in the absence of any commercial or financial relationships that could be construed as a potential conflict of interest.

APPENDIX

Calculation Formula of Gait Symmetry Indices

1. The phase symmetry index (IDps) (Yang et al., 2001; Wang et al., 2005; Jin and Zhang, 2011; Gouwanda, 2014; Wu and Pan, 2014) is calculated to evaluate the symmetry of the left and right leg gaits by the time phase of the gait cycle.

$$\mathrm{IDps} = \sqrt{\frac{T_0}{T}}\left(0.62\frac{S_\mathrm{s}}{s_\mathrm{m}} + 0.38\frac{W_s}{W_m}\right), \tag{1}$$

where T_0 is the average of the gait cycle of healthy people; T is the gait cycle of the measured object; S_s and S_m are the minimum and maximum values, respectively, of the single leg support period; and W_s and W_m are the minimum and maximum values, respectively, of the single leg swing period. The different gait cycles of the left and right legs are divided into the left relative symmetry index (IDpsL) and the right relative symmetry index (IDpsR).

2. The F-step size symmetry index in the Cartesian coordinate system, which is a comprehensive symmetry index based on the Fitts' law (Yang et al., 2001; Wang et al., 2005; Jin and Zhang, 2011; Gouwanda, 2014; Wu and Pan, 2014), is calculated as follows:

$$\mathrm{IDsp} = \frac{log_2(2ST_1/ST_{l0})/t_1}{log_2(2ST_r/ST_{r0})/t_r}, \tag{2}$$

where ST_1 and ST_r are the stride lengths of the left and right legs, respectively; ST_{l0} and $ST_{\mathrm{r}0}$ are the step by step precision error values of the left and right legs, respectively, of a healthy person with a normal gait; and t_1 and t_r are the swing period of the left and right legs, respectively.

3. The step size symmetry index (Yang et al., 2001; Wang et al., 2005; Jin and Zhang, 2011; Gouwanda, 2014; Wu and Pan, 2014) in polar coordinates (IDspθ and IDspρ) is calculated using the following equations:

$$\mathrm{IDsp}\theta = \frac{log_2(2\theta_{ST_s}/\theta_{ST_0})/t_s}{log_2(2\theta_{ST_m}/\theta_{ST_0})/t_m}\text{and} \tag{3}$$

$$\mathrm{IDsp}\rho = \frac{log_2(2\rho_{ST_s}/\rho_{ST_0})/t_s}{log_2(2\rho_{ST_m}/\rho_{ST_0})/t_m}, \tag{4}$$

where θ and ρ are the absolute values of the difference between the polar angle and the polar diameter of the toe during motion and at the end of the motion relative to the hip joint, respectively; $\theta_{ST\mathrm{s}}$ and $\rho_{ST\mathrm{s}}$ are the smaller values of the spans; $\theta_{ST\mathrm{m}}$ and $\rho_{ST\mathrm{m}}$ are the larger values among the stride lengths; t_s and t_m are the smaller and larger side step execution times, respectively, of $\log_2(2\theta_{ST}/\theta_{ST0})/t$; and θ_{ST0} and ρ_{ST0} are the precision error values of the normal step size of the normal person.

4. The asymmetry index (ASI) (Yang et al., 2001; Wang et al., 2005; Jin and Zhang, 2011; Gouwanda, 2014; Kutilek et al., 2014; Wu and Pan, 2014) is calculated using the following equation:

$$\mathrm{ASI} = |\frac{2\left(X_\mathrm{L} - X_\mathrm{R}\right)}{X_\mathrm{L} + X_\mathrm{R}}| \times 100\%, \tag{5}$$

where X_L and X_R are the support times of the single support phase of the left and right feet, respectively.

Formula of WPCO

In the calculation, if the original signal undergoes wavelet transform and the instantaneous wavelet phase is at a certain frequency f and time t_n as (Yang et al., 2001)

$$\emptyset_k\left(f, t_n\right) = \arctan\left[\frac{b_k\left(f, t_n\right)}{a_k\left(f, t_n\right)}\right], \tag{6}$$

then the instantaneous phase difference between these two signals is

$$\triangle\emptyset\left(f, t_n\right) = \emptyset_1\left(f, t_n\right) - \emptyset_2\left(f, t_n\right). \tag{7}$$

Averaging $\cos\triangle\emptyset\left(f, t_n\right)$ and $\sin\triangle\emptyset\left(f, t_n\right)$ in the time domain, the following is obtained:

$$< \cos\triangle\emptyset\left(f\right) >= \frac{1}{N}\sum_{n-1}^{N}\cos\triangle\emptyset(f, t_n) \tag{8}$$

$$< \sin\triangle\emptyset\left(f\right) >= \frac{1}{N}\sum_{n-1}^{N}\sin\triangle\emptyset(f, t_n) \tag{9}$$

Therefore, the definition of WPCO is

$$C_\phi\left(f\right) = \sqrt{\left\langle cos\ \phi\left(f,\ t\right)\right\rangle^2 + \left\langle sin\ \Delta\phi\ (f)\right\rangle^2}. \tag{10}$$

frontiers in Aging Neuroscience

ORIGINAL RESEARCH
published: 25 June 2021
doi: 10.3389/fnagi.2021.671351

Altered Functional Connectivity of the Basal Nucleus of Meynert in Subjective Cognitive Impairment, Early Mild Cognitive Impairment, and Late Mild Cognitive Impairment

Wenwen Xu[1†], *Jiang Rao*[2†], *Yu Song*[1], *Shanshan Chen*[1], *Chen Xue*[3], *Guanjie Hu*[4,5], *Xingjian Lin*[1*] and *Jiu Chen*[4,5*]

[1] Department of Neurology, The Affiliated Brain Hospital of Nanjing Medical University, Nanjing, China, [2] Department of Rehabilitation, The Affiliated Brain Hospital of Nanjing Medical University, Nanjing, China, [3] Department of Radiology, The Affiliated Brain Hospital of Nanjing Medical University, Nanjing, China, [4] Institute of Neuropsychiatry, The Affiliated Brain Hospital of Nanjing Medical University, Nanjing, China, [5] Institute of Brain Functional Imaging, Nanjing Medical University, Nanjing, China

OPEN ACCESS

Edited by:
Fermín Segovia,
University of Granada, Spain

Reviewed by:
Yu-Chen Chen,
Nanjing Medical University, China
Carlos Ayala Grosso,
Instituto Venezolano de Investigaciones Cientificas, IVIC, Venezuela
Zhiqun Wang,
Aerospace Center Hospital, China

***Correspondence:**
Xingjian Lin
linxingjian@njmu.edu.cn
Jiu Chen
ericcst@aliyun.com

[†] These authors have contributed equally to this work and share first authorship

Received: 23 February 2021
Accepted: 11 May 2021
Published: 25 June 2021

Citation:
Xu W, Rao J, Song Y, Chen S, Xue C, Hu G, Lin X and Chen J (2021) Altered Functional Connectivity of the Basal Nucleus of Meynert in Subjective Cognitive Impairment, Early Mild Cognitive Impairment, and Late Mild Cognitive Impairment. Front. Aging Neurosci. 13:671351. doi: 10.3389/fnagi.2021.671351

Background: The spectrum of early Alzheimer's disease (AD) is thought to include subjective cognitive impairment, early mild cognitive impairment (eMCI), and late mild cognitive impairment (lMCI). Choline dysfunction affects the early progression of AD, in which the basal nucleus of Meynert (BNM) is primarily responsible for cortical cholinergic innervation. The aims of this study were to determine the abnormal patterns of BNM-functional connectivity (BNM-FC) in the preclinical AD spectrum (SCD, eMCI, and lMCI) and further explore the relationships between these alterations and neuropsychological measures.

Methods: Resting-state functional magnetic resonance imaging (rs-fMRI) was used to investigate FC based on a seed mask (BNM mask) in 28 healthy controls (HC), 30 SCD, 24 eMCI, and 25 lMCI patients. Furthermore, the relationship between altered FC and neurocognitive performance was examined by a correlation analysis. The receiver operating characteristic (ROC) curve of abnormal BNM-FC was used to specifically determine the classification ability to differentiate the early AD disease spectrum relative to HC (SCD and HC, eMCI and HC, lMCI and HC) and pairs of groups in the AD disease spectrum (eMCI and SCD, lMCI and SCD, eMCI and lMCI).

Results: Compared with HC, SCD patients showed increased FC in the bilateral SMA and decreased FC in the bilateral cerebellum and middle frontal gyrus (MFG), eMCI patients showed significantly decreased FC in the bilateral precuneus, and lMCI individuals showed decreased FC in the right lingual gyrus. Compared with the SCD group, the eMCI group showed decreased FC in the right superior frontal gyrus (SFG), while the lMCI group showed decreased FC in the left middle temporal gyrus (MTG). Compared with the eMCI group, the lMCI group showed decreased FC in the right hippocampus. Interestingly, abnormal FC was associated with certain cognitive domains and functions including episodic memory, executive function, information processing

speed, and visuospatial function in the disease groups. BNM-FC of SFG in distinguishing eMCI from SCD; BNM-FC of MTG in distinguishing lMCI from SCD; BNM-FC of the MTG, hippocampus, and cerebellum in distinguishing SCD from HC; and BNM-FC of the hippocampus and MFG in distinguishing eMCI from lMCI have high sensitivity and specificity.

Conclusions: The abnormal BNM-FC patterns can characterize the early disease spectrum of AD (SCD, eMCI, and lMCI) and are closely related to the cognitive domains. These new and reliable findings will provide a new perspective in identifying the early disease spectrum of AD and further strengthen the role of cholinergic theory in AD.

Keywords: early mild cognitive impairment, late mild cognitive impairment, subjective cognitive impairment, basal nucleus of Meynert, functional connectivity, basal forebrain

INTRODUCTION

Subjective cognitive impairment (SCD), characterized by a condition where self-aware cognitive function is diminished, is reported to be a very early stage of the preclinical AD spectrum (Lautenschlager et al., 2019). Numerous credible studies proved that healthy people with SCD have a higher risk of conversion to amnestic mild cognitive impairment (aMCI) and dementia, the progression rate of which is twice than healthy people without SCD per year (Lautenschlager et al., 2019). As a subtype of MCI, aMCI, defined by exact existing memory disorders, is considered to be the distinctive transitional stage converting to AD (Csukly et al., 2016). Given the more refined early diagnosis and discrimination, aMCI is categorized into early MCI (eMCI) and late MCI (lMCI) according to the severity of the memory impairment assessed by neuropsychological examinations (Edmonds et al., 2019). Neuroimaging has been recognized as a good indicator of the pathologic progression of AD (Chen S. et al., 2020). As a result, the brain imaging characteristics of the preclinical stages of the AD spectrum including SCD, eMCI, and lMCI are worth further studying.

To explain the pathogenesis of AD with a hypothesis is limited and difficult (Barage and Sonawane, 2015). The pathogenesis of AD is very complex and has not yet been fully elucidated (Barage and Sonawane, 2015). The known pathogenesis is associated with cholinergic deficiency, gene mutation, oxidative stress, free radical injury, and inflammatory immune injury (Chen, 2018). At present, the mainstream view early recognized internationally is the cholinergic hypothesis, that is, neurocholinergic neuronal degeneration or disruption of the cholinergic system in the brain (Hampel et al., 2019). Acetylcholine (ACh), a neurotransmitter linked with learning, memory, and neuromodulation, is provided from the basal forebrain (BF) to the neocortex, hippocampus, and amygdala (Hampel et al., 2019). In addition, four overlapping cell groups (Ch1–Ch4) are contained in the BF system (Liu et al., 2015). Supported by relevant literature, a broad band of cell clusters named the basal nucleus of Meynert (BNM) is located in the BF (Gratwicke et al., 2020). Specifically, BNM is an anatomical structure corresponding to the Ch4 group which is the largest group of four groups. In the very early course of the neurodegenerative disease, previous studies have confirmed that downregulation of cholinergic markers exactly occurs (Fotiou et al., 2015). Thus, as the key hub for cholinergic energy, the study of BNM shows the great significance of cholinergic deficiency which might represent an etiological marker of cognitive impairment in the early stage of AD.

Increasing neuroimaging techniques such as resting-state functional magnetic resonance imaging (fMRI) are being applied to assess brain alterations in SCD, MCI, and AD patients to further understand the pathogenesis and progression (Fotiou et al., 2015). The disruption of neural circuit connectivities within the default mode network (DMN), executive control network (ECN), and salience network has been deeply demonstrated (Xu et al., 2020). Based on the stereotaxic map of the BNM constructed by Zaborszky et al., two latest studies show that functional disconnection exists in the BNM with insula/claustrum, leading to cognitive decline (Li et al., 2014). A study assessed volume reductions of the cholinergic basal forebrain nuclei in SCD subjects on 3D-T1-weighted MR images based on a postmortem-derived atlas (Scheef et al., 2019). Decreased volume of BNM in AD has been further reported in AD and MCI patients. Postmortem studies also have shown evidence that neuronal loss in the BNM are selectively vulnerable to degeneration in AD (Grothe et al., 2012). Dubois et al. (2016) conformed even if the criteria for cognitive impairment are not met that the diagnosis of preclinical AD can be made as long as the presence of biomarkers of amyloid beta and tau is detected by pathology. In other words, AD-specific pathological changes such as neuroimaging markers and biochemical pathological markers occur in the human brain decades before clinical symptoms appear (Tan et al., 2014). Moreover, the degree of BNM atrophy shows a linear correlation with amyloid-beta burden from the *in vivo* MRI outcomings, which is the other important pathologic mechanism of AD (Grothe et al., 2013). Therefore, as an important anatomical structure in cholinergic theory, whether in terms of structure or function, the alteration of BNM in early AD spectrum in detail deserves attention.

So far, although evidence can only support the differences in the FC of the BNM in AD and MCI, there has been no study of BNM in the detailed early AD spectrum (Li et al., 2017). Hence, it is important to determine alterations in BNM-functional connectivity (BNM-FC) in individuals in the early

disease spectrum of AD and to explore the relationships between BNM-FC and neuropsychological scores. We hypothesize that (1) abnormal BNM-FC among the early AD spectrum can be detected and continuous disruption of brain functional networks during disease progression can be explored, (2) these abnormal FCs are linked with impairments in different cognitive domains, and (3) the ability of these abnormal brain regions to classify the early AD disease spectrum is highly specific and sensitive.

METHOD

Participants

A total of 116 elderly individuals participated in our study, including 30 HC, 30 SCD, 28 eMCI, and 28 lMCI. All of the participant data came from our in-home database: the Nanjing Brain Hospital-Alzheimer's Disease Spectrum Neuroimaging Project (NBH-ADsnp) (Nanjing, China). **Supplementary Materials** summarized specific information about NBH-ADsnp in detail. Seven of them were ruled out because of no MRI data and two of them were excluded due to the effect of head motion (cumulative translation or rotation >3.0 mm or 3.0°) (Xue et al., 2020). At last, 107 individuals were included (28 HC, 30 SCD, 24 eMCI, and 25 lMCI) in the present study. Relevant exclusion criteria and inclusion criteria were documented in the **Supplementary Materials**.

Neurocognitive Assessments

All participants underwent comprehensive and standard neurocognitive assessments to evaluate their cognitive function, including general cognitive functions, episodic memory, executive function, information processing speed, and visual spatial domains (Gu et al., 2017; Chen J. et al., 2020). Comprehensive division and evaluation details were summarized in the **Supplementary Materials**.

MRI Data Acquisition

Detailed MRI data acquisition parameters involved in the NBH-ADsnp database were listed in **Supplementary Materials**.

MRI Data Preprocessing

On the basis of Statistical Parametric Mapping (SPM8), fMRI data were preprocessed by MATLAB2013b and Data Processing and Analysis for Brain Imaging (DPABI). In summary, the concrete steps of image preprocessing were provided in the **Supplementary Materials**. Overall, slice-timing and head motion correction, realignment, nuisance covariate regression, normalization, smoothing, and filtering were a series of steps in the process.

Functional Connectivity Analysis

A seed-based FC analysis was performed to explore the alternation of AD early disease spectrum (Li et al., 2017). The FC method based on seed voxel analysis can identify the brain regions that are related to the function of the seed voxel selected initially (Bell et al., 2019). If the brain regions and seed regions show a high degree of time-domain consistency, it can be considered that these brain regions and seed brain regions together form a network related to a certain brain function (Joel et al., 2011). The identification and fabrication of seed points for BNM were summarized in the **Supplementary Materials**.

Statistical Analyses

SPSS 19 was used to analyze clinical data and neuropsychological measures. The analysis of variance (ANOVA), the multimodal general linear model (GLM), and the chi-square test were conducted to compare the demographic and neurocognitive data among groups, including the HC, SCD, eMCI, and lMCI. The Bonferroni correction was used for *post-hoc* comparisons. The p-value was set as <0.05 for significant differences.

One-way ANOVA analysis was performed to determine the differential brain regions among the four groups with the control of the influence of age, gender, and education level. Then, the two-sample t-test was used for comparing differential BNM-FC in any two of the four groups based on the mask resulted from ANOVA analyses after controlling for the effects of age, gender, and level of education. Results within-group were thresholded at voxel level $p < 0.05$ [Gaussian random field (GRF) corrected] and cluster size >50 voxels. The FC values of the altered regions were extracted with DPABI.

Notably, four cognitive domains were divided from the neuropsychological tests (**Supplementary Materials**). These original psychometric scores were converted to standardized Z-values. These initial psychological scores were converted to standardized Z-values, which were then added together to obtain the cognitive domain average (Gao et al., 2018; Chen et al., 2019). A correlation analysis was conducted between altered BNM-FC and cognitive domains (Bonferroni corrected, $p < 0.05$).

In addition, the ability of altered BNM-FC in specific brain regions to differentiate and classify the spectrum of early AD diseases was realized by ROC curve (Pei et al., 2018). First, the FC value and group number were analyzed by binary regression to obtain the prediction probability. Then, the ROC curve of the prediction probability and the group was analyzed. The FC values of multiple brain regions were synthesized during binary regression analysis to obtain a new prediction probability.

RESULTS

Demographic and Neurocognitive Characteristics

The demographic and neurocognitive information of all participants, including 28 HC (mean age 62.43 ± 13.39), 30 SCD (mean age 66.23 ± 14.01), 24 eMCI (mean age 62.96 ± 13.97), and 25 lMCI (mean age 66.28 ± 15.06) individuals, can be found in **Table 1**. As expected, our results showed significant differences in cognitive performance between pairs of the comparison groups. Compared with HC, both the SCD group and the eMCI group showed lower MDRS-2 and MoCA and showed higher SCD-Q scores. In addition, the eMCI group also showed lower EM score and IPS score than the HC group and the SCD group. Compared with the eMCI group, the lMCI group exhibited significantly lower MDRS-2, MoCA, EM score, and VF score. The lMCI group also showed lower EF score and

TABLE 1 | Demographics and clinical measures of HC and patients with SCD, eMCI, and lMCI.

	HC $N = 28$	SCD $N = 30$	eMCI $N = 24$	lMCI $N = 25$	F-values (χ^2)	p-values
Age (years)	62.43 ± 13.39	66.23 ± 14.01	62.96 ± 13.97	66.28 ± 15.06	1.918	0.131
Gender (m/f)	15/13	7/23	7/17	7/15	6.523	0.089
Education (years)	12.64 ± 3.20	12.05 ± 2.77*	11.46 ± 3.35*	11.16 ± 3.44$^{\&}$	1.665	0.179
MMSE	28.57 ± 5.09	27.97 ± 4.80	27.33 ± 5.41	26.76 ± 5.13	9.977	<0.001
MDRS-2	141.89 ± 26.03	139.60 ± 25.05*	137.42 ± 27.49*	135.56 ± 26.75$^{\&}$	11.037	<0.001
MoCA	26.08 ± 5.25	24.50 ± 4.57*	23.17 ± 5.04*	21.72 ± 4.82$^{\&}$	13.464	<0.001
SCD-Q	3.31 ± 1.39	6.52 ± 1.28*	4.66 ± 2.07*	5.62 ± 1.80$^{*\#}$	21.861	<0.001
Composite Z-scores of each cognitive						
EM	0.00 ± 0.69	−0.01 ± 0.54	−0.17 ± 0.60$^{*\#}$	−0.76 ± 0.77$^{\&}$	13.230	<0.001
IPS	0.00 ± 0.61	0.05 ± 0.44	−0.17 ± 0.59$^{\#}$	0.29 ± 0.67	3.501	0.018
EF	0.00 ± 0.55	0.24 ± 0.74	−0.23 ± 0.65	0.03 ± 0.61$^{\#}$	4.269	0.007
VF	0.00 ± 0.78	0.28 ± 0.64	−0.14 ± 1.04	−0.35 ± 0.92$^{\&}$	3.270	0.024

*Numbers are given as means (standard deviation, SD) unless stated otherwise. Scores reflect the number of correct items unless stated otherwise. Significant group differences were found at $p < 0.05$ (ANOVA test and multivariable general linear model), Bonferroni corrected. Between-group comparisons were further utilized to reveal specific alterations among matched groups (*compared with HC, $^{\#}$compared with SCD, $^{\&}$compared with eMCI).*

MMSE, Mini-Mental State Exam; MDRS-2, Mattis Dementia Rating Scale-2; MoCA, the Montreal Cognitive Assessment test; SCD-Q, Subjective Cognitive Decline Questionnaire; HC, healthy controls; SCD, subjective cognitive decline; eMCI, early mild cognitive impairment; lMCI, late mild cognitive impairment; EM, episodic memory; EF, executive function; VF, visuospatial function; IPS, information processing speed.

SCD-Q score than the SCD group and higher SCD-Q score than the HC group (all $p < 0.05$).

The ANOVA analysis showed three significantly altered brain regions among the four groups, including the left hippocampus, bilateral cerebellum, and bilateral supplementary motor area (SMA). Compared with HC, eMCI patients showed significantly decreased BNM-FC in the bilateral precuneus (PCUN), lMCI individuals showed decreased BNM-FC in the right lingual gyrus (LING), and SCD patients showed increased BNM-FC in the bilateral SMA and decreased BNM-FC in the bilateral cerebellum and middle frontal gyrus (MFG). Compared with the SCD group, the eMCI group showed decreased BNM-FC in the right superior frontal gyrus (SFG), while the lMCI group showed decreased BNM-FC in the left middle temporal gyrus (MTG). Compared with the eMCI group, the lMCI group showed decreased BNM-FC in the right hippocampus. All the results were based on controlling for age, gender, and level of education (GRF corrected, cluster size $\geq$50 mm^3, $p < 0.05$) (**Figure 1** and **Table 2**).

Behavioral Significance of the Abnormal Functional Connectivity

In the groups consisting of eMCI and lMCI, the analysis showed that the altered FC between the BNM and the right hippocampus is positively correlated with EM ($r = 0.314$, $p = 0.028$). Altered FC between the BNM and the right MFG was positively correlated with EM ($r = 0.268$, $p = 0.049$). Compared with SCD subjects, BNM-FC in the right MTG of lMCI subjects was negatively correlated with IPS ($r = -0.281$, $p = 0.037$). Compared with HC, BNM-FC in bilateral SMA of SCD subjects was positively correlated with VF ($r = 0.450$, $p = 0.012$). Age, gender, and years of education were used as covariates for all these results. There was no statistically significant correlation (Bonferroni corrected, $p < 0.05$) between the cognition domains and the remaining areas (**Figure 2**).

Classification Results

To further illustrate the classification performance of altered BNM-FC and their combination, we plot their ROC curves and presented their AUC values, respectively (**Figure 3**). AUC values for BNM-FC in the MFG, SMA, and cerebellum and their combination were 0.744, 0.758, 0.767, and 0.848. AUC values for BNM-FC in the MTG were 0.835. AUC values for BNM-FC in the SFG were 0.806. AUC values for BNM-FC in the MFG and hippocampus and their combination were 0.757, 0.830, and 0.862.

DISCUSSION

In this present study, we first used a seed-based method to examine the BNM-FC for the early AD spectrum (SCD, eMCI, and lMCI) and explored the relationship between altered BNM-FC and cognitive function. The main results were summarized below: (1) abnormal BNM-FC in the frontal lobe, occipital lobe, and cerebellum was indicated in the AD disease spectrum (SCD, eMCI, and lMCI) relative to HC, and there was abnormal BNM-FC in the frontal lobe and temporal lobe between pairwise comparisons in the disease group. (2) From HC to SCD, and then to eMCI, the BNM-FC in the ECN was damaged; from SCD to eMCI, and then to lMCI, the BNM-FC in the DMN was damaged. (3) These abnormal BNM-FCs were confirmed to be associated with different cognitive domains impairment. (4) Furthermore, the ROC analyses of abnormal BNM-FC could accurately determine the classification ability of differentiating SCD from HC, SCD from eMCI, SCD from lMCI, and eMCI from lMCI. The findings supported cholinergic dysfunction as an

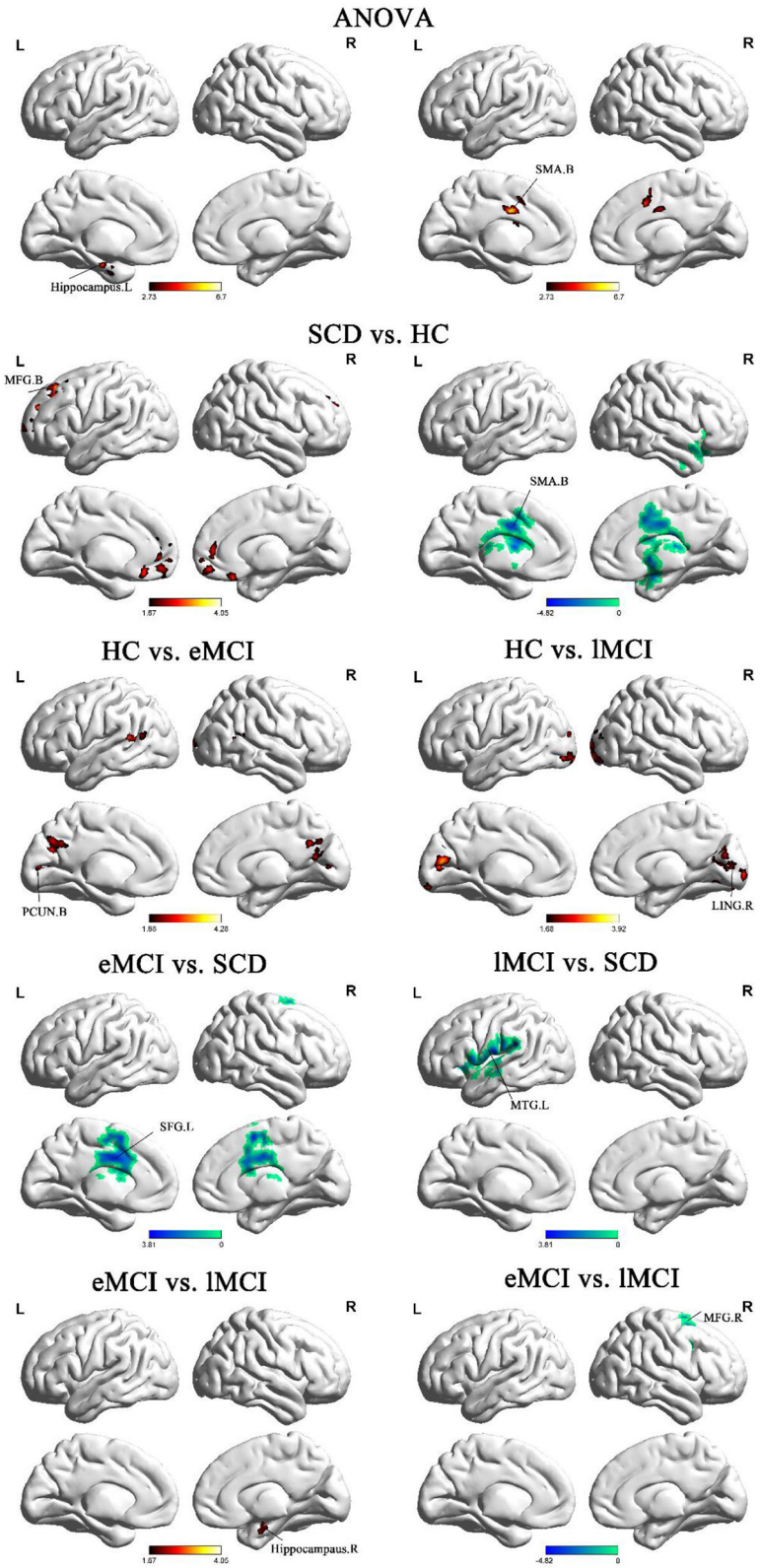

FIGURE 1 | Brain regions exhibiting significant differences in BNM-FC based on analysis of variance (ANOVA) analysis and two-sample *t*-tests. Age, gender, and years of education were used as covariates for all these results. GRF corrected, cluster size ≥50 mm^3, $p < 0.05$. eMCI, early mild cognitive impairment; lMCI, late mild cognitive impairment; SCD, subjective cognitive decline; HC, healthy controls; SMA, supplementary motor area; PCUN, precuneus; SFG, superior frontal gyrus; MFG, middle frontal gyrus; MTG, middle temporal gyrus; LING, lingual gyrus; L, left hemisphere; R, right hemisphere; B, bilateral hemisphere.

TABLE 2 | Regions of BNM-FC based on analysis of variance (ANOVA) analysis and two-sample *t*-tests.

Region	MNI			*F/t*	Cluster number
	x	*Y*	*z*		
ANOVA					
L hippocampus	−21	3	−12	6.7027	61
B cerebellum	−12	−60	−54	8.0209	140
B supplementary motor area	−9	−12	33	6.9442	195
eMCI<HC					
B precuneus	−33	−75	0	4.286	1,098
lMCI<HC					
R lingual gyrus	18	−84	3	3.9196	1,521
SCD>HC					
B supplementary motor area	−9	−12	33	−4.8206	1,032
SCD<HC					
B middle frontal gyrus	−18	33	48	3.8688	1,177
B cerebellum	−12	−54	−51	4.0489	451
eMCI>lMCI					
R hippocampus	27	−6	−24	3.6856	151
eMCI<lMCI					
R middle frontal gyrus	30	9	54	−3.3575	118
eMCI<SCD					
R superior frontal gyrus	−9	−12	36	−3.8082	638
lMCI<SCD					
L middle temporal gyrus	−66	−21	24	−4.5037	306

The x, y, z coordinates are the primary peak locations in the MNI space. Cluster size >50 mm^3 in ANOVA analysis, $p < 0.05$; cluster size >50 mm^3 in the two-sample t-test, $p < 0.05$, GRF corrected.

eMCI, early mild cognitive impairment; lMCI, late mild cognitive impairment; SCD, subjective cognitive decline; HC, healthy controls; MNI, Montreal Neurological Institute; L, left hemisphere; R, right hemisphere; B, bilateral hemisphere.

important etiological mechanism of the early disease spectrum of AD.

The Pattern of Abnormal BNM-FC in the AD Disease Spectrum Relative to HC

As a new concept in the field of dementia, SCD is a transitional stage between healthy state and MCI, with a high risk of becoming a pathological state (Hill et al., 2017). In the absence of objective clinical evidence to support cognitive impairment, SCD appears to be indistinguishable from normal aging (Rabin et al., 2017). However, some potential alterations did exist in patients with SCD in functional imaging (Eliassen et al., 2017). Compared with the HC group, the SCD group showed increased BNM-FC in bilateral SMA and decreased BNM-FC in bilateral MFG and cerebellum. The MFG region, which is a part of the dorsal lateral prefrontal cortex, is in charge of working memory and executive cognitive functions (Liu G. et al., 2020). Self-perceived abnormalities in the performance of daily life were the most common complaints, which may be associated with the damage of the MFG (Vega et al., 2016). Damage to the cerebellum has been a neglected point in the AD disease spectrum (Qi et al., 2019). Cerebro-cerebellar loops have been confirmed to have a great influence on cognition (Sierra et al., 2016). The decline of BNM-FC in these two brain regions indicated that brain function had changed in SCD patients, but the cognitive impairment was not obvious. The area under the curve of the MFG was 0.744, the area under the curve of the cerebellum was 0.767, the area under the curve of the SMA was 0.758, and the area under the curve of their combined value was 0.848. From these data, it can be known that the BNM-FCs of these three brain regions are able to distinguish between SCD and HC. As a result, more attention must be paid to the specific brain regions of SCD patients with close follow-up. As for the increase of compensatory motor area, it can be understood as a compensatory situation after the loss of executive function and cerebellar balance function.

Compared with the HC group, increased BNM-FC in bilateral PCUN was indicated in the eMCI group, and increased BNM-FC in the right LING was shown in the lMCI group. Meanwhile, differences between the two disease groups were also significant. As the precursor stage of AD, the eMCI group indicated in the results of this paper that bilateral PCUN was the first to be affected. As part of the posterior parietal cortex, PCUN is involved in episodic memory, visual space, self-related information processing, metacognition, consciousness, and other processes (Koch et al., 2018). The clinical symptoms of eMCI are mild and have a little impact on life (Edmonds et al., 2019). However, previous articles have confirmed that PCUN may gradually alter as early as about 10–20 years before the onset of cognitive impairment, which is not difficult

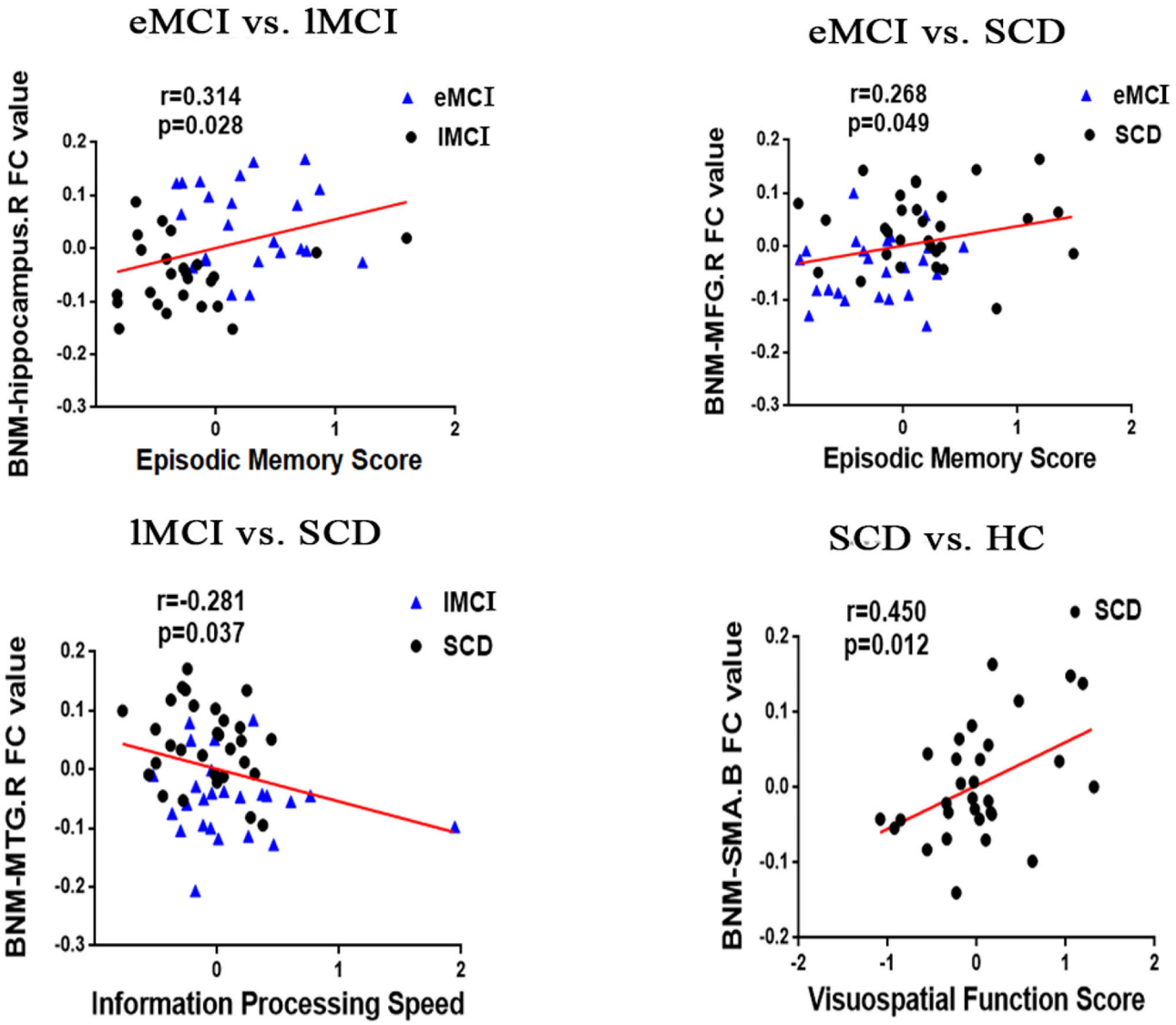

FIGURE 2 | Significant associations between altered BNM-FC and cognitive function including episodic memory, executive function, and information processing speed (Bonferroni corrected, $p < 0.05$). Age, gender, and years of education were used as covariates for all these results. eMCI, early mild cognitive impairment; lMCI, late mild cognitive impairment; SCD, subjective cognitive decline; HC, healthy controls; SMA, supplementary motor area; SFG, superior frontal gyrus; MFG, middle frontal gyrus; L, left hemisphere; R, right hemisphere; B, bilateral hemisphere.

to understand, because AD is a disease related to genes and inheritance (Bateman et al., 2012; Riedel et al., 2016). LING, which is the core of visual network, is responsible for processing visual memory and logical analysis (Lenoir and Siéroff, 2019). As we know, lMCI is the aggravating stage of eMCI. In addition to simple memory damage, visual processing damage is more prominent, which may lead to misperception and miscommunication with the outside world (Liu et al., 2017). Overall, patients with eMCI have early impairments in episodic memory and information processing, while patients with lMCI may have more severe impairments in visual processing.

The Pattern of Abnormal BNM-FC Between Pairs of Comparison Groups in the AD Disease Spectrum

Interestingly, in the process of disease transformation (from SCD to eMCI), decreased BNM-FC in the SFG was observed. According to the statistics of studies, most patients diagnosed with eMCI mainly complain of emotional and personality changes in addition to memory decline, which is consistent with the alteration of the SFG. That is to say, when the illness state is reached, a change in personality follows (Liu Y. et al., 2020). The evidence supporting our inference is also the ROC curve, with an area under the curve of 0.806, which indicates that the

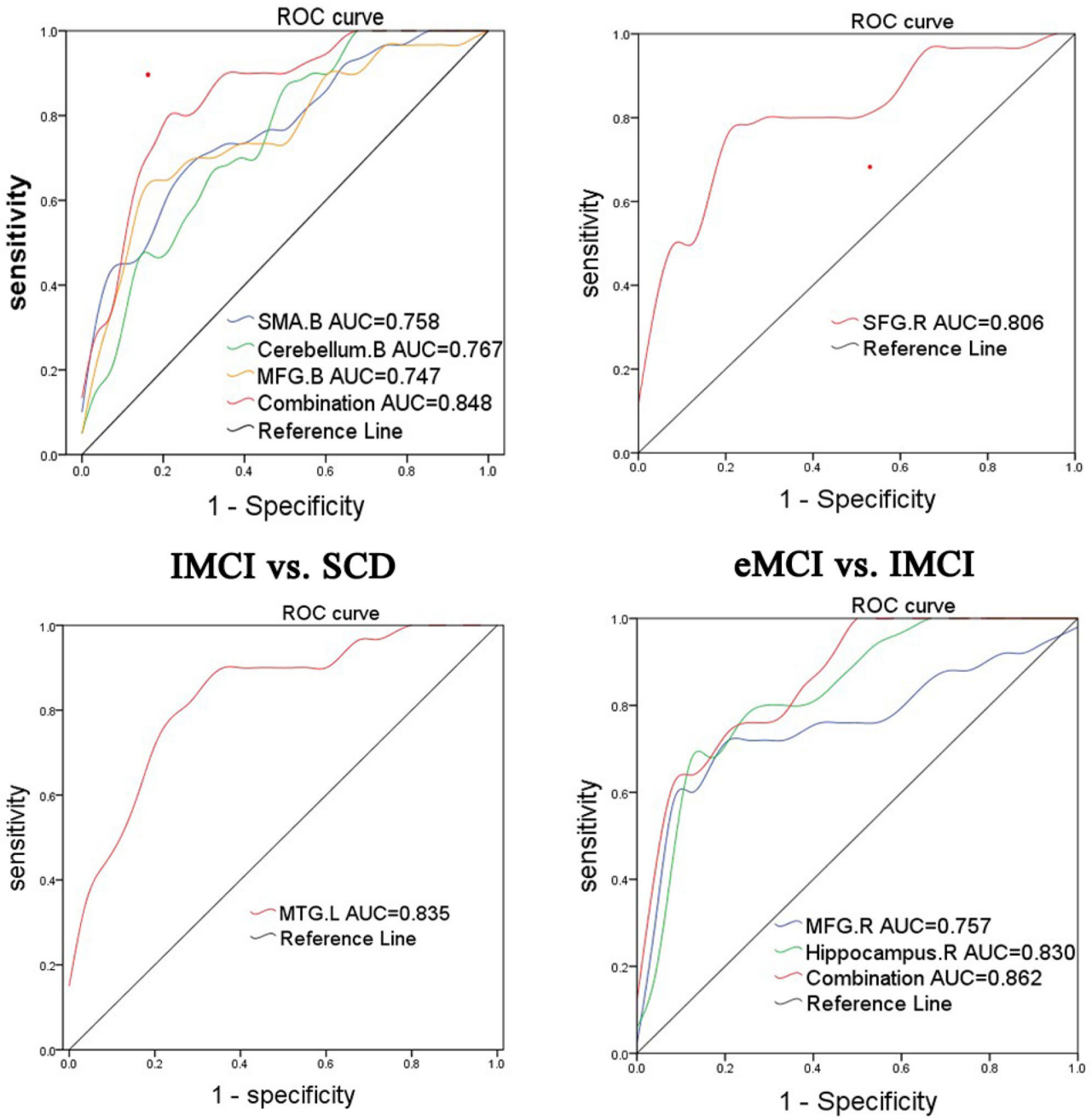

FIGURE 3 | Receiver operating characteristic (ROC) curves of different groups were identified in specific brain areas. eMCI, early mild cognitive impairment; lMCI, late mild cognitive impairment; SCD, subjective cognitive decline; HC, healthy controls; SMA, supplementary motor area; SFG, superior frontal gyrus; MFG, middle frontal gyrus; MTG, middle temporal gyrus; L, left hemisphere; R, right hemisphere; B, bilateral hemisphere.

SFG has certain accuracy in distinguishing SCD from eMCI. In addition, MTG attenuation was observed in the transition from SCD to lMCI. Notably, MTG is a brain region with complex and diverse functions in memory processing (Gao et al., 2020). The results suggested that the biggest difference between subhealth and advanced development is in memory. Memory impairment is persistent and increases with the course of the disease until it progresses to AD, an irreversible mental impairment (Gao et al., 2020). The area of the ROC curve was 0.835, showing that the MTG is reliable in distinguishing SCD from lMCI.

In terms of the differentiation of the two subtypes of aMCI, we found that with the progression of aMCI (from eMCI to lMCI), decreased BNM-FC in the hippocampus and MFG could be detected. Located in the medial temporal lobe, the hippocampus plays a role in short-term memory, long-term memory, and spatial orientation (Chen et al., 2015). LMCI is the closest prodrome to AD, and hippocampal destruction can be predicted to undoubtedly cause disturbance to daily life, with a higher probability of turning into irreversible AD (Lisman et al., 2017). Previous evidence indicated that during the transformation from eMCI to lMCI, the hippocampal volume changed significantly, which is consistent with our findings (Hong et al., 2015). There has been numerous research on the hippocampus, but the results of our paper indicated that the hippocampus is a target of attention in terms of MCI conversion and progression. The area under the curve of the MFG was 83.0%, the area under the curve of the hippocampus was 73.7%, and the area under the curve of their combined value was 86.2%. Both the functional connectivity values of individual brain regions and the comprehensive functional connectivity values show specificity and sensitivity in distinguishing between eMCI and lMCI.

Damaged Networks During Disease Progression

In the pairwise comparison, we found abnormal BNM-FC and further summarized some rules. The SCD group showed decreased BNM-FC in the MFG relative to the HC group, the eMCI group showed decreased BNM-FC in the MFG relative to the SCD group, and the lMCI group showed decreased BNM-FC in the MFG relative to the eMCI group. This result indicated that BNM-FCs in the frontal gyrus are continuously weakened during the transformation of a healthy state into eMCI. The SFG and MFG belong to the executive control network (ECN), which is involved in the regulation of cognition and behavior (Qi et al., 2010). Therefore, we can speculate that BNM-FCs in the ECN are disconnected in the qualitative change process from HCs to SCD, then to eMCI and then to lMCI.

Meanwhile, the eMCI group showed decreased BNM-FC in the hippocampus relative to the SCD group, and the lMCI group showed decreased BNM-FC in the MTG relative to the SCD group. The MTG and hippocampus pertain to DMN, which is an important index to evaluate the level of consciousness of patients (Grieder et al., 2018). In Alzheimer's disease, the DMN is the first to be compromised by amyloid deposition caused by the course of the disease (Grieder et al., 2018). In conclusion, whether the transition is from SCD to eMCI or lMCI, there is persistent temporal lobe damage and connectivity disruption between the BNM and DMN.

Correlation Between BNM-FC and Cognitive Domains

Meanwhile, our findings indicated that episodic memory is positively correlated with BNM-FC in the hippocampus and MFG. Information processing speed is negatively correlated with BNM-FC in the MTG. Visuospatial function is negatively correlated with BNM-FC in the SMA. These results suggested that the abnormal BNM-FCs we found were specific and highly correlated with cognitive domains. From this, we can speculate that these abnormal BNM-FCs can be used as specific imaging markers in the AD early spectrum and further illustrate that AD is a disconnection syndrome.

Limitation

Although the results of our article have been of great value, there are still some limitations that deserve our attention. First, differences in age and education among the four groups are inevitable. In order to avoid interference caused by these factors, we used age, sex, and education level as covariables in the statistical analysis. Overall, our results are fairly reliable. Second, this paper based on a cross-sectional design is a study of a small sample size. However, high-quality patient data rarely interfered with the paper's results. Further patient recruitment is ongoing and follow-up is being synchronized. We will make every effort to avoid possible deviations and seek more precise results.

CONCLUSION

The abnormal BNM-FC patterns can characterize the spectrum of early AD (SCD, eMCI, and lMCI) and are closely related to the cognitive domains. These new and reliable findings will provide a new perspective in identifying the early disease spectrum of AD and further strengthen the role of cholinergic theory in AD.

DATA AVAILABILITY STATEMENT

The datasets presented in this article are not readily available because none. Requests to access the datasets should be directed to 1074914057@qq.com.

ETHICS STATEMENT

The studies involving human participants were reviewed and approved by the responsible Human Participants Ethics Committee of the Affiliated Brain Hospital of Nanjing Medical University. The patients/participants provided their written informed consent to participate in this study. Written informed consent was obtained from the individual(s) for the publication of any potentially identifiable images or data included in this article.

AUTHOR CONTRIBUTIONS

All authors listed have made a substantial, direct and intellectual contribution to the work, and approved it for publication.

FUNDING

This study was supported by the National Natural Science Foundation of China (No. 81701675); the Key Project supported by the Medical Science and Technology Development Foundation, Nanjing Department of Health (No. JQX18005); the Cooperative Research Project of Southeast University-Nanjing

Medical University (No. 2018DN0031); the Key Research and Development Plan (Social Development) Project of Jiangsu Province (No. BE2018608); and the Innovation and Entrepreneurship Training Program for College Students in Jiangsu Province (Nos. 201810312061X and 201910312035Z).

SUPPLEMENTARY MATERIAL

The Supplementary Material for this article can be found online at: https://www.frontiersin.org/articles/10.3389/fnagi.2021.671351/full#supplementary-material

REFERENCES

Barage, S. H., and Sonawane, K. D. (2015). Amyloid cascade hypothesis: pathogenesis and therapeutic strategies in Alzheimer's disease. *Neuropeptides* 52, 1–18. doi: 10.1016/j.npep.2015.06.008

Bateman, R. J., Xiong, C., Benzinger, T. L., Fagan, A. M., Goate, A., Fox, N. C., et al. (2012). Clinical and biomarker changes in dominantly inherited Alzheimer's disease. *N. Engl. J. Med.* 367, 795–804. doi: 10.1056/NEJMoa1202753

Bell, C. S., Mohd Khairi, N., Ding, Z., and Wilkes, D. M. (2019). Bayesian framework for robust seed-based correlation analysis. *Med. Phys.* 46, 3055–3066. doi: 10.1002/mp.13522

Chen, H., Iinuma, M., Onozuka, M., and Kubo, K. Y. (2015). Chewing maintains hippocampus-dependent cognitive function. *Int. J. Med. Sci.* 12, 502–509. doi: 10.7150/ijms.11911

Chen, J., Chen, G., Shu, H., Chen, G., Ward, B., Wang, Z., et al. (2019). Predicting progression from mild cognitive impairment to Alzheimer's disease on an individual subject basis by applying the CARE index across different independent cohorts. *Aging* 11, 2185–2201. doi: 10.18632/aging.101883

Chen, J., Yan, Y., Gu, L., Gao, L., and Zhang, Z. J. B. t. (2020). Electrophysiological processes on motor imagery mediate the association between increased gray matter volume and cognition in amnestic mild cognitive impairment. *Brain Topogr.* 33, 255–266. doi: 10.1007/s10548-019-00742-8

Chen, S., Xu, W., Xue, C., Hu, G., Ma, W., Qi, W., et al. (2020). Voxelwise meta-analysis of gray matter abnormalities in mild cognitive impairment and subjective cognitive decline using activation likelihood estimation. *J. Alzheimers Dis.* 77, 1495–1512. doi: 10.3233/JAD-200659

Chen, Y. G. (2018). Research progress in the pathogenesis of Alzheimer's disease. *Chin. Med. J.* 131, 1618–1624. doi: 10.4103/0366-6999.235112

Csukly, G., Sirály, E., Fodor, Z., Horváth, A., Salacz, P., Hidasi, Z., et al. (2016). The differentiation of amnestic type MCI from the non-amnestic types by structural MRI. *Front. Aging Neurosci.* 8:52. doi: 10.3389/fnagi.2016.00052

Dubois, B., Hampel, H., Feldman, H. H., Scheltens, P., Aisen, P., Andrieu, S., et al. (2016). Preclinical Alzheimer's disease: definition, natural history, and diagnostic criteria. *Alzheimers Dement.* 12, 292–323. doi: 10.1016/j.jalz.2016.02.002

Edmonds, E. C., McDonald, C. R., Marshall, A., Thomas, K. R., Eppig, J., Weigand, A. J., et al. (2019). Early versus late MCI: Improved MCI staging using a neuropsychological approach. *Alzheimers Dement.* 15, 699–708. doi: 10.1016/j.jalz.2018.12.009

Eliassen, C. F., Reinvang, I., Selnes, P., Grambaite, R., Fladby, T., and Hessen, E. (2017). Biomarkers in subtypes of mild cognitive impairment and subjective cognitive decline. *Brain Behav.* 7:e00776. doi: 10.1002/brb3.776

Fotiou, D., Kaltsatou, A., Tsiptsios, D., and Nakou, M. (2015). Evaluation of the cholinergic hypothesis in Alzheimer's disease with neuropsychological methods. *Aging Clin. Exp. Res.* 27, 727–733. doi: 10.1007/s40520-015-0321-8

Gao, L., Chen, J., Gu, L., Shu, H., Wang, Z., Liu, D., et al. (2018). Effects of gender and apolipoprotein E on novelty MMN and P3a in healthy elderly and amnestic mild cognitive impairment. *Front. Aging Neurosci.* 10:256. doi: 10.3389/fnagi.2018.00256

Gao, L., Gu, L., Shu, H., Chen, J., Zhu, J., Wang, B., et al. (2020). The reduced left hippocampal volume related to the delayed P300 latency in amnestic mild cognitive impairment. *Psychol. Med.* 2020, 1–9. doi: 10.1017/S0033291720000811

Gratwicke, J., Oswal, A., Akram, H., Jahanshahi, M., Hariz, M., Zrinzo, L., et al. (2020). Resting state activity and connectivity of the nucleus basalis of Meynert and globus pallidus in Lewy body dementia and Parkinson's disease dementia. *Neuroimage* 221:117184. doi: 10.1016/j.neuroimage.2020.117184

Grieder, M., Wang, D. J. J., Dierks, T., Wahlund, L. O., and Jann, K. (2018). Default mode network complexity and cognitive decline in mild Alzheimer's disease. *Front. Neurosci.* 12:770. doi: 10.3389/fnins.2018.00770

Grothe, M., Heinsen, H., and Teipel, S. (2013). Longitudinal measures of cholinergic forebrain atrophy in the transition from healthy aging to Alzheimer's disease. *Neurobiol. Aging* 34, 1210–1220. doi: 10.1016/j.neurobiolaging.2012.10.018

Grothe, M., Heinsen, H., and Teipel, S. J. (2012). Atrophy of the cholinergic Basal forebrain over the adult age range and in early stages of Alzheimer's disease. *Biol. Psychiatry* 71, 805–813. doi: 10.1016/j.biopsych.2011.06.019

Gu, L. H., Chen, J., Gao, L. J., Shu, H., Wang, Z., Liu, D., et al. (2017). The effect of apolipoprotein E ε4 (APOE ε4) on visuospatial working memory in healthy elderly and amnestic mild cognitive impairment patients: an event-related potentials study. *Front. Aging Neurosci.* 9:145. doi: 10.3389/fnagi.2017.00145

Hampel, H., Mesulam, M. M., Cuello, A. C., Khachaturian, A. S., Vergallo, A., Farlow, M. R., et al. (2019). Revisiting the cholinergic hypothesis in Alzheimer's disease: emerging evidence from translational and clinical research. *J. Prev. Alzheimers Dis.* 6, 2–15. doi: 10.14283/jpad.2018.43

Hill, N. L., McDermott, C., Mogle, J., Munoz, E., DePasquale, N., Wion, R., et al. (2017). Subjective cognitive impairment and quality of life: a systematic review. *Int. Psychogeriatr.* 29, 1965–1977. doi: 10.1017/S1041610217001636

Hong, Y. J., Yoon, B., Shim, Y. S., Ahn, K. J., Yang, D. W., and Lee, J. H. (2015). Gray and white matter degenerations in subjective memory impairment: comparisons with normal controls and mild cognitive impairment. *J. Korean Med. Sci.* 30, 1652–1658. doi: 10.3346/jkms.2015.30.11.1652

Joel, S. E., Caffo, B. S., van Zijl, P. C., and Pekar, J. J. (2011). On the relationship between seed-based and ICA-based measures of functional connectivity. *Magn. Reson. Med.* 66, 644–657. doi: 10.1002/mrm.22818

Koch, G., Bonnì, S., Pellicciari, M. C., Casula, E. P., Mancini, M., Esposito, R., et al. (2018). Transcranial magnetic stimulation of the precuneus enhances memory and neural activity in prodromal Alzheimer's disease. *Neuroimage* 169, 302–311. doi: 10.1016/j.neuroimage.2017.12.048

Lautenschlager, N. T., Cox, K. L., and Ellis, K. A. (2019). Physical activity for cognitive health: what advice can we give to older adults with subjective cognitive decline and mild cognitive impairment? *Dialog. Clin. Neurosci.* 21, 61–68. doi: 10.31887/DCNS.2019.21.1/nilautenschlager

Lenoir, H., and Siéroff, É. (2019). Visual perceptual disorders in Alzheimer's disease. *Geriatr. Psychol. Neuropsychiatr. Vieil.* 17, 307–316. doi: 10.1684/pnv.2019.0815

Li, C. S., Ide, J. S., Zhang, S., Hu, S., Chao, H. H., and Zaborszky, L. (2014). Resting state functional connectivity of the basal nucleus of Meynert in humans: in comparison to the ventral striatum and the effects of age. *Neuroimage* 97, 321–332. doi: 10.1016/j.neuroimage.2014.04.019

Li, H., Jia, X., Qi, Z., Fan, X., Ma, T., Ni, H., et al. (2017). Altered functional connectivity of the basal nucleus of Meynert in mild cognitive impairment: a resting-state fMRI study. *Front. Aging Neurosci.* 9:127. doi: 10.3389/fnagi.2017.00127

Lisman, J., Buzsáki, G., Eichenbaum, H., Nadel, L., Ranganath, C., and Redish, A. D. (2017). Viewpoints: how the hippocampus contributes to memory, navigation and cognition. *Nat. Neurosci.* 20, 1434–1447. doi: 10.1038/nn.4661

Liu, A. K., Chang, R. C., Pearce, R. K., and Gentleman, S. M. (2015). Nucleus basalis of Meynert revisited: anatomy, history and differential involvement in Alzheimer's and Parkinson's disease. *Acta Neuropathol.* 129, 527–540. doi: 10.1007/s00401-015-1392-5

Liu, G., Jiao, K., Zhong, Y., Hao, Z., Wang, C., Xu, H., et al. (2020). The alteration of cognitive function networks in remitted patients with major depressive disorder: an independent component analysis. *Behav. Brain Res.* 400:113018. doi: 10.1016/j.bbr.2020.113018

Liu, X., Chen, W., Hou, H., Chen, X., Zhang, J., Liu, J., et al. (2017). Decreased functional connectivity between the dorsal anterior cingulate cortex and lingual gyrus in Alzheimer's disease patients with depression. *Behav. Brain Res.* 326, 132–138. doi: 10.1016/j.bbr.2017.01.037

Liu, Y., Hu, G., Yu, Y., Jiang, Z., Yang, K., Hu, X., et al. (2020). Structural and functional reorganization within cognitive control network associated with protection of executive function in patients with unilateral frontal gliomas. *Front. Oncol.* 10:794. doi: 10.3389/fonc.2020.00794

Pei, S., Guan, J., and Zhou, S. (2018). Classifying early and late mild cognitive impairment stages of Alzheimer's disease by fusing default mode networks extracted with multiple seeds. *BMC Bioinform.* 19:523. doi: 10.1186/s12859-018-2528-0

Qi, Z., An, Y., Zhang, M., Li, H. J., and Lu, J. (2019). Altered cerebro-cerebellar limbic network in AD spectrum: a resting-state fMRI study. *Front. Neural Circ.* 13:72. doi: 10.3389/fncir.2019.00072

Qi, Z., Wu, X., Wang, Z., Zhang, N., Dong, H., Yao, L., et al. (2010). Impairment and compensation coexist in amnestic MCI default mode network. *Neuroimage.* 50, 48–55. doi: 10.1016/j.neuroimage.2009.12.025

Rabin, L. A., Smart, C. M., and Amariglio, R. E. (2017). Subjective cognitive decline in preclinical Alzheimer's disease. *Annu. Rev. Clin. Psychol.* 13, 369–396. doi: 10.1146/annurev-clinpsy-032816-045136

Riedel, B. C., Thompson, P. M., and Brinton, R. D. (2016). Age, APOE and sex: triad of risk of Alzheimer's disease. *J. Steroid. Biochem. Mol. Biol.* 160, 134–147. doi: 10.1016/j.jsbmb.2016.03.012

Scheef, L., Grothe, M. J., Koppara, A., Daamen, M., Boecker, H., Biersack, H., et al. (2019). Subregional volume reduction of the cholinergic forebrain in subjective cognitive decline (SCD). *Neuroimage Clin.* 21:101612. doi: 10.1016/j.nicl.2018.101612

Sierra, M., Gelpi, E., Martí, M. J., and Compta, Y. (2016). Lewy- and Alzheimer-type pathologies in midbrain and cerebellum across the Lewy body disorders spectrum. *Neuropathol. Appl. Neurobiol.* 42, 451–462. doi: 10.1111/nan.12308

Tan, C. C., Yu, J. T., and Tan, L. (2014). Biomarkers for preclinical Alzheimer's disease. *J. Alzheimers Dis.* 42, 1051–1069. doi: 10.3233/JAD-140843

Vega, J. N., Zurkovsky, L., Albert, K., Melo, A., Boyd, B., Dumas, J., et al. (2016). Altered brain connectivity in early postmenopausal women with subjective cognitive impairment. *Front. Neurosci.* 10:433. doi: 10.3389/fnins.2016.00433

Xu, W., Chen, S., Xue, C., Hu, G., Ma, W., Qi, W., et al. (2020). Functional MRI-specific alterations in executive control network in mild cognitive impairment: an ALE meta-analysis. *Front. Aging Neurosci.* 12:578863. doi: 10.3389/fnagi.2020.578863

Xue, C., Sun, H., Hu, G., Qi, W., Yue, Y., Rao, J., et al. (2020). Disrupted patterns of rich-club and diverse-club organizations in subjective cognitive decline and amnestic mild cognitive impairment. *Front. Neurosci.* 14:575652. doi: 10.3389/fnins.2020.575652

Conflict of Interest: The authors declare that the research was conducted in the absence of any commercial or financial relationships that could be construed as a potential conflict of interest.

The reviewer Y-CC declared a shared affiliation, with no collaboration, with the authors to the handling editor at the time of the review.

frontiers in Aging Neuroscience

ORIGINAL RESEARCH
published: 01 July 2021
doi: 10.3389/fnagi.2021.696735

Distinctive Association of the Functional Connectivity of the Posterior Cingulate Cortex on Memory Performances in Early and Late Amnestic Mild Cognitive Impairment Patients

*Dong Woo Kang[1], Sheng-Min Wang[2], Yoo Hyun Um[3], Hae-Ran Na[2], Nak-Young Kim[4], Chang Uk Lee[1] and Hyun Kook Lim[2]**

[1] Department of Psychiatry, Seoul St. Mary's Hospital, College of Medicine, The Catholic University of Korea, Seoul, South Korea, [2] Department of Psychiatry, Yeouido St. Mary's Hospital, College of Medicine, The Catholic University of Korea, Seoul, South Korea, [3] Department of Psychiatry, St. Vincent's Hospital, College of Medicine, The Catholic University of Korea, Suwon, South Korea, [4] Department of Psychiatry, Keyo Hospital, Uiwang, South Korea

OPEN ACCESS

Edited by:
Stephen D. Ginsberg,
Nathan Kline Institute for Psychiatric Research, United States

Reviewed by:
Muthuswamy Anusuyadevi,
Bharathidasan University, India
Kyu-Man Han,
Korea University, South Korea

***Correspondence:**
Hyun Kook Lim
drblues@catholic.ac.kr

Received: 17 April 2021
Accepted: 31 May 2021
Published: 01 July 2021

Citation:
Kang DW, Wang S-M, Um YH, Na H-R, Kim N-Y, Lee CU and Lim HK (2021) Distinctive Association of the Functional Connectivity of the Posterior Cingulate Cortex on Memory Performances in Early and Late Amnestic Mild Cognitive Impairment Patients. Front. Aging Neurosci. 13:696735. doi: 10.3389/fnagi.2021.696735

Background: Attempts have been made to explore the biological basis of neurodegeneration in the amnestic mild cognitive impairment (MCI) stage, subdivided by memory performance. However, few studies have evaluated the differential impact of functional connectivity (FC) on memory performances in early- and late-MCI patients.

Objective: This study aims to explore the difference in FC of the posterior cingulate cortex (PCC) among healthy controls (HC) (n = 37), early-MCI patients (n = 30), and late-MCI patients (n = 35) and to evaluate a group-memory performance interaction against the FC of PCC.

Methods: The subjects underwent resting-state functional MRI scanning and a battery of neuropsychological tests.

Results: A significant difference among the three groups was found in FC between the PCC (seed region) and bilateral crus cerebellum, right superior medial frontal gyrus, superior temporal gyrus, and left middle cingulate gyrus (Monte Carlo simulation-corrected $p < 0.01$; cluster $p < 0.05$). Additionally, the early-MCI patients displayed higher FC values than the HC and late-MCI patients in the right superior medial frontal gyrus, cerebellum crus 1, and left cerebellum crus 2 (Bonferroni-corrected $p < 0.05$). Furthermore, there was a significant group-memory performance interaction (HC *vs*. early MCI *vs*. late MCI) for the FC between PCC and bilateral crus cerebellum, right superior medial frontal gyrus, superior temporal gyrus, and left middle cingulate gyrus (Bonferroni-corrected $p < 0.05$).

Conclusion: These findings contribute to the biological implications of early- and late-MCI stages, categorized by evaluating the impairment of memory performance. Additionally, comprehensively analyzing the structural differences in the subdivided amnestic MCI (aMCI) stages could deepen our understanding of these biological meanings.

Keywords: functional connectivity, early mild cognitive impairment, late mild cognitive impairment, posterior cingulate cortex, memory performance

INTRODUCTION

Mild cognitive impairment (MCI) is considered a prodromal stage of Alzheimer's disease (AD), with subjective and objective cognitive decline but preserved ability to perform independent daily activities (Petersen and Negash, 2008). In particular, amnestic MCI (aMCI) patients, whose main symptom is a decrease in memory function among cognitive function items, are reported to progress to dementia at a rate of 10–15% every year (Gauthier et al., 2006). Recently, the aMCI stage has been subdivided into early and late MCI based on the degree of delayed memory recall impairment (Jessen et al., 2014). It is estimated that early MCI reflects an earlier stage of AD progression, and late MCI is reported to have a higher risk for AD progression than early MCI (Jessen et al., 2014). Furthermore, attempts have been made to explore the biological basis of neurodegeneration in the aMCI stage, subdivided based on memory performance. In our previous study, cortical atrophy in healthy controls (HC), early-MCI patients, and late-MCI patients was compared by whole-brain analysis (Kang et al., 2019). We found that early-MCI patients show a significant atrophy in the right middle temporal gyrus compared with that in HC, and late-MCI patients showed a greater atrophy in the left fusiform gyrus than did early-MCI patients. Additionally, it has been established that the association between brain volume and memory decline in these regions is significantly different depending on MCI subdivided stage (Kang et al., 2019). With regard to resting-state brain functional connectivity (FC), a representative biomarker for AD progression (Liu et al., 2008), the mean FC value of the default-mode network (DMN) has shown a significant difference among HC, early-MCI patients, and late-MCI patients (Lee et al., 2016). However, it was difficult to identify patterns showing differences between the three groups by only confirming the regions showing differences in mean DMN FC between two of the three groups. Moreover, since the interaction between group and cognitive function was not analyzed, the differential relationship between FC and cognitive function was not evaluated as the prodromal stage progressed (Lee et al., 2016). Finally, because FC was evaluated only within the DMN, it was impossible to evaluate FC between other brain regions. A previous study that performed seed-based FC analysis using the thalamus as a seed region has indicated that FC between regions such as the bilateral superior temporal gyrus, right fusiform gyrus, and thalamus decreased in early and late MCI compared to that in HC (Cai et al., 2015). However, FC between the left FG, bilateral precuneus, and thalamus was increased. The thalamus-seeded FC difference was confirmed between early and late MCI. However, no significant association was found between FC and cognitive function (Cai et al., 2015). This study did not also evaluate whether this relationship varies with the progression of AD stage.

The posterior cingulate cortex (PCC) is a hub region of the DMN, showing the highest metabolic rates in healthy older adults compared to other brain regions (Raichle and Snyder, 2007), and is vulnerable to amyloid-beta deposition induced by an increased neuronal activity of this brain region in the early phases of AD (Zott et al., 2019). Prior research has demonstrated that intra-regional FC and inter-regional FC of PCC reflect AD progression (Liu et al., 2008). In addition, another previous study has found decreased FC of PCC with the temporal cortex but increased FC with the frontal cortex in aMCI patients compared to cognitively intact healthy older adults (Bai et al., 2009). Moreover, FC between PCC and the middle temporal gyrus shows a significant correlation with working memory and executive function in aMCI patients (Bai et al., 2009). Despite the clinical implications of PCC in prodromal AD, there has been little discussion about the functional brain changes in early- and late-aMCI stages. Furthermore, there has also been no study to examine the variation in correlation between memory performance and FC in the aMCI stage according to subdivided aMCI stage. Through an investigation of these unexplored issues, we hope to gain a deeper understanding of how changes in brain function in early- and late-MCI stages interact with cognitive decline.

In this study, we aimed to compare the FC from the PCC between cognitively healthy older adults, early-aMCI patients, and late-aMCI patients by whole-brain analysis. In addition, this paper assesses whether the association between the FC of PCC with regions of interest (ROIs) and memory performance differs according to the subdivided aMCI stage of early and late aMCI.

MATERIALS AND METHODS

Participants

One hundred two subjects were included in this study [37 subjects in the healthy control group (age range: 72–78 years), 30 subjects with early MCI (age range: 71–82 years), and 35 subjects with late MCI (age range: 69–82 years)]. The subjects were recruited from the Catholic Geriatric Brain MRI database, which was built through the outpatient psycho-geriatric clinic of Seoul Saint Mary's Hospital located in Seoul, South Korea, from October 2016 to July 2018. The cognitive functions of all subjects were assessed with the Korean version of the Consortium to Establish a Registry for AD (CERAD-K) (Lee et al., 2002). The measures

included assessment in verbal fluency (VF), the 15-item Boston Naming Test (BNT), the Korean version of the Mini-Mental State Examination (MMSE-K) (Park, 1989), word list memory (WLM), word list recall (WLR), word list recognition (WLRc), constructional praxis (CP), and constructional recall (CR). In addition, total memory (TM) domain scores were obtained by summing the scores from the CERAD-K, WLM, WLR, and WLRc. Patients with MCI met Peterson's criteria of (1) memory complaint corroborated by an informant, (2) objective memory impairment for age, level of education, and sex, (3) essentially preserved general cognitive function, (4) mostly intact functional activities, and (5) no dementia. All MCI patients had an overall clinical dementia rating of 0.5 (Morris, 1993). The classifications of late MCI and early MCI were as follows: subjects classified with late MCI reported memory impairment, demonstrated by memory performance scores greater than 1.5 standard deviations (SDs) below the respective age-, education-, and sex-specific normative mean on the CERAD-K WLR; on the other hand, subjects classified with early MCI had performance scores between 1.5 and 1.0 SDs below the normative mean. Concise descriptions of the tests and the review process are described in the **Supplementary Material**. We excluded participants with any history of alcoholism, drug abuse, head trauma, or psychiatric disorders; those with multiple vascular risk factors, extensive cerebrovascular disease, or taking any psychotropic medications (e.g., cholinesterase inhibitors, antidepressants, benzodiazepines, and antipsychotics) were excluded. The inclusion criteria for elderly HCs were as follows: (1) older than 60 years of age, (2) within 1.0 SD for the CERAD-K WLR and within 1.5 SDs on the other domains of the CERAD-K, and (3) a clinical dementia rating score of 0. The study was conducted under the ethical and safety guidelines set forth by the Institutional Review Board of The Catholic University of Korea, which approved all study procedures. Informed and written consent was obtained from all participants.

MRI Acquisition

Imaging data were collected in the Department of Radiology of Seoul Saint Mary's Hospital at The Catholic University of Korea using a 3T Siemens Verio machine and an eight-channel Siemens head coil (Siemens Medical Solutions, Erlangen, Germany). The parameters used for T1-weighted volumetric magnetization-prepared rapid gradient-echo scan sequences were echo time = 2.5 ms, repetition time = 1,900 ms, inversion time = 900 ms, field of view = 250 mm, matrix = 256 × 256, and voxel size = 1.0 × 1.0 × 1.0 mm^3. The resting-state functional images were collected using a T2-weighted gradient-echo sequence with the following parameters: TR = 2,490 ms, TE = 30 ms, matrix = 128 × 128 × 29, and voxel size = 2 × 2 × 3 mm^3. One hundred fifty volumes were acquired over 5 min with the instruction: "Keep your eyes closed and think of nothing in particular."

Image Preprocessing

We used the Data Processing Assistant for Resting-State fMRI (DPARSF) (Chao-Gan and Yu-Feng, 2010), which is based on Statistical Parametric Mapping (SPM[1]), to preprocess the fMRI images. Slice timing and realignment for motion corrections were performed on the images. Subjects with excessive head motion (cumulative translation or rotation > 2 mm or 2°) were excluded. To prevent group-related differences caused by microscopic head motion, we compared framewise displacement (FD) between groups. The mean FD scores did not differ between groups ($p > 0.05$, two-sample t-test), and they were further used as covariates for group comparisons. For spatial registration, the T1-weighted image was co-registered to the mean resting-state functional MRI based on rigid body transformation. For spatial normalization, the International Consortium for Brain Mapping template was applied (resampling voxel size = 3 × 3 × 3 mm^3) and fitted to the "East Asian brain." After this, functional images were spatially smoothed with a 6-mm full-width at half-maximum Gaussian kernel.

We further processed our functional data so they fit the FC analysis with the DPARSF. Linear trends were removed from the functional images, and data were filtered with a temporal band-pass of 0.01–0.08 Hz. This filtering reduces low-frequency drift as well as physiological high-frequency respiratory and cardiac noise (Biswal et al., 1995).

[1]http://www.fil.ion.ucl.ac.uk/spm

TABLE 1 | Demographic and clinical characteristics of the study participants.

	Control group (n = 37)	Early-mild cognitive impairment (MCI) group (n = 30)	Late MCI group (n = 35)	P-value
Age (years)	73.9 ± 2.0 (72–78)	76.9 ± 4.3 (71–82)	77.3 ± 4.1 (69–82)	<0.001
Sex (M/F,%)	40.5: 59.5	53.3: 46.7	45.7: 54.3	0.579
Education (years)	10.8 ± 4.0 (4–16)	9.0 ± 4.8 (2–20)	9.6 ± 4.3 (2–16)	0.259
APOE ε4 carrier (n,%)	8 (21.6%)	13 (43.3%)	14 (40.0%)	0.121
MMSE-K	27.1 ± 1.7 (24–30)	21.7 ± 4.3 (14–30)	21.7 ± 4.5 (11–29)	<0.001
CERAD-K WLM	17.8 ± 3.3 (12–25)	12.8 ± 4.4 (6–20)	10.6 ± 4.1 (3–19)	<0.001
CERAD-K WLR	6.0 ± 1.7 (4–9)	2.5 ± 0.8 (2–5)	0.9 ± 1.0 (0–3)	<0.001
CERAD-K WLRc	9.2 ± 0.8 (8–10)	6.6 ± 2.2 (3–10)	5.2 ± 2.6 (0–10)	<0.001
CERAD-K TM	33.0 ± 5.0 (25–47)	21.9 ± 6.0 (12–32)	16.7 ± 5.7 (6–29)	<0.001

The data are presented as mean ± SD (minimum–maximum) unless indicated otherwise. MMSE-K, Korean version of the Mini-Mental Status Examination; CERAD-K, Korean version of the Consortium to Establish a Registry for Alzheimer's disease; WLM, word list memory; WLR, word list recall; WLRc, word list recognition; TM, total scores of memory domains, including CERAD-K WLM, WLR, and WLRc.

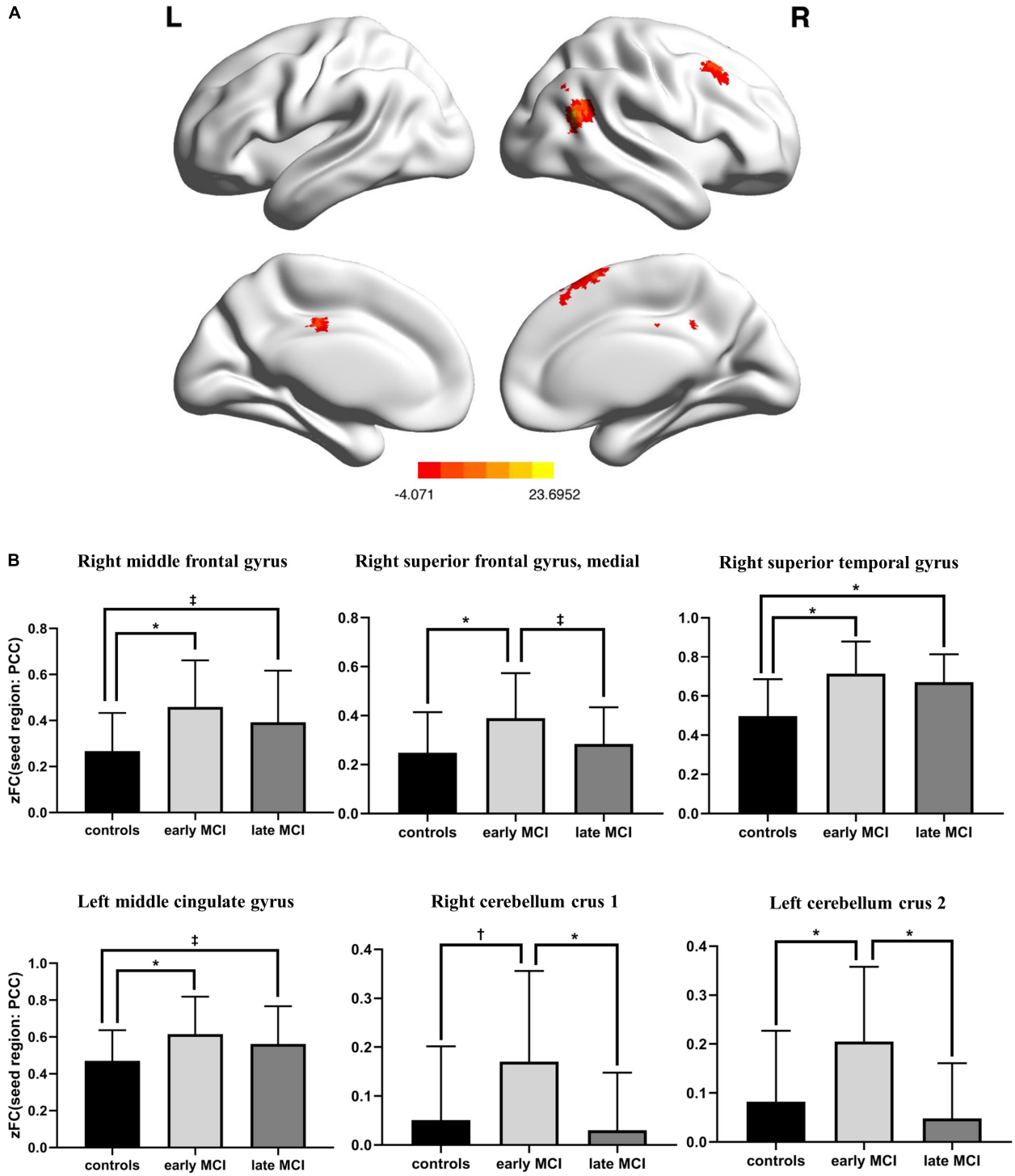

FIGURE 1 | (A) Brain regions where the functional connectivity of the posterior cingulate cortex showed significant differences among control subjects, early-mild cognitive impairment (MCI) patients, and late-MCI patients (ANCOVA, Monte Carlo simulation-corrected $p < 0.01$). **(B)** Difference in functional connectivity from the posterior cingulate cortex among control subjects, early-MCI patients, and late-MCI patients (Bonferroni *post hoc* tests). *Bonferroni-corrected $P < 0.001$; †Bonferroni-corrected $P < 0.01$; ‡Bonferroni-corrected $P < 0.05$.

Functional Connectivity Analyses

Seed-based FC analysis was used to construct resting-state networks. A spherical ROI (radius = 6 mm) was centered at the given coordinates within the PCC as a seed region [(MNI) space: 0, −51, and 29] (Greicius et al., 2003; Sestieri et al., 2011). For each subject, the mean time series of each seed region was computed as the reference time course for each network. Pearson cross-correlation analysis was performed between the seed time course and the time course of the whole-brain voxels. A Fisher's z-transformation was applied to improve the normality of the correlation coefficients (Wang et al., 2006). Finally, the individual maps of each network were obtained.

Statistical Analysis

Statistical analyses for demographic data were performed with R software (version 2.15.3). Normality assumptions were tested for all continuous variables using the Kolmogorov–Smirnov test. All variables were normally distributed. One-way ANOVA and chi-square (χ^2) test were used to assess potential differences between the HC, early-MCI, and late-MCI groups for all demographic variables. All statistical analyses used a two-tailed level of 0.05 for defining statistical significance. We conducted a whole-brain voxel-wise analysis of between-group differences in FC with a general linear model using SPM8, controlling for age, sex, education years, apolipoprotein E (*APOE*) genotype, and voxel-wise gray matter (GM) volume (Oakes et al., 2007). The process of obtaining GM intensity maps in the MNI space is described in the **Supplementary Material**. Multiple corrections were performed using cluster-extent correction (AlphaSim) as implemented by Data Processing and Analysis for Brain Imaging, and the following parameters were set: $p < 0.01$ for statistical significance in individual voxel threshold comparison, 1,000 Monte Carlo simulations, and $p < 0.01$ as the effective threshold for cluster-extent correction. Subsequently, the identified brain regions showing significant differences in FC compared to that of the seed region or between groups were extracted as ROIs. In *post hoc* procedures, Z-transformed FC (zFC) values between seed regions and ROIs were used to compare region-specific differences in FC between groups (HC *vs*. early MCI, HC *vs*. late MCI, and early MCI *vs*. late MCI), with Bonferroni multiple testing correction.

To assess the main effect of the interaction between group and cognitive performance on zFC values between the PCC and ROIs, we used multiple regression analyses after adjusting for age, sex, education years, and *APOE* genotype. We applied a threshold of $\alpha = 0.05$ to consider regression weights significant, and we additionally accounted for multiple testing using the Bonferroni correction for each hypothesis.

RESULTS

Baseline Demographic and Clinical Data

Table 1 shows the baseline demographic data for the different subject groups. There were no significant differences in sex, years of education, and *APOE* ε4 genotype between the control, early-MCI, and late-MCI groups. However, there was a significant difference in age across groups ($p < 0.001$). As expected based on the inclusion criteria, the groups differed in memory performance test scores (MMSE-K, CERAD-K WLM, WLR, WLRc, and TM) ($p < 0.001$). Concerning non-amnestic cognitive functions, there were significant differences in CERAD-K VF, BNT, CR ($p < 0.001$), and CP scores across groups ($p = 0.024$) (see **Supplementary Table 1**).

Group Differences in Functional Connectivity: Whole-Brain Voxel-Based Analysis

There was a significant difference in the zFC of PCC with right middle frontal gyrus, superior medial frontal gyrus, superior temporal gyrus, left middle cingulate gyrus, right cerebellum crus 1, and left cerebellum crus 2 among HC, early-MCI patients, and late-MCI patients (**Figure 1A** and **Table 2**). Additionally, in the right middle frontal gyrus, superior temporal gyrus, and left middle cingulate gyrus, early- and late-MCI groups showed significantly higher zFC values than the HC (Bonferroni-corrected $p < 0.05$), but there was no significant difference between early- and late-MCI patients (**Figure 1B**). In the right superior medial frontal gyrus, cerebellum crus 1, and left cerebellum crus 2, the early-MCI patients displayed higher zFC values than the HC and late-MCI patients (Bonferroni-corrected $p < 0.05$, **Figure 1B**).

Interaction of Memory Performances and Functional Connectivity Between PCC and ROIs

With regard to the CERAD-K WLM, we found a significant group interaction for zFC scores of PCC with the right superior

TABLE 2 | Anatomical locations of regions showing significant differences in functional connectivity from the posterior cingulate cortex among control subjects, early-mild cognitive impairment (MCI) patients, and late-MCI patients.

Region	L/R	Cluster (voxel count)	Peak *F* value	Peak MNI coordinates (*x*, *y*, *z*)		
Middle frontal gyrus	R	60	11.0123	39	18	42
Superior frontal gyrus, medial	R	53	10.2437	9	30	51
Superior temporal gyrus	R	189	23.6952	45	−57	21
Middle cingulate gyrus	L	95	10.4025	−3	−21	36
Cerebellum crus 1	R	83	9.8205	21	−66	−33
Cerebellum crus 2	L	300	11.2579	0	−81	−33

FC, functional connectivity; PCC, posterior cingulate cortex; L, left; R, right.

temporal gyrus, right cerebellum crus 1, and left cerebellum crus 2. When we applied the Bonferroni correction, the results remained significant only for the zFC values of PCC with the left cerebellum crus 2. Concerning the CERAD-K WLR, there was a significant group interaction for the zFC scores of PCC with the right superior medial frontal gyrus, superior temporal gyrus, left middle cingulate gyrus, right cerebellum crus 1, and left cerebellum crus 2. With Bonferroni multiple testing correction, the results remained significant for the zFC values with the right superior medial frontal gyrus, right cerebellum crus 1, and left cerebellum crus 2. In addition, there was a significant group interaction between the CERAD-K WLRc score and the zFC of PCC with the right middle frontal gyrus, superior medial frontal gyrus, superior temporal gyrus, left middle cingulate gyrus, right cerebellum crus 1, and left cerebellum crus 2. However, after performing Bonferroni correction, a significant

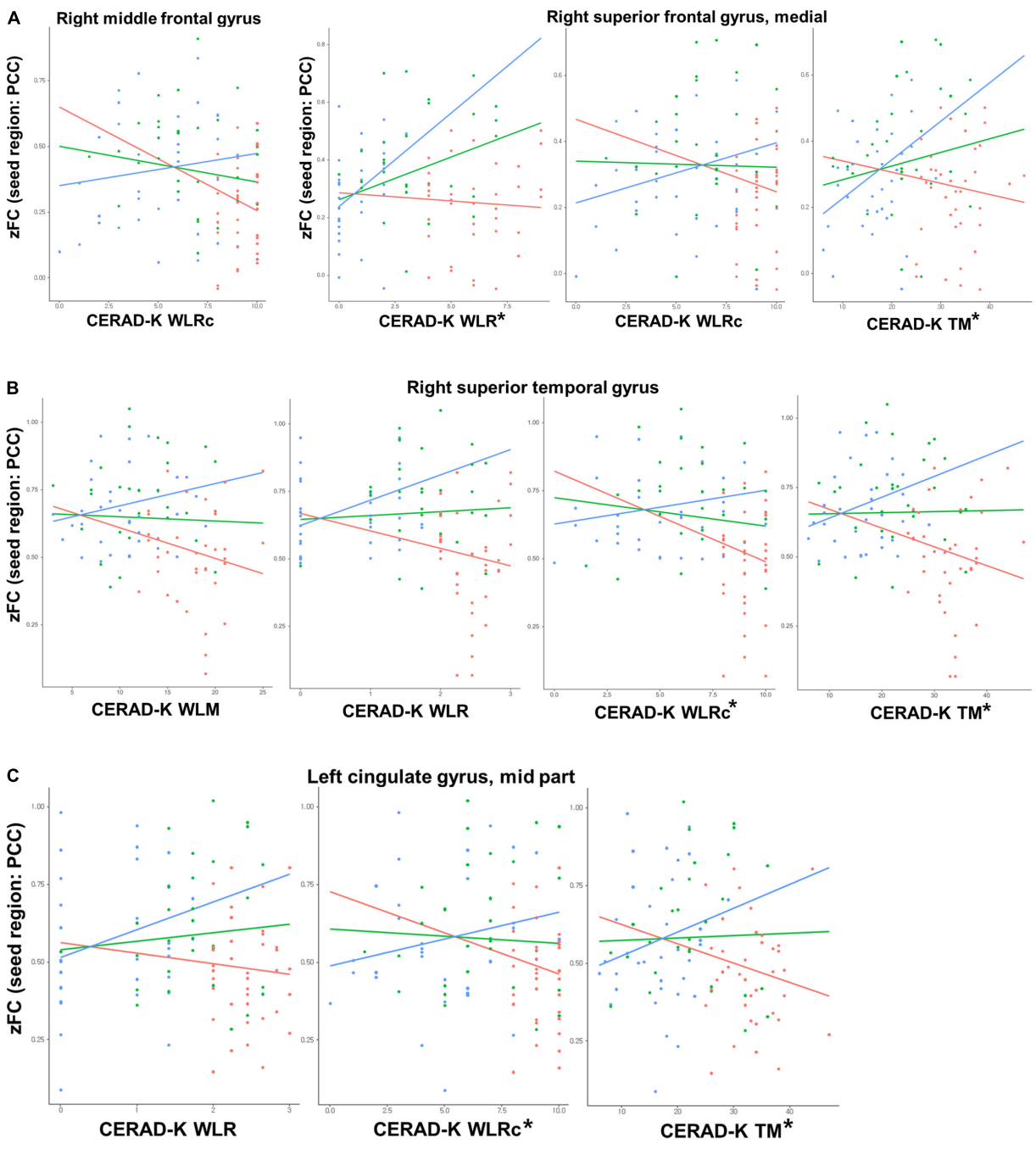

FIGURE 2 | Continued

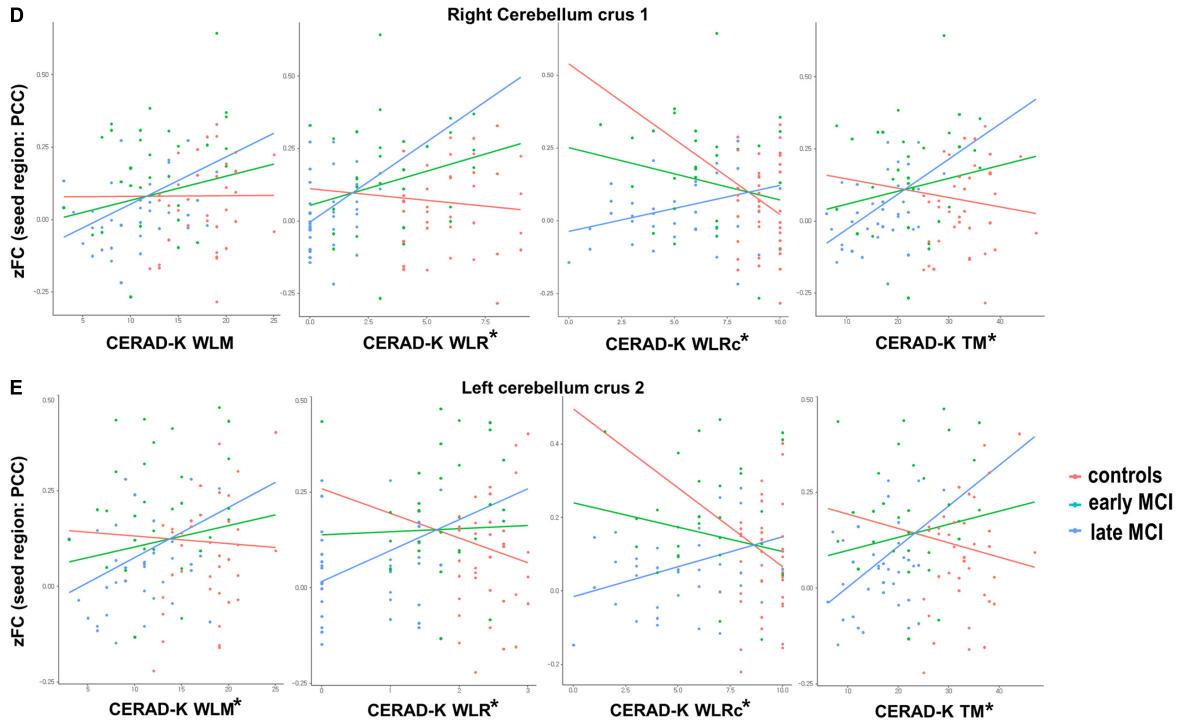

FIGURE 2 | Significant group [healthy control *vs*. early-mild cognitive impairment (MCI) *vs*. late MCI] by cognitive performance interactions for functional connectivity between posterior cingulate cortex and **(A)** right frontal lobe, **(B)** right superior temporal gyrus, **(C)** left cingulate gyrus—mid part, and **(D,E)** bilateral cerebellum. CERAD-K, Korean version of the Consortium to Establish a Registry for Alzheimer's disease; VF, verbal fluency; BNT, Boston Naming Test; WLM, word list memory; WLR, word list recall; CR, constructional recall; TM, total scores of memory domains, including CERAD-K WLM, WLR, and WLRc; *Bonferroni-corrected $P < 0.05$ by multiple regression analysis.

interaction remained only for zFC values with the right superior temporal gyrus, left middle cingulate gyrus, right cerebellum crus 1, and left cerebellum crus 2. Lastly, there was a significant group interaction between the CERAD-K TM score and the zFC with the right superior medial frontal gyrus, superior temporal gyrus, left middle cingulate gyrus, right cerebellum crus 1, and left cerebellum crus 2 after Bonferroni correction. **Figure 2** provides an overview of significant group-memory performance interactions on FC between PCC and ROIs (HC *vs*. early MCI *vs*. late MCI).

DISCUSSION

The current study sets out to evaluate brain regions showing a significant difference in FC from the PCC, the representative hub region of the DMN, between cognitively intact older adults and early- and late-aMCI patients by whole-brain analysis. In addition, this research explored whether the relationships between the FC of PCC with ROIs and memory performance differ according to the progression of prodromal AD.

The early-MCI patients displayed a higher zFC from the PCC in the right superior medial frontal gyrus and bilateral cerebellum crus than did the HC and late-MCI patients. Additionally, the highest zFC was found from the PCC with the right middle frontal gyrus, superior temporal gyrus, and left middle cingulate gyrus in the early-MCI group, while the difference between early- and late-MCI groups was not significant. In a previous study that analyzed the mean FC of DMN through independent component analysis (ICA), contrary to the results of the present study, the early-MCI patients showed a lower FC of DMN than did HC (Lee et al., 2016). However, in agreement with the present study, the late-MCI patients showed a lower FC than that of early-MCI patients (Lee et al., 2016). However, the previous study had extracted only the FC values within the DMN brain regions through the ICA and not FC with other brain regions (Lee et al., 2016). These results, therefore, need to be interpreted with caution. Additionally, another previous study presented different results in longitudinal change in FC among subdivided MCI stages (Zhan et al., 2016). In this prior paper, the degree of change in the nodal FC of the right putamen was smallest in late MCI, and that in the nodal FC of the right insula was smallest in early MCI (Zhan et al., 2016). Moreover, the inter-network FC between the DMN and salience network decreased sequentially as CN progressed to late MCI (Zhan et al., 2016). However, considering that the average disease duration for MCI stage is roughly 4 years at the average age of the participants in the previous study (mean age of 70) (Vermunt et al., 2019), the follow-up period of 6 months is not sufficient, and the sample size is small. Therefore, it is important to consider the possible bias for interpreting these results.

Concerning the ROIs, the right superior medial frontal gyrus of MCI patients has been demonstrated to have a higher FC with the right middle fusiform gyrus during face matching tasks compared to that of the HC group (Bokde et al., 2006). Additionally, increased intra-regional brain activity in this brain region has been suggested to perform a compensatory role in the progression of AD (Yuan et al., 2016). Furthermore, previous results on increased activity in this ROI with higher levels of education might support this compensatory function (Boller et al., 2017). Given the impacts of Aβ retention and *APOE* ε4 allele genotype on the increased functional activity of this ROI (Oh et al., 2014; Wang et al., 2015), further studies with these AD risk factors should be undertaken.

The cerebellum crus, another ROI, belongs to lobule VII of the posterior lobe of the cerebellum (D'Mello and Stoodley, 2015), where abundant Aβ retention and increased microglia are observed in AD patients (Sjöbeck and Englund, 2001; Wang et al., 2002). In the present study, FC between the PCC and bilateral cerebellum crus showed inverse-U-shaped change patterns in all groups. Previous research has found increased FC of the posterior cerebellum with the temporal and parietal cortex at baseline but greater decreased FC between the posterior cerebellum and the aforementioned ROIs after 20 months (Bai et al., 2011). That change in FC over time might have contributed to the inverse U-shaped curve found in the current study. Additionally, previous research has suggested that the posterior cerebellum might have a compensatory role against functional impairment of the hippocampus, given the negative association between changes in the intra-regional activity of these two brain regions (Bai et al., 2011).

The present study found a differential relationship between memory performance and FC from PCC with ROIs according to MCI stage. Although the present study is cross-sectional and cognitive decline does not necessarily indicate progression of AD with associated decreased memory performance, the HC group showed increased FC, while the MCI group showed decreased FC in most of the ROIs. In addition, the linear regression coefficient between FC and memory performance was higher in the late-MCI group. These results indicate that the compensatory role of FC weakens as HC progress to late MCI. Furthermore, the highest FC of early-MCI patients in various ROIs could be induced by other factors, including Aβ accumulation (Zott et al., 2019), rather than by a compensatory mechanism (Wang et al., 2006; Yuan et al., 2016). In this regard, further studies considering these variables are needed. These results are of clinical significance in that there have been few previous studies examining the interaction between memory performance and FC in subdivided MCI stages. In a previous paper, although participants in HC and early- and late-MCI groups have exhibited a positive association between the mean FC of DMN and cognitive function, such as memory performance and executive function, it was uncertain whether this association varies by group (Lee et al., 2016).

Among the ROIs that showed a significant group-memory performance interaction for FC from PCC, a previous study has shown that the brain activity of the medial superior frontal gyrus is increased by memory encoding strategy training, supporting the compensatory function of this brain region (Kirchhoff et al., 2012). Concerning the superior temporal gyrus, the FC with the hippocampus was disrupted in mild AD compared to the normal group (Wang et al., 2006). In the current results, a decrease in FC with cognitive decline was not noticeable in early-MCI patients but significantly decreased in late-MCI patients, showing a pattern similar to that of AD. In addition, the middle cingulate cortex, another significant ROI, has been reported to be a critical hub region of the salience (SAL) network (Xie et al., 2012). Therefore, the FC between the PCC and the middle cingulate cortex observed in this study could reflect the internetwork connectivity between the DMN and the SAL network. Furthermore, the previous study has shown that the change in DMN–SAL inter-network connectivity is disrupted with progression from CN to the late MCI stage, and a disrupted inter-network connectivity shows a significant relationship with cognitive dysfunction (Zhan et al., 2016). However, since this previous study did not examine the group-by-FC-change interaction for cognitive decline, additional studies are needed to confirm whether significant differences exist in this relationship depending on subdivided MCI stage. In another prior study that analyzed the difference in FC of DMN between HC and aMCI groups, the activity of the middle cingulate cortex was increased in the aMCI group, but there was no significant association with cognitive function (Jin et al., 2012). However, considering the small sample size of the previous research, caution must be applied when interpreting the results. FC between the posterior cerebellum and DMN has been associated with cognitive function in AD patients (Zheng et al., 2017), similar to the positive association found in late-MCI patients in the present study. However, few studies have explored the differential association of FC with memory performance at the subdivided aMCI stage. Given the results of the present study, it might be assumed that the activated compensatory mechanism in the HC group weakens as aMCI progresses.

This study was limited by the absence of analysis of AD pathology, including Aβ and tau deposits, which have been demonstrated to affect cognitive decline and functional brain changes throughout the trajectory of AD (Canuet et al., 2015; Sperling et al., 2019). Therefore, further investigation and experimentation with these AD pathologies are recommended to understand the role of functional brain change in the subdivided stages of prodromal AD.

CONCLUSION

The purpose of the current study was to determine the difference in FC from PCC, the hub region of the DMN, between HC and early- and late-MCI patients and to assess the differential association of FC with memory performance according to the subdivided stage of aMCI. This study illustrated a significant difference in FC from PCC to several brain regions, which is known to have a compensatory role against cognitive decline and confirmed the significant memory performance-by-group interaction for FC between PCC and ROIs. These findings contribute to the biological implications of the early- and late-aMCI stages, which are categorized by evaluating the impairment

of memory performance. Additionally, complementing the aforementioned limitations and comprehensively analyzing the results of structural differences in subdivided aMCI stages could deepen our understanding of these biological meanings.

DATA AVAILABILITY STATEMENT

The datasets generated or analyzed during the current study are not publicly available due to Patient Data Management Protocol of Seoul Saint Mary's Hospital but are available from the corresponding author on reasonable request.

ETHICS STATEMENT

The studies involving human participants were reviewed and approved by the Institutional Review Board of The Catholic University of Korea. The patients/participants provided their written informed consent to participate in this study.

AUTHOR CONTRIBUTIONS

DK contributed to the conceptualization, methodology, data curation, writing—original draft, visualization, formal analysis, and funding acquisition. S-MW and YU contributed to the methodology, data curation, and writing—review and editing. H-RN contributed to the investigation and visualization. N-YK contributed to the methodology and data curation. CL contributed to the conceptualization and supervision. HL contributed to the conceptualization, methodology, writing—review and editing, supervision, project administration, and funding acquisition. All authors contributed to the article and approved the submitted version.

FUNDING

This work was supported by the National Research Foundation of Korea grants funded by the Korean government (Ministry of Science and ICT) (Nos. 2019R1A2C2009100 and 2019R1C1C1007608). The funders had no role in the study design, data collection and analysis, decision to publish, or preparation of the manuscript.

SUPPLEMENTARY MATERIAL

The Supplementary Material for this article can be found online at: https://www.frontiersin.org/articles/10.3389/fnagi.2021.696735/full#supplementary-material

REFERENCES

Bai, F., Liao, W., Watson, D. R., Shi, Y., Yuan, Y., Cohen, A. D., et al. (2011). Mapping the altered patterns of cerebellar resting-state function in longitudinal amnestic mild cognitive impairment patients. *J. Alzheimers Dis.* 23, 87–99. doi: 10.3233/jad-2010-101533

Bai, F., Watson, D. R., Yu, H., Shi, Y., Yuan, Y., and Zhang, Z. (2009). Abnormal resting-state functional connectivity of posterior cingulate cortex in amnestic type mild cognitive impairment. *Brain Res.* 1302, 167–174. doi: 10.1016/j.brainres.2009.09.028

Biswal, B., Yetkin, F. Z., Haughton, V. M., and Hyde, J. S. (1995). Functional connectivity in the motor cortex of resting human brain using echo-planar MRI. *Magn. Reson. Med.* 34, 537–541. doi: 10.1002/mrm.1910340409

Bokde, A., Lopez-Bayo, P., Meindl, T., Pechler, S., Born, C., Faltraco, F., et al. (2006). Functional connectivity of the fusiform gyrus during a face-matching task in subjects with mild cognitive impairment. *Brain* 129, 1113–1124. doi: 10.1093/brain/awl051

Boller, B., Mellah, S., Ducharme-Laliberté, G., and Belleville, S. (2017). Relationships between years of education, regional grey matter volumes, and working memory-related brain activity in healthy older adults. *Brain Imaging Behav.* 11, 304–317. doi: 10.1007/s11682-016-9621-7

Cai, S., Huang, L., Zou, J., Jing, L., Zhai, B., Ji, G., et al. (2015). Changes in thalamic connectivity in the early and late stages of amnestic mild cognitive impairment: a resting-state functional magnetic resonance study from ADNI. *PLoS One* 10:e0115573. doi: 10.1371/journal.pone.0115573

Canuet, L., Pusil, S., López, M. E., Bajo, R., Pineda-Pardo, J., Cuesta, P., et al. (2015). Network Disruption and Cerebrospinal Fluid Amyloid-Beta and Phospho-Tau Levels in Mild Cognitive Impairment. *J. Neurosci.* 35, 10325–10330. doi: 10.1523/jneurosci.0704-15.2015

Chao-Gan, Y., and Yu-Feng, Z. (2010). DPARSF: a MATLAB Toolbox for "Pipeline" Data Analysis of Resting-State fMRI. *Front. Syst. Neurosci.* 4:13. doi: 10.3389/fnsys.2010.00013

D'Mello, A. M., and Stoodley, C. J. (2015). Cerebro-cerebellar circuits in autism spectrum disorder. *Front. Neurosci.* 9:408. doi: 10.3389/fnins.2015.00408

Gauthier, S., Reisberg, B., Zaudig, M., Petersen, R. C., Ritchie, K., Broich, K., et al. (2006). Mild cognitive impairment. *Lancet* 367, 1262–1270.

Greicius, M. D., Krasnow, B., Reiss, A. L., and Menon, V. (2003). Functional connectivity in the resting brain: a network analysis of the default mode hypothesis. *Proc. Natl. Acad. Sci. U. S. A.* 100, 253–258.

Jessen, F., Wolfsgruber, S., Wiese, B., Bickel, H., Mösch, E., Kaduszkiewicz, H., et al. (2014). AD dementia risk in late MCI, in early MCI, and in subjective memory impairment. *Alzheimers Dement.* 10, 76–83. doi: 10.1016/j.jalz.2012.09.017

Jin, M., Pelak, V. S., and Cordes, D. (2012). Aberrant default mode network in subjects with amnestic mild cognitive impairment using resting-state functional MRI. *Magn. Reson. Imaging* 30, 48–61. doi: 10.1016/j.mri.2011.07.007

Kang, D. W., Lim, H. K., Joo, S.-H., Lee, N. R., and Lee, C. U. (2019). Differential associations between volumes of atrophic cortical brain regions and memory performances in early and late mild cognitive impairment. *Front. Aging Neurosci.* 11:245. doi: 10.3389/fnagi.2019.00245

Kirchhoff, B., Anderson, B., Barch, D., and Jacoby, L. (2012). Cognitive and neural effects of semantic encoding strategy training in older adults. *Cereb. Cortex* 22, 788–799. doi: 10.1093/cercor/bhr129

Lee, E.-S., Yoo, K., Lee, Y.-B., Chung, J., Lim, J.-E., Yoon, B., et al. (2016). Default mode network functional connectivity in early and late mild cognitive impairment. *Alzheimer Dis. Assoc. Disord.* 30, 289–296. doi: 10.1097/wad.0000000000000143

Lee, J. H., Lee, K. U., Lee, D. Y., Kim, K. W., Jhoo, J. H., Kim, J. H., et al. (2002). Development of the Korean version of the Consortium to Establish a Registry for Alzheimer's Disease Assessment Packet (CERAD-K): clinical and neuropsychological assessment batteries. *J. Gerontol. B Psychol. Sci. Soc. Sci.* 57, 47–53.

Liu, Y., Wang, K., Chunshui, Y., He, Y., Zhou, Y., Liang, M., et al. (2008). Regional homogeneity, functional connectivity and imaging markers of Alzheimer's disease: a review of resting-state fMRI studies. *Neuropsychologia* 46, 1648–1656. doi: 10.1016/j.neuropsychologia.2008.01.027

Morris, J. C. (1993). The Clinical Dementia Rating (CDR): current version and scoring rules. *Neurology* 43, 2412–2414.

Oakes, T. R., Fox, A. S., Johnstone, T., Chung, M. K., Kalin, N., and Davidson, R. J. (2007). Integrating VBM into the General Linear Model with voxelwise anatomical covariates. *Neuroimage* 34, 500–508. doi: 10.1016/j.neuroimage.2006.10.007

Oh, H., Habeck, C., Madison, C., and Jagust, W. (2014). Covarying alterations in Aβ deposition, glucose metabolism, and gray matter volume in cognitively normal elderly. *Hum. Brain Mapp.* 35, 297–308. doi: 10.1002/hbm.22173

Park, J.-H. (1989). Standardization of korean version of the mini-mental state examination (MMSE-K) for use in the elderly. Part II. diagnostic validity. *J. Korean Neuropsychiatr. Assoc.* 28, 508–513.

Petersen, R. C., and Negash, S. (2008). Mild cognitive impairment: an overview. *CNS Spectr.* 13:45.

Raichle, M. E., and Snyder, A. Z. (2007). A default mode of brain function: a brief history of an evolving idea. *Neuroimage* 37, 1083–1090. doi: 10.1016/j.neuroimage.2007.02.041

Sestieri, C., Corbetta, M., Romani, G. L., and Shulman, G. L. (2011). Episodic memory retrieval, parietal cortex, and the default mode network: functional and topographic analyses. *J. Neurosci.* 31, 4407–4420. doi: 10.1523/jneurosci.3335-10.2011

Sjöbeck, M., and Englund, E. (2001). Alzheimer's disease and the cerebellum: a morphologic study on neuronal and glial changes. *Dement. Geriatr. Cogn. Disord.* 12, 211–218. doi: 10.1159/000051260

Sperling, R. A., Mormino, E. C., Schultz, A. P., Betensky, R. A., Papp, K. V., Amariglio, R. E., et al. (2019). The impact of amyloid-beta and tau on prospective cognitive decline in older individuals. *Ann. Neurol.* 85, 181–193.

Vermunt, L., Sikkes, S. A., Van Den Hout, A., Handels, R., Bos, I., Van Der Flier, W. M., et al. (2019). Duration of preclinical, prodromal, and dementia stages of Alzheimer's disease in relation to age, sex, and APOE genotype. *Alzheimers Dement.* 15, 888–898. doi: 10.1016/j.jalz.2019.04.001

Wang, H.-Y., D'andrea, M. R., and Nagele, R. G. (2002). Cerebellar diffuse amyloid plaques are derived from dendritic Aβ42 accumulations in Purkinje cells. *Neurobiol. Aging* 23, 213–223. doi: 10.1016/s0197-4580(01)00279-2

Wang, L., Zang, Y., He, Y., Liang, M., Zhang, X., Tian, L., et al. (2006). Changes in hippocampal connectivity in the early stages of Alzheimer's disease: evidence from resting state fMRI. *Neuroimage* 31, 496–504. doi: 10.1016/j.neuroimage.2005.12.033

Wang, X., Wang, J., He, Y., Li, H., Yuan, H., Evans, A., et al. (2015). Apolipoprotein E ε4 modulates cognitive profiles, hippocampal volume, and resting-state functional connectivity in Alzheimer's disease. *J. Alzheimers Dis.* 45, 781–795. doi: 10.3233/jad-142556

Xie, C., Bai, F., Yu, H., Shi, Y., Yuan, Y., Chen, G., et al. (2012). Abnormal insula functional network is associated with episodic memory decline in amnestic mild cognitive impairment. *Neuroimage* 63, 320–327. doi: 10.1016/j.neuroimage.2012.06.062

Yuan, X., Han, Y., Wei, Y., Xia, M., Sheng, C., Jia, J., et al. (2016). Regional homogeneity changes in amnestic mild cognitive impairment patients. *Neurosci. Lett.* 629, 1–8. doi: 10.1016/j.neulet.2016.06.047

Zhan, Y., Ma, J., Alexander-Bloch, A. F., Xu, K., Cui, Y., Feng, Q., et al. (2016). Longitudinal study of impaired intra-and inter-network brain connectivity in subjects at high risk for Alzheimer's disease. *J. Alzheimers Dis.* 52, 913–927. doi: 10.3233/jad-160008

Zheng, W., Liu, X., Song, H., Li, K., and Wang, Z. (2017). Altered Functional Connectivity of Cognitive-Related Cerebellar Subregions in Alzheimer's Disease. *Front. Aging Neurosci.* 9:143. doi: 10.3389/fnagi.2017.00143

Zott, B., Simon, M. M., Hong, W., Unger, F., Chen-Engerer, H.-J., Frosch, M. P., et al. (2019). A vicious cycle of β amyloid–dependent neuronal hyperactivation. *Science* 365, 559–565. doi: 10.1126/science.aay0198

Conflict of Interest: The authors declare that the research was conducted in the absence of any commercial or financial relationships that could be construed as a potential conflict of interest.

frontiers in Aging Neuroscience

ORIGINAL RESEARCH
published: 13 August 2021
doi: 10.3389/fnagi.2021.724267

Using Fractional Amplitude of Low-Frequency Fluctuations and Functional Connectivity in Patients With Post-stroke Cognitive Impairment for a Simulated Stimulation Program

Sirui Wang[1†], Bo Rao[2†], Linglong Chen[2†], Zhuo Chen[1], Pinyan Fang[2], Guofu Miao[1], Haibo Xu[2] and Weijing Liao[1*]*

[1] Department of Rehabilitation Medicine, Zhongnan Hospital of Wuhan University, Wuhan, China, [2] Department of Radiology, Zhongnan Hospital of Wuhan University, Wuhan, China

OPEN ACCESS

Edited by:
Mingxia Liu,
University of North Carolina at Chapel Hill, United States

Reviewed by:
Daniele Corbo,
University of Brescia, Italy
Dongren Yao,
Massachusetts General Hospital and Harvard Medical School, United States

***Correspondence:**
Haibo Xu
xuhaibo@whu.edu.cn
Weijing Liao
weijingliaorehab@163.com

[†] These authors have contributed equally to this work and share first authorship

Received: *12 June 2021*
Accepted: *22 July 2021*
Published: *13 August 2021*

Citation:
Wang S, Rao B, Chen L, Chen Z, Fang P, Miao G, Xu H and Liao W (2021) Using Fractional Amplitude of Low-Frequency Fluctuations and Functional Connectivity in Patients With Post-stroke Cognitive Impairment for a Simulated Stimulation Program. Front. Aging Neurosci. 13:724267. doi: 10.3389/fnagi.2021.724267

Stroke causes alterations in local spontaneous neuronal activity and related networks functional connectivity. We hypothesized that these changes occur in patients with post-stroke cognitive impairment (PSCI). Fractional amplitude of low-frequency fluctuations (fALFF) was calculated in 36 patients with cognitive impairment, including 16 patients with hemorrhagic stroke (hPSCI group), 20 patients with ischemic stroke (iPSCI group). Twenty healthy volunteers closely matched to the patient groups with respect to age and gender were selected as the healthy control group (HC group). Regions with significant alteration were regarded as regions of interest (ROIs) using the one-way analysis of variance, and then the seed-based functional connectivity (FC) with other regions in the brain was analyzed. Pearson correlation analyses were performed to investigate the correlation between functional indexes and cognitive performance in patients with PSCI. Our results showed that fALFF values of bilateral posterior cingulate cortex (PCC)/precuneus and bilateral anterior cingulate cortex in the hPSCI group were lower than those in the HC group. Compared with the HC group, fALFF values were lower in the superior frontal gyrus and basal ganglia in the iPSCI group. Correlation analysis showed that the fALFF value of left PCC was positively correlated with MMSE scores and MoCA scores in hPSCI. Besides, the reduction of seed-based FC values was reported, especially in regions of the default-mode network (DMN) and the salience network (SN). Abnormalities of spontaneous brain activity and functional connectivity are observed in PSCI patients. The decreased fALFF and FC values in DMN of patients with hemorrhagic and SN of patients with ischemic stroke may be the pathological mechanism of cognitive impairment. Besides, we showed how to use fALFF values and functional connectivity maps to specify a target map on the cortical surface for repetitive transcranial magnetic stimulation (rTMS).

Keywords: post-stroke cognitive impairment, fractional amplitude of low-frequency fluctuations, seed-based functional connectivity, default-mode network, salience network

INTRODUCTION

Post-stroke cognitive impairment (PSCI) is a common functional disorder after stroke, including executive dysfunction, attention disorders, memory impairment, language disorders, and visual space impairment (Iadecola et al., 2019). About 30 % of stroke patients have varying degrees of cognitive impairment, but the prevalence varies between the regions, races, and diagnostic criteria (Sun et al., 2014). Besides, PSCI is an independent predictor of the recurrence of ischemic stroke (Kwon et al., 2020), which seriously affects patients' quality of life and increases families' financial burden (Park et al., 2013).

Cognitive impairment after stroke cannot be well-explained by the size and location of the lesion. The damage caused by stroke extends beyond the local area and may disrupt the entire brain network (Rehme and Grefkes, 2013). The spontaneous neural activity and functional connectivity (FC) of the brain provide a primary method for detecting mechanisms of cognitive impairment. However, until now, how these changes in patients with PSCI are still unclear. Resting-state functional magnetic resonance imaging (rs-fMRI) is an effective method for evaluating neurological function based on blood oxygen level-dependent (BOLD) signal (Wang et al., 2020a). As a non-invasive examination method, rs-fMRI can obtain brain information by analyzing the low-frequency amplitude of the BOLD signals, enabling us to understand the brain changes in patients with PSCI. Most previous studies used independent component analysis (ICA), which explores the changes of the independent brain spontaneous activity to interpret the rs-fMRI signals (De Luca et al., 2006). Tuladhar et al. found decreased FC in the left medial temporal lobe, posterior cingulate cortex (PCC), and medial prefrontal cortex (mPFC) areas within the default mode network (DMN) in stroke patients, which suggested that this may explain the occurrence of cognitive impairment after stroke (Tuladhar et al., 2013). Ding et al. used the ICA analysis to identify the DMN and found significantly decreased FC in the PCC/precuneus in patients with or without cognitive impairment after stroke, but FC in the mPFC increased (Ding et al., 2014). Jiang et al. found decreased FC in the right mPFC and precuneus in patients with acute brainstem stroke by ICA (Jiang et al., 2018). This result was in accordance with Chen's, which provided a new idea for the neural mechanism of cognitive impairment after an ischemic brainstem stroke (Chen et al., 2019).

Different from ICA analysis, functional connectivity analysis can reflect the time consistency of spontaneous low-frequency fluctuations between different regions. Moreover, the seed-based functional connectivity can probe specific brain networks. This approach is less frequently used to study cognitive impairment after stroke. Ding et al. used the seed-based FC to explore the pathogenesis of subcortical vascular cognitive impairment. He found that the frontal lobe and subcortical region were essential, especially the FC value between the PCC and thalamus may be associated with the severity of the disease (Ding et al., 2015). However, the seed points are selected by experience using seed-based FC to explore the strength of association between brain regions.

Furthermore, Zang et al. proposed the amplitude low-frequency fluctuation (ALFF) method, which was defined as the sum of the signal spectrum amplitudes of each voxel in the low-frequency range, reflecting the intensity of local brain spontaneous activity (Zang et al., 2007). However, ALFF is easily affected by other physiological noises. Zou et al. proposed another calculating method called the fractional amplitude of low-frequency fluctuation (fALFF), which was defined as the ratio of ALFF to the sum of a given low-frequency band. Compared with ALFF, fALFF can effectively reduce the interference of physiological signals such as intracranial venous sinus and cerebrospinal fluid, thus significantly improve the sensitivity and specificity of detecting brain spontaneous activity (Zou et al., 2008). For instance, the fALFF analysis has been widely applied in Alzheimer's disease (Yang et al., 2018), mild cognitive impairment (Pan et al., 2017), and amnestic mild cognitive impairment (Zhou et al., 2020), but only a few studies used it in PSCI.

In this study, we used the fALFF method in conjunction with seed-based FC to explore the differences among different types of strokes and the healthy control group. We hypothesized that stroke causes changes in local spontaneous neuronal activity and functional connectivity of connected networks, and these changes are associated with cognitive impairment. We also explored the correlation between functional indexes and cognitive performance in patients with PSCI using the Pearson correlation analysis. Besides, we assumed that repetitive transcranial magnetic stimulation (rTMS) could indirectly activate or inhibit the regions where the fALFF values were abnormal, and stimulation targets were chosen based on the functional connectivity maps. We aim to characterize fALFF and seed-based FC changes among different types of strokes and healthy control group, and show how to use fALFF values and functional connectivity maps to specify a target map on the cortical surface for the rTMS.

MATERIALS AND METHODS

Participants

A total of 36 Chinese patients with PSCI were recruited from November 2019 to December 2020, including 16 patients with hemorrhagic stroke (hPSCI group), 20 patients with ischemic stroke (iPSCI group). These patients were all recruited from the Department of Neurological Rehabilitation in Zhongnan Hospital of Wuhan University. Twenty healthy volunteers closely matched to the patient groups with respect to age and gender were selected as the healthy control group (HC group), which were enrolled from the community by advertisements.

Abbreviations: PSCI, post-stroke cognitive impairment; hPSCI, hemorrhagic stroke with cognitive impairment; iPSCI, ischemic stroke with cognitive impairment; HC, healthy control; fALFF, fractional amplitude of low-frequency fluctuations; ROI, regions of interest; FC, functional connectivity; rTMS, repetitive transcranial magnetic stimulation; PCC, posterior cingulate cortex; DMN, default-mode network; SN, salience network; rs-fMRI, resting-state functional magnetic resonance imaging; ICA, independent component analysis; mPFC, medial prefrontal cortex; ALFF, amplitude low-frequency fluctuation; MoCA, Montreal Cognitive Assessment; MMSE, Mini-Mental State Examination; ACC, anterior cingulate cortex; SFG, superior frontal gyrus; MNI, Montreal Neurological Institute; CEN, central executive network; DLPFC, dorsolateral prefrontal cortex.

The inclusion criteria for PSCI included the following: (1) stroke patients following the cerebral apoplexy diagnostic criteria approved by the fourth National Cerebrovascular Diseases Academic Conference in 1995 confirmed by CT or MRI; (2) first-ever stroke, early subacute period within 7days to 3 months (Bernhardt et al., 2017); (3) 30 to 80 years old (Jiang et al., 2018; Yin et al., 2020); (4) cognitive impairment with at least one cognitive domain impaired, Montreal Cognitive Assessment (MoCA) < 26 (Yin et al., 2020); (5) right-handed; (6) there was no severe aphasia and could complete the cognitive test; (7) lesion volume no more than 30 cm^3 (Wang et al., 2020b); and (8) voluntarily participated and signed the informed consent form. The exclusion criteria for PSCI and healthy volunteers included the following: (1) unstable vital signs; (2) post-operative craniotomy or skull defect; (3) other brain diseases such as Parkinson's disease, encephalitis, dementia, intracranial space-occupying lesions, intracranial inflammation; (4) pre-stroke cognitive impairment such as Alzheimer's disease; (5) any mental illness that may interfere the cognitive assessment; and (6) contraindications for MRI scanning.

Behavioral Assessment

The neuropsychological tests were conducted by professional therapists. All subjects underwent two extensive neuropsychological tests, including the Beijing version of the Montreal Cognitive Assessment (MoCA) and the Chinese version of the Mini-Mental State Examination (MMSE).

Data Acquisition

All resting-state fMRI and T1-weighted images were obtained on a MAGNETOM Trio 3.0 T MR scanner (Siemens, Germany). Participants were instructed to rest with closed eyes and stay awake. Resting-state images were acquired by a gradient echo planar imaging (EPI) sequence: TR/TE = 2,000/30 ms, FOV = 240 × 240 mm, flip angle (FA) = 78°, matrix = 64 × 64, thickness = 4.0 mm, number of slices = 35, and voxel size = 2.4 × 2.4 × 2.4 mm^3. High-resolution sagittal T1-weighted images were collected with a three-dimensional magnetization-prepared rapid gradient echo (3D-MPRAGE) sequence: TR/TE = 2,000/2.3 ms, thickness = 1.0 mm, FA = 8°, FOV = 225 × 240 mm and voxel size = 1 × 1 × 1 mm^3.

Data Pre-processing

Preprocessing of the data was conducted using DPABI software (Yan et al., 2016) (http://rfmri.org/dpabi) based on SPM 12 (http://www.fil.ion.ucl.ac.uk/spm) in MATLAB environment (Mathworks, Natick, MA, USA). Preprocessing procedures included 10 steps: (1) the NIFTI format conversion from DICOM; (2) the removal of the first 10 time points; (3) the slice timing correction; (4) realignment correction for head motion; (5) the coregistration of the structural and functional images; (6) the spatial normalization to the standard Montreal Neurological Institute (MNI) space with 3 × 3 × 3 mm^3 resample; (7) the smoothing with a 4 × 4 × 4 mm^3 full-width-half-maximum (FWHM) Gaussian kernel; (8) the nuisance regression out of the Friston 24 motion parameters and the white matter and cerebrospinal fluid signals (Friston et al., 1996); (9) the removal of linear trends; (10) 0.01–0.08 low-frequency filter (Biswal et al., 1995). Finally, no subject was excluded for more than 2° angular displacement or 2 mm head motion.

fALFF Calculation

fALFF calculation was performed using DPABI software in MATLAB. Each voxel's time series were transformed to the frequency domain for the power spectrum with a fast Fourier transform (FFT). After computing each frequency's square root in the power spectrum, the averaged square root across 0.01–0.08 Hz is ALFF (Zang et al., 2007). fALFF is calculated by ALFF (0.01–0.08 Hz) relative to the full frequency range (0.01–0.25 Hz) (Zou et al., 2008). All fALFF values were standardized using mean division.

FC Analysis

The seed-based FCs were calculated using DPABI software. The clusters of the between-group differences in fALFF were set as seeds (region of interest, ROI). After extracting the mean time series of the ROI, the Pearson correlation coefficients were computed between the ROI and all voxels within the brain. Fisher's z-transformation of the results was conducted for statistical analysis.

Optimization of rTMS for Cortical FC Pattern

After setting the ROI, we computed the Pearson correlation coefficients between the ROI and all voxels within the brain and done the average of the group. The cluster and peak points with the largest correlation coefficient between the ROI were selected. If the fALFF value of the ROI was lower than the HC group, activated rTMS should be applied in the area with a positive correlation coefficient with ROI, and inhibited rTMS should be applied in the area with a negative correlation coefficient with ROI. The functional connection mode diagram was displayed by Brainnet Viewer software (v1.6, http://www.nitrc.org/projects/bnv/). The therapeutic targets were displayed by SimNIBS software (v3.2.2, https://simnibs.drcmr.dk). Our approach is partially referenced from Ruffini's article (Ruffini et al., 2014).

Statistical Analysis

The general demographic and clinical variables were analyzed with SPSS software (Version 23.0). The Shapiro-Wilk (S-W) test was applied for the normality of the distribution of scale scores. Age, years of education, MMSE, MoCA of the hemorrhagic, ischemic, and control groups, expressed as mean ± standard deviation, were analyzed by one-way analysis of variance (ANOVA). Two sample *t*-test was used for the duration of the disease. A chi-square test was conducted to compare sex and the number of lesions. The significance level was set to be equal to 0.05.

The statistical analyses of the fALFF and FC data were performed using DPABI software. The fALFF and seed-based FCs of the hemorrhagic, ischemic, and control groups were analyzed by one-way ANOVA, and a two-sample *t*-test was used as *post-hoc* analysis for the significant clusters of the between-group

TABLE 1 | Demographic, clinical, and neuropsychological data in cognitive impairment group after hemorrhagic stroke (hPSCI group), the cognitive impairment group after ischemic stroke (iPSCI group) and healthy control group (HC group).

Variable	hPSCI ($n = 16$)	iPSCI ($n = 20$)	HC ($n = 20$)	p-value
Age (years)	60.38 ± 9.78	55.80 ± 10.89	60.30 ± 6.67	0.22
Sex (male/female)	12/4	17/3	14/6	0.62
Education (years)	11.31 ± 3.22	12.05 ± 2.98	11.95 ± 2.80	0.74
Disease duration (days)	49.69 ± 20.11	37.95 ± 24.20	–	0.13
Number of lesions (single/multiple)	13/3	12/8	–	0.16
MMSE	20.69 ± 4.66[a]	18.60 ± 5.73[a]	29.35 ± 0.75	<0.001
MoCA	16.62 ± 4.57[a]	15.76 ± 5.20[a]	29.10 ± 1.17	<0.001

One-way ANOVA with post-hoc test was used for age, years of education, MMSE scores, MOCA scores among three groups; Two sample t-test was used for the duration of the disease; A chi-square test was conducted to compare sex and number of lesions; MMSE, Mini-Mental State Examination; MoCA, Montreal Cognitive Assessment Scale; [a]Significant compared to HC.

differences [Gaussian random field (GRF) correction, cluster-level $p < 0.05$, voxel-level $p < 0.001$, two tail]. Age, sex, years of education, disease duration, number of lesions, and head motion parameters were included as covariates in all functional data analyses. Finally, the correlations between the fALFF and seed-based FC values of these significant clusters and clinical variables in patients were performed using Pearson correlation analysis ($p < 0.05$, uncorrected).

RESULTS

Demographic and Clinical Results

As shown in **Table 1**, there were no significant differences in age, sex and education level among the three groups ($p > 0.05$). No significant difference was found in the duration of the disease between the hPSCI group and the iPSCI group ($p > 0.05$). There were significant differences in the scores of MMSE and MoCA between the stroke group and the HC group. However, there was no significant difference between the hPSCI group and the iPSCI group.

fALFF Differences Between Groups

Significant differences in fALFF values were found between the stroke and HC groups, but not between the hPSCI and iPSCI groups.

fALFF values of bilateral posterior cingulate cortex/precuneus and bilateral anterior cingulate cortex (ACC) in the hPSCI group were lower than those in the HC group. In contrast, fALFF values of bilateral cerebellar subarea 9 and cerebellar vermis 10 increased in patients with cognitive impairment after hemorrhagic stroke (**Figure 1A**, **Table 2**).

Compared with the HC group, fALFF values in the iPSCI group were lower in the left caudate, left putamen, right dorsolateral superior frontal gyrus, and right medial superior frontal gyrus. Moreover, fALFF values of bilateral cerebellar subarea 9 and cerebellar vermis 10 were higher than those in the HC group (**Figure 1B**, **Table 3**).

Seed-Based FC

As shown above, the brain areas that showed significant clusters of the between-group differences in fALFF were set as ROIs, including PCC, ACC, putamen, and superior frontal gyrus (SFG). It was found that there was a significant difference in FC values between the stroke and HC groups, but not between the hPSCI and iPSCI groups.

When PCC was used as the ROI, our study showed that the FC values between the PCC and some brain regions were decreased in patients with hemorrhagic stroke, including the bilateral precuneus, left superior parietal lobule, and middle cingulate gyrus (**Figure 2A**, **Supplementary Table 1**). When ACC was selected as ROI, our results revealed decreased functional connection of the ACC and some brain regions, such as the bilateral superior marginal gyrus, the left superior temporal gyrus, the right superior parietal gyrus, the right inferior parietal lobule, and the right angular gyrus (**Figure 2B**, **Supplementary Table 1**).

In the iPSCI group, decreased FC values were found between the putamen and the right insular lobe and between the putamen and the right inferior frontal gyrus of the opercular in patients with ischemic stroke (**Figure 2C**, **Supplementary Table 2**). Besides, FC values between the SFG and the bilateral crus 1 and crus 2 of the cerebellum were significantly increased (**Figure 2D**, **Supplementary Table 2**).

Correlation Analysis

Correlation analysis showed that the fALFF value of the left PCC was positively correlated with MMSE scores and MoCA scores in the hPSCI group (**Figures 3A,B**). We also found a positive relationship between the MoCA scores and the FC values in ACC and the right superior marginal gyrus (**Figures 4A,B**).

Optimization of rTMS for Cortical FC Pattern

The average functional connection pattern map between ROI and the whole brain was obtained after the group average (**Figure 5A**). As a result of the previous two-sample T-test post-host analysis, it was found that the fALLF values of the PCC and ACC in the hPSCI group were lower than those in the HC group. Thus, when selected PCC and ACC as ROIs, the target of activated rTMS therapy was the cluster that had a positive correlation coefficient with the ROIs (the peak MNI coordinates for PCC was: $x = 51$, $y = -47$, $z = 29$; the peak MNI coordinates

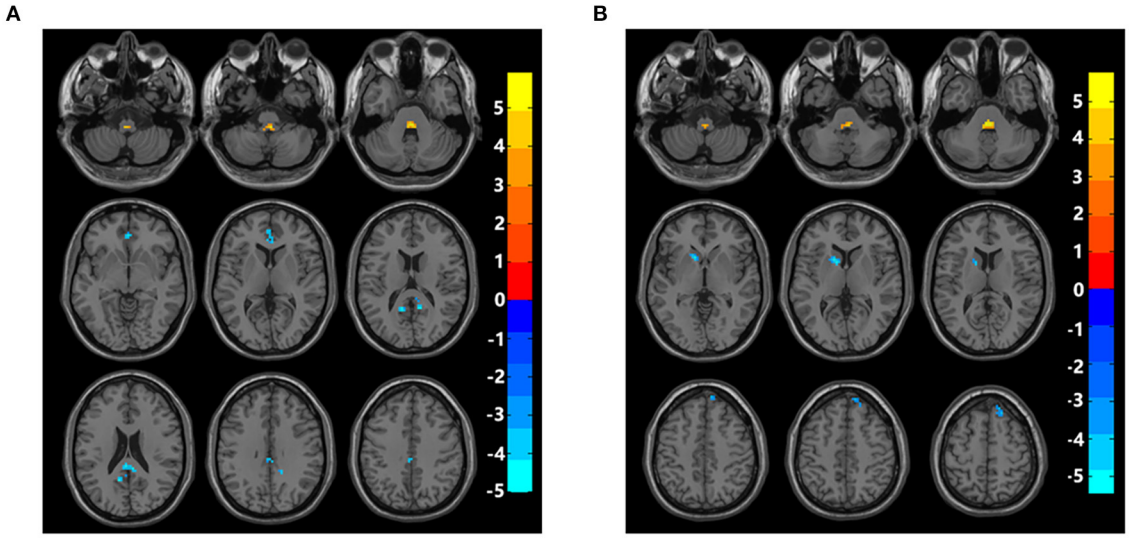

FIGURE 1 | Brain maps of fALFF differences. **(A)** Differences of fALFF between cognitive impairment group after hemorrhagic stroke and healthy control group. **(B)** Differences of fALFF between cognitive impairment group after ischemic stroke and healthy control group. fALFF, fractional amplitude of low-frequency fluctuations; Gaussian random field correction, cluster-level $p < 0.05$, voxel-level $p < 0.001$. The color bar represents T statistics. The red areas represent the regions which have increased fALFF, while the blue ones represent the regions which have decreased fALFF.

TABLE 2 | Comparisons of fALFF between cognitive impairment group after hemorrhagic stroke (hPSCI group) and healthy control group (HC group).

	Region	Cluster	MNI coordinates			*T*-value
			X	Y	Z	
hPSCI<HC		132	12	−42	33	3.29
	Bilateral PCC	45				
	Precuneus	31				
		40	0	33	6	3.31
	Bilateral ACC	27				
hPSCI>HC		46	0	33	6	5.93
	Right cerebelum_9	2				
	Vermis_10	1				

X, Y, Z, coordinates of peak locations in the MNI space. MNI, Montreal Neurological Institute; PCC, posterior cingulate cortex; ACC, anterior cingulate cortex; Gaussian random field correction, cluster-level p < 0.05, voxel-level p < 0.001.

for ACC was: x = −20, y = 47, z = 38), while the target of inhibited rTMS therapy was the cluster which had a negative correlation coefficient with the ROIs (the peak MNI coordinates for PCC was: x = 65, y = −29, z = 37; the peak MNI coordinates for ACC was: x = 61, y = −34, z = 47).

It was found that the fALLF values of the putamen and SFG in the iPSCI group were lower than those in the HC group. When selected putamen and SFG as ROIs: activated rTMS therapy should be applied in the cluster, which had a positive correlation coefficient with the putamen (the peak MNI coordinates for putamen was: x = 54, y = −27, z = −10), while activated rTMS can directly stimulate SFG. Moreover, inhibited rTMS therapy should be applied in the cluster which had a negative correlation coefficient with the ROIs (the peak MNI coordinates for putamen was: x = 46, y = 50, z = 13; the peak MNI coordinates for SFG was: x = 61, y = −36, z = 48) (**Figures 5B,C**).

DISCUSSION

The goal of our study was to characterize the changes of fALFF and seed-based FC among different types of strokes and the healthy control group. No significant differences were found between the hPSCI and iPSCI groups in terms of MMSE scores, MoCA scores, fALFF values, and FC values by *post-hoc t*-tests. Different stroke categories affected different networks. Our results showed that the fALFF values of PCC and ACC belonging to the DMN were decreased in the hPSCI group compared

TABLE 3 | Comparisons of fALFF between cognitive impairment group after ischemic stroke (iPSCI group) and healthy control group (HC group).

	Region	Cluster	MNI coordinates			T value
			X	Y	Z	
iPSCI<HC		59	−18	−15	9	3.31
	Left caudate	33				
	Left putamen	16				
		28	28	58	42	3.30
	Right dorsolateral SFG	14				
	Right medial SFG	13				
		63	0	−36	−36	5.80
iPSCI>HC	Bilateral cerebelum_9	2				
	Vermis_10	9				

X, Y, Z, coordinates of peak locations in the MNI space. MNI, Montreal Neurological Institute; SFG, superior frontal gyrus; Gaussian random field correction, cluster-level $p < 0.05$, voxel-level $p < 0.001$.

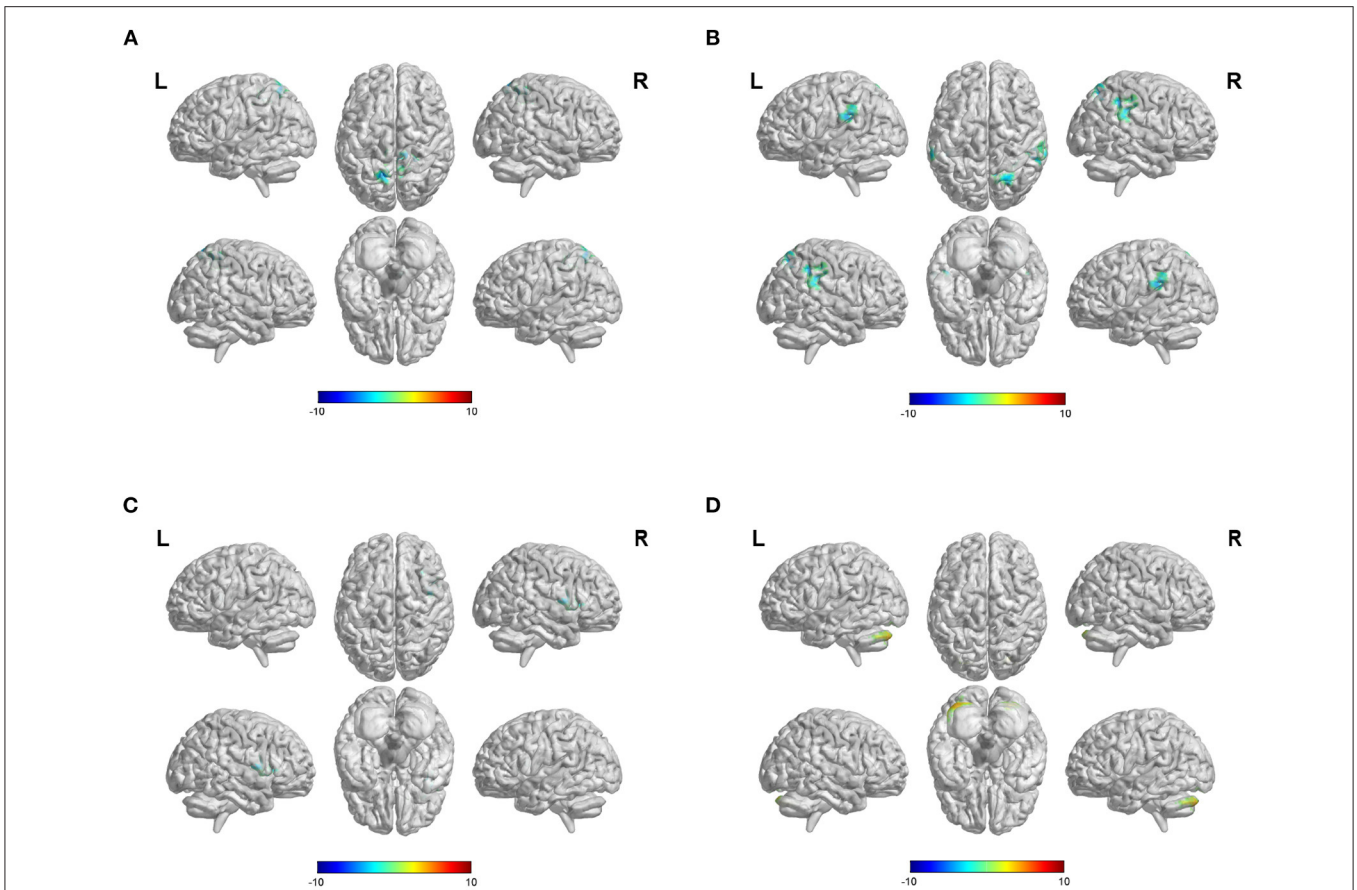

FIGURE 2 | Difference of FC values when select different ROIs. **(A)** Differences of FC values in the posterior cingulate cortex (PCC). **(B)** Differences of FC values in the anterior cingulate cortex (ACC). **(C)** Differences of FC values in the putamen. **(D)** Differences of FC values in the superior frontal gyrus (SFG). FC, functional connectivity; ROI, region of interest; Gaussian random field correction, voxel-level $p < 0.001$, cluster size >100 voxels; The color bar represents *T* statistics. The red areas represent the regions which have increased FC, while the blue ones represent the regions which have decreased FC.

to the HC group. The fALFF values of putamen and SFG, which, respectively, belong to the salience network (SN) and DMN, were decreased in the iPSCI group compared to the HC group. Meanwhile, we studied the seed-based FCs, suggesting that abnormal alterations in the DMN and SN may play a core role in the cognition impairment associated with stroke.

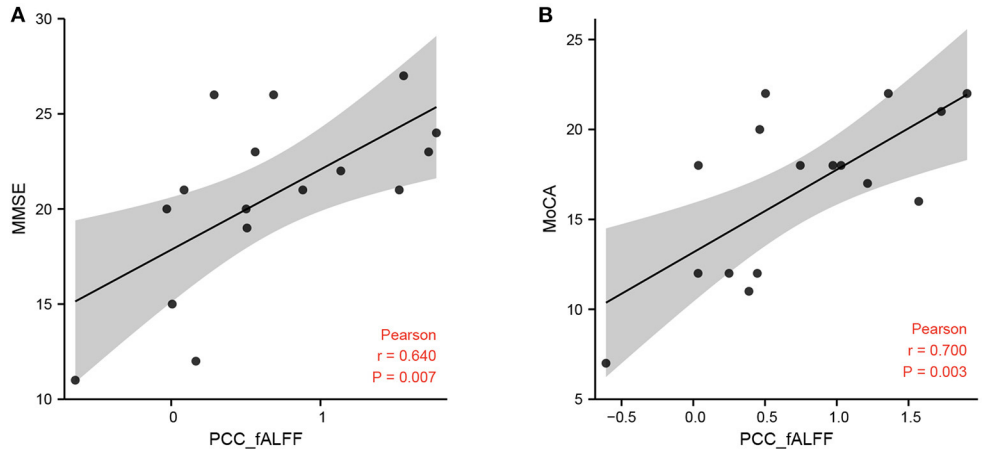

FIGURE 3 | Correlation between fALFF and MMSE, MoCA scores. **(A)** Correlation between the fALFF value of the left PCC and MMSE scores in cognitive impairment group after hemorrhagic stroke (hPSCI group). **(B)** Correlation between the fALFF value of the left PCC and MoCA scores in hPSCI group. fALFF, fractional amplitude of low-frequency fluctuations; MMSE, Mini-Mental State Examination; MoCA, Montreal Cognitive Assessment Scale.

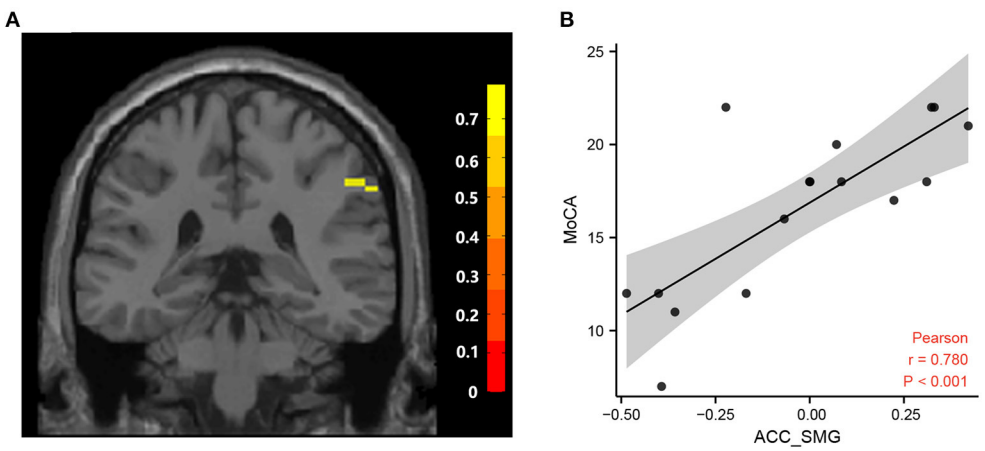

FIGURE 4 | Correlation between FC and MoCA scores. **(A)** Brain areas positively correlated with MoCA scores. A significant cluster in the SMG (57, −39, 39) (The color bar represents T statistics). **(B)** Correlation between the MoCA scores and FC values in ACC and the right superior marginal gyrus in cognitive impairment group after hemorrhagic stroke. FC, functional connectivity; MoCA, Montreal Cognitive Assessment Scale; ACC, anterior cingulate cortex; SMG, superior marginal gyrus.

fALFF Differences Between the hPSCI Group and HC Group

The fALFF values of bilateral PCC/precuneus and bilateral ACC in the hPSCI group were lower than those in the HC group. The PCC/precuneus is considered an important node of the DMN and an important part of the limbic system, which plays a central role in episodic memory and short-term memory (Raichle, 2015). Several neuroimaging studies had shown that there were structural and functional abnormalities in PCC, and recent studies found abnormal ALFF values in the PCC in patients with cognitive impairment (Liang et al., 2014; Pan et al., 2017; Fan et al., 2019). Our results also showed that the fALFF values in the PCC/precuneus were significantly decreased in the hPSCI group comparing to the HC group. Our results increased the evidence for changes in the PCC/precuneus and further indicated that fALFF values in the PCC reflect the damaged global cognitive function in patients with PSCI. The importance of PCC was supposed by the positive correlation between the fALFF values in the left PCC and the MMSE scores and MoCA scores.

The ACC is related to attention control and emotional processing (Bush et al., 2000). Li et al. found decreased ACC function in patients with subcortical ischemic cognitive impairment companies with poor attention control ability (Li et al., 2012). In our study, the fALFF values of bilateral ACC in patients with hemorrhagic stroke were lower than those in healthy controls, indicating that spontaneous neuronal activity was weakened in the ACC region. Besides, some studies have

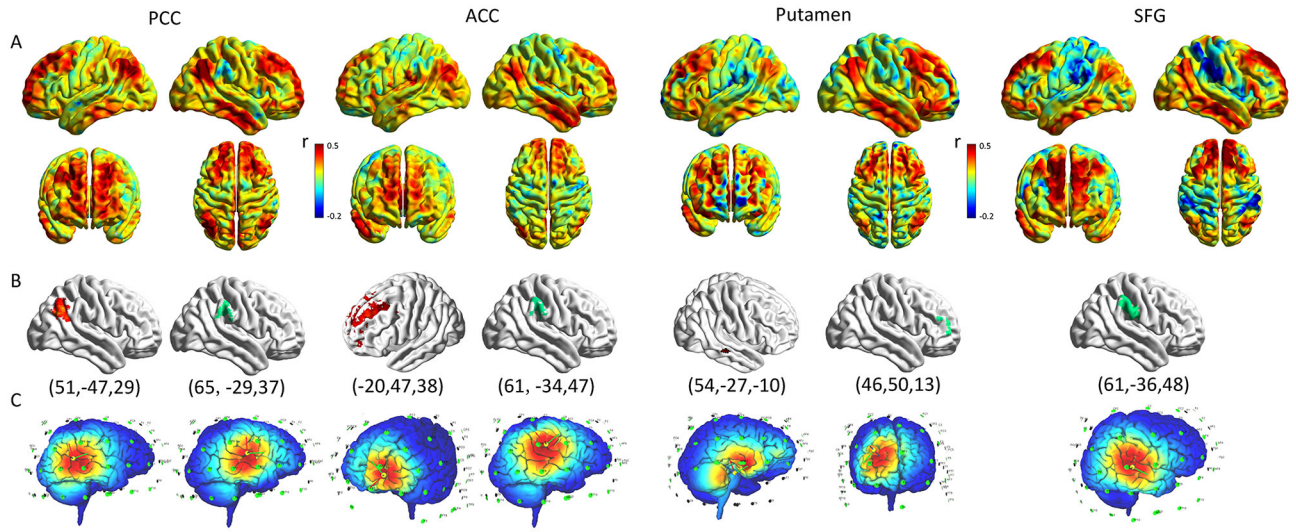

FIGURE 5 | Optimization of rTMS for cortical functional connectivity pattern. **(A)** The pattern map of the connection between ROIs and whole brain. **(B)** The cluster with the maximum correlation coefficient with ROI in the cortex (Red represents positive correlation, green represents negative correlation; The peak coordinates are shown below the graph). **(C)** The rTMS treatment coordinates according to the functional connection pattern diagram (The target of activated rTMS therapy was the cluster which had a positive correlation coefficient with the ROIs, the target of inhibited rTMS therapy was the cluster which had a negative correlation coefficient with the ROIs). rTMS, repetitive transcranial magnetic stimulation; ROI, region of interest; PCC, posterior cingulate cortex; ACC, anterior cingulate cortex; SFG, superior frontal gyrus.

shown that exercise intervention can increase the value of ALFF in the ACC and improve cognitive function (Qi et al., 2019).

The PCC/precuneus and ACC are all important hubs of the DMN related to maintaining cognitive function in the resting state (Buckner and DiNicola, 2019). At present, the researches on rs-fMRI of PSCI are mainly focused on DMN. Both ICA and seed-based FC have found the impairment of the DMN in PSCI patients, which is in line with our research results (Tuladhar et al., 2013; Ding et al., 2014).

fALFF Differences Between the iPSCI Group and HC Group

We found that fALFF values of the left caudate, left putamen, the right dorsolateral superior frontal gyrus, and the right medial superior frontal gyrus in the iPSCI group were lower than those in the HC group. The caudate and putamen belong to the striatum, the largest input nucleus to the basal ganglia, and receive a large input from the neocortex and thalamus (Graybiel, 2004). According to the current knowledge on basal ganglia circuits, cortico-basal ganglia circuits carry motor information and cognitive function (Milardi et al., 2019). The striatum belongs to the SN, involving memory and learning, and the basal ganglia play a crucial role in decision making (Thibaut, 2016). The atrophy of the caudate nucleus destroys the frontalstriatal network, which is the central node of executive function in patients with subcortical ischemic vascular dementia (Riley et al., 2011). Han et al. reported that the decrease of ALFF in basal ganglia might be related to cognitive impairment in patients with amnesia mild cognitive impairment (Han et al., 2011). Zhang et al. explored the association between PSCI patients and specific effective network connectivity in the prefrontal–basal ganglia circuit and found decreased effective connectivity of the prefrontal–basal ganglia circuit (Zhang et al., 2020). Our results showed that the fALFF values of left putamen and caudate in patients with ischemic stroke were lower than that in healthy controls, which may be related to the damage to the prefrontal-basal ganglia circuit.

Besides, the SFG is closely related to cognitive function, emotional regulation, and social cognition (Briggs et al., 2020). One study found that SFG may coordinate working memory, and using intracranial electric stimulation of left SFG enhanced working memory (Alagapan et al., 2019). In our study, the fALFF values of the dorsolateral superior frontal gyrus belonging to the central executive network (CEN) and the medial superior frontal gyrus belonging to the DMN were lower than the HC group. Our results indicated that the decrease of spontaneous neural activity in the right SFG might be associated with cognitive dysfunction.

fALFF Differences Between the hPSCI Group and iPSCI Group

No significant differences in fALFF values were found between the hPSCI group and the iPSCI group. To get some more information about the structural differences between the two subgroups, we done the voxel-based morphometry (VBM) analysis using the FSL-VBM toolbox. We processed all images using the default parameters of the toolboxes. Regional changes were assessed using permutation-based non-parametric testing with 5,000 random permutations. The threshold for significance

was $p < 0.05$, using the threshold-free cluster enhancement (TFCE) method with family wise-error (FWE) correction for multiple comparisons. However, we found no difference among the three groups. We found no significant differences in fALFF values between the hPSCI group and the iPSCI group. We speculated that this might be related to the pattern of stroke injury. Hemorrhagic stroke is caused by the rupture of a blood vessel, resulting in mechanical tissue rupture and hematoma formation, followed by a secondary process of injury (Kitago and Ratan, 2017). While ischemic stroke is due to loss of blood supply, resulting in cell death and loss of neuronal function (Kuriakose and Xiao, 2020). Although there are differences in the pathophysiology of hemorrhagic and ischemic strokes, they ultimately lead to apoptosis and neuronal necrosis. Though our results showed that fALFF values are not different across stroke subtypes, future studies should further investigate fALFF differences based on the subtypes of stroke and locations of injury in a larger sample. Maybe we could provide more evidence by using longitudinal MRI data from a large sample of stroke patients coupled with modern voxel-based analyses methods and functional MRI in the future.

Interestingly, we found that the fALFF values in the cerebellar hemisphere and cerebellar vermis were increased in both the hPSCI and iPSCI groups. Also, recent studies have found that the cerebellum is part of cognitive, and emotional circuits, participating in various activities such as attention, executive function and social emotion (Stoodley et al., 2016). The mechanism of cognitive impairment caused by cerebellar injury may be the abnormal functional connection between the cerebellum and the brain (Schmahmann, 2019). Previous studies have shown that the damage of the right cerebellar subarea 9 can lead to poor Boston naming test scores (Marien et al., 2014). Our study showed that the fALFF values of right cerebellar subregion 9 and cerebellar vermis 10 in both PSCI groups were higher than those in healthy controls, which may be due to the compensatory effect of the cerebellum. This further illustrated that the cerebellum played an important role in cognitive function, providing a new idea for future intervention.

Seed-Based FC Between the hPSCI Group and HC Group

Our study showed that the FC values between the PCC and some brain regions were decreased in patients with hemorrhagic stroke, including the bilateral precuneus, left superior parietal lobule, and middle cingulate gyrus. The precuneus belongs to the DMN, participating in the processing of episodic memory (Li et al., 2019). The superior parietal lobule belongs to the CEN, and the middle cingulate gyrus belongs to the sensorimotor network. The reduction of FC between PCC and precuneus and left superior parietal gyrus may decrease memory and cognitive processing speed. Our result revealed reduced FC, which showed the impairment of the synchronization of these regions.

Our results also showed the decreased functional connection of the ACC and some brain regions, such as the bilateral superior marginal gyrus, the left superior temporal gyrus, the right superior parietal gyrus, the right inferior parietal lobule, and the right angular gyrus. The supramarginal gyrus, the inferior parietal lobule, and the angular gyrus are all components of the posterior parietal cortex, which all belong to DMN. The posterior parietal cortex combines information imported from different brain regions (Whitlock, 2017). Our study showed that decreased FC values were found between the ACC and the posterior parietal cortex, suggesting the damage of the DMN. We also found a positive relationship between the MoCA scores and the FC values in ACC and the right superior marginal gyrus, indicating that synchronization of ACC and right supramarginal gyrus was associated with cognitive impairment. In addition, the superior temporal gyrus belongs to the SN, which is very important for extracting meaningful language features from the speech input. The left superior temporal especially gyrus plays an important role in language comprehension and language production (Yi et al., 2019). The decrease of FC in the superior temporal gyrus may be related to the impairment of patients' semantic processing function. Li et al. showed that the PSCI patients got higher fALFF values in the superior temporal gyrus after rTMS treatment accompanied by corresponding cognition improvement (Li et al., 2020).

Seed-Based FC Between the iPSCI Group and HC Group

This study showed decreased FC values between the putamen and the right insular lobe and between the putamen and the inferior frontal gyrus of the opercular in patients with infarct stroke. The putamen and insular are all components of SN. Insular plays a major role in SN, regulating the interactive competition between the DMN and CEN in cognitive information processing (Fox et al., 2005). One study showed that the modulation mode of the SN in patients with mild cognitive impairment was damaged, and the degree of network damage was significantly associated with the decline of overall cognitive function (Chand et al., 2017). Our results showed reduced synchronization of the putamen and insular, possibly suggesting a declining coordination role of the SN. The inferior frontal gyrus of the opercular is part of the Broca region, belonging to the CEN. Unlike the DMN, the CEN focuses on external attention-dependent tasks. It plays a critical role in participating in advanced cognition (Koechlin and Summerfield, 2007). Our result showed the impairment of the synchronization of the putamen and the inferior frontal gyrus, which may be related to language expression disorders. However, some studies have found that patients with mild Alzheimer's disease had increased FC within the CEN (Balachandar et al., 2015). Further research is needed on the change of CEN after stroke.

Interestingly, our study showed that the FC values between the SFG and the bilateral crus 1 and crus 2 of the cerebellum were significantly increased. The cerebellum is currently thought to play an essential role in cognitive function. The cerebellum is not an independent subcortical system, which may interrelate the network with basal ganglia and cerebral

cortex (Bostan and Strick, 2018). The cerebellum connects many different thalamus regions, and the thalamus connects the broader areas of the cerebral cortex, including the frontal lobe and the posterior parietal cortex (Mitoma et al., 2020). Alteration in one brain region can influence the complex resting-state network, and enhanced cerebellar functional connections may provide a compensatory mechanism in cognitive impairment.

Optimization of rTMS for Cortical FC Pattern

Effective treatment for PSCI has not been identified yet, and the therapeutic effect of routine cognition training is limited. rTMS is a non-invasive and relatively safe technique that has been used in cognition impairment (Fisicaro et al., 2019). Several studies have shown the efficacy of TMS in improving cognition function in patients with PSCI (Liu et al., 2020; Tsai et al., 2020). They found that rTMS can improve attention, memory, executive and overall cognitive function after stroke (Hara et al., 2021). However, the evidence of the stimulation site and frequency of rTMS on the treatment of cognitive impairment after stroke is not convincing. Most studies selected the dorsolateral prefrontal cortex (DLPFC) as the stimulation target. The theoretical basis that they chose DLPFC as the stimulation target was not sufficient.

In this study, we showed how to use fALFF values and functional connectivity maps to specify a target map on the cortical surface for excitatory or inhibitory stimulation. According to the results of fALFF changes, we could find the abnormal regions. However, these regions were deep in the brain beyond the stimulation depth of rTMS. We can stimulate the region which had a significant correlation coefficient with the ROI. Our study found that the fALFF values of the PCC, ACC, putamen, and SFG were lower than the HC group. Thus, we speculated that activating these abnormal regions may improve cognitive function, but rTMS cannot stimulate PCC, ACC, and putamen directly. We are supposed to indirectly activate the abnormal regions by finding peak points on the brain's surface through seed-based functional connectivity. We stimulated two regions simultaneously with activated and inhibited rTMS to indirectly activate the abnormal regions. The target of activated rTMS therapy was the peak point which had a positive correlation coefficient with the ROI. The target of inhibited rTMS therapy was the peak point which had a negative correlation coefficient with the ROI. We hope to achieve individualized rTMS intervention through this method.

Limitations

This study has some limitations. Firstly, we did not separate the subgroup due to stroke locations to discuss the impact of locations on spontaneous brain activity because of the small sample size. Different topography of hemorrhagic and ischemic stroke may have different effects on brain activity, so the relationship between location and the spontaneous brain activity was needed with a larger sample in the future. Secondly, we only set up a healthy control group. Stroke patients with non-cognitive impairment should also be set up as a control group. Thirdly, we excluded patients with pre-stroke cognitive impairment such as Alzheimer's disease, but it was not clear how much the cognitive status differed before the stroke. Fourthly, we cannot dynamically observe the changes of fALFF over time in PSCI patients based on the cross-sectional study. In the future, we will study the dynamic changes of fALFF and its relationship with cognitive function in a large sample of PSCI patients to provide a basis for the diagnosis and treatment of PSCI. Moreover, there was no rTMS treatment in this study, the feasibility of the individualized rTMS intervention based on functional connectivity should be verified in the future.

CONCLUSIONS

Abnormalities of spontaneous brain activity and functional connectivity are observed in post-stroke cognitive impairment. Hemorrhagic and ischemic stroke affect different networks. This study shows that fALFF values of the PCC and the ACC within the DMN were decreased in hPSCI patients, while the SFG and the putamen which, respectively, belong to the DMN and SN, were decreased in iPSCI patients. The decreased fALFF and FC values may be the pathological mechanism of cognitive impairment. These neuroimaging indexes may serve as biomarkers for the evaluation of post-stroke cognitive impairment. Besides, individualize rTMS intervention based on functional connectivity may improve cognitive function.

DATA AVAILABILITY STATEMENT

The original contributions presented in the study are included in the article/**Supplementary Material**, further inquiries can be directed to the corresponding authors.

ETHICS STATEMENT

The studies involving human participants were reviewed and approved by the Medical Research Ethics Committee and Institutional Review Board of Zhongnan Hospital (2019012). The patients/participants provided their written informed consent to participate in this study.

AUTHOR CONTRIBUTIONS

SW: conceptualization, methodology, formal analysis, and writing original draft preparation. BR: conceptualization, formal analysis, and writing—review & editing. LC: formal analysis, visualization, and writing—review & editing. PF and GM: investigation. HX and WL: supervision. All authors have read and approved the final manuscript.

FUNDING

This study was supported by the National Key Technology Research and Development Program of China (2018YFC2002300).

ACKNOWLEDGMENTS

Thanks to those who helped us in our department for helps during this study. Thanks to all the patients who participated.

SUPPLEMENTARY MATERIAL

The Supplementary Material for this article can be found online at: https://www.frontiersin.org/articles/10.3389/fnagi.2021.724267/full#supplementary-material

REFERENCES

Alagapan, S., Lustenberger, C., Hadar, E., Shin, H. W., and Frhlich, F. (2019). Low-frequency direct cortical stimulation of left superior frontal gyrus enhances working memory performance. *Neuroimage* 184, 697–706. doi: 10.1016/j.neuroimage.2018.09.064

Balachandar, R., John, J. P., Saini, J., Kumar, K. J., Joshi, H., Sadanand, S., et al. (2015). A study of structural and functional connectivity in early Alzheimer's disease using rest fMRI and diffusion tensor imaging. *Int. J. Geriatr. Psychiatry* 30, 497–504. doi: 10.1002/gps.4168

Bernhardt, J., Hayward, K. S., Kwakkel, G., Ward, N. S., Wolf, S. L., Borschmann, K., et al. (2017). Agreed definitions and a shared vision for new standards in stroke recovery research: the stroke recovery and rehabilitation roundtable taskforce. *Int. J. Stroke* 12, 444–450. doi: 10.1177/1747493017711816

Biswal, B., Yetkin, F. Z., Haughton, V. M., and Hyde, J. S. (1995). Functional connectivity in the motor cortex of resting human brain using echo-planar MRI. *Magn. Reson. Med.* 34, 537–541. doi: 10.1002/mrm.1910340409

Bostan, A. C., and Strick, P. L. (2018). The basal ganglia and the cerebellum: nodes in an integrated network. *Nat. Rev. Neurosci.* 19, 338–350. doi: 10.1038/s41583-018-0002-7

Briggs, R. G., Khan, A. B., Chakraborty, A. R., Abraham, C. J., Anderson, C. D., Karas, P. J., et al. (2020). Anatomy and white matter connections of the superior frontal gyrus. *Clin. Anat.* 33, 823–832. doi: 10.1002/ca.23523

Buckner, R. L., and DiNicola, L. M. (2019). The brain's default network: updated anatomy, physiology and evolving insights. *Nat. Rev. Neurosci.* 20, 593–608. doi: 10.1038/s41583-019-0212-7

Bush, G., Luu, P., and Posner, M. I. (2000). Cognitive and emotional influences in anterior cingulate cortex. *Trends Cogn. Sci.* 4, 215–222. doi: 10.1016/S1364-6613(00)01483-2

Chand, G. B., Wu, J., Hajjar, I., and Qiu, D. (2017). Interactions of the salience network and its subsystems with the default-mode and the central-executive networks in normal aging and mild cognitive impairment. *Brain Connect.* 7, 401–412. doi: 10.1089/brain.2017.0509

Chen, H., Shi, M., Zhang, H., Zhang, Y. D., Geng, W., Jiang, L., et al. (2019). Different patterns of functional connectivity alterations within the default-mode network and sensorimotor network in basal ganglia and pontine stroke. *Med. Sci. Monit.* 25, 9585–9593. doi: 10.12659/MSM.918185

De Luca, M., Beckmann, C. F., De Stefano, N., Matthews, P. M., and Smith, S. M. (2006). fMRI resting state networks define distinct modes of long-distance interactions in the human brain. *Neuroimage* 29, 1359–1367. doi: 10.1016/j.neuroimage.2005.08.035

Ding, W., Cao, W., Wang, Y., Sun, Y., Chen, X., Zhou, Y., et al. (2015). Altered functional connectivity in patients with subcortical vascular cognitive impairment–a resting-state functional magnetic resonance imaging study. *PLoS ONE* 10:e0138180. doi: 10.1371/journal.pone.0138180

Ding, X., Li, C. Y., Wang, Q. S., Du, F. Z., Ke, Z. W., Peng, F., et al. (2014). Patterns in default-mode network connectivity for determining outcomes in cognitive function in acute stroke patients. *Neuroscience* 277, 637–646. doi: 10.1016/j.neuroscience.2014.07.060

Fan, L., Hu, J., Ma, W., Wang, D., Yao, Q., and Shi, J. (2019). Altered baseline activity and connectivity associated with cognitive impairment following acute cerebellar infarction: a resting-state fMRI study. *Neurosci. Lett.* 692, 199–203. doi: 10.1016/j.neulet.2018.11.007

Fisicaro, F., Lanza, G., Grasso, A. A., Pennisi, G., Bella, R., Paulus, W., et al. (2019). Repetitive transcranial magnetic stimulation in stroke rehabilitation: review of the current evidence and pitfalls. *Ther. Adv. Neurol. Disord.* 12:1756286419878317. doi: 10.1177/1756286419878317

Fox, M. D., Snyder, A. Z., Vincent, J. L., Corbetta, M., Van Essen, D. C., and Raichle, M. E. (2005). The human brain is intrinsically organized into dynamic, anticorrelated functional networks. *Proc. Natl. Acad. Sci. U.S.A.* 102, 9673–9678. doi: 10.1073/pnas.0504136102

Friston, K. J., Williams, S., Howard, R., Frackowiak, R. S., and Turner, R. (1996). Movement-related effects in fMRI time-series. *Magn. Reson. Med.* 35, 346–355. doi: 10.1002/mrm.1910350312

Graybiel, A. M. (2004). Network-level neuroplasticity in cortico-basal ganglia pathways. *Parkinsonism Relat. Disord.* 10, 293–296. doi: 10.1016/j.parkreldis.2004.03.007

Han, Y., Wang, J., Zhao, Z., Min, B., Lu, J., Li, K., et al. (2011). Frequency-dependent changes in the amplitude of low-frequency fluctuations in amnestic mild cognitive impairment: a resting-state fMRI study. *Neuroimage* 55, 287–295. doi: 10.1016/j.neuroimage.2010.11.059

Hara, T., Shanmugalingam, A., McIntyre, A., and Burhan, A. M. (2021). The effect of non-invasive brain stimulation (NIBS) on attention and memory function in stroke rehabilitation patients: a systematic review and meta-analysis. *Diagnostics* 11:227. doi: 10.3390/diagnostics11020227

Iadecola, C., Duering, M., Hachinski, V., Joutel, A., Pendlebury, S. T., Schneider, J. A., et al. (2019). Vascular cognitive impairment and dementia: JACC scientific expert panel. *J. Am. Coll. Cardiol.* 73, 3326–3344. doi: 10.1016/j.jacc.2019.04.034

Jiang, L., Geng, W., Chen, H., Zhang, H., Bo, F., Mao, C. N., et al. (2018). Decreased functional connectivity within the default-mode network in acute brainstem ischemic stroke. *Eur. J. Radiol.* 105, 221–226. doi: 10.1016/j.ejrad.2018.06.018

Kitago, T., and Ratan, R. R. (2017). Rehabilitation following hemorrhagic stroke: building the case for stroke-subtype specific recovery therapies. *F1000Res* 6:2044. doi: 10.12688/f1000research.11913.1

Koechlin, E., and Summerfield, C. (2007). An information theoretical approach to prefrontal executive function. *Trends Cogn. Sci.* 11, 229–235. doi: 10.1016/j.tics.2007.04.005

Kuriakose, D., and Xiao, Z. (2020). Pathophysiology and treatment of stroke: present status and future perspectives. *Int. J. Mol. Sci.* 21:7609. doi: 10.3390/ijms21207609

Kwon, H. S., Lee, D., Lee, M. H., Yu, S., Lim, J. S., Yu, K. H., et al. (2020). Post-stroke cognitive impairment as an independent predictor of ischemic stroke recurrence: PICASSO sub-study. *J Neurol.* 267, 688–693. doi: 10.1007/s00415-019-09630-4

Li, C., Zheng, J., and Wang, J. (2012). An fMRI study of prefrontal cortical function in subcortical ischemic vascular cognitive impairment. *Am. J. Alzheimers. Dis. Other Demen.* 27, 490–495. doi: 10.1177/1533317512455841

Li, R., Utevsky, A. V., Huettel, S. A., Braams, B. R., Peters, S., Crone, E. A., et al. (2019). Developmental maturation of the precuneus as a functional core of the default mode network. *J. Cogn. Neurosci.* 31, 1506–1519. doi: 10.1162/jocn_a_01426

Li, Y., Luo, H., Yu, Q., Yin, L., Li, K., Li, Y., et al. (2020). Cerebral functional manipulation of repetitive transcranial magnetic stimulation in cognitive impairment patients after stroke: an fMRI study. *Front. Neurol.* 11:977. doi: 10.3389/fneur.2020.00977

Liang, P., Xiang, J., Liang, H., Qi, Z., Li, K., and Alzheimer's Disease NeuroImaging, I. (2014). Altered amplitude of low-frequency fluctuations in early and late mild cognitive impairment and Alzheimer's disease. *Curr. Alzheimer Res.* 11, 389–398. doi: 10.2174/1567205011666140331225335

Liu, Y., Yin, M., Luo, J., Huang, L., Zhang, S., Pan, C., et al. (2020). Effects of transcranial magnetic stimulation on the performance of the activities of daily living and attention function after stroke: a randomized controlled trial. *Clin. Rehabil.* 34, 1465–1473. doi: 10.1177/0269215520946386

Marien, P., Ackermann, H., Adamaszek, M., Barwood, C. H., Beaton, A., Desmond, J., et al. (2014). Consensus paper: language and the cerebellum: an ongoing enigma. *Cerebellum* 13, 386–410. doi: 10.1007/s12311-013-0540-5

Milardi, D., Quartarone, A., Bramanti, A., Anastasi, G., Bertino, S., Basile, G. A., et al. (2019). The cortico-basal ganglia-cerebellar network: past, present and future perspectives. *Front. Syst. Neurosci.* 13:61. doi: 10.3389/fnsys.2019.00061

Mitoma, H., Buffo, A., Gelfo, F., Guell, X., Fuca, E., Kakei, S., et al. (2020). Consensus paper. Cerebellar reserve: from cerebellar physiology to cerebellar disorders. *Cerebellum* 19, 131–153. doi: 10.1007/s12311-019-01091-9

Pan, P., Zhu, L., Yu, T., Shi, H., Zhang, B., Qin, R., et al. (2017). Aberrant spontaneous low-frequency brain activity in amnestic mild cognitive impairment: a meta-analysis of resting-state fMRI studies. *Ageing Res. Rev.* 35, 12–21. doi: 10.1016/j.arr.2016.12.001

Park, J. H., Kim, B. J., Bae, H. J., Lee, J., Lee, J., Han, M. K., et al. (2013). Impact of post-stroke cognitive impairment with no dementia on health-related quality of life. *J. Stroke* 15, 49–56. doi: 10.5853/jos.2013.15.1.49

Qi, M., Zhu, Y., Zhang, L., Wu, T., and Wang, J. (2019). The effect of aerobic dance intervention on brain spontaneous activity in older adults with mild cognitive impairment: a resting-state functional MRI study. *Exp. Ther. Med.* 17, 715–722. doi: 10.3892/etm.2018.7006

Raichle, M. E. (2015). The brain's default mode network. *Annu. Rev. Neurosci.* 38, 433–447. doi: 10.1146/annurev-neuro-071013-014030

Rehme, A. K., and Grefkes, C. (2013). Cerebral network disorders after stroke: evidence from imaging-based connectivity analyses of active and resting brain states in humans. *J. Physiol.* 591, 17–31. doi: 10.1113/jphysiol.2012.243469

Riley, J. D., Moore, S., Cramer, S. C., and Lin, J. J. (2011). Caudate atrophy and impaired frontostriatal connections are linked to executive dysfunction in temporal lobe epilepsy. *Epilepsy Behav.* 21, 80–87. doi: 10.1016/j.yebeh.2011.03.013

Ruffini, G., Fox, M. D., Ripolles, O., Miranda, P. C., and Pascual-Leone, A. (2014). Optimization of multifocal transcranial current stimulation for weighted cortical pattern targeting from realistic modeling of electric fields. *Neuroimage* 89, 216–225. doi: 10.1016/j.neuroimage.2013.12.002

Schmahmann, J. D. (2019). The cerebellum and cognition. *Neurosci. Lett.* 688, 62–75. doi: 10.1016/j.neulet.2018.07.005

Stoodley, C. J., MacMore, J. P., Makris, N., Sherman, J. C., and Schmahmann, J. D. (2016). Location of lesion determines motor vs. cognitive consequences in patients with cerebellar stroke. *Neuroimage Clin.* 12, 765–775. doi: 10.1016/j.nicl.2016.10.013

Sun, J. H., Tan, L., and Yu, J. T. (2014). Post-stroke cognitive impairment: epidemiology, mechanisms and management. *Ann. Transl. Med.* 2:80. doi: 10.3978/j.issn.2305-5839.2014.08.05

Thibaut, F. (2016). Basal ganglia play a crucial role in decision making. *Dialogues Clin. Neurosci.* 18:3. doi: 10.31887/DCNS.2016.18.1/fthibaut

Tsai, P. Y., Lin, W. S., Tsai, K. T., Kuo, C. Y., and Lin, P. H. (2020). High-frequency versus theta burst transcranial magnetic stimulation for the treatment of poststroke cognitive impairment in humans. *J. Psychiatry Neurosci.* 45, 262–270. doi: 10.1503/jpn.190060

Tuladhar, A. M., Snaphaan, L., Shumskaya, E., Rijpkema, M., Fernandez, G., Norris, D. G., et al. (2013). Default mode network connectivity in stroke patients. *PLoS ONE* 8:e66556. doi: 10.1371/journal.pone.0066556

Wang, R., Liu, N., Tao, Y. Y., Gong, X. Q., Zheng, J., Yang, C., et al. (2020a). The application of rs-fMRI in vascular cognitive impairment. *Front. Neurol.* 11:951. doi: 10.3389/fneur.2020.00951

Wang, X., Wang, H., Xiong, X., Sun, C., Zhu, B., Xu, Y., et al. (2020b). Motor imagery training after stroke increases slow-5 oscillations and functional connectivity in the ipsilesional inferior parietal lobule. *Neurorehabil. Neural Repair* 34, 321–332. doi: 10.1177/1545968319899919

Whitlock, J. R. (2017). Posterior parietal cortex. *Curr. Biol.* 27, R691–5. doi: 10.1016/j.cub.2017.06.007

Yan, C. G., Wang, X. D., Zuo, X. N., and Zang, Y. F. (2016). DPABI: data processing & analysis for (resting-state) brain imaging. *Neuroinformatics* 14, 339–351. doi: 10.1007/s12021-016-9299-4

Yang, L., Yan, Y., Wang, Y., Hu, X., Lu, J., Chan, P., et al. (2018). Gradual disturbances of the amplitude of low-frequency fluctuations (ALFF) and fractional ALFF in alzheimer spectrum. *Front. Neurosci.* 12:975. doi: 10.3389/fnins.2018.00975

Yi, H. G., Leonard, M. K., and Chang, E. F. (2019). the encoding of speech sounds in the superior temporal gyrus. *Neuron* 102, 1096–1110. doi: 10.1016/j.neuron.2019.04.023

Yin, M., Liu, Y., Zhang, L., Zheng, H., Peng, L., Ai, Y., et al. (2020). Effects of rTMS treatment on cognitive impairment and resting-state brain activity in stroke patients: a randomized clinical trial. *Front. Neural Circuits* 14:563777. doi: 10.3389/fncir.2020.563777

Zang, Y. F., He, Y., Zhu, C. Z., Cao, Q. J., Sui, M. Q., Liang, M., et al. (2007). Altered baseline brain activity in children with ADHD revealed by resting-state functional MRI. *Brain Dev.* 29, 83–91. doi: 10.1016/j.braindev.2006.07.002

Zhang, J., Li, Z., Cao, X., Zuo, L., Wen, W., Zhu, W., et al. (2020). Altered prefrontal-basal ganglia effective connectivity in patients with poststroke cognitive impairment. *Front. Neurol.* 11:577482. doi: 10.3389/fneur.2020.577482

Zhou, Q. H., Wang, K., Zhang, X. M., Wang, L., and Liu, J. H. (2020). Differential regional brain spontaneous activity in subgroups of mild cognitive impairment. *Front. Hum. Neurosci.* 14:2. doi: 10.3389/fnhum.2020.00002

Zou, Q. H., Zhu, C. Z., Yang, Y., Zuo, X. N., Long, X. Y., Cao, Q. J., et al. (2008). An improved approach to detection of amplitude of low-frequency fluctuation (ALFF) for resting-state fMRI: fractional ALFF. *J. Neurosci. Methods* 172, 137–141. doi: 10.1016/j.jneumeth.2008.04.012

Conflict of Interest: The authors declare that the research was conducted in the absence of any commercial or financial relationships that could be construed as a potential conflict of interest.

Publisher's Note: All claims expressed in this article are solely those of the authors and do not necessarily represent those of their affiliated organizations, or those of the publisher, the editors and the reviewers. Any product that may be evaluated in this article, or claim that may be made by its manufacturer, is not guaranteed or endorsed by the publisher.

frontiers in Aging Neuroscience

ORIGINAL RESEARCH
published: 18 August 2021
doi: 10.3389/fnagi.2021.694254

The Cognitive Connectome in Healthy Aging

Eloy Garcia-Cabello[1], Lissett Gonzalez-Burgos[1,2], Joana B. Pereira[2,3], Juan Andres Hernández-Cabrera[1], Eric Westman[2,4], Giovanni Volpe[5], José Barroso[1†] and Daniel Ferreira[1,2,6†]*

[1]Department of Clinical Psychology, Psychobiology and Methodology, Faculty of Psychology, University of La Laguna, La Laguna, Spain, [2]Division of Clinical Geriatrics, Center for Alzheimer Research, Department of Neurobiology, Care Sciences, and Society, Karolinska Institutet, Stockholm, Sweden, [3]Clinical Memory Research Unit, Department of Clinical Sciences, Lund University, Lund, Sweden, [4]Department of Neuroimaging, Centre for Neuroimaging Sciences, Institute of Psychiatry, Psychology and Neuroscience, King's College London, London, United Kingdom, [5]Department of Physics, University of Gothenburg, Gothenburg, Sweden, [6]Department of Radiology, Mayo Clinic, Rochester, MN, United States

Objectives: Cognitive aging has been extensively investigated using both univariate and multivariate analyses. Sophisticated multivariate approaches such as graph theory could potentially capture unknown complex associations between multiple cognitive variables. The aim of this study was to assess whether cognition is organized into a structure that could be called the "cognitive connectome," and whether such connectome differs between age groups.

Methods: A total of 334 cognitively unimpaired individuals were stratified into early-middle-age (37–50 years, *n* = 110), late-middle-age (51–64 years, *n* = 106), and elderly (65–78 years, *n* = 118) groups. We built cognitive networks from 47 cognitive variables for each age group using graph theory and compared the groups using different global and nodal graph measures.

Results: We identified a cognitive connectome characterized by five modules: verbal memory, visual memory—visuospatial abilities, procedural memory, executive—premotor functions, and processing speed. The elderly group showed reduced transitivity and average strength as well as increased global efficiency compared with the early-middle-age group. The late-middle-age group showed reduced global and local efficiency and modularity compared with the early-middle-age group. Nodal analyses showed the important role of executive functions and processing speed in explaining the differences between age groups.

Conclusions: We identified a cognitive connectome that is rather stable during aging in cognitively healthy individuals, with the observed differences highlighting the important role of executive functions and processing speed. We translated the connectome concept from the neuroimaging field to cognitive data, demonstrating its potential to advance our understanding of the complexity of cognitive aging.

Keywords: connectome, cognition, aging, graph theory, compensation, differentiation

OPEN ACCESS

Edited by:
Cosimo Urgesi, University of Udine, Italy

Reviewed by:
Melissa Lamar, Rush University Medical Center, United States
Talitha Best, Central Queensland University, Australia

***Correspondence:**
Daniel Ferreira
daniel.ferreira.padilla@.ki.se

† These authors share senior authorship

Received: *12 April 2021*
Accepted: *23 July 2021*
Published: *18 August 2021*

Citation:
Garcia-Cabello E, Gonzalez-Burgos L, Pereira JB, Hernández-Cabrera JA, Westman E, Volpe G, Barroso J and Ferreira D (2021) The Cognitive Connectome in Healthy Aging. Front. Aging Neurosci. 13:694254. doi: 10.3389/fnagi.2021.694254

INTRODUCTION

Cognitive aging has been extensively investigated. A common approach has been to focus on how a particular cognitive function changes over time or differs across age groups, using univariate methods for data analysis (West, 2001; Tisserand and Jolles, 2003; Lachman, 2004; Schroeder and Salthouse, 2004; Schaie, 2005; Salthouse, 2009, 2010, 2016; Harada et al., 2013; Ferreira et al., 2015; Reas et al., 2017; Oschwald et al., 2019). While this approach has provided important insight on age-related cognitive decline, cognitive functions are highly interrelated with each other through complex associations, possibly in a dynamic manner across ages, i.e., these inter-relations may differ across age groups. Capturing such complex associations is difficult when focussing on a particular cognitive function in isolation, as conventionally done with univariate analysis. This motivated the development and use of multivariate approaches, facilitating a deeper and more integrated understanding of cognitive aging (Salthouse and Ferrer-Caja, 2003; Viroli, 2012; Hoogendam et al., 2014; Habeck et al., 2015; Nielsen and Wilms, 2015; Salthouse et al., 2015; Machado et al., 2018). Previous multivariate studies have informed on the complex association between cognitive performance and key demographic, clinical, and neuroimaging variables. However, it is still largely unknown how cognitive domains and cognitive components are organized and interrelated with each other, forming a structure that could be called the "cognitive connectome." Further, whether this cognitive connectome changes during aging has not been investigated so far. Within the connectome field of neuroscience (Bullmore and Sporns, 2021), graph theory has recently emerged as a promising technique to investigate complex associations in the data, both in normal and pathological aging.

Graph theory enables the analysis of complex inter-relationships between multiple measures. Although graph theory has been extensively applied to neuroimaging data in the field of aging (Zhu et al., 2012; Jung et al., 2018; Chong et al., 2019; Lee et al., 2019; Xia et al., 2019), to our knowledge only one study has applied graph theory on cognitive data in an aging study (Gonzalez-Burgos et al., 2020). In that study, Gonzalez-Burgos et al. (2020) studied compensation of age-related differences in verbal fluency and demonstrated the potential of graph theory to investigate cognitive aging, as an alternative to other multivariate methods such as random forest analysis or orthogonal partial least squares to latent structures (Machado et al., 2018; Gonzalez-Burgos et al., 2020). To our knowledge, four other previous studies applied graph theory on cognitive data, in other fields than normal aging: three studies investigated children with epilepsy (Garcia-Ramos et al., 2015, 2016; Kellermann et al., 2015), and another study investigated neurological patients with different etiologies (Jonker et al., 2019). Hence, translating the concept of connectome from the neuroimaging field to cognitive data (i.e., the "cognitive connectome") is timely and is expected to provide relevant new insights on how human cognition is organized. This step is warranted in order to understand the behavioral outcomes of the well-studied brain connectome in neuroimaging research (Van den Heuvel and Sporns, 2019; Bullmore and Sporns, 2021). This understanding could have various implications, both for research and clinical work in normal and pathological aging.

The overall goal of the current study was to investigate cognitive aging with graph theory using a large set of cognitive measures (47 variables) in three groups of age spanning from 37 to 78 years (early-middle-age = 37–50 years; late-middle-age = 51–64 years, and elderly = 65–78 years). The first aim was to investigate how multiple cognitive domains and cognitive components are interrelated with each other in the whole cohort, forming a cognitive connectome independent of age. To address this first aim, we applied modular analyses using graph theory. The second aim was to investigate whether this cognitive connectome differs between groups of early-middle-age, late-middle-age, and elderly individuals. To address this second aim, we also applied modular analyses using graph theory, across the three groups of age. The third aim was to gain a deeper understanding of network features underlying age-related differences in the cognitive connectome. To address this third aim, we quantified and analyzed global and nodal measures from the three age groups. Based on previous studies from our group (Ferreira et al., 2015; Machado et al., 2018) and other groups (Lachman, 2004; Willis et al., 2010), we hypothesized that differences between the two middle-age groups would be modest, but the differences would be more prominent when comparing middle-age groups with the elderly group. We anticipated more disconnected cognitive networks in the elderly group, with an important role of executive functions and processing speed in network differences, as predicted by the executive and processing speed theories of cognitive aging (Salthouse, 1996; West, 1996).

MATERIALS AND METHODS

Participants

A total of 334 participants were selected from the GENIC (Group of Neuropsychological Studies of the Canary Islands) database (Ferreira et al., 2017). All individuals were native Spanish speakers from the Canary Islands, with ages between 37 and 78 years and a balanced distribution of sex across age. For the current study, participants were selected according to the following criteria: (1) No dementia according to a Mini-Mental State Examination (MMSE) score $\geq$24, a Blessed Dementia Rating Scale (BDRS) score $<$4, and a Functional Activities Questionnaire (FAQ) score $<$6; (2) No mild cognitive impairment based on consensus diagnosis from two experienced neuropsychologists, following Winblad et al. (2004) criteria applied on comprehensive neuropsychological assessment (Ferreira et al., 2015) and age-, sex-, and education-corrected normative data; (3) Right-handed manual preference as assessed by the Edinburgh Handedness Inventory. We applied this criterion because some cognitive functions such as language abilities (Springer et al., 1999), visuospatial functions (Zaidel, 1990; Kong et al., 2018), or attention (Heilman, 1995) are lateralized and so, the "cognitive connectome" could be different in left-handed individuals; (4) No abnormal findings such as stroke, tumors, or hippocampal sclerosis on MRI according

to an experienced neuroradiologist; and (5) No neurologic or psychiatric disorders, systemic diseases with neuropsychological consequences, or history of substance abuse. An exception was made for the BDRS. Although the BDRS scale cut-off for abnormality is frequently established at ≥4 points (Blessed et al., 1968; Erkinjuntti et al., 1988), the "changes in personality, interests and drive" subscale may influence the BDRS total score and does not necessarily reflect functional impairment. With the aim of excluding only individuals with functional impairment, we included those participants with total BDRS scores ≥4 (n = 15) if: (a) 70% or higher percentage of the BDRS total score resulted from the "changes in personality, interests and drive" subscale; and (b) if a score ≤1.5 was obtained in the other two subscales ("changes in performance of everyday activities" and "changes in habits"). The same procedure has been applied in previous studies (Cedres et al., 2019; Gonzalez-Burgos et al., 2020). Participation was completely voluntary and all subjects gave written informed consent in accordance with the Declaration of Helsinki. The study was approved by the local ethics committee of the University of La Laguna (Spain).

Cognitive Assessment

A comprehensive neuropsychological protocol was applied covering the following cognitive domains: processing speed, attention, executive functions, premotor functions, episodic memory, procedural memory, visuoconstructive, visuoperceptive, and visuospatial functions, and language. The protocol is fully detailed in **Supplementary Table 1** and described elsewhere (Ferreira et al., 2015). In addition, the MMSE (Folstein et al., 1975) was used as a measure of global cognition, and the BDRS (Blessed et al., 1968) and the FAQ (Pfeffer et al., 1982) were used as measures of functional status. The Wechsler Adult Intelligence Scale (WAIS-III) Information subtest (Wechsler, 1997a) was scored and used as an indicator of crystallized intelligence.

Graph Analysis

All cognitive variables detailed in **Table 1A** were selected as the nodes to construct the network constituting the cognitive connectome.

Regarding our first aim of investigating an age-independent cognitive connectome in the whole cohort, all cognitive variables were corrected for age and crystallized intelligence (WAIS-III Information subtest) by using multiple linear regression prior to network construction. The resulting residual values were used for network construction. We controlled the age because we aimed to investigate an age-independent cognitive connectome, and we also controlled for crystallized intelligence because it is known to have a strong impact on cognitive performance (Ferreira et al., 2016).

Regarding our second aim of investigating whether the cognitive connectome differs between age groups of early-middle-age, late-middle-age, and elderly individuals, new cognitive networks were built separately for each age group by controlling only for the effect of crystallized intelligence, using multiple linear regression prior to network construction. Again, the resulting residual values were used for network construction.

The edges between the nodes were calculated through matrices of Pearson correlation coefficients from each pair of nodes. Matrices were binarized by thresholding the correlation coefficients at a range of densities from 15% to 50% of connections, in steps of 1%. This ensured the exclusion of disconnected networks (densities below 15%) and random topologies (densities above 50%, when the small-world index became close to 1). Network topologies were compared across this range of densities. Results from global graph measures were reported across all densities. Results from nodal graph measures were considered also across all densities but reported only at the median density (30%), to simplify reporting and as a common procedure to represent the whole range of densities (Pereira et al., 2018; Ferreira et al., 2019). Both self-connections and negative correlations were excluded.

Regarding our third aim of gaining a deeper understanding of the network features underlying potential age-related differences in the cognitive connectome, the nodal and global graph measures described below were calculated. Some graph measures have been reported to be unstable, especially in small cohorts (Mårtensson et al., 2018). To circumvent this issue, we aimed for age groups larger than those in studies shown to be reproducible (Welton et al., 2015), and selected graph measures that are stable according to Mårtensson et al. (2018).

Figure 1 shows a graphical representation of the nodal graph measures included in this study. The nodal *global efficiency*, the *local efficiency*, and the *participation* coefficient, which were calculated from the binary networks across the different densities. In addition, we also included the *nodal strength*, which was calculated from the weighted network (before binarization). The nodal *global efficiency* is the average of the inverse shortest path length from a node to all other nodes in the network. The *local efficiency* is the global efficiency of a node calculated on the subgraph created by the node's neighbors. The *participation* coefficient quantifies the relation between the number of edges connecting a node outside its community and its total number of edges. The *nodal strength* is the sum of the weights of all edges connected to a node.

Figure 2 shows a graphical representation of the global graph measures included in this study: the *average global efficiency*, the *average local efficiency*, the *transitivity*, and the *modularity*. All these measures were calculated in the binary networks across the different densities. In addition, we also included the *average strength*, which was calculated from the weighted network (before binarization). Global measures such as the *average global efficiency*, the *average local efficiency*, and the *average strength* represent the mean of all nodes across the whole network for each nodal measure. The *transitivity* refers to the fraction of a node's neighbors that are also neighbors of each other in the whole network, normalized by the whole network. Hence, the *transitivity* reflects how well the nodes are connected to nearby nodes forming cliques. The *modularity* is a quantitative measure that reflects the extent to which a graph can be divided into clearly separate

TABLE 1 | Cognitive variables and cognitive modules.

(A) Cognitive variables included as the nodes in graph analysis		(B) Cognitive modules from modular analysis with the Newman algorithm
LM A-Immediate	TAVEC 1st trial	**Verbal Memory Module**
LM B1-Immediate	TAVEC Learning	
LM B2-Immediate	TAVEC Interference	
LM A-Delay	TAVEC Short delay	
LM B-Delay	TAVEC Short delay-Clues	
LM A-Recognition	TAVEC Long delay	
LM B- Recognition	TAVEC Long delay-Clues	
VR I-Total Score	8/30 Long delay	**Visual Memory and Visuospatial Module**
VR II-Total Score	FRT	
VR-Copying	JLOT-First half	
VR- Total Recognition	JLOT-Second half	
8/30 1st trial	BNT	
8/30 Learning	Spatial Span backward	
8/30 Interference	Block Design Total	
8/30 Short delay		
STROOP Words	Digit Span forward	**Executive Functions and Premotor Functions Module**
STROOP Colors	Digit Span backward	
STROOP Inhibition	Spatial Span forward	
Phonemic fluency	Luria's HAM Right	
Semantic fluency	Luria's HAM Left	
Action fluency	Luria's—Coordination	
PCV Decision time	CTT-Part 1	**Processing Speed Module**
PCV Motor time		
HT 1st trial	HT Long delay	**Procedural Memory Module**
HT Learning		

The table shows the cognitive variables used as the nodes in the network construction (A). The table also shows the cognitive variables included in each of the different cognitive modules (B). Please see **Supplementary Table 1** *for more information about cognitive variables and tests. LM, Logical Memory; FRT, Facial Recognition Test; JLOT, Judgment of Line Orientation Test; VR, Visual Reproduction; BNT, Boston Naming Test; HT, Hanoi Tower; PCV, PC-Vienna System; CTT, Color Trails Test.*

communities (that is, subgraphs or modules). In addition, complementary modular analyses were performed using the Newman algorithm (Newman, 2004) to provide qualitative information on how cognitive variables are organized into specific communities.

Statistical Analysis

To address the aims of the current study, we stratified individuals into three age groups by dividing the whole age range from 37 to 78 years into equidistant groups with an age range of 13 years each: an early-middle-age group (37–50 years) treated as the reference group, a late-middle-age group (51–64 years), and an elderly group (65–78 years). We favored three age groups because three is the smallest number of groups to test for non-linear group differences. In particular, we used ANCOVA (see below) to test both linear and non-linear trends in cognitive performance across age groups. Also, we ensured that the resulting groups had sizes larger than previous studies shown to be reproducible (Welton et al., 2015). We further confirmed that the sizes of the age groups provided enough power for the comparisons using ANCOVA (see below).

Because graph analysis is based on correlations, cognitive variables that showed low variability were excluded from the analysis. More specifically, among all variables included in our comprehensive neuropsychological protocol (Ferreira et al., 2015), we excluded error variables, the PASAT (Gronwall, 1977), recognition variables in all our memory tests, and the discrimination test from Visual Reproduction (Wechsler, 1997b). This gave a total of 47 cognitive variables included in our graph analysis (**Table 1A**). We ensured that the selection of 47 cognitive variables covered all cognitive domains and their subcomponents. Further, missing data could not be accommodated in our software, and given the multivariate nature of graph theory, individuals with at least one missing value in any of the included 47 cognitive variables were excluded from this study. We used the *BRAPH software version 1.0.0* (Mijalkov et al., 2017) for graph analysis and *R Studio version 0.99.483* with the *ULLRToolbox* for statistical analyses.

The widely used Newman algorithm (Newman, 2004) was implemented for modular analyses, to reduce the set of 47 cognitive variables down to a few modules (**Table 1B**). This analysis also served as our computational method to identify cognitive connectomes. Since different algorithms can produce different modular solutions and thus affect the identification of the cognitive connectome, we replicated all our analyses with another widely used method: the Louvain algorithm (Blondel et al., 2008). Pearson's correlation was used to test the relationship between educative level and crystallized intelligence (WAIS-III Information subtest). ANCOVA and Chi square tests were used for continuous and categorical variables, respectively. A p-value <0.05 was deemed significant in all analyses. In addition, the false discovery rate (FDR) adjustment was used at $p \leq 0.05$ (two-tailed) for analyses involving nodal graph measures (Genovese et al., 2002).

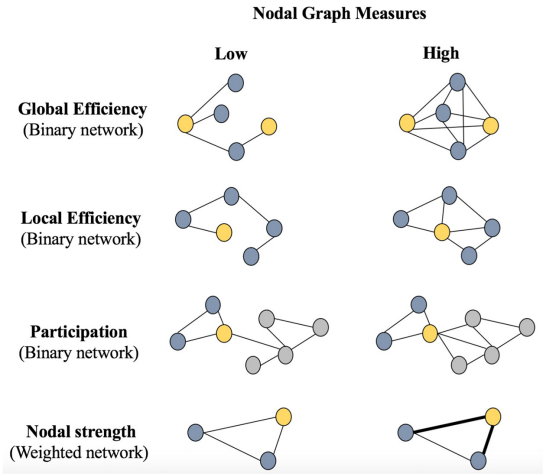

FIGURE 1 | Schematic representation of nodal graph measures. Circles represent nodes and edges represent connections between the nodes. The Global Efficiency panel represents a less efficient connectivity between the two yellow nodes (left: two steps between yellow nodes) vs. a more efficient connectivity between the two yellow nodes (right: multiple connections of one and two steps between yellow nodes). The Local Efficiency panel represents a less efficient connectivity between the yellow node and all other nodes (left: only one connection) vs. a more efficient connectivity between the yellow node and all other nodes (right: four connections). The Participation panel represents two communities (blue and gray); the yellow node belongs to the blue community and has less connections (edges) with the gray community in the left part of the panel (low participation) than in the right part of the panel (high participation). The nodal strength panel represents the intensity of the connectivity of the yellow node with its connections, where thinner connections (left) represent a lower strength and thicker connections (right) represent a higher strength. Parentheses indicate whether binary or weighted networks were used for each nodal measure.

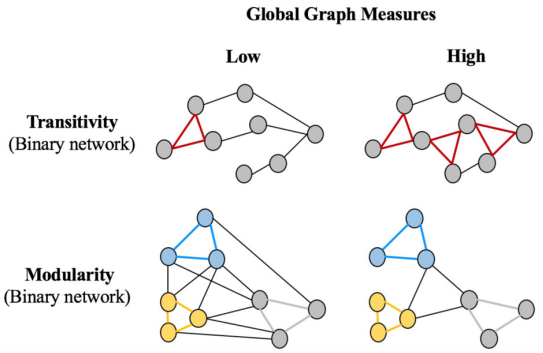

FIGURE 2 | Schematic representation of global graph measures. Circles represent nodes and edges represent connections between the nodes. The Transitivity is the number of triangles in a network, with the left panel showing a lower transitivity (one triangle), vs. the right panel showing a higher transitivity (three triangles). The Modularity panel shows that there are three modules (blue, yellow and gray), which can be less clearly divided into separate communities on the left part (high between-module connectivity relative to within-module connectivity: low modularity) than on the right part (low between-module connectivity relative to within-module connectivity: high modularity). Parentheses indicate that binary networks were used for the Transitivity and Modularity global measures. The global measures of Global Efficiency, Local Efficiency and Average Strength were also used in this study but are not represented in this Figure because they are similar to the representation in **Figure 1**, but for the global network instead of the local network.

RESULTS

Key Characteristics of the Whole Cohort and the Three Age Groups

Table 2 shows the key characteristics of the whole cohort (N = 334) and the three age groups. Briefly, there were no group differences in sex distribution, but educative level and scores in crystallized intelligence (WAIS-III Information subtest) differed across ages. Hence, we controlled for the effects of the educative level/WAIS-III Information subtest when investigating cognitive performance across age groups. Since there was a strong correlation between the educative level and WAIS-III Information subtest (r = 0.7, p < 0.001), we favored the continuous nature of WAIS-III Information subtest to be used as a covariate in further analyses. In order to characterize cognitive profile across age groups, the set of 47 cognitive variables were reduced into five cognitive domains or modules using modular analysis with the Newman algorithm. After controlling for the WAIS-III Information subtest in ANCOVA, we observed lower MMSE scores and lower performance in all the five cognitive modules with increasing age (**Table 2**, **Figure 3**). More specifically, we observed a significant linear trend in executive and premotor functions, verbal memory, visual memory, and visuospatial measures. This means that the magnitude of the difference between the early-middle-age group and the late-middle-age group was similar to the magnitude of the difference between the late-middle-age group and the elderly group. In contrast, we observed a significant quadratic trend in procedural memory and processing speed, indicating comparable performance between the two middle-age groups, and significantly worse performance in the elderly group. All tests with ANCOVA showed power values of 1 or close to 1, indicating good statistical power.

Aim 1—Age-Independent Cognitive Connectome

To investigate how cognitive domains and cognitive components are organized and interrelated with each other (i.e., to determine the "cognitive connectome"), independently of age, we corrected our 47 cognitive variables by de-trending the effects of age and WAIS-III Information subtest. The age-independent cognitive connectome was then investigated through a modular analysis (Newman algorithm) performed on the 47 de-trended cognitive variables. As it can be seen in **Figure 4**, memory variables of verbal nature clustered together forming a first module. Memory variables of visual nature clustered together and with visuospatial measures, forming a second module. Executive and premotor functions also clustered together, forming the third module. Variables of procedural memory and processing speed formed the fourth and fifth small separate modules, respectively. Between-module correlations were observed between the modules of verbal memory, visual memory—visuospatial measures, and executive—premotor measures. However, procedural memory and processing speed modules showed

TABLE 2 | Key characteristics of the whole cohort and the three age groups.

	Whole cohort (*N* = 334)	Early-middle-age (*n* = 110)	Late-middle-age (*n* = 106)	Elderly (*n* = 118)	
	M(SD)/count(%)	M(SD)/count(%)	M(SD)/count(%)	M(SD)/count(%)	*p*-value
Age (years) (min-max)	57.85 (11.2) (37–78)	44.6 (3.4)[a,b] (37–50)	57.8 (4.4)[b] (51–64)	70.2 (3.8) (65–78)	<0.001
Sex (female, count (%))	188 (56.0%)	58 (52.7%)	63 (59.4%)	67 (56.8%)	0.61
Education level					
Illiteracy	4	0	0	4	<0.001
Unfinished primary studies	43	2	6	35	
Completed primary studies	120	48	31	41	
Completed secondary studies	73	34	20	19	
University studies	94	26	49	19	
WAIS-III Information	15.3 (6.3)	15.7 (5.8)[a,b]	17.6 (6.4)[b]	12.9 (5.9)	<0.001
MMSE	28.5 (1.5)	29 (1.3)[a,b]	28.6 (1.4)[b]	27.9 (1.6)	<0.001
Verbal memory module	0 (1)	0.3 (0.6)[a,b]	0.2 (0.7)[b]	−0.5 (0.6)	<0.001
Visual memory and visuospatial module	0 (1)	0.4 (0.4)[a,b]	0.1 (0.5)[b]	−0.5 (0.6)	<0.001
Executive and premotor functions module	0 (1)	0.4 (0.5)[a,b]	0.2 (0.7)[b]	−0.6 (0.6)	<0.001
Processing speed module	0 (1)	−0.5 (0.4)[a,b]	−0.2 (0.5)[b]	0.7 (0.8)	<0.001
Procedural memory module	0 (1)	0.0 (0.7)	0.1 (0.8)[b]	−0.1 (0.7)	<0.05

The table shows mean (SD) except for sex and education level, where count (%) is shown. The five cognitive modules were obtained using the Newman algorithm in the whole cohort when reducing the set of 47 cognitive variables into modules. All 47 cognitive variables had previously been corrected for age and crystallized intelligence (WAIS-III Information subtest). The three age groups were then compared across modules to investigate age-related differences in cognitive performance. ANCOVA with crystallized intelligence (WAIS-III Information subtest) as a covariate was used to test between-group differences in MMSE and cognitive modules. Processing speed is an inverse measure so that a higher score denotes a worse performance. [a]Significantly different from the Late-middle-age group. [b]Significantly different from the Elderly group. MMSE, Mini-Mental State Examination. WAIS, Wechsler Adult Intelligence Scale.

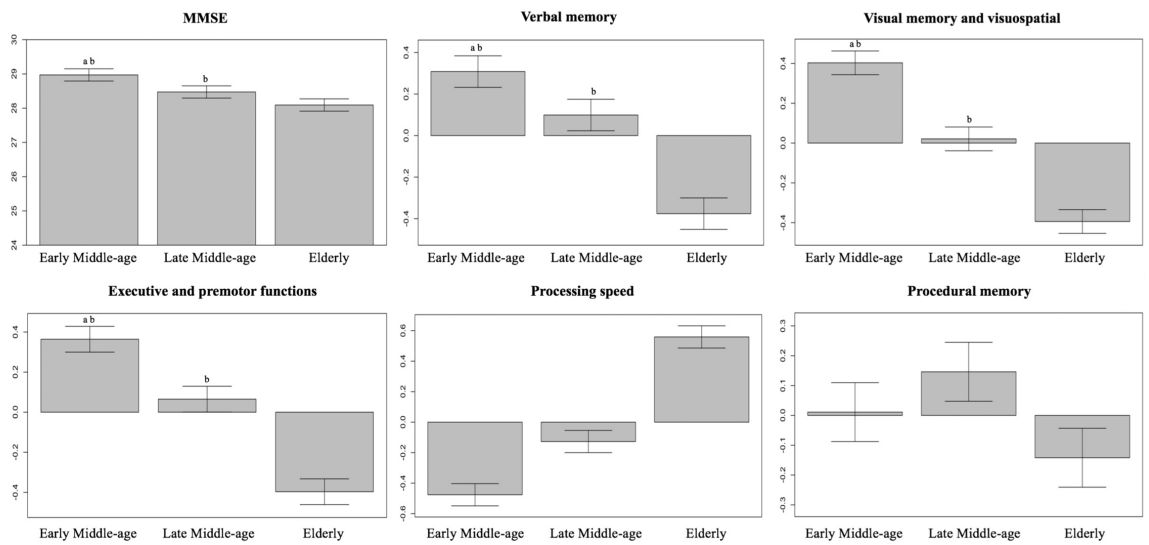

FIGURE 3 | Differences in cognitive performance across age groups. Between-group differences in MMSE and cognitive modules were analyzed using ANCOVA with crystalized intelligence (WAIS-III Information subtest) as a covariate. Processing speed is an inverse measure, so that a higher score denotes a worse performance. Whiskers show 95% confidence intervals. [a]Significantly different from the late-middle-age group. [b]Significantly different from the elderly group. MMSE, Mini-Mental State Examination.

weak almost non-existent between-module correlations. The Louvain algorithm showed the same results except for procedural memory and processing speed modules converging into one single module (**Supplementary Figure 1**).

Aim 2—Age-Related Differences in the Cognitive Connectome

We then investigated whether the cognitive connectome differs across age groups of early-middle-age, late-middle-age, and elderly individuals. This time, performance in our 47 cognitive variables were corrected only for WAIS-III Information, by de-trending its effect.

Firstly, we visually inspected the five modules from the age-independent cognitive connectome fixed across the three age groups, in order to describe the correlation matrices used for the quantitative analyses of global and nodal measures described below (**Figure 5**, see **Supplementary Figures 2–4** for matrices with larger size). The correlation matrix in

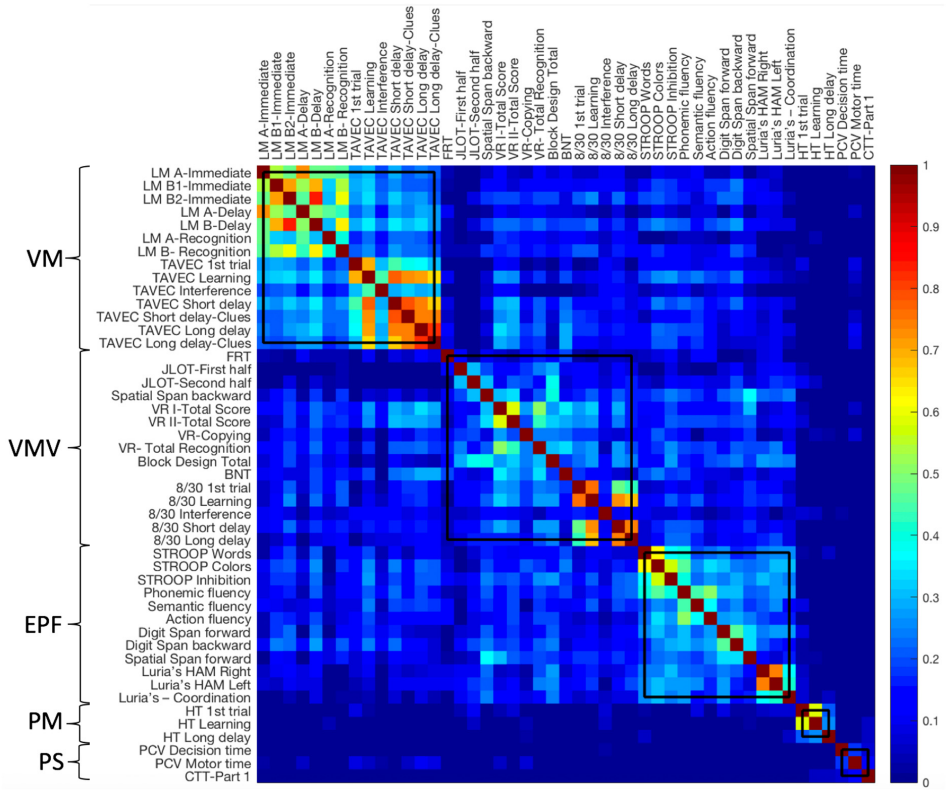

FIGURE 4 | Age-independent cognitive connectome in the whole cohort. Weighted correlation matrix in the whole cohort (N = 334) sorted out by cognitive modules obtained with the Newman algorithm. Pearson's correlation coefficients were used to build the matrix. The color bar indicates the strength of the Pearson's correlation coefficients: colder colors represent weaker correlations, while warmer colors represent stronger correlations. PM, procedural Memory module; VM, verbal memory module; PS, processing speed module; VMV, visual memory and visuospatial abilities module; EPF, executive functions and premotor functions module; LM, logical memory; FRT, facial recognition test; JLOT, judgment of line orientation test; VR, visual reproduction; BNT, boston naming test; HT, hanoi tower; PCV, PC-Vienna System; CTT, color trails test.

the early-middle-age group was very similar to that of the age-independent cognitive connectome. Nonetheless, in the early-middle-age group, the visual memory—visuospatial module showed stronger between-module correlations with executive—premotor and verbal memory modules. Likewise, the correlation matrix of the late-middle-age group was similar to that of the early-middle-age group, although with a tendency to show weaker within-module correlations in the visual memory—visuospatial module, stronger within-module correlations in verbal memory and executive—premotor modules, and stronger between-module correlations of the executive—premotor module with verbal memory and visual memory—visuospatial modules. The elderly group showed overall weaker correlations than the other two age groups. However, the elderly group was the only group where processing speed variables showed correlations with cognitive variables from other modules.

Secondly, in order to quantify the differences described on visual inspection of correlation matrices, we conducted new modular analyses (Newman algorithm), separately within each age group. These modular analyses tested whether different cognitive modules emerge in each age group. Our results showed rather similar cognitive connectomes across the three age groups. The most notable differences were observed in visual and executive domains, which emerged as only one module in the early-middle-age group, but split into two separate modules in late-middle-age and elderly groups (**Figure 6**). Likewise, while verbal memory and processing speed were separate modules in early-middle-age and late-middle-age groups, the two modules converged into one single module in the elderly group (**Figure 6**). The Louvain algorithm showed very similar results. The only exception was that in the elderly group, the procedural memory module converged with the visual memory—visuospatial module instead of converging with the executive—premotor module (**Supplementary Figure 6**).

Aim 3—Global and Nodal Network Differences in the Cognitive Connectome Across Age Groups

We compared global and nodal network measures calculated from correlation matrices of early-middle-age, late-middle-age, and elderly groups. Significant densities are detailed between brackets in the following sentences. Regarding global network

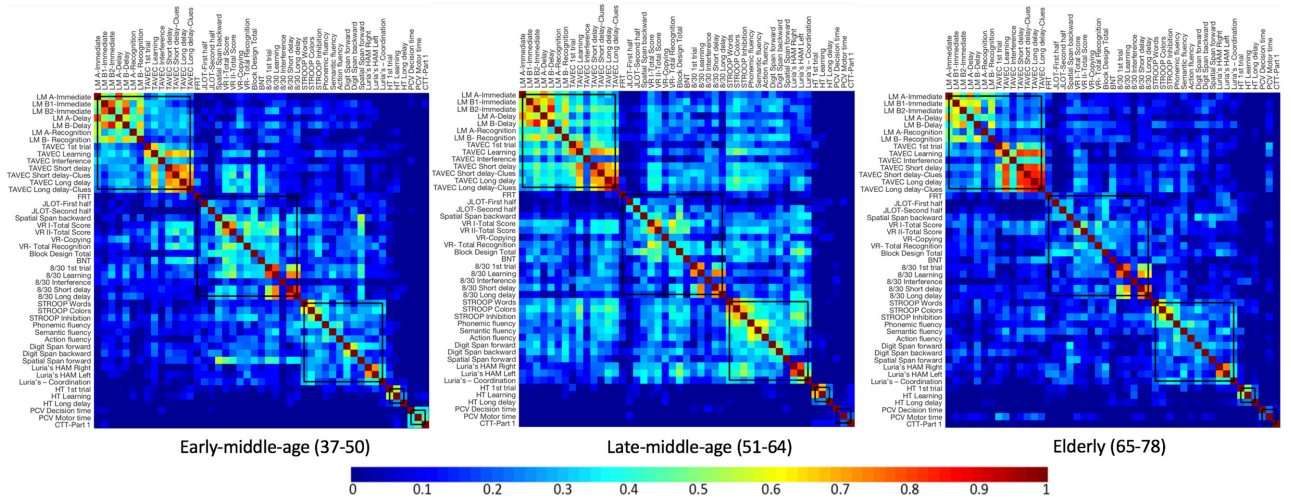

FIGURE 5 | Correlation matrices for each age group, keeping the five modules from the whole cohort fixed. Newman algorithm was used for modular analysis. Pearson's correlation coefficients were used to build the matrix. The color bar indicates the strength of the Pearson's correlation coefficients: colder colors represent weaker correlations, while warmer colors represent stronger correlations. See **Supplementary Figures 2–4** for matrices with larger size and labelled regions. LM, Logical Memory; FRT, Facial Recognition Test; JLOT, Judgment of Line Orientation Test; VR, Visual Reproduction; BNT, Boston Naming Test; HT, Hanoi Tower; PCV, PC-Vienna System; CTT, Color Trails Test.

measures, the elderly group showed decreased transitivity in all densities (15%–50%) and increased average global efficiency measures (17%–39%) when compared with the reference early-middle-age group (**Table 3**, **Figure 7**). The late-middle-age group showed decreased average global efficiency (32%–36%; 38%–43%), average local efficiency (16%–18%; 20%–25%), and modularity measures (19%–24%; 28%–47%) when compared with the reference early-middle-age group (**Table 3**, **Figure 7**). The comparison between the elderly group and the late-middle-age group showed that the elderly group had increased average global efficiency (19%–50%) and modularity measures (19%–24%; 29%–43%) and decreased average strength and transitivity measures (26%–50%; **Table 3**, **Figure 7**).

Regarding nodal network measures, the elderly group showed a decrease in local efficiency and nodal strength in processing speed variables and an increase in global efficiency in procedural memory and processing speed variables, when compared with the reference early-middle-age group (**Table 4**). Further, the elderly group showed an increase in the participation coefficient in executive and visuospatial variables, compared with the reference early-middle-age group. The late-middle-age group showed a decrease in local efficiency and an increase in the participation coefficient in processing speed when compared with the reference early-middle-age group. Finally, the comparison between elderly and late-middle-age groups showed that the elderly group had an increase in global efficiency in processing speed and visuoperceptive variables and an increase in the strength in processing speed variables. Further, the elderly group showed a decrease in local efficiency in executive variables, when compared with the late-middle-age group.

DISCUSSION

We investigated how multiple cognitive domains and cognitive components are interrelated with each other, forming a cognitive connectome. We also investigated whether this cognitive connectome and its network characteristics differ between early-middle-age, late-middle-age, and elderly groups. Our results showed a cognitive connectome that illustrates the organization of cognitive functions and cognitive components into five modules. This cognitive connectome was rather stable across age groups but some differences were observed in the modular organization, the strength of correlations between cognitive variables, and the characteristics of the networks. Our results support the relevance of executive functions and processing speed in cognitive aging, and stress the potential of graph theory to unravel the complex organization of cognition.

Our first aim was to investigate how multiple cognitive domains and cognitive components are interrelated with each other, forming a cognitive connectome. We wanted to identify a cognitive connectome that is independent of age and other relevant confounding factors such as crystallized intelligence. To that end, we regressed out the effect of age and crystallized intelligence previous to our modular analysis. We identified a cognitive connectome that included five modules: verbal memory, visual memory—visuospatial functions, procedural memory, processing speed, and executive—premotor functions. These modules fit with the cognitive structure reported in the study by Salthouse and Ferrer-Caja (2003), which included "space" abilities (similar to our visual memory—visuospatial module), reasoning (similar to our executive module), verbal memory, and processing speed. Despite the extensive literature on cognitive aging, we are not aware of studies that had an

FIGURE 6 | Cognitive variables included in each cognitive module for each age group. The alluvial plot shows how each cognitive variable flows across the cognitive modules in each age group. The Newman algorithm was used for modular analysis. Each cognitive module is represented with a different color: blue color represents an executive and premotor, visual memory and visuospatial functions module; green color represents a procedural memory and processing speed module; pink color represents a verbal memory module; red color represents an executive functions module; orange color represents a premotor functions, visual memory and visuospatial functions module; turquoise color represents a procedural memory, executive and premotor functions module; yellow color represents a visual memory and visuospatial functions module; and violet color represents a verbal memory and processing speed module. Schematic representation of cognitive modules using Newman and Louvain algorithms are detailed in **Supplementary Figures 5, 6**, respectively.

TABLE 3 | Differences in global network measures from the cognitive connectome across age groups.

	Early-middle-age vs. Elderly	Early-middle-age vs. Late-middle-age	Late-middle-age vs. Elderly
Av. Strength	n.s	n.s	↓
Transitivity	↓	n.s	↓
Global Efficiency	↑	↓	↑
Local Efficiency	n.s	↓	n.s
Modularity	n.s	↓	↑

*The table shows an overview of the results from global graph analyses. Please, see **Figure 7** for more details about quantitative results. Each column shows the between-group differences in global network measures, with the first group as the reference group in the comparison: higher values in the second group in the comparison are indicated with an upwards arrow (e.g., in the "Early-middle-age vs. Elderly" comparison, an upwards arrow indicates that the Elderly group had a higher global efficiency than the Early-middle-age group), lower values in the second group in the comparison are indicated with a downwards arrow, and n.s denotes non-significant results. Results were considered significant when $p \leq 0.05$ (two-tailed).*

explicit focus on the complex inter-relations between cognitive domains and cognitive components, apart from the study of Salthouse and Ferrer-Caja (2003). However, several studies that applied analytical methods for the reduction of cognitive data are of interest in this discussion. Using different approaches such as factorial analysis (Mitchell et al., 2012; Viroli, 2012; Hayden et al., 2014; Mungas et al., 2014; Nielsen and Wilms, 2015; Salthouse et al., 2015; Rizio and Diaz, 2016) and principal component

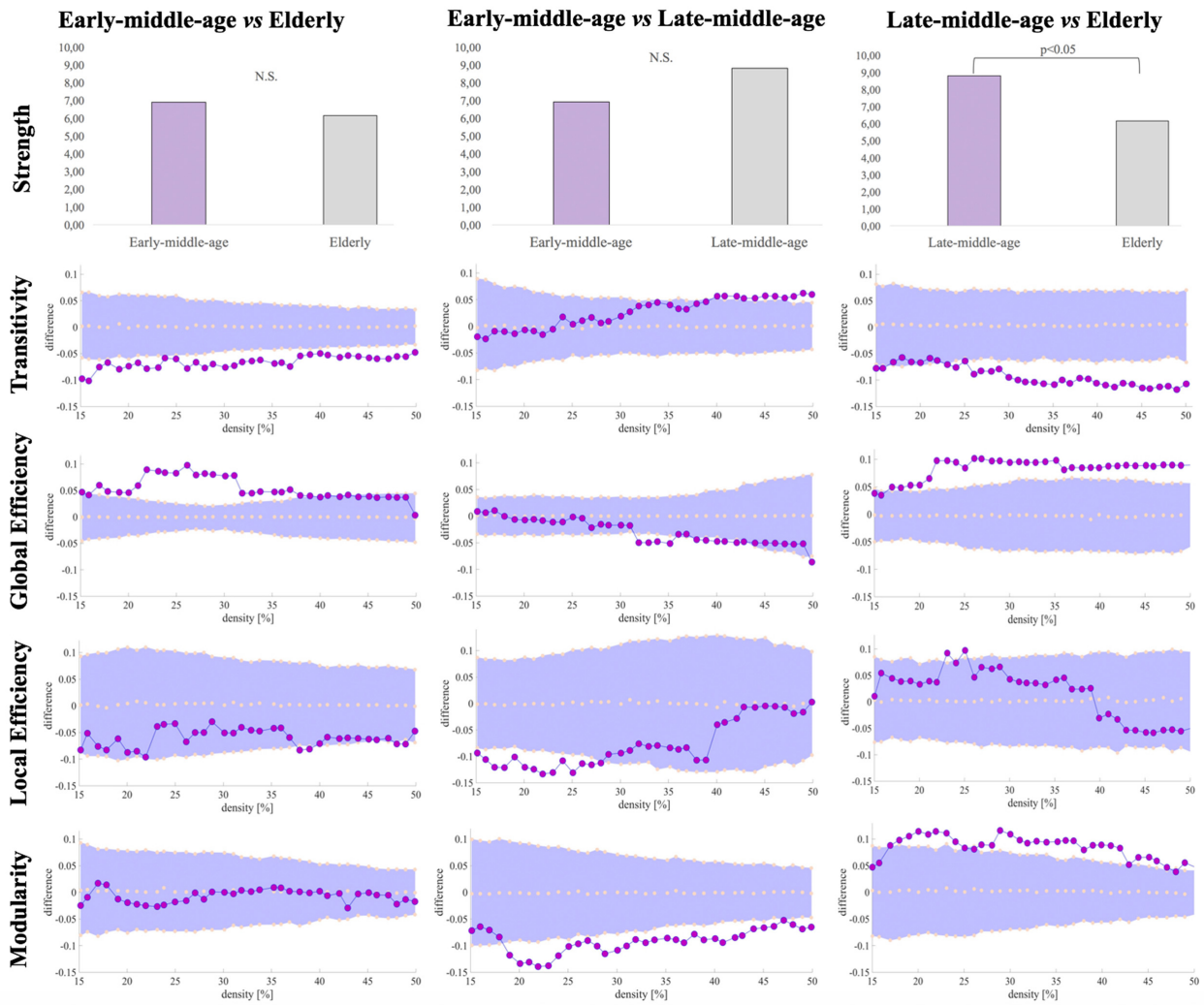

FIGURE 7 | Global network differences in the cognitive connectome across age groups. Figures illustrating modularity, local efficiency, global efficiency and transitivity measures display network densities on the x-axis, spanning from min = 15% to max = 50%, in steps of 1%. Between-group differences in network measures are displayed on the y-axis. Between-group differences are significant when the red circles fall out of the purple-shaded area. N.S., non-significant ($P > 0.05$).

analysis (Oh et al., 2012; Costa et al., 2013; Aribisala et al., 2014; Fellows and Schmitter-Edgecombe, 2015), four factors (i.e., modules) form the most frequently reported cognitive structure across all these studies. Among these four factors, verbal memory, executive function, and processing speed are the most common factors across studies. The fact that a rather stable solution of modules has repeatedly been reported irrespectively of the cohort, age range, cognitive tests used, and analytical method employed, highlights the potential existence of a universal cognitive connectome, as we have designated in our study. Future works should apply graph theory on cognitive data in other cohorts to further corroborate this idea.

Our second aim was to investigate whether this cognitive connectome differs across early-middle-age, late-middle-age, and elderly groups. Our modular analyses as well as visual inspection of the correlation matrices showed modest differences in the cognitive connectome across age groups. Specifically, the early-middle-age group showed a cognitive connectome of three modules with moderate correlations both between-modules and within-modules. The late-middle-age group showed a cognitive connectome of four modules with stronger correlations both between-modules and within-modules, especially involving executive functions. In contrast, the elderly group showed a cognitive connectome of three modules with weaker correlations, but there was a unique correlation of processing speed with other modules. These overall similarities in the cognitive connectome across age groups were also highlighted by Salthouse and Ferrer-Caja (2003), who found a similar cognitive structure when stratifying the sample by age groups. These results support the hypothesis of a stable cognitive connectome across the adulthood and older ages in healthy aging. The increase in modules from three in the early-middle-age group to four in the late-middle-age

TABLE 4 | Differences in nodal network measures from the cognitive connectome across age groups.

		Early-middle-age vs. Elderly	Early-middle-age vs. Late-middle-age	Late-middle-age vs. Elderly
Global Efficiency	PCV Motor time	↑(0.006)	n.s	↑(<0.001)
	PCV Decision time	↑(0.006)	n.s	↑(<0.001)
	CTT-Part 1	↓(0.006)	n.s	n.s
	HT 1st trial	↑(0.006)	n.s	n.s
	HT Learning	↑(0.006)	n.s	n.s
	HT Long delay	↑(0.006)	n.s	n.s
	FRT	n.s	n.s	↑(<0.001)
Local Efficiency	PCV Motor time	n.s	↓(<0.001)	n.s
	PCV Decision time	↓(<0.001)	↓(<0.001)	n.s
	HT Long delay	↑(<0.001)	n.s	↑(<0.001)
	CTT-Part 1	↓(<0.001)	↓(<0.001)	n.s
	STROOP Words	↓(<0.001)	n.s	n.s
	STROOP Inhibition	n.s	n.s	↓(<0.001)
	Semantic fluency	n.s	n.s	↓(<0.001)
Participation	STROOP Words	n.s	↑(0.003)	n.s
	STROOP Colors	↑(0.006)	↑(0.003)	n.s
	STROOP Inhibition	↑(0.006)	n.s	n.s
	Block Design Total	↑(0.006)	n.s	n.s
Nodal Strength	PCV Motor time	↑(<0.001)	n.s	↑(<0.001)
	PCV Decision time	↓(<0.001)	n.s	n.s
	CTT-Part 1	↓(<0.001)	n.s	n.s

Each column shows between-group differences in local network measures, with the first group as the reference group in the comparison: higher values in the second group in the comparison are indicated with an upwards arrow (e.g., in the "Early-middle-age vs. Elderly" comparison, an upwards arrow indicates that PCV motor time shows a higher global efficiency in the Elderly group than the Early-middle-age group), lower values in the second group in the comparison are indicated with a downwards arrow, and n.s denotes non-significant results. False discovery rate (FDR) adjustment was used at $p \leq 0.05$ (two-tailed) for analyses. FDR adjusted p-value within parentheses. PCV, PC-Vienna System; CTT, Color Trails Test; HT, Hanoi Tower; FRT, Facial Recognition Test.

group could be interpreted as a compensatory mechanism related to de-differentiation processes during the late-middle-age (Baltes et al., 1980; Hülür et al., 2015; Gonzalez-Burgos et al., 2019). This would help to partially maintain cognitive performance during late-middle age, as observed in our data. The reduction in cognitive performance in the elderly, particularly in processing speed and procedural memory, together with the decrease in modules from four in the late-middle-age group to three in the elderly group and the prominent finding of differentiation (weak correlations among variables) further support this interpretation and suggest an aberrant organization in the elderly (Park et al., 2004; Reuter-Lorenz and Cappell, 2008; Sleimen-Malkoun et al., 2014; Gonzalez-Burgos et al., 2019, 2021).

Other observations in regard to our second aim are that in the late-middle-age group, visual and executive domains split into two separate modules. In previous studies using the current cohort, we observed that visual abilities are among the cognitive domains that are most strongly associated with age (Machado et al., 2018). In turn, executive functions showed less prominent associations with age (Machado et al., 2018), suggesting that executive functions may be important to maintain high cognitive performance during late-middle-age adulthood (Park and Reuter-Lorenz, 2009; Gonzalez-Burgos et al., 2019). This interpretation is further supported in our current study by the observation of weaker within-module correlations in the visual module, stronger within-module correlations in the executive module, and stronger between-module correlations between the executive and the visual modules.

Our third aim was to gain a deeper understanding of the network features underlying age-related differences in the cognitive connectome of early-middle-age, late-middle-age, and elderly groups. Briefly, our findings showed that the late-middle-age group was less efficient and had a decreased modularity than the early-middle-age group. The elderly group showed decreased transitivity and higher efficiency than the other age groups. The comparison between elderly and late-middle-age groups showed that the elderly group had increased modularity and decreased average strength. We interpret these findings as follows. Regarding the late-middle-age group, the decrease in modularity could be explained by the stronger between-module correlations, which support our interpretation above as a de-differentiation process during late-middle-age (Baltes et al., 1980; Hülür et al., 2015; Gonzalez-Burgos et al., 2019). However, this pattern does not seem to promote the formation of local modules, which could explain the decrease in both global and local efficiency measures (Van den Heuvel and Sporns, 2019; Bullmore and Sporns, 2021). This finding may seem contradictory at first, but we recently demonstrated that reduced efficiency is a characteristic of individuals with higher cognitive performance (Gonzalez-Burgos et al., 2021). This interpretation is further supported in our current study by the observation that increased global efficiency was related to lower cognitive performance in the elderly group. In our current study, this occurred in the context of decreased transitivity and average strength, explained by a pattern of weak or non-existent correlations across most variables. We discussed this finding above as prominent cognitive differentiation suggestive of an aberrant organization in the elderly (Gonzalez-Burgos et al., 2019, 2021). The increased modularity in the elderly may be driven by the merging of processing speed and verbal memory measures in one module, and the less de-differentiated pattern of correlations as compared with the late-middle-

age group. This finding highlights the role of processing speed in the elderly (Salthouse, 1996; Schaie, 2005; Robitaille et al., 2013), as a potential compensatory mechanism on top of the prominent role of executive functions. What we observed is that elderly individuals with better processing speed managed to keep a higher performance in verbal memory. The nodal network analyses highlighted once again the important role of executive functions in late-middle-age individuals, and the role of processing speed in the elderly (Salthouse, 1996; West, 1996; Schaie, 2005; Robitaille et al., 2013).

Altogether, our current findings support two of the main theories of aging, which postulate that executive functions and processing speed drive cognitive aging (Salthouse, 1996; West, 1996). The role of the frontal lobe and its connections with other cortical and subcortical regions is the neural substrate common to these two theories of aging. While our study is on cognitive data, we could speculate that our modular organization may reflect the differentiated nature of cortical circuitry including frontal-parietal brain networks (executive—premotor module; Nowrangi et al., 2014), separate left and right medial temporal networks (verbal and visual memory modules, respectively; Squire and Bayley, 2007), and dorsolateral prefrontal networks (procedural memory module; Alexander et al., 1986). Further, this modular organization may also reflect the integrity of the brain white matter overall (processing speed module; Gunning-Dixon and Raz, 2000; Kloppenborg et al., 2014). An important contribution of our study is that we have helped to unravel the roles of executive functions and processing speed at different age groups. In particular, we demonstrated that executive functions seem to have a more prominent role during late-middle-age and elderly, whereas processing speed seems to be more relevant during the elderly.

The current study has some limitations. We performed the modular analysis with the Newman algorithm as a means to identify the cognitive connectome. The modular solution obtained with this algorithm could differ from that obtained with other methods. To minimize this problem, we also applied another popular algorithm for modular analysis: the Louvain algorithm (Blondel et al., 2008). We obtained very similar modular solutions both with Newman and Louvain algorithms, which cross-validates our findings. Furthermore, as discussed above, similar solutions have been reported using other methods such as factorial analysis and principal component analysis. This suggests that the cognitive connectome may be quite universal and does not depend on cohort, age range, cognitive tests used, or analytical method employed. Although we removed some cognitive variables from our graph analysis due to methodological reasons, the information captured in the removed variables is likely contained in variables remaining in our graph (e.g., the component reflected by the removed discrimination test from Visual Reproduction is very likely contained in other visual discrimination tests such as the Facial Recognition Test (FRT), which was retained in our graph analysis). Hence, despite methodological choices, we believe our current findings are generalizable. Future studies should test the cognitive connectome in pathological populations, and investigate whether the variables removed in this study on healthy individuals (e.g., errors) provide relevant information in such populations. Another limitation is that we analyzed cross-sectional data to investigate cognitive aging. Hence, substantiating our current results using longitudinal designs is warranted. Finally, we have demonstrated the potential of graph theory analysis on cognitive data to investigate complex associations between multiple cognitive domains and cognitive components. We interpreted our results following the principles of connectivity proposed by Van den Heuvel and Sporns (2019), which are primarily based on functional magnetic resonance imaging data. However, the field of graph theory applied to cognitive data is in its infancy, and more progress is needed to assess whether principles and interpretations need to be adjusted and new measures developed.

In conclusion, we identified a cognitive connectome that is rather stable across age in cognitively healthy individuals. Nonetheless, several differences in network features were observed, highlighting the important role of executive functions during the late-middle-age adulthood, as well as the role of processing speed during the elderly. A novelty of our study is the use of graph theory to investigate what we called the cognitive connectome. We translated the connectome concept from the neuroimaging field (Van den Heuvel and Sporns, 2019) to cognitive data, demonstrating its potential to advance our understanding of the complexity of cognitive aging. We hope that this step opens new possibilities and encourages future studies to validate and help to establish this new concept. One of the next challenges will be to integrate the well-studied brain connectome from structural and functional neuroimaging studies (Van den Heuvel and Sporns, 2019; Bullmore and Sporns, 2021), with the cognitive connectome investigated in the current study. Understanding that integration could have several important implications, both for research and clinical work in normal and pathological aging.

DATA AVAILABILITY STATEMENT

The authors of this study are willing to share the generated dataset in order to promote transparency and replicability of research, upon reasonable request from qualified researchers. Requests to access the datasets should be directed to DF, daniel.ferreira.padilla@ki.se.

ETHICS STATEMENT

The studies involving human participants were reviewed and approved by CEIBA; local ethics committee of the University of La Laguna (Spain). The patients/participants provided their written informed consent to participate in this study.

AUTHOR CONTRIBUTIONS

EG-C contributed to the design of the study, organized the database, performed statistical analyses, contributed to the interpretation of the results, and wrote the first draft of the manuscript. LG-B contributed to organize the database,

interpretation of the results, and revised the final version of the manuscript. JP contributed to the interpretation of the results, and revised the final version of the manuscript. JH-C contributed to the statistical analysis, and revised the final version of the manuscript. EW obtained funding, co-supervised the study, and revised the final version of the manuscript. GV contributed to the interpretation of the results, and revised the final version of the manuscript. JB contributed to the conception and design of the study, obtained funding, co-supervised the study, and revised the final version of the manuscript. DF contributed to the the conception and design of the study, wrote sections of the manuscript, contributed to the interpretation of the results, obtained funding, and supervised the study. All authors contributed to the article and approved the submitted version.

FUNDING

This research was funded by Estrategia de Especialización Inteligente de Canarias RIS3 de la Consejería de Economía, Industria, Comercio y Conocimiento del Gobierno de Canarias, co-funded by Programa Operativo FEDER Canarias 2014–2020 (ProID2020010063); the research grant Formación de Profesorado Universitario (FPU) from Ministerio de Educación, Cultura y Deporte (convocatoria 2019; FPU-19/00656); funding by Agencia Canaria de Investigación, Innovación y Sociedad de la Información de la Consejería de Economía, Industria, Comercio y Conocimiento y por el Fondo Social Europeo (FSE) Programa Operativo Integrado de Canarias 2014–2020, Eje 3 Tema prioritario 74 (85%); funding for Research and Geriatric Diseases at Karolinska Institutet; Demensfonden; Gamla Tjanarinnor; Sigurd och Elsa Goljes Minne Stiftelse; and Gun and Bertil Stohnes Stiftelse. Funders had no role in the study design nor the collection, analysis, and interpretation of data, writing of the report, or decision to submit the manuscript for publication.

ACKNOWLEDGMENTS

Data used in the preparation of this article is part of the GENIC-database (Group of Neuropsychological Studies of the Canary Islands, University of La Laguna, Spain. Principal investigator: Dr. José Barroso, contact: daniel.ferreira.padilla@ki.se). The following collaborators contributed to the GENIC- database but did not participate in the analysis or writing of this report (in alphabetic order by family name): Nira Cedrés, Rut Correia, Patricia Díaz, Aída Figueroa, Nerea Figueroa, Teodoro González, Zaira González, Cathaysa Hernández, Edith Hernández, Nira Jiménez, Judith López, Cándida Lozano, Alejandra Machado, María Mata, Yaiza Molina, Antonieta Nieto, María Sabucedo, Elena Sirumal, Marta Suárez, Manuel Urbano, and Pedro Velasco.

SUPPLEMENTARY MATERIAL

The Supplementary Material for this article can be found online at: https://www.frontiersin.org/articles/10.3389/fnagi.2021.694254/full#supplementary-material.

REFERENCES

Alexander, G. E., DeLong, M. R., and Strick, P. L. (1986). Parallel organization of functionally segregated circuits linking basal ganglia and cortex. *Annu. Rev. Neurosci.* 9, 357–381. doi: 10.1146/annurev.ne.09.030186.002041

Aribisala, B. S., Royle, N. A., Valdés Hernández, M. C., Murray, C., Penke, L., Gow, A., et al. (2014). Potential effect of skull thickening on the associations between cognition and brain atrophy in ageing. *Age Ageing* 43, 712–716. doi: 10.1093/ageing/afu070

Baltes, P. B., Cornelius, S. W., Spiro, A., Nesselroade, J. R., and Willis, S. L. (1980). Integration versus differentiation of fluid/crytallized intelligence in old age. *Dev. Psychol.* 16, 625–635. doi: 10.1037/0012-1649.16.6.625

Blessed, G., Tomlinson, B. E., and Roth, M. (1968). The association between quantitative measures of dementia and of senile change in the cerebral grey matter of elderly subjects. *Br. J. Psychiatry* 114, 797–811. doi: 10.1192/bjp.114.512.797

Blondel, V. D., Guillaume, J. L., Lambiotte, R., and Lefebvre, E. (2008). Fast unfolding of communities in large networks. *J. Stat. Mech.* 10:P10008. doi: 10.1088/1742-5468/2008/10/p10008

Bullmore, E., and Sporns, O. (2021). The economy of brain network organization. *Nat. Rev. Neurosci.* 13, 336–349. doi: 10.1038/nrn3214

Cedres, N., Machado, A., Molina, Y., Diaz-Galvan, P., Hernández-Cabrera, J. A., Barroso, J., et al. (2019). Subjective cognitive decline below and above the age of 60: a multivariate study on neuroimaging, cognitive, clinical and demographic measures. *J. Alzheimers Dis.* 68, 295–309. doi: 10.3233/JAD-180720

Chong, J. S. X., Ng, K. K., Tandi, J., Wang, C., Poh, J. H., Lo, J. C., et al. (2019). Longitudinal changes in the cerebral cortex functional organization of healthy elderly. *J. Neurosci.* 39, 5534–5550. doi: 10.1523/JNEUROSCI.1451-18.2019

Costa, P. S., Santos, N. C., Cunha, P., Palha, J. A., and Sousa, N. (2013). The use of bayesian latent class cluster models to classify patterns of cognitive performance in healthy ageing. *PLoS One* 8:e71940. doi: 10.1371/journal.pone.0071940

Erkinjuntti, T., Hokkanen, L., Sulkava, R., and Palo, J. (1988). The Blessed Dementia Scale as a screening test for dementia. *Int. J. Geriatr. Psychiatry* 3, 267–273. doi: 10.1002/gps.930030406

Fellows, R. P., and Schmitter-Edgecombe, M. (2015). Between-domain cognitive dispersion and functional abilities in older adults. *J. Clin. Exp. Neuropsychol.* 37, 1013–1023. doi: 10.1080/13803395.2015.1050360

Ferreira, D., Bartrés-Faz, D., Nygren, L., Rundkvist, L. J., Molina, Y., Machado, A., et al. (2016). Different reserve proxies confer overlapping and unique endurance to cortical thinning in healthy middle-aged adults. *Behav. Brain Res.* 311, 375–383. doi: 10.1016/j.bbr.2016.05.061

Ferreira, D., Correia, R., Nieto, A., Machado, A., Molina, Y., and Barroso, J. (2015). Cognitive decline before the age of 50 can be detected with sensitive cognitive measures. *Psicothema* 27, 216–222. doi: 10.7334/psicothema2014.192

Ferreira, D., Machado, A., Molina, Y., Nieto, A., Correia, R., Westman, E., et al. (2017). Cognitive variability during middle-age: possible association with neurodegeneration and cognitive reserve. *Front. Aging Neurosci.* 9:188. doi: 10.3389/fnagi.2017.00188

Ferreira, D., Pereira, J. B., Volpe, G., and Westman, E. (2019). Subtypes of Alzheimer's disease display distinct network abnormalities extending beyond their pattern of brain atrophy. *Front. Neurol.* 10:524. doi: 10.3389/fneur.2019.00524

Folstein, M. F., Folstein, S. E., and McHugh, P. R. (1975). "Mini-mental state". A practical method for grading the cognitive state of patients for the clinician. *J. Psychiatr. Res.* 12, 189–198. doi: 10.1016/0022-3956(75)90026-6

Garcia-Ramos, C., Lin, J. J., Kellermann, T. S., Bonilha, L., Prabhakaran, V., and Hermann, B. P. (2016). Graph theory and cognition: a complementary

avenue for examining neuropsychological status in epilepsy. *Epilepsy Behav.* 64, 329–335. doi: 10.1016/j.yebeh.2016.02.032

Garcia-Ramos, C., Lin, J. J., Prabhakaran, V., and Hermann, B. P. (2015). Developmental reorganization of the cognitive network in pediatric epilepsy. *PLoS One* 10:e0141186. doi: 10.1371/journal.pone.0141186

Genovese, C. R., Lazar, N. A., and Nichols, T. (2002). Thresholding of statistical maps in functional neuroimaging using the false discovery rate. *NeuroImage* 15, 870–878. doi: 10.1006/nimg.2001.1037

Gonzalez-Burgos, L., Barroso, J., and Ferreira, D. (2020). Cognitive reserve and network efficiency as compensatory mechanisms of the effect of aging on phonemic fluency. *Aging* 12, 23351–23378. doi: 10.18632/aging.202177

Gonzalez-Burgos, L., Hernández-Cabrera, J. A., Westman, E., Barroso, J., and Ferreira, D. (2019). Cognitive compensatory mechanisms in normal aging: a study on verbal fluency and the contribution of other cognitive functions. *Aging* 11, 4090–4106. doi: 10.18632/aging.102040

Gonzalez-Burgos, L., Pereira, J. B., Mohanty, R., Barroso, J., Westman, E., and Ferreira, D. (2021). Cortical networks underpinning compensation of verbal fluency in normal aging. *Cereb. Cortex* 31, 3832–3845. doi: 10.1093/cercor/bhab052

Gronwall, D. (1977). Paced auditory serial-addition task: a measure of recovery from concussion. *Percept. Mot. Skills* 44, 367–373. doi: 10.2466/pms.1977.44.2.367

Gunning-Dixon, F. M., and Raz, N. (2000). The cognitive correlates of white matter abnormalities in normal aging: a quantitative review. *Neuropsychology* 14, 224–232. doi: 10.1037//0894-4105.14.2.224

Habeck, C., Steffener, J., Barulli, D., Gazes, Y., Razlighi, Q., Shaked, D., et al. (2015). Making cognitive latent variables manifest: distinct neural networks for fluid reasoning and processing speed. *J. Cogn. Neurosci.* 27, 1249–1258. doi: 10.1162/jocn_a_00778

Harada, C. N., Natelson Love, M. C., and Triebel, K. L. (2013). Normal cognitive aging. *Clin. Geriatr. Med.* 29, 737–752. doi: 10.1016/j.cger.2013.07.002

Hayden, K. M., Kuchibhatla, M., Romero, H. R., Plassman, B. L., Burke, J. R., Browndyke, J. N., et al. (2014). Pre-clinical cognitive phenotypes for Alzheimer disease: a latent profile approach. *Am. J. Geriatr. Psychiatry* 22, 1364–1374. doi: 10.1016/j.jagp.2013.07.008

Heilman, K. M. (1995). "Attentional asymmetries," in *Brain Asymmetry*, eds R. J. Davidson and K. Hugdahl (Massachussetts, MA: MIT Press), 217–234.

Hoogendam, Y. Y., Hofman, A., van der Geest, J. N., van der Lugt, A., and Ikram, M. A. (2014). Patterns of cognitive function in aging: the Rotterdam Study. *Eur. J. Epidemiol.* 29, 133–140. doi: 10.1007/s10654-014-9885-4

Hülür, G., Ram, N., Willis, S. L., Schaie, K. W., and Gerstorf, D. (2015). Cognitive dedifferentiation with increasing age and proximity of death: within-person evidence from the Seattle Longitudinal Study. *Psychol. Aging* 30, 311–323. doi: 10.1037/a0039260

Jonker, F., Weeda, W., Rauwerda, K., and Scherder, E. (2019). The bridge between cognition and behavior in acquired brain injury: a graph theoretical approach. *Brain Behav.* 9:e01208. doi: 10.1002/brb3.1208

Jung, J., Visser, M., Binney, R. J., and Lambon Ralph, M. A. (2018). Establishing the cognitive signature of human brain networks derived from structural and functional connectivity. *Brain Struct. Funct.* 223, 4023–4038. doi: 10.1007/s00429-018-1734-x

Kellermann, T. S., Bonilha, L., Lin, J. J., and Hermann, B. P. (2015). Mapping the landscape of cognitive development in children with epilepsy. *Cortex* 66, 1–8. doi: 10.1016/j.cortex.2015.02.001

Kloppenborg, R. P., Nederkoorn, P. J., Geerlings, M. I., and van den Berg, E. (2014). Presence and progression of white matter hyperintensities and cognition: a meta-analysis. *Neurology* 82, 2127–2138. doi: 10.1212/WNL.0000000000000505

Kong, X.-Z., Mathias, S. R., Guadalupe, T., ENIGMA Laterality Working Group, Glahn, D. C., Franke, B., et al. (2018). Mapping cortical brain asymmetry in 17,141 healthy individuals worldwide *via* the ENIGMA Consortium. *Proc. Natl. Acad. Sci. U S A* 115, E5154–E5163. doi: 10.1073/pnas.1718418115

Lachman, M. E. (2004). Development in midlife. *Annu. Rev. Psychol.* 55, 305–331. doi: 10.1146/annurev.psych.55.090902.141521

Lee, D. H., Lee, P., Seo, S. W., Roh, J. H., Oh, M., Oh, J. S., et al. (2019). Neural substrates of cognitive reserve in Alzheimer's disease spectrum and normal aging. *NeuroImage* 186, 690–702. doi: 10.1016/j.neuroimage.2018.11.053

Machado, A., Barroso, J., Molina, Y., Nieto, A., Díaz-Flores, L., Westman, E., et al. (2018). Proposal for a hierarchical, multidimensional, and multivariate approach to investigate cognitive aging. *Neurobiol. Aging* 71, 179–188. doi: 10.1016/j.neurobiolaging.2018.07.017

Mårtensson, G., Pereira, J. B., Mecocci, P., Vellas, B., Tsolaki, M., Koszewska, I., et al. (2018). Stability of graph theoretical measures in structural brain networks in Alzheimer's disease. *Sci. Rep.* 8:11592. doi: 10.1038/s41598-018-29927-0

Mijalkov, M., Kakaei, E., Pereira, J. B., Westman, E., Volpe, G., and Alzheimer's Disease Neuroimaging Initiative. (2017). BRAPH: a graph theory software for the analysis of brain connectivity. *PLoS One* 12:e0178798. doi: 10.1371/journal.pone.0178798

Mitchell, M. B., Shaughnessy, L. W., Shirk, S. D., Yang, F. M., and Atri, A. (2012). Neuropsychological test performance and cognitive reserve in healthy aging and the Alzheimer's disease spectrum: a theoretically driven factor analysis. *J. Int. Neuropsychol. Soc.* 18, 1071–1080. doi: 10.1017/S1355617712000859

Mungas, D., Heaton, R., Tulsky, D., Zelazo, P. D., Slotkin, J., Blitz, D., et al. (2014). Factor structure, convergent validity, and discriminant validity of the NIH Toolbox Cognitive Health Battery (NIHTB-CHB) in adults. *J. Int. Neuropsychol. Soc.* 20, 579–587. doi: 10.1017/S1355617714000307

Newman, M. E. (2004). Fast algorithm for detecting community structure in networks. *Phys. Rev. E Stat. Nonlin. Soft. Matter Phys.* 69:066133. doi: 10.1103/PhysRevE.69.066133

Nielsen, S., and Wilms, L. I. (2015). Cognitive aging on latent constructs for visual processing capacity: a novel structural equation modeling framework with causal assumptions based on a theory of visual attention. *Front. Psychol.* 5:1596. doi: 10.3389/fpsyg.2014.01596

Nowrangi, M. A., Lyketsos, C., Rao, V., and Munro, C. A. (2014). Systematic review of neuroimaging correlates of executive functioning: converging evidence from different clinical populations. *J. Neuropsychiatry Clin. Neurosci.* 26, 114–125. doi: 10.1176/appi.neuropsych.12070176

Oh, H., Madison, C., Haight, T. J., Markley, C., and Jagust, W. J. (2012). Effects of age and β-amyloid on cognitive changes in normal elderly people. *Neurobiol. Aging* 33, 2746–2755. doi: 10.1016/j.neurobiolaging.2012.02.008

Oschwald, J., Guye, S., Liem, F., Rast, P., Willis, S., Röcke, C., et al. (2019). Brain structure and cognitive ability in healthy aging: a review on longitudinal correlated change. *Rev. Neurosci.* 31, 1–57. doi: 10.1515/revneuro-2018-0096

Park, D. C., Polk, T. A., Park, R., Minear, M., Savage, A., and Smith, M. R. (2004). Aging reduces neural specialization in ventral visual cortex. *Proc. Natl. Acad. Sci. U S A* 101, 13091–13095. doi: 10.1073/pnas.0405148101

Park, D. C., and Reuter-Lorenz, P. (2009). The adaptive brain: aging and neurocognitive scaffolding. *Annu. Rev. Psychol.* 60, 173–196. doi: 10.1146/annurev.psych.59.103006.093656

Pereira, J. B., Strandberg, T. O., Palmqvist, S., Volpe, G., van Westen, D., Westman, E., et al. (2018). Amyloid network topology characterizes the progression of Alzheimer's disease during the predementia stages. *Cereb. Cortex* 28, 340–349. doi: 10.1093/cercor/bhx294

Pfeffer, R. I., Kurosaki, T. T., Harrah, C. H. Jr., Chance, J. M., and Filos, S. (1982). Measurement of functional activities in older adults in the community. *J. Gerontol.* 37, 323–329. doi: 10.1093/geronj/37.3.323

Reas, E. T., Laughlin, G. A., Bergstrom, J., Kritz-Silverstein, D., Barrett-Connor, E., and McEvoy, L. K. (2017). Effects of sex and education on cognitive change over a 27-year period in older adults: the rancho bernardo study. *Am. J. Geriatr. Psychiatry* 25, 889–899. doi: 10.1016/j.jagp.2017.03.008

Reuter-Lorenz, P. A., and Cappell, K. A. (2008). Neurocognitive aging and the compensation hypothesis. *Curr. Dir. Psychol. Sci.* 17, 177–182. doi: 10.1111/j.1467-8721.2008.00570.x

Rizio, A. A., and Diaz, M. T. (2016). Language, aging and cognition: frontal aslant tract and superior longitudinal fasciculus contribute toward working memory performance in older adults. *NeuroReport* 27, 689–693. doi: 10.1097/WNR.0000000000000597

Robitaille, A., Piccinin, A. M., Muniz-Terrera, G., Hoffman, L., Johansson, B., Deeg, D., et al. (2013). Longitudinal mediation of processing speed on age-related change in memory and fluid intelligence. *Psychol. Aging* 28, 887–901. doi: 10.1037/a0033316

Salthouse, T. A. (1996). The processing-speed theory of adult age differences in cognition. *Psychol. Rev.* 103, 403–428. doi: 10.1037/0033-295x.103.3.403

Salthouse, T. A. (2009). When does age-related cognitive decline begin? *Neurobiol. Aging* 30, 507–514. doi: 10.1016/j.neurobiolaging.2008.09.023

Salthouse, T. A. (2010). Selective review of cognitive aging. *J. Int. Neuropsychol. Soc.* 16, 754–760. doi: 10.1017/S1355617710000706

Salthouse, T. A. (2016). Continuity of cognitive change across adulthood. *Psychon. Bull. Rev.* 23, 932–939. doi: 10.3758/s13423-015-0910-8

Salthouse, T. A., and Ferrer-Caja, E. (2003). What needs to be explained to account for age-related effects on multiple cognitive variables? *Psychol. Aging* 18, 91–110. doi: 10.1037/0882-7974.18.1.91

Salthouse, T. A., Habeck, C., Razlighi, Q., Barulli, D., Gazes, Y., and Stern, Y. (2015). Breadth and age-dependency of relations between cortical thickness and cognition. *Neurobiol. Aging* 36, 3020–3028. doi: 10.1016/j.neurobiolaging.2015.08.011

Schaie, K. W. (2005). What can we learn from longitudinal studies of adult development? *Res. Hum. Dev.* 2, 133–158. doi: 10.1207/s15427617rhd0203_4

Schroeder, D. H., and Salthouse, T. A. (2004). Age-related effects on cognition between 20 and 50 years of age. *Pers. Individual Differences* 36, 393–404. doi: 10.1016/s0191-8869(03)00104-1

Sleimen-Malkoun, R., Temprado, J. J., and Hong, S. L. (2014). Aging induced loss of complexity and dedifferentiation: consequences for coordination dynamics within and between brain, muscular and behavioral levels. *Front. Aging Neurosci.* 6:140. doi: 10.3389/fnagi.2014.00140

Springer, J. A., Binder, J. R., Hammeke, T. A., Swanson, S. J., Frost, J. A., Bellgowan, P. S., et al. (1999). Language dominance in neurologically normal and epilepsy subjects: a functional MRI study. *Brain* 122, 2033–2046. doi: 10.1093/brain/122.11.2033

Squire, L. R., and Bayley, P. J. (2007). The neuroscience of remote memory. *Curr. Opin. Neurobiol.* 17, 185–196. doi: 10.1016/j.conb.2007.02.006

Tisserand, D. J., and Jolles, J. (2003). Special issue on the involment of prefrontal networks in cognitive ageing. *Cortex* 39, 1107–1128. doi: 10.1016/S0010-9452(08)70880-3

Van den Heuvel, M. P., and Sporns, O. (2019). A cross-disorder connectome landscape of brain dysconnectivity. *Nat. Rev. Neurosci.* 20, 435–446. doi: 10.1038/s41583-019-0177-6

Viroli, C. (2012). Using factor mixture analysis to model heterogeneity, cognitive structure, and determinants of dementia: an application to the Aging, Demographics, and Memory Study. *Stat. Med.* 31, 2110–2122. doi: 10.1002/sim.5320

Wechsler, D. (1997a). *Wechsler Adult Intelligence Scale—Administration and Scoring Manual.* 3rd Edn. San Antonio, TX: The Psychological Corporation.

Wechsler, D. (1997b). *Wechsler Memory Scale—Third Edition Technical Manual.* 3rd Edn. San Antonio, TX: The Psychological Corporation.

Welton, T., Kent, D. A., Auer, D. P., and Dineen, R. A. (2015). Reproducibility of graph-theoretic brain network metrics: a systematic review. *Brain Connect.* 5, 193–202. doi: 10.1089/brain.2014.0313

West, R. (2001). The transient nature of executive control processes in younger and older adults. *Eur. J. Cogn. Psychol.* 13, 91–105. doi: 10.1080/09541440042000232

West, R. L. (1996). An application of prefrontal cortex function theory to cognitive aging. *Psychol. Bull.* 120, 272–292. doi: 10.1037/0033-2909.120.2.272

Willis, S. L., Martin, M., and Rocke, C. (2010). Longitudinal perspectives on midlife development: stability and change. *Eur. J. Ageing* 7, 131–134. doi: 10.1007/s10433-010-0162-4

Winblad, B., Palmer, K., Kivipelto, M., Jelic, V., Fratiglioni, L., Wahlund, L. O., et al. (2004). Mild cognitive impairment—beyond controversies, towards a consensus: report of the international working group on mild cognitive impairment. *J. Intern. Med.* 256, 240–246. doi: 10.1111/j.1365-2796.2004.01380.x

Xia, Y., Chen, Q., Shi, L., Li, M. Z., Gong, W., Chen, H., et al. (2019). Tracking the dynamic functional connectivity structure of the human brain across the adult lifespan. *Hum. Brain Mapp.* 40, 717–728. doi: 10.1002/hbm.24385

Zaidel, D. W. (1990). "Memory and spatial cognition following commissurotomy," in *Handbook of Neuropsychology, vol 4*, eds F. Boller and J. Grafman (Amsterdam: Elsevier).

Zhu, W., Wen, W., He, Y., Xia, A., Anstey, K. J., and Sachdev, P. (2012). Changing topological patterns in normal aging using large-scale structural networks. *Neurobiol. Aging* 33, 899–913. doi: 10.1016/j.neurobiolaging.2010.06.022

Conflict of Interest: The authors declare that the research was conducted in the absence of any commercial or financial relationships that could be construed as a potential conflict of interest.

Publisher's Note: All claims expressed in this article are solely those of the authors and do not necessarily represent those of their affiliated organizations, or those of the publisher, the editors and the reviewers. Any product that may be evaluated in this article, or claim that may be made by its manufacturer, is not guaranteed or endorsed by the publisher.

frontiers | Frontiers in Aging Neuroscience

ORIGINAL RESEARCH
published: 30 May 2022
doi: 10.3389/fnagi.2022.863580

Still Wanting to Win: Reward System Stability in Healthy Aging

Laura Opitz[1,2†], Franziska Wagner[1,2,3†], Jenny Rogenz[1,2], Johanna Maas[1,2], Alexander Schmidt[1,2], Stefan Brodoehl[1,2] and Carsten M. Klingner[1,2]*

[1] Hans Berger Department of Neurology, Jena University Hospital, Jena, Germany, [2] Biomagnetic Center, Jena University Hospital, Jena, Germany, [3] Clinician Scientist Program OrganAge, Jena University Hospital, Jena, Germany

Healthy aging is accompanied by multi-faceted changes. Especially within the brain, healthy aging exerts substantial impetus on core parts of cognitive and motivational networks. Rewards comprise basic needs, such as food, sleep, and social contact. Thus, a functionally intact reward system remains indispensable for elderly people to cope with everyday life and adapt to their changing environment. Research shows that reward system function is better preserved in the elderly than most cognitive functions. To investigate the compensatory mechanisms providing reward system stability in aging, we employed a well-established reward paradigm (Monetary Incentive Delay Task) in groups of young and old participants while undergoing EEG measurement. As a new approach, we applied EEG connectivity analyses to assess cortical reward-related network connectivity. At the behavioral level, our results confirm that the function of the reward system is preserved in old age. The mechanisms identified for maintaining reward system function in old age do not fit into previously described models of cognitive aging. Overall, older adults exhibit lower reward-related connectivity modulation, higher reliance on posterior and right-lateralized brain areas than younger adults, and connectivity modulation in the opposite direction than younger adults, with usually greater connectivity during non-reward compared to reward conditions. We believe that the reward system has unique compensatory mechanisms distinct from other cognitive functions, probably due to its etymologically very early origin. In summary, this study provides important new insights into cortical reward network connectivity in healthy aging.

Keywords: healthy aging, EEG, reward, functional connectivity, HAROLD, PASA

OPEN ACCESS

Edited by:
Cosimo Urgesi,
University of Udine, Italy

Reviewed by:
Bhoomika Kar,
Allahabad University, India
Holly Jeanne Bowen,
Southern Methodist University, United States

***Correspondence:**
Franziska Wagner
franziska.wagner@med.uni-jena.de

† These authors have contributed equally to this work and share first authorship

Specialty section:
This article was submitted to Neurocognitive Aging and Behavior, a section of the journal Frontiers in Aging Neuroscience

Received: *27 January 2022*
Accepted: *14 April 2022*
Published: *30 May 2022*

Citation:
Opitz L, Wagner F, Rogenz J, Maas J, Schmidt A, Brodoehl S and Klingner CM (2022) Still Wanting to Win: Reward System Stability in Healthy Aging. Front. Aging Neurosci. 14:863580. doi: 10.3389/fnagi.2022.863580

Abbreviations: BDI-II, Beck Depression Inventory II; C, Central; DPSS, discrete prolate spheroidal sequences; EEG, Electroencephalography; EQ-5D, European quality of life 5 dimensions; FCL, Frontocentral left; FCR, Frontocentral right; FDR, False discovery rate; FL, Frontal left; FP, Frontopolar; FPCN, Frontoparietal control network; FR, Frontal right; GEE, Generalized estimating equations; HAROLD, Hemispheric asymmetry reduction in older adults; ICA, Independent component analysis; MEG, Magnetoencephalography; MID, Monetary incentive delay task; MoCA, Montreal cognitive assessment; mPFC, Medial prefrontal cortex; O, Occipital; OFC, Orbitofrontal cortex; PASA, Posterior-anterior shift in aging; PL, Parietal left; POC, Parietooccipital central; POL, Parietooccipital left; POR, Parietooccipital right; PR, Parietal right; py, pack years of smoking; RT, Reaction time; SF-36, Short form-36 health survey; SST, Socioemotional selectivity theory; TL, Temporal left; TR, Temporal right; VAN, Ventral attention network.

INTRODUCTION

In a globally aging society, understanding motivational and cognitive processes in the elderly are of growing importance. A functionally intact reward system remains indispensable in healthy aging to succeed in daily life. Reward prediction and receiving are involved in every part of an individual's behavior, shaping its actions to obtain rewards and avoid punishment (Schultz, 1998; Wise, 2004; Berridge and Kringelbach, 2008). Reward measurably improves cognitive performance and decision-making in humans (Spaniol et al., 2014; Cohen et al., 2016; Cox and Witten, 2019; Bowen et al., 2020). Cognition is inseparably intertwined with reward processing (Pessoa and Engelmann, 2010). Rewards exert extensive influences on behavior, mediating multi-faceted cognitive processes (Braver et al., 2014). In this way, reward-based enhancement of cognitive performance is conveyed through cognitive control processes (Jimura et al., 2010; Pessoa and Engelmann, 2010). Cognitive as well as reward functions critically rely on cortical areas like the PFC and parietal cortex, serving the integration of reward and cognitive control networks (Pessoa and Engelmann, 2010; Braver et al., 2014; Chau et al., 2018). Across these links, the reward network functionally interacts with cognition-related large-scale networks like the frontoparietal control network (FPCN), default network (DN), and ventral and dorsal attention network (VAN, DAN) (Raichle et al., 2001; Corbetta and Shulman, 2002; Vincent et al., 2008; Spaniol et al., 2015; Parro et al., 2018). The reward system's core part is the mesocorticolimbic dopamine system, comprising projections of midbrain dopamine neurons to cortical structures, such as the medial prefrontal (mPFC) and orbitofrontal cortex (OFC) (Wise, 2004; Björklund and Dunnett, 2007; Lammel et al., 2008; Haber and Knutson, 2010; Ikemoto, 2010).

All the structures and mechanisms involved are subject to age-related changes. For instance, brain volume decreases with age up to 0.5% per year at the age of 60 (Hedman et al., 2012); locally pronounced in prefrontal areas (Gordon et al., 2008; Raz et al., 2010; Zanto and Gazzaley, 2019). Furthermore, the most important neurotransmitter in the reward system, the dopamine system (Wise, 2002; Schultz, 2007) declines with age (Fearnley and Lees, 1991; Backman et al., 2006; Li et al., 2009; Karrer et al., 2017).

These multilayered structural changes inevitably affect related brain functions, not only in the reward system but also in a wide range of cognitive areas. Interestingly, not all cognitive domains are equally affected by age-related changes (Lyoo and Yoon, 2017).

Recent studies have indicated that the reward system's function is less affected by age-related changes than other highly interconnected functions like fluid cognitive domains (Blum et al., 2018; Tryon et al., 2020). Reward sensitivity remains preserved in age as older people are able to exhibit enhanced performance (Spaniol et al., 2015; Castel et al., 2016; Yee et al., 2019) and restoration of age-impaired cognitive abilities under incentive motivation (Ferdinand and Czernochowski, 2018). With respect to this divergency, however, it remains an open question how the aging brain manages to preserve the functionality of the reward system despite the cellular and molecular changes affecting its core parts. In general, older adults attempt to preserve their cognitive abilities with reduced resources by employing compensatory mechanisms. These compensatory mechanisms are well-observed in fMRI brain network alterations in older adults that comprise hypo- and hyperactivations in specific patterns that have been summarized in several models. Three of these models characterizing mechanisms of cognitive aging are the HAROLD (Hemispheric Asymmetry Reduction in Older Adults) (Cabeza, 2002), the PASA (posterior-anterior shift in aging) model (Davis et al., 2008), and the theory of frontoparietal control network (FPCN) hyperactivation (Reuter-Lorenz and Park, 2014; Li et al., 2015). The HAROLD model describes bilateral frontal cortical activation in older adults in comparison to lateralized frontal cortical activation in younger adults (Cabeza, 2002; Cabeza et al., 2018). PASA coherently describes a prefrontal over-related to an occipital underrecruitment in older compared to younger adults (Davis et al., 2008). FPCN network hyperactivation, HAROLD, and PASA all have been found to be associated with improved cognitive performance in healthy aging (Li et al., 2015). Qualifying that, HAROLD and PASA or FPCN hyperactivation to date have been tested using demanding cognitive tasks. Additionally, these models have been proposed to reflect aging mechanisms in salience networks (Jacques et al., 2013). Compensatory reorganization of cognitive networks during reward processing has already been reported in healthy aging (Spaniol et al., 2015). It remains unclear which compensatory mechanisms underlie reward system function in healthy aging and whether these models are able to explain preserved reward system stability.

We performed a study contrasting older and younger participant groups in a monetary incentive delay task (MID) using electroencephalography (EEG) (Knutson et al., 2000). Reward-guided acting can be separated into two distinct temporal phases, the prediction and the receiving phases. The MID allows to dissociate both phases. In the prediction phase, a reward-predicting stimulus elicits specific approach behavior, serving the obtaining of a reward (Schultz, 2006). Reward receipt is accompanied by pleasure, known as hedonia (Berridge and Kringelbach, 2015; Becker et al., 2019). EEG offers a high temporal resolution and, therefore, provides detailed information on the time course of neuronal information processing (Andrä and Nowak, 2007). Rapidly changing network states can be investigated by employing functional connectivity analyses (Friston, 2011; Fries, 2015; Meyer et al., 2021).

Studies investigating reward processing in healthy aging largely confirmed the notion of preserved reward sensitivity in older adults. In EEG studies, reward prediction has been related to increased frontal theta power (Doñamayor et al., 2012; Gruber et al., 2013), whereas reward consumption was associated with high-beta oscillations (20-35 Hz) in younger adults (Marco-Pallarés et al., 2015). Only one study investigated age-related effects of incentives on brain oscillations, reporting increased frontocentral and parietooccipital theta power for reward anticipation in older but not younger adults (Steiger and Bunzeck, 2017). To date, no EEG studies investigating

aging effects on the reward system with complex functional connectivity analyses, especially in the context of compensation, have been published (Meyer et al., 2021).

This study aims to further understand the neural mechanisms providing for generally stable reward system function in the elderly. Therefore, we first hypothesized a behaviorally preserved reward system function in older adults. For investigating reward-based modulation of large-scale brain networks, functional brain connectivity analyses were employed. Based on previous studies, diminished neuronal reward effects on older adults are expected. We hypothesized altered responses to occur in reward-related frequency bands: in the alpha band due to its involvement in attentional processes (Sadaghiani and Kleinschmidt, 2016) and reward prediction (Heuer et al., 2017); in the delta band as it has been associated with reward, motivation, and salience detection (Knyazev, 2012); in the theta and high-beta bands for their roles in reward feedback processing (Luft, 2014; Andreou et al., 2017; Glazer et al., 2018). Furthermore, we especially focused on compensatory mechanisms within the reward system and changes in cognition-related networks during reward processing in older adults. Due to the close link between reward processing and cognition, we propose established functional compensatory mechanisms of cognitive control (i.e., HAROLD, PASA, and FPCN hyperactivation) to apply to preserved reward system function in healthy aging.

MATERIALS AND METHODS

Participants

This study was comprised of 46 healthy volunteers (**Table 1**) with no history of neurological or psychiatric disease, who were divided into 2 groups according to their age. The younger group comprised 22 subjects (13 women), aged 18 to 33 years (mean, 24.59 ± 3.96), and the older group, 24 subjects (13 women), aged 62 to 86 years (mean, 69.42 ± 5.85). Prior to the monetary incentive delay task (MID), the subjects had undergone an assessment with an anamnesis questionnaire and standardized questionnaires (Edinburgh Handedness Inventory, BDI-II, SF-36 (Kirchberger, 2000), EQ-5D (EuroQol Group, 1990), and the MoCA (Nasreddine et al., 2005) test for the older group (**Table 1**). All the subjects were right-handed according to the Edinburgh Handedness Inventory (Oldfield, 1971). We explicitly tested for the presence of depressive symptoms and included only the subjects with a BDI-II Score $< = 14$ points (Beck et al., 1996). Further exclusion criteria were sight defects, substance dependence, and current ingestion of psychopharmaca. From the initial sample of 49 subjects, data of three subjects had to be excluded from analysis because of red-green color blindness (one subject), technical errors (2 subjects). All experiments were approved by the local ethics committee, and all the subjects provided written informed consent in accordance with the Declaration of Helsinki.

Stimuli and Procedure

In this study, we utilized the monetary incentive delay task (MID), which is the most frequently used paradigm for examining reward system function (Knutson et al., 2000). In this paradigm, scalable monetary cues indicate possible rewards that can be earned by a fast response to a target.

The here employed version of the MID task (**Figure 1**) consisted of 450 trials (300 trials for the older group), subdivided into three blocks of 150 (100) trials with short breaks in between (**Figure 1**). Each trial randomly started with one of the three following reward incentive cues:

> A circle with one line indicated a possible gain of 3 cents.
> A circle with two lines, indicating a possible gain of 30 cents.
> A triangle, indicating a possible gain of 0 cent. Cue were shown for 250 ms each. The trials cued with a triangle (0 cent - gain) served as the neutral control condition.

The participants were told to hit the answer button with their right index fingers as fast as possible as soon as a white square (the target) appeared on the screen afterward. Between the cue and the target, a fixation cross with randomized duration (750-1,250 ms) was presented. Target duration adapted to individual reaction times, resulting in a predestined hit rate of 75%. Performance feedback was presented by a green laughing smiley if the time limit was not exceeded. A red sad smiley appeared otherwise. Afterward, pictures of coins visualized monetary rewards. Both feedback screens had duration of 1,000 ms each. For investigating neural mechanisms of reward prediction error, in 50 (33 for the older group) trials, unexpectedly, no monetary rewards were distributed. Gain cues preceded these trials, and the participants hit in time (positive feedback), but, on the last screen, a gray coin was displayed (not analyzed in this study). The participants received a start budget of 20€ (30€) and could earn about 30€ (20€). They were told in the beginning that the money they earned (**Table 1**) would be paid as an expense allowance by non-cash payment afterward. Test persons performed a short training session in advance.

Measurements took place in a magnetically shielded chamber of the Biomagnetic Centre, Compartment of Neurology, in the University Hospital of Friedrich-Schiller-University Jena. EEG was conducted using MEG-compatible 60-channel EEG caps (Waveguard, ANT). Stimuli were presented on a screen in the chamber using Presentation (Neurobehavioral Systems, Inc., Berkeley, CA., United States, Version 16.3). The participants

TABLE 1 | An overview of test person groups and assessment.

	YOUNG GROUP	OLD GROUP
Participants	22	24
Sex	13 female, 9 male	13 female, 11 male
Age	18-33 years (mean 24.59 ± 3.96)	62-86 years (mean 69.42 ± 5.85)
BDI-II	median 1.5 points (IQR = 6, range 0-11)	median 4.0 points (IQR = 7, range 0-13)
MoCA	–	mean score 25.75 ± 2.07 (range 21-29 points)
Mean money gain in €	52.69 ± 1.18 (range, 50.09 – 55.25)	51.45 ± 1.57 (48.66 – 54.75)

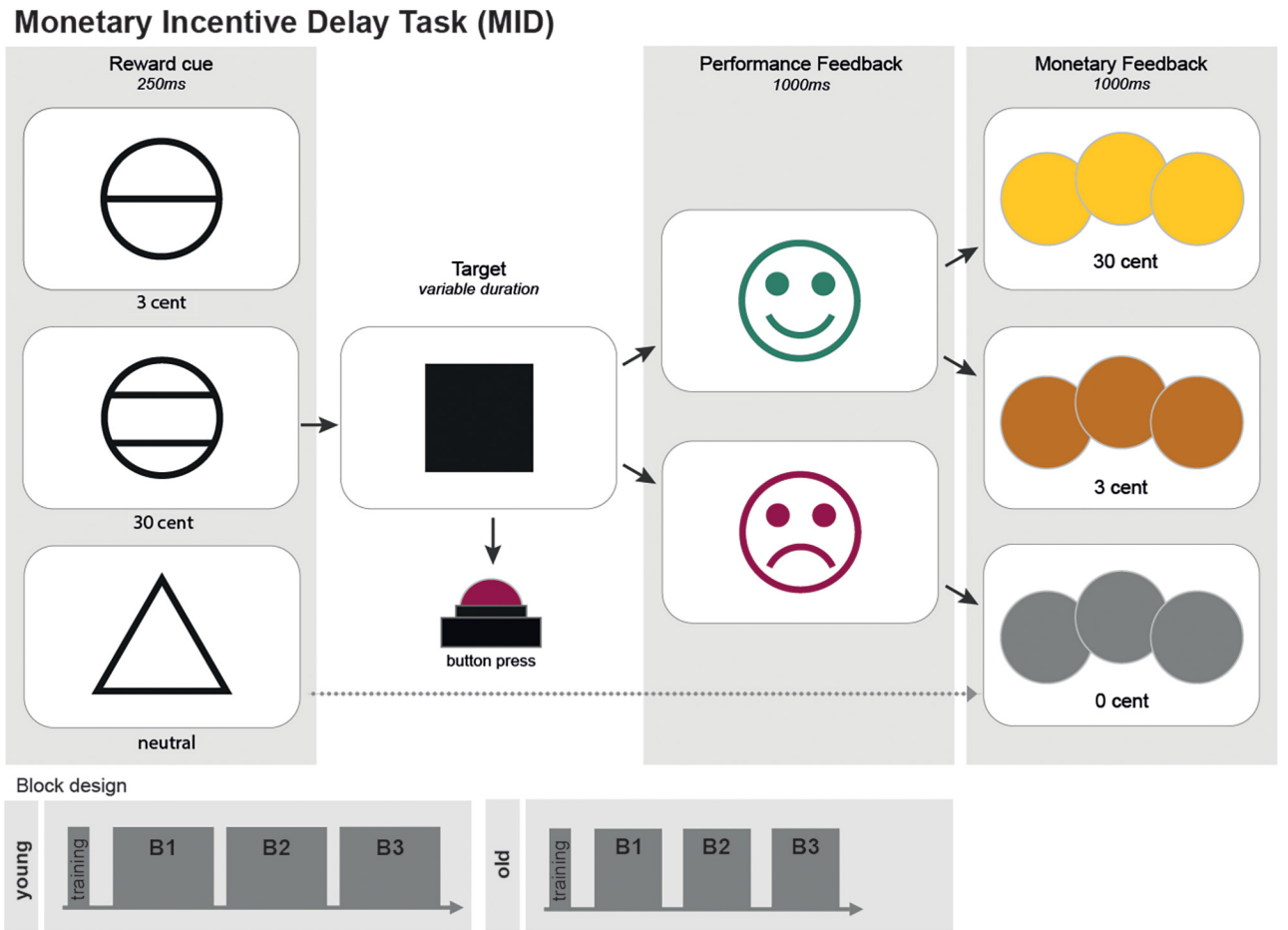

FIGURE 1 | A scheme of the monetary incentive delay task (MID). The MID consisted of 450 trials (300 trials for the older group) separated into three blocks. Each trial randomly started with one of the three following reward incentive cues: a circle with one line indicated a possible gain of 3 cents; a circle with two lines, indicating a possible gain of 30 cents; and a triangle, indicating a possible gain of 0 cent. The cues were shown for 250 ms each. The trials cued with a triangle (0 cent-gain) served as the neutral control condition. Between the cue and the target, a fixation cross with randomized duration (750-1,250 ms) was presented. Target duration was adapted to individual reaction times, resulting in a predestined hit rate of 75%. Performance feedback was presented by a green laughing smiley if the time limit was not exceeded. A red sad smiley appeared otherwise. Afterward, pictures of coins visualized monetary rewards. Both feedback screens had duration of 1,000 ms each.

responded with a keyboard (a LUMItouch photon control optical response pad). The participants had sufficient or corrected-to-normal vision.

Preprocessing of EEG Data

EEG data were acquired using a sampling rate of 1 kHz. A bandpass filter for.1–1,000 Hz was applied. Measurement data were preprocessed with the MatLab fieldtrip toolbox (Oostenveld et al., 2011). Measurement files were segmented into trials lasting from −.5 to 1. s around the trigger onset. These trials were entirely employed for subsequent analyses. The data were downsampled to 500 Hz and then submitted to a visual artifact correction method, reject visual. Bad EEG channels and trials with artifacts were removed. An independent component analysis (ICA) was performed to correct for eyeblink and heartbeat artifacts, as well as electric noise. Finally, a bandpass filter for.1–100 Hz was applied. To provide analysis with respect to functional segregation of cortical areas, EEG channels were anatomically divided into 14 groups corresponding to their underlying brain regions (**Figures 2A,B**).

Connectivity analyses (Friston, 2011; Sakkalis, 2011) were applied by estimating coherence with the fieldtrip toolbox (Oostenveld et al., 2011), employing a non-parametric approach event-related for frequencies of 1. to 40 Hz (in 1-Hz steps) for all combinations of channel groups (Pereda et al., 2005). First, data were Fast Fourier transformed (Cooley and Tukey, 1965) using DPSS (discrete prolate spheroidal sequences) as a tapering function. Then, the cross-spectral density (**Formula 1**)

FORMULA 1 | Calculation of cross-spectral density of Fourier-transformed data X (f) and Y (f) (Kida et al., 2015).

$$G_{xy}(f) = X(f)\,Y^{T}(f)$$

A

EEG CHANNEL GROUPS		EEG ELECTRODES
Frontopolar	FP	FPz, FZ
Frontal left	FL	FP1, AF3, AF7, F7
Frontal right	FR	FP2, AF4, AF8, F8
Temporal left	TL	FT9, FT7, T7, TP7, TP9, P7
Temporal right	TR	FT10, FT8, T8, TP8, TP10, P8
Frontocentral left	FCL	F1, F3, FC1, FC5
Frontocentral right	FCR	F2, F4, FC2, FC6
Parietal left	PL	C1, C3, C5, CP1, CP3, CP5
Parietal right	PR	C2, C4, C6, CP2, CP4, CP6
Central	C	FCz, Cz, CPz
Parietooccipital left	POL	P1, P3, PO3
Parietooccipital right	POR	P2, P4, PO4
Parietooccipital central	POC	Pz, POz
Occipital	O	Oz, O1, O2, PO7, PO8

B

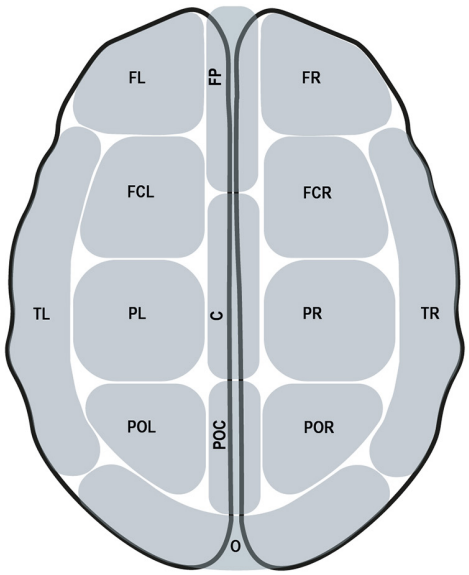

FIGURE 2 | EEG channel groups **(A),** an overview of EEG channels and their assignment to regional channel groups. **(B)** Simplified scheme of EEG channel groups defined in 2 **(A)**.

was computed from frequency domain data. Finally, using the cross-spectral density matrix, the coherence coefficient $C_{XY}(f)$ for signals X and Y representing pairwise channel-group combinations was calculated (**Formula 2**)[1].

As coherence analysis here was conducted on the channel group level, spatial resolution was reduced in advance to serve asgreater reliability of results. Averaging of signals across these regional channel groups facilitates dissociation of adjacent regions and reduces short-interelectrode-distance volume conduction effects. Consequently, genuine coherence results can be expected for inter-regional coherence, especially for non-adjacent channel groups (Srinivasan et al., 2007; Fries, 2015).

Statistical Analysis

Coherence results were analyzed using R (Version 4.1.1/Kick Things) (R Core Team, 2020) and RStudio (Version 2021.09.0 Build 351) (RStudio Team, 2020). Coherence coefficients of each channel combination were averaged across frequency bands (alpha, 8–12 Hz; beta, 13–30 Hz; delta, 0.5–3 Hz; theta, 4–7 Hz) (Engel and Fries, 2010). We were interested in group differences in the connectedness between prespecified channel groups (channel groups = networks) (**Figure 2**). To access the between network connectivity, the connectivity between each combination of channels of the two networks was estimated and averaged for each participant. Afterward, coherence values were transformed into a z-score by Fisher's z-transformation. This analysis was performed separately for each experimental condition, resulting in one averaged value per network-condition subject. Within-group comparisons of the between network connectivity were performed by a paired *t*-test between the experimental conditions. To account for between-group differences, Welch's two sample *t*-test was used by entering the connectivity difference between experimental conditions for each subject. All results were corrected for multiple comparison by using the false discovery rate (FDR).

Statistical analyses of questionnaire data were conducted using SPSS software (Version 27, IBM). If the normal distribution was not given, nonparametric tests were employed. Reaction times were resolved by excluding misses and values below 150 ms as well as all reaction times above 414 ms (75. quartile plus 3*IQR) as outliers (Baayen and Milin, 2010; Marković et al., 2019).

To analyze reaction times, generalized estimating equations (GEE) assuming a normal-distributed response (Liang and Zeger, 1986; Højsgaard et al., 2005) were calculated using R (Version 4.1.1/Kick Things) (R Core Team, 2020) and RStudio (Version 2021.09.0 Build 351) (RStudio Team, 2020). The goal of GEE is to draw inferences from the population by accounting for the within-subject correlation of longitudinal data. Ignoring these correlations would lead to regression estimates, being more widely scattered around the true population means. It is an extension of the generalized linear model (GLM) to correlated data, enabling the calculation of valid standard errors of the parameter estimates.

Based on the three parameters cue (reward incentive; control, 3ct, 30ct), block (B1, B2, B3), and group (young and old) and their interaction terms, different parameter combinations were tested as well as the two different most reliable correlation structures

[1]https://www.fieldtriptoolbox.org/tutorial/connectivity/

FORMULA 2 | Coherence coefficient; x (t), y (t) - time series; Gxy (f) - cross-spectral density of x and y; Gxx (f), Gyy (f) - autospectral densities of x and y (Kida et al., 2015).

$$C_{xy}(f) = \frac{|G_{xy}(f)|^2}{G_{xx}(f)\,G_{xy}(f)}$$

(AR1, exchangeable) to find the most suitable GEE model for the data. After testing different models (**Supplementary Table 2**) Model M3 has the lowest Model selection criteria values and is used for further analyses (**Supplementary Tables 3, 4**).

RESULTS

The participants performed the MID task while undergoing EEG measurement and reaction time recording. Reward sensitivity is considered as faster reaction times with increasing reward.

Behavioral Data

Analyzing reaction times, mean reaction times decreased with increasing monetary incentives in the younger and in the older group (control, 3 ct, 30 ct, **Figure 3A**, full data: **Supplementary Table 1**). **Figure 3A** gives an overview of the data, showing significant reward-related reaction time reduction within both groups (Mann-Whitney-U-Test). Notably, there was a higher standard deviation in RTs in the older group, being a well-known finding (Woods et al., 2015).

The GEE model revealed significant reward-related reaction time reduction effects within both groups (**Figure 3B** model contrasts, **Figure 3E** estimated marginal means, see **Supplementary Table 3** for exact values). But there were no significant differences in the cue contrast between both groups (**Figure 3B**).

According to the model, the participants of the older group generally reacted 46.66 ms (SE = 10.3, CI: 26.5-66.8, $p < .001$) slower than the participants of the younger group. Analyzing reaction times considering the blocks revealed that the older adults significantly improved reaction times from Blocks B1 to B3 and from B2 to B3. These improvements were significantly higher in comparison to younger adults (**Figure 3C** model contrasts, **Figure 3F** estimated marginal means, see **Supplementary Table 4** for exact values). Younger adults only exhibited a significant improvement between Blocks B1 and B2, not significantly differing from the older group. Older adults show higher hit rates than younger adults during the second and the third block across all conditions (**Figure 3D**). In an additional regression analysis, no significant effect of the factor age on reaction time differences between conditions could be found (**Supplementary Figure 1**).

Effects of Rewards on Frontal Intra- and Internet Work Connectivity

For investigating reward effects, a within-group comparison of the neutral vs. high-reward cue (0 ct vs. 30 ct) and neutral vs. high-reward feedback (0 ct vs. 30 ct) (**Figures 4A,B**) was conducted. Important network centers of the reward system are represented in the prefrontal cortex (Kringelbach, 2005; Tobler et al., 2009; Doñamayor et al., 2012; Li et al., 2016). Thus, we expected higher reward-related frontal connectivity. All frontal channel groups (FR, FL, FP, FCL, FCR, see **Figure 2**) and all remaining channel groups each were summarized into a new EEG channel group. Connectivity among the five frontal channel groups and between the newlydefined frontal and non-frontal channel groups was assessed (**Figure 4A**).

First, the reward cue effect on frontal connectivity was analyzed. In the young group, coherence within the frontal group (mean = 0.434 vs. 0.421; $p = 0.012$; df = 21) and frontal-non-frontal coherence was significantly higher in the alpha band for the reward cue (mean = 0.405 vs. 0.391; $p = 0.002$; df = 21). In the beta band, a non-significant tendency for higher coherence during the reward cue appeared within the frontal group ($p = 0.070$) and between the frontal and non-frontal groups ($p = 0.056$). In the older group, no significant differences existed for frontal-nonfrontal coherence and coherence among frontal channel groups. There was a non-significant tendency for lower coherence during the reward cue among the nonfrontal channel groups in the delta band ($p = 0.061$) (**Figure 4B**). In a finer-grained regional analysis, significant changes only appeared in the alpha and delta bands of the young group (**Supplementary Figure 2**).

Group Differences of Reward Effects on Interregional Connectivity

Interregional connectivity modulation was compared between groups to test for group differences of reward effects (**Figure 4C**).

Significant differences could exclusively be found in the delta band, where a mixed picture concerning differences in coherence between neutral and reward cues appeared (**Figure 4D**). Reward-based modulation was higher in the older group for frontocentral right and parietal right with parietooccipital and occipital channel groups. In detail, this applied for FCR with POR and O; and PR with POC and O. Modulation was higher in the younger group for FCR with POL and POC. Noteworthy, younger and older adults exhibited connectivity modulations in different directions, such as coherence increased for reward compared to neutral cues in the younger group, whereas it decreased in the older group. In this way, coherence was significantly different between PR and POL; both groups modulated it in the same absolute value, but in different directions.

Application of Cognitive Aging Models on Reward Processing in Healthy Aging

HAROLD

In case of the HAROLD model (hemispheric asymmetry reduction in older adults) (Cabeza, 2002), frontal connectivity within and between the frontal areas of both hemispheres was assessed and compared between groups for the cue events. Therefore, two new channel groups were defined, including all frontal cortical channel groups of the left or right hemispheres (left: FL, FCL; right: FR, FCR) (**Figures 2**, **5A**).

In the delta band, the older group exhibited lower reward-based coherence modulation within the left frontal [mean = −0.041 vs. 0.019; p (uncorr) = 0.046; df = 30.1] and the right frontal channel group [mean = −0.05 vs. 0.009; p (uncorr) = 0.017; df = 41.8]. The younger group exhibited higher reward-based coherence modulation in frontal left with all other channel groups in the alpha band (mean = 0.013 vs −0.07; $p = 0.038$; df = 32). In the high-beta band, the older group similarly showed lower differences in coherence within the right frontal channel group [mean = 0.014 vs.

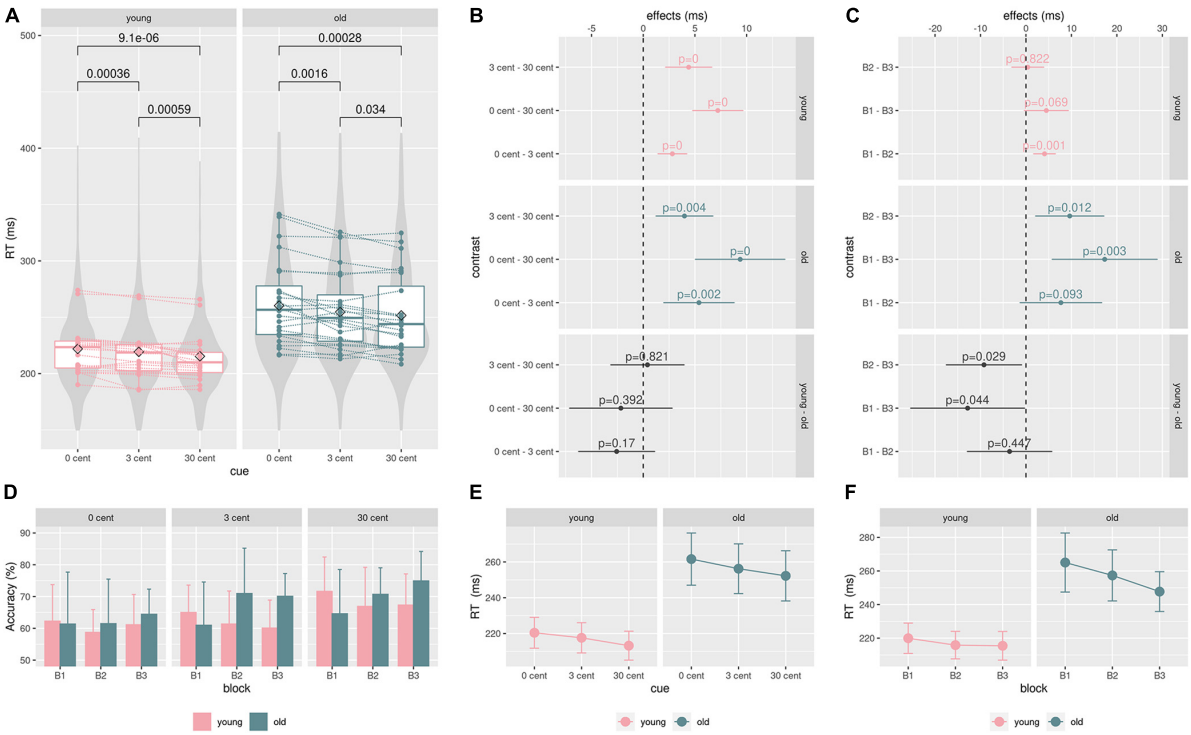

FIGURE 3 | Behavioral data: **(A)**, Boxplot: single mean reaction time data, lines/points correspond to different participants. P-values from the paired Mann-Whitney U-Test show significant reward-related reaction time speeding within both groups. Violin plots are based on single reaction time data. **(B)** and **(E)**, the GEE model results for effects of the groups (young, old) and the cue (0 ct, 3 ct, 30 ct) on reaction times. Reaction time differences between cues did not significantly differ between groups. **(D)**, a hit rate (accuracy) in percent for each block and condition. Older adults show higher hit rates than younger adults during the second and third blocks across all conditions. **(C)** and **(F)**, analyzing the effect of the blocks on reaction times showed that the older adults significantly improved performance from Blocks B1 to B3 and B2 to B3. These improvements are significantly higher in comparison to the younger adults. The younger adults showed only a significant improvement between Blocks B1 and B2, not significantly differing from the older group; color code: green = old, pink = young, gray = contrast.

0.003; p (uncorr) = 0.035; df = 40.5] than the younger group. In the high-beta band, there was a non-significant result for higher modulation in the younger group between frontal right and other channel groups (p = 0.062) (**Figure 5B**,a). To investigate hemispheric asymmetry, the difference in reward-based coherence modulation of the frontal left and the frontal right channels was compared between the older and the younger groups, revealing no significant results (**Figure 5B**,b).

PASA

For testing the PASA (posterior-anterior shift in aging) model (Davis et al., 2008), an analysis of connectivity between and among frontal and occipital channel groups was conducted and compared between the older and the younger groups for the cue events. Therefore, frontal channel groups (FP, FR, FL, FCR, FCL) and parietooccipital and occipital channel groups (POC, POL, POR, and O) were summarized into two new groups (**Figures 2**, **5A**).

The difference between conditions was greater in the older compared to the younger group for coherence among occipital channel groups in the delta band [mean = 0.001 vs. −0.01; p (uncorr) = 0.044; df = 33] and in the theta band [mean =0 .001 vs. −0.006; p (uncorr) = 0.043; df = 29.3]. In both cases, coherence was modulated reversely in older adults so that it decreased during reward cues. In the beta band, the older adults showed higher coherence modulation between occipital and all other channel groups (mean = 0.001 vs. −0.004; p = 0.045; df = 37.4). In the high-beta band, the older group exhibited a significantly higher reward-based modulation in coherence between frontal and occipital groups [mean = 0.003 vs. −0.006; p (uncorr) = 0.039; df = 34.2] and a marginally non-significant result for differences in coherence among occipital channel groups [p (uncorr) = 0.059]. In the beta band, two non-significant results pointed to a greater difference in coherence between frontal and occipital groups [p (uncorr) = 0.061] and in coherence among occipital channel groups [p (uncorr) = 0.052] in the older group. A non-significant tendency appeared in the alpha band, indicating lower differences between conditions in coherence between frontal and occipital groups [p (uncorr) = 0.066] and between frontal and remaining channel groups (p = 0.060) coherence in the older group (**Figure 5B**,a). Comparing the difference in reward-based modulation of frontal and occipital coherence between groups, no significant results appeared (**Figure 5B**,b).

Frontoparietal Control Network

To investigate connectivity between frontal and parietal areas for the cue events, four new channel groups were defined: a frontal

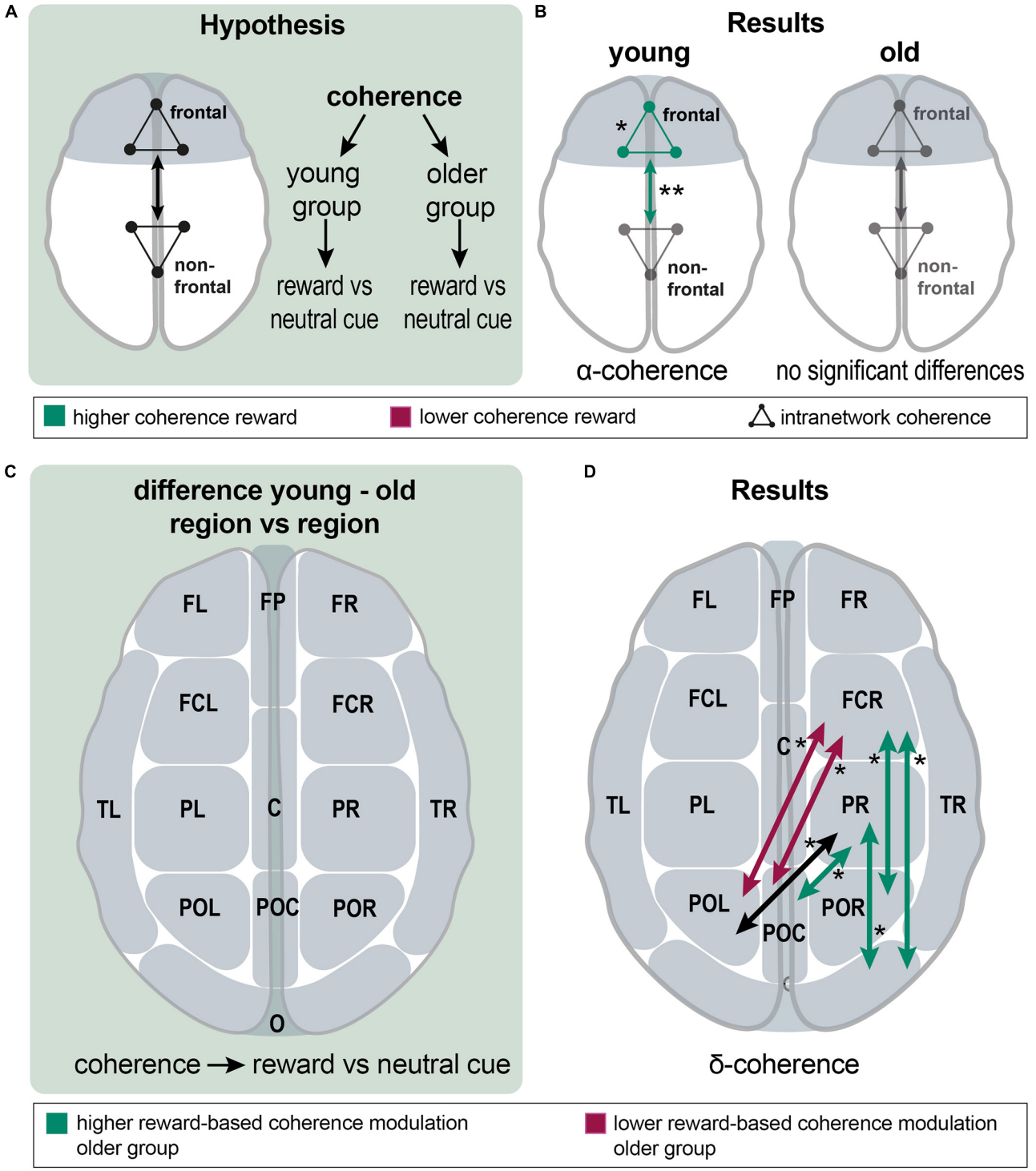

FIGURE 4 | Analysis of reward effects on frontal intra- and internetwork connectivity and of group differences in reward effect on interregional connectivity; **(A),** a schematic overview over the analyzing procedure: Within-group coherence was analyzed for the reward vs. neutral cue contrast between frontal and non-frontal EEG channel groups. **(B),** Results show a higher frontal network and higher frontal-nonfrontal alpha-band coherence during the reward cue. There were no significant differences in the older group. **(C),** A schematic overview of the analyzing procedure: Between group comparison of interregional coherence for the reward vs. neutral cue contrast. **(D),** Results: significant differences appeared in the delta band; reward-based modulation was higher in the older group for frontocentral right and parietal right with parietooccipital and occipital channel groups. In detail, this applied to FCR with POR and O; and PR with POC and O (green arrows). Modulation was higher in the younger group for FCR with POL and POC (red arrows). Coherence was significantly different between PR and POL; both groups modulated it in the same absolute value, but in different directions (a black arrow). Asterisks: one asterisk: $p \leq 0.05$; two asterisks: $p \leq 0.01$.

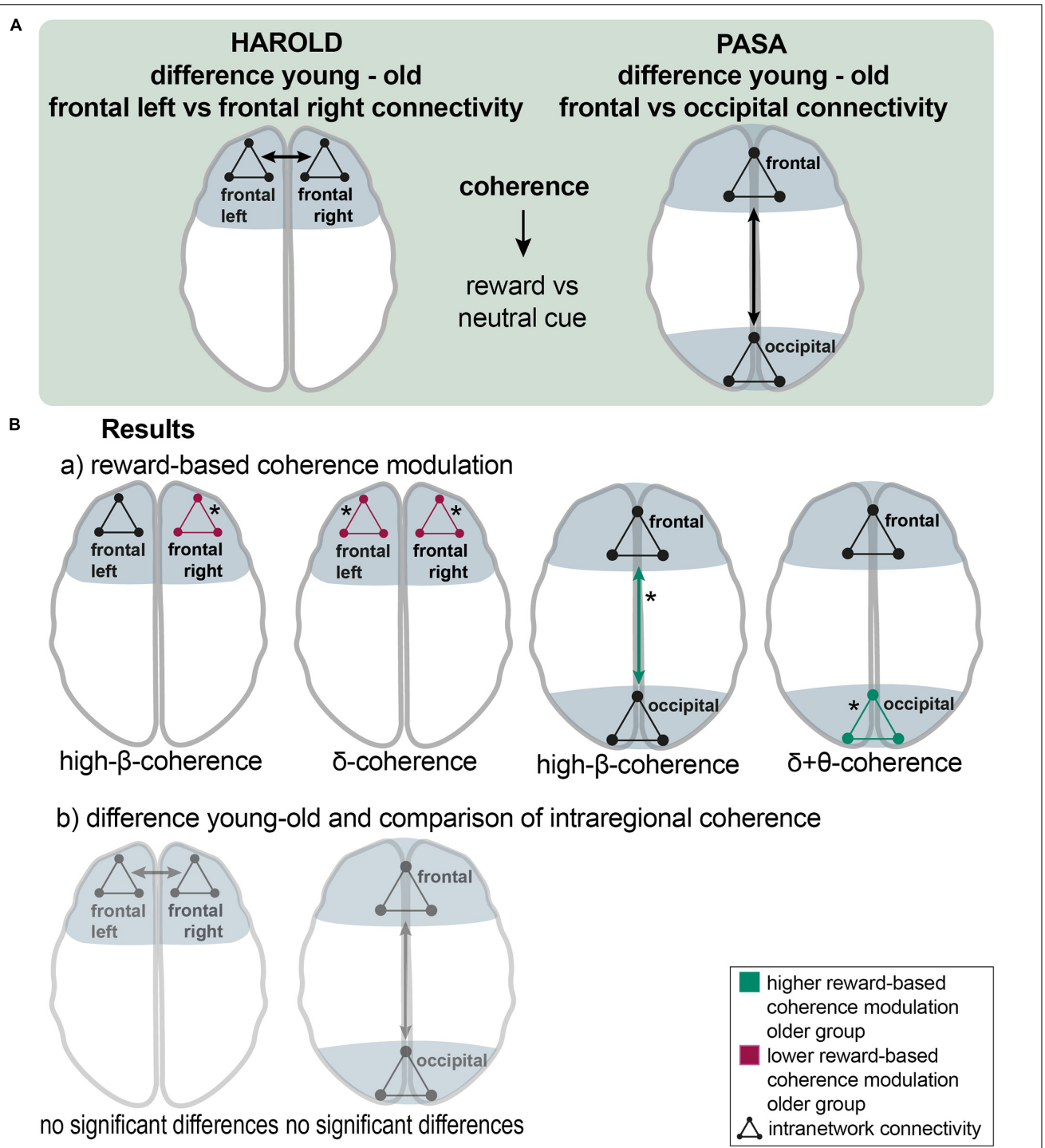

FIGURE 5 | The HAROLD and PASA effect during reward processing: **(A),** a schematic overview of the analyzing procedure: Testing HAROLD (left side), group differences in coherence between frontal left and frontal right channel groups were assessed for the reward vs. neutral cue contrast. Testing PASA (right side), group differences in coherence between frontal and occipital channel groups were assessed for the reward vs. neutral cue contrast. **(B),** Results: a) HAROLD in the delta band, the older group exhibited lower reward-based coherence modulation within the left frontal and the right frontal channel groups. In the high-beta band, the older group showed lower differences in coherence within the right frontal channel group than the younger group (red arrows). PASA - the difference between conditions was greater in the older compared to the younger group for coherence among occipital channel groups in the delta band and in the theta band. In the high-beta band, the older group exhibited a significantly higher reward-based modulation in coherence between frontal and occipital groups (green arrows). b) HAROLD - to investigate hemispheric asymmetry, the difference in reward-based coherence modulation of the frontal left and the frontal right channels was compared between the older and the younger groups, revealing no significant results. PASA - comparing the difference in reward-based modulation of frontal and occipital coherence between groups, no significant results appeared. Asterisks: one asterisk: $p \leq 0.05$.

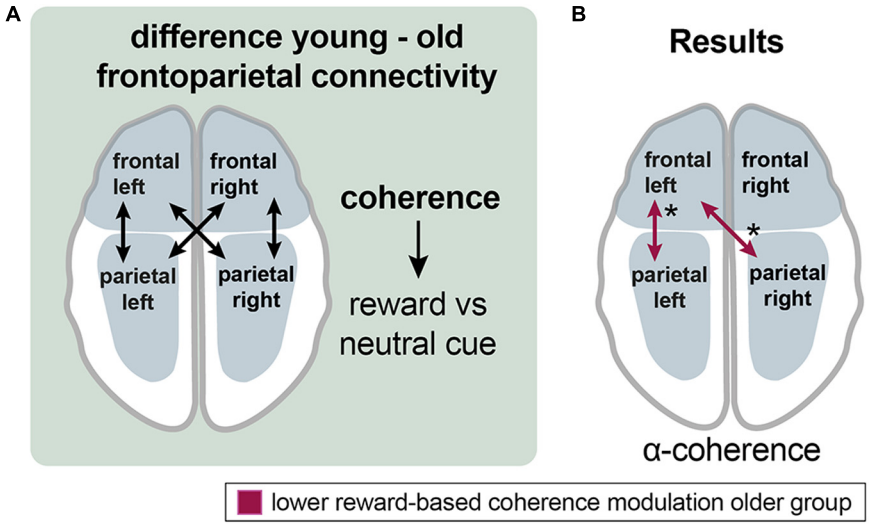

FIGURE 6 | Aging effects on the frontoparietal control network during reward processing**. (A)** Analyzing the procedure scheme: group differences in coherence between frontal and parietal channel groups were assessed for the reward vs. neutral cue contrast. **(B)** Results: Older adults exhibited lower reward-related frontoparietal left and frontal left-parietal right coherence modulation in the alpha band (red arrows). Asterisks: one asterisk: $p \leq 0.05$.

right (FR, FCR), a frontal left (FL, FCL), a parietal left (PL, POL), and a parietal right channel group (PR, POR) (**Figures 2**, **6A**).

In the alpha band, the older group exhibited lower left frontoparietal [mean = 0.013 vs. −0.005; p (uncorr) = 0.043; df = 35.3] and left frontal with right parietal [mean = 0.015 vs. −0.01; p (uncorr) = 0.032; df = 34.1] reward-based coherence modulation compared to the younger group (**Figure 6B**).

Questionnaire

Analysis of questionnaire data amounted to the following results (**Table 1**). To test for depressive symptoms, the BDI-II score was chosen. Across subjects, the median BDI-II score (Beck et al., 1996) was 1.5 (IQR = 6; range, 0-11) in the younger and 4 (IQR = 7; range, 0-13) in the older group. The Mann-Whitney U-Test for independent samples ($p = 0.349$; U = 222) showed no significant difference between groups. Concerning the MoCA test (Nasreddine et al., 2005), the mean score was 25.75 (SD = 2.07; range, 21-29 points), slightly below the original cut-off score of 26 points (results < 26 indicate cognitive impairment) (Nasreddine et al., 2005). Test results showed a normal distribution (Shapiro-Wilk Test, $p = .349$). However, no participant was excluded based on the results of the MoCA test. Moreover, we carefully checked for correct understanding and execution.

For hedonia assessment, the items stress, gambling behavior, religiosity, pack-years of smoking (py), and alcohol consumption (Saunders et al., 1993) of the anamnesis questionnaire were evaluated. For religiosity and stress, the participants had to answer on a scale from 1 to 10 (1 – not stressed/not religious, 10 – high stress/very religious). Both groups did not differ in concerns of religiosity ($p = 0.319$; U = 211.5) and alcohol consumption ($p = 0.781$; U = 248). Significant differences for the items stress ($p \leq 0.000$; U = 57.5) and py ($p = 0.045$; U = 182.5) were found, revealing that the younger participants suffered significantly more from stress and smoked significantly less than the older participants.

DISCUSSION

Behaviorally Robust Reward Sensitivity in Older Age

In line with our hypothesis, we did not find a significant effect of age on reward-dependent modulation of reaction times (RTs). Younger and older adults significantly decreased their reaction times with increasing reward (**Figure 3** and **Supplementary Table 1**). The decrease in reaction times with an increasing monetary incentive reflects an intact reward sensitivity in aging. This overall stability might be an explanation for well-known psychological changes in aging. Older adults tend to aim at preserving resources, preventing negative outcomes and maintaining their emotional well-being. This refers to socioemotional selectivity theory (SST), which emphasizes older adults' most prioritized goals of sustaining positive affect due to perceiving their further lifetime as limited (Carstensen et al., 1999). Thus, older people pay more attention to positive compared to negative stimuli. This so-called "positivity effect" explains an empirical phenomenon, stating that information processing exhibits a positive bias in aging (Mather and Carstensen, 2005; Reed et al., 2014).

Our results of a preserved sensitivity in older adults are in line with most aging aging studies employing the monetary incentive delay task (MID) (Samanez-Larkin et al., 2007; Rademacher et al., 2014; Vink et al., 2015). However, some studies reported a preserved but reduced or total lack of reward sensitivity in older adults (Spaniol et al., 2015; Dhingra et al., 2020). An explanation for these differences could be the differing number

of trials and investigated subjects (Samanez-Larkin et al., 2014; Yee et al., 2019). Studies reporting reduced reward sensitivity generally conduct fewer trials and, often, foregoing training sessions prior to the actual experiment (Spaniol et al., 2015; Dhingra et al., 2020). These differences indicate that older adults might need a longer time for getting used to a task so that differences in task performance stand out when the experimental duration is shorter. Although this training effect might account for reports of significant differences in age-related reward sensitivity, it is, nevertheless, possible that there is a small effect of age on reward sensitivity that might require a high number of participants and long experiment duration to become statistically significant. Longer experiment durations, however, increase the risk that any measured effects are no longer primarily due to the principal performance of the reward system but to faster age-related exhaustibility of the attentional system. Regardless of these methodological difficulties, a possible effect of age on the functionality of the reward system must be small compared to other cognitive and behavioral domains (particularly in comparison to the age-related decrease in RTs). Thus, it remains an open question how the aging brain manages to preserve reward system functionality despite the cellular and molecular changes affecting its core parts. Here, we conducted further analyses to address the question of what compensatory mechanisms are used to maintain reward system function in the elderly.

Here, we used EEG connectivity measures to clarify this question. To our best knowledge, no previous study investigated the aging reward system with EEG connectivity measures (Meyer et al., 2021). Connectivity analyses further improve the understanding of reward network integrity and communication of cortical brain areas during reward processing (Sakkalis, 2011) and were here performed with particular focus on the prefrontal cortex as a center for important network hubs of the reward system (Kringelbach, 2005; Tobler et al., 2009; Doñamayor et al., 2012; Li et al., 2016).

Reward Prediction in Young and Older Adults

Younger and older adults showed different reward-related connectivity patterns (**Figure 4B** and **Supplementary Figure 2**). During reward prediction, the younger adults showed significantly higher coherence in the alpha band and lower coherence in the delta band (**Figure 4B** and **Supplementary Figure 2**), while, in the older group, there was no significant reward-based modulation of coherence. The distribution of alpha-band changes is in line with the current literature, suggesting altered activity within the frontoparietal control network (Sadaghiani and Kleinschmidt, 2016; Lepage and Vijayan, 2017) and the ventral attention network (VAN) (Solís-Vivanco et al., 2021). Both have been found to be involved in the reorientation of attention and the maintenance of selective attention (Corbetta and Shulman, 2002; Mengotti et al., 2020). Thus, our findings imply that younger adults show enhanced recruitment of FPCN and VAN as a sign of cognitive control and increased attention in a rewarding context (Corbetta and Shulman, 2002; Persichetti et al., 2015). With respect to the decreased delta band coherence, it has been suggested that the cues elicited a "cognitive reward" and, therefore, caused a reward feedback-like delta band response (Bromberg-Martin and Hikosaka, 2009; Wang et al., 2016). Taken together, changes in alpha-band coherence might suggest increases in cognitive control and attention in a rewarding context in young adults, while delta band coherence during non-reward cues in younger adults may resemble a negative reward due to the absence of a possible monetary gain. The absence of such a modulation in older adults might reflect their reduced ability to flexibly recruit cognitive control mechanisms in response to varying incentives (Huizeling et al., 2021).

Significant changes in the delta band were also found by comparing the reward-related connectivity patterns between older and younger adults (**Figure 4D**).

Analysis of Group Differences in Reward Effects on Interregional Connectivity

Comparing the reward-related connectivity patterns between older and younger adults, significant differences only emerged during the cue events in the delta band. The younger adults exhibited higher reward-based modulation of coherence in the frontal right with parietooccipital left channel groups (**Figure 4D**). Older adults exhibited higher frontoparietal right and parietooccipital coherence modulation. Noteworthy, younger and older adults exhibited connectivity modulations in different directions, such as coherence increased for reward compared to neutral cues in the younger group, whereas it decreased in the older group (**Figure 4D**).

According to the function of delta oscillations, they support the idea of older adults' altered pathways of detecting and processing salient stimuli (Knyazev, 2007; Knyazev, 2012; Daitch et al., 2013; Güntekin and Başar, 2016). Especially, older adults' higher reward-related coherence modulation in the delta band resembles the ventral attention network (VAN) (Corbetta and Shulman, 2002). It consists of the temporoparietal junction and middle and inferior frontal gyrus, exhibiting a right-lateralized activation. The VAN also underlies connectivity alterations in aging, although studies disagree on their direction and magnitude (Li et al., 2015; Kurth et al., 2016; Deslauriers et al., 2017; ElShafei et al., 2020). One study reported increased connectivity within the VAN in older adults, which is in line with our findings (Deslauriers et al., 2017). These age differences in the reward-related network connectivity likely reflect compensatory mechanisms employed by the aging brain to maintain behavioral reward system function.

Application of Cognitive Aging Models on Reward Processing

Age-related cognitive network alterations are well-observed by fMRI in older adults and comprise hypo- and hyperactivations in specific patterns that have been summarized in distinct models. Their functional effect has been interpreted in the sense of dedifferentiation and compensation (Sala-Llonch et al., 2015).

Two of the best established compensatory models are the HAROLD (Hemispheric Asymmetry Reduction in Older Adults) (Cabeza, 2002) and the PASA (posterior-anterior shift in aging) model (Davis et al., 2008). Furthermore, frontoparietal control network (FPCN) hyperactivation has been observed in older adults during cognitively demanding tasks (Reuter-Lorenz and Park, 2014; Li et al., 2015). The FPCN exerts a paramount role in organizing cognitive control and goal-directed behavior (Spreng et al., 2010; Parro et al., 2018). Due to the close link between reward processing and cognition, we propose the involvement of HAROLD, PASA, and FPCN compensatory mechanisms in preserved reward system function in healthy aging. These compensatory models have been tested successfully with EEG connectivity analyses elsewhere (Rosjat et al., 2018; Rosjat et al., 2021).

Now, these models of cognitive aging were tested regarding their applicability to the aging reward system (**Figure 5A**) (Cabeza, 2002; Reuter-Lorenz and Mikels, 2006; Davis et al., 2008; Reuter-Lorenz and Park, 2014; Festini et al., 2018).

First, the HAROLD theory (Hemispheric Asymmetry Reduction in Older Adults) was applied (**Figure 5B**). It suggests the bilateral recruitment of prefrontal brain areas in older adults compared to a predominantly lateralized activity in younger adults during the same cognitive task as a compensatory mechanism (Cabeza, 2002; Cabeza and Dennis, 2012). The additional activation is related to performance improvements in older adults (Cabeza and Dennis, 2012). In the delta and high-beta bands, the older group showed lower reward-related modulation of bilateral intrahemispheric frontal coherence than the younger group during the cue events. However, the direct test for hemispheric asymmetry yielded no significant results (**Figure 5B**,b). Hemispheric asymmetry reduction in older adults has been reported during cognitive tasks across studies (Hogan et al., 2012; Learmonth et al., 2017; Kenney et al., 2019; Rosjat et al., 2021). The here presented results do not show an apparent HAROLD effect. A possible explanation might be that older adults rely less on the frontal cortex for reward processing, as indicated by the results reported above. Nevertheless, a HAROLD effect could be observable in other cortical areas that were not analyzed here (Kenney et al., 2019).

Another consistently observed pattern describes a prefrontal over- related to an occipital underrecruitment in older compared to younger adults, resulting in the PASA model (Davis et al., 2008; **Figure 5A**). The additional prefrontal activation in older adults is argued to be a compensatory mechanism for age-related occipitotemporal deficits in the processing of sensory stimuli (Grady et al., 1994). Evidence indicates that occipital activity is negatively correlated with frontal activity, and the latter correlates positively with cognitive performance, providing a mechanism for compensation (Davis et al., 2008; Cabeza and Dennis, 2012). During the cue events, the older adults exhibited higher reward-based modulation of occipital coherence in the delta and theta bands and of fronto-occipital coherence in the high-beta band. Contrary to the PASA hypothesis, the results show higher reward-related occipital coherence modulation in the older group during reward anticipation. This is in line with the above-reported results, indicating that older adults rely less on frontal cortical areas during reward processing. Explicit comparison of frontal relative to occipital connectivity between groups amounted to no significant differences (**Figure 5B,b**). Thus, the results show no clear PASA effect. Nevertheless, the higher fronto-occipital coherence modulation in the older group could comply with a PASA effect (Rosjat et al., 2021). The PASA phenomenon has been described during cognitive tasks across studies (Huizeling et al., 2021; Rosjat et al., 2021; Seider et al., 2021). According to the PASA hypothesis, declined occipital activation is due to older adults' sensory processing deficits.

To sum up, we found no evidence that the HAROLD or PASA model explains significant portions of age-related compensatory mechanisms in the reward system, indicating that they might only apply to specific cognitive tasks, and not to the aging reward system.

Lower Reward-Related Frontoparietal Control Network Modulation in Aging

Studies to date especially focused on aging effects on the reward system itself, whereby neglecting incentive-based modulation of the previously described large-scale brain networks (Spaniol et al., 2015). Reward-dependent performance improvement is mediated by the interaction of the reward system with large-scale cognition-related networks, such as the FPCN or the VAN, by implementing cognitive control (Spaniol et al., 2015; Parro et al., 2018). Incentive-based overrecruitment of the default-mode network and cognitive control regions in older compared to younger adults together with similar reward-network activation in both groups has been reported (Spaniol et al., 2015).

An underlying mechanism of performance enhancement under reward conditions is the functional interaction of the reward network with cognition-related large-scale networks like the frontoparietal control network (FPCN) (Vincent et al., 2008), default network (DN), and ventral and dorsal attention network (VAN, DAN). These are engaged, respectively, and disengaged and interconnected during the performance of cognitive tasks, according to task demands (Spaniol et al., 2015; Parro et al., 2018). Importantly, the older adults achieved equal performance as the younger adults when activation levels in the frontoparietal control network were higher (Li et al., 2015). Therefore, we hypothesized frontoparietal hyperactivation in the older adults as a compensatory mechanism for functional deficits of other brain areas (Reuter-Lorenz and Park, 2014), implementing pronouncement of cognitive control processes (Parro et al., 2018). Testing reward-related frontoparietal coherence modulation (**Figure 6A**), the older group showed lower reward-based modulation of left frontoparietal and left frontal with right parietal alpha-band coherence during cue events (**Figure 6B**). Thus, our hypothesis could not be confirmed as the opposite effect was observed.

Conclusively, we found age-related compensatory mechanisms that did not fit to predescribed age-related compensatory mechanisms of other cognitive domains. Thus, we propose that different neural mechanisms underlie the preserved behavioral function of the aging reward system. One reason for this could be the large evolutionary gap in development between

the reward system and higher cognitive functions. Evolutionary preserved reward-related delta oscillations support this idea (Knyazev, 2012). Further evidence shows that salience networks underlie less age-related decline compared to other cognitive networks (Zhang et al., 2014). For instance, fear as another important evolutionary skill for survival has also been found to be relatively stable in healthy aging (LaBar et al., 2004).

Methodical Limitations

Possible limitations may have been the small number of test persons. To identify older participants with mild cognitive impairment up to dementia, the MoCA test was conducted, resulting in a mean score of 25.75 (range, 21-29) (**Table 1**). The original cut-off for a normal result is $\geq$ 26 points, which has often been criticized for being too conservative (Thomann et al., 2018); therefore, no participant was excluded based on this test.

Task performance in the MID may be compromised by a large number of trials, especially in EEG studies and the monotonous course of the MID (Bjork et al., 2010). Additionally, the ability to maintain attention might be reduced in older adults. Consequently, the number of trials was reduced in the older group. According to Spaniol et al., the MID only requires low task-performance skills (Spaniol et al., 2015). Therefore, they argue that aging effects on incentive processing are less confounded by aging effects on task performance (Spaniol et al., 2015). This idea is supported by studies reporting equal performance of younger and older adults in the MID using explicit reward cues, which do not require learning (Samanez-Larkin et al., 2007). Thus, the here used MID is a convenient paradigm for investigating aging of the reward system (Spaniol et al., 2015). As our aim was to shed light on aging effects on the reward system itself and reduce the influence of aged cognitive abilities, the MID is the most appropriate paradigm as it requires low cognitive processing while eliciting robust reward network activation (Spaniol et al., 2015). Although HAROLD and PASA have previously mainly been used to explain compensation in the field of cognitive aging, both were successfully tested in studies investigating risk-taking or emotional perception, being closely related to reward processing (Lee et al., 2008; Jacques et al., 2013). Furthermore, due to the close link between reward and cognitive networks, we assumed that comparable compensatory mechanisms might occur in the aging reward system.

Another point is the use of money as a secondary reward (Bonner and Sprinkle, 2002; Knutson and Wimmer, 2007; Kohls et al., 2009; Knutson and Heinz, 2015). Highly varying individual attitudes should not be neglected (Lutz and Widmer, 2014), including the participants' current financial situation. In addition, older adults, in general, seem to prefer social and positive affective rewards over monetary rewards (Rademacher et al., 2014; Samanez-Larkin and Knutson, 2015; Dhingra et al., 2020).

Limitations of EEG are mainly represented by volume conduction, the extension of electric fields in tissues surrounding the brain, leading to low-pass spatial filtering of signals (Srinivasan et al., 1998; Nunez and Srinivasan, 2006; Srinivasan et al., 2007; Kayser and Tenke, 2015b; Bastos and Schoffelen, 2016). In case of coherence, the abovementioned spatial filtering caused by volume conduction is the main reason for artificial coherence results between EEG channels, which can be reduced by surface Laplacian transform (Srinivasan et al., 1998). Disadvantageously, it distorts signals from extensive sources and may compromise genuine coherence from widespread neural activities over a greater distance (Srinivasan et al., 1998; Nunez and Srinivasan, 2006; Srinivasan et al., 2007; Kayser and Tenke, 2015a,b). As this method was not applied in this study, especially significant coherence results of adjacent regions have to be interpreted cautiously. In sum, when interpreted carefully, coherence offers a valuable and frequently used method for investigating neuronal communication (Srinivasan et al., 2007; Fries, 2015; Bastos and Schoffelen, 2016).

CONCLUSION

In the current study we found that (1) older adults show greater reliance on posterior cortical areas for reward processing, (2) reward-related connectivity modulation tends to be lower in older adults, and (3) older adults modulate connectivity in the opposite direction than younger adults, with usually greater connectivity during non-reward compared to reward conditions. Furthermore, our data indicate that older adults show a more right-lateralized reward-related connectivity, in contrast to younger adults who rely more on left-hemispheric connectivity. These findings provide important new insights into age-related changes in cortical connectivity in the reward system. The mechanisms identified for maintaining reward system function in old age did not fit into previously described models of cognitive aging. We infer that the reward system has unique compensatory mechanisms distinct from other cognitive functions. Nevertheless, further studies are needed to fully understand the complexity of changes in the reward system in healthy aging.

DATA AVAILABILITY STATEMENT

The raw data supporting the conclusions of this article will be made available by the authors, without undue reservation.

ETHICS STATEMENT

The studies involving human participant were reviewed and approved by Ethics Committee of the University Hospital Jena, Germany (REST:2019-1473-BO). The participants provided their written informed consent to participate in this study.

AUTHOR CONTRIBUTIONS

LO, FW, JR, JM, AS, and SB contributed to the acquisition and analysis of data. LO, FW, and CK drafted a significant portion of the manuscript and figures. LO and FW conceived the initial idea and contributed equally. All authors read and improved the final manuscript. The manuscript is part of the thesis of LO.

FUNDING

FW was supported by the Deutsche Forschungsgemeinschaft (DFG, German Research Foundation) Clinician Scientist Program OrganAge funding number 413668513 and by the Interdisciplinary Center of Clinical Research of the Medical Faculty Jena.

ACKNOWLEDGMENTS

We thank the staff of the department of neurology.

SUPPLEMENTARY MATERIAL

The Supplementary Material for this article can be found online at: https://www.frontiersin.org/articles/10.3389/fnagi.2022.863580/full#supplementary-material

Supplementary Figure 1 | Pearson's partial correlation analysis, based on single mean values of the participants, for all three RT differences versus age, controlling for the non-participating reward condition in the difference (left: 3–30 cent, controling for 0 cent, middle: 0–30 cent, controlling for 3 cent, right: 0–3 cent, controlling for 30 cent), no significant effect could be found.

Supplementary Figure 2 | Analysis of interregional analysis within the young group for the reward vs neutral cue. **(A)** Corrplot with FDR-corrected *p*-values for the alpha band; **(B)** Corrplot with FDR-corrected *p*-values for the delta band.

REFERENCES

Andrä, W., and Nowak, H. (2007). *Magnetism in MedicineA Handbook*, 2nd Edn. Berlin: Wiley-VCH Verlag GmbH & Co. KGaA.

Andreou, C., Frielinghaus, H., Rauh, J., Mussmann, M., Vauth, S., Braun, P., et al. (2017). Theta and high-beta networks for feedback processing: a simultaneous EEG-fMRI study in healthy male subjects. *Transl. Psychiatry* 7:e1016. doi: 10.1038/tp.2016.287

Baayen, R. H., and Milin, P. (2010). Analyzing reaction times. *Int. J. Psychol. Res.* 3, 12–28. doi: 10.21500/20112084.807

Backman, L., Nyberg, L., Lindenberger, U., Li, S. C., and Farde, L. (2006). The correlative triad among aging, dopamine, and cognition: current status and future prospects. *Neurosci. Biobehav. Rev.* 30, 791–807. doi: 10.1016/j.neubiorev.2006.06.005

Bastos, A. M., and Schoffelen, J.-M. (2016). A tutorial review of functional connectivity analysis methods and their interpretational pitfalls. *Front. Syst. Neurosci.* 9:175. doi: 10.3389/fnsys.2015.00175

Beck, A. T., Steer, R. A., and Brown, G. K. (1996). *BDI-II, Beck Depression Inventory : Manual*. San Antonio, TX: Psychological Corporation.

Becker, S., Brascher, A. K., Bannister, S., Bensafi, M., Calma-Birling, D., Chan, R. C. K., et al. (2019). The role of hedonics in the Human Affectome. *Neurosci. Biobehav. Rev.* 102, 221–241. doi: 10.1016/j.neubiorev.2019.05.003

Berridge, K. C., and Kringelbach, M. L. (2008). Affective neuroscience of pleasure: reward in humans and animals. *Psychopharmacology* 199, 457–480. doi: 10.1007/s00213-008-1099-6

Berridge, K. C., and Kringelbach, M. L. (2015). Pleasure systems in the brain. *Neuron* 86, 646–664. doi: 10.1016/j.neuron.2015.02.018

Bjork, J. M., Smith, A. R., Chen, G., and Hommer, D. W. (2010). Adolescents, adults and rewards: comparing motivational neurocircuitry recruitment using fMRI. *PLoS One* 5:e11440. doi: 10.1371/journal.pone.0011440

Björklund, A., and Dunnett, S. B. (2007). Dopamine neuron systems in the brain: an update. *Trends Neurosci.* 30, 194–202. doi: 10.1016/j.tins.2007.03.006

Blum, K., Gondré-Lewis, M., Steinberg, B., Elman, I., Baron, D., Modestino, E. J., et al. (2018). Our evolved unique pleasure circuit makes humans different from apes: reconsideration of data derived from animal studies. *J. Syst. Integr. Neurosci.* 4:e11440. doi: 10.1371/journal.pone.0011440

Bonner, S. E., and Sprinkle, G. B. (2002). The effects of monetary incentives on effort and task performance: theories, evidence, and a framework for research. *Account. Organ. Soc.* 27, 303–345. doi: 10.1016/s0361-3682(01)00052-6

Bowen, H. J., Gallant, S. N., and Moon, D. H. (2020). Influence of reward motivation on directed forgetting in younger and older adults. *Front. Psychol.* 11:1764. doi: 10.3389/fpsyg.2020.01764

Braver, T. S., Krug, M. K., Chiew, K. S., Kool, W., Westbrook, J. A., Clement, N. J., et al. (2014). Mechanisms of motivation–cognition interaction: challenges and opportunities. *Cogn. Affect. Behav. Neurosci.* 14, 443–472. doi: 10.3758/s13415-014-0300-0

Bromberg-Martin, E. S., and Hikosaka, O. (2009). Midbrain dopamine neurons signal preference for advance information about upcoming rewards. *Neuron* 63, 119–126. doi: 10.1016/j.neuron.2009.06.009

Cabeza, R. (2002). Hemispheric asymmetry reduction in older adults: the HAROLD model. *Psychol. Aging* 17, 85–100. doi: 10.1037/0882-7974.17.1.85

Cabeza, R., Albert, M., Belleville, S., Craik, F. I. M., Duarte, A., Grady, C. L., et al. (2018). Maintenance, reserve and compensation: the cognitive neuroscience of healthy ageing. *Nat. Rev. Neurosci.* 19, 701–710. doi: 10.1038/s41583-018-0068-2

Cabeza, R., and Dennis, N. A. (2012). *Frontal Lobes and Aging. Principles of Frontal Lobes Function*. (New York, NY: Oxford University Press), 628–652.

Carstensen, L. L., Isaacowitz, D. M., and Charles, S. T. (1999). Taking time seriously: a theory of socioemotional selectivity. *Am. Psychol.* 54, 165–181. doi: 10.1037//0003-066x.54.3.165

Castel, A. D., Friedman, M. C., Mcgillivray, S., Flores, C. C., Murayama, K., Kerr, T., et al. (2016). I owe you: age-related similarities and differences in associative memory for gains and losses. *Aging Neuropsychol. Cogn.* 23, 549–565. doi: 10.1080/13825585.2015.1130214

Chau, B. K. H., Jarvis, H., Law, C.-K., and Chong, T. T.-J. (2018). Dopamine and reward: a view from the prefrontal cortex. *Behav. Pharmacol.* 29, 569–583. doi: 10.1097/FBP.0000000000000424

Cohen, M. S., Rissman, J., Suthana, N. A., Castel, A. D., and Knowlton, B. J. (2016). Effects of aging on value-directed modulation of semantic network activity during verbal learning. *Neuroimage* 125, 1046–1062. doi: 10.1016/j.neuroimage.2015.07.079

Cooley, J. W., and Tukey, J. W. (1965). An algorithm for the machine calculation of complex Fourier series. *Math. Comput.* 19, 297–301. doi: 10.1090/s0025-5718-1965-0178586-1

Corbetta, M., and Shulman, G. L. (2002). Control of goal-directed and stimulus-driven attention in the brain. *Nat. Rev. Neurosci.* 3, 201–215. doi: 10.1038/nrn755

Cox, J., and Witten, I. B. (2019). Striatal circuits for reward learning and decision-making. *Nat. Rev. Neurosci.* 20, 482–494. doi: 10.1038/s41583-019-0189-2

Daitch, A. L., Sharma, M., Roland, J. L., Astafiev, S. V., Bundy, D. T., Gaona, C. M., et al. (2013). Frequency-specific mechanism links human brain networks for spatial attention. *Proc. Natl. Acad. Sci. U.S.A.* 110, 19585–19590. doi: 10.1073/pnas.1307947110

Davis, S. W., Dennis, N. A., Daselaar, S. M., Fleck, M. S., and Cabeza, R. (2008). Que PASA? The posterior-anterior shift in aging. *Cereb. Cortex* 18, 1201–1209. doi: 10.1093/cercor/bhm155

Deslauriers, J., Ansado, J., Marrelec, G., Provost, J. S., and Joanette, Y. (2017). Increase of posterior connectivity in aging within the Ventral Attention Network: a functional connectivity analysis using independent component analysis. *Brain Res.* 1657, 288–296. doi: 10.1016/j.brainres.2016.12.017

Dhingra, I., Zhang, S., Zhornitsky, S., Le, T. M., Wang, W., Chao, H. H., et al. (2020). The effects of age on reward magnitude processing in the monetary incentive delay task. *Neuroimage* 207:116368. doi: 10.1016/j.neuroimage.2019.116368

Doñamayor, N., Schoenfeld, M. A., and Münte, T. F. (2012). Magneto- and electroencephalographic manifestations of reward anticipation and delivery. *Neuroimage* 62, 17–29. doi: 10.1016/j.neuroimage.2012.04.038

ElShafei, H. A., Fornoni, L., Masson, R., Bertrand, O., and Bidet-Caulet, A. (2020). Age-related modulations of alpha and gamma brain activities underlying

anticipation and distraction. *PLoS One* 15:e0229334. doi: 10.1371/journal.pone.0229334

Engel, A. K., and Fries, P. (2010). Beta-band oscillations–signalling the status quo? *Curr. Opin. Neurobiol.* 20, 156–165. doi: 10.1016/j.conb.2010.02.015

EuroQol Group (1990). EuroQol–a new facility for the measurement of health-related quality of life. *Health Policy* 16, 199–208. doi: 10.1016/0168-8510(90)90421-9

Fearnley, J. M., and Lees, A. J. (1991). Ageing and Parkinson's disease: substantia nigra regional selectivity. *Brain* 114(Pt. 5), 2283–2301. doi: 10.1093/brain/114.5.2283

Ferdinand, N. K., and Czernochowski, D. (2018). Motivational influences on performance monitoring and cognitive control across the adult lifespan. *Front. Psychol.* 9:1018. doi: 10.3389/fpsyg.2018.01018

Festini, S. B., Zahodne, L., and Reuter-Lorenz, P. A. (2018). *Theoretical Perspectives on Age Differences in Brain Activation: HAROLD, PASA, CRUNCH—How Do They STAC Up?* Oxford: Oxford University Press.

Fries, P. (2015). Rhythms for cognition: communication through coherence. *Neuron* 88, 220–235. doi: 10.1016/j.neuron.2015.09.034

Friston, K. J. (2011). Functional and effective connectivity: a review. *Brain Connect.* 1, 13–36. doi: 10.1089/brain.2011.0008

Glazer, J. E., Kelley, N. J., Pornpattananangkul, N., Mittal, V. A., and Nusslock, R. (2018). Beyond the FRN: Broadening the time-course of EEG and ERP components implicated in reward processing. *Int. J. Psychophysiol.* 132, 184–202. doi: 10.1016/j.ijpsycho.2018.02.002

Gordon, B. A., Rykhlevskaia, E. I., Brumback, C. R., Lee, Y., Elavsky, S., Konopack, J. F., et al. (2008). Neuroanatomical correlates of aging, cardiopulmonary fitness level, and education. *Psychophysiology* 45, 825–838. doi: 10.1111/j.1469-8986.2008.00676.x

Grady, C. L., Maisog, J. M., Horwitz, B., Ungerleider, L. G., Mentis, M. J., Salerno, J. A., et al. (1994). Age-related changes in cortical blood flow activation during visual processing of faces and location. *J. Neurosci.* 14, 1450–1462. doi: 10.1523/JNEUROSCI.14-03-01450.1994

Gruber, M. J., Watrous, A. J., Ekstrom, A. D., Ranganath, C., and Otten, L. J. (2013). Expected reward modulates encoding-related theta activity before an event. *Neuroimage* 64, 68–74. doi: 10.1016/j.neuroimage.2012.07.064

Güntekin, B., and Başar, E. (2016). Review of evoked and event-related delta responses in the human brain. *Int. J. Psychophysiol.* 103, 43–52. doi: 10.1016/j.ijpsycho.2015.02.001

Haber, S. N., and Knutson, B. (2010). The reward circuit: linking primate anatomy and human imaging. *Neuropsychopharmacology* 35, 4–26. doi: 10.1038/npp.2009.129

Hedman, A. M., Van Haren, N. E. M., Schnack, H. G., Kahn, R. S., and Hulshoff Pol, H. E. (2012). Human brain changes across the life span: A review of 56 longitudinal magnetic resonance imaging studies. *Hum. Brain Mapp.* 33, 1987–2002. doi: 10.1002/hbm.21334

Heuer, A., Wolf, C., Schütz, A. C., and Schubö, A. (2017). The necessity to choose causes reward-related anticipatory biasing: parieto-occipital alpha-band oscillations reveal suppression of low-value targets. *Sci. Rep.* 7:14318. doi: 10.1038/s41598-017-14742-w

Hogan, M. J., Kilmartin, L., Keane, M., Collins, P., Staff, R. T., Kaiser, J., et al. (2012). Electrophysiological entropy in younger adults, older controls and older cognitively declined adults. *Brain Res.* 1445, 1–10. doi: 10.1016/j.brainres.2012.01.027

Højsgaard, S., Yan, J., and Halekoh, U. (2005). The R package GEEPACK for generalized estimating equations. *J. Stat. Softw.* 15, 1–11. doi: 10.18637/jss.v015.i02

Huizeling, E., Wang, H., Holland, C., and Kessler, K. (2021). Changes in theta and alpha oscillatory signatures of attentional control in older and middle age. *Eur. J. Neurosci.* 54, 4314–4337. doi: 10.1111/ejn.15259

Ikemoto, S. (2010). Brain reward circuitry beyond the mesolimbic dopamine system: a neurobiological theory. *Neurosci. Biobehav. Rev.* 35, 129–150. doi: 10.1016/j.neubiorev.2010.02.001

Jacques, P. L. S., Winecoff, A., and Cabeza, R. (2013). "Emotion and aging: linking neural mechanisms to psychological theory," in *The Cambridge Handbook of Human Affective Neuroscience*, eds J. Armony and P. Vuilleumier (Cambridge: Cambridge University Press).

Jimura, K., Locke, H. S., and Braver, T. S. (2010). Prefrontal cortex mediation of cognitive enhancement in rewarding motivational contexts. *Proc. Natl. Acad. Sci. U.S.A.* 107, 8871–8876. doi: 10.1073/pnas.1002007107

Karrer, T. M., Josef, A. K., Mata, R., Morris, E. D., and Samanez-Larkin, G. R. (2017). Reduced dopamine receptors and transporters but not synthesis capacity in normal aging adults: a meta-analysis. *Neurobiol. Aging* 57, 36–46. doi: 10.1016/j.neurobiolaging.2017.05.006

Kayser, J., and Tenke, C. E. (2015a). Issues and considerations for using the scalp surface Laplacian in EEG/ERP research: a tutorial review. *Int. J. Psychophysiol.* 97, 189–209. doi: 10.1016/j.ijpsycho.2015.04.012

Kayser, J., and Tenke, C. E. (2015b). On the benefits of using surface Laplacian (current source density) methodology in electrophysiology. *Int. J. Psychophysiol.* 97, 171–173. doi: 10.1016/j.ijpsycho.2015.06.001

Kenney, J. P. M., Ward, C., Gallen, D., Roche, R. A. P., Dockree, P., Hohensen, N., et al. (2019). Self-initiated learning reveals memory performance and electrophysiological differences between younger, older and older adults with relative memory impairment. *Eur. J. Neurosci.* 50, 3855–3872. doi: 10.1111/ejn.14530

Kida, T., Tanaka, E., and Kakigi, R. (2015). Multi-dimensional dynamics of human electromagnetic brain activity. *Front. Hum. Neurosci.* 9:713. doi: 10.3389/fnhum.2015.00713

Kirchberger, I. (2000). "Der SF-36-Fragebogen zum Gesundheitszustand: Anwendung, Auswertung und Interpretation," in *Lebensqualität und Gesundheitsökonomie in der Medizin*, eds U. Ravens-Sieberer and A. Cieza (Landsberg: ecomed), 73–85.

Knutson, B., and Heinz, A. (2015). Probing psychiatric symptoms with the monetary incentive delay task. *Biol. Psychiatry* 77, 418–420. doi: 10.1016/j.biopsych.2014.12.022

Knutson, B., Westdorp, A., Kaiser, E., and Hommer, D. (2000). FMRI visualization of brain activity during a monetary incentive delay task. *Neuroimage* 12, 20–27. doi: 10.1006/nimg.2000.0593

Knutson, B., and Wimmer, G. E. (2007). Splitting the difference: How does the brain code reward episodes? *Ann. N. Y. Acad. Sci.* 1104, 54–69. doi: 10.1196/annals.1390.020

Knyazev, G. G. (2007). Motivation, emotion, and their inhibitory control mirrored in brain oscillations. *Neurosci. Biobehav. Rev.* 31, 377–395. doi: 10.1016/j.neubiorev.2006.10.004

Knyazev, G. G. (2012). EEG delta oscillations as a correlate of basic homeostatic and motivational processes. *Neurosci. Biobehav. Rev.* 36, 677–695. doi: 10.1016/j.neubiorev.2011.10.002

Kohls, G., Peltzer, J., Herpertz-Dahlmann, B., and Konrad, K. (2009). Differential effects of social and non-social reward on response inhibition in children and adolescents. *Dev. Sci.* 12, 614–625. doi: 10.1111/j.1467-7687.2009.00816.x

Kringelbach, M. L. (2005). The human orbitofrontal cortex: Linking reward to hedonic experience. *Nat. Rev. Neurosci.* 6, 691–702. doi: 10.1038/nrn1747

Kurth, S., Majerus, S., Bastin, C., Collette, F., Jaspar, M., Bahri, M. A., et al. (2016). Effects of aging on task- and stimulus-related cerebral attention networks. *Neurobiol. Aging* 44, 85–95. doi: 10.1016/j.neurobiolaging.2016.04.015

LaBar, K., Cook, C., Torpey, D., and Welsh-Bohmer, K. (2004). Impact of healthy aging on awareness and fear conditioning. *Behav. Neurosci.* 118, 905–915. doi: 10.1037/0735-7044.118.5.905

Lammel, S., Hetzel, A., Hackel, O., Jones, I., Liss, B., and Roeper, J. (2008). Unique properties of mesoprefrontal neurons within a dual mesocorticolimbic dopamine system. *Neuron* 57, 760–773. doi: 10.1016/j.neuron.2008.01.022

Learmonth, G., Benwell, C., Thut, G., and Harvey, M. (2017). Age-related reduction of hemispheric lateralisation for spatial attention: An EEG study. *Neuroimage* 153, 139–151. doi: 10.1016/j.neuroimage.2017.03.050

Lee, T. M. C., Leung, A. W. S., Fox, P. T., Gao, J.-H., and Chan, C. C. H. (2008). Age-related differences in neural activities during risk taking as revealed by functional MRI. *Soc. Cogn. Affect. Neurosci.* 3, 7–15. doi: 10.1093/scan/nsm033

Lepage, K. Q., and Vijayan, S. (2017). The relationship between coherence and the phase-locking value. *J. Theor. Biol.* 435, 106–109. doi: 10.1016/j.jtbi.2017.08.029

Li, H. J., Hou, X. H., Liu, H. H., Yue, C. L., Lu, G. M., and Zuo, X. N. (2015). Putting age-related task activation into large-scale brain networks: A meta-analysis of 114 fMRI studies on healthy aging. *Neurosci. Biobehav. Rev.* 57, 156–174. doi: 10.1016/j.neubiorev.2015.08.013

Li, S.-C., Lindenberger, U., Nyberg, L., Heekeren, H. R., and Bäckman, L. (2009). "Dopaminergic modulation of cognition in human aging," in *Imaging the Aging Brain*, eds W. Jagust and M. D'Esposito (New York, NY: Oxford University Press).

Li, Y., Vanni-Mercier, G., Isnard, J., Mauguiere, F., and Dreher, J. C. (2016). The neural dynamics of reward value and risk coding in the human orbitofrontal cortex. *Brain* 139, 1295–1309. doi: 10.1093/brain/awv409

Liang, K.-Y., and Zeger, S. L. (1986). Longitudinal data analysis using generalized linear models. *Biometrika* 73, 13–22. doi: 10.1093/biomet/73.1.13

Luft, C. D. (2014). Learning from feedback: the neural mechanisms of feedback processing facilitating better performance. *Behav. Brain Res.* 261, 356–368. doi: 10.1016/j.bbr.2013.12.043

Lutz, K., and Widmer, M. (2014). What can the monetary incentive delay task tell us about the neural processing of reward and punishment? *Neurosci. Neuroecon.* 3, 33–45. doi: 10.2147/nan.s38864

Lyoo, Y., and Yoon, S. (2017). Brain network correlates of emotional aging. *Sci. Rep.* 7:15576. doi: 10.1038/s41598-017-15572-6

Marco-Pallarés, J., Münte, T. F., and Rodríguez-Fornells, A. (2015). The role of high-frequency oscillatory activity in reward processing and learning. *Neurosci. Biobehav. Rev.* 49, 1–7. doi: 10.1016/j.neubiorev.2014.11.014

Marković, S., Vuckovic, G., and Jankovic, R. (2019). Simple visual reaction time in students of Academy of Criminalistic and Police Studies. *Bezbednost Beograd* 61, 25–39. doi: 10.5937/bezbednost1901025m

Mather, M., and Carstensen, L. L. (2005). Aging and motivated cognition: the positivity effect in attention and memory. *Trends Cogn. Sci.* 9, 496–502. doi: 10.1016/j.tics.2005.08.005

Mengotti, P., Käsbauer, A.-S., Fink, G. R., and Vossel, S. (2020). Lateralization, functional specialization, and dysfunction of attentional networks. *Cortex* 132, 206–222. doi: 10.1016/j.cortex.2020.08.022

Meyer, G. M., Marco-Pallarés, J., Boulinguez, P., and Sescousse, G. (2021). Electrophysiological underpinnings of reward processing: Are we exploiting the full potential of EEG? *Neuroimage* 242:118478. doi: 10.1016/j.neuroimage.2021.118478

Nasreddine, Z. S., Phillips, N. A., Bedirian, V., Charbonneau, S., Whitehead, V., Collin, I., et al. (2005). The Montreal Cognitive Assessment, MoCA: a brief screening tool for mild cognitive impairment. *J. Am. Geriatr. Soc.* 53, 695–699. doi: 10.1111/j.1532-5415.2005.53221.x

Nunez, P. L., and Srinivasan, R. (2006). *Electric Fields of the Brain: The Neurophysics of EEG*. Oxford: Oxford University Press.

Oldfield, R. C. (1971). The assessment and analysis of handedness: the edinburgh inventory. *Neuropsychologia* 9, 97–113. doi: 10.1016/0028-3932(71)90067-4

Oostenveld, R., Fries, P., Maris, E., and Schoffelen, J. M. (2011). FieldTrip: open source software for advanced analysis of MEG, EEG, and invasive electrophysiological data. *Comput. Intell. Neurosci.* 2011:156869. doi: 10.1155/2011/156869

Parro, C., Dixon, M. L., and Christoff, K. (2018). The neural basis of motivational influences on cognitive control. *Hum. Brain Mapp.* 39, 5097–5111. doi: 10.1002/hbm.24348

Pereda, E., Quiroga, R. Q., and Bhattacharya, J. (2005). Nonlinear multivariate analysis of neurophysiological signals. *Prog. Neurobiol.* 77, 1–37. doi: 10.1016/j.pneurobio.2005.10.003

Persichetti, A. S., Aguirre, G. K., and Thompson-Schill, S. L. (2015). Value is in the eye of the beholder: early visual cortex codes monetary value of objects during a diverted attention task. *J. Cogn. Neurosci.* 27, 893–901. doi: 10.1162/jocn_a_00760

Pessoa, L., and Engelmann, J. (2010). Embedding reward signals into perception and cognition. *Front. Neurosci.* 4:17. doi: 10.3389/fnins.2010.00017

R Core Team (2020). *R: A Language and Environment for Statistical Computing*. Vienna: R Foundation for Statistical Computing.

Rademacher, L., Salama, A., Grunder, G., and Spreckelmeyer, K. N. (2014). Differential patterns of nucleus accumbens activation during anticipation of monetary and social reward in young and older adults. *Soc. Cogn. Affect. Neurosci.* 9, 825–831. doi: 10.1093/scan/nst047

Raichle, M. E., Macleod, A. M., Snyder, A. Z., Powers, W. J., Gusnard, D. A., and Shulman, G. L. (2001). A default mode of brain function. *Proc. Natl. Acad. Sci. U.S.A.* 98, 676–682.

Raz, N., Ghisletta, P., Rodrigue, K. M., Kennedy, K. M., and Lindenberger, U. (2010). Trajectories of brain aging in middle-aged and older adults: regional and individual differences. *Neuroimage* 51, 501–511. doi: 10.1016/j.neuroimage.2010.03.020

Reed, A. E., Chan, L., and Mikels, J. A. (2014). Meta-analysis of the age-related positivity effect: age differences in preferences for positive over negative information. *Psychol. Aging* 29, 1–15. doi: 10.1037/a0035194

Reuter-Lorenz, P. A., and Mikels, J. A. (2006). "The aging mind and brain: implications of enduring plasticity for behavioral and cultural change," in *Lifespan Development and the Brain: The Perspective of Biocultural Co-Constructivism*, eds P. B. Baltes, P. A. Reuter-Lorenz and F. Rösler (Cambridge: Cambridge University Press), 255–276. doi: 10.1017/cbo9780511499722.014

Reuter-Lorenz, P. A., and Park, D. C. (2014). How does it STAC up? Revisiting the scaffolding theory of aging and cognition. *Neuropsychol. Rev.* 24, 355–370. doi: 10.1007/s11065-014-9270-9

Rosjat, N., Liu, L., Wang, B. A., Popovych, S., Tóth, T., Viswanathan, S., et al. (2018). Aging-associated changes of movement-related functional connectivity in the human brain. *Neuropsychologia* 117, 520–529. doi: 10.1016/j.neuropsychologia.2018.07.006

Rosjat, N., Wang, B. A., Liu, L., Fink, G. R., and Daun, S. (2021). Stimulus transformation into motor action: Dynamic graph analysis reveals a posterior-to-anterior shift in brain network communication of older subjects. *Hum. Brain Mapp.* 42, 1547–1563. doi: 10.1002/hbm.25313

RStudio Team (2020). *RStudio: Integrated Development Environment for R*. Boston, MA: RStudio.

Sadaghiani, S., and Kleinschmidt, A. (2016). Brain networks and α-oscillations: structural and functional foundations of cognitive control. *Trends Cogn. Sci.* 20, 805–817. doi: 10.1016/j.tics.2016.09.004

Sakkalis, V. (2011). Review of advanced techniques for the estimation of brain connectivity measured with EEG/MEG. *Comput. Biol. Med.* 41, 1110–1117. doi: 10.1016/j.compbiomed.2011.06.020

Sala-Llonch, R., Bartrés-Faz, D., and Junqué, C. (2015). Reorganization of brain networks in aging: a review of functional connectivity studies. *Front. Psychol.* 6:663. doi: 10.3389/fpsyg.2015.00663

Samanez-Larkin, G. R., Gibbs, S. E., Khanna, K., Nielsen, L., Carstensen, L. L., and Knutson, B. (2007). Anticipation of monetary gain but not loss in healthy older adults. *Nat. Neurosci.* 10, 787–791. doi: 10.1038/nn1894

Samanez-Larkin, G. R., and Knutson, B. (2015). Decision making in the ageing brain: changes in affective and motivational circuits. *Nat. Rev. Neurosci.* 16, 278–289. doi: 10.1038/nrn3917

Samanez-Larkin, G. R., Worthy, D. A., Mata, R., Mcclure, S. M., and Knutson, B. (2014). Adult age differences in frontostriatal representation of prediction error but not reward outcome. *Cogn. Affect. Behav. Neurosci.* 14, 672–682. doi: 10.3758/s13415-014-0297-4

Saunders, J. B., Aasland, O. G., Babor, T. F., De La Fuente, J. R., and Grant, M. (1993). Development of the alcohol use disorders identification test (AUDIT): WHO collaborative project on early detection of persons with harmful alcohol consumption–II. *Addiction* 88, 791–804. doi: 10.1111/j.1360-0443.1993.tb02093.x

Schultz, W. (1998). Predictive reward signal of dopamine neurons. *J. Neurophysiol.* 80, 1–27. doi: 10.1152/jn.1998.80.1.1

Schultz, W. (2006). Behavioral theories and the neurophysiology of reward. *Annu. Rev. Psychol.* 57, 87–115. doi: 10.1146/annurev.psych.56.091103.070229

Schultz, W. (2007). Behavioral dopamine signals. *Trends Neurosci.* 30, 203–210. doi: 10.1016/j.tins.2007.03.007

Seider, T. R., Porges, E. C., Woods, A. J., and Cohen, R. A. (2021). An fMRI study of age-associated changes in basic visual discrimination. *Brain Imaging Behav.* 15, 917–929. doi: 10.1007/s11682-020-00301-x

Solís-Vivanco, R., Jensen, O., and Bonnefond, M. (2021). New insights on the ventral attention network: active suppression and involuntary recruitment during a bimodal task. *Hum. Brain Mapp.* 42, 1699–1713. doi: 10.1002/hbm.25322

Spaniol, J., Bowen, H. J., Wegier, P., and Grady, C. (2015). Neural responses to monetary incentives in younger and older adults. *Brain Res.* 1612, 70–82. doi: 10.1016/j.brainres.2014.09.063

Spaniol, J., Schain, C., and Bowen, H. J. (2014). Reward-enhanced memory in younger and older adults. *J. Gerontol. B Psychol. Sci. Soc. Sci.* 69, 730–740. doi: 10.1093/geronb/gbt044

Spreng, R. N., Stevens, W. D., Chamberlain, J. P., Gilmore, A. W., and Schacter, D. L. (2010). Default network activity, coupled with the frontoparietal control

network, supports goal-directed cognition. *Neuroimage* 53, 303–317. doi: 10.1016/j.neuroimage.2010.06.016

Srinivasan, R., Nunez, P. L., and Silberstein, R. B. (1998). Spatial filtering and neocortical dynamics: estimates of EEG coherence. *IEEE Trans. Biomed. Eng.* 45, 814–826. doi: 10.1109/10.686789

Srinivasan, R., Winter, W. R., Ding, J., and Nunez, P. L. (2007). EEG and MEG coherence: measures of functional connectivity at distinct spatial scales of neocortical dynamics. *J. Neurosci. Methods* 166, 41–52. doi: 10.1016/j.jneumeth.2007.06.026

Steiger, T. K., and Bunzeck, N. (2017). Reward dependent invigoration relates to theta oscillations and is predicted by dopaminergic midbrain integrity in healthy elderly. *Front. Aging Neurosci.* 9:1. doi: 10.3389/fnagi.2017.00001

Thomann, A. E., Goettel, N., Monsch, R. J., Berres, M., Jahn, T., Steiner, L. A., et al. (2018). The montreal cognitive assessment: normative data from a german-speaking cohort and comparison with international normative samples. *J. Alzheimers Dis.* 64, 643–655. doi: 10.3233/JAD-180080

Tobler, P. N., Christopoulos, G. I., O'doherty, J. P., Dolan, R. J., and Schultz, W. (2009). Risk-dependent reward value signal in human prefrontal cortex. *Proc. Natl. Acad. Sci. U.S.A.* 106, 7185–7190. doi: 10.1073/pnas.0809599106

Tryon, V. L., Baker, P. M., Long, J. M., Rapp, P. R., and Mizumori, S. J. Y. (2020). Loss of sensitivity to rewards by dopamine neurons may underlie age-related increased probability discounting. *Front. Aging Neurosci.* 12:49. doi: 10.3389/fnagi.2020.00049

Vincent, J. L., Kahn, I., Snyder, A. Z., Raichle, M. E., and Buckner, R. L. (2008). Evidence for a frontoparietal control system revealed by intrinsic functional connectivity. *J. Neurophysiol.* 100, 3328–3342. doi: 10.1152/jn.90355.2008

Vink, M., Kleerekooper, I., Van Den Wildenberg, W. P., and Kahn, R. S. (2015). Impact of aging on frontostriatal reward processing. *Hum. Brain Mapp.* 36, 2305–2317. doi: 10.1002/hbm.22771

Wang, J., Chen, Z., Peng, X., Yang, T., Li, P., Cong, F., et al. (2016).). To Know or Not to Know? Theta and delta reflect complementary information about an advanced cue before feedback in decision-making. *Front. Psychol.* 7:1556. doi: 10.3389/fpsyg.2016.01556

Wise, R. A. (2002). Brain reward circuitry: insights from unsensed incentives. *Neuron* 36, 229–240. doi: 10.1016/s0896-6273(02)00965-0

Wise, R. A. (2004). Dopamine, learning and motivation. *Nat. Rev. Neurosci.* 5, 483–494. doi: 10.1038/nrn1406

Woods, D. L., Wyma, J. M., Yund, E. W., Herron, T. J., and Reed, B. (2015). Factors influencing the latency of simple reaction time. *Front. Hum. Neurosci.* 9:131. doi: 10.3389/fnhum.2015.00131

Yee, D. M., Adams, S., Beck, A., and Braver, T. S. (2019). Age-related differences in motivational integration and cognitive control. *Cogn. Affect. Behav. Neurosci.* 19, 692–714. doi: 10.3758/s13415-019-00713-3

Zanto, T. P., and Gazzaley, A. (2019). Aging of the frontal lobe. *Handb. Clinical Neurol.*. 163, 369–389. doi: 10.1016/B978-0-12-804281-6.00020-3

Zhang, H.-Y., Chen, W.-X., Jiao, Y., Xu, Y., Zhang, X.-R., and Wu, J.-T. (2014). Selective vulnerability related to aging in large-scale resting brain networks. *PLoS One* 9:e108807. doi: 10.1371/journal.pone.0108807

Conflict of Interest: The authors declare that the research was conducted in the absence of any commercial or financial relationships that could be construed as a potential conflict of interest.

Publisher's Note: All claims expressed in this article are solely those of the authors and do not necessarily represent those of their affiliated organizations, or those of the publisher, the editors and the reviewers. Any product that may be evaluated in this article, or claim that may be made by its manufacturer, is not guaranteed or endorsed by the publisher.

frontiers | Frontiers in Aging Neuroscience

TYPE Original Research
PUBLISHED 10 August 2022
DOI 10.3389/fnagi.2022.959394

OPEN ACCESS

EDITED BY
Fermín Segovia,
University of Granada, Spain

REVIEWED BY
Jinglei Lv,
The University of Sydney, Australia
Valentina Bessi,
University of Florence, Italy

*CORRESPONDENCE
Yuan Yang
yuan.yang-2@ou.edu

SPECIALTY SECTION
This article was submitted to Neurocognitive Aging and Behavior, a section of the journal Frontiers in Aging Neuroscience

RECEIVED 01 June 2022
ACCEPTED 19 July 2022
PUBLISHED 10 August 2022

CITATION
Williamson J, Yabluchanskiy A, Mukli P, Wu DH, Sonntag W, Ciro C and Yang Y (2022) Sex differences in brain functional connectivity of hippocampus in mild cognitive impairment.
Front. Aging Neurosci. 14:959394.
doi: 10.3389/fnagi.2022.959394

Sex differences in brain functional connectivity of hippocampus in mild cognitive impairment

Jordan Williamson[1], Andriy Yabluchanskiy[2], Peter Mukli[2], Dee H. Wu[3,4,5,6], William Sonntag[2], Carrie Ciro[7] and Yuan Yang[1,4,7,8,9]*

[1]Neural Control and Rehabilitation Laboratory, Stephenson School of Biomedical Engineering, University of Oklahoma, Norman, OK, United States, [2]Vascular Cognitive Impairment and Neurodegeneration Program, Oklahoma Center for Geroscience and Healthy Brain Aging, Department of Biochemistry and Molecular Biology, University of Oklahoma Health Sciences Center, Oklahoma City, OK, United States, [3]Department of Radiological Science and Medical Physics, University of Oklahoma Health Science Center, Oklahoma City, OK, United States, [4]Data Institute for Societal Challenges, University of Oklahoma, Norman, OK, United States, [5]School of Computer Science, Gallogly College of Engineering, University of Oklahoma, Norman, OK, United States, [6]School of Electrical and Computer Engineering, Gallogly College of Engineering, University of Oklahoma, Norman, OK, United States, [7]Department of Rehabilitation Sciences, University of Oklahoma Health Science Center, Oklahoma City, OK, United States, [8]School of Electrical and Computer Engineering, University of Oklahoma, Tulsa, OK, United States, [9]Department of Physical Therapy and Human Movement Sciences, Northwestern University, Chicago, IL, United States

Mild cognitive impairment (MCI) is the prodromal stage of Alzheimer's Disease (AD). Prior research shows that females are more impacted by MCI than males. On average females have a greater incidence rate of any dementia and current evidence suggests that they suffer greater cognitive deterioration than males in the same disease stage. Recent research has linked these sex differences to neuroimaging markers of brain pathology, such as hippocampal volumes. Specifically, the rate of hippocampal atrophy affects the progression of AD in females more than males. This study was designed to extend our understanding of the sex-related differences in the brain of participants with MCI. Specifically, we investigated the difference in the hippocampal connectivity to different areas of the brain. The Resting State fMRI and T2 MRI of cognitively normal individuals (n = 40, female = 20) and individuals with MCI (n = 40, female = 20) from the Alzheimer's Disease Neuroimaging Initiative (ADNI) were analyzed using the Functional Connectivity Toolbox (CONN). Our results demonstrate that connectivity of hippocampus to the precuneus cortex and brain stem was significantly stronger in males than in females. These results improve our current understanding of the role of hippocampus-precuneus cortex and hippocampus-brainstem connectivity in sex differences in MCI. Understanding the contribution of impaired functional connectivity

sex differences may aid in the development of sex specific precision medicine to manipulate hippocampal-precuneus cortex and hippocampal-brainstem connectivity to decrease the progression of MCI to AD.

KEYWORDS

mild cognitive impairment, sex difference, hippocampus, functional connectivity, Alzheimer's disease

Introduction

According to the CDC, there are 6.2 million people in the United States living with Alzheimer's Disease (AD) in 2021 (Centers for Disease Control and Prevention, 2021). This disease disproportionately affects females as they constitute more than two-thirds of the AD population (Snyder et al., 2016). The higher prevalence of AD in females has been attributed to females having greater longevity compared to males (Guerreiro and Bras, 2015). Since age is the greatest risk factor for the development of AD, it would be reasonable to state that more females would live long enough to develop AD. However, increasing evidence suggests there are other factors contribute to the sex-specific risk of AD such as genetics, hormonal differences, rate of depression, education level, and sleep disturbances (Andrew and Tierney, 2018; Mielke, 2019; Pearce et al., 2022).

The most important predictor is mild cognitive impairment (MCI) that always precedes AD, usually years before meeting the diagnostic criteria of clinical dementia (Petersen, 2004). MCI is defined as cognitive decline greater than expected for a given age but does not notably interfere with daily activities (Salmon, 2011). Current clinical evidence demonstrates about a 20% annual conversion rate of MCI to AD and that more than half of the individuals with MCI progress to dementia within 5 years (Gauthier et al., 2006; Davatzikos et al., 2011; López et al., 2020; McGrattan et al., 2022). In addition to prevalence differences, females experience greater cognitive deterioration than males in the same disease stage (Alzheimer's Association, 2016) that are also present in individuals with MCI (Sohn et al., 2018). Compared to males with AD, females perform worse on a variety of neuropsychological tasks and have greater total brain atrophy and temporal lobe degeneration (Henderson and Buckwalter, 1994; Chapman et al., 2011; Gumus et al., 2021). Magnetic resonance imaging (MRI) data collected through the Alzheimer's Disease Neuroimaging Initiative (ADNI) study attested to the faster atrophic rate (Hua et al., 2010). The hippocampus is also known to be affected at the earliest stages of MCI, even before a diagnosis can be made (Braak and Braak, 1995), and hippocampal atrophy has been found to affect the progression of AD only in females (Burke et al., 2019). Recent research revealed additional brain imaging markers that may also contribute to the sex differences in AD and are specifically present in individuals with MCI and that reduced hippocampal volume and any microhemorrhage, regardless of location, are the best MRI features to predict the transition from pre-MCI to MCI (Ferretti et al., 2018; Jiang et al., 2022). Cavedo et al. (2018) found that males with MCI had a higher anterior cingulate cortex amyloid load and glucose hypometabolism in the precuneus, posterior cingulate, and inferior parietal cortex. Similar findings have been reported among cognitively normal adults (Rahman et al., 2020) suggesting that males have a higher brain resilience. However, the role of sex-related differences in hippocampal connectivity during MCI has not been elucidated yet.

This study was designed to extend the understanding of the mechanism underlying the sex differences in pathophysiological biomarkers in individuals with MCI. Our hypothesis was that hippocampal functional connectivity (FC) to the precuneus cortex and the brain stem shows sex-and MCI-specific differences. The FC of the hippocampus will be analyzed and compared between females and males with MCI, as well as cognitively normal females and males as controls.

Materials and methods

Data source

The data for this study were extracted from the ADNI[1], which is a publicly accessible dataset available at adni.loni.usc.edu. Launched in 2003, ADNI is a longitudinal, multi-site, cohort study, led by Principal Investigator Michael W. Weiner, MD. The original study, ADNI-1, has been extended three times and the database contains subject data from ADNI-1, ADNI-GO, ADNI-2, and ADNI-3. The overall goal of the studies was to evaluate whether serial magnetic resonance imaging (MRI), positron emission tomography (PET), other biological markers, and clinical and neuropsychological assessment can be combined to measure the progression of mild cognitive impairment (MCI) and early Alzheimer's disease (AD). For up-to-date information, see www.adni-info.org.

1 https://adni.loni.usc.edu/

Screening process

The data were screened for subjects with MCI. To eliminate multiple images from the same subject, the data included early MCI (EMCI), late MCI (LMCI), or MCI from the 1-year subject visit of ADNI-1, ADNI-GO, ADNI-2, and ADNI-3. Subjects' selection was also limited to those with data collected from resting-state functional magnetic resonance imaging (rs-fMRI) and 3.0-Tesla T2 magnetic resonance imaging. A similar search methodology was applied for cognitively normal (CN) subjects. The screening resulted in a total of 40 MCI females, 42 MCI males, 25 CN females, and 20 CN males. To balance the number of subjects in each group, 20 of each group were randomly selected for the study. Demographics of MCI subjects are provided in **Table 1**. This includes age, Apolipoprotein E (ApoE) genotype, the Mini Mental State Examination (MMSE), the Geriatric Depression (GD) Scale, the Global Clinical Dementia Rating (CDR), and the Functional Activities Questionnaire (FAQ), and the Neuropsychiatric Inventory Questionnaire (NPI-Q). IBM SPSS (IBM Corp. Armonk, NY, United States) was used to run independent *t*-tests to ensure there was not a statistically significant sex difference in age, MMSE, GD Scale, CDR, FAQ and NPI-Q ($P > 0.05$). If normal distribution could not be assumed based on the Shapiro–Wilk test, a non-parametric Mann–Whitney test was performed. These values are provided in **Table 1**.

Analysis of functional connectivity and statistical testing

The subject's original rs-fMRI and MRI images (NiFTI format) were imported into the NITRC Functional Connectivity Toolbox (CONN) version 20b (Whitfield-Gabrieli and Nieto-Castanon, 2012). CONN utilizes SPM12 (Welcome Department of Cognitive Neurology, United Kingdom) and MATLAB R2020a (MathWorks, Natick, MA, United States) in its processes and by default a combination of the Harvard-Oxford atlas (HOA distributed with FSL[2]) (Smith et al., 2004; Woolrich et al., 2009; Jenkinson et al., 2012) and the Automated Anatomical Labeling (AAL) atlas (Tzourio-Mazoyer et al., 2002).

The images were processed through the default functional and structural preprocessing pipeline as detailed in Nieto-Castanon (2020). This included realignment, slice timing correction, coregistration/normalization, segmentation, outlier detection, and smoothing. Additionally, this step extracted the blood-oxygen-level dependent (BOLD) time series from the regions of interest (ROIs) and at the voxels. Next, the images were denoised to remove confounding effects from the BOLD signal through linear regression and band-pass filtering. A quality assurance check was made after the denoising to ensure normalization and that there were no visible artifacts in the data.

A seed-to-voxel analysis was conducted for each subject. This analysis created a seed-based connectivity (SBC) map between the ROI (left or right hippocampus) to every voxel of the brain. The SBC map is computed as the Fisher-transformed bivariant correlation coefficients between the ROI BOLD time series and each individual voxel BOLD time series (Whitfield-Gabrieli and Nieto-Castanon, 2012). The mathematical relationship to construct the SBC is shown below

$$r(x) = \frac{\int S(x,t)\,R(t)\,dt}{\left(\int R^2(t)\,dt \int S^2(x,t)\,dt\right)^{1/2}}$$

$$Z(x) = tanh^{-1}(r(x))$$

where R is the average ROI BOLD timeseries, S is the BOLD timeseries at each voxel, r is the spatial map of Pearson correlation coefficients, and Z is the SBC map of the Fisher-transformed correlation coefficients for the ROI. Finally, *F*-tests were conducted between the SBC maps to compare differences between groups. For a cortical area to be considered significant, the toolbox used the Gaussian Random Field theory parametric statistics, with a cluster threshold $p < 0.05$ (FDR-corrected) and voxel threshold $p < 0.001$ (uncorrected) to control the type I error in multiple comparisons (Worsley et al., 1996). Additionally, the area must have been over 800 voxels large or cover more than 80 percent of a given atlas (specific brain area).

Results

The brain regions identified to be significantly different between the MCI and CN groups are shown in **Table 2**. The left and right para hippocampal gyrus, hippocampus, and amygdala all had significant between-group differences in both sexes. The regions that had a sex-specific were the Precuneus Cortex and the Brainstem, observed only in males.

In MCI, males showed significantly stronger connectivity of the right or left hippocampus to the left or right precuneus cortex, respectively. This difference is shown visually by comparing boxes A and D (see **Figures 1–3**). There was also a sex specific difference detected in the brain stem. This is visualized in **Figure 3**.

Discussion

This study supports that there are sex differences in pathophysiological biomarkers of the brain in MCI. Specifically, it extends our current understanding of the role of the hippocampus in these differences. We demonstrate that

2 http://www.fmrib.ox.ac.uk/fsl/

hippocampal functional connectivity differs to the precuneus cortex and the brain stem between males and females.

The differences found between the MCI and cognitively normal groups across sexes (posterior para hippocampal gyrus, hippocampus, and amygdala) are consistent with prior studies. The posterior para hippocampal gyrus is the cortical ridge in the medial temporal lobe. It contains the hippocampus (covering it medially) and amygdala (covering

TABLE 1 Mild cognitive impairment subject demographics.

ID	Sex	Age	ApoE genotype	MMSE	GD Scale	CDR	FAQ	NPI-Q
S001	F	74	ε3 ε3	26	6	0.5	0	3
S002	F	65	ε4 ε4	25	1	0.5	1	1
S003	F	71	ε4 ε4	29	0	0.5	0	0
S004	F	80	ε3 ε3	25	1	0.5	0	1
S005	F	70	ε3 ε3	30	5	0.5	0	-
S006	F	65	ε4 ε4	27	7	1.0	30	10
S007	F	79	ε3 ε3	29	0	0.5	4	2
S008	F	58	ε3 ε4	30	1	0.5	0	3
S009	F	76	ε3 ε4	26	7	0.5	4	8
S010	F	61	ε3 ε3	29	3	0.5	5	0
S011	F	72	ε3 ε4	28	2	1.0	19	16
S012	F	72	ε3 ε3	28	5	0.5	0	0
S013	F	84	ε3 ε3	28	6	0.5	8	0
S014	F	69	ε3 ε3	26	1	0.5	0	0
S015	F	72	ε3 ε3	30	2	0.5	0	3
S016	F	72	ε3 ε4	28	0	0.5	6	4
S017	F	81	ε3 ε4	25	2	0.5	7	3
S018	F	77	ε3 ε3	29	1	0.5	0	2
S019	F	67	ε3 ε3	29	2	0.5	0	0
S020	F	63	ε3 ε3	29	1	0.5	1	1
S021	M	68	ε3 ε4	29	0	0.5	2	3
S022	M	72	ε3 ε4	29	0	0.5	12	4
S023	M	62	ε4 ε4	29	0	0.5	0	0
S024	M	58	ε3 ε3	25	0	0.5	1	2
S025	M	74	ε3 ε4	28	2	0.5	3	2
S026	M	63	ε2 ε3	30	1	0.5	1	2
S027	M	90	ε3 ε3	26	2	0.5	4	11
S028	M	86	ε3 ε3	25	1	0.5	6	3
S029	M	87	ε3 ε4	29	1.	1.0	10	12
S030	M	70	ε2 ε4	28	2	0.5	2	8
S031	M	74	ε2 ε3	30	3	0.5	0	2
S032	M	75	ε3 ε4	27	5	1.0	21	7
S033	M	69	ε3 ε3	27	1	0.5	0	1
S034	M	74	ε3 ε3	29	2	1	0	0
S035	M	77	ε2 ε3	28	6	0.5	7	8.0
S036	M	80	ε3 ε4	21	3	1.0	22	4
S037	M	73	ε3 ε4	30	2	0.5	2	2
S038	M	76	ε3 ε3	30	1	0.5	1	1
S039	M	62	ε4 ε4	27	5	0.5	3	7
S040	M	76	ε3 ε3	23	5	0.5	3	4
Female μ ± SD		**71 ± 7.1**	-	**27.7 ± 1.7**	**2.5 ± 2.4**	**0.55 ± 0.16**	**4.4 ± 7.7**	**3.0 ± 4.1**
Male μ ± SD		**73 ± 8.5**	-	**27.5 ± 2.5**	**2.1 ± 1.9**	**0.6 ± 0.21**	**5.0 ± 6.5**	**4.1 ± 3.5**
Between sex *t*-tests		***P* = 0.44**	-	***P* = 0.95**	***P* = 0.58**	***P* = 0.38**	***P* = 0.22**	***P* = 0.12**

Bold values represented by Mean±STD and *p*-values.

it anteromedially) (Goel, 2015). These structures are highly integrated and significant in the process of associative memory (Weniger et al., 2004). It has been shown that functional connectivity between the hippocampus and amygdala to different regions of the brain is disrupted in MCI (Wang et al., 2011; Ortner et al., 2016). This is consistent with our findings.

The role of the precuneus cortex is consistent with other literature highlighting its importance in the development of AD. The precuneus cortex is in the posteromedial portion of the parietal lobe. This area has a central role in a wide range of integrated tasks, including visuo-spatial imagery, episodic memory retrieval, and self-processing operations (Cavanna and Trimble, 2006). The precuneus cortex has been shown to have significantly greater activation in MCI, compared to controls, during visual encoding memory tasks (Rami et al., 2012). Prior studies have shown that functional connectivity between the hippocampus and precuneus cortex differs between individuals with early AD and healthy controls (Kim et al., 2013; Yokoi et al., 2018). However, these studies do not extend to differences between sexes. It has been shown that in individuals with subjective memory complaints, males compared to females had glucose hypometabolism in the precuneus cortex (Cavedo et al., 2018). Our findings extend this knowledge of differences between males and females in the precuneus cortex and show that the effect of MCI on the hippocampal-precuneus cortex functional connectivity may be contributing to the high prevalence of MCI in females.

TABLE 2 Brain regions with a significant difference between mild cognitive impairment and cognitively normal for each sex.

Sex	ROI	Brain area (Atlas)	% Atlas covered	# Of voxels
Female (FMCI v FCN)	Right Hippocampus	Left Posterior Para Hippocampal Gyrus	89%	346
		Right Posterior Para Hippocampal Gyrus	89%	283
		Right Hippocampus	100%	342
		Left Hippocampus	94%	318
		Right Amygdala	100%	342
		Left Amygdala	97%	318
	Left Hippocampus	Left Posterior Para Hippocampal Gyrus	91%	354
		Right Posterior Para Hippocampal Gyrus	90%	288
		Right Hippocampus	98%	684
		Left Hippocampus	100%	761
		Right Amygdala	94%	322
		Left Amygdala	100%	327
Male (MMCI v MCN)	Right Hippocampus	Brain Stem	24%	1001
		Precuneus Cortex	18%	993
		Left Posterior Para Hippocampal Gyrus	97%	380
		Right Posterior Para Hippocampal Gyrus	97%	308
		Right Hippocampus	98%	685
		Left Hippocampus	100%	760
		Right Amygdala	100%	342
		Left Amygdala	100%	327
	Left Hippocampus	Brain Stem	20%	829
		Precuneus Cortex	20%	1132
		Left Posterior Para Hippocampal Gyrus	92%	358
		Right Posterior Para Hippocampal Gyrus	94%	299
		Right Hippocampus	98%	685
		Left Hippocampus	100%	760
		Right Amygdala	99%	337
		Left Amygdala	100%	327

10.3389/fnagi.2022.959394

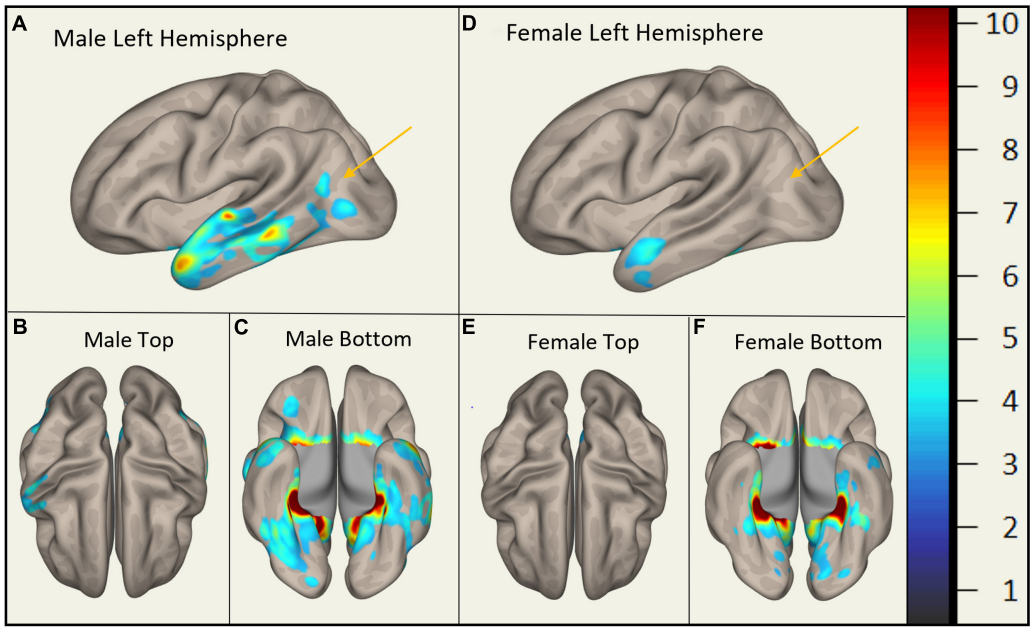

FIGURE 1
Sex-Specific Pathological Features with Right Hippocampus as ROI. Highlighted display the statistically significant cortical regions between mild cognitive impairment (MCI) and cognitively normal (CN) ($p < 0.001$) normalized to a 1–10 scale. Orange arrows indicate the areas of difference at the precuneus cortex. Panels **(A–C)** display MMCI v MCN. Panels **(D–F)** display FMCI v FCN.

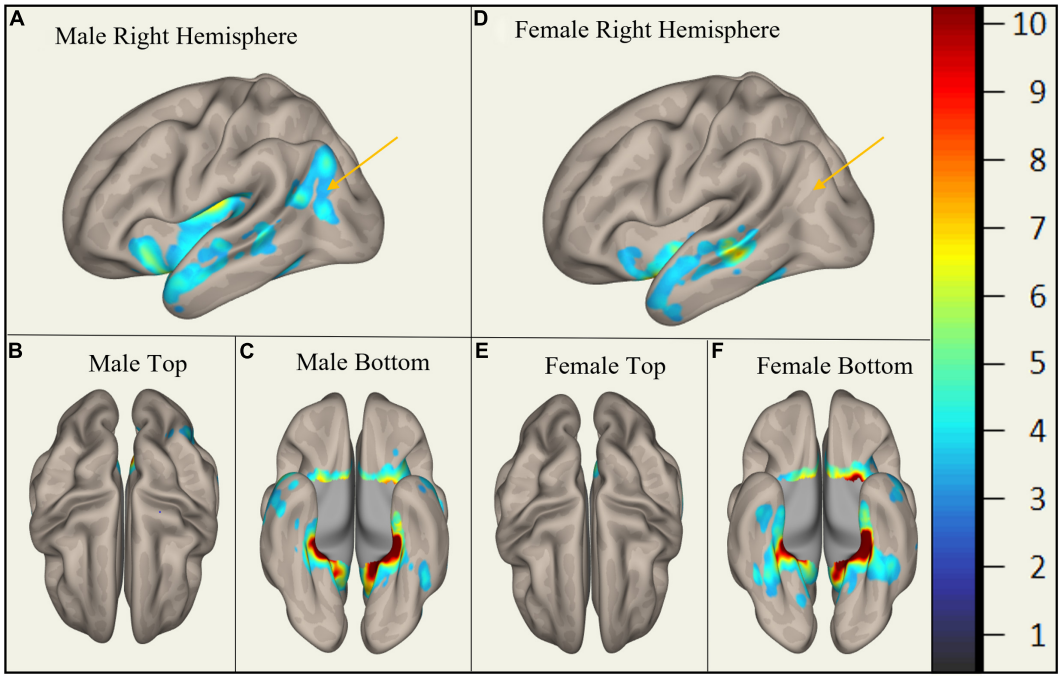

FIGURE 2
Sex-Specific Pathological Features with Left Hippocampus as ROI. Highlighted areas display the statistically significant cortical regions between mild cognitive impairment (MCI) and cognitively normal (CN) ($p < 0.001$) normalized to a 1–10 scale. Orange arrows indicate the area of difference at the precuneus cortex. Panels **(A–C)** display MMCI v MCN. Panels **(D–F)** display FMCI v FCN.

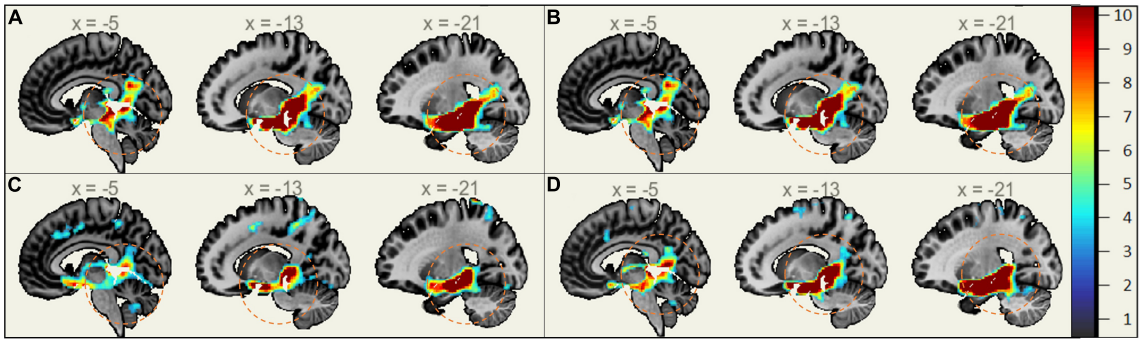

FIGURE 3
Sex-Specific Pathological Features Sagittal View. Highlighted Areas display the statistically significant regions between cognitively normal (CN) and mild cognitive impairment (MCI) ($p < 0.001$) normalized to a 1–10 scale. Orange circles indicate the area of difference in the brain stem and provide size reference between subplots. **(A)** Right Hippocampus ROI MMCI v MCN. **(B)** Left Hippocampus ROI MMCI v MCN. **(C)** Right Hippocampus ROI FMCI v FCN. **(D)** Left Hippocampus ROI FMCI v FCN.

Previous studies observed that functional connectivity of the locus coeruleus (LC) and the ventral tegmental area (VTA) in the midbrain of the brain stem differ in individuals with AD and MCI. Specifically, the connectivity between the VTA and the para hippocampal gyrus and cerebellar vermis were associated with the occurrence of neuropsychiatric symptoms of AD (Serra et al., 2018). Other studies showed that reduced connectivity between the LC and para hippocampal gyrus in MCI was correlated with memory performance (Jacobs et al., 2015). The difference in functional connectivity seen between males and females in this study extends these known connectivity differences seen between MCI and controls to an additional sex difference. This may be a factor in the observed worse neuropsychological tasks seen in females.

The sex differences observed in MCI have also been attributed to other factors besides functional connectivity. For example, cognitive reserve, referring to education and premorbid intelligence (IQ), is associated with the progression of MCI to AD (Osone et al., 2014). Furthermore, Giacomucci et al. (2022) reported that sex interacts with cognitive reserve and influences the onset and severity of subjective cognitive decline. Additionally, sex differences in the progression of AD from MCI have been correlated with the ApoE ε4 allele, a well-known risk factor for AD. It has been observed that ApoE ε4 is only significantly correlated to the progression of AD in females (Kim et al., 2015).

In summary, these findings are significant as they expand our current understanding of the role of the hippocampus-precuneus cortex and hippocampus-brainstem connectivity in sex differences in MCI. Understanding these sex differences in pathophysiology may aid in the development of sex-specific precision medicine to manipulate hippocampal-precuneus cortex and hippocampal-brainstem connectivity to decrease the progression of MCI to AD. Our findings provide the rationale for sex-specific interventions such as cognitive training (Hardcastle et al., 2022) and neuro-navigation guided, targeted non-invasive brain stimulation (Mackenbach et al., 2020; Yang et al., 2021) or their combination (Vecchio et al., 2022).

Limitations and Future Work are related to this study's number of subjects. While this research provides preliminary findings on sex differences in functional connectivity of the hippocampus in individuals with MCI, the small sample size (n = 80) is a limitation. Therefore, future work includes increasing sample size in a larger database, as well as expanding functional connectivity from other regions of interest for MCI, in addition to the hippocampus. Furthermore, studies such as these could be furthered by combining mentioned risk factors such as cognitive reserve or genetic differences to explore if there is any connection.

Data availability statement

The original contributions presented in this study are included in the article/supplementary material, further inquiries can be directed to the corresponding author/s.

Author contributions

JW conducted the study and drafted the manuscript. YY contributed to conceptualization, problem solving, and guidance during the conduction of the study. AY, PM, DW, WS, CC, and YY participated in editing the manuscript. All authors contributed to the article and approved the submitted version.

Funding

This research was supported by a seed grant from the Vice President for Research and Partnerships of the University

of Oklahoma and the Data Institute for Societal Challenges. This work was also supported by the Oklahoma Center for the Advancement of Science and Technology (OCAST) Health Research Program HR21-164, the American Heart Association (#966924), Oklahoma Shared Clinical and Translational Resources (U54GM104938) with an Institutional Development Award from National Institute of General Medical Sciences, NIA-supported Geroscience Training Program in Oklahoma (T32AG052363), Oklahoma Nathan Shock Center (P30AG050911), and Cellular and Molecular GeroScience CoBRE (P20GM125528).

Acknowledgments

We would like to thank Mr. Runfeng Tian for his help and suggestion in data preprocessing. Data collection and sharing for this project was funded by the Alzheimer's Disease Neuroimaging Initiative (ADNI) (National Institutes of Health Grant U01 AG024904) and DOD ADNI (Department of Defense award number: W81XWH-12-2-0012). ADNI is funded by the National Institute on Aging, the National Institute of Biomedical Imaging and Bioengineering, and through generous contributions from the following: AbbVie, Alzheimer's Association; Alzheimer's Drug Discovery Foundation; Araclon Biotech; BioClinica, Inc.; Biogen; Bristol-Myers Squibb Company; CereSpir, Inc.; Cogstate; Eisai Inc.; Elan Pharmaceuticals, Inc.; Eli Lilly and Company; EuroImmun; F. Hoffmann-La Roche Ltd and its affiliated company Genentech, Inc.; Fujirebio; GE Healthcare; IXICO Ltd.; Janssen Alzheimer Immunotherapy Research and Development, LLC.; Johnson & Johnson Pharmaceutical Research and Development LLC.; Lumosity; Lundbeck; Merck and Co., Inc.; Meso Scale Diagnostics, LLC.; NeuroRx Research; Neurotrack Technologies; Novartis Pharmaceuticals Corporation; Pfizer Inc.; Piramal Imaging; Servier; Takeda Pharmaceutical Company; and Transition Therapeutics. The Canadian Institutes of Health Research is providing funds to support ADNI clinical sites in Canada. Private sector contributions are facilitated by the Foundation for the National Institutes of Health (www.fnih.org). The grantee organization is the Northern California Institute for Research and Education, and the study is coordinated by the Alzheimer's Therapeutic Research Institute at the University of Southern California. ADNI data are disseminated by the Laboratory for Neuro Imaging at the University of Southern California.

Conflict of interest

The authors declare that the research was conducted in the absence of any commercial or financial relationships that could be construed as a potential conflict of interest.

Publisher's note

References

Alzheimer's Association (2016). 2016 Alzheimer's disease facts and figures. *Alzheimers Dement.* 12, 459–509. doi: 10.1016/j.jalz.2016.03.001

Andrew, M. K., and Tierney, M. C. (2018). The puzzle of sex, gender and Alzheimer's disease: Why are women more often affected than men? *Womens Health* 14:1745506518817995. doi: 10.1177/1745506518817995

Braak, H., and Braak, E. (1995). Staging of Alzheimer's disease- related neurofibrillary changes. *Neurobiol. Aging.* 16, 271–278. doi: 10.1016/0197-4580(95)00021-6

Burke, S. L., Tianyan, H., Fava, N. M., Li, T., Rodriguez, M. J., Schuldiner, K. L., et al. (2019). Sex differences in the development of mild cognitive impairment and probable Alzheimer's disease as predicted by the hippocampal volume or white matter hyperintensities. *J. Women Aging* 31, 140–164. doi: 10.1080/08952841.2018.1419476

Cavanna, A. E., and Trimble, M. R. (2006). The precuneus: A review of its functional anatomy and behavioral correlates. *Brain* 129, 564–583. doi: 10.1093/brain/awl004

Cavedo, E., Chiesa, P. A., Houot, M., Ferretti, M. T., Grothe, M. J., Teipel, S. J., et al. (2018). Sex differences in functional and molecular neuroimaging biomarkers of Alzheimer's disease in cognitively normal older adults with subjective memory complaints. *Alzheimers Dement.* 14, 1204–1215. doi: 10.1016/j.jalz.2018.05.014

Centers for Disease Control and Prevention (2021). *Alzheimer's Disease.* Available online at: https://www.cdc.gov/dotw/alzheimers/index.html (accessed March 9, 2022).

Chapman, R. M., Mapstone, M., Gardner, M. N., Sandoval, T. C., McCrary, J. W., Guillily, M. D., et al. (2011). Women have farther to fall: Gender differences between normal elderly and Alzheimer's disease in verbal memory engender better detection of Alzheimer's disease in women. *J. Int. Neuropsychol. Soc.* 17, 654–662. doi: 10.1017/S1355617711000452

Davatzikos, C., Bhatt, P., Shaw, L. M., Batmanghelich, K. N., and Trojanowski, J. Q. (2011). Prediction of MCI to AD conversion, via MRI, CSF biomarkers, and pattern classification. *Neurobiol. Aging* 32, 2322.e19–27. doi: 10.1016/j.neurobiolaging.2010.05.023

Ferretti, M., Iulita, M. F., Cavedo, E., Chiesa, P. A., Schumacher Dimech, A., Santuccione Chadha, A., et al. (2018). Sex differences in Alzheimer disease–the gateway to precision medicine. *Nat. Rev. Neurol.* 14, 457–469. doi: 10.1038/s41582-018-0032-9

Gauthier, S., Reisberg, B., Zaudig, M., Petersen, R. C., Ritchie, K., Broich, K., et al. (2006). Mild cognitive impairment. *Lancet* 367, 1262–1270. doi: 10.1016/S0140-6736(06)68542-5

Giacomucci, G., Mazzeo, S., Padiglioni, S., Bagnoli, S., Belloni, L., Ferrari, C., et al. (2022). Gender differences in cognitive reserve: Implication for subjective

cognitive decline in women. *Neurol. Sci.* 43, 2499–2508. doi: 10.1007/s10072-021-05644-x

Goel, A. (2015). *Parahippocampal Gyrus*. Available online at: https://doi.org/10.53347/rID-34499 (accessed May 20, 2022).

Guerreiro, R., and Bras, J. (2015). The age factor in Alzheimer's disease. *Genome Med.* 7, 1–3. doi: 10.1186/s13073-015-0232-5

Gumus, M., Multani, N., Mack, M. L., and Tartaglia, M. C. (2021). Progression of neuropsychiatric symptoms in young-onset versus late-onset Alzheimer's disease. *Geroscience*. 43, 213–223. doi: 10.1007/s11357-020-00304-y

Hardcastle, C., Hausman, H. K., Kraft, J. N., Albizu, A., O'Shea, A., Boutzoukas, E. M., et al. (2022). Proximal improvement and higher-order resting state network change after multidomain cognitive training intervention in healthy older adults. *Geroscience* 44, 1011–1027. doi: 10.1007/s11357-022-00535-1

Henderson, V. W., and Buckwalter, J. G. (1994). Cognitive deficits of men and women with Alzheimer's disease. *Neurology* 44, 90–96. doi: 10.1212/WNL.44.1.90

Hua, X., Hibar, D. P., Lee, S., Toga, A. W., Jack, C. R. Jr., Weiner, M. W., et al. (2010). Sex and age differences in atrophic rates: An ADNI study with n = 1368 MRI scans. *Neurobiol. Aging* 31, 1463–1480. doi: 10.1016/j.neurobiolaging.2010.04.033

Jacobs, H. I. L., Wiese, S., van de Ven, V., Gronenschild, E. H., Verhey, F. R., Matthews, P. M., et al. (2015). Relevance of parahippocampal-locus coeruleus connectivity to memory in early dementia. *Neurobiol. Aging* 36, 618–626. doi: 10.1016/j.neurobiolaging.2014.10.041

Jenkinson, M., Beckmann, C. F., Behrens, T. E., Woolrich, M. W., and Smith, S. M. (2012). FSL. *Neuroimage* 62, 782–790. doi: 10.1016/j.neuroimage.2011.09.015

Jiang, J., Sheng, C., Chen, G., Liu, C., Jin, S., Li, L., et al. (2022). Alzheimer's disease neuroimaging initiative. Glucose metabolism patterns: A potential index to characterize brain ageing and predict high conversion risk into cognitive impairment. *Geroscience*. doi: 10.1007/s11357-022-00588-2

Kim, J., Kim, Y. H., and Lee, J. H. (2013). Hippocampus–precuneus functional connectivity as an early sign of Alzheimer's disease: A preliminary study using structural and functional magnetic resonance imaging data. *Brain Res.* 1495, 18–29. doi: 10.1016/j.brainres.2012.12.011

Kim, S., Kim, M. J. S., Kim, H. S., Kang, S. W., Lim, W., Myung, W., et al. (2015). Gender differences in risk factors for transition from mild cognitive impairment to Alzheimer's disease: A CREDOS study. *Compr. Psychiatry* 62, 114–122. doi: 10.1016/j.comppsych.2015.07.002

López, M. E., Turrero, A., Cuesta, P., Rodríguez-Rojo, I. C., Barabash, A., Marcos, A., et al. (2020). A multivariate model of time to conversion from mild cognitive impairment to Alzheimer's disease. *Geroscience*. 42, 1715–1732. doi: 10.1007/s11357-020-00260-7

Mackenbach, C., Tian, R., and Yang, Y. (2020). "Effects of electrode configurations and injected current intensity on the electrical field of transcranial direct current stimulation: A simulation study," in *Proceedings of the 2020 42nd Annual International Conference of the IEEE Engineering in Medicine & Biology Society* (Montreal, QC: EMBC), 3517–3520. doi: 10.1109/EMBC44109.2020.9176686

McGrattan, A. M., Pakpahan, E., Siervo, M., Mohan, D., Reidpath, D. D., Prina, M., et al. (2022). Risk of conversion from mild cognitive impairment to dementia in low-and-middle-income countries: A systematic review and meta-analysis. *Alzheimers Assoc.* 8:e12267. doi: 10.1002/trc2.12267

Mielke, M. M. (2019). Sex and gender differences in Alzheimer's disease dementia. *Psychiatr. Times* 35, 14–17.

Nieto-Castanon, A. (2020). *Handbook of Functional Connectivity Magnetic Resonance Imaging Methods in CONN*. Boston, MA: Hilbert Press.doi: 10.56441/hilbertpress.2207.6598

Ortner, M., Pasquini, L., Barat, M., Alexopoulos, P., Grimmer, T., Förster, S., et al. (2016). Progressively disrupted intrinsic functional connectivity of basolateral amygdala in very early Alzheimer's disease. *Front. Neurol.* 7:132. doi: 10.3389/fneur.2016.00132

Osone, A., Arai, R., Hakamada, R., and Shimoda, K. (2014). Impact of cognitive reserve on the progression of mild cognitive impairment to Alzheimer's disease in Japan. *Geriatr. Gerontol. Int.* 15, 428–234. doi: 10.1111/ggi.12292

Pearce, E. E., Alsaggaf, R., Katta, S., Dagnall, C., Aubert, G., Hicks, B. D., et al. (2022). Telomere length and epigenetic clocks as markers of cellular aging: A comparative study. *Geroscience* 44, 1861–1869. doi: 10.1007/s11357-022-00586-4

Petersen, R. C. (2004). Mild cognitive impairment as a diagnostic entity. *J. Intern. Med.* 256, 183–194. doi: 10.1111/j.1365-2796.2004.01388.x

Rahman, A., Schelbaum, E., Hoffman, K., Diaz, I., Hristov, H., Andrews, R., et al. (2020). Sex-driven modifiers of Alzheimer risk a multimodality brain imaging study. *Neurology* 95, e166–e178. doi: 10.1212/WNL.0000000000009781

Rami, L., Sala-Llonch , R., Solé-Padullés , C., Fortea, J., Olives, J., Lladó, A., et al. (2012). Distinct functional activity of the precuneus and posterior cingulate cortex during encoding in the preclinical stage of Alzheimer's disease. *J. Alzheimers Dis.* 31, 517–526. doi: 10.3233/JAD-2012-120223

Salmon, D. P. (2011). Neuropsychological features of mild cognitive impairment and preclinical Alzheimer's disease. *Curr. Top. Behav. Neurosci.* 10, 187–212. doi: 10.1007/7854_2011_171

Serra, L., Di Domenico, C., D'Amelio, M., Dipasquale, O., Marra, C., Mercuri, N. B., et al. (2018). In vivo mapping of brainstem nuclei functional connectivity disruption in Alzheimer's disease. *Neurobiol. Aging* 72, 72–82. doi: 10.1016/j.neurobiolaging.2018.08.012

Smith, S. M., Jenkinson, M. W., Woolrich, C. F., Beckmann, T. E. J., Behrens, H., Johansen-Berg, P. R., et al. (2004). Advances in functional and structural MR image analysis and implementation as FSL. *Neuroimage* 23, 208–219. doi: 10.1016/j.neuroimage.2004.07.051

Snyder, H. M., Asthana, S., Bain, L., Brinton, R., Craft, S., Dubal, D. B., et al. (2016). Sex biology contributions to vulnerability to Alzheimer's disease: A think tank convened by the women's Alzheimer's research initiative. *Alzheimers Dement.* 12, 1186–1196. doi: 10.1016/j.jalz.2016.08.004

Sohn, D., Shpanskaya, K., Lucas, J. E., Petrella, J. R., Saykin, A. J., Tanzi, R. E., et al. (2018). "Sex differences in cognitive decline in subjects with high likelihood of mild cognitive impairment due to Alzheimer's disease. *Sci. Rep.* 8:7490. doi: 10.1038/s41598-018-25377-w

Tzourio-Mazoyer, N., Landeau, B., Papathanassiou, D., Crivello, F., Etard, O., Delcroix, N., et al. (2002). Automated anatomical labeling of activations in SPM using a macroscopic anatomical parcellation of the MNI MRI single-subject brain. *Neuroimage* 15, 273–289. doi: 10.1006/nimg.2001.0978

Vecchio, F., Quaranta, D., Pappalettera, C., Di Iorio, R., L'Abbate, F., et al. (2022). Neuronavigated magnetic stimulation combined with cognitive training for Alzheimer's patients: An EEG graph study. *Geroscience* 44, 159–172. doi: 10.1007/s11357-021-00508-w

Wang, Z., Liang, P., Jia, X., Qi, Z., Yu, L., Yang, Y., et al. (2011). Baseline and longitudinal patterns of hippocampal connectivity in mild cognitive impairment: Evidence from resting state fMRI. *J. Neurol. Sci.* 309, 79–85. doi: 10.1016/j.jns.2011.07.017

Weniger, G., Boucsein, K., and Irle, E. (2004). Impaired associative memory in temporal lobe epilepsy subjects after lesions of hippocampus, parahippocampal gyrus, and amygdala. *Hippocampus* 14, 785–796. doi: 10.1002/hipo.10216

Whitfield-Gabrieli, S., and Nieto-Castanon, A. (2012). Conn: A functional connectivity toolbox for correlated and anticorrelated brain networks. *Brain Connect.* 2, 125–141. doi: 10.1089/brain.2012.0073

Woolrich, M. W., Jbabdi, S., Patenaude, B., Chappell, M., Makni, S., Behrens, T., et al. (2009). Bayesian analysis of neuroimaging data in FSL. *Neuroimage* 45, S173–S186. doi: 10.1016/j.neuroimage.2008.10.055

Worsley, K. J., Marrett, S., Neelin, P., Vandal, A. C., Friston, K. J., and Evans, A. C. (1996). A unified statistical approach for determining significant signals in images of cerebral activation. *Hum. Brain Mapp.* 4, 58–73.Yang, Y., Sidorov, E., and Dewald, J. P. (2021). Targeted tDCS reduces the expression of the upper limb flexion synergy in chronic hemiparetic stroke. *Arch. Phys. Med. Rehabil.* 102:e10.

Yang, Y., Sidorov, E. V., and Dewald, J. P. (2021). Targeted tDCS reduces the expression of the upper limb flexion synergy in chronic hemiparetic stroke. *Arch. Phys. Med. Rehabil.* 102:e10. doi: 10.1016/j.apmr.2021.07.418

Yokoi, T., Watanabe, H., Yamaguchi, H., Bagarinao, E., Masuda, M., Imai, K., et al. (2018). Involvement of the precuneus/posterior cingulate cortex is significant for the development of Alzheimer's disease: A PET (THK5351, PiB) and resting fMRI study. *Front. Aging Neurosci.* 10:304. doi: 10.3389/fnagi.2018.00304

frontiers | Frontiers in Aging Neuroscience

TYPE Original Research
PUBLISHED 17 August 2022
DOI 10.3389/fnagi.2022.905035

OPEN ACCESS

EDITED BY
Fermín Segovia,
University of Granada, Spain

REVIEWED BY
Yoo Hyun Um,
Catholic University of Korea,
South Korea
Xia Li,
Shanghai Jiao Tong University, China

*CORRESPONDENCE
Jiao Liu
liujiao0415@outlook.com

†These authors have contributed equally to this work and share first authorship

SPECIALTY SECTION
This article was submitted to Neurocognitive Aging and Behavior, a section of the journal Frontiers in Aging Neuroscience

RECEIVED 26 March 2022
ACCEPTED 25 July 2022
PUBLISHED 17 August 2022

CITATION
Chen R, Cai G, Xu S, Sun Q, Luo J, Wang Y, Li M, Lin H and Liu J (2022) Body mass index related to executive function and hippocampal subregion volume in subjective cognitive decline. *Front. Aging Neurosci.* 14:905035. doi: 10.3389/fnagi.2022.905035

Body mass index related to executive function and hippocampal subregion volume in subjective cognitive decline

Ruilin Chen[1,2†], Guiyan Cai[1,2†], Shurui Xu[1,2†], Qianqian Sun[2], Jia Luo[2], Yajun Wang[1,2], Ming Li[3], Hui Lin[4] and Jiao Liu[1,5,6,7*]

[1]National-Local Joint Engineering Research Center of Rehabilitation Medicine Technology, Fujian University of Traditional Chinese Medicine, Fuzhou, China, [2]College of Rehabilitation Medicine, Fujian University of Traditional Chinese Medicine, Fuzhou, China, [3]Affiliated Rehabilitation Hospital, Fujian University of Traditional Chinese Medicine, Fuzhou, China, [4]Department of Physical Education, Fujian University of Traditional Chinese Medicine, Fuzhou, China, [5]Fujian Key Laboratory of Rehabilitation Technology, Fuzhou, China, [6]Traditional Chinese Medicine Rehabilitation Research Center of State Administration of Traditional Chinese Medicine, Fujian University of Traditional Chinese Medicine, Fuzhou, China, [7]Key Laboratory of Orthopedics and Traumatology of Traditional Chinese Medicine and Rehabilitation, Ministry of Education, Fujian University of Traditional Chinese Medicine, Fuzhou, China

Objective: This study aims to explore whether body mass index (BMI) level affects the executive function and hippocampal subregion volume of subjective cognitive decline (SCD).

Materials and methods: A total of 111 participants were included in the analysis, including SCD (38 of normal BMI, 27 of overweight and obesity) and normal cognitive control (NC) (29 of normal BMI, 17 of overweight and obesity). All subjects underwent the Chinese version of the Stroop Color-Word Test (SCWT) to measure the executive function and a high-resolution 3D T1 structural image acquisition. Two-way ANOVA was used to examine the differences in executive function and gray matter volume in hippocampal subregions under different BMI levels between the SCD and NC.

Result: The subdimensions of executive function in which different BMI levels interact with SCD and NC include inhibition control function [SCWT C-B reaction time(s): $F_{(1,104)} = 5.732$, $p = 0.018$], and the hippocampal subregion volume of CA1 [$F_{(1,99)} = 8.607$, $p = 0.004$], hippocampal tail [$F_{(1,99)} = 4.077$, $p = 0.046$], and molecular layer [$F_{(1,99)} = 6.309$, $p = 0.014$]. After correction by Bonferroni method, the population × BMI interaction only had a significant effect on the CA1 ($p = 0.004$). Further analysis found that the SCWT C-B reaction time of SCD was significantly longer than NC no matter whether it is at the normal BMI level [$F_{(1,104)} = 4.325$, $p = 0.040$] or the high BMI level [$F_{(1,104)} = 21.530$, $p < 0.001$], and the inhibitory control function of SCD was worse than that of NC. In the normal BMI group, gray matter volume in the hippocampal subregion (CA1) of SCD was significantly smaller than that of NC [$F_{(1,99)} = 4.938$, $p = 0.029$]. For patients with SCD, the high BMI group had

worse inhibitory control function [$F_{(1,104)}$ = 13.499, p < 0.001] and greater CA1 volume compared with the normal BMI group [$F_{(1,99)}$ = 7.619, p = 0.007].

Conclusion: The BMI level is related to the inhibition control function and the gray matter volume of CA1 subregion in SCD. Overweight seems to increase the gray matter volume of CA1 in the elderly with SCD, but it is not enough to compensate for the damage to executive function caused by the disease. These data provide new insights into the relationship between BMI level and executive function of SCD from the perspective of imaging.

KEYWORDS

subjective cognitive decline, executive function, inhibition control function, hippocampal subregion, CA1

Introduction

Subjective cognitive decline (SCD) refers to the decline in subjective memory or cognitive function, but there is no obvious cognitive dysfunction and no obvious impairment of daily living ability in objective behavioral examination (Jessen et al., 2014). SCD is a state between normal aging and mild cognitive impairment (MCI), which is considered to be one of the most initial cognitive change in the pathogenesis of Alzheimer's disease (AD) (Jessen et al., 2020). A recent study found that the prevalence of SCD in the elderly population > 50 years was 26.6% (Liew, 2019), and SCD increased the risk of progression to MCI in the elderly by 1.73 times and the risk of progression to AD by 1.9 times (Pike et al., 2021).

One variable that may play an important role in the development of AD is obesity, which is associated with numerous deleterious health conditions (Mallorquí-Bagué et al., 2018; Piché et al., 2020) including late-life dementia (Kivipelto et al., 2018). Body mass index (BMI), one measure of obesity, has a complex relationship with cognitive function in the elderly. Previous studies found that the cognitive dimensions of BMI's impact are different across clinical stages of AD. For instance, in dementia or MCI stage of AD, a higher BMI is related to the worse overall cognitive function, memory, attention, and executive function in the elderly (Calderón-Garcidueñas et al., 2019; Sanchez-Flack et al., 2021). In the elderly population with normal cognitive status, higher BMI predicts worse executive function (Gunstad et al., 2007; Beyer et al., 2017), while BMI is not significantly associated with attention and memory dimensions (Schmeidler et al., 2019). These studies suggested that different from other cognitive dimensions the effects of BMI on executive function may appear to be present throughout different clinical stages of AD. However, the relationship between BMI and executive function in SCD (an early stage of AD) is unclear. In addition, our previous preliminary study found that overweight and obese patients with SCD had a worse executive function compared with patients with SCD in the normal weight group (Xu et al., 2021). However, a previous study lacked further investigation in normal controls (NCs) to check the interaction of BMI level and disease on executive function in patients with SCD. In addition, the underlying mechanism is also unclear.

Neuroimaging studies have suggested early AD-like structural brain alterations in SCD (Pini and Wennberg, 2021). The hippocampus plays a critical role in cognition (Lisman et al., 2017). A previous study found that SCD exhibits a consistent pattern of hippocampal atrophy (Chen et al., 2021). Some studies have observed a decreased hippocampal volume in individuals with SCD both at baseline and during a significant longitudinal decline (Scheef et al., 2012; Sánchez-Benavides et al., 2018; van Rooden et al., 2018; Yue et al., 2018), with an annual decrease of 1.9% (Cherbuin et al., 2015; Wang et al., 2020). The hippocampus is composed of multiple subregions such as the dentate gyrus (DG), cornu ammonis (CA) region, and subiculum (SUB), all of which play specific roles in the circuits of the hippocampus (O'Keefe et al., 2007). For example, the CA1 subregion and the entorhinal cortex can represent a variety of different information (time, space, etc.), and the SUB, as a transition region between the two subregions, can accept the direct input of synapses in CA1 subregion and project it to different cortex and subcortical regions (Matsumoto et al., 2019); CA1, CA2/3, and DG play complementary roles in supporting episodic memory by allowing one to remember specific items, as well as their relationships, within a shared context (Dimsdale-Zucker et al., 2018). With the progression of AD, the volume of hippocampal subregions shows an obvious decreasing trend (Zhao et al., 2019). Studies have found that in people with risk of AD smaller volumes of the hippocampal fimbria, presubiculum, and SUB showed the associations with poor performance on executive function (Evans et al., 2018). While in patients with MCI, smaller hippocampal subregion (CA1) volume is associated with worse

executive function (Suo et al., 2017). However, the relationship between the hippocampal subregion and the executive function subdimension in SCD is still not clear.

It is worth mentioning that the hippocampus is a key structure involved in body weight regulation (Davidson et al., 2007; Kanoski and Grill, 2017). Neuroimaging studies incorporating structural magnetic resonance imaging (MRI) reported that patients with AD with higher BMI levels have a smaller hippocampal volume (Ly et al., 2021). However, the relationship between BMI and cognitive function/hippocampal volume in different stages of AD is inconsistent. Kivimäki et al. (2018) reported that when BMI was assessed > 20 years before the diagnosis of dementia, a higher BMI was associated with an increased risk of dementia, whereas when BMI was assessed < 10 years before the diagnosis, a lower BMI predicted dementia. In addition, studies reported that overweight/obesity was positively correlated with the hippocampal volume of subjects (Widya et al., 2011; Ma et al., 2019). Animal experiments show that obesity affects the hippocampal subregion (CA1, CA3) of rats with pre-AD and MCI models (Ivanova et al., 2020). However, it is unclear what the effects are of different BMIs on the volume of the hippocampal subregion in the elderly with SCD and whether there is an interactive effect between the BMI and disease condition on the volume of hippocampal subregions.

This study aims to compare the difference in executive function of the elderly SCD and NC with different BMI levels and explore whether there are differences in hippocampal subregions related to BMI levels in different cognitive states. We hypothesized that the effect of BMI level on executive function in patients with SCD may be related especially to the hippocampal subregion gray matter volume.

Materials and methods

Participants

In this study, we recruited 111 elderly subjects aged > 60 years, who voluntarily participated in a free questionnaire survey and physical examination in communities in Fuzhou, Fujian Province, including 65 elderly people with SCD and 46 elderly NC. The SCD and NC participants were divided into normal BMI group and overweight/obesity (high BMI) group according to the Chinese adult overweight and obesity prevention and control guidelines (China Obesity Working Group, 2004) (normal weight, BMI between 18.5 and 23.9 kg/m^2; overweight and obese, BMI ≥ 24.0 kg/m^2). This study was approved by the Medical Ethics Committee of the Affiliated Rehabilitation Hospital of Fujian University of Traditional Chinese Medicine. All participants signed an informed consent form before taking the tests.

Inclusion criteria of SCD included (1) meeting the SCD conceptual framework proposed by Jessen et al. (2014) and China AD Preclinical Alliance (Ying Han, 2018); (2) aged 60–75 years; (3) BMI ≥ 18.5 kg/m^2; and (4) informed consent, voluntary participation. The SCD conceptual framework was as follows: (1) subjective decline in memory rather than other domains of cognition; (2) onset of SCD within the last 5 years; (3) age at SCD onset of at least 60 years; (4) worries associated with SCD; (5) worse self-perceived memory than others in the same age group; and (6) absence of objective clinical impairment of MCI, Montreal Cognitive Assessment (MoCA) (Nasreddine et al., 2005) total score ≥ 26 (Langa and Levine, 2014).

Normal cognitive control inclusion criteria included (1) normal activities of daily living; (2) no self-SCD and no obvious memory impairment; (3) normal cognitive testing (MoCA score ≥ 26 points); (4) no significant behavioral and language impairments; (5) aged 60–75 years; (6) BMI ≥ 18.5 kg/m^2; and (7) informed consent, voluntary participation.

Subjective cognitive decline and NC exclusion criteria included (1) hypertensive patients with uncontrolled blood pressure; (2) history of alcohol and drug abuse; (3) severe anxiety and depression, as indicated by the Hamilton Depression Scale (HAMD) (Hamilton, 1960) score > 24 points or Hamilton Anxiety Scale (HAMA) (Hamilton, 1959) score > 29 points; (4) decline in cognitive function caused by other diseases (such as mental diseases and poisoning); and (5) unable to cooperate with the tester due to other physiological and psychological reasons.

Clinical assessment

In the form of a questionnaire, the basic demographic data of the subjects (age, gender, BMI, years of education) and medical history (hypertension, hyperlipidemia, type II diabetes mellitus [T2DM], etc.), as well as medication history, were recorded in detail by professionally trained assessors. Medication history refers to the last 3-month routine medication self-reported by subjects when receiving the questionnaire of this study. We mainly recorded the use of drugs that control hypertension, hyperlipidemia, and T2DM. In addition, any other medication the participant used within the last 3 months was also recorded.

Neuropsychological assessment

Montreal Cognitive Assessment was used to assess the global cognitive function of subjects, with a total score of 30 points (the higher the score, the better the global cognitive function). HAMD and HAMA were used to assess the severity of depression and anxiety.

The Stroop Color-Word Test (SCWT) (Golden and Golden, 1981) evaluates the executive function. The SCWT version (Xu et al., 2021) adopted in this study consists of three cards, each with 24 characters. SCWT A is composed of red, yellow, blue, or green dots; SCWT B is composed of Chinese characters printed in the same color (red, yellow, blue, or green, the color of the characters is consistent with the meaning of the word); and SCWT C prints four kinds of Chinese characters with different colors (red, yellow, blue, or green, the color of the characters is inconsistent with the meaning of the word, such as "yellow" printed in red color). The longer the response time of each card, the worse the execution function (Wecker et al., 2000; Homack and Riccio, 2004). The analysis indicators are the reaction time of each card and the SCWT C-B reaction time. A larger SCWT C-B reaction time represents greater interference from conflicting response sets or poorer inhibitory control (Scarpina and Tagini, 2017; Rabi et al., 2020).

Brain imaging acquisition

The brain MRI data were acquired on a 3.0 T Prisma scanner system (Siemens Medical Solutions, Erlangen, Germany) with a 64–channel head coil. Before MRI scanning, inform the precautions of MRI scanning again and sign the consent form for MRI scanning. Confirm that the subjects have no scanning contraindications such as metal implants and claustrophobia. Ask the subjects to stay still during the scanning process, use rubber earplugs and soft head pads to reduce noise, and fix the position of the head. If they feel uncomfortable, press the alarm in their hand to instruct the staff to stop the scanning. The T1–MPRAGE images were collected using the following parameters: field of view, 256 mm * 256 mm; repetition time, 2,300 ms; echo time, 2.94 ms; flip angle, 15°; slice thickness, 1 mm; and slices, 160. In addition, all subjects in this study were screened with an appropriate MRI scan (T2-weighted sequence) to check the vascular injuries such as stroke and brain tumor before initiation of the study. None of the eligible subjects included had obvious vascular lesions.

Brain imaging processing

The T1 image data were preprocessed using the MRIconvert (a toolbox for image data conversion, version 2.0 Rev. 235[1]) and FreeSurfer software (a toolbox for image data analysis, version 7.1.0[2]) under the Lunix system.

The FreeSurfer 7.1.0 software was used to extract the hippocampal volume in the subcortical nucleus segmentation file of each subject generated by pretreatment. During segmentation, the image of each subject is first converted from the individual space to the FreeSurfer standard space to ensure accurate segmentation, and then the hippocampus of each subject is divided into 19 regions according to the hippocampal subregion segmentation template on the official website of FreeSurfer.[3] According to **Supplementary Table 1**, the subdivided 19 regions were combined into hippocampal tail, hippocampal fissure, fimbria, parasubiculum, subiculum, presubiculum, CA1, CA3, CA4, molecular layer, granule cell layer, and molecular layer of the dentate gyrus (GC-ML-DG) and hippocampal amygdala transition area (HATA), the 12 hippocampal subregions, and CA2 is always included in CA3 (Fischl, 2012; Iglesias et al., 2015; **Supplementary Figure 1**).

Statistical analysis

Behavioral data analysis

Analysis was performed using the SPSS software (version 26.0 for Windows, IL, United States). The categorical variables are expressed by the number of cases *n* (%), and the comparison between groups was performed using chi-square test. The continuous variables are expressed as mean ± SD, and the comparison between groups was performed using one-way ANOVA. If $p < 0.05$, the difference was considered to be statistically significant, and the *post hoc* comparison was performed using Fisher's least significant difference method.

Two-way ANOVA was used for the comparison between groups of SCWT test (the first factor was population grouping and the second factor was BMI grouping, to explore the main effects of population grouping and BMI grouping and the interaction between them). Age, gender, and years of education were used as covariates; $p < 0.05$ was considered to be statistically significant. When there is an interaction between population grouping and BMI grouping, simple main effect and paired comparative analysis were used to further study whether different populations and different BMI improve or reduce executive function.

Brain imaging analysis

The volume of each subject's hippocampal subregion was extracted and analyzed by two-way ANOVA based on region of interest (ROI) level (the first factor is population grouping and the second factor is BMI grouping) with the total hippocampal volume, intracranial volume, age/gender/years of education/hypertension/hyperlipidemia/T2DM as covariates. The brain regions with interactive gray matter volume

1 https://www.softpedia.com/get/Science-CAD/MRIConvert.shtml

2 http://surfer.nmr.mgh.harvard.edu

3 https://surfer.nmr.mgh.harvard.edu/fswiki/HippocampalSubfieldsAndNucleiOfAmygdala

differences were obtained, and the interaction effects between them were further analyzed using the SPSS 26.0 software. When there is an interaction between population grouping and BMI grouping, simple main effect and paired comparative analysis were used to further study whether different populations and different BMI increase or decrease the gray matter volume of hippocampal subregions. For the brain area with significant interaction, the association between the gray matter volume and the corresponding score of SCWT test was done using the partial correlation analysis with age, gender, and years of education as covariates. Multiple comparisons were corrected using Bonferroni method.

Results

Demographic characteristics

The comparison of general demographic data and personal medical history of each group (i.e., NC-normal BMI, NC-high BMI, SCD-normal BMI, SCD-high BMI) is shown in Table 1. The results of intergroup comparison showed that no significant group difference was found among the general demographic data of the four groups except BMI. After adjusting for age, gender, and years of education, the mean MoCA score of subjects with SCD included in this study was $27.40 \pm 1.07 \geq 26$, which suggested that there was no obvious objective index abnormality.

Neuropsychological characteristics

Montreal Cognitive Assessment score, HAMD score, and HAMA score of each group (NC-normal BMI, NC-high BMI, SCD-normal BMI, and SCD-high BMI) are compared in Table 1. The results of intergroup comparison showed that there was no significant difference in MOCA score, HAMD score, and HAMA score among the four groups ($p > 0.05$).

The comparison of SCWT scores of each group is shown in Table 2. We observed significant interaction effects for SCWT C reaction time (s) [$F_{(1,104)} = 8.017$, $p = 0.006$, partial $\eta^2 = 0.072$] and SCWT C-B reaction time (s) [$F_{(1,104)} = 5.732$, $p = 0.018$, partial $\eta^2 = 0.052$], as well as significant population main effects [SCWT C reaction time (s): $F_{(1,104)} = 32.745$, $p < 0.001$; SCWT C-B reaction time (s): $F_{(1,104)} = 23.411$, $p < 0.001$] and BMI main effects [SCWT C reaction time (s): $F_{(1,104)} = 7.593$, $p = 0.007$; SCWT C-B reaction time (s): $F_{(1,104)} = 5.33$, $p = 0.023$], respectively.

Post hoc analysis showed that the SCWT C reaction time (s) and SCWT C-B reaction time (s) of the SCD-normal BMI group were significantly larger than the NC-normal BMI group, which indicates that the inhibitory control function of the SCD-normal BMI group was worse than the NC-normal BMI group [SCWT C reaction time (s): $F_{(1,104)} = 6.050$, $p = 0.016$; SCWT C-B reaction time (s): $F_{(1,104)} = 4.325$, $p = 0.040$]. The SCWT C-B reaction time (s) of SCD-high BMI group was significantly higher than the NC-high BMI group, indicating that the inhibitory control function of the SCD-high BMI group was worse than the NC-high BMI group [SCWT C reaction time (s): $F_{(1,104)} = 30.115$, $p < 0.001$; SCWT C-B reaction time (s): $F_{(1,104)} = 21.530$, $p < 0.001$]. The SCWT C reaction time (s) and SCWT C-B reaction time (s) of the SCD-normal BMI group were significantly smaller than the SCD-high BMI group, suggesting that the inhibitory control function of the SCD-normal BMI group was better than those of the SCD-high BMI group [SCWT C reaction time (s): $F_{(1,104)} = 19.053$, $p < 0.001$; SCWT C-B reaction time (s): $F_{(1,104)} = 13.499$, $p < 0.001$]. There was no significant difference in the inhibitory control function [SCWT C reaction time (s): $p = 0.982 > 0.05$; SCWT C-B reaction time (s): $p = 0.973 > 0.05$] between the NC-normal BMI group and the NC-high BMI group. The results of SCWT C reaction time (s) and SCWT C-B reaction time (s) are given in Tables 2, 3.

For SCWT A reaction time (s) and SCWT B reaction time (s), we did not find significant differences in the interaction terms between population grouping and BMI grouping ($p > 0.05$; see Table 2).

Brain imaging characteristics

A comparison of hippocampal subregion volume among the four groups is shown in Table 4. ANOVA showed that the population × BMI interaction had a significant effect on CA1 [$F_{(1,99)} = 8.607$, $p = 0.004$, partial $\eta^2 = 0.080$], molecular layer [$F_{(1,99)} = 6.309$, $p = 0.014$, partial $\eta^2 = 0.060$], and hippocampal tail [$F_{(1,99)} = 4.077$, $p = 0.046$, partial $\eta^2 = 0.040$]. *Post hoc* analysis showed that compared with SCD-normal BMI, CA1 [$F_{(1,99)} = 7.619$, $p = 0.007$], molecular layer [$F_{(1,99)} = 6.351$, $p = 0.013$], and hippocampal tail [$F_{(1,99)} = 4.481$, $p = 0.037$] volumes were larger in the SCD-high BMI group. The volume of CA1 [$F_{(1,99)} = 4.938$, $p = 0.029$] was smaller in the SCD-normal BMI group compared with the NC-normal BMI group. For other hippocampal subregions (hippocampal tail, hippocampal fissure, fimbria, parasubiculum, subiculum, presubiculum, CA3, CA4, GC-ML-DG, HATA), we did not find significant differences in the interaction term between population grouping and BMI grouping ($p > 0.05$; see Table 5).

After correction by Bonferroni's method, ANOVA showed that the population × BMI interaction had a significant effect on CA1. *Post hoc* analysis showed that in the normal BMI group gray matter volume was decreased in CA1 of SCD compared with NC; in the SCD population, gray matter volume of CA1 in the high BMI group was significantly increased compared with normal BMI (see Figure 1). In the NC population, we

TABLE 1 Demographics, disease medical history, and cognitive features of participants.

	NC		SCD		$F/Z/\chi^2$	*P*-value
	Normal BMI (*n* = 29)	High BMI (*n* = 17)	Normal BMI (*n* = 38)	High BMI (*n* = 27)		
Age (years)[a]	66.24 ± 4.57	68.53 ± 4.05	65.39 ± 4.72	65.85 ± 4.61	6.459	0.091
Gender [*n* (%)][b]					7.184	0.066
Male	6 (20.7)	6 (35.3)	10 (26.3)	28 (73.7)		
Female	23 (79.3)	11 (64.7)	28 (73.7)	13 (48.1)		
BMI (kg/m^2)[a]	21.60 ± 1.64	26.23 ± 1.76	21.81 ± 1.37	25.90 ± 2.64	79.395	<0.001
Education (years)[a]	11.12 ± 2.45	11.56 ± 2.32	12.54 ± 2.81	12.28 ± 2.58	1.916	0.131
Hypertension [*n* (%)][b]	7 (24.1)	9 (52.9)	14 (36.8)	14 (51.9)	5.977	0.113
Hyperlipidemia [*n* (%)][b]	5 (17.2)	5 (29.4)	5 (13.2)	5 (18.5)	2.118	0.548
T2DM [*n* (%)][b]	5 (17.2)	3 (17.6)	9 (23.7)	6 (22.2)	0.552	0.907
Medicine [*n* (%)][b]	13 (44.8)	9 (52.9)	20 (52.6)	17 (63.0)	1.855	0.603
MoCA score[a]	26.97 ± 1.05	27.59 ± 1.12	27.53 ± 1.03	27.22 ± 1.12	7.045	0.070
HAMD score[a]	2.55 ± 2.10	1.94 ± 2.14	3.47 ± 2.55	2.26 ± 2.18	6.548	0.088
HAMA score[a]	3.28 ± 2.58	2.76 ± 1.95	3.00 ± 1.79	3.04 ± 1.48	1.042	0.791

[a]Continuous variable, one-way ANOVA is adopted, and mean ± SD is used for statistical description.
[b]Categorical variables were statistically described by chi-square test, and *n* (%) is used for statistical description.
BMI, body mass index; T2DM, type II diabetes mellitus; MoCA, the Montreal Cognitive Assessment; HAMD, the Hamilton Depression Scale; HAMA, the Hamilton Anxiety Scale. Medicine: medication history refers to the last 3-month routine medication self-reported by subjects when receiving the questionnaire of this study, and mainly records the use of drugs that control hypertension, hyperlipidemia, and T2DM. In addition, any other medications the participant has used within the last 3 months were also recorded.

TABLE 2 Comparison of SCWT response time of participants.

	NC		SCD		*F*	interaction *P*-value	η^2
	Normal BMI (*n* = 29)	High BMI (*n* = 17)	Normal BMI (*n* = 38)	High BMI (*n* = 27)			
SCWT A reaction time(s)[a]	15.72 ± 3.24	15.05 ± 3.56	18.61 ± 4.42	20.97 ± 6.46	1.954	0.165	0.018
SCWT B reaction time(s)[a]	19.42 ± 4.65	20.01 ± 4.96	22.26 ± 5.34	28.82 ± 13.08	3.163	0.078	0.030
SCWT C reaction time(s)[a,b]	33.01 ± 9.22	34.96 ± 10.28	38.88 ± 12.80	53.67 ± 13.22	8.017	0.006	0.072
SCWT C-B reaction time(s)[a,b]	13.59 ± 7.63	14.95 ± 8.15	17.73 ± 10.83	28.65 ± 13.31	5.732	0.018	0.052

[a]Continuous variable, two-way ANOVA is adopted, and mean ± SD is used for statistical description; the unit is seconds.
[b]There is an interaction between population grouping and BMI grouping after correction by Bonferroni method.
SCWT, the Stroop Color-Word Test.
The two-way ANOVA was carried out with age, gender, and years of education as covariates.

did not observe any significant effect of changes in BMI level on CA1 gray matter volume ($p > 0.05$). In the high BMI population, we did not observe any significant difference in CA1 gray matter volume between the SCD and NC population ($p > 0.05$).

TABLE 3 *Post hoc* analysis of SCWT tests with interactions.

		Normal BMI	High BMI	NC	SCD
SCWT C reaction time(s)[a]	*F*	6.050	30.115	0.001	19.053
	P	0.016	<0.001	0.982	<0.001
SCWT C-B reaction time(s)[a]	*F*	4.325	21.530	0.001	13.499
	P	0.040	<0.001	0.973	<0.001

[a]There is an interaction between population grouping and BMI grouping.
SCWT, the Stroop Color-Word Test.
The two-way ANOVA was carried out with age, gender, and years of education as covariates.

After correction by the Bonferroni method, we did not find significant correlation between gray matter volume changes in CA1 and SCWT C reaction time (s) ($p > 0.05/4$) or CA1 and SCWT C-B reaction time (s) ($p > 0.05/4$; see Supplementary Tables 2, 3).

Discussion

This study compared the effects of different BMI levels (high BMI and normal BMI) and different populations (SCD and NC) on executive function and hippocampal subregion volume. Our results showed significant interaction effects between the

TABLE 4 Comparison of the gray matter volume of hippocampal subregions.

	NC		SCD		*F*	interaction *P*-value	η^2
	Normal BMI (*n* = 29)	High BMI (*n* = 17)	Normal BMI (*n* = 38)	High BMI (*n* = 27)			
Fimbria[a]	140.02 ± 27.68	136.88 ± 42.62	140.71 ± 42.62	135.30 ± 30.08	0.468	0.496	0.005
Hippocampal tail[a]	1131.37 ± 148.57	1124.49 ± 145.31	1211.41 ± 145.31	1174.71 ± 150.21	4.077	0.046	0.040
Hippocampal fissure[a]	311.08 ± 57.45	332.80 ± 43.91	313.00 ± 43.91	334.24 ± 61.54	0.085	0.771	0.001
Parasubiculum[a]	118.63 ± 22.72	128.19 ± 39.14	125.66 ± 39.14	129.06 ± 26.69	0.565	0.454	0.006
HATA[a]	372.18 ± 42.04	365.76 ± 61.01	385.50 ± 61.01	383.93 ± 47.42	0.356	0.552	0.004
Subiculum[a]	875.96 ± 88.15	864.50 ± 108.60	900.03 ± 108.6	911.20 ± 99.37	0.002	0.961	0.000
Presubiculum[a]	578.68 ± 61.11	587.29 ± 91.56	603.47 ± 91.56	599.56 ± 72.49	1.342	0.249	0.013
CA1[a,b]	1261.17 ± 173.97	1191.34 ± 173.97	1229.23 ± 149.79	1319.61 ± 157.07	8.607	0.004	0.080
CA3[a]	395.54 ± 58.86	390.07 ± 68.34	414.46 ± 56.01	433.96 ± 57.62	0.479	0.490	0.005
CA4[a]	464.64 ± 52.40	459.88 ± 64.73	489.89 ± 48.30	502.93 ± 53.16	0.256	0.614	0.003
Molecular layer[a]	1069.42 ± 112.25	1045.28 ± 149.39	1107.70 ± 117.61	1139.04 ± 124.48	6.309	0.014	0.060
GC-ML-DG[a]	535.52 ± 62.95	524.13 ± 78.41	562.64 ± 60.00	576.00 ± 67.07	0.723	0.397	0.007

[a]Continuous variable, two-way ANOVA is adopted, and mean ± SD is used for statistical description; the unit of volume is cubic millimeter.
[b]There is an interaction between population grouping and BMI grouping after correction by Bonferroni method.
HATA, hippocampal amygdala transition area; CA, cornu ammonis; GC-ML-DG, granule cell layer and molecular layer of the dentate gyrus.
The two-way ANOVA was carried out with age, gender, years of education, hypertension, hyperlipidemia, type II diabetes mellitus, whole hippocampus volume, and intracranial volume as covariates.

population group and BMI group in the executive function (inhibitory control function) and hippocampal subregion (CA1) gray matter volume. In addition, we found significant main effects in the BMI group and population group. Our results suggested that SCD has a worse executive function (inhibitory control function) than NC regardless of the BMI level, but overweight and obesity aggravate the degree of impairment of executive function in the elderly with SCD. For the normal BMI subgroup, the CA1 volume of SCD was smaller than that of NC. Furthermore, we found that in the SCD population the CA1 gray matter volume of high BMI was larger than that of normal BMI.

The present results suggest that SCD has a worse executive function (inhibitory control function) than NC in both overweight/obese and normal weight, which is partly consistent with previous studies. A study from Spain (López-Higes et al., 2017) showed that the executive function test (use the Stroop interference index to test) performance scores in the elderly with SCD were lower than healthy controls. This study found that the worse executive function of SCD compared with NC is mainly manifested in inhibitory control function. Although repeating the results of previous studies, this study considered the effect of BMI on patients with SCD and found that elevated BMI aggravated the impairment of inhibitory control function in patients with SCD. A meta-analysis (Yang Y. et al., 2018) showed that individuals who are overweight have deficits in working memory and inhibitory control function. Inhibitory control is an important subdimension of executive function (Dempster, 1992; Bjorklund and Harnishfeger, 1995). The impairment of inhibitory control functions has been identified as the most affected function in the subdomain of MCI executive function (Traykov et al., 2007; Brandt et al., 2009; Johns et al., 2012). These results may be explained from a neurophysiological perspective. Inhibitory-controlled behavior was found to be electrophysiologically correlated in patients with MCI, and neurocognitive mechanisms associated with response inhibition (No Go P300) were impaired in patients with MCI compared with healthy controls (López Zunini et al., 2016). In the preclinical stage of MCI, SCD may also have the same neurocognitive impairment as MCI, so we observed worse inhibitory control function in SCD compared with healthy subjects. As for the impact of BMI on the executive function of SCD, studies have shown that overweight or obesity can significantly reduce brain blood flow, lead to insufficient cerebral

TABLE 5 *Post hoc* analysis of hippocampal subregions with interactions.

		Normal BMI	High BMI	NC	SCD
CA1[a,b]	*F*	4.938	3.500	2.140	7.619
	P	0.029	0.064	0.147	0.007
Molecular layer[a]	*F*	2.726	3.253	1.260	6.351
	P	0.102	0.074	0.264	0.013
Hippocampal tail[a]	*F*	3.113	1.208	0.684	4.481
	P	0.818	0.274	0.410	0.037

[a]There is an interaction between population grouping and BMI grouping before correction by Bonferroni method.
[b]There is an interaction between population grouping and BMI grouping after correction by Bonferroni method.
The two-way ANOVA was carried out with age, gender, years of education, hypertension, hyperlipidemia, type II diabetes mellitus, whole hippocampus volume, and intracranial volume as covariates.

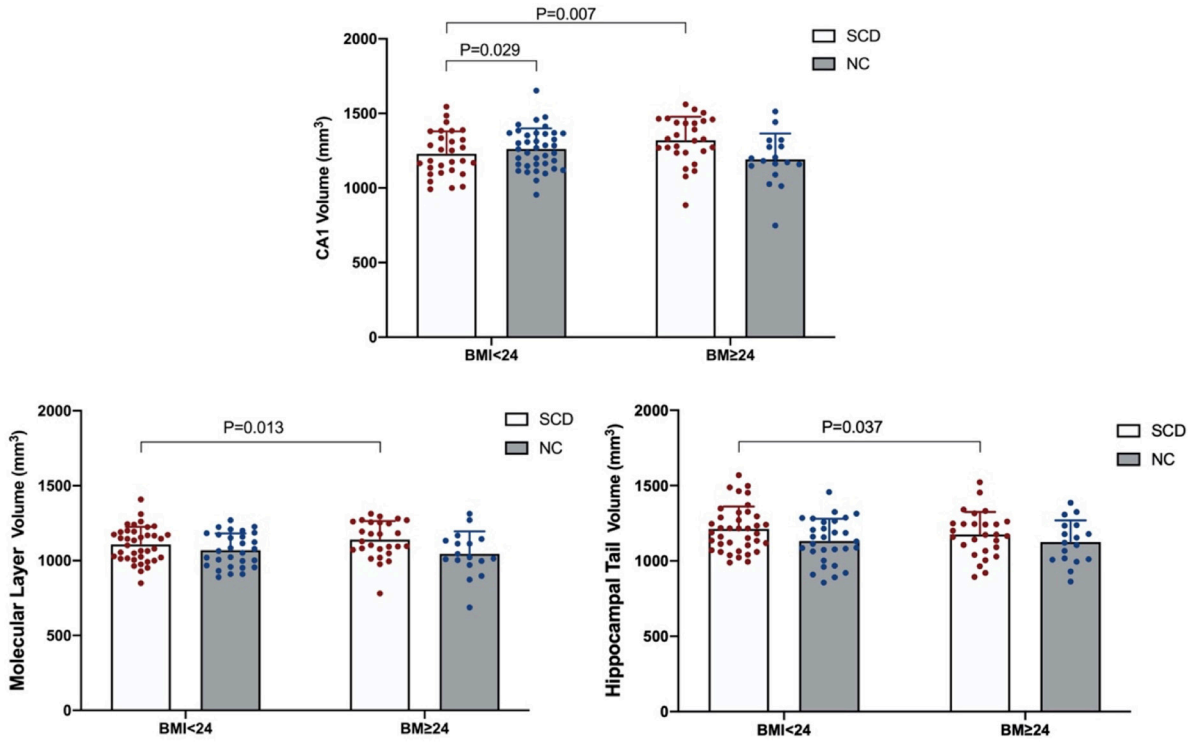

FIGURE 1
Significant population × BMI interaction effect on gray matter volume in the hippocampal subregion.

perfusion, with the brain lacking enough oxygen and nutrients for a long time, which is the early mechanism of AD (Knight et al., 2021), and is also related to worse executive function (Alosco et al., 2012). This may explain why the increase in BMI leads to the aggravation of executive function impairment in patients with SCD.

In addition, we also found a significant interaction between population grouping and BMI grouping in the hippocampal subregion (CA1), and the hippocampal subregion of CA1 significant atrophy in SCD compared with NC. A recent study (Worker et al., 2018) showed that patients with AD experience greater hippocampal subregional atrophy over time compared to NC subjects, including CA1, molecular layer, CA3, hippocampal tail, fissure, and presubiculum, among which CA1 and molecular layer is more obvious. We also found atrophy in the molecular layer of the hippocampus in SCD before Bonferroni correction, which is partly consistent with a previous study. The results seem plausible as the most distinctive AD-related neuron loss was seen in the CA1 region of the hippocampus, and the neuronal loss in CA1 is not an age-related phenomenon but rather characterizes an overt AD process (West et al., 1994). Some studies considered a sequential pattern of atrophy starting within entorhinal and transentorhinal areas and moving to CA1 and eventually other hippocampus subregions (Csernansky et al., 2005; Apostolova et al., 2010). SCD showed a similar pattern of volume atrophy in the hippocampal subregion as AD, preferentially and mainly involving the CA1 region (Perrotin et al., 2015). These findings may be related to the unique structure and function of hippocampal CA1. The CA1 region of the hippocampus maintains its neuroplastic flexibility well into adulthood and plays an important role in external and internal demands to serve cognitive processes (Walhovd et al., 2014b). However, studies have found that brain regions with high neuroplasticity are more prone to neurodegeneration (Neill, 2012; Bufill et al., 2013). The ability of CA1 may increase its vulnerability to neurotoxic effects, ultimately leading to structural atrophy and functional decline (Walhovd et al., 2014a; Nemeth et al., 2017). Deposition of Aβ occurs in the neocortex and hippocampus many years before the onset of clinical symptoms of AD (Sadigh-Eteghad et al., 2015), while the CA1 area is highly sensitive to pathological changes (Pluta et al., 2021). We therefore speculate that the loss of CA1 volume in subjects with SCD may be significantly associated with neuroplasticity in the hippocampal CA1 region.

It is worth mentioning that the result of this study also showed that the hippocampal subregion (CA1) volume of high BMI index in SCD is significantly higher than that of normal BMI population. A recent longitudinal imaging study (Sun et al., 2020) found that higher BMI in AD populations was

associated with larger hippocampus volumes, which is partly consistent with the present result. Sun et al. (2020) pointed out that subjects with higher BMI showed a significant lower Aβ load using PET imaging. Previous studies have suggested that Aβ peptide deposition triggers tau hyperphosphorylation and aggregation in the form of neurofibrillary tangles, and these aggregates lead to inflammation, synaptic damage, neuronal loss, and thus decrease the brain volume (Nelson et al., 2012; He et al., 2018; Vogel et al., 2020; Roda et al., 2022). The accumulation of Aβ pathology enhances hippocampal atrophy in pre-AD (Gordon et al., 2016; Wang et al., 2016). In addition, in contrast to previous study, we found that the increased hippocampal volume caused by the increase in BMI is mainly in the CA1 area. A previous study found that medium and large Aβ plaques are significantly more numerous in CA1 than in other hippocampal subregions (Ugolini et al., 2018), and CA1 may be the most vulnerable region of the hippocampus to neuronal loss (Padurariu et al., 2012; Yang X. et al., 2018). We therefore reasoned that the increased CA1 volume in high-BMI subjects with SCD might be partly mediated by obesity reducing the accumulation of Aβ in the hippocampus.

However, the compensatory increase in CA1 volume in patients with SCD in this study does not appear to be sufficient to compensate for the impairment of executive function in patients with SCD, which is manifested by worse performance on executive function tests in patients with SCD compared with NC. Recent studies have shown that the hippocampus plays an important role in appetite and weight regulation (Alosco et al., 2017; Hsu et al., 2018; Li et al., 2021), and is crucial in the mediation of executive function (Li et al., 2019). Obesity, however, can lead to impaired executive function (Willeumier et al., 2011; Davidson et al., 2019). The results of this study may be explained by the leptin synthesized and secreted by adipocytes. Leptin is transported across the blood–brain barrier (BBB) *via* a saturable transport system (Banks, 2004) and is a potent modulator of excitatory synaptic transmission at hippocampal CA1 synapses (Irving and Harvey, 2014, 2021). Consequently, the ability of leptin to regulate excitatory synaptic efficacy at CA1 synapses suggests that leptin is likely to influence cognition processes (Hamilton and Harvey, 2021; Harvey, 2022). However, leptin transport across the BBB is impaired in high BMI phenotypes (Banks et al., 1999), which has an adverse effect on the synaptic transmission of hippocampal CA1 (Grillo et al., 2011). Furthermore, circulating leptin levels were significantly reduced in patients with cognitive impairment (Power et al., 2001; Johnston et al., 2014), which may explain why patients with SCD have increased CA1 gray matter volume and impaired executive function.

In this study, we did not find significant association between gray matter volume changes in CA1 and inhibitory control function. Previous studies have found that the impairment of executive function is not always correlated with the change of hippocampal subregion volume that is partly consistent with our results. Ge et al. (2021) showed that the volume of hippocampal subregions such as CA1 gradually decreased from the amyloid-negative group to the amyloid-positive group in the elderly people (including 87 individuals with normal cognition, 46 with MCI, and 10 with AD), and as amyloid pathology persisted, impairment of executive function was more significantly associated with changes in hippocampal tau lesions/volume. There seems to be a threshold effect in the relationship between hippocampal atrophy and executive function (Oosterman et al., 2012), that is, severe to very severe but not moderate hippocampal atrophy is associated with lower executive function. We speculate that due to the SCD in the preclinical stage of AD, its behavioral or brain pathological changes are not very serious, resulting in the weak correlation between executive function and hippocampal CA1 volume. Further study is needed to confirm this hypothesis.

This study has several limitations. First, the subjects we included did not contain any BMI level such as lower than 18.5 kg/m^2, so it was impossible to examine the effects of insufficient body mass on executive function and hippocampal subregion. Secondly, the sample size included in this study is insufficient, which may lead to the instability of the research results. Furthermore, this is a cross-sectional study, and it is impossible to follow the subjects for a long time to observe the changes, correlations, and possible causes of cognitive function and hippocampal subregions caused by different BMI with the development of disease and age. Further longitudinal study should be done.

Conclusion

Our results showed that higher BMI was associated with lower levels of executive function in the SCD and larger hippocampal subregion (CA1) gray matter volume. These associations suggest that obesity increases hippocampal gray matter volume in the elderly with SCD but is not sufficient to compensate for the impairment of executive function caused by the disease. Future studies are necessary to better elucidate these associations from the perspective of other mechanisms.

Data availability statement

The raw data supporting the conclusions of this article will be made available by the authors, without undue reservation.

Ethics statement

The studies involving human participants were reviewed and approved by Medical Ethics Committee of the

Affiliated Rehabilitation Hospital of Fujian University of Traditional Chinese Medicine, Fuzhou, Fujian, China. The patients/participants provided their written informed consent to participate in this study. Written informed consent was obtained from the individual(s) for the publication of any potentially identifiable images or data included in this article.

Author contributions

JLi: experimental design, analysis, and manuscript preparation and revision. RC: data analysis and manuscript preparation and revision. GC and SX: data collection and data analysis. QS and JLu: data collection. YW, ML, and HL: data analysis. All authors contributed to drafting the manuscript and have read and approved the final manuscript.

Funding

This study was supported by the National Natural Science Foundation of China (grant no. 81904270), the Natural Science Foundation of Fujian Province (grant no. 2019J01362), the Educational Department of Fujian Province Outstanding Youth Scientific Research Talent Cultivation Program (grant no. MinJiaoKe [2018] 47), and the Science and Technology Platform Construction Project of Fujian Science and Technology Department (grant no. 2015Y2001).

Acknowledgments

We thank the Affiliated Rehabilitation Hospital, Fujian University of Traditional Chinese Medicine, for assistance.

Conflict of interest

The authors declare that the research was conducted in the absence of any commercial or financial relationships that could be construed as a potential conflict of interest.

Publisher's note

All claims expressed in this article are solely those of the authors and do not necessarily represent those of their affiliated organizations, or those of the publisher, the editors and the reviewers. Any product that may be evaluated in this article, or claim that may be made by its manufacturer, is not guaranteed or endorsed by the publisher.

Supplementary material

The Supplementary Material for this article can be found online at: https://www.frontiersin.org/articles/10.3389/fnagi.2022.905035/full#supplementary-material

References

Alosco, M. L., Duskin, J., Besser, L. M., Martin, B., Chaisson, C. E., Gunstad, J., et al. (2017). Modeling the relationships among late-life body mass index, cerebrovascular disease, and Alzheimer's disease neuropathology in an autopsy sample of 1,421 subjects from the national Alzheimer's coordinating center data set. *J. Alzheimers Dis.* 57, 953–968. doi: 10.3233/JAD-161205

Alosco, M. L., Spitznagel, M. B., Raz, N., Cohen, R., Sweet, L. H., Colbert, L. H., et al. (2012). Obesity interacts with cerebral hypoperfusion to exacerbate cognitive impairment in older adults with heart failure. *Cerebrovasc. Dis. Extra* 2, 88–98. doi: 10.1159/000343222

Apostolova, L. G., Mosconi, L., Thompson, P. M., Green, A. E., Hwang, K. S., Ramirez, A., et al. (2010). Subregional hippocampal atrophy predicts Alzheimer's dementia in the cognitively normal. *Neurobiol. Aging* 31, 1077–1088. doi: 10.1016/j.neurobiolaging.2008.08.008

Banks, W. A. (2004). The many lives of leptin. *Peptides* 25, 331–338. doi: 10.1016/j.peptides.2004.02.014

Banks, W. A., DiPalma, C. R., and Farrell, C. L. (1999). Impaired transport of leptin across the blood-brain barrier in obesity. *Peptides* 20, 1341–1345. doi: 10.1016/s0196-9781(99)00139-4

Beyer, F., Kharabian Masouleh, S., Huntenburg, J. M., Lampe, L., Luck, T., Riedel-Heller, S. G., et al. (2017). Higher body mass index is associated with reduced posterior default mode connectivity in older adults. *Hum. Brain Mapp.* 38, 3502–3515. doi: 10.1002/hbm.23605

Bjorklund, D. F., and Harnishfeger, K. K. (1995). "The evolution of inhibition mechanisms and their role in human cognition and behavior," in *Interference and inhibition in cognition*, eds F. N. Dempster and C. J. Brainerd (San Diego, CA: Academic Press), 141–173.

Brandt, J., Aretouli, E., Neijstrom, E., Samek, J., Manning, K., Albert, M. S., et al. (2009). Selectivity of executive function deficits in mild cognitive impairment. *Neuropsychology* 23, 607–618.

Bufill, E., Blesa, R., and Augustí, J. (2013). Alzheimer's disease: An evolutionary approach. *J. Anthropol. Sci.* 91, 135–157.

Calderón-Garcidueñas, L., Mukherjee, P. S., Kulesza, R. J., Torres-Jardón, R., Hernández-Luna, J., Ávila-Cervantes, R., et al. (2019). Mild cognitive impairment and dementia involving multiple cognitive domains in Mexican Urbanites. *J. Alzheimers Dis.* 68, 1113–1123. doi: 10.3233/jad-181208

Chen, B., Wang, Q., Zhong, X., Mai, N., Zhang, M., Zhou, H., et al. (2021). Structural and functional abnormalities of olfactory-related regions in subjective cognitive decline, mild cognitive impairment and Alzheimer's disease. *Int. J. Neuropsychopharmacol.* 25, 361–374. doi: 10.1093/ijnp/pyab091

Cherbuin, N., Sargent-Cox, K., Fraser, M., Sachdev, P., and Anstey, K. J. (2015). Being overweight is associated with hippocampal atrophy: The PATH through life study. *Int. J. Obes.* 39, 1509–1514. doi: 10.1038/ijo.2015.106

China Obesity Working Group (2004). Guidelines for the prevention and control of overweight and obesity in Chinese adults (excerpt). *Acta Nutr. Sin.* 26, 1–4.

Csernansky, J. G., Wang, L., Swank, J., Miller, J. P., Gado, M., McKeel, D., et al. (2005). Preclinical detection of Alzheimer's disease: Hippocampal shape and volume predict dementia onset in the elderly. *Neuroimage* 25, 783–792. doi: 10.1016/j.neuroimage.2004.12.036

Davidson, T. L., Jones, S., Roy, M., and Stevenson, R. J. (2019). The cognitive control of eating and body weight: It's more than what you "Think". *Front. Psychol.* 10:62. doi: 10.3389/fpsyg.2019.00062

Davidson, T. L., Kanoski, S. E., Schier, L. A., Clegg, D. J., and Benoit, S. C. (2007). A potential role for the hippocampus in energy intake and body weight regulation. *Curr. Opin. Pharmacol.* 7, 613–616. doi: 10.1016/j.coph.2007.10.008

Dempster, F. N. (1992). The rise and fall of the inhibitory mechanism: Toward a unified theory of cognitive development and aging. *Dev. Rev.* 12, 45–75.

Dimsdale-Zucker, H. R., Ritchey, M., Ekstrom, A. D., Yonelinas, A. P., and Ranganath, C. (2018). CA1 and CA3 differentially support spontaneous retrieval of episodic contexts within human hippocampal subfields. *Nat. Commun.* 9, 294–294. doi: 10.1038/s41467-017-02752-1

Evans, T. E., Adams, H. H. H., Licher, S., Wolters, F. J., van der Lugt, A., Ikram, M. K., et al. (2018). Subregional volumes of the hippocampus in relation to cognitive function and risk of dementia. *Neuroimage* 178, 129–135. doi: 10.1016/j.neuroimage.2018.05.041

Fischl, B. (2012). FreeSurfer. *Neuroimage* 62, 774–781. doi: 10.1016/j.neuroimage.2012.01.021

Ge, X., Zhang, D., Qiao, Y., Zhang, J., Xu, J., and Zheng, Y. (2021). Association of Tau pathology with clinical symptoms in the subfields of hippocampal formation. *Front. Aging Neurosci.* 13:672077. doi: 10.3389/fnagi.2021.672077

Golden, C., and Golden, C. (1981). *Stroop color and word test: A manual for clinical and experimental uses*. Wood Dale, IL: Stoelting Company.

Gordon, B. A., Blazey, T., Su, Y., Fagan, A. M., Holtzman, D. M., Morris, J. C., et al. (2016). Longitudinal β-amyloid deposition and hippocampal volume in preclinical Alzheimer disease and suspected non-Alzheimer disease pathophysiology. *JAMA Neurol.* 73, 1192–1200. doi: 10.1001/jamaneurol.2016.2642

Grillo, C. A., Piroli, G. G., Evans, A. N., Macht, V. A., Wilson, S. P., Scott, K. A., et al. (2011). Obesity/hyperleptinemic phenotype adversely affects hippocampal plasticity: Effects of dietary restriction. *Physiol. Behav.* 104, 235–241. doi: 10.1016/j.physbeh.2010.10.020

Gunstad, J., Paul, R. H., Cohen, R. A., Tate, D. F., Spitznagel, M. B., and Gordon, E. (2007). Elevated body mass index is associated with executive dysfunction in otherwise healthy adults. *Compr. Psychiatry* 48, 57–61. doi: 10.1016/j.comppsych.2006.05.001

Hamilton, K., and Harvey, J. (2021). Leptin regulation of hippocampal synaptic function in health and disease. *Vitam. Horm.* 115, 105–127. doi: 10.1016/bs.vh.2020.12.006

Hamilton, M. (1959). The assessment of anxiety states by rating. *Br. J. Med. Psychol.* 32, 50–55.

Hamilton, M. (1960). A rating scale for depression. *J. Neurol. Neurosurg. Psychiatry* 23, 56–62. doi: 10.1136/jnnp.23.1.56

Harvey, J. (2022). Leptin regulation of synaptic function at hippocampal TA-CA1 and SC-CA1 synapses. *Vitam. Horm.* 118, 315–336. doi: 10.1016/bs.vh.2021.12.002

He, Z., Guo, J. L., McBride, J. D., Narasimhan, S., Kim, H., Changolkar, L., et al. (2018). Amyloid-β plaques enhance Alzheimer's brain tau-seeded pathologies by facilitating neuritic plaque tau aggregation. *Nat. Med.* 24, 29–38. doi: 10.1038/nm.4443

Homack, S., and Riccio, C. A. (2004). A meta-analysis of the sensitivity and specificity of the Stroop color and word test with children. *Arch. Clin. Neuropsychol.* 19, 725–743. doi: 10.1016/j.acn.2003.09.003

Hsu, T. M., Noble, E. E., Reiner, D. J., Liu, C. M., Suarez, A. N., Konanur, V. R., et al. (2018). Hippocampus ghrelin receptor signaling promotes socially-mediated learned food preference. *Neuropharmacology* 131, 487–496. doi: 10.1016/j.neuropharm.2017.11.039

Iglesias, J. E., Augustinack, J. C., Nguyen, K., Player, C. M., Player, A., Wright, M., et al. (2015). A computational atlas of the hippocampal formation using ex vivo, ultra-high resolution MRI. *Neuroimage* 115, 115–137. doi: 10.1016/j.neuroimage.2015.04.042

Irving, A., and Harvey, J. (2021). Regulation of hippocampal synaptic function by the metabolic hormone leptin: Implications for health and disease. *Prog. Lipid Res.* 82:101098. doi: 10.1016/j.plipres.2021.101098

Irving, A. J., and Harvey, J. (2014). Leptin regulation of hippocampal synaptic function in health and disease. *Philos. Trans. R Soc. Lond. B Biol. Sci.* 369:20130155. doi: 10.1098/rstb.2013.0155

Ivanova, N., Liu, Q., Agca, C., Agca, Y., Noble, E. G., Whitehead, S. N., et al. (2020). White matter inflammation and cognitive function in a co-morbid metabolic syndrome and prodromal Alzheimer's disease rat model. *J. Neuroinflamm.* 17, 29. doi: 10.1186/s12974-020-1698-7

Jessen, F., Amariglio, R. E., Boxtel, M. V., Breteler, M., Ceccaldi, M., Chételat, G., et al. (2014). A conceptual framework for research on subjective cognitive decline in preclinical Alzheimer's disease. *Alzheimers Dement.* 10, 844–852.

Jessen, F., Amariglio, R. E., Buckley, R. F., van der Flier, W. M., Han, Y., Molinuevo, J. L., et al. (2020). The characterisation of subjective cognitive decline. *Lancet* 19, 271–278. doi: 10.1016/S1474-4422(19)30368-0

Johns, E. K., Phillips, N. A., Belleville, S., Goupil, D., Babins, L., Kelner, N., et al. (2012). The profile of executive functioning in amnestic mild cognitive impairment: Disproportionate deficits in inhibitory control. *J. Int. Neuropsychol. Soc.* 18, 541–555. doi: 10.1017/S1355617712000069

Johnston, J. M., Hu, W. T., Fardo, D. W., Greco, S. J., Perry, G., Montine, T. J., et al. (2014). Low plasma leptin in cognitively impaired ADNI subjects: Gender differences and diagnostic and therapeutic potential. *Curr. Alzheimer Res.* 11, 165–174. doi: 10.2174/1567205010666131212114156

Kanoski, S. E., and Grill, H. J. (2017). Hippocampus contributions to food intake control: Mnemonic, neuroanatomical, and endocrine mechanisms. *Biol. Psychiatry* 81, 748–756. doi: 10.1016/j.biopsych.2015.09.011

Kivimäki, M., Luukkonen, R., Batty, G. D., Ferrie, J. E., Pentti, J., Nyberg, S. T., et al. (2018). Body mass index and risk of dementia: Analysis of individual-level data from 1.3 million individuals. *Alzheimers Dement.* 14, 601–609. doi: 10.1016/j.jalz.2017.09.016

Kivipelto, M., Mangialasche, F., and Ngandu, T. (2018). Lifestyle interventions to prevent cognitive impairment, dementia and Alzheimer disease. *Nat. Rev. Neurol.* 14, 653–666. doi: 10.1038/s41582-018-0070-3

Knight, S. P., Laird, E., Williamson, W., O'Connor, J., Newman, L., Carey, D., et al. (2021). Obesity is associated with reduced cerebral blood flow – Modified by physical activity. *Neurobiol. Aging* 105, 35–47. doi: 10.1016/j.neurobiolaging.2021.04.008

Langa, K. M., and Levine, D. A. (2014). The diagnosis and management of mild cognitive impairment: A clinical review. *JAMA* 312, 2551–2561. doi: 10.1001/jama.2014.13806

Li, G., Hu, Y., Zhang, W., Ding, Y., Wang, Y., Wang, J., et al. (2021). Resting activity of the hippocampus and amygdala in obese individuals predicts their response to food cues. *Addict. Biol.* 26:e12974. doi: 10.1111/adb.12974

Li, Y., Shen, M., Stockton, M. E., and Zhao, X. (2019). Hippocampal deficits in neurodevelopmental disorders. *Neurobiol. Learn. Memory* 165:106945. doi: 10.1016/j.nlm.2018.10.001

Liew, T. M. (2019). Depression, subjective cognitive decline, and the risk of neurocognitive disorders. *Alzheimers Res. Ther.* 11:70. doi: 10.1186/s13195-019-0527-7

Lisman, J., Buzsáki, G., Eichenbaum, H., Nadel, L., Ranganath, C., and Redish, A. D. (2017). Viewpoints: How the hippocampus contributes to memory, navigation and cognition. *Nat. Neurosci.* 20, 1434–1447. doi: 10.1038/nn.4661

López Zunini, R. A., Knoefel, F., Lord, C., Breau, M., Sweet, L., Goubran, R., et al. (2016). P300 amplitude alterations during inhibitory control in persons with mild cognitive impairment. *Brain Res.* 1646, 241–248. doi: 10.1016/j.brainres.2016.06.005

López-Higes, R., Prados, J. M., Rubio, S., Montejo, P., and Del Río, D. (2017). Executive functions and linguistic performance in SCD older adults and healthy controls. *Neuropsychol. Dev. Cogn. B Aging Neuropsychol. Cogn.* 24, 717–734. doi: 10.1080/13825585.2016.1256370

Ly, M., Raji, C. A., Yu, G. Z., Wang, Q., Wang, Y., Schindler, S. E., et al. (2021). Obesity and white matter neuroinflammation related edema in Alzheimer' disease dementia biomarker negative cognitively normal individuals. *J. Alzheimers Dis.* 79, 1801–1811. doi: 10.3233/JAD-201242

Ma, L.-Z., Huang, Y.-Y., Wang, Z.-T., Li, J.-Q., Hou, X.-H., Shen, X.-N., et al. (2019). Metabolically healthy obesity reduces the risk of Alzheimer's disease in elders: A longitudinal study. *Aging* 11, 10939–10951. doi: 10.18632/aging.102496

Mallorquí-Bagué, N., Lozano-Madrid, M., Toledo, E., Corella, D., Salas-Salvadó, J., Cuenca-Royo, A., et al. (2018). Type 2 diabetes and cognitive impairment in an older population with overweight or obesity and metabolic syndrome: Baseline cross-sectional analysis of the PREDIMED-plus study. *Sci. Rep.* 8:16128. doi: 10.1038/s41598-018-33843-8

Matsumoto, N., Kitanishi, T., and Mizuseki, K. (2019). The subiculum: Unique hippocampal hub and more. *Neurosci. Res.* 143, 1–12. doi: 10.1016/j.neures.2018.08.002

Nasreddine, Z. S., Phillips, N. A., Bédirian, V., Charbonneau, S., and Chertkow, H. (2005). The montreal cognitive assessment, MoCA: A brief screening tool for mild cognitive impairment. *J. Am. Geriatr. Soc.* 53, 695–699. doi: 10.1111/j.1532-5415.2005.53221.x

Neill, D. (2012). Should Alzheimer's disease be equated with human brain ageing?: A maladaptive interaction between brain evolution and senescence. *Ageing Res. Rev.* 11, 104–122. doi: 10.1016/j.arr.2011.06.004

Nelson, P. T., Alafuzoff, I., Bigio, E. H., Bouras, C., Braak, H., Cairns, N. J., et al. (2012). Correlation of Alzheimer disease neuropathologic changes with cognitive

status: A review of the literature. *J. Neuropathol. Exp. Neurol.* 71, 362–381. doi: 10.1097/NEN.0b013e31825018f7

Nemeth, V. L., Must, A., Horvath, S., Király, A., Kincses, Z. T., and Vécsei, L. (2017). Gender-specific degeneration of dementia-related subcortical structures throughout the lifespan. *J. Alzheimers dis.* 55, 865–880. doi: 10.3233/JAD-160812

O'Keefe, J., Morris, R., Andersen, P., Bliss, T., and Amaral, D. G. (2007). *The hippocampus book*. Oxford: Oxford University Press.

Oosterman, J. M., Oosterveld, S., Rikkert, M. G., Claassen, J. A., and Kessels, R. P. (2012). Medial temporal lobe atrophy relates to executive dysfunction in Alzheimer's disease. *Int. Psychogeriatr.* 24, 1474–1482. doi: 10.1017/s1041610212000506

Padurariu, M., Ciobica, A., Mavroudis, I., Fotiou, D., and Baloyannis, S. (2012). Hippocampal neuronal loss in the CA1 and CA3 areas of Alzheimer's disease patients. *Psychiatria Danubina* 24, 152–158.

Perrotin, A., de Flores, R., Lamberton, F., Poisnel, G., La Joie, R., de la Sayette, V., et al. (2015). Hippocampal subfield volumetry and 3D surface mapping in subjective cognitive decline. *J. Alzheimers Dis.* 48, S141–S150. doi: 10.3233/JAD-150087

Piché, M.-E., Tchernof, A., and Després, J.-P. (2020). Obesity phenotypes, diabetes, and cardiovascular diseases. *Circ. Res.* 126, 1477–1500. doi: 10.1161/CIRCRESAHA.120.316101

Pike, K. E., Cavuoto, M. G., Li, L., Wright, B. J., and Kinsella, G. J. (2021). Subjective cognitive decline: Level of risk for future dementia and mild cognitive impairment, a meta-analysis of longitudinal studies. *Neuropsychol. Rev.* doi: 10.1007/s11065-021-09522-3 [Epub ahead of print].

Pini, L., and Wennberg, A. M. (2021). Structural imaging outcomes in subjective cognitive decline: Community vs. clinical-based samples. *Exp. Gerontol.* 145:111216. doi: 10.1016/j.exger.2020.111216

Pluta, R., Ouyang, L., Januszewski, S., Li, Y., and Czuczwar, S. J. (2021). Participation of amyloid and tau protein in post-ischemic neurodegeneration of the hippocampus of a nature identical to Alzheimer's disease. *Int. J. Mol. Sci.* 22:2460. doi: 10.3390/ijms22052460

Power, D. A., Noel, J., Collins, R., and O'Neill, D. (2001). Circulating leptin levels and weight loss in Alzheimer's disease patients. *Dement. Geriatr. Cogn. Disord.* 12, 167–170. doi: 10.1159/000051252

Rabi, R., Vasquez, B. P., Alain, C., Hasher, L., Belleville, S., and Anderson, N. D. (2020). Inhibitory control deficits in individuals with amnestic mild cognitive impairment: A meta-analysis. *Neuropsychol. Rev.* 30, 97–125. doi: 10.1007/s11065-020-09428-6

Roda, A. R., Serra-Mir, G., Montoliu-Gaya, L., Tiessler, L., and Villegas, S. (2022). Amyloid-beta peptide and tau protein crosstalk in Alzheimer's disease. *Neural Regen. Res.* 17, 1666–1674. doi: 10.4103/1673-5374.332127

Sadigh-Eteghad, S., Sabermarouf, B., Majdi, A., Talebi, M., Farhoudi, M., and Mahmoudi, J. (2015). Amyloid-beta: A crucial factor in Alzheimer's disease. *Med. Princ. Pract.* 24, 1–10. doi: 10.1159/000369101

Sánchez-Benavides, G., Grau-Rivera, O., Suárez-Calvet, M., Minguillon, C., Cacciaglia, R., Gramunt, N., et al. (2018). Brain and cognitive correlates of subjective cognitive decline-plus features in a population-based cohort. *Alzheimers Res. Ther.* 10:123. doi: 10.1186/s13195-018-0449-9

Sanchez-Flack, J. C., Tussing-Humphreys, L., Lamar, M., Fantuzzi, G., Schiffer, L., Blumstein, L., et al. (2021). Building research in diet and cognition (BRIDGE): Baseline characteristics of older obese African American adults in a randomized controlled trial to examine the effect of the Mediterranean diet with and without weight loss on cognitive functioning. *Prev. Med. Rep.* 22:101302. doi: 10.1016/j.pmedr.2020.101302

Scarpina, F., and Tagini, S. (2017). The stroop color and word test. *Front. Psychol.* 8:557. doi: 10.3389/fpsyg.2017.00557

Scheef, L., Spottke, A., Daerr, M., Joe, A., Striepens, N., Kölsch, H., et al. (2012). Glucose metabolism, gray matter structure, and memory decline in subjective memory impairment. *Neurology* 79, 1332–1339. doi: 10.1212/WNL.0b013e31826c1a8d

Schmeidler, J., Mastrogiacomo, C. N., Beeri, M. S., Rosendorff, C., and Silverman, J. M. (2019). Distinct age-related associations for body mass index and cognition in cognitively healthy very old veterans. *Int. Psychogeriatr.* 31, 895–899. doi: 10.1017/s1041610218001412

Sun, Z., Wang, Z.-T., Sun, F.-R., Shen, X.-N., Xu, W., Ma, Y.-H., et al. (2020). Late-life obesity is a protective factor for prodromal Alzheimer's disease: A longitudinal study. *Aging* 12, 2005–2017. doi: 10.18632/aging.102738

Suo, C., Gates, N., Fiatarone Singh, M., Saigal, N., Wilson, G. C., Meiklejohn, J., et al. (2017). Midlife managerial experience is linked to late life hippocampal morphology and function. *Brain Imaging Behav.* 11, 333–345. doi: 10.1007/s11682-016-9649-8

Traykov, L., Raoux, N., Latour, F., Gallo, L., Hanon, O., Baudic, S., et al. (2007). Executive functions deficit in mild cognitive impairment. *Cogn. Behav. Neurol.* 20, 219–224.

Ugolini, F., Lana, D., Nardiello, P., Nosi, D., Pantano, D., Casamenti, F., et al. (2018). Different patterns of neurodegeneration and glia activation in CA1 and CA3 hippocampal regions of TgCRND8 Mice. *Front. Aging Neurosci.* 10:372. doi: 10.3389/fnagi.2018.00372

van Rooden, S., van den Berg-Huysmans, A. A., Croll, P. H., Labadie, G., Hayes, J. M., Viviano, R., et al. (2018). Subjective cognitive decline is associated with greater white matter hyperintensity volume. *J. Alzheimers Dis.* 66, 1283–1294. doi: 10.3233/JAD-180285

Vogel, J. W., Iturria-Medina, Y., Strandberg, O. T., Smith, R., Levitis, E., Evans, A. C., et al. (2020). Spread of pathological tau proteins through communicating neurons in human Alzheimer's disease. *Nat. Commun.* 11:2612. doi: 10.1038/s41467-020-15701-2

Walhovd, K. B., Tamnes, C. K., and Fjell, A. M. (2014b). Brain structural maturation and the foundations of cognitive behavioral development. *Curr. Opin. Neurol.* 27, 176–184. doi: 10.1097/WCO.0000000000000074

Walhovd, K. B., Fjell, A. M., and Espeseth, T. (2014a). Cognitive decline and brain pathology in aging – Need for a dimensional, lifespan and systems vulnerability view. *Scand. J. Psychol.* 55, 244–254. doi: 10.1111/sjop.12120

Wang, L., Benzinger, T. L., Su, Y., Christensen, J., Friedrichsen, K., Aldea, P., et al. (2016). Evaluation of tau imaging in staging Alzheimer disease and revealing interactions between β-amyloid and tauopathy. *JAMA Neurol.* 73, 1070–1077. doi: 10.1001/jamaneurol.2016.2078

Wang, X., Huang, W., Su, L., Xing, Y., Jessen, F., Sun, Y., et al. (2020). Neuroimaging advances regarding subjective cognitive decline in preclinical Alzheimer's disease. *Mol. Neurodegen.* 15:55. doi: 10.1186/s13024-020-00395-3

Wecker, N. S., Kramer, J. H., Wisniewski, A., Delis, D. C., and Kaplan, E. (2000). Age effects on executive ability. *Neuropsychology* 14, 409–414. doi: 10.1037//0894-4105.14.3.409

West, M. J., Coleman, P. D., Flood, D. G., and Troncoso, J. C. (1994). Differences in the pattern of hippocampal neuronal loss in normal ageing and Alzheimer's disease. *Lancet* 344, 769–772. doi: 10.1016/s0140-6736(94)92338-8

Widya, R. L., de Roos, A., Trompet, S., de Craen, A. J., Westendorp, R. G., Smit, J. W., et al. (2011). Increased amygdalar and hippocampal volumes in elderly obese individuals with or at risk of cardiovascular disease. *Am. J. Clin. Nutr.* 93, 1190–1195. doi: 10.3945/ajcn.110.006304

Willeumier, K. C., Taylor, D. V., and Amen, D. G. (2011). Elevated BMI is associated with decreased blood flow in the prefrontal cortex using SPECT imaging in healthy adults. *Obesity (Silver Spring, MD)* 19, 1095–1097. doi: 10.1038/oby.2011.16

Worker, A., Dima, D., Combes, A., Crum, W. R., Streffer, J., Einstein, S., et al. (2018). Test-retest reliability and longitudinal analysis of automated hippocampal subregion volumes in healthy ageing and Alzheimer's disease populations. *Hum. Brain Mapp.* 39, 1743–1754. doi: 10.1002/hbm.23948

Xu, S., Jia, L., Ruilin, C., Guiyan, C., and Jiao, L. (2021). Correlation between different BMI levels and executive function in patients with subjective cognitive decline. *Modern Prev. Med.* 48, 3247–3253. doi: 10.26355/eurrev_201712_13937

Yang, Y., Shields, G. S., Guo, C., and Liu, Y. (2018). Executive function performance in obesity and overweight individuals: A meta-analysis and review. *Neurosci. Biobehav. Rev.* 84, 225–244. doi: 10.1016/j.neubiorev.2017.11.020

Yang, X., Yao, C., Tian, T., Li, X., Yan, H., Wu, J., et al. (2018). A novel mechanism of memory loss in Alzheimer's disease mice via the degeneration of entorhinal-CA1 synapses. *Mol. Psychiatry* 23, 199–210. doi: 10.1038/mp.2016.151

Ying Han. (2018). Recommendations for diagnosis and treatment of subjective cognitive decline due to preclinical Alzheimer disease in China. *J. China Clin. Med. Imaging* 29, 5–5. doi: 10.1136/bmjopen-2018-028317

Yue, L., Wang, T., Wang, J., Li, G., Wang, J., Li, X., et al. (2018). Asymmetry of hippocampus and amygdala defect in subjective cognitive decline among the community dwelling Chinese. *Front. Psychiatry* 9:226. doi: 10.3389/fpsyt.2018.00226

Zhao, W., Wang, X., Yin, C., He, M., Li, S., and Han, Y. (2019). Trajectories of the hippocampal subfields atrophy in the Alzheimer's disease: A structural imaging study. *Front. Neuroinform.* 13:13. doi: 10.3389/fninf.2019.00013

frontiers | Frontiers in Aging Neuroscience

TYPE Original Research
PUBLISHED 15 September 2022
DOI 10.3389/fnagi.2022.933567

OPEN ACCESS

EDITED BY
Cosimo Urgesi,
University of Udine, Italy

REVIEWED BY
Huafeng Liu,
Zhejiang University, China
Zhiyong Zhao,
Zhejiang University, China

*CORRESPONDENCE
Yongxin Li
yxin-li@163.com
Ping Wu
wuping_33@163.com
Jiaxu Chen
chenjiaxu@hotmail.com

SPECIALTY SECTION
This article was submitted to Neurocognitive Aging and Behavior, a section of the journal Frontiers in Aging Neuroscience

RECEIVED 01 May 2022
ACCEPTED 16 August 2022
PUBLISHED 15 September 2022

CITATION
Li Y, Yu Z, Wu P and Chen J (2022) Ability of an altered functional coupling between resting-state networks to predict behavioral outcomes in subcortical ischemic stroke: A longitudinal study. *Front. Aging Neurosci.* 14:933567. doi: 10.3389/fnagi.2022.933567

Ability of an altered functional coupling between resting-state networks to predict behavioral outcomes in subcortical ischemic stroke: A longitudinal study

Yongxin Li[1]*, Zeyun Yu[2], Ping Wu[2]* and Jiaxu Chen[1]*

[1]Guangzhou Key Laboratory of Formula-Pattern of Traditional Chinese Medicine, Formula-Pattern Research Center, School of Traditional Chinese Medicine, Jinan University, Guangzhou, China, [2]Acupuncture and Tuina School/Third Teaching Hospital, Chengdu University of Traditional Chinese Medicine, Chengdu, China

Stroke can be viewed as an acute disruption of an individual's connectome caused by a focal or widespread loss of blood flow. Although individuals exhibit connectivity changes in multiple functional networks after stroke, the neural mechanisms that underlie the longitudinal reorganization of the connectivity patterns are still unclear. The study aimed to determine whether brain network connectivity patterns after stroke can predict longitudinal behavioral outcomes. Nineteen patients with stroke with subcortical lesions underwent two sessions of resting-state functional magnetic resonance imaging scanning at a 1-month interval. By independent component analysis, the functional connectivity within and between multiple brain networks (including the default mode network, the dorsal attention network, the limbic network, the visual network, and the frontoparietal network) was disrupted after stroke and partial recovery at the second time point. Additionally, regression analyses revealed that the connectivity between the limbic and dorsal attention networks at the first time point showed sufficient reliability in predicting the clinical scores (Fugl-Meyer Assessment and Neurological Deficit Scores) at the second time point. The overall findings suggest that functional coupling between the dorsal attention and limbic networks after stroke can be regarded as a biomarker to predict longitudinal clinical outcomes in motor function and the degree of neurological functional deficit. Overall, the present study provided a novel opportunity to improve prognostic ability after subcortical strokes.

KEYWORDS

functional MRI, subcortical stroke, independent component analysis, functional network connectivity, recovery prediction

Introduction

Stroke is one of the most frequent causes of chronic disability worldwide. Unlike many other neurological disorders, a stroke appears suddenly in the brain system. Most stroke cases are ischemic or caused by a lack of blood supply to cerebral tissue due to embolic occlusion of a cerebral artery (Rehme and Grefkes, 2013). Aphasia and motor deficits are particularly prevalent long-term disabilities after stroke significantly impacting public health. Thus, understanding the neurobiological factors determining functional outcomes would offer insights into stroke treatment approaches. Functional magnetic resonance imaging (fMRI) can provide a non-invasive means to understand the neural mechanisms of brain reorganization after stroke (Ovadia-Caro et al., 2014).

Stroke can be viewed as an acute disruption of an individual's connectome caused by a focal or widespread loss of blood flow. Patients with ischemic stroke showed functional and structural reorganization of perilesional and remote brain regions. Using a connectivity-based approach can provide unique opportunities to study the effect of a stroke on brain recovery (Grefkes and Fink, 2014). Previous studies reported disruptions in functional brain connections between distinctive cortical areas following strokes (Grefkes and Ward, 2014; Mirzaei and Adeli, 2016; Chen et al., 2021). For example, several studies on stroke demonstrated reduced functional connectivity between the bilateral motor regions (Carter et al., 2010, 2012a; Wang et al., 2010; Min et al., 2020). Abnormal interhemispheric functional connectivity patterns within the motor network were correlated with motor deficits after strokes (Baldassarre et al., 2016; Li et al., 2016). Although the effects of stroke on the functional networks of the brain were mainly focused on the motor network, patients with stroke also exhibited significant changes in functional connectivity in other subnetworks, such as the frontoparietal network (FPN) (Nomura et al., 2010; Hordacre et al., 2021), the default mode network (DMN) (Tuladhar et al., 2013; Jiang et al., 2018), the attention-related network (Zhao et al., 2018a), and the visual network (VIS) (Park et al., 2011). A previous neuroimaging study showed a double dissociation between an abnormal functional connectivity pattern and attention and motor deficits in patients with a right hemisphere stroke (Baldassarre et al., 2016). Abnormal patterns in the brain networks after a stroke can reflect the corresponding behavioral deficits. Additionally, changes in the internetwork functional connectivity of multiple networks following strokes were also investigated (Wang et al., 2014; Zhao et al., 2018b). Patients with stroke demonstrated alterations in both motor-visual networks and other high-order motor-cognitive networks. Together, these findings consistently demonstrate extensive changes in the functional network organization in patients with stroke.

Recently, the effects of the intervention on network organization in patients with stroke were also investigated to understand the recovery of motor or other cognitive functions (Bajaj et al., 2015; Zheng et al., 2016; Sinha et al., 2021). For example, a previous study on strokes revealed functional restoration of the brain's motor-execution network after a combination of mental practice and physical therapy (Bajaj et al., 2015). Three weeks of upper limb rehabilitation therapy in patients with stroke can result in an increase in interhemispheric communication among motor areas, which is accompanied by improvements in behavioral performance (James et al., 2009). Our recent studies, which used a longitudinal design, revealed that motor-related networks and motor function in patients with subcortical stroke showed recovery after 1 month of clinical treatment (Li et al., 2016, 2017, 2021). However, all of these previous studies were focused only on the intervention effect of interactions between brain regions within a subnetwork; few studies used neuroimaging to detect longitudinal changes in interactions between networks during the recovery process in patients with stroke.

Thus, the present study aimed to examine the longitudinal changes in the functional organization within and between resting-state networks of the whole brain in patients with chronic subcortical stroke. For this purpose, we employed a method called independent component analysis (ICA) to construct functional brain networks. ICA is a data-driven approach for delineating spatially independent patterns of coherent signals (van de Ven et al., 2004). The interactions within and between multiple brain networks can be measured directly (Zhao et al., 2018b). Previous studies on certain neurological disorders, such as schizophrenia and depression, indicated that ICA can efficiently detect intra- and inter-network connectivity patterns (Salman et al., 2019; Maglanoc et al., 2020). A recent stroke study used this resting-state fMRI method to assess hypoperfusion (Hu et al., 2021). Until now, only a few studies used the ICA method to investigate both intra- and inter-network connectivity changes in functional deficits after strokes (Wang et al., 2014; Zhao et al., 2018b; Chen et al., 2019). These previous studies used ICA to detect functional connectivity alterations within and between multiple networks in patients with stroke, but longitudinal changes in the organization of the brain were not investigated. In the present study, we applied the ICA method to resting-state fMRI data to investigate the functional recovery process within and between resting-state networks in stroke. Because stroke symptoms may reflect dysfunction across multiple systems, changes in the functional pattern of the brain after strokes have important implications for cognitive recovery (Carter et al., 2012b; Grefkes and Fink, 2020). We hypothesized the following: (1) disrupted functional organization within and between functional networks would be detected in patients with subcortical stroke, (2) disrupted functional organization in patients would be restored after a period of time, and (3) functional connectivity between networks in patients with stroke would reflect the patients' clinical recovery.

Materials and methods

Subjects

We collected 21 subcortical adult patients with stroke from the Department of Neurology of the First Affiliated Hospital of Chengdu University of Traditional Chinese Medicine in China and 17 healthy controls in the present study. The present study was designed and carried out a few years ago. The sample size selection was referred to by the previous studies (Lindenberg et al., 2012; Wang et al., 2012, 2014), in which the general sample size of subjects in these previous neuroimaging studies of each group was from 15 to 30. We discarded data of two participants (one patient and one control) because of incomplete imaging data. Data of one patient were discarded because of head movement during the MRI scan. Therefore, 19 adult patients with stroke (eight women; mean age ± SD: 64.74 ± 12.42 years) were included in the final analysis. All patients were diagnosed with unimanual motor deficits due to subcortical ischemic lesions. Patients were included in the study based on the following criteria: (1) first-ever ischemic stroke with right-handedness before stroke; (2) strictly subcortical lesions and absence of other white matter pathology as verified by structural MRI; (3) time interval of at least 3 weeks between stroke onset and the time of study enrollment; (4) no additional psychiatric or neurological disorders; (5) absence of neglect, aphasia, and dementia; and (6) no subsequent cerebral ischemia. None of the patients had undergone any other experimental therapy before enrollment in this study. Resting-state fMRI data of all patients were collected at two time points: before and 1 month after the antiplatelet therapy. Clinical scores were assessed for these patients at the above two time points. Sixteen healthy subjects (six women, mean age ± SD: 64.75 ± 10.51 years) without any history of neurological or psychiatric disorders were included in the final analysis. All of the control subjects were right-handed. The participants in the control group were well matched to the patients with stroke with regard to age, gender, and handedness. All control subjects were scanned only one time, on the day they were recruited. **Table 1** provides detailed information on both groups. The protocol was approved by the Ethics Committee of Chengdu University of Traditional Chinese Medicine (no. 2011KL-002), and the research was carried out in accordance with the Declaration of Helsinki. Written informed consent was obtained from each subject prior to the study.

Clinical assessments

Antiplatelet therapy was administered to all the patients (75 mg of clopidogrel one time each day taken orally and 10 mg of Erigeron breviscapus injection). Additionally, citicoline (0.5 g, daily) was injected intravenously to improve the clinical outcome following ischemic stroke. Drug therapy was conducted for 1 month (30 days) for each patient. Information on the Fugl-Meyer Assessment (FMA) and the Neurological Deficit Scores (NDS) was assessed two times from all patients on the days the imaging data were collected. FMA has been widely used to evaluate the motor functions of patients with stroke (Gladstone et al., 2002). Higher FMA scores indicate milder impairments in motor function. NDS constitutes an observational assessment of the severity of neurological functional deficits and stroke severity. This score resembles the NIHSS score, which is used in clinical practice. A paired *t*-test was conducted to determine whether the clinical scores of the patients with stroke had changed between the two time points.

Image acquisition

All images were obtained using a 3T Siemens scanner (MAGNETOM Trio Tim, Siemens, Germany) at the West China Hospital MRI Center, Chengdu, China. During the scanning process, foam cushions were used to reduce head movements and scanner noise. Whole-brain resting-state fMRI was performed using an echo-planar imaging (EPI) sequence: 30 interleaved axial slices; slice thickness = 5 mm; matrix = 64 × 64; repetition time = 2 s; echo time = 30 ms; flip angle = 90°; field-of-view (FOV) = 240 mm × 240 mm; and 180 volume; three-dimensional T1-weighted structural MRI was performed using a spin-echo planar image sequence with the following parameters: repetition time/echo time = 1,900 ms/2.26 ms; flip angle = 9°; in-plane matrix resolution = 256 × 256; slices = 176; field of view = 256 mm × 256 mm; and voxel size = 1 mm × 1 mm × 1 mm. The head coil and foam cushions were used during scanning to reduce head movement. During the acquisition of the imaging data, the participants were instructed to remain awake, remain motionless, keep their eyes closed, and try not to think about anything in particular.

Lesion mapping

The lesion location for each patient on the T1-weighted MRI images was determined by one experienced neuroradiologist. We manually outlined the lesion profiles on the T1-weighted MRI images slice by slice using MRIcron software, and we generated a lesion mask for each patient. Then, for each patient, the T1 structural image was normalized to the MNI template, and the resulting parameter file was used to normalize the lesion mask. After spatial normalization, the lesion mask of each patient was normalized to MNI spaces (see **Supplementary Figure 1A** and **Supplementary Table 1**). The individual masks were used to evaluate the lesion volume of each patient. To ensure that all lesions were on the same hemisphere, the imaging data of two patients who had lesions on the right hemisphere were flipped from right to left along the midsagittal line.

TABLE 1 Demographic and clinical information data of the subjects.

Characteristics	Patient group (n = 19, Mean ± SD)		Control group (n = 16, Mean ± SD)	Statistics	P-value
Gender (men/women)	11/8		10/6	$\chi^2(1) = 0.077$	0.782
Age (ages)	64.74 ± 12.42		64.75 ± 10.51	$t(33) = -0.003$	0.997
Duration of illness (days)	55.53 ± 46.75		\	\	\
Lesion sizes (cm^3)	0.85 ± 0.19		\	\	\
FMA_pre_post	Pre: 84.26 ± 4.05	Post: 91.53 ± 4.06	\	$t(18) = -10.08$	0.000
NDS_pre_post	Pre: 23.26 ± 4.28	Post: 14.21 ± 5.17	\	$t(18) = 12.96$	0.000

Summary values are reported as the means ± standard deviation. Duration of illness refers to how long the patients were enrolled after the stroke. FMA, Fugl-Meyer Motor Assessment; NDS, neurological deficit scores.

Additionally, the imaging data from the control subject matched the two patients who were midsagittally oriented. The union of all individual lesion masks was used to construct a group lesion map for the patients (see **Supplementary Figure 1B**). This overlapped lesion map helped us to see all patients' lesion distribution.

Imaging processing and group-independent component analysis

The resting-state fMRI data were processed using the Statistical Parametric Mapping (SPM8[1]) package. The preprocessing steps included slice timing, spatial realignment, normalization into the Montreal Neurological Institute template, and smoothing (6 mm FWHM). Slice timing and head motion correction were performed, and a mean functional image was obtained for each participant. The excessive motion was defined as more than 3 mm of translation or greater than a 3° rotation in any direction. The mean framewise displacement (FD) was computed by averaging the FD of each participant across the time points. The participants were excluded if the mean FD was less than 0.5 mm or more than 20% of all time points with FD values exceeding 0.5 mm. Only one patient was excluded due to excessive motion, and no participant was excluded due to excessive FD. Then, the mean FD values for the remaining participants were included for the comparison between the patients and healthy subjects. No significant differences were found between groups of FD (Stroke_1st: 0.19 ± 0.07, Stroke_2nd: 0.20 ± 0.08, Controls: 0.19 ± 0.11, $F = 0.088$, $p = 0.916$). Each participant's T1-weighted structural image was co-registered to their mean functional image and then segmented. The functional images were then normalized to the standard Montreal Neurological Institute space using the T1 image unified segmentation; they were then resampled to 3 mm and smoothed using a 6-mm full-width at half maximum Gaussian smoothing kernel. The preprocessed resting state data of all of the participants were analyzed using ICA as implemented in the GIFT software[2] (Calhoun et al., 2001). Spatial ICA analysis is a data-driven approach performed using a group ICA in the GIFT. This method extracts the non-overlapping spatial maps with temporally coherent time courses that maximize independence. We used the standard procedure in GIFT. The preprocessed data from all participants were concatenated into a single dataset. Data reduction was conducted using principal component analysis to reduce the dimensions of the functional data. ICA was performed to decompose the grouped data into 28 independent components using an Infomax algorithm (Bell and Sejnowski, 1995). This step was repeated 20 times using the ICASSO algorithm to assess independent components' repeatability or stability (ICs). Aggregate spatial maps were estimated as the modes of the component clusters. ICs and time courses for each participant were back-reconstructed.

A systematic procedure was used to diagnose the artifacts and identify the functional networks. We used the cortical parcelation maps of the Yeo2011 resting state network[3] as a template and multiple linear regression, as implemented in the spatial sorting function of GIFT, to compare the spatial pattern of each IC with these templates. The functional "Component Labeller" module in the GIFT toolbox was used to produce a txt file containing a correlation index. Components with a higher correlation (larger than 0.2) with these maps of Yeo2011 templates were considered the most related components. The reason for selecting this correlation criterion is based on previous references, in which a reasonable choice of correlation value was studied between ICs from different datasets (Smith et al., 2009; Fu et al., 2019). Some components were excluded from the remainder of the analysis because they correlated with motion artifacts or spatial maps that included the white matter, the ventricular system, or the cerebral spinal fluid or because they had irregular time course spectral power. As a result, the

1 http://www.fil.ion.ucl.ac.uk/spm

2 http://mialab.mrn.org/software/gift

3 https://surfer.nmr.mgh.harvard.edu/fswiki/CorticalParcellation_Yeo2011

potential components of interest (19 ICs) were identified by the above process.

Functional network connectivity analysis

To detect the functional organization within and between functional networks after a stroke, functional network connectivity (FNC) analysis was performed. Before calculating the FNC between the time courses of the ICs, postprocessing procedures on the time courses were performed to remove the remaining noise sources, such as detrending linear, multiple regressions of the Friston 24 realignment parameters, and filtering (a bandpass filter of 0.01–0.1 Hz). Then, we calculated the FNC using the Pearson correlation coefficients between the time courses of the ICs. To normalize the variance in the correlation values, all of the resulting correlation coefficients were transformed into z-scores using Fisher's z-transformation. The normalized correlation value of each pair was regarded as the network edges. An FNC matrix with a dimension of 19×19 was created for each subject. In the present study, these selected ICs were categorized into seven functional domains based on the Yeo2011 template: VIS, somatomotor network (SMN), dorsal attention network (DAN), ventral attention network (VAN), limbic network (LIM), FPN, and DMN (see **Supplementary Figure 2A**). Here, network connectivity was defined as the connectivity between these seven subnetworks (such as FNC between one IC of the DAN and one IC of the DMN). Network connectivity was defined as the connectivity among the components belonging to one subnetwork (such as the FNC between two ICs of the DMN).

We used a network-based statistic (NBS) approach for the functional connectivity networks to localize the specific connected components, which reflects the functional connections that differed between each pair of groups (Zalesky et al., 2010). A set of suprathreshold links among all the connected components was defined using the NBS method. The non-parametric permutation method was used to estimate the significance of each component (5000 permutations). Analyses were controlled for age, gender, duration of illness, and lesion size. The threshold (edge $p < 0.05$ and component $p < 0.05$) was adopted to address the multiple comparisons in the functional connectivity.

We further examined whether FNC changes after stroke can predict the recovery of clinical performance. This step focused on those functional connections between ICs with significant group differences. We performed linear regression analyses to determine those functional connections at the first time point to assess their ability to predict clinical performance (FMA and NDS) at the second time point. The regression model was considered significant at a p-value < 0.05. The Bonferroni method also corrected the regression results based on the pairs of ICs showing significant changes in FNC in patients with stroke. This process was performed using the SPSS statistical software (version 20.0, IBM Inc., Armonk, NY, United States).

Results

Behavioral data

No significant differences between the patients and the normal controls were observed in the sexes and ages (**Table 1**). Between the two time points of the patient group, the FMA score was significantly increased (paired t-test: $t = -10.08$, $p < 0.001$) from 84.26 ± 4.05 (first time point) to 91.53 ± 4.06 (second time point). The severity of the neurological functional deficit after stroke was assessed by the NDS and showed a significant decrease (pair T: $t = 12.96$, $p < 0.001$) from 23.26 ± 4.28 (first time point) to 14.21 ± 5.17 (second time point).

Group independent component analysis and identification of potential interest components

The spatial maps of potential interest components were identified for group ICA (**Figure 1**). Nine ICs were excluded, and nineteen potential components of interest were identified in group ICA. These selected ICs were categorized into seven functional domains: VIS, SMN, DAN, VAN, LIM, FPN, and DMN (see **Supplementary Figure 2B**).

Between-group differences in functional network connectivity

The NBS approach was conducted for the functional connectivity networks between each pair of groups, and the statistical results demonstrated specific FNC alterations in patients with stroke. Paired t-test analysis of the patients with stroke demonstrated that the FNC within networks showed a significant increase at the second time point (Paired t-test, patients 1st vs. 2nd: FPN_IC5-FPN_IC13, $t = -2.41$, $p = 0.021$; LIM_IC11-LIM_IC20, $t = -2.07$, $p = 0.045$, LIM_IC18-LIM_IC20, $t = -2.56$, $p = 0.014$). The significant within-network changes in FNC in patients with stroke are shown in **Figure 2**.

As displayed in **Figure 3**, the FNCs between the DMN and DAN showed a significant decrease in the patients with stroke compared with the controls (two sample t-test, 1st patient vs. control: IC4-IC25, $t = -2.05$, $p = 0.046$; IC8-IC25, $t = -2.59$, $p = 0.014$; IC9-IC25, $t = -3.99$, $p = 0.0003$; IC27-IC25, $t = -3.15$, $p = 0.0035$; IC17-IC16, $t = -2.64$, $p = 0.012$; IC27-IC16, $t = -3.33$, $p = 0.0021$). Significant increases in FNCs between the DMN and DAN were found from the 1st to the 2nd patients with stroke

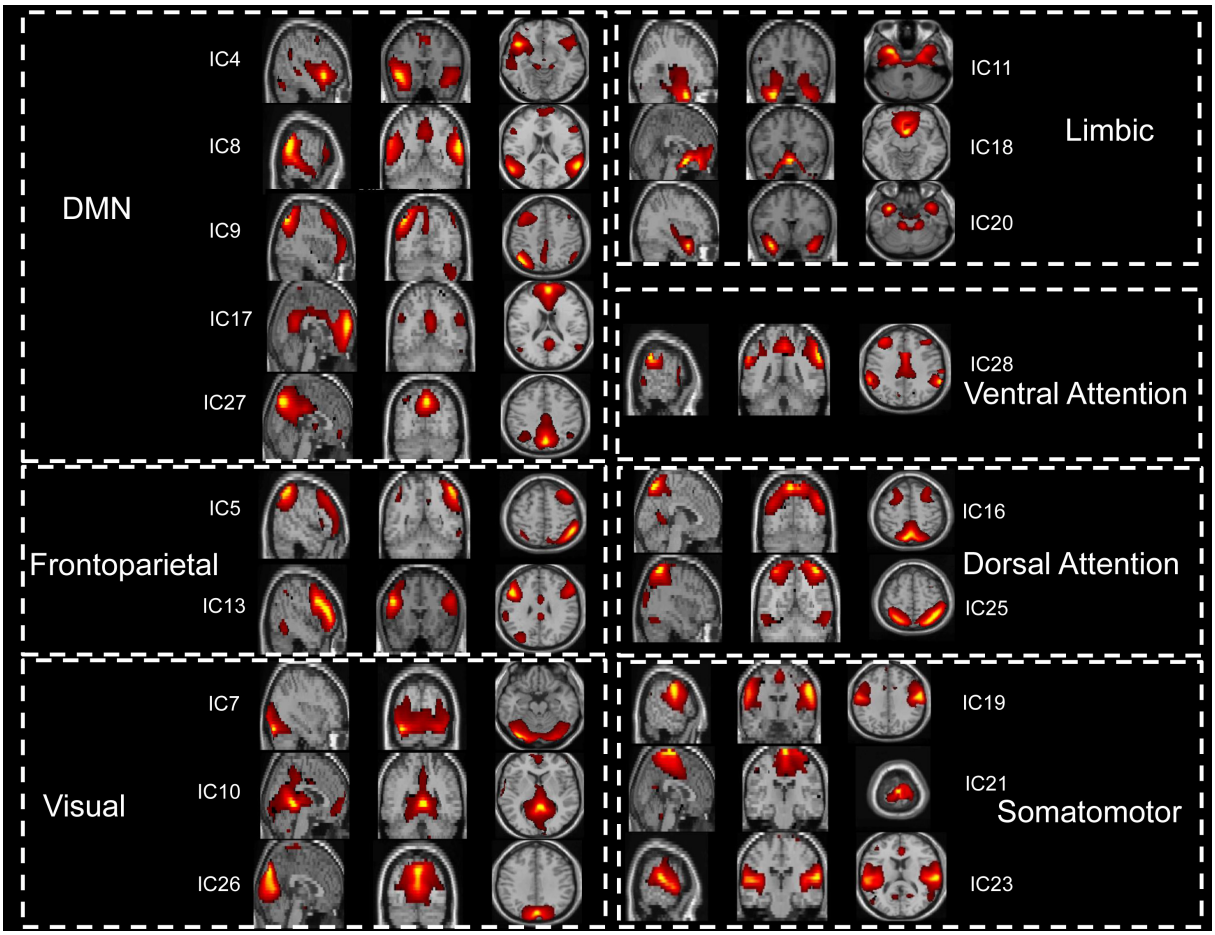

FIGURE 1
The 19 functionally relevant resting-state networks. IC, independent component; DMN, default mode network.

(Paired *t*-test, patients 1st vs. 2nd: IC4-IC25, $t = -2.68$, $p = 0.011$; IC8-IC25, $t = -2.08$, $p = 0.045$; IC9-IC25, $t = -2.90$, $p = 0.006$; IC27-IC25, $t = -2.62$, $p = 0.013$; IC17-IC16, $t = -2.12$, $p = 0.041$; IC27-IC16, $t = -2.42$, $p = 0.021$). No significant differences were detected in FNCs (DMN-DAN) between the controls and the patients with stroke at the second time point.

According to Figure 4, decreased FNCs between networks were also observed in the patients with stroke at the first time point (two sample *t*-test between 1st patient vs. control: DAN_IC25- VIS_IC10, $t = -2.22$, $p = 0.033$; SMN_IC21-VIS_IC10, $t = -2.41$, $p = 0.021$; DAN_IC16-LIM_IC20, $t = -3.38$, $p = 0.0018$; DAN_IC25-LIM_IC20, $t = -2.96$, $p = 0.0056$; DMN_IC27-LIM_IC20, $t = -3.43$, $p = 0.0035$). Paired *t*-test analysis of the patients with stroke revealed that the FNCs between these networks increased from the first to the second time point (Paired *t*-test, patients 1st vs. 2nd: DAN_IC25-VIS_IC10, $t = -3.05$, $p = 0.0043$; SMN_IC21-VIS_IC10, $t = -2.88$, $p = 0.0067$; DAN_IC16-LIM_IC20, $t = -2.55$, $p = 0.015$; DAN_IC25-LIM_IC20, $t = -2.11$, $p = 0.042$; DMN_IC27-LIM_IC20, $t = -2.21$, $p = 0.034$). There was no longer a significant difference in the FNCs between the controls and the patients at the second time point.

Regression analyses to predict clinical scores

In the present study, 14 pairs of ICs showed significant changes in the FNC in patients with stroke. The regression involving the FNC values between the DAN and the LIM (IC16-IC20) at the first time point produced a predictive regression of the FMA values at the second time point ($R^2 = 0.412$, $p = 0.003$, see Figure 5A). This regression result ($p = 0.003$) could withstand the Bonferroni correction (threshold at 0.0036 = 0.05/14). At the same time, the regression involving the FNC values between the DAN and the LIM (IC16-IC20) at the first time point also produced a predictive regression of the NDS values at the second time point ($R^2 = 0.234$, $p = 0.036$, see Figure 5B). This regression result could not withstand the Bonferroni correction (threshold at 0.0036 = 0.05/14).

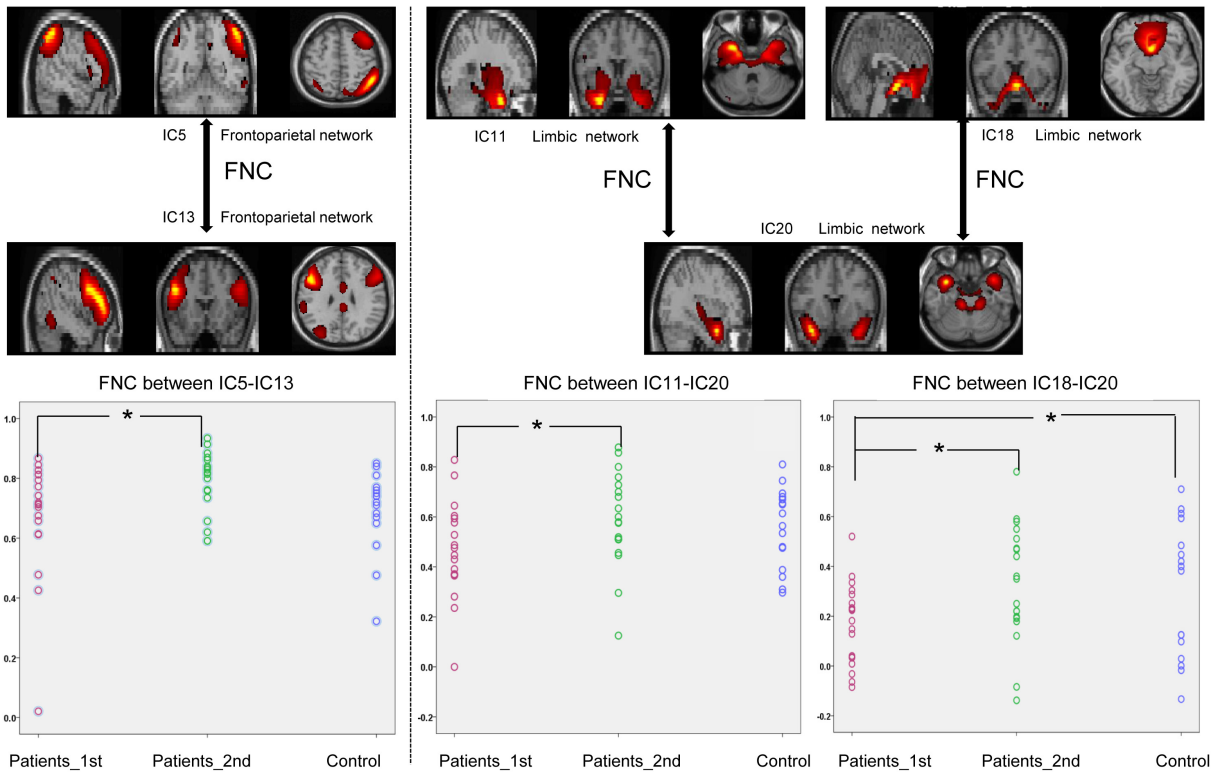

FIGURE 2
Significantly enhanced within-network connectivity of patients with subcortical ischemic stroke with a 1-month follow-up. IC, independent component; Patients_1st, patients with stroke' results at the first time point; Patients_2nd, patients with stroke' results at the second time point. Significant changes in the FNC between groups: $*p < 0.05$.

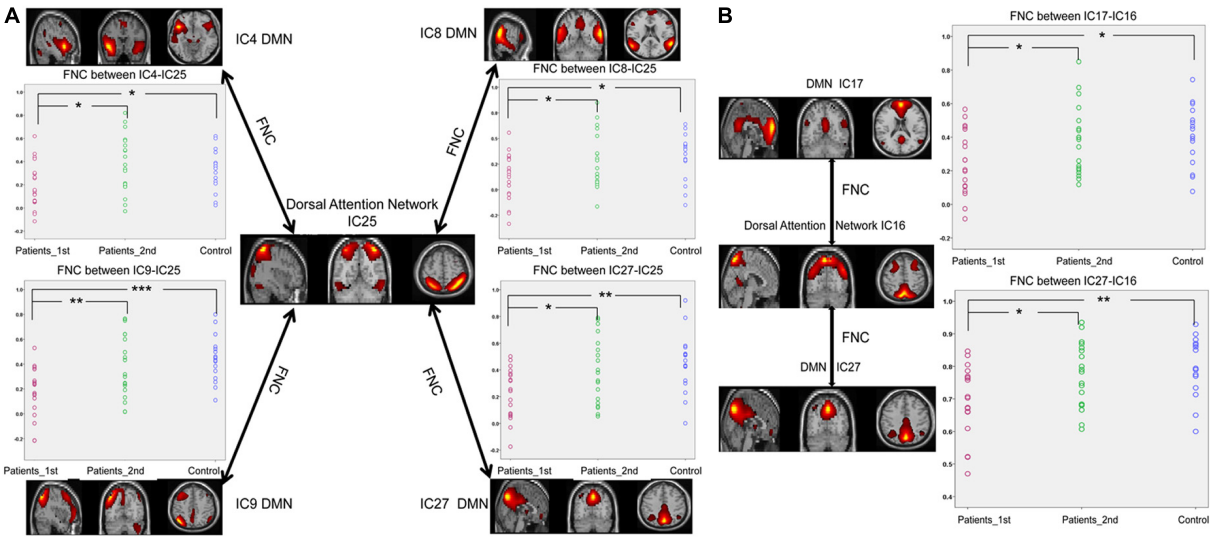

FIGURE 3
Significantly enhanced FNCs between the DAN and DMN in subcortical ischemic stroke patients with 1-month follow-up. **(A)** The FNCs between the DAN (IC25) and the DMN (IC4, IC8, IC9, IC27). **(B)** The FNCs between the DAN (IC16) and the DMN (IC17, IC27). IC, independent component; Patients_1st, stroke patients' results at the first time point; Patients_2nd, stroke patients' results at the second time point; DMN, default mode network. Significant changes in the FNC between groups: $*p < 0.05$; $**p < 0.01$; $***p < 0.001$.

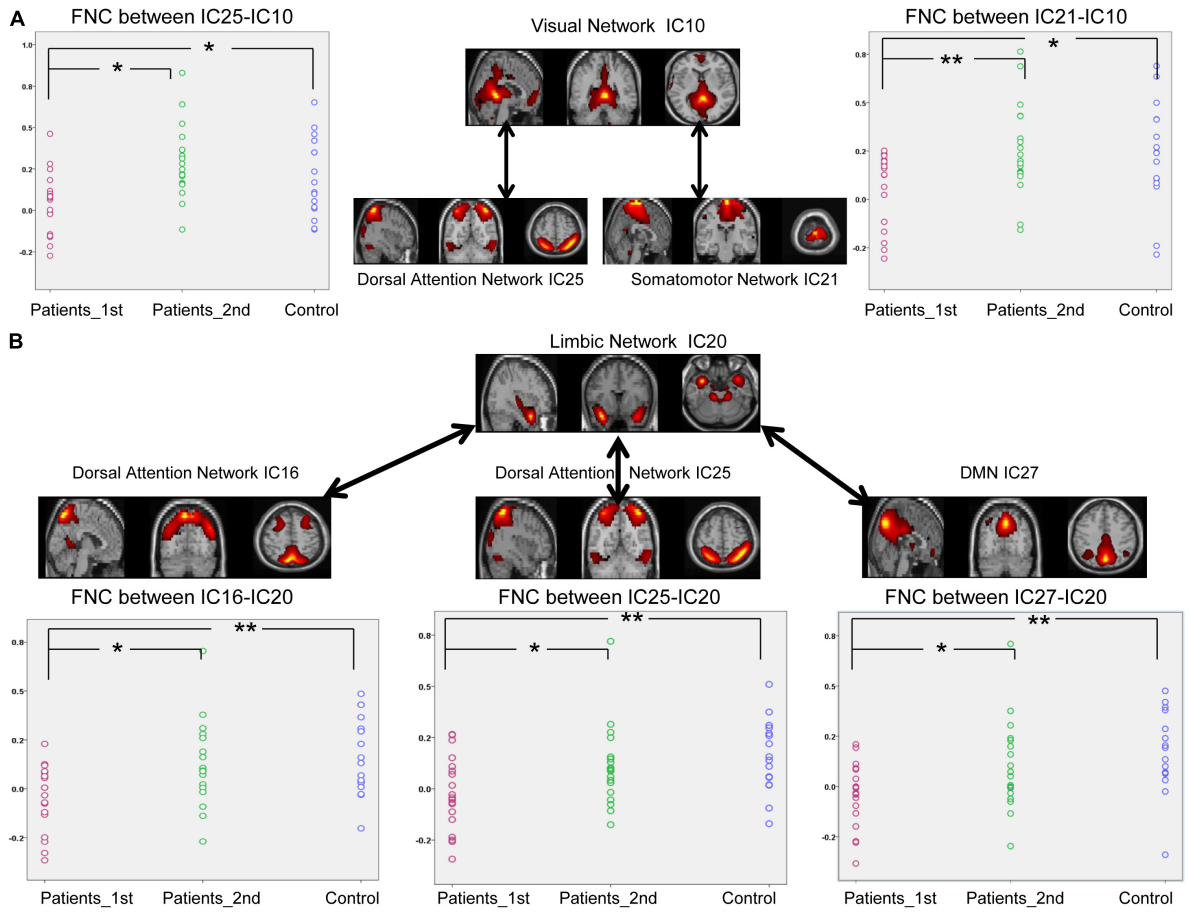

FIGURE 4
Significantly enhanced between-network connectivity of subcortical ischemic stroke patients with a 1-month follow-up. **(A)** The FNCs between the VIS (IC10) and the VAN (IC25) or between the VIS (IC10) and SMN (IC21). **(B)** The FNCs between the LIM (IC20) and the VAN (IC16, IC25) or between the LIM (IC20) and DMN (IC27). IC, independent component; Patients_1st, stroke patients' results at the first time point; Patients_2nd, stroke patients' results at the second time point. Significant changes of FNC between groups: $*p < 0.05$; $**p < 0.01$.

Discussion

The present study employed the FNC analysis to investigate the changes within and between brain networks with a longitudinal design. We further explored the potential predictive ability of functional recovery using functional coupling between resting-state networks after stroke. Our results demonstrated the following: (a) the FNCs within and between multiple brain networks were disrupted after strokes, (b) these disrupted FNCs were restored to a nearly normal level 1 month later, and (c) the FNC between the DAN and the LIM at the first time point yielded a predictive regression associated with the later clinical performance. These overall findings suggest that longitudinal changes in FNCs within and between networks can provide relevant information on brain recovery after stroke. The regression analyses suggest that internetwork functional coupling after stroke can predict the recovery of neurological functional ability.

Altered functional network connectivity after subcortical strokes

Relative to the normal controls, the patients with stroke exhibited a significant decrease in the internetwork functional coupling between multiple networks (including the DAN, DMN, LIM, VIS, and SMN). Our results are consistent with previous studies that reported decreased functional connectivity within and between the resting state networks in patients with stroke (Wang et al., 2014; Bajaj et al., 2015; Baldassarre et al., 2016). Here, we found that patients with stroke exhibited decreased internetwork FNC between the DAN and DMN. The DAN is an identified functional brain network that includes regions in the posterior parietal cortex, the frontal eye fields, and the visual area of MT + (Corbetta and Shulman, 2002). Previous studies showed that this subnetwork is related to unilateral spatial neglect (Carter et al., 2010). A previous study in patients with stroke demonstrated a significant decrease in

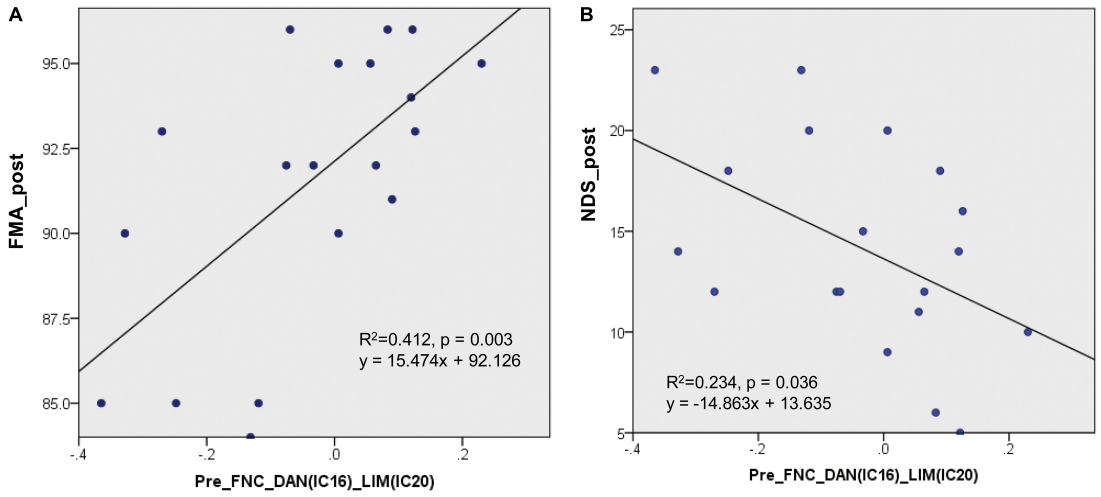

FIGURE 5
Regression results of the FNC at the first time point to predict the clinical assessment performance at the second time point. **(A)** The regression involving the FNC values between the DAN and LIM (IC16-IC20) at the first time point produced a predictive regression of the FMA values at the second time point (R^2 = 0.412, p = 0.003). **(B)** The regression involving the FNC values between the DAN and LIM (IC16-IC20) at the first time point produced a predictive regression of the NDS values at the second time point (R^2 = 0.234, p = 0.036).

the interhemispheric functional connectivity in the DAN and motor networks (Baldassarre et al., 2016). The DMN is an important resting-state functional network of the brain and is composed of a set of functionally highly connected regions (Raichle et al., 2001). Previous resting-state functional studies on patients with stroke commonly observed DMN disruption (Tuladhar et al., 2013). Resting-state functional connectivity impairments of the DMN in ischemic patients with stroke were associated with the patient's cognitive decline (Dacosta-Aguayo et al., 2015). The abnormalities of the resting-state functional connectivity in the DAN and the DMN are the effects of strokes on brain networks. Functional disruptions in these networks are linked to impairment of the patients' cognitive functions, such as attention and motor functions. Thus, the decreased connectivity found in this study between the DAN and the DMN is consistent with these previous studies and reflects abnormal functional interactions among the DAN and the DMN.

Decreased internetwork connectivity among the VIS, DAN, and SMN was also observed in patients after stroke. The VIS is a subnetwork related to visual attention and receives top–down modulation from the frontal and parietal areas (Bressler et al., 2008). A previous study in patients with stroke showed abnormal activity in the visual occipital region, which is explained as a non-effective compensatory reorganization of motor deficits after stroke (Park et al., 2011). Motor deficits can also explain the disrupted coupling between the VIS and SMN in our results in patients with stroke. The limbic network is a system that includes the amygdala, the hippocampus, the cingulate gyrus, the hypothalamus, and the fornix. The hippocampus is essential for memory formation. The amygdala is thought to be important for processing emotions. The limbic system serves various functions, such as memory and emotions (Rolls, 2015). A previous study on poststroke depression demonstrated that the functional connections of the limbic system were reduced (Shi et al., 2017). The significant decrease in the FNC between the LIM and the DAN and between the LIM and the DMN may be the neuroimaging expression of their behavioral deficits after stroke. In the real world, patients with stroke rarely experience damage to only their motor function. A previous study revealed that emotional difficulties and memory deficits after stroke are common (Kneebone, 2016). All these physical or cognitive deficits and brain neuroimaging damage in ischemic stroke are induced by the deprivation of blood supply. The widely detected decrease in the FNC between networks may imply that stroke-induced alterations can occur in multiple functional systems. This view can also be supported by a previous graph theory study showing that the topological organization of the brain networks is altered in patients with stroke (Gratton et al., 2012).

The recovery process in the functional network connectivity after a stroke

A stroke can induce a long-term motor or language disability, significantly reducing the quality of life of patients with stroke. Previous neuroimaging studies focused on cerebral reorganization following spontaneous motor recovery and demonstrated that all patients with stroke experience at least some predictable degree of functional motor recovery

within the first few months after a stroke (Park et al., 2011; Carter et al., 2012b; Xu et al., 2014). This spontaneous functional recovery may be associated with functional and structural reorganization of the related subnetworks of the brain. In addition to spontaneous recovery, specific therapeutic intervention is another main method for determining the mechanism that underlies recovery after stroke. Previous studies demonstrated that intervention studies can provide further insights into the causal relationships between behavior and connectivity (Grefkes and Fink, 2011). In the present study, we used the ICA method to investigate the recovery process in brain functional patterns after a stroke. As expected, the depressed internetwork FNCs of the DAN, the DMN, the LIM, the VIS, and the SMN were enhanced from the first to the second time point in the patient group. No significant difference in internetwork FNCs was detected between the controls and the patients at the second time point. The results were consistent with previous findings, in that the intrinsic functional connectivity patterns in chronic patients with stroke showed plasticity with clinical intervention (Bajaj et al., 2015; Li et al., 2015a, 2017; Zheng et al., 2016). Enhanced between-network functional connectivity may be induced by vascular repair after antiplatelet therapy or spontaneous recovery. Platelets can adhere to damaged blood vessels and agglutinate locally (Yardumian et al., 1986). Citicoline is a neuroprotective agent and a membrane phospholipid biosynthesis medium that can reduce cerebral vascular resistance, increase cerebral blood flow, improve brain function, and promote brain function recovery (Adibhatla, 2013). In the present study, patients with stroke were treated with antiplatelet therapy. The disruptions in the brain functions of patients with stroke were relieved at the second time point. Antiplatelet therapy may be the potential factor that induced this recovery. However, the present study included only one patient group with antiplatelet therapy. One patient group without any therapy should be included in this experiment to determine whether this recovery was induced by therapy alone. A previous study showed that spontaneous recovery could be seen in the first few months after a first-ever stroke (Ramsey et al., 2017). The stroke duration of all the patients in the present study falls within this time frame. Thus, the improvements in the FNC may also be due to spontaneous recovery. The restored FNC patterns of the present study only suggest an enhanced coupling between the cognitive networks. Future research should consider this question and improve our design to determine which factor is the reason for the present results.

Most previous studies on the longitudinal changes in stroke focused on the recovery of motor-related networks (James et al., 2009; Bajaj et al., 2015; Li et al., 2017). Our study is unique in our assessment of the functional reconfiguration of multiple networks in strokes with a longitudinal design. The reason is that cerebral stroke leave patients with significant psychological and physical impairments, such as motor, language, attention, and memory deficits. In the present study, we observed a significant increase in the functional coupling among the motor, visual, attention, and limbic subnetworks. Such changes in internetwork coupling in strokes can provide a new understanding of the ability for clinical recovery.

Regression analyses

Notably, the FNC between the DAN and the LIM in patients with stroke showed a predictive regression with their posttreatment clinical scores. This regression result between the FNC score and the FMA score may suggest that the network coupling between the DAN and the LIM before treatment can reflect the recovery degree of the patients' motor function ability. The present result was consistent with our expectation that the functional connectivity between networks in stroke would reflect the degree of the patients' clinical recovery later. A previous study revealed that oscillatory brain activity during the rehabilitative intervention could be considered a biomarker of motor recovery in chronic stroke (Ray et al., 2020). The topological organization of the brain networks was altered in patients with stroke, and the abnormal nodal degree was positively correlated with the FMA score (Zhang et al., 2017). The topological properties of the brain can reflect motor impairment in patients with stroke (Li et al., 2021). The regression result between the FNC and the FMA is consistent with that of these previous studies. It implies that patients with stroke with few disruptions in the functional coupling between the DAN and the LIM would better recover their motor ability. Additionally, we observed that the functional coupling of the DAN and the LIM in patients with stroke showed a predictive regression with the NDS score at the second time point. Our previous study revealed that the FMA scores significantly and negatively correlated with the DNS scores in patients with stroke (Li et al., 2015b). This result may suggest that patients with stroke with few disruptions of their functional coupling between the DAN and the LIM would exhibit good neurological functional recovery. Thus, the functional coupling between the DAN and LIM can be regarded as a biomarker for predicting neurological function recovery in stroke. The functional coupling between the DAN and the LIM can be used to evaluate prognosis before stroke treatment.

Although significant neuroimaging-behavior relationships were detected in the present study, the FNC within the motor network did not show any predictive regression with the clinical behavioral scores. Previous studies revealed that the functional connectivity between the motor regions can predict the recovery of patients' motor ability (Park et al., 2011; Rehme et al., 2011; Min et al., 2020; Li et al., 2021). The possible reason for this inconsistency may be that the motor components in the present

study did not divide the bilateral regions. We used the mean signal of the bilateral motor regions to calculate the functional connectivity within the motor network. Our calculation of within-motor ICs could not detect the functional connectivity between the bilateral motor regions. Future studies should pay more attention to this question.

Limitations

There were several potential limitations to this study. First, our analysis did not indicate increased FNC between subnetworks. This result is not consistent with that of a previous study that found both an increase and a decrease in the FNC among multiple networks (Zhao et al., 2018b). This inconsistency may be because the components used to select the template differed between the two studies. Future studies should reduce the template selection methods to obtain the final results. Second, the sample size was relatively small, and the acquisition time of our resting-state fMRI data was relatively short. This small sample size would limit the statistical power for detecting longitudinal changes in brain functional coupling. The short acquisition time may affect the quality of the imaging data. Future studies with a larger sample set are required to investigate the replicability of our findings. Third, the experimental design must be optimized. The present design cannot demonstrate whether the significant recovery was induced by the treatment or by spontaneous recovery. Thus, a group of patients with stroke who have not received any intervention should be included in the design. Finally, the patients in the current study had a wide range of duration of illness, which may affect our statistical results. Future studies would need to control the duration of illness of the patients.

Conclusion

Using a longitudinal design, we investigated the changes in brain network patterns in patients with subcortical strokes. The patients with stroke demonstrated disruption in the FNC among multiple functional networks. The disrupted FNCs were restored to their normal level 1 month later. The results provided insights into the neural mechanisms of brain functional recovery after stroke. Moreover, the regression analyses revealed that the FNC between the DAN and LIM in patients with stroke showed predictive regression with their clinical scores 1 month later. Functional coupling between the DAN and LIM after stroke can be regarded as a biomarker for predicting the recovery of a patient's motor function and the degree of neurological functional deficit. Overall, these findings may provide a novel opportunity to improve the prognostic ability of subcortical strokes. Future studies may benefit from including more information in the analysis to predict prognoses in stroke.

Data availability statement

The original contributions presented in this study are included in the article/**Supplementary material**, further inquiries can be directed to the corresponding author YL, yxin-li@163.com.

Ethics statement

The studies involving human participants were reviewed and approved by the Ethics Committee of Chengdu University of Traditional Chinese Medicine. The patients/participants provided their written informed consent to participate in this study.

Author contributions

YL and PW designed the experiment, analyzed the data, and drafted this manuscript for the work. ZY and PW helped to acquire the clinical and fMRI data. JC helped to revise the manuscript critically for important intellectual content. YL, PW, and JC provided the financial support, reviewed the manuscript, and provided final approval for the manuscript to be published. All authors read and approved the final manuscript.

Funding

This research received funding from the National Natural Science Foundation of China (81601483 and 81072864). This research was also supported by the Medical Science and Technology Research Foundation of Guangdong Province (A2021076), the Guang Zhou Science and Technology Project (202201011812), the Administration of Traditional Chinese Medicine of Guangdong Province (20221099), the Key-Area Research and Development Program of Guangdong Province (No. 2020B1111100001), and the Huang Zhendong Research Fund for Traditional Chinese Medicine of Jinan University.

Acknowledgments

The authors are grateful to the patients who participated in the study. The authors are also thank Qie-zhu Wu in the West China Hospital MRI Center for his cooperation in data collection and analysis.

Conflict of interest

The authors declare that the research was conducted in the absence of any commercial or financial relationships that could be construed as a potential conflict of interest.

Publisher's note

All claims expressed in this article are solely those of the authors and do not necessarily represent those of their affiliated organizations, or those of the publisher, the editors and the reviewers. Any product that may be evaluated in this article, or claim that may be made by its manufacturer, is not guaranteed or endorsed by the publisher.

Supplementary material

The Supplementary Material for this article can be found online at: https://www.frontiersin.org/articles/10.3389/fnagi.2022.933567/full#supplementary-material

SUPPLEMENTARY FIGURE 1
Lesion maps. **(A)** This figure demonstrates the locations of the lesions in the standard space of each patient included in this study. **(B)** This figure is the merged lesion map of all patients, in which all lesion maps were overlapped to produce this patient group lesion map. The right hemisphere lesions of two patients were flipped to the left hemisphere. The *n* values of the color bar in this map represent the number of patients. For example, one region showed yellow; in this region, the corresponding *n* value is 5, suggesting that five patients have lesions.

SUPPLEMENTARY FIGURE 2
Spatial maps. **(A)** The seven spatial maps of Yeo2011 reference networks, **(B)** spatial maps of the 19 independent components grouped into seven domains and compared to the Yeo 2011 reference networks.

References

Adibhatla, R. M. (2013). Citicoline in stroke and TBI clinical trials. *Nat. Rev. Neurol.* 9:173.

Bajaj, S., Butler, A. J., Drake, D., and Dhamala, M. (2015). Functional organization and restoration of the brain motor-execution network after stroke and rehabilitation. *Front. Hum. Neurosci.* 9:173. doi: 10.3389/fnhum.2015.00173

Baldassarre, A., Ramsey, L., Rengachary, J., Zinn, K., Siegel, J. S., Metcalf, N. V., et al. (2016). Dissociated functional connectivity profiles for motor and attention deficits in acute right-hemisphere stroke. *Brain* 139, 2024–2038. doi: 10.1093/brain/aww107

Bell, A. J., and Sejnowski, T. J. (1995). An information-maximization approach to blind separation and blind deconvolution. *Neural Comput.* 7, 1129–1159. doi: 10.1162/neco.1995.7.6.1129

Bressler, S. L., Tang, W., Sylvester, C. M., Shulman, G. L., and Corbetta, M. (2008). Top-down control of human visual cortex by frontal and parietal cortex in anticipatory visual spatial attention. *J. Neurosci.* 28, 10056–10061.

Calhoun, V., Adali, T., Pearlson, G., and Pekar, J. (2001). A method for making group inferences from functional MRI data using independent component analysis. *Hum. Brain Mapp.* 14, 140–151.

Carter, A. R., Astafiev, S. V., Lang, C. E., Connor, L. T., Rengachary, J., Strube, M. J., et al. (2010). Resting interhemispheric functional magnetic resonance imaging connectivity predicts performance after stroke. *Ann. Neurol.* 67, 365–375.

Carter, A. R., Patel, K. R., Astafiev, S. V., Snyder, A. Z., Rengachary, J., Strube, M. J., et al. (2012a). Upstream dysfunction of somatomotor functional connectivity after corticospinal damage in stroke. *Neurorehabil. Neural Repair* 26, 7–19. doi: 10.1177/1545968311411054

Carter, A. R., Shulman, G. L., and Corbetta, M. (2012b). Why use a connectivity-based approach to study stroke and recovery of function? *Neuroimage* 62, 2271–2280. doi: 10.1016/j.neuroimage.2012.02.070

Chen, H. Y., Shi, M. Y., Zhang, H., Zhang, Y. D., Geng, W., Jiang, L., et al. (2019). Different patterns of functional connectivity alterations within the default-mode network and sensorimotor network in basal ganglia and pontine stroke. *Med. Sci. Monit.* 25, 9585–9593. doi: 10.12659/MSM.918185

Chen, X., Chen, L., Zheng, S., Wang, H., Dai, Y., Chen, Z., et al. (2021). Disrupted brain connectivity networks in aphasia revealed by resting-state fMRI. *Front. Aging Neurosci.* 13:666301. doi: 10.3389/fnagi.2021.666301

Corbetta, M., and Shulman, G. L. (2002). Control of goal-directed and stimulus-driven attention in the brain. *Nat. Rev. Neurosci.* 3, 201–215.

Dacosta-Aguayo, R., Graña, M., Iturria-Medina, Y., Fernández-Andújar, M., López-Cancio, E., Cáceres, C., et al. (2015). Impairment of functional integration of the default mode network correlates with cognitive outcome at three months after stroke. *Hum. Brain Mapp.* 36, 577–590.

Fu, Z., Caprihan, A., Chen, J., Du, Y., Adair, J. C., Sui, J., et al. (2019). Altered static and dynamic functional network connectivity in Alzheimer's disease and subcortical ischemic vascular disease: shared and specific brain connectivity abnormalities. *Hum. Brain Mapp.* 40, 3203–3221. doi: 10.1002/hbm.24591

Gladstone, D. J., Danells, C. J., and Black, S. E. (2002). The fugl-meyer assessment of motor recovery after stroke: a critical review of its measurement properties. *Neurorehabil. Neural Repair* 16, 232–240. doi: 10.1177/154596802401105171

Gratton, C., Nomura, E. M., Pérez, F., and D'Esposito, M. (2012). Focal brain lesions to critical locations cause widespread disruption of the modular organization of the brain. *J. Cogn. Neurosci.* 24, 1275–1285. doi: 10.1162/jocn_a_00222

Grefkes, C., and Fink, G. R. (2011). Reorganization of cerebral networks after stroke: new insights from neuroimaging with connectivity approaches. *Brain* 134, 1264–1276. doi: 10.1093/brain/awr033

Grefkes, C., and Fink, G. R. (2014). Connectivity-based approaches in stroke and recovery of function. *Lancet Neurol.* 13, 206–216.

Grefkes, C., and Fink, G. R. (2020). Recovery from stroke: current concepts and future perspectives. *Neurol. Res. Pract.* 2:17.

Grefkes, C., and Ward, N. S. (2014). Cortical reorganization after stroke: how much and how functional? *Neuroscientist* 20, 56–70.

Hordacre, B., Lotze, M., Jenkinson, M., Lazari, A., Barras, C. D., Boyd, L., et al. (2021). Fronto-parietal involvement in chronic stroke motor performance when corticospinal tract integrity is compromised. *Neuroimage Clin.* 29:102558. doi: 10.1016/j.nicl.2021.102558

Hu, J.-Y., Kirilina, E., Nierhaus, T., Ovadia-Caro, S., Livne, M., Villringer, K., et al. (2021). A novel approach for assessing hypoperfusion in stroke using spatial independent component analysis of resting-state fMRI. *Hum. Brain Mapp.* 42, 5204–5216. doi: 10.1002/hbm.25610

James, G. A., Lu, Z.-L., VanMeter, J. W., Sathian, K., Hu, X. P., and Butler, A. J. (2009). Changes in resting state effective connectivity in the motor network following rehabilitation of upper extremity poststroke paresis. *Top. Stroke Rehabil.* 16, 270–281. doi: 10.1310/tsr1604-270

Jiang, L., Geng, W., Chen, H., Zhang, H., Bo, F., Mao, C.-N., et al. (2018). Decreased functional connectivity within the default-mode network in acute brainstem ischemic stroke. *Eur. J. Radiol.* 105, 221–226. doi: 10.1016/j.ejrad.2018.06.018

Kneebone, I. I. (2016). A framework to support cognitive behavior therapy for emotional disorder after stroke. *Cogn. Behav. Pract.* 23, 99–109. doi: 10.1186/s13012-016-0452-0

Li, Y., Wang, D., Zhang, H., Wang, Y., Wu, P., Zhang, H., et al. (2016). Changes of brain connectivity in the primary motor cortex after subcortical stroke: a multimodal magnetic resonance imaging study. *Medicine* 95:2579.

Li, Y., Wang, Y., Zhang, H., Wu, P., and Huang, W. (2015a). The effect of acupuncture on the motor function and white matter microstructure

in ischemic patients with stroke. *Evid. Based Complement. Alternat. Med.* 2015:164792.

Li, Y., Wu, P., Liang, F., and Huang, W. (2015b). The microstructural status of the corpus callosum is associated with the degree of motor function and neurological deficit in patients with stroke. *PLoS One* 10:e0122615. doi: 10.1371/journal.pone.0122615

Li, Y., Yu, Z., Wu, P., and Chen, J. (2021). The disrupted topological properties of structural networks showed recovery in ischemic patients with stroke: a longitudinal design study. *BMC Neurosci.* 22:47. doi: 10.1186/s12868-021-00652-1

Li, Y. X., Wang, Y., Liao, C. X., Huang, W. H., and Wu, P. (2017). Longitudinal brain functional connectivity changes of the cortical motor-related network in subcortical patients with stroke with acupuncture treatment. *Neural Plast.* 2017:5816263. doi: 10.1155/2017/5816263

Lindenberg, R., Zhu, L. L., Rüber, T., and Schlaug, G. (2012). Predicting functional motor potential in chronic patients with stroke using diffusion tensor imaging. *Hum. Brain Mapp.* 33, 1040–1051.

Maglanoc, L. A., Kaufmann, T., Jonassen, R., Hilland, E., Beck, D., Landro, N. I., et al. (2020). Multimodal fusion of structural and functional brain imaging in depression using linked independent component analysis. *Hum. Brain Mapp.* 41, 241–255. doi: 10.1002/hbm.24802

Min, Y. S., Park, J. W., Park, E., Kim, A. R., Cha, H., Gwak, D. W., et al. (2020). Interhemispheric functional connectivity in the primary motor cortex assessed by resting-state functional magnetic resonance imaging aids long-term recovery prediction among subacute patients with stroke with severe hand weakness. *J. Clin. Med.* 9:975. doi: 10.3390/jcm9040975

Mirzaei, G., and Adeli, H. (2016). Resting state functional magnetic resonance imaging processing techniques in stroke studies. *Rev. Neurosci.* 27, 871–885.

Nomura, E. M., Gratton, C., Visser, R. M., Kayser, A., Perez, F., and D'Esposito, M. (2010). Double dissociation of two cognitive control networks in patients with focal brain lesions. *Proc. Natl. Acad. Sci. U.S.A.* 107, 12017–12022. doi: 10.1073/pnas.1002431107

Ovadia-Caro, S., Margulies, D. S., and Villringer, A. (2014). The value of resting-state functional magnetic resonance imaging in stroke. *Stroke* 45, 2818–2824.

Park, C. H., Chang, W. H., Ohn, S. H., Kim, S. T., Bang, O. Y., Pascual-Leone, A., et al. (2011). Longitudinal changes of resting-state functional connectivity during motor recovery after stroke. *Stroke* 42, 1357–1362.

Raichle, M. E., MacLeod, A. M., Snyder, A. Z., Powers, W. J., Gusnard, D. A., and Shulman, G. L. (2001). A default mode of brain function. *Proc. Natl. Acad. Sci. U.S.A.* 98, 676–682.

Ramsey, L. E., Siegel, J. S., Lang, C. E., Strube, M., Shulman, G. L., and Corbetta, M. (2017). Behavioural clusters and predictors of performance during recovery from stroke. *Nat. Hum. Behav.* 1:0038.

Ray, A. M., Figueiredo, T. D. C., Lopez-Larraz, E., Birbaumer, N., and Ramos-Murguialday, A. (2020). Brain oscillatory activity as a biomarker of motor recovery in chronic stroke. *Hum. Brain Mapp.* 41, 1296–1308. doi: 10.1002/hbm.24876

Rehme, A. K., Eickhoff, S. B., Wang, L. E., Fink, G. R., and Grefkes, C. (2011). Dynamic causal modeling of cortical activity from the acute to the chronic stage after stroke. *Neuroimage* 55, 1147–1158. doi: 10.1016/j.neuroimage.2011.01.014

Rehme, A. K., and Grefkes, C. (2013). Cerebral network disorders after stroke: evidence from imaging-based connectivity analyses of active and resting brain states in humans. *J. Physiol.* 591, 17–31. doi: 10.1113/jphysiol.2012.243469

Rolls, E. T. (2015). Limbic systems for emotion and for memory, but no single limbic system. *Cortex* 62, 119–157.

Salman, M. S., Du, Y., Lin, D., Fu, Z., Fedorov, A., Damaraju, E., et al. (2019). Group ICA for identifying biomarkers in schizophrenia: 'Adaptive' networks via spatially constrained ICA show more sensitivity to group differences than spatio-temporal regression. *NeuroImage Clin.* 22:101747. doi: 10.1016/j.nicl.2019.101747

Shi, Y., Zeng, Y., Wu, L., Liu, Z., Zhang, S., Yang, J., et al. (2017). A study of the brain functional network of post-stroke depression in three different lesion locations. *Sci. Rep.* 7:14795. doi: 10.1038/s41598-017-14675-4

Sinha, A. M., Nair, V. A., and Prabhakaran, V. (2021). Brain-computer interface training with functional electrical stimulation: facilitating changes in interhemispheric functional connectivity and motor outcomes post-stroke. *Front. Neurosci.* 15:670953. doi: 10.3389/fnins.2021.670953

Smith, S. M., Fox, P. T., Miller, K. L., Glahn, D. C., Fox, P. M., Mackay, C. E., et al. (2009). Correspondence of the brain's functional architecture during activation and rest. *Proc. Natl. Acad. Sci. U.S.A.* 106, 13040–13045.

Tuladhar, A. M., Snaphaan, L., Shumskaya, E., Rijpkema, M., Fernandez, G., Norris, D. G., et al. (2013). Default mode network connectivity in patients with stroke. *PLoS One* 8:e66556. doi: 10.1371/journal.pone.0066556

van de Ven, V. G., Formisano, E., Prvulovic, D., Roeder, C. H., and Linden, D. E. (2004). Functional connectivity as revealed by spatial independent component analysis of fMRI measurements during rest. *Hum. Brain Mapp.* 22, 165–178.

Wang, C., Qin, W., Zhang, J., Tian, T., Li, Y., Meng, L., et al. (2014). Altered functional organization within and between resting-state networks in chronic subcortical infarction. *J. Cereb. Blood Flow Metab.* 34, 597–605. doi: 10.1038/jcbfm.2013.238

Wang, L., Yu, C., Chen, H., Qin, W., He, Y., Fan, F., et al. (2010). Dynamic functional reorganization of the motor execution network after stroke. *Brain* 133, 1224–1238.

Wang, L. E., Tittgemeyer, M., Imperati, D., Diekhoff, S., Ameli, M., Fink, G. R., et al. (2012). Degeneration of corpus callosum and recovery of motor function after stroke: a multimodal magnetic resonance imaging study. *Hum. Brain Mapp.* 33, 2941–2956. doi: 10.1002/hbm.21417

Xu, H., Qin, W., Chen, H., Jiang, L., Li, K., and Yu, C. (2014). Contribution of the resting-state functional connectivity of the contralesional primary sensorimotor cortex to motor recovery after subcortical stroke. *PLoS One* 9:e84729. doi: 10.1371/journal.pone.0084729

Yardumian, D. A., Mackie, I. J., and Machin, S. J. (1986). Laboratory investigation of platelet function: a review of methodology. *J. Clin. Pathol.* 39, 701–712.

Zalesky, A., Fornito, A., and Bullmore, E. T. (2010). Network-based statistic: identifying differences in brain networks. *Neuroimage* 53, 1197–1207.

Zhang, J., Zhang, Y., Wang, L., Sang, L., Yang, J., Yan, R., et al. (2017). Disrupted structural and functional connectivity networks in ischemic patients with stroke. *Neuroscience* 364, 212–225.

Zhao, Z., Tang, C., Yin, D., Wu, J., Gong, J., Sun, L., et al. (2018a). Frequency-specific alterations of regional homogeneity in subcortical patients with stroke with different outcomes in hand function. *Hum. Brain Mapp.* 39, 4373–4384. doi: 10.1002/hbm.24277

Zhao, Z., Wu, J., Fan, M., Yin, D., Tang, C., Gong, J., et al. (2018b). Altered intra- and inter-network functional coupling of resting-state networks associated with motor dysfunction in stroke. *Hum. Brain Mapp.* 39, 3388–3397. doi: 10.1002/hbm.24183

Zheng, X., Sun, L., Yin, D., Jia, J., Zhao, Z., Jiang, Y., et al. (2016). The plasticity of intrinsic functional connectivity patterns associated with rehabilitation intervention in chronic patients with stroke. *Neuroradiology* 58, 417–427. doi: 10.1007/s00234-016-1647-4

frontiers | Frontiers in Aging Neuroscience

TYPE Original Research
PUBLISHED 06 October 2022
DOI 10.3389/fnagi.2022.936661

OPEN ACCESS

EDITED BY
Fermín Segovia,
University of Granada, Spain

REVIEWED BY
Otmar Bock,
German Sport University Cologne, Germany
Cristina Fernandez-Baizan,
University of Oviedo, Spain

*CORRESPONDENCE
Luis Eudave
leudave@unav.es
María A. Pastor
mapastor@unav.es

SPECIALTY SECTION
This article was submitted to Neurocognitive Aging and Behavior, a section of the journal Frontiers in Aging Neuroscience

RECEIVED 05 May 2022
ACCEPTED 09 September 2022
PUBLISHED 06 October 2022

CITATION
Eudave L, Martínez M, Luis EO and Pastor MA (2022) Egocentric distance perception in older adults: Results from a functional magnetic resonance imaging and driving simulator study. *Front. Aging Neurosci.* 14:936661. doi: 10.3389/fnagi.2022.936661

Egocentric distance perception in older adults: Results from a functional magnetic resonance imaging and driving simulator study

Luis Eudave[1,2]*, Martín Martínez[1,2], Elkin O. Luis[1,2] and María A. Pastor[1]*

[1]Neuroimaging Laboratory, Division of Neurosciences, Centre for Applied Medical Research, University of Navarra, Pamplona, Spain, [2]School of Education and Psychology, University of Navarra, Pamplona, Spain

The ability to appropriately perceive distances in activities of daily living, such as driving, is necessary when performing complex maneuvers. With aging, certain driving behaviors and cognitive functions change; however, it remains unknown if egocentric distance perception (EDP) performance is altered and whether its neural activity also changes as we grow older. To that end, 19 young and 17 older healthy adults drove in a driving simulator and performed an functional magnetic resonance imaging (fMRI) experiment where we presented adults with an EDP task. We discovered that (a) EDP task performance was similar between groups, with higher response times in older adults; (b) older adults showed higher prefrontal and parietal activation; and (c) higher functional connectivity within frontal and parietal-occipital-cerebellar networks; and (d) an association between EDP performance and hard braking behaviors in the driving simulator was found. In conclusion, EDP functioning remains largely intact with aging, possibly due to an extended and effective rearrangement in functional brain resources, and may play a role in braking behaviors while driving.

KEYWORDS

egocentric distance perception, fMRI, driving, simulator, older adults

Introduction

Egocentric distance perception (EDP) refers to the distance perceived between the observer and the stimulus. The EDP of a stimulus or an object in a 3D scene is determined by a set of optical variables called distance cues (Foley, 1977). These include, but are not limited to, depth, size, perspective, contrast, texture, shadows, surface inclination, or even gravity (Clément et al., 2016). It is usually considered that within an image, objects are close and scenes are distant. Thus, distant objects or scenes would occupy the upper half of the visual field, while closer objects take the lower half in addition to the fovea.

There are two types of EDP tasks: those based on a verbal answer and those based on action. The first type requires a verbally emitted response and includes the calculation

of distances in metric units. The second type implies an action directed to the visual information that was presented just before the action. A common example of the latter is walking blindfolded toward the position of a previously presented object. These tasks assume that the action is controlled by a visual representation of the physical space. Although the neurological substrate underlying both types of EDP tasks has not been studied, we can assume that both processes transform visual signals in different ways and therefore use different resources (Milner and Goodale, 2008).

These studies on EDP are usually carried out in "real" physical places, both outdoors (garden and street) and indoors (rooms and corridors). There are also digital modalities in which scenes and objects are shown on a computer screen: some use optical illusions to simulate depth within the scene (Amit et al., 2012), while others show pairs of images of the same stimulus but at different distances (Parkinson et al., 2014; Persichetti and Dilks, 2016). This modality, displayed on a computer screen, could prove useful when studying situations where the perception of great distances is necessary, such as when driving a car on a highway. Studies comparing performance between real-world and PC-generated tasks (including virtual reality) show mixed results: some have found differences in performance (Adamo et al., 2012; Kimura et al., 2017), while in others both modalities show similar patterns of underestimation (Creem-Regehr et al., 2005; Kunz et al., 2009; Li et al., 2011; Hettinger and Haas, n.d.). This is relevant, since an EDP task "virtual analog" is needed when exploring its neural basis using functional magnetic resonance imaging (fMRI).

Driving is a complex daily-life activity that makes use of several cognitive abilities. For instance, when evaluating on-road fitness-to-drive, the best discriminative tests employed were the Ergovision Movement Perception subtest and Useful Field of View (UFOW), which have good discriminative ability to predict the performance of older drivers on a driving simulator, the Benton Line Orientation Task, Clock Drawing task, Driver Scanning, and the UFOW divided and selective attention subtests. These tests evaluate different aspects of perception, cognitive flexibility, attention, and spatial construction (Mathias and Lucas, 2009). Other functions, such as other executive functions, memory, or perceptual abilities, are also required for driving (Whelihan et al., 2005; Mäntylä et al., 2009; León-Domínguez et al., 2017). Some of these cognitive abilities deteriorate with aging, but only deficits in visuospatial abilities have been consistently associated with impaired driving, both real and simulated, in older adults (Reger et al., 2004; Hoffman et al., 2005; Mathias and Lucas, 2009). Investigating the mediating mechanisms of visuospatial abilities in driving is important since its deficit has been associated with real-world crashes and performance in a driving simulator in older adults (Anderson et al., 2005) and patients with cognitive impairment (Apolinario et al., 2009).

The study of EDP in aging has been little explored. It has been found that while young volunteers underestimated distances, older volunteers over 70 years of age did not and, surprisingly, had better accuracy (Bian and Andersen, 2013). To explain these results, the authors argue that this effect may be due to the fact that older adults have more knowledge about the egocentric distance from real scenes (Zhou et al., 2016), as a result of greater experience throughout life. Another explanation is the participants' "height" effect, in which older adults have reached their height for a longer time than younger adults and therefore can make better distance estimates, even after controlling for height (Ooi and He, 2007; Zhou et al., 2016).

Other studies have reported alternate results. Gajewski et al. (2015) obtained egocentric distance detection thresholds for each subject; the results showed thresholds to be higher in older volunteers than in younger adults. However, the distance perception accuracy between both groups was similar, even when allowed to take a longer glance and when multiple stimuli appeared instead of one. They attributed these higher thresholds in older adults as necessary to extract useful information from the scene. In general, they conclude that this function is not impaired in older adults, and that the representation of space formed from memory plays an important role in this group. A subsequent study found support for this hypothesis (Wallin et al., 2017). Finally, Ruggiero et al. (2016) found slower and less accurate responses to egocentric distance judgments in participants above 70 years old, although this might be dependent on variables, such as scene context and sex, may affect the perception of distances in older adults (Norman et al., 2018).

Overall, previous studies indicate that EDP might be preserved in older age; however, the brain mechanisms involved in this task remain unclear. To date, there are few functional neuroimaging studies that have studied the neural correlates of EDP, and none included an older adult population. Activation of the lateral occipital cortex was found when stimuli were presented close and the parahippocampal area of places when presented further away (Amit et al., 2012). Using the perception of egocentric distance specific to scenes, not only to images of objects, activity was found in the retrosplenial complex in addition to the occipital lateral cortex but not in the parahippocampal area of places (Persichetti and Dilks, 2016). The right inferior parietal lobe (IPL) and areas from the default mode network (DMN) have also been found to be activated in tasks where spatial, temporal, and social perception of distance is examined (for example, "a close friend" and "a year from now"), which reinforces its role as an integrator of the perception of distance in a broader sense (Parkinson et al., 2014; Peer et al., 2015). It is important to note that functional connectivity networks of EDP have not been explored so far.

Studying how these activations change as we age could be of practical relevance, since an increased activation might reflect an increased cognitive demand, which might degrade EDP performance when executed in a complex everyday situation, such as car driving, and not as an isolated laboratory paradigm (Venkatesan et al., 2018). This is important since distance perception is attributed to be a perceptual mechanism of driving

behaviors that may prevent accidents, especially in driving conditions, such as nighttime or foggy weather (Cavallo et al., 2001, 2007).

To date, there are a few functional neuroimaging studies that have studied the neural correlates of EDP, and none included an older adult population. In general, results report activations from the occipital V3d/V3A areas, and further objects were in pairs of images with stimuli at different distances (Berryhill, 2009). Activation from the lateral occipital cortex was found when stimuli were presented close and from the parahippocampal area of places when presented further away (Amit et al., 2012). Using the perception of egocentric distance specific to scenes, not only to images of objects, activity was found in the retrosplenial complex in addition to the occipital lateral cortex but not in the parahippocampal area of places (Persichetti and Dilks, 2016). The right inferior parietal lobe (IPL) and areas from the default mode network (DMN) have also been found to be activated in tasks where spatial, temporal, and social perception of distance is examined (for example, "a close friend" and "a year from now"), which reinforces its role as an integrator of the perception of distance in a broader sense (Parkinson et al., 2014; Peer et al., 2015). It is important to note that functional connectivity networks of EDP have not been explored so far.

Therefore, in this study, we aimed to explore the neural correlates of EDP in older adults as compared to younger adults using fMRI, and how performance impacts both populations on a common activity of daily living like car driving using a driving simulator. Our hypotheses for this experiment are as follows: (1) EDP performance is comparable between young and older adults, (2) a difference will be observed in brain activity and connectivity between groups, and (3) there will be a connection between EDP performance and driving behavior.

Materials and methods

Participants

A total of 36 volunteers were recruited and classified into two groups: 19 young subjects (YS, 11 men, 30.5 ± 4.5 years old [descriptive results will continue to be presented in the mean ± standard deviation format] and a mean 8.8 years of driving experience) and 17 older subjects (OS, 14 men, 66.5 ± 4.7 years old and a mean of 44.7 years of driving experience). The sample size and our EDP task design were calculated using POBE (v1.1), a Matlab-based program for the optimal design of blocked experiments (Maus and van Breukelen, 2014).

Subjects in the YS group included volunteers aged from 22 to 40 years old, and in the OS group, volunteers more than 60 years of age were recruited (range 61–72 years). All participants were right-handedly tested with the Edinburgh inventory (Oldfield, 1971). Exclusion criteria included those associated with MRI use (metallic implants, claustrophobia, etc.), the presence of neurological, cognitive, or visual dysfunction, current pharmacological treatment modulating the central nervous system, and abnormal findings on the participants' structural MRI scan.

Volunteers were mostly recruited from the University of Navarra's studentship and alumni. All participants had higher education; we requested information about studies or professions using their ability to visualize and spatial judgment, finding engineering training and profession in similar percentage in both groups (percentage of professions in YS was as follows: Life Sciences 43%, Education and Psychology 21%, Social Sciences 24%, and Engineering 12%; percentage of professions in OS was as follows: Life Sciences 23%, Education and Psychology 37%, Law and Social Sciences 28%, and Engineering 12%). All but two YS volunteers were research-naive and had never participated in any research study before. The experimental protocol was approved by the University of Navarra Research Ethics Committee. Subjects signed a written informed consent before participating in the study.

Driving simulator setup and evaluation

The driving simulator setup used in this study (Signos, Prometeo Innovations C) consisted of a PC, a 40-inch TV, the Logitech G25 Driving Wheel, Pedals and Stick, and a racing seat (Supplementary Image 1). The screen was positioned 1 m in front of the driver while seated and displayed a simulated first-person view from the inside of a Toyota Yaris driver's seat. The driving session consisted of a 40-min evaluation where participants had to follow a set of pre-defined verbal instructions given by an automated voice, like a GPS system (e.g., "at the roundabout and take the second exit") through a three-stage circuit (Supplementary Image 2) while driving as they would in a real car. The first stage took place in an urban environment that included traffic lights, different speed limits, pedestrians crossing the street, slow traffic, and a roundabout crossing that lasted for approximately 2.4 km. The second stage was done on a highway where participants had to drive for 11.6 km (round trip) with a 120 km/h speed limit. In the third stage, participants had to drive through a two-lane mountain road (9.6 km, roundtrip) with traffic and different speed limits. Prior to the examination, subjects were allowed to practice driving on "free mode" for up to 20 min, in order to get familiarized with the simulator controls and sensitivity to steering, accelerating, and braking. No systematic monitoring was carried out for simulator sickness symptoms during the experiment. The participants were requested to stop the trial in case they experienced any uncomfortable symptoms. They were asked to communicate any symptoms or simulator sickness and their intensity after the experiment.

A total of 27 telemetric parameters were registered during each driving evaluation, which were related to how fast the participant was driving (total session time, % of time moving,

% of time above the speed limit, and mean speed at 40, 50, 80, 100, and 120 km/h limit areas), pedal management (time with gas pedal pressed over 75%, % of time with gas pedal pressed over 75%, time braking, % of time braking, time with brake pedal pressed over 75%, % of time with brake pedal pressed over 75%), number of >5 s brakes (brake pedal pressed over 5 s), number of >10 s brakes (brake pedal pressed over 10 s), steering (number of 60°–90°, 90°–180°, 180°–270°, and 270°–360° steers in 0.5 s), and traffic violations (two wheel sidewalk invasion, collision with other cars or objects, yellow or red traffic light skips, runovers, and restarts). After each driving session, a log file including these parameters was created, from which data were then extracted and analyzed.

Functional magnetic resonance imaging experimental setup and design

The EDP task was built using the Unity (v5, 2015) game engine. The objective of this experiment was to determine the participants' ability to estimate the distance of a vehicle from the observer and to determine whether it was closer or farther when compared to another vehicle within a naturalistic driving scenario (**Figure 1**). Each cycle (14 in total) began a rest period (Rest) where subjects were asked to keep their gaze fixed on a central cross for 15 s. They were then presented with a block of the Task condition, which consisted of a series of three trials each of which contained two images. Each image represented the point of view of a driver inside a Peugeot 207, driving on a straight road with a mountainous background and was presented for 1,500 ms. In the first image (reference image), a vehicle (car or truck, to avoid participants using stimuli size as a cue) was presented in front of the observer, on the road at one of the 14 different possible distances (from 10 to 140 virtual meters, in virtual meters, in 10-m intervals) which was assigned pseudo-randomly. Then, a second image was presented but with a new vehicle (car or truck) at a shorter or longer distance than the previous vehicle, but never at more than two intervals (10 or 20 m apart) away. At the end of the presentation, a response window of 2,000 ms was left in which the participant had to answer the question "which of the two vehicles was the furthest?" by pressing the first (left-most button) of the button box if he/she thought the first vehicle was farther away, or by pressing the second button (from left to right) if he/she thought the second vehicle was the furthest. Subsequently, a block of the Control condition was presented, where the subject was requested to detect a single image presented during 3,000 ms, which resembled the one in Task, but "pixelated" (by reducing the original resolution from 1,280 × 720p to 128 × 72p) in such a way that it was still possible to recognize the context of the image (driving on a road in a scenario with mountains) but not how far were vehicles from each other. The spatial distribution, chromatic scale, and shapes of objects in the scene were similar but with a lower resolution, which would prevent the participants to estimate the distance between the vehicles. At the end of this image, a 2,000 ms response window was presented where the subject was asked to press any button in response to detecting the stimulus. The duration of each Task and Control block was 15 s, for a total of 45 s per cycle (Rest = 15 s, Task = 15 s, and Control = 15 s) which was repeated 14 times. The total duration of the experiment was 10 min and 30 s. Participants practiced briefly before entering the scanner to be familiarized with the task.

Each of the 42 EDP trials was classified into groups of 14 according to the maximum distance from the observer in each of the comparisons: Close if it was 60 m, Mid if it was 100 m, and Far if it was 140 m away.

Egocentric distance perception performance variables

In this study, two behavioral variables were individually assessed: Accuracy (AC), defined as the percentage of correct

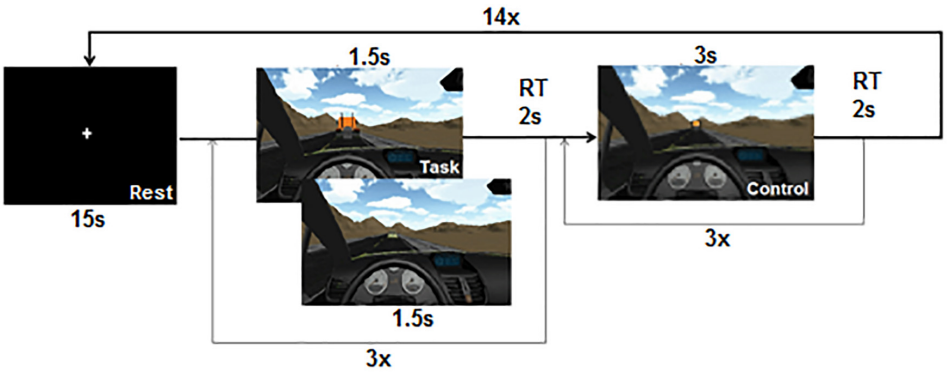

FIGURE 1
Egocentric distance perception functional magnetic resonance imaging (fMRI) paradigm. At each TASK trial participants were instructed to answer in which of the images the vehicle was the furthest (first or second). RT, response time window.

responses, and response time (RT), defined as the average time between the stimulus offset and each of the participants' correct responses in each trial. Normality and homogeneity tests were performed on both variables.

Behavioral statistical analysis

To compare values of AC and RT between groups, two mixed ANOVAs (factors Group, with levels YS and OS, and Distance with levels Near [up to 60 m], Mid [up to 100 m], and Far [up to 140 m]) were conducted to test the effect of AC and RT on groups at different distances.

To understand the relationship between the series of variables delivered by our driving simulator, we performed an exploratory factor analysis test which included the 27 telemetric variables in order to find the main factors that could better explain data variance. Specifically, we ran a parallel analysis, with orthogonal rotation (varimax) and a loading threshold of 0.6. Factors obtained by the EFA were then correlated to our EDP performance variables to explore a possible association between EDP and driving in our simulator. All behavioral statistical analyses were conducted using the JASP software (JASP Team, 2021, v0.15).

Functional magnetic resonance imaging data acquisition and analysis

BOLD fMRI studies were performed on a 3.0 Tesla MR scanner (Siemens TRIO, Germany) using a 16-channel head coil. A total of 210 whole-brain functional volumes using a T2*-weighted gradient echo-planar imaging (EPI) sequence (repetition time/echo time [TR/TE] = 3,000/30 ms, field of view [FOV] = 192 × 192 mm^2, flip angle = 30°, 48 slices, and resolution = 3 × 3 × 3 mm^3) were acquired during each session in an interleaved fashion. A total of three initial "dummy" volumes were discarded due to scanner stabilization.

The anatomical image was obtained using a whole-brain T1-weighted MPRAGE sequence [TR/TE = 1620/3 ms, inversion time (TI) = 950 ms, FOV = 250 × 187 × 160 mm^3, flip angle = 15°, 160 slices, and resolution = 1 × 1 × 1 mm^3]. No fat suppression was employed.

Mass univariate data analysis was done using SPM12 (r6225, Wellcome Department of Imaging Neuroscience, UCL, London). To detect and correct severe motion or artifacts, we completed preliminary visual checks using Check Reg. Conventional preprocessing pipeline steps were followed. First, slice time correction was applied, taking slice 25 as the reference slice. EPI images were then motion-corrected and realigned to the first volume of the series and co-registered to the anatomical image. Functional and anatomical images were then normalized to the coordinates of the Montreal Neurological Institute (MNI) template, version ICBM-152. A three-dimensional Gaussian smoothing kernel of 8 mm full width at half maximum (FWHM) was applied to the EPI images.

Statistical analysis was performed following the General Linear Model (GLM) and modeled with the canonical double-gamma hemodynamic response function (HRF). At the first-level analysis, two Conditions (Task and Control) were modeled for all participants in both Groups (YS and OS). In both Conditions, only the timeframe between the stimulus onset and the subsequent 2 s was modeled into the design matrix. The 24-parameter Volterra expansion motion regressors (Friston et al., 1996) were included in the design matrix to control for head movements generated during image acquisition. All participants' Task and Control contrasts were obtained and exported for further analysis.

Second-level analyses comparing Task > Control between groups were done using a two-factor ANOVA, where task-related differences in brain activity between Groups (YS > OS, OS > YS) and mutual coactivations (Global conjunction, positive and negative YS∩OS) were obtained using a primary threshold of $p < 0.001$ and corrected for multiple comparisons using the Family-wise error (FWE, $p < 0.05$) method at the cluster level Anatomical cerebral activations were defined at the peak activation maxima.

To evaluate the effect of performance on brain activations, we included AC and RT as second-level covariates.

Regions of interest definition and functional connectivity analysis

Regions of interest (ROI) were obtained by extracting the coordinates of peak activations in each significant cluster from the fMRI analysis and selecting its corresponding ROI from CONN's default atlas (Harvard-Oxford cortical and subcortical atlas and the AAL atlas for cerebellar areas).

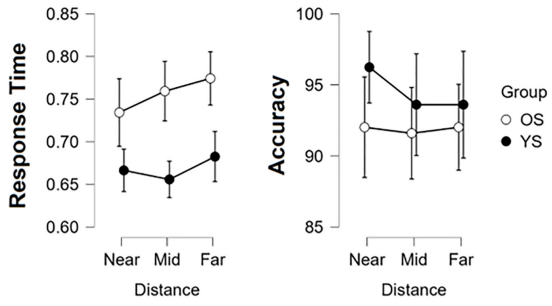

FIGURE 2
Egocentric distance perception performance results. Response Time **(left)** and Accuracy **(right)** were compared by groups (YS, young subjects and OS, older subjects) and within Distance; circles indicate the mean and whiskers the 95% confidence interval.

Non-smoothed images were used and analyzed using the CONN 16.b Functional Connectivity Toolbox (Whitfield-Gabrieli and Nieto-Castanon, 2012). Our pipeline analysis included the following steps: BOLD data smoothing (8 mm), despiking, and bandpass filtering (0.008-inf) in order to avoid "spillage" between blocks and conditions. White matter, cerebrospinal fluid, and movement parameters were treated as nuisance regressors. Also, main Condition effects were removed from the signal in order to avoid task-related coactivation effects. Then, we conducted a gPPI-based ROI-to-ROI analysis that allowed us to measure changes in functional connectivity that covaried with the experimental factors.

Results

Egocentric distance perception performance

Results from our mixed two-way ANOVA analysis for AC and RT are summarized in **Figure 2**. Despite consistent higher RT across conditions in the OS, no significant effects of Group [$F(1,34) = 1.254$, $p = 0.271$], Distance [$F(2,68) = 0.555$, $p = 0.576$], or interactions [$F(2,68) = 0.406$, $p = 0.668$] were found. In AC, non-significant effects of Group [$F(1,34) = 3.28$, $p = 0.079$] and Distance [$F(2,68) = 2.059$, $p = 0.135$], as well as their interactions [$F(2,68) = 0.799$, $p = 0.454$], were found.

Driving simulator results

Results of the driving simulator performance are detailed in **Table 1**. The exploratory factor analysis indicated that 22 variables (with no cross-loadings) surpassed the loading threshold, which was intentionally set high due to the relative number of variables. Bartlett's Test of Sphericity was significant ($\chi^2 = 1313.283$, $p < 0.001$), demonstrating the adequacy of our data. Five uncorrelated factors were identified, which explained 72.2% of the variability of our data. The relationship between variables within each factor allowed for appropriate labeling: driving Speed, which included variables related to the time it took the participant to finish the driving session, average speed while driving, and yellow light skips; Steering, which included sudden steering at any angle; Dexterity, which included variables related to traffic violations and speeding; Braking, associated with braking variables; and Hard Braking, which was related with hard brake pressing parameters. From these factors and their variables, we created composite scores to compare results between groups and explore an association with performance in the EDP task. These scores were based on the sum of the mean value of every variable in each factor, weighted by its loading value.

When compared by groups, only the factor Speed showed a significant difference between YS and OS. Within this factor, the YS showed a significantly lower total session time, higher % of time above the speed limit, and higher mean speed at 80 km/h, 100 km/h, and 120 km/h zones. These results were corrected for multiple comparisons using the Bonferroni method.

Relationship between egocentric distance perception performance and driving factors

Pearson correlations between EDP performance variables (RT and AC) and driving factors (Speed, Steering, Dexterity, Braking, and Hard Braking) showed a significant association between AC and Hard Braking ($r = -0.673$, $p < 0.001$), where higher AC correlated with lower Hard Braking scores (less time and % of time pressing with brake pedal beyond 75%).

Functional magnetic resonance imaging analysis results

Conjunction analysis for activations (Task > Control contrast) between groups (**Figure 3** and **Table 2**) showed bilateral precentral, supplementary motor area (SMA), and posterior parietal coactivations, along with activity in occipital, cerebellar, basal ganglia, thalamic, and brainstem areas. Deactivations (Control > Task contrast) were also found in default mode network (DMN) regions (posterior cingulate and medial frontal cortex).

Significant differential activations between groups were only found in the contrast OS > YS where the OS hyperactivated bilateral frontal (mainly the SMA and prefrontal cortex) and parietal regions (precuneus), as well as in the basal ganglia (putamen and pallidum).

When exploring the effect of performance (AC and RT), we found no significant correlation with brain activations.

Connectivity analysis results

ROI-to-ROI functional connectivity analysis revealed increased connectivity in the OS group within nodes in the occipital cortex (middle and superior occipital gyri, fusiform cortex) and between other parietal (precuneus), cerebellar (lobules VI and IX), and brainstem nodes as well as within frontal (SMA, precentral, and middle frontal gyri) nodes (**Figure 4**).

Discussion

Results from our driving simulator show a previously observed driving pattern in the elderly, characterized by

TABLE 1 Driving simulator factor and telemetry data.

	YS	OS	YS vs. OS		
	M ± SD	M ± SD	*W*-test	*P*-value	Effect size
Speed	3.051 ± 4.35	−3.41 ± 4.071	42	<0.001*	−0.74
Total session time	2023.763 ± 225.278	2426.559 ± 330.012	279	<0.001*	0.728
% Time above speed limit	4.619 ± 3.561	1.755 ± 1.187	57	<0.001*	−0.647
Mean speed at 40 km/h zone	31.607 ± 3.537	26.844 ± 6.16	76	0.007	−0.529
Mean speed at 50 km/h zone	16.65 ± 3.076	14.376 ± 1.888	84	0.015	−0.48
Mean speed at 80 km/h zone	50.503 ± 5.813	43.317 ± 5.842	60	0.001*	−0.628
Mean speed at 100 km/h zone	49.007 ± 9.479	38.714 ± 5.413	59	<0.001*	−0.635
Mean speed at 120 km/h zone	95.11 ± 12.156	76.155 ± 11.986	44	<0.001*	−0.728
Yellow traffic light skips	1.842 ± 1.344	3.235 ± 1.985	239.5	0.012	0.483
Steering	−0.629 ± 1.078	0.703 ± 4.545	193	0.326	0.195
60–90° steers in 0.5 s	58.368 ± 18.031	71 ± 42.27	194	0.31	0.201
90–180° steers in 0.5 s	38.474 ± 14.331	46.941 ± 37.046	171	0.775	0.059
180–270° steers in 0.5 s	2.842 ± 2.588	4.824 ± 8.338	180.5	0.55	0.118
270–360° steers in 0.5 s	0.105 ± 0.315	0.588 ± 1.326	185.5	0.251	0.149
Dexterity	0.033 ± 3.511	−0.037 ± 1.845	192	0.342	0.189
Time w/gas pedal > 75%	61.963 ± 65.315	48.382 ± 36.503	157.5	0.912	−0.025
% Time w/gas pedal > 75%	1.684 ± 1.94	0.989 ± 0.769	142	0.547	−0.121
Collisions w/other cars	0.526 ± 0.905	0.412 ± 0.712	155.5	0.83	−0.037
Two wheel sidewalk invasion	58 ± 25.153	71.588 ± 17.836	241	0.012	0.492
Collisions w/other objects	3.895 ± 3.799	5 ± 3.791	198.5	0.244	0.229
Braking	0.18 ± 1.354	−0.202 ± 2.109	124	0.241	−0.232
Time braking	261.132 ± 82.111	260.412 ± 154.588	139	0.486	−0.139
% Time braking	13.061 ± 4.473	10.733 ± 5.735	104.5	0.073	−0.353
Hard braking	−0.07 ± 1.4	0.078 ± 3.176	129	0.311	−0.201
% Time moving	87.648 ± 2.953	88.038 ± 5.655	200.5	0.222	0.241
Time w/brake pedal > 75%	3.632 ± 7.654	5.324 ± 16.622	171.5	0.736	0.062
% Time w/brake pedal > 75%	0.091 ± 0.189	0.113 ± 0.357	163	0.971	0.009
>5 s brakes	2.421 ± 1.953	1.824 ± 1.286	140	0.495	−0.133
>10 s brakes	6.684 ± 2.907	4.588 ± 3.001	96	0.038	−0.406
Red traffic light skips	1.895 ± 2.158	3.824 ± 6.55	207	0.139	0.282
Run overs	0.158 ± 0.501	0.235 ± 0.437	180.5	0.365	0.118
Restarts	5.158 ± 0.834	4.412 ± 0.618	82.5	0.008	−0.489

Mann–Whitney *U* test. Effect size by rank-biserial correlation. *Significant values after Bonferroni correction. YS, young subjects; OS, older subjects.

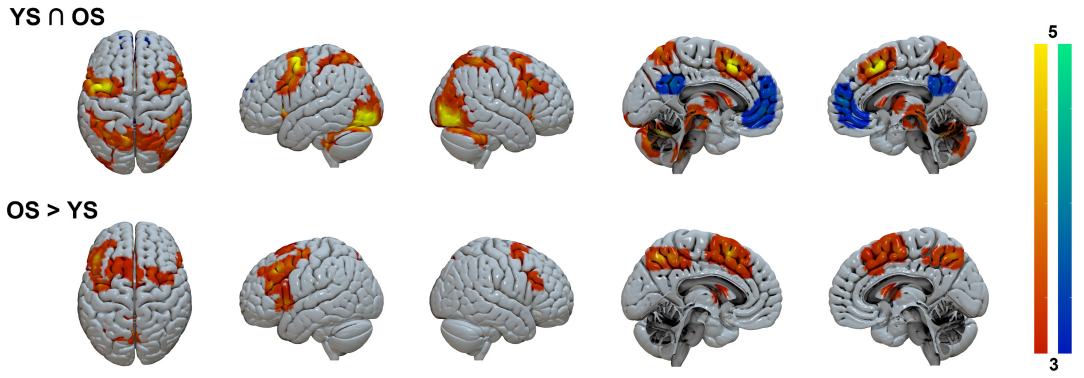

FIGURE 3
Task > Control shared and differential activation patterns between groups. Color-coded activation (hot) and deactivation (winter) parametrical maps. Clusters were FWE-corrected at $p < 0.05$. YS, young subjects; OS, older subjects.

TABLE 2 Shared and differential activation in Task > Control contrast.

Contrast	Cluster size	Region	MNI coordinates			*t*-Value
			x	*y*	*z*	
YS ∩ OS (pos)	9075	Right middle occipital gyrus	32	−70	28	8.23
		Right supramarginal gyrus	44	−36	44	7.82
		Right inferior occipital gyrus	38	−80	−6	7.66
		Right inferior parietal lobule	34	−44	42	7.1
		Right cerebellum (Lobule VI)	28	−60	−28	7.02
		Right superior parietal lobule	20	−62	52	6.61
		Right cerebellum (Crus 1)	44	−54	−32	5.67
		Left cerebellum (Crus 1)	−6	−72	−26	5.09
		Right inferior temporal gyrus	52	−50	−8	4.92
		Right fusiform gyrus	40	−48	−18	4.89
		Right cerebellum (Lobule VI)	6	−70	−24	4.62
	8554	Left inferior occipital gyrus	−36	−84	−10	8.7
		Left inferior parietal lobule	−34	−46	46	8.44
		Left superior occipital gyrus	−26	−68	32	7.13
		Left middle occipital gyrus	−40	−66	2	6.88
		Left precuneus	−14	−62	54	6.74
		Left fusiform gyrus	−38	−58	−14	6.37
		Left cerebellum (Lobule VI)	−34	−50	−30	5.4
		Left cerebellum (Lobule IX)	−12	−46	−48	4.69
		Left superior parietal lobule	−32	−58	64	4.28
	3325	Left SMA	0	18	48	7.22
		Left inferior frontal gyrus (p. Opercularis)	−44	4	26	6.85
		Left precentral gyrus	−42	2	54	5.94
		Left middle frontal gyrus	−36	2	64	5.62
		Left middle cingulate cortex	−12	22	34	4.7
		Left SMA	−8	8	58	4.53
		Left inferior frontal gyrus (p. Triangularis)	−58	20	28	3.91
		Right middle cingulate cortex	10	26	34	3.89
		Left frontal superior gyrus	−22	2	74	3.41
	2575	Left insula	−32	20	2	8.39
		Right insula	32	22	2	7.65
		Left putamen	−20	6	6	5.18
		Left thalamus	−12	−10	4	4.9
		Left thalamus	−18	−8	0	4.85
		Right thalamus	10	−6	4	4.24
		Right pallidum	14	8	−2	4.11
	954	Right inferior frontal gyrus (p. Opercularis)	46	8	26	6.98
	573	Right precentral gyrus	34	2	52	5.2
	429	Brainstem	8	−26	−8	4.86
		Brainstem	−4	−24	−12	4.61
YS ∩ OS (neg)	1099	Left anterior cingulate cortex	−8	50	0	5.19
		Right superior frontal medial gyrus	6	58	10	4.75
		Left superior frontal medial gyrus	−8	58	18	4.69
	371	Right posterior cingulate cortex	8	−48	28	4.58
		Left posterior cingulate cortex	−8	−48	30	4.57
OS > YS	5509	Left precentral gyrus	−38	6	38	6.75
		Left middle frontal gyrus	−42	22	40	5.71

(Continued)

TABLE 2 (Continued)

Contrast	Cluster size	Region	MNI coordinates			*t*-Value
			x	*y*	*z*	
		Left SMA	−6	16	54	5.39
		Left inferior frontal gyrus (p. Triangularis)	−52	16	0	4.87
		Right superior frontal gyrus	14	12	52	4.74
		Left superior frontal medial gyrus	−8	26	40	4.72
		Left superior frontal gyrus	−18	10	48	4.63
		Left precentral gyrus	36	0	52	4.47
		Right precentral gyrus	32	−2	48	4.39
		Right middle cingulate cortex	8	20	38	4.27
		Right SMA	6	−4	54	4.18
	967	Left precuneus	−2	−64	50	5.09
		Right precuneus	10	−68	52	4.14
		Left inferior parietal lobule	−28	−54	40	3.92
		Left superior parietal lobule	−22	−66	44	3.84
	399	Right inferior frontal gyrus (p. Opercularis)	42	18	30	4.76
	383	Right pallidum	14	0	6	4.99
	322	Left putamen	−22	10	8	4.28
		Left pallidum	−12	0	4	4.28

Clusters are corrected for multiple comparisons using FWE. YS, young subjects; OS, older subjects.

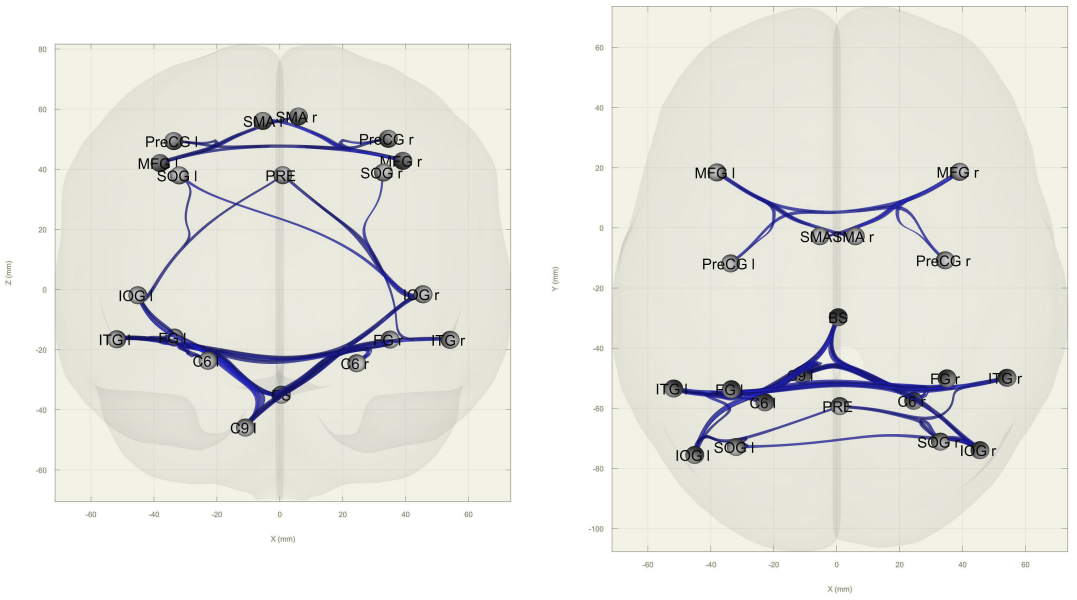

FIGURE 4
Between-group differences in ROI-to-ROI functional connectivity. Blue edges indicate higher connectivity in older subjects when compared to younger subjects between nodes (in gray). Edges are FDR-corrected at $p < 0.05$ at the cluster level (connection threshold: $p < 0.05$). **Left:** coronal view; **right:** axial view.

generalized slower driving. Vehicle telemetry data allowed us to identify five different driving factors or behaviors. The relative perception of distances remains largely intact with advancing age, with similar performance in both groups of age. To associate our simulator and behavioral data, we found that task accuracy was negatively correlated to the Hard Braking behavior (better AC, less hard brake pedal pressing). Functionally, EDP was related in both groups to activation of frontoparietal, cerebellar, and subcortical structures and deactivation of the DMN. Meanwhile, the OS hyperactivated prefrontal, precentral,

and posterior parietal regions, along with the basal ganglia. Our connectivity analysis presented increased connectivity within the frontal and a parieto-occipital-cerebellar network exclusively in the elderly.

Egocentric distance perception is preserved in older adults

When comparing the average values of precision in the EDP, we found no differences between age groups; these results held even across the three different egocentric distances. These findings are in accordance with previous research on EDP and aging, which indicate that this function is preserved in accordance with some studies where this effect remains even when accounting for attentional differences between age groups (Bian and Andersen, 2013) or could even improve by having more experience as people grow older (Gajewski et al., 2015; Wallin et al., 2017).

It is important to note that when participants estimate distances, they might also do it from the allocentric frame of reference where the observer's position is irrelevant to distance estimation (e.g., "the truck is behind the car"). Allocentric distance perception has not been as thoroughly studied as its egocentric counterpart, especially in older adults; however, it has been found that allocentric navigation and wayfinding might be impaired in healthy aging, particularly in 3D scenes (Colombo et al., 2017; Ladyka-Wojcik and Barense, 2021).

Driving behavior and egocentric distance perception

The main significant result from telemetric data was that older adults drove at a lower speed when compared to younger adults, a usual finding when evaluating driving behaviors in aging (Shinar et al., 2005; Cantin et al., 2009; Thompson et al., 2012; Keay et al., 2013; Eudave et al., 2018; Wechsler et al., 2018). In an attempt to associate EDP and driving performance, we found that higher accuracy in the EDP task is associated with a reduction in the Hard Braking behavior in our simulator. Although this relationship has not been reported before, it is possible that preserved EDP functioning is necessary to correctly estimate how distant other moving objects, such as cars, are from the viewer, which would then help elicit the correct response to a sudden decrease in that distance, such as fully pressing the brake pedal.

Egocentric distance perception functional correlates

Common activation between young and older adults when performing the egocentric distance perception task revealed the use of both the ventral (middle and inferior occipital gyri, and fusiform gyrus) and dorsal (inferior parietal lobe and posterior parietal cortex) visual pathways. The activation of these areas may correspond to merely visual aspects, such as the distance that separates two objects (Berryhill, 2009), if the object is closer or further away (Amit et al., 2012) or if the stimulus to be compared is an object or a scene (Persichetti and Dilks, 2016). Activations of bilateral frontal cortical regions are also found to be active during short-term memory encoding and retrieval of 3D objects (Baumann et al., 2010), useful when reproducing perceived distances (Wiener et al., 2016). DMN involvement was observed in this EDP task by deactivating the precuneus and medial frontal cortex, regions that can participate in the projection of oneself in time and space, thus helping in distance estimation (Buckner and Carroll, 2007; Peer et al., 2015). A definitive role of the cerebellum in EDP is unknown, although it has been related to other aspects of visuospatial cognition. The cerebellum takes part in the representation of the body in space by participating in hippocampal spatial navigation. Using the L7-PKCI transgenic model mice, whose protein kinase C activity is specifically inhibited in the Purkinje cells, a deficit in the use of self-motion cues and inability to detect the relevant features of the environment were found without motor coordination deficits (Rochefort et al., 2013; Lefort et al., 2015). Lastly, our EDP task also involved the basal ganglia. Classical studies have found that the basal ganglia (specifically, caudate nucleus) are involved in the egocentric frame of reference (Cook and Kesner, 1988). The role of the putamen in the computation of egocentric coordinates was initially demonstrated in neurophysiological studies (Cavada and Goldman-Rakic, 1991; Graziano and Gross, 1993) and may modulate the degree to which participants overestimate or underestimate distances (Wiener et al., 2016). The reciprocal relationship of the caudate nucleus and putamen with the cerebral cortex mediates egocentric memory, the relationship between the individual and its environment (White, 1997).

Frontoparietal activation as attempted compensation in older adults

The hyperactivation pattern in older adults showed greater recruitment of parietal and frontal areas, as well as the basal ganglia. This effect corresponds to findings found in other cognitive paradigms where older adults use more frontoparietal resources (Grady et al., 2016), including visuospatial paradigms (Madden et al., 2017). This increase in cortical activity tends to be proportional with age (Kennedy et al., 2015), and despite it being predominantly prefrontal and right-sided, this pattern can also be more diffuse and multimodal, employing different associative areas. Typically, these changes in brain activity have been correlated to task performance, accomplishing a "successful" compensation (Cabeza and Dennis, 2013). However, in our study, this hyperactivation in older adults did

not correlate with parameters of task performance, a finding that could be attributed to "attempted" compensation, where activity is instead related to structural brain decline and task demands. In this study, the EDP task could have been more demanding in older adults given limited neural resources or cognitive processing capacity (Scheller et al., 2014).

Areas belonging to this hyperactivation pattern in the OS correspond to findings in functional connectivity, where we detected an increase between frontal nodes and between parietal, visual, and cerebellar nodes when compared to younger adults. To the best of our knowledge, there are no studies examining the functional connectivity of the EDP in both young and older adults. In monkeys, it has been shown that the posterior parietal cortex projects to the cerebellar hemispheres *via* the pontine nucleus, which could contribute substantially to multisensory integration (Glickstein, 2003). It is possible that this increase in connectivity in the OA is part of a compensatory network, necessary to sustain cognitive skills. In a visual working memory experiment, Burianová et al. (2015) found that while young adults are able to modulate baseline connectivity as cognitive load increases, older adults are not, and instead display a predominantly frontal compensatory network which also includes the inferior parietal lobe. This could be attributed to an increase in connectivity within (frontoparietal) networks that comes with aging, a parameter that has been found to predict task skills (Grady et al., 2016). Additionally, this increase in connectivity might also be a consequence of the depletion of the participants' cognitive reserve, which also increases with task difficulty (Bastin et al., 2012). This supports our "functional compensation" findings, since the EDP task was relatively easy allowing these extra resources to intervene and possibly sustain young-like performance.

Limitations and future direction

As with other driving simulator studies, our simulator might have introduced bias, since it does not exactly portray the act and experience of real driving. Also, our driving task might have proven difficult for some drivers since it required navigation in a complex environment while also following instructions, with a relatively short training session. Additionally, despite these throwbacks, we believe that this naturalistic approach to driving allowed for reliable telemetry data collection. Also, some of our participants (mostly older adults) experienced mild symptoms of simulator sickness (eye strain and dizziness).

An important caveat is that our task intended to evaluate EDP from a set of static images; however, distance perception is usually carried out in a dynamic fashion, especially in the context of movement, such as car driving, where the subjects' point of view is constantly changing and updating. Also, future studies should include the evaluation of the allocentric frame of reference which, as stated previously, might be impaired in older adults and be involved in distance perception.

Another limitation and future work of this study is the validation of the factor analysis and its relationship with EDP performance in an independent sample that could not be performed due to the limited sample size in this study. Also, the few female participants did not allow for an analysis of the differences between the sexes.

Conclusion

In conclusion, performance in egocentric distance perception was similar between young and older adults. Both groups showed consistent accuracies and response times independent of how far the vehicle was from the viewer. Driving in a simulator confirmed previous findings of generally slower driving in older adults. Additionally, five driving behaviors were identified by means of an EFA; from these, Hard Breaking behaviors when driving were associated with how accurate participants were in the EDP task. Neuroimaging results identified the hyperactivation of frontoparietal and basal ganglia in older adults, along with increased connectivity within frontal nodes and between a posterior network comprised of posterior parietal, occipital, and cerebellar nodes.

Data availability statement

The raw data supporting the conclusions of this article will be made available by the authors, without undue reservation.

Ethics statement

The studies involving human participants were reviewed and approved by the University of Navarra Research Ethics Committee. The patients/participants provided their written informed consent to participate in this study.

Author contributions

LE and MP contributed to the conception and design of the study. LE, MM, EL, and MP collected participant data. LE organized data and performed all analyses. LE and MP interpreted the results and wrote the first draft of the manuscript. All authors contributed to the manuscript revision, read, and approved the submitted version.

Funding

This work was funded by the Fundación Caja Navarra grant (Ref: FBCN 15/70757) for biomedical research. LE was financially supported by a grant from the University of Navarra Friends Association.

Conflict of interest

The authors declare that the research was conducted in the absence of any commercial or financial relationships that could be construed as a potential conflict of interest.

Publisher's note

All claims expressed in this article are solely those of the authors and do not necessarily represent those of their affiliated organizations, or those of the publisher, the editors and the reviewers. Any product that may be evaluated in this article, or claim that may be made by its manufacturer, is not guaranteed or endorsed by the publisher.

Supplementary material

The Supplementary Material for this article can be found online at: https://www.frontiersin.org/articles/10.3389/fnagi.2022.936661/full#supplementary-material

References

Adamo, D. E., Briceño, E. M., Sindone, J. A., Alexander, N. B., and Moffat, S. D. (2012). Age differences in virtual environment and real world path integration. *Front. Aging Neurosci.* 4:26. doi: 10.3389/fnagi.2012.00026

Amit, E., Mehoudar, E., Trope, Y., and Yovel, G. (2012). Do object-category selective regions in the ventral visual stream represent perceived distance information? *Brain Cogn.* 80, 201–213. doi: 10.1016/j.bandc.2012.06.006

Anderson, S. W., Rizzo, M., Shi, Q., Uc, E. Y., and Dawson, J. D. (2005). "Cognitive abilities related to driving performance in a simulator and crashing on the road," in *Driving Assessment 2005 : Proceedings of the 3rd International Driving Symposium on Human Factors in Driver Assessment, Training, and Vehicle Design*, (Rockport, AZ: University of Iowa).

Apolinario, D., Magaldi, R. M., Busse, A. L., Lopes, L., da, C., Kasai, J. Y. T., et al. (2009). Cognitive impairment and driving: a review of the literature. *Dement. Neuropsychol.* 3, 283–290. doi: 10.1590/S1980-57642009DN30400004

Bastin, C., Yakushev, I., Bahri, M. A., Fellgiebel, A., Eustache, F., Landeau, B., et al. (2012). Cognitive reserve impacts on inter-individual variability in resting-state cerebral metabolism in normal aging. *NeuroImage* 63, 713–722. doi: 10.1016/j.neuroimage.2012.06.074

Baumann, O., Chan, E., and Mattingley, J. B. (2010). Dissociable neural circuits for encoding and retrieval of object locations during active navigation in humans. *NeuroImage* 49, 2816–2825. doi: 10.1016/j.neuroimage.2009.10.021

Berryhill, M. (2009). The representation of object distance: evidence from neuroimaging and neuropsychology. *Front. Hum. Neurosci.* 3:2009. doi: 10.3389/neuro.09.043.2009

Bian, Z., and Andersen, G. J. (2013). Aging and the perception of egocentric distance. *Psychol. Aging* 28, 813–825. doi: 10.1037/a0030991

Buckner, R. L., and Carroll, D. C. (2007). Self-projection and the brain. *Trends Cogn. Sci.* 11, 49–57. doi: 10.1016/j.tics.2006.11.004

Burianová, H., Marstaller, L., Choupan, J., Sepehrband, F., Ziaei, M., and Reutens, D. (2015). The relation of structural integrity and task-related functional connectivity in the aging brain. *Neurobiol. Aging* 36, 2830–2837. doi: 10.1016/j.neurobiolaging.2015.07.006

Cabeza, R., and Dennis, N. A. (2013). "Frontal lobes and aging: deterioration and compensation," in *Principles of Frontal Lobe Function*, eds D. T. Stuss and R. T. Knight (Oxford: Oxford University Press), doi: 10.1093/med/9780199837755.003.0044

Cantin, V., Lavallière, M., Simoneau, M., and Teasdale, N. (2009). Mental workload when driving in a simulator: effects of age and driving complexity. *Accid. Anal. Prev.* 41, 763–771. doi: 10.1016/j.aap.2009.03.019

Cavada, C., and Goldman-Rakic, P. S. (1991). Topographic segregation of corticostriatal projections from posterior parietal subdivisions in the macaque monkey. *Neuroscience* 42, 683–696. doi: 10.1016/0306-4522(91)90037-O

Cavallo, V., Caro, S., Dore, J., Colomb, M., and Dumont, E. (2007). "Risky driving in fog : psychological explanations," in *Proceedings of the 14th International Conference on Road Safety on Four Continents*, (Bangkok).

Cavallo, V., Colomb, M., and Doré, J. (2001). Distance perception of vehicle rear lights in fog. *Hum. Factors J. Hum. Factors Ergon. Soc.* 43, 442–451. doi: 10.1518/001872001775898197

Clément, G., Loureiro, N., Sousa, D., and Zandvliet, A. (2016). Perception of egocentric distance during gravitational changes in parabolic flight. *PLoS One* 11:e0159422. doi: 10.1371/journal.pone.0159422

Colombo, D., Serino, S., Tuena, C., Pedroli, E., Dakanalis, A., Cipresso, P., et al. (2017). Egocentric and allocentric spatial reference frames in aging: a systematic review. *Neurosci. Biobehav. Rev.* 80, 605–621. doi: 10.1016/j.neubiorev.2017.07.012

Cook, D., and Kesner, R. P. (1988). Caudate nucleus and memory for egocentric localization. *Behav. Neural Biol.* 49, 332–343. doi: 10.1016/S0163-1047(88)90338-X

Creem-Regehr, S. H., Willemsent, P., Goochl, A. A., and Thompson, W. B. (2005). The influence of restricted viewing conditions on egocentric distance perception: implications for real and virtual indoor environments. *Perception* 34, 191–204. doi: 10.1068/p5144

Eudave, L., Martínez, M., Luis, E. O., and Pastor, M. A. (2018). Default-mode network dynamics are restricted during high speed discrimination in healthy aging: associations with neurocognitive status and simulated driving behavior. *Hum. Brain Mapp.* 39, 4196–4212. doi: 10.1002/hbm.24240

Foley, J. M. (1977). Effect of distance information and range on two indices of visually perceived distance. *Perception* 6, 449–460. doi: 10.1068/p060449

Friston, K. J., Williams, S., Howard, R., Frackowiak, R. S., and Turner, R. (1996). Movement-related effects in fMRI time-series. *Magn. Reson. Med.* 35, 346–355.

Gajewski, D. A., Wallin, C. P., and Philbeck, J. W. (2015). The effects of age and set size on the fast extraction of egocentric distance. *Vis. Cogn.* 23, 957–988. doi: 10.1080/13506285.2015.1132803

Glickstein, M. (2003). Subcortical projections of the parietal lobes. *Adv. Neurol.* 93, 43–55.

Grady, C., Sarraf, S., Saverino, C., and Campbell, K. (2016). Age differences in the functional interactions among the default, frontoparietal control, and dorsal attention networks. *Neurobiol. Aging* 41, 159–172. doi: 10.1016/j.neurobiolaging.2016.02.020

Graziano, M. S. A., and Gross, C. G. (1993). A bimodal map of space: somatosensory receptive fields in the macaque putamen with corresponding visual receptive fields. *Exp. Brain Res.* 97, 96–109. doi: 10.1007/BF00228820

Hettinger, L. J., and Haas, M. (n.d.). *Virtual and Adaptive Environments: Applications, Implications, and Human Performance Issues*.

Hoffman, L., McDowd, J. M., Atchley, P., and Dubinsky, R. (2005). The role of visual attention in predicting driving impairment in older adults. *Psychol. Aging* 20, 610–622. doi: 10.1037/0882-7974.20.4.610

JASP Team (2021). JASP (Version 0.15) [Computer software]. Available online at: https://jasp-stats.org/JASP

Keay, L., Munoz, B., Duncan, D. D., Hahn, D., Baldwin, K., Turano, K. A., et al. (2013). Older drivers and rapid deceleration events: salisbury eye evaluation driving study. *Accid. Anal. Prev.* 58, 279–285. doi: 10.1016/j.aap.2012.06.002

Kennedy, K. M., Rodrigue, K. M., Bischof, G. N., Hebrank, A. C., Reuter-Lorenz, P. A., and Park, D. C. (2015). Age trajectories of functional activation under conditions of low and high processing demands: an adult lifespan fMRI study of the aging brain. *NeuroImage* 104, 21–34. doi: 10.1016/j.neuroimage.2014.09.056

Kimura, K., Reichert, J. F., Olson, A., Pouya, O. R., Wang, X., Moussavi, Z., et al. (2017). Orientation in virtual reality does not fully measure up to the real-world. *Sci. Rep.* 7:18109. doi: 10.1038/s41598-017-18289-8

Kunz, B. R., Wouters, L., Smith, D., Thompson, W. B., and Creem-Regehr, S. H. (2009). Revisiting the effect of quality of graphics on distance judgments in virtual environments: a comparison of verbal reports and blind walking. *Atten. Percept. Psychophys.* 71, 1284–1293. doi: 10.3758/APP.71.6.1284

Ladyka-Wojcik, N., and Barense, M. D. (2021). Reframing spatial frames of reference: what can aging tell us about egocentric and allocentric navigation? *WIREs Cogn. Sci.* 12:e1549. doi: 10.1002/wcs.1549

Lefort, J. M., Rochefort, C., and Rondi-Reig, L. (2015). Cerebellar contribution to spatial navigation: new insights into potential mechanisms. *Cerebellum* 14, 59–62. doi: 10.1007/s12311-015-0653-0

León-Domínguez, U., Solís-Marcos, I., Barrio-Álvarez, E., Barroso y Martín, J. M., and León-Carrión, J. (2017). Safe driving and executive functions in healthy middle-aged drivers. *Appl. Neuropsychol.* 24, 395–403. doi: 10.1080/23279095.2015.1137296

Li, Z., Phillips, J., and Durgin, F. H. (2011). The underestimation of egocentric distance: evidence from frontal matching tasks. *Atten. Percept. Psychophys.* 73, 2205–2217. doi: 10.3758/s13414-011-0170-2

Madden, D. J., Parks, E. L., Tallman, C. W., Boylan, M. A., Hoagey, D. A., Cocjin, S. B., et al. (2017). Frontoparietal activation during visual conjunction search: effects of bottom-up guidance and adult age. *Hum. Brain Mapp.* 38, 2128–2149. doi: 10.1002/hbm.23509

Mäntylä, T., Karlsson, M. J., and Marklund, M. (2009). Executive control functions in simulated driving. *Appl. Neuropsychol.* 16, 11–18. doi: 10.1080/09084280802644086

Mathias, J. L., and Lucas, L. K. (2009). Cognitive predictors of unsafe driving in older drivers: a meta-analysis. *Int. Psychogeriatr.* 21, 637–653. doi: 10.1017/S1041610209009119

Maus, B., and van Breukelen, G. J. P. (2014). POBE : a computer program for optimal design of multi-subject blocked fMRI experiments. *J. Stat. Softw.* 56, 1–24. doi: 10.18637/jss.v056.i09

Milner, A. D., and Goodale, M. A. (2008). Two visual systems re-viewed. *Neuropsychologia* 46, 774–785. doi: 10.1016/j.neuropsychologia.2007.10.005

Norman, J. F., Dowell, C. J., Higginbotham, A. J., Fedorka, N. W., and Norman, H. F. (2018). Sex and age modulate the visual perception of distance. *Atten. Percept. Psychophys.* 80, 2022–2032. doi: 10.3758/s13414-018-1542-7

Oldfield, R. C. (1971). The assessment and analysis of handedness: the Edinburgh inventory. *Neuropsychologia* 9, 97–113. doi: 10.1016/0028-3932(71)90067-4

Ooi, T. L., and He, Z. J. (2007). A distance judgment function based on space perception mechanisms: revisiting Gilinsky's (1951) equation. *Psychol. Rev.* 114, 441–454. doi: 10.1037/0033-295X.114.2.441

Parkinson, C., Liu, S., and Wheatley, T. (2014). A common cortical metric for spatial, temporal, and social distance. *J. Neurosci.* 34, 1979–1987. doi: 10.1523/JNEUROSCI.2159-13.2014

Peer, M., Salomon, R., Goldberg, I., Blanke, O., and Arzy, S. (2015). Brain system for mental orientation in space, time, and person. *Proc. Natl. Acad. Sci. U S A.* 112, 11072–11077. doi: 10.1073/pnas.1504242112

Persichetti, A. S., and Dilks, D. D. (2016). Perceived egocentric distance sensitivity and invariance across scene-selective cortex. *Cortex* 77, 155–163. doi: 10.1016/j.cortex.2016.02.006

Reger, M. A., Welsh, R. K., Watson, G. S., Cholerton, B., Baker, L. D., and Craft, S. (2004). The relationship between neuropsychological functioning and driving ability in dementia: a meta-analysis. *Neuropsychology* 18, 85–93. doi: 10.1037/0894-4105.18.1.85

Rochefort, C., Lefort, J., and Rondi-Reig, L. (2013). The cerebellum: a new key structure in the navigation system. *Front. Neural Circuits* 7:35. doi: 10.3389/fncir.2013.00035

Ruggiero, G., D'Errico, O., and Iachini, T. (2016). Development of egocentric and allocentric spatial representations from childhood to elderly age. *Psychol. Res.* 80, 259–272. doi: 10.1007/s00426-015-0658-9

Scheller, E., Minkova, L., Leitner, M., and Klöppel, S. (2014). Attempted and successful compensation in preclinical and early manifest neurodegeneration-a review of task fMRI studies. *Front. Psychiatry* 5:132. doi: 10.3389/fpsyt.2014.00132

Shinar, D., Tractinsky, N., and Compton, R. (2005). Effects of practice, age, and task demands, on interference from a phone task while driving. *Accid. Anal. Prev.* 37, 315–326. doi: 10.1016/j.aap.2004.09.007

Thompson, K. R., Johnson, A. M., Emerson, J. L., Dawson, J. D., Boer, E. R., and Rizzo, M. (2012). Distracted driving in elderly and middle-aged drivers. *Accid. Anal. Prev.* 45, 711–717. doi: 10.1016/j.aap.2011.09.040

Venkatesan, U. M., Festa, E. K., Ott, B. R., and Heindel, W. C. (2018). Differential contributions of selective attention and sensory integration to driving performance in healthy aging and alzheimer's disease. *J. Int. Neuropsychol. Soc.* 24, 486–497. doi: 10.1017/S1355617717001291

Wallin, C. P., Gajewski, D. A., Teplitz, R. W., Jaidzeka, S. M., and Philbeck, J. W. (2017). The roles for prior visual experience and age on the extraction of egocentric distance. *J. Gerontol. - Ser. B Psychol. Sci. Soc. Sci.* 72, 91–99. doi: 10.1093/geronb/gbw089

Wechsler, K., Drescher, U., Janouch, C., Haeger, M., Voelcker-Rehage, C., and Bock, O. (2018). Multitasking during simulated car driving: a comparison of young and older persons. *Front. Psychol.* 9:910. doi: 10.3389/fpsyg.2018.00910

Whelihan, W. M., DiCarlo, M. A., and Paul, R. H. (2005). The relationship of neuropsychological functioning to driving competence in older persons with early cognitive decline. *Arch. Clin. Neuropsychol.* 20, 217–228. doi: 10.1016/j.acn.2004.07.002

White, N. M. (1997). Mnemonic functions of the basal ganglia. *Curr. Opin. Neurobiol.* 7, 164–169. doi: 10.1016/S0959-4388(97)80004-9

Whitfield-Gabrieli, S., and Nieto-Castanon, A. (2012). Conn : a functional connectivity toolbox for correlated and anticorrelated brain networks. *Brain Connect.* 2, 125–141. doi: 10.1089/brain.2012.0073

Wiener, M., Michaelis, K., and Thompson, J. C. (2016). Functional correlates of likelihood and prior representations in a virtual distance task: prior and likelihood in virtual distance. *Hum. Brain Mapp.* 37, 3172–3187. doi: 10.1002/hbm.23232

Zhou, L., Ooi, T. L., and He, Z. J. (2016). Intrinsic spatial knowledge about terrestrial ecology favors the tall for judging distance. *Sci. Adv.* 2:e1501070. doi: 10.1126/sciadv.1501070

frontiers | Frontiers in Aging Neuroscience

TYPE Original Research
PUBLISHED 25 October 2022
DOI 10.3389/fnagi.2022.977917

OPEN ACCESS

EDITED BY
Cosimo Urgesi,
University of Udine, Italy

REVIEWED BY
Feng Liu,
Tianjin Medical University General Hospital, China
Sy Duong-Quy,
Lam Dong Medical College, Vietnam
Khue Bui,
University of Medicine and Pharmacy at Ho Chi Minh City, Vietnam

*CORRESPONDENCE
Dechang Peng
pengdcdoctor@163.com

SPECIALTY SECTION
This article was submitted to Neurocognitive Aging and Behavior, a section of the journal Frontiers in Aging Neuroscience

RECEIVED 25 June 2022
ACCEPTED 26 September 2022
PUBLISHED 25 October 2022

CITATION
Li H, Li L, Li K, Li P, Xie W, Zeng Y, Kong L, Long T, Huang L, Liu X, Shu Y, Zeng L and Peng D (2022) Abnormal dynamic functional network connectivity in male obstructive sleep apnea with mild cognitive impairment: A data-driven functional magnetic resonance imaging study. *Front. Aging Neurosci.* 14:977917. doi: 10.3389/fnagi.2022.977917

Abnormal dynamic functional network connectivity in male obstructive sleep apnea with mild cognitive impairment: A data-driven functional magnetic resonance imaging study

Haijun Li[1,2], Lan Li[3], Kunyao Li[1], Panmei Li[1], Wei Xie[1], Yaping Zeng[1], Linghong Kong[1], Ting Long[1], Ling Huang[1], Xiang Liu[1], Yongqiang Shu[1], Li Zeng[1] and Dechang Peng[1,2]*

[1]Medical Imaging Center, The First Affiliated Hospital of Nanchang University, Nanchang, China, [2]PET Center, The First Affiliated Hospital of Nanchang University, Nanchang, China, [3]Department of Infection Management, Jiangxi Provincial Maternal and Child Health Hospital, Nanchang, China

Objective: The purpose of this study was to investigate the dynamic functional network connectivity (FNC) and its relationship with cognitive function in obstructive sleep apnea (OSA) patients from normal cognition (OSA-NC) to mild cognitive impairment (OSA-MCI).

Materials and methods: Eighty-two male OSA patients and 48 male healthy controls (HC) were included in this study. OSA patients were classified to OSA-MCI (n = 41) and OSA-NC (n = 41) based on cognitive assessments. The independent component analysis was used to determine resting-state functional networks. Then, a sliding-window approach was used to construct the dynamic FNC, and differences in temporal properties of dynamic FNC and functional connectivity strength were compared between OSA patients and the HC. Furthermore, the relationship between temporal properties and clinical assessments were analyzed in OSA patients.

Results: Two different connectivity states were identified, namely, State I with stronger connectivity and lower frequency, and State II with lower connectivity and relatively higher frequency. Compared to HC, OSA patients had a longer mean dwell time and higher fractional window in stronger connectivity State I, and opposite result were found in State II, which was mainly reflected in OSA-MCI patients. The number of transitions was an increasing trend and positively correlated with cognitive assessment in OSA-MCI patients. Compared with HC, OSA patients showed extensive abnormal functional connectivity in stronger connected State I and less reduced functional connectivity in lower connected State II, which were mainly located in the salience network, default mode network, and executive control network.

Conclusion: Our study found that OSA patients showed abnormal dynamic FNC properties, which was a continuous trend from HC, and OSA-NC to OSA-MCI, and OSA patients showed abnormal dynamic functional connectivity strength. The number of transformations was associated with cognitive impairment in OSA-MCI patients, which may provide new insights into the neural mechanisms in OSA patients.

KEYWORDS

obstructive sleep apnea, dynamic functional connectivity, mild cognitive impairment, independent component analysis, brain network

Introduction

Obstructive sleep apnea (OSA) is the most common sleep-respiratory disorder, but it is often overlooked by people (Franklin and Lindberg, 2015). The incidence of OSA in adult populations was reported to be approximately 6–38%, and was higher in the elderly and obese populations (Senaratna et al., 2017). A growing number of studies have shown that OSA is a clinical syndrome, leading to multisystem diseases, such as hypertension, osteoporosis, diabetes, depression, and anxiety, among which cognitive impairment has gradually become a concern for scholars (Vanek et al., 2020). Cognitive disorders associated with OSA mainly include disorders in memory, execution, vigilance, and so on (Olaithe et al., 2018). OSA is considered one of the potential independent risk factors for Alzheimer's disease (Liguori et al., 2021). Therefore, the potential neural mechanisms of cognitive impairment in OSA patients should have important roles in the treatment and prevention of diseases.

Many neuroimaging studies have used magnetic resonance imaging (MRI) techniques to explore the neural basis of OSA, partly providing a theoretical basis for understanding the underlying neural mechanisms (Huang et al., 2019; Lee et al., 2019; Yan et al., 2021). In recent years, our research group has conducted a series of neuroimaging studies of OSA patients. Compared with healthy controls (HC), we found default mode network (DMN) dysfunction and frontal adaptive compensatory response in OSA patients (Li et al., 2015), and further study found that frequency-specific local spontaneous neural activity can be reversed in the temporal lobe, parietal lobe, and brainstem areas after short-term continuous positive airway pressure (CPAP) treatment (Li et al., 2021), which provided additional information on the underlying neural mechanisms of OSA-related cognitive impairment and potential neuroimaging markers for clinical treatment. In resting-state functional connectivity (FC) studies, we found abnormal FC between insular subregions and multiple other related brain regions involved in cognitive, emotional, and sensorimotor networks (Kong et al., 2022). In addition, abnormal FC between hippocampal subregions and sensorimotor network, frontoparietal network and default mode network-related brain regions were found in OSA patients (Liu et al., 2022). The local integration and integrity of brain connectivity may be disrupted from small-world networks, which can be used as quantitative physiological indicators to assist with clinical diagnosis (Chen et al., 2017). We found significantly reduced regional degree centrality values in the left middle occipital gyrus, posterior cingulate, left superior frontal gyrus and bilateral inferior parietal lobe, and increased degree centrality values in the right orbitofrontal cortex, bilateral posterior cerebellum, bilateral lenticular nucleus, hippocampus, and inferior temporal gyrus, contributing to our understanding of the neurological features of OSA at the whole-brain network level (Li H. et al., 2016). Meanwhile, after short-term CPAP treatment, OSA patients have increased degree centrality values in some brain areas such as frontal lobe, temporal lobe, and insular lobe (Li et al., 2022). CPAP treatment can effectively reverses the functional network damage caused by OSA and provides potential neuroimaging markers for CPAP treatment evaluation. Other researcher have found that OSA patients have complex and abnormal resting-state FC in different brain areas, including the cerebellum, frontal lobe, parietal lobe, temporal lobe, occipital lobe, limbic system, and basal ganglia. These abnormal FC may result in inadequate self-discipline, executive, cognitive, emotional, and sensorimotor responses (Park et al., 2016). Recently, scholars have found that patients with OSA mainly affect the cerebrocerebellar pathway, and that was associated with sleep fragmentation and hypoxia, which was thought to be involved in the cognitive decline in OSA (Park et al., 2022). The study found that after 3 months of short-term CPAP treatment, abnormal sleep, and mood scores in OSA patients significantly decreased to normal levels, meanwhile, spontaneous brain activity was decreased in autonomic and

somatosensory control areas such as thalamus, putamen, posterior central gyrus, and insula, and increased in the cognitive and affective regulatory regions (Song et al., 2022). The above functional MRI (fMRI) studies were all based on the intrinsic brain activity in the resting-state of the classical frequency band, ignoring the temporal variability and failing to provide the necessary information to understand the spatiotemporal features of information processing in the human brain.

Compared with regional homogeneity, amplitude of low frequency fluctuation and FC, independent component analysis (ICA) is a data-driven processing method of resting-state fMRI, without *a priori* assumptions, it can be used to divide resting-state fMRI data into multiple functional networks and to further analyze these resting-state networks (Hu et al., 2019). The ICA methods have been widely used in neuroscience studies, such as sleep disorders (Luo et al., 2022), Parkinson's disease (Zhou et al., 2020), Alzheimer's disease (Soheili-Nezhad et al., 2020), etc. Zhang et al. (2013) used the ICA approach have identified seven brain networks and found that OSA specifically affects resting-state FC in cognitive and sensorimotor-related brain networks, suggesting that it is a promising tool for monitoring of neurological defects and disease progression. Some scholars have proposed that dynamic functional network connectivity (FNC) can reflect transient and periodic whole-brain temporal coupling patterns (Elton and Gao, 2015). For dynamic FNC analysis, covariance calculated across the entire sliding time window for all participants and then clustering the covariance into several brain connectivity states, can be used to explore their temporal variability and network connectivity strength (Fu et al., 2018). The dynamic FNC alterations are associated with specific cognitive states, psychiatric disorders, and neurological disorders [e.g., Alzheimer's disease (Zhao et al., 2022), major depressive disorder (Xue et al., 2020), idiopathic generalized epilepsy (Liu et al., 2017), and Parkinson's disease (Fiorenzato et al., 2019)], providing spatiotemporal features for understanding neural mechanisms. However, there has been no report of combining ICA with dynamic FNC to explore the neural mechanism in OSA patients.

Based on these findings, we hypothesized that the dynamic FNC and FC strength in OSA patients were changes, and altered temporal properties of the dynamic FNC in OSA was associated with the cognitive status. Therefore, we first used the ICA method to determine the resting-state functional networks. Second, we constructed dynamic FNC based on resting-state network components identified by the ICA and compared the differences between groups. Finally, the relationship between temporal properties and clinical evaluation was explored to reveal the underlying neural mechanism of cognitive impairment in patients with OSA.

Materials and methods

Subjects

All subjects were recruited from the sleep monitoring room at the respiratory or otolaryngology department of the First Affiliated Hospital of Nanchang University from August 2015 to June 2018. The diagnostic criteria of OSA were based on the American Academy of Sleep Medicine Clinical Practice Guideline (2007) (Collop et al., 2007). The inclusion criteria for OSA were apnea-hypopnea index (AHI) > 15/hour, male, age 20–60, and right-handedness. An AHI < 5 defined as the HC group. The exclusion criteria for OSA patients and HC were as follows: (1) other sleep disorders; (2) history of diabetes or respiratory diseases; (3) history of neurodegenerative disease, brain tumors, epilepsy, and traumatic brain injury; (4) abuse of illicit drugs or intake of psychoactive medications; and (5) MRI contraindications, such as metallic implants in the body, and claustrophobia.

Polysomnography

Before polysomnography (PSG) monitoring, all participants were asked not to drink coffee or alcohol. All subjects underwent overnight PSG (from 22:00 to 6:00 the next morning) using the Respironics LE-Series physiological monitoring system (Alice 5 LE, Respironics, Orlando, FL, USA). PSG monitoring included a standard electrooculogram, electrocardiogram, electrocardiogram, electromyogram, snoring, body position, nasal and oral airflow, thoracic and abdominal respiratory movements, and oxygen saturation (SaO_2), and total sleep time, sleep latency, sleep efficiency, sleep stages, arousal index, and respiratory events were recorded. See our previous study for the details (Li et al., 2021). According to the American Academy of Sleep Medicine manual, hypopnea was defined as a 30% or greater drop in airflow, lasting ≥ 10 s, accompanied by 4% or greater oxygen desaturation. Obstructive apnea was described as a continuous reduction in airflow ≥ 90% for ≥ 10 s along with evident respiratory effort. The AHI was defined as the sum of apnea and hypopnea events per hour during sleep.

Neuropsychological assessment

All participants completed the Montreal Cognitive Assessment (MoCA) and the Epworth Sleepiness Scale (ESS) assessment. The MoCA, which assesses cognitive domains including naming, visuospatial skills, executive function, attentional, language, delayed memory, abstraction, and orientation, was used to assess cognitive function. The MoCA total score is 30, with a score below 26 was considered mild

cognitive impairment, and one point is added as a correction if the years of education are less than 12 (Nasreddine et al., 2005). The ESS is a very simple questionnaire for the self-assessment of daytime sleepiness, including eight different conditions, each with a score of 0–3, and the total score ranges from 0 to 24, and a total score of more than 6 indicates drowsiness (Johns, 1991).

Imaging data acquisition and preprocessing

All subjects were scanned using the 3.0 Tesla MRI system with an 8-channel phased-array head coil (Siemens, Munich, Germany). Before MRI scans, all subjects were told to close their eyes, not to think about anything, and not to fall asleep. First, conventional axial T2-weighted imaging and axial T1-weighted imaging were performed. Then, three-dimensional high-resolution T1-weighted images were collected. Finally, blood oxygen level-dependent fMRI data were collected using an echo-planar imaging sequence and each functional contained 240 volumes. Detailed scanning parameters are shown in **Supplementary Table 1**. Foam pads and earplugs were used to reduce patient head movement and scanner noise during scanning. Two senior radiologists read the images to exclude gross lesions and motion artifacts.

The Statistical Parametric Mapping (SPM12[1]) and Data Processing and Analysis for Brain Imaging (DPABI[2]) software were used to preprocess fMRI data, which were run on MATLAB 2018b (Mathworks, Natick, MA, USA). Image preprocessing mainly includes the following steps: data from DICOM to NII format; the first 10 time points was removed in order to acclimate the participants to the environment; slice timing correction and head motion correction was performed, and subjects whose head motion with maximum displacement (x, y, z) of more than 2.0 mm and maximum angular rotation (x, y, z) of more than 2.0° was excluded; three-dimensional T1 imaging was segmented into gray matter, white matter and cerebrospinal fluid with the Diffeomorphic Anatomical Registration Through Exponentiated Lie algebra (DARTEL); the rs-fMRI images were normalized to the Montreal Neurological Institute space with DARTEL and resampled to 3 mm × 3 mm × 3 mm voxels; the images were spatially smoothed using a Gaussian kernel of 6 mm full-width at half-maximum. We excluded 8 OSA patients as for head motion criterion. Finally, 82 male OSA patients and 48 male HC were included in the analysis.

Group independent component analysis and resting-state network identification

After data preprocessing, we used the group ICA function of the fMRI Toolbox (GIFT v4.0c[3]) to decompose the data into a group-level spatial function independent component. First, principal component analysis was performed to reduce the data dimension for subject specificity. The minimum description length standard was used to automatically estimate the number of independent components (ICs) (resulting in 44 ICs) for all participants. Second, to ensure the reliability and stability of the ICs, the infomax algorithm with ICASSO was run by repeating 20 times (Wang et al., 2020). Finally, the subject-specific spatial maps and time courses were back-reconstructed using group ICA, and the results were converted to a z score for display. Based on previous studies (Allen et al., 2014; Damaraju et al., 2014) and a publicly available atlas by the Functional Imaging in Neuropsychiatric Disorders Laboratory,[4] 25 meaningful ICs were identified and were classified into eight functional networks by visual observation of the ICA results. The detailed information and spatial maps of the ICs are listed in **Supplementary Table 2** and **Supplementary Figure 1**.

According to Allen et al.'s (2014) study, we performed additional postprocessing on the 25 ICs to reduce the remaining noise. The 3dDespike algorithm[5] was used for linear drift, filtered using a fifth order Butterworth filter with a 0.15 Hz high frequencies cut-off. Finally, we regressed out the movement parameters.

Dynamic functional network connectivity analysis

The sliding window technique is the most common method to study dynamic FNC (Kim et al., 2017). We computed this analysis using the temporal dynamic FNC toolbox V1.0a in GIFT. First, a sliding time window approach with a window size set to 30 TRs with a Gaussian and steps of 1 TR was used to compute the dynamic FNC between all ICs time courses. A total of 26,000 windowed FNC matrices (130 subjects × 200 matrices) were produced. Then, the k-means clustering algorithm (using the squared Euclidean distance method with a maximum of 500 iterations and 150 replicate dynamic FNC windows) was conducted on the windowed FNC matrices (Malhi et al., 2019). To estimate the optimal number of clusters, a cluster validity analysis was performed using

1 https://www.fil.ion.ucl.ac.uk/spm/software/spm12/

2 http://rfmri.org/dpabi

3 https://trendscenter.org/software/gift/

4 http://findlab.stanford.edu/functional_ROIs.html

5 http://afni.nimh.nih.gov/afni

gap and silhouette statistics on the samples of all subjects (resulting is 2).

Statistical analysis

For demographic and clinical data, the Kolmogorov-Smirnov test was used to test the normality of the data. One-way analysis of variance (ANOVA) was used to assess differences between the three groups, a $p < 0.05$ was considered to be statistically significant, and the *post-hoc* t-test was used to compare differences between any two groups, Bonferroni correction.

For the dynamic FNC, we investigated the temporal properties of dynamic FNC states by computing the mean dwell time and fractional windows in each state, as well as the number of transitions from one state to another. One-way ANOVA was used to compare each of the 300 mean dynamic FNC correlations ($25 \times 24/2$) from each of the 2 states between the three groups (HC, OSA-NC, OSA-MCI), age, years of education, and head motion as covariates. In addition, three dynamic FNC indices were extracted from all two states of each subject (Jiang et al., 2020), namely, the fractional window of each state, mean dwell time, and number of transitions. Fractional window indicates the percentage of time spent in each state out of the total time, mean dwell time reflects the average length of time the subjects spent in a certain state, and number of transitions refers to the number of times a subject switched between different states. These indices were compared by the two sample t-test, and $p < 0.05$ was considered statistically significant. The two sample t-test were used to compare the connectivity strength of each state between OSA and HC ($p < 0.01$, FDR correction).

The dynamic FNC values, such as fractional window, mean dwell time, and number of transitions, were analyzed for correlation with clinical data using Pearson correlations (such as MoCA, ESS, PSG) in OSA patients. The $p < 0.05$ was considered statistically significant.

Results

Population and clinical characteristics

According to the grading criteria, the 82 OSA patients were divided into 41 OSA-NC and 41 OSA-MCI. All of the clinical data conformed to the normal distribution. The clinical data are shown in Table 1. One-way ANOVA showed that no significant differences were found in age, years of education, and FD, and significant differences in BMI, AHI, nadir SaO_2, mean SaO_2, AI, ESS, and MoCA were found between three groups. The detailed results of the *post-hoc* t-test are shown in Table 1.

TABLE 1 Population and clinical data in OSA patients and HC.

Characteristic	HC ($n = 48$)	OSA-NC ($n = 41$)	OSA-MCI ($n = 41$)	*F* value	*P*-value	HC vs. OSA-NC *P*-value	HC vs. OSA-MCI *P*-value	OSA-NC vs. OSA-MCI *P*-value
Age, years	41.2 ± 10.1	38.9 ± 9.8	40.4 ± 10.8	1.558	0.234	0.568	0.785	0.686
BMI, Kg/m2	20.6 ± 1.6	26.7 ± 3.8	27.1 ± 3.2	60.002	< 0.001	< 0.001	< 0.001	0.915
Education, years	11.6 ± 3.1	12.6 ± 3.3	11.2 ± 3.6	1.762	0.761	0.561	0.885	0.212
AHI, /h	2.4 ± 1.3	50.3 ± 19.0	53.2 ± 23.1	130.605	< 0.001	< 0.001	< 0.001	0.915
Nadir SaO_2, %	92.9 ± 3.3	68.2 ± 12.7	72.2 ± 11.3	83.395	< 0.001	< 0.001	< 0.001	0.199
Mean SaO_2, %	96.2 ± 2.3	91.3 ± 5.3	92.3 ± 3.5	20.669	< 0.001	< 0.001	< 0.001	0.799
AI, /hour	11.6 ± 2.9	34.6 ± 23.0	32.6 ± 23.8	21.194	< 0.001	< 0.001	< 0.001	0.945
ESS, scores	3.1 ± 1.5	9.6 ± 4.8	11.7 ± 4.2	67.453	< 0.001	< 0.001	< 0.001	0.033
MoCA, scores	27.3 ± 1.7	27.4 ± 1.2	22.5 ± 2.8	84.889	< 0.001	0.986	< 0.001	< 0.001
Mean FD, mm	0.20 ± 0.11	0.24 ± 0.12	0.25 ± 0.12	1.751	0.178	0.550	0.234	0.967

OSA, obstructive sleep apnea; HC, health controls; BMI, body mass index; AHI, apnea hypopnea index; SaO_2, oxygen saturation; AI, arousal index; ESS, Epworth Sleepiness Scale; MoCA, Montreal Cognitive Assessment; FD, framewise displacement.

Resting-state intrinsic functional network connectivity

The spatial maps of all 25 ICs are summarized in Figure 1. The functional networks were divided into the auditory network (AN) (IC42), DMN (IC2, IC12, IC14, IC18, IC36), executive control network (ECN) (IC9, IC10, IC22, IC28, IC33, IC41), language network (LN) (IC17, IC32), sensorimotor network (SMN) (IC35, IC39), salience network (SN) (IC19, IC24, IC44), visual network (VN) (IC6, IC13, IC16, IC25, IC30), and cerebellar networks (CBN) (IC23). The averaged static FNC matrix between 25 ICs of all subjects is shown in Figure 2A. The single sample *t*-test results of all subjects are shown in Figure 2B. The stronger connections were mainly located in AN, DMN, ECN, LN, SMN, SN, and VN.

Dynamic functional network connectivity alterations

According to the estimate results of cluster status using gap and silhouette statistic criterion, all the participants time-varying dynamic FNC was clustered into two different states by k-means clustering (k = 2). State I was characterized by less frequency (33%) and the presence of stronger connectivity in all networks, except for the CBN; State II was characterized by more frequency (67%) and relatively weaker connectivity (Figure 3).

The state- and group-specific cluster center obtained by the k-means cluster analysis (k = 2) are shown in Figure 4. We observed that in the HC and all OSA patients, State I, integrated state with stronger connectivity within and between networks located mostly in the network (AN, DMN, ECN, LN, SMN, SN, VN); while State II, segregated state with relatively weaker connectivity within networks and anti-correlation connections between the ECN, SMN, and DMN.

The differences of temporal properties of dynamic FNC between OSA patients and HC are shown in Table 2 and Figure 5. In OSA patients, State I occurred 17% more often than in HC, paralleled by a proportional reduction of State II. In OSA-MCI patients, State I was more frequently observed than that in HC (OSA-MCI: 0.44 ± 0.35, HC: 0.22 ± 0.26, p = 0.003). OSA-MCI showed a significantly longer mean dwell time in State I (OSA-MCI: 45.4 ± 51.6, HC: 19.9 ± 21.2, p = 0.008). However, the opposite results were shown in State II. There were no significant differences between HC and OSA-NC. The number of transitions in the three groups were 2.5 ± 2.4, 2.6 ± 1.9, 2.8 ± 2.6, respectively ($p > 0.05$).

We further compared the strength of connection in the two states between all OSA patients and HC groups, and the results are shown in Figure 6. In the State I, OSA patients observed 2 stronger connections and 11 lower connections compared to HC, which included 4 within-network connections (1 enhanced connections within ECN; and 3 lower connections within SN and ECN), and 9 between-networks connections (1 enhanced connections between DMN-SN, and 8 lower connections between DMN-ECN, DMN-SN, VN-SN, SN-ECN, SMN-LN, LN-ECN). In the State II, compared with HC, OSA patients showed 4 lower connections, including 1 within-network connections (ECN) and 3 between-network connections (AN-ECN, AN-CBN, and DMN-ECN).

Correlation results

Unfortunately, no significant correlation between the dynamic FNC of temporal properties (mean dwell time, fractional windows, and number of transitions) and clinical data using Pearson correlation analysis was found in all OSA patients. However, in OSA-MCI patients, we found that the mean dwell time in State I and State II was positively correlated with the AHI and AI, the fractional windows were positively associated with the AHI and AI. The number of transitions was negatively correlated with the MoCA in OSA-MCI patients. Detailed related results are shown in Table 3.

Discussion

In this study, we used a data-driven ICA approach to clarify the intrinsic network components in OSA patients and for the first time to explored dynamic FNC patterns in patients with OSA ranging from normal cognition to mild cognitive impairment using sliding windows and the k-means clustering method. Our main findings were as follows: (1) Two different connectivity states were determined in all subjects, namely, State II, segregated state with weaker connectivity and high frequency, State I, integrated state with stronger connectivity and low frequency; (2) Compared with HC, OSA-MCI patients appear more frequent and had longer mean dwell time in stronger connected State I, and lower connected State II appears less frequently and has a shorter mean dwell time; However, there was no significant difference between the OSA-NC and HC. In OSA-MCI patients, there was a trend to increase in number of transitions, and was positively correlated with cognitive assessment; (3) OSA patients showed more abnormal FC in stronger connected State I and showed less reduced FC in lower connected State II. These results suggested that alterations in dynamic FC patterns were associated with the presence of MCI in OSA, providing new insights into understanding neurocognitive mechanisms in patients with OSA.

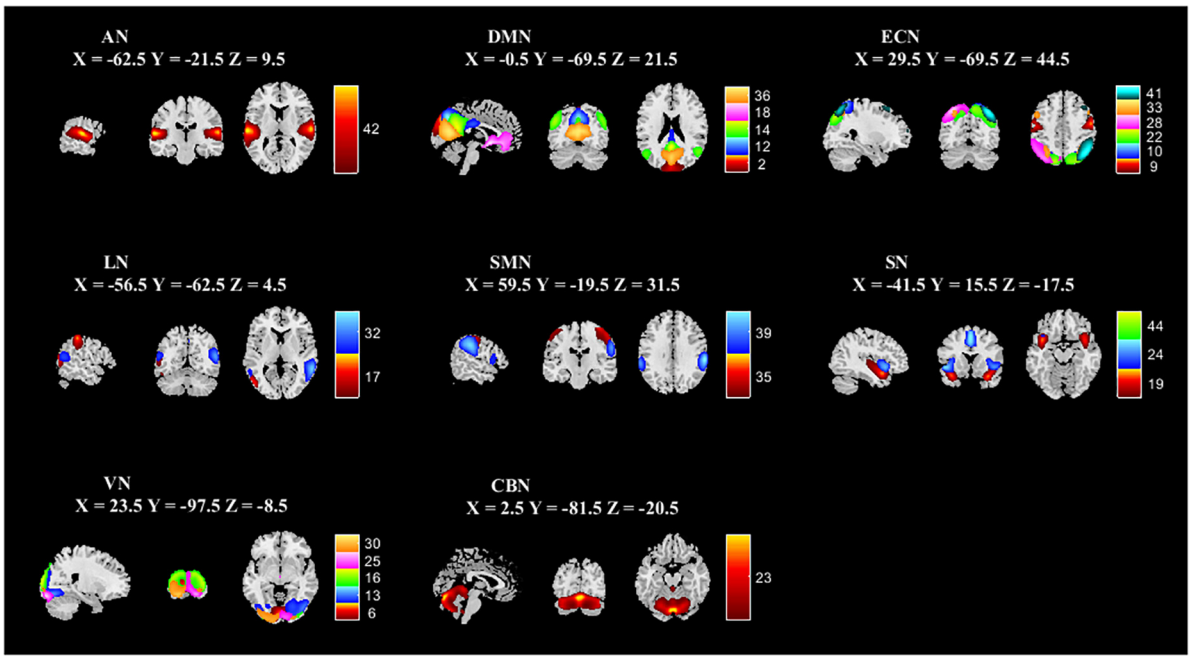

FIGURE 1
Spatial independent component analysis was used to identify independent components. Independent component spatial maps divided on eight functional networks (AN, DMN, ECN, LN, SMN, SN, VN, and CBN) based on their anatomical and functional properties. ICA, independent component analysis; AN, auditory network; DMN, default mode network; ECN, executive control network; LN, language network; SMN, sensorimotor network; SN, salience network; VN, visual network; CBN, cerebellar network.

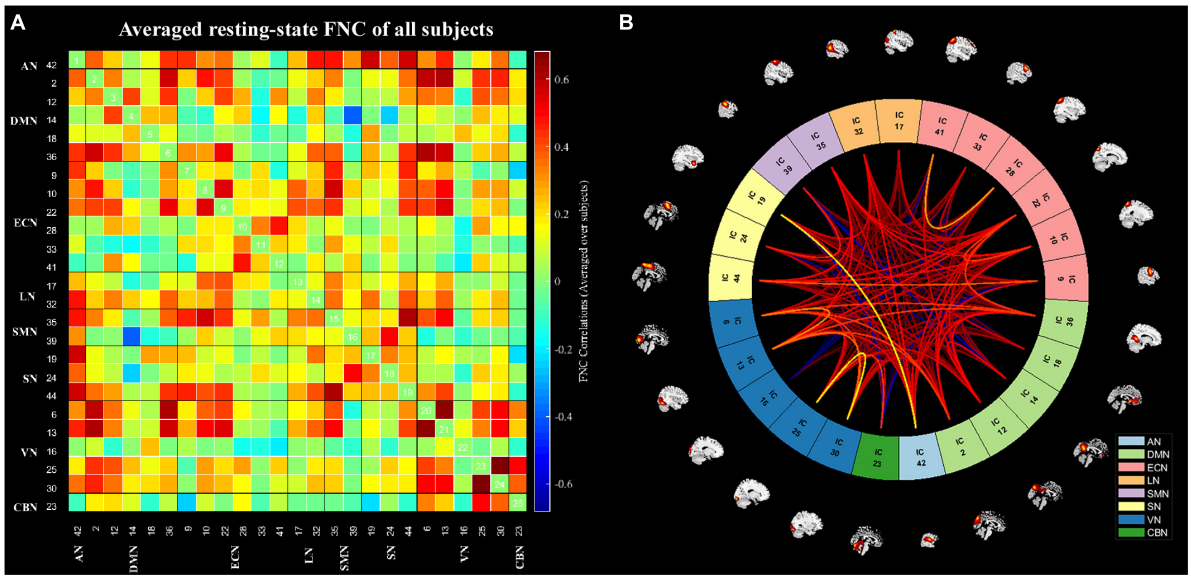

FIGURE 2
The static functional network connectivity results. **(A)** The averages static functional network connectivity matrices of all subjects between independent components pairs was produced in entire resting-state time courses. **(B)** The mean static functional network connectivity of all subjects in eight network (single sample *t*-test) ($p < 0.01$, FDR correction). AN, auditory network; DMN, default mode network; ECN, executive control network; LN, language network; SMN, sensorimotor network; SN, salience network; VN, visual network; CBN, cerebellar network.

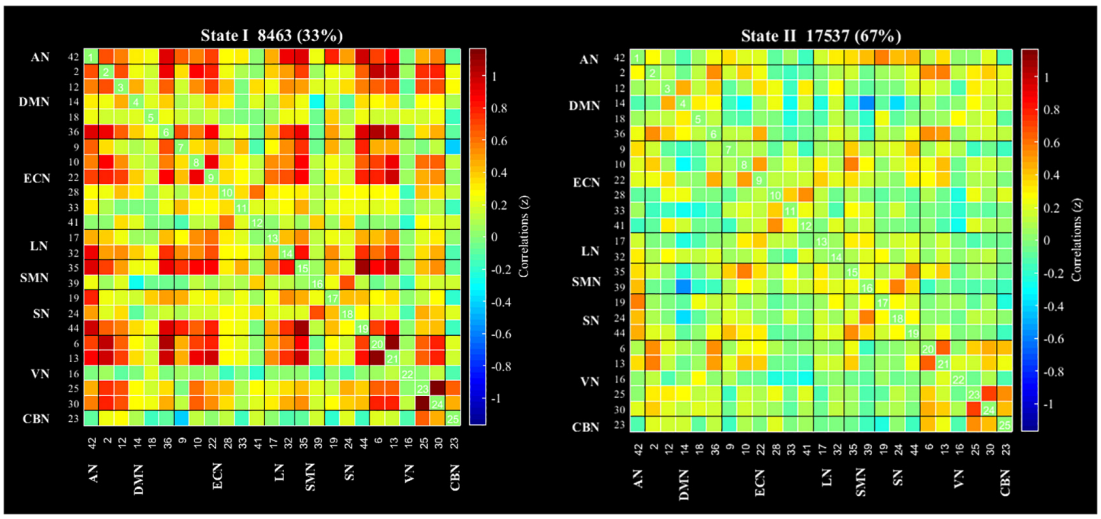

FIGURE 3
Results of the clustering analysis per state. Cluster centroids for each state of all participant. The total number of occurrences and percentage of total occurrences are listed in each cluster. AN, auditory network; DMN, default mode network; ECN, executive control network; LN, language network; SMN, sensorimotor network; SN, salience network; VN, visual network; CBN, cerebellar network.

In this study, we found that the incidence of lower connectivity in State II in OSA patients was lower than that in HC, along with reduced mean dwell time, while the incidence of stronger connectivity in State I was higher than that in HC. In previous studies of acute sleep deprivation, increased subcortical-cortical frequency was found after acute sleep deprivation, instead, another low connectivity state significantly reduced frequency, reflecting changes in the dynamics of mental activity in the brain after sleep loss (Li et al., 2020). Other studies found that patients with Parkinson's disease-MCI had significantly reduced time spent in state characterized by low connectivity compared with HC, while these differences were not found in Parkinson's disease-NC patients, suggesting that dynamic FC patterns may be related to the presence of MCI in Parkinson's disease patients (Díez-Cirarda et al., 2018). Previous studies of dynamic FC in patients with schizophrenia found that medication-naive schizophrenia patients had shorter mean dwell time and fewer fractional windows in sparse connectivity, and longer mean dwell time and more fractional windows in intermediate connectivity, suggesting associations with brain network temporal dynamics (Lottman et al., 2017). This study analyzed the changes in dynamic FNC patterns in OSA patients from normal cognition to mild cognitive impairment. The results showed that the frequency of State II characterized by lower connectivity was 22% lower in OSA-MCI patients than that in HC, but not in the OSA-NC group, indicating that OSA patients need higher network integration. Meanwhile, we found that the mean dwell time and fractional windows in State I and II were positively associated with the AHI and AI in OSA-MCI patients, which suggested that the temporal variability of the brain functional network was related to disease severity in OSA patients.

Furthermore, compared to the HC group, there was no significant difference in the number of transitions between the states in OSA patients, but there was a tendency toward an increase in the number of transitions in OSA from normal cognition to mild cognitive impairment. Previous studies on Parkinson's disease found no significant difference in status transition in Parkinson's disease patients without diagnosed MCI compared to HC (Kim et al., 2017), but showed a significantly increased number of transitions in patients with Parkinson's disease-MCI (Díez-Cirarda et al., 2018), which indicated that gradual dysfunctional patterns may exist in Parkinson's disease patients. Another study of major depressive disorder found no significant difference but a slight increase in the number of transitions in major depressive disorder patients compared with HC (Yao et al., 2019). The results of this study were similar to findings on Parkinson's disease and major depressive disorder. In OSA-MCI patients, increasing the number of transitions was positively correlated with MoCA score, indicating that dynamic network conversion may provide potential neural markers for cognitive deterioration in OSA.

We further compared the strength of connections in different states between OSA patients and the HC. We observed that compared with HC, OSA patients showed extensive abnormal FC in stronger connected State I and less reduced FC in lower connected State II, mainly in intranetwork connectivity (SN and ECN) and internetwork connectivity (mainly between DMN, ECN, and SN). Human cognitive function relies on efficient coordination between multiple interacting large-scale

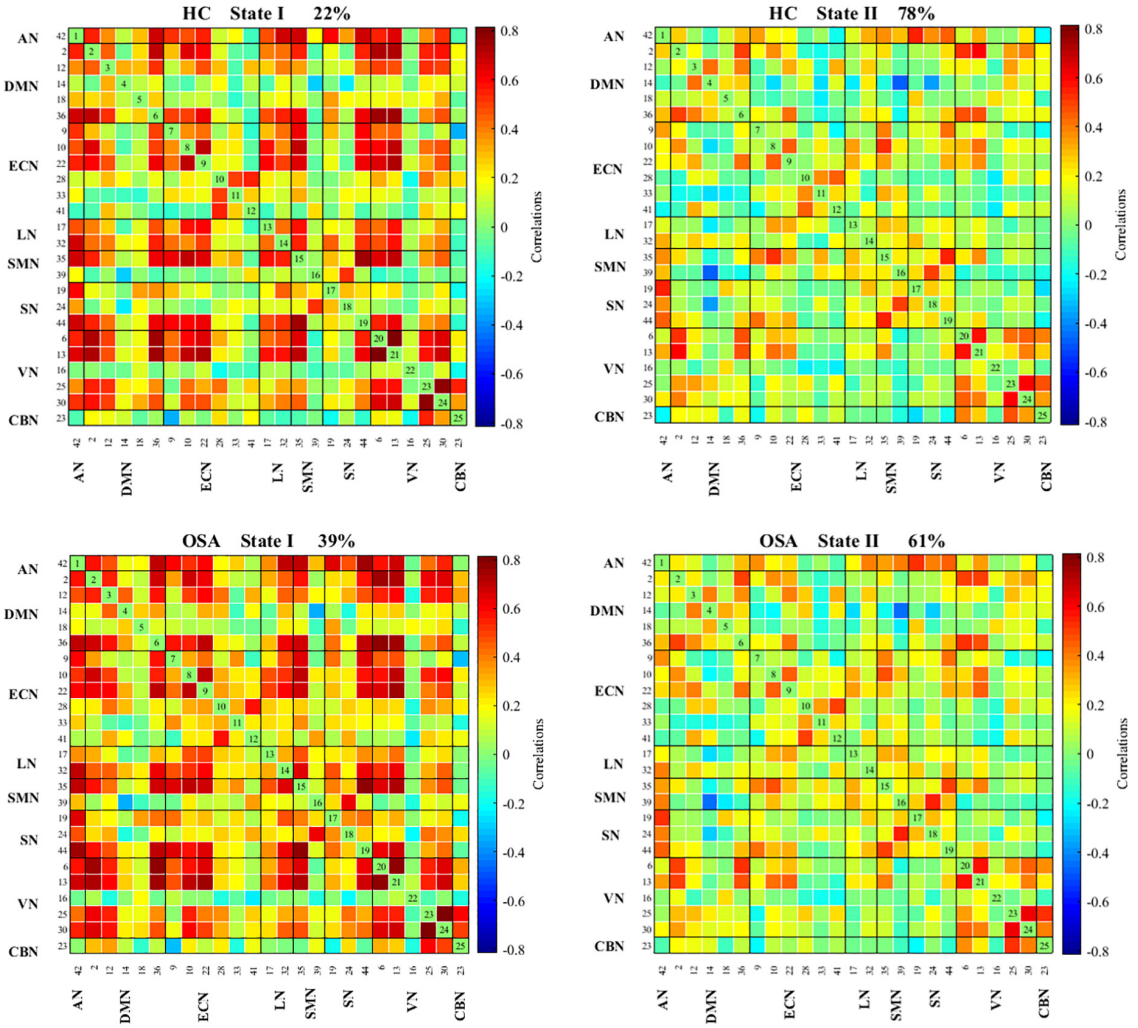

FIGURE 4
Functional connectivity state results. Group functional network connectivity matrices for each state (percentage of total occurrences for State I and II: 22 and 78% in the healthy controls and 39 and 61% in the OSA groups, respectively). There are significant statistical differences between two groups ($p < 0.05$). AN, auditory network; DMN, default mode network; ECN, executive control network; LN, language network; SMN, sensorimotor network; SN, salience network; VN, visual network; CBN, cerebellar network.

functional brain networks, in which the ECN, DMN, and SN are core networks for high-level cognitive activity. The SN is mainly composed of the dorsal anterior cingulate cortex and insular cortex, and is used to identify the most relevant stimuli in internal and external stimuli and switch to the corresponding network processing, while also participating in various cognitive functions, such as attention control, conflict monitoring, error monitoring and detection (Kerns et al., 2004; Seeley et al., 2007). The ECN is mainly composed of the dorsolateral prefrontal cortex and the posterior parietal cortex, which plays an important role in emotional and adaptive cognitive control. The DMN includes medial prefrontal cortex and posterior cingulate cortex, which are mainly responsible for autobiographical memory and self-reference processing, and episodic memory. Studies have shown that an important function of the SN is to adjust the flexible interactive switching between the activation and withdrawal of the DMN and the ECN (Sridharan et al., 2008). Specifically, in a self-related psychological task, SN induces DMN activation and ECN inactivation, while in a cognitive demands task, SN induced activation of ECN and inactivation of DMN (Chiong et al., 2013). Previous literature has described alterations in ECN activation and DMN inactivation during working memory tasks in patients with OSA (Prilipko et al., 2011). Previous studies found significant positive FC between the SN and ECN, and negative FC between the SN and DMN. This selective impairment of resting-state FC between the SN and the DMN, which may be the potential basis for cognitive impairment in OSA patients (Zhang et al., 2015). Studies have also shown the functional separation of the ECN and

TABLE 2 The dynamic FNC temporal properties between OSA patients and HC groups.

Properties	State	HC	OSA-NC	OSA-MCI	HC vs. OSA-NC *P*-value	HC vs. OSA-MCI *P*-value	OSA-NC vs. OSA-MCI *P*-value
Mean dwell time	I	19.9 ± 21.2	32.3 ± 37.1	45.4 ± 51.6	0.112	**0.008**	0.337
	II	108.7 ± 74.0	88.2 ± 72.0	82.1 ± 78.4	0.182	**0.022**	0.271
Fractional windows	I	0.22 ± 0.26	0.33 ± 0.32	0.44 ± 0.35	0.113	**0.003**	0.189
	II	0.78 ± 0.26	0.67 ± 0.32	0.56 ± 0.35	0.113	**0.003**	0.189
Number of transitions		2.5 ± 2.4	2.6 ± 1.9	2.8 ± 2.6	0.599	0.571	0.869

OSA, obstructive sleep apnea; HC, health controls; OSA-NC, obstructive sleep apnea with normal cognition; OSA-MCI, obstructive sleep apnea with mild cognitive impairment; FNC, functional network connectivity. The bold values indicates statistical significance.

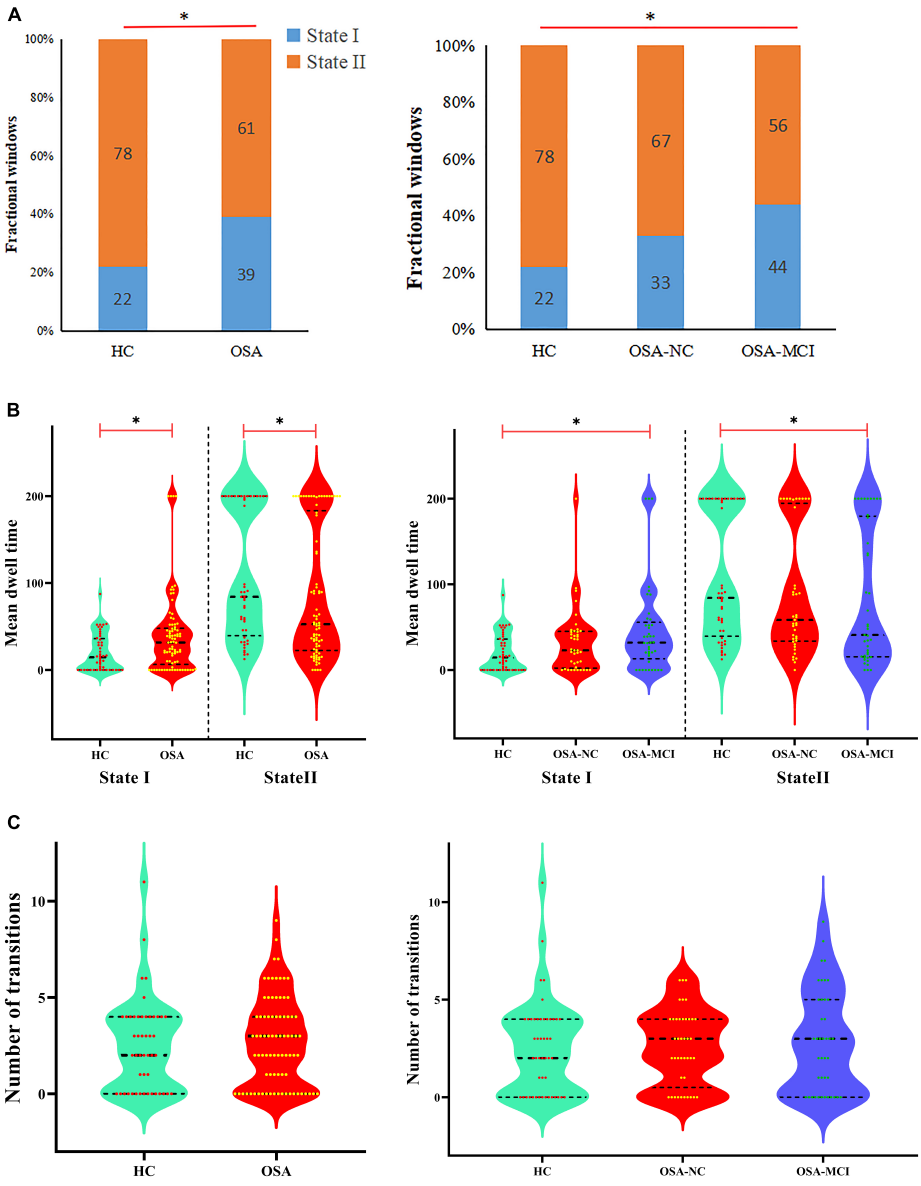

FIGURE 5
Temporal properties of dynamic functional network connectivity states for the OSA and HC groups. **(A)** Percentage of total time subjects spent in each state. **(B)** Mean dwell time and **(C)** number of transitions between states were plotted using violin plots. Horizontal black dotted lines indicate group medians and inter-quartile range. *$p < 0.05$. OSA, obstructive sleep apnea; HC, healthy control; MCI, mild cognitive impairment; NC, normal cognitive.

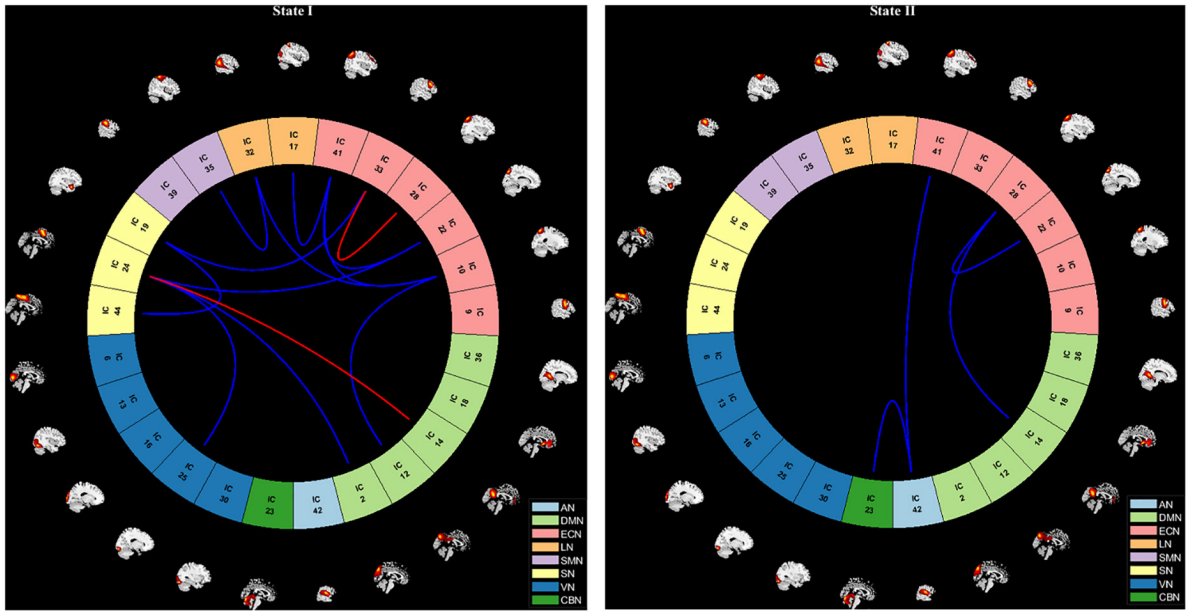

FIGURE 6
Visualization of functional network connectivity differences in two states ($p < 0.01$, FDR correction). The red line represents increased functional connectivity and the blue line represents decreased functional connectivity in OSA patients. AN, auditory network; DMN, default mode network; ECN, executive control network; LN, language network; SMN, sensorimotor network; SN, salience network; VN, visual network; CBN, cerebellar network.

DMN brain regions in OSA patients (Harper et al., 1985). Our previous study found reduced DMN network connectivity and topological reorganization in patients with OSA (Li H. J. et al., 2016; Chen et al., 2018), which may underlie the cognitive deficits in patients with OSA. Some scholars have also found that the FC of the SN, bilateral ECN and DMN in OSA patients is decreased, which is related to autonomic disorders, suggesting that autonomic dysfunction in OSA is associated with central autonomic network alterations (Lin et al., 2020). Similar to these findings, this study found that OSA patients had lower connections within the SN and ECN, and internetwork connections between the DMN, ECN and SN, indicating that FNC was separated and integration ability decreased, which may be the basis of advanced cognitive impairment in OSA patients, and further supplemented the mechanism of cognitive impairment in OSA from a dynamic perspective of OSA patients.

Moreover, our study also found that VN-SN, SMN-LN, LN-ECN, AN-ECN, and AN-CBN network connections were decreased in OSA patients. The AN, SMN, VN, and LN are low-level perceptual networks that mainly receive external stimuli and play a central role in information

TABLE 3 Correlations between temporal properties of dynamic FNC and clinical characteristics in OSA-MCI patients.

		AHI	Nadir SaO_2	Mean SaO_2	AI	Sleep efficiency	ESS	MoCA
Mean dwell time in State I	*r* value	0.323	−0.200	−0.257	0.383	0.006	0.020	0.058
	p-value	**0.040**	0.210	0.105	**0.014**	0.969	0.902	0.721
Mean dwell time in State II	*r* value	−0.325	0.210	0.160	−0.32	0.162	−0.183	0.162
	p-value	**0.038**	0.187	0.317	**0.041**	0.311	0.252	0.312
Fractional windows in State I	*r* value	0.363	−0.238	−0.248	0.376	−0.066	0.143	−0.143
	p-value	**0.020**	0.134	0.118	**0.016**	0.682	0.373	0.372
Fractional windows in State II	*r* value	−0.363	0.238	0.248	−0.376	0.066	−0.143	0.143
	p-value	**0.020**	0.134	0.118	**0.016**	0.682	0.373	0.372
Number of transitions	*r* value	0.139	0.013	0.156	−0.086	−0.199	0.135	−0.326
	p-value	0.387	0.937	0.331	0.595	0.212	0.399	**0.038**

AHI, apnea hypopnea index; SaO_2, oxygen saturation; AI, arousal index; ESS, Epworth Sleepiness Scale; MoCA, Montreal Cognitive Assessment. The bold values indicates statistical significance.

transmission in the external environment (Shang et al., 2014). The reduced FC between the VN and the SN may reflect that the OSA exhibits poor visual information processing power. The reduced functional network of SMN-LN, LN-ECN, and AN-ECN indicate decreased receptivity to external stimuli, which affects higher cognitive function.

Some limitations should be considered in our study. First, due to gender differences in outpatients, we collected more male OSA patients, while female and children OSA patients were collected in smaller numbers, so female and children patients were excluded from our analysis. It is difficult to generalize this conclusion to the whole OSA population. Second, similar to most ICA studies thus far that have focused on gray matter, while ignoring the physiological significance of white matter signals, our study only explored changes in the temporal properties of dynamic FNC in gray matter. However, recent studies have confirmed that white matter fMRI signals contain rich spatiotemporal information similar to those found in gray matter (Wang et al., 2022). Finally, our study is only a cross-sectional study, and it is not clear how CPAP therapy affects the dynamic FNC attributes in OSA patients. In the future, female and children with OSA should be included, the dynamic FNC of white matter brain regions may provide additional information from whole brain network, and longitudinal studies would provide more information for clinical treatment.

Conclusion

This study was the first to use the combined ICA and dynamic FNC methods to investigate dynamic temporal properties in OSA patients from normal cognition to mild cognitive impairment. In OSA-MCI patients, we found that temporal properties of dynamic FNC (mean dwell time and fractional window) were altered, and number of transformations were associated with cognitive state. It was also found that OSA patients showed abnormal high-level cognitive network connections in the stronger connected State I, mainly between the SN, DMN, and ECN. These abnormalities may be neuroimaging mechanisms in OSA-MCI patients, providing new insights into our understanding of cognitive impairment in OSA patients, and future studies should consider using dynamic FNC to predict MCI in OSA.

Data availability statement

The raw data supporting the conclusions of this article will be made available by the authors, without undue reservation.

Ethics statement

This study was approved by the Medical Ethics Committee of the First Affiliated Hospital of Nanchang University. The participants signed written informed consent forms, in accordance with the Declaration of Helsinki. The patients/participants provided their written informed consent to participate in this study.

Author contributions

DP guided and designed the MRI experiment. HL analyzed the resting-state fMRI data. LL performed statistical analysis. HL and LL wrote the manuscript. KL, PL, WX, YZ, LK, TL, LH, XL, LZ, and YS collected the resting fMRI data and clinical data. HL and DP reviewed and revised the manuscript. All authors contributed to the article and approved the submitted version.

Funding

This study was supported by the National Natural Science Foundation of China (Grant No. 81860307), the Natural Science Foundation Project of Jiangxi, China (Grant Nos. 20202BABL216036 and 20181ACB20023), Education Department Project of Jiangxi Province, China (Grant Nos. GJJ160035 and GJJ190133), and Department of Health Project and Jiangxi Province, China (Grant No. 202210211).

Conflict of interest

The authors declare that the research was conducted in the absence of any commercial or financial relationships that could be construed as a potential conflict of interest.

Publisher's note

Supplementary material

The Supplementary Material for this article can be found online at: https://www.frontiersin.org/articles/10.3389/fnagi.2022.977917/full#supplementary-material

References

Allen, E. A., Damaraju, E., Plis, S. M., Erhardt, E. B., Eichele, T., and Calhoun, V. D. (2014). Tracking whole-brain connectivity dynamics in the resting state. *Cereb. Cortex* 24, 663–676. doi: 10.1093/cercor/bhs352

Chen, L. T., Fan, X. L., Li, H. J., Nie, S., Gong, H. H., Zhang, W., et al. (2017). Disrupted small-world brain functional network topology in male patients with severe obstructive sleep apnea revealed by resting-state fMRI. *Neuropsychiatr. Dis. Treat.* 13, 1471–1482. doi: 10.2147/NDT.S135426

Chen, L., Fan, X., Li, H., Ye, C., Yu, H., Gong, H., et al. (2018). Topological reorganization of the default mode network in severe male obstructive sleep apnea. *Front. Neurol.* 9:363. doi: 10.3389/fneur.2018.00363

Chiong, W., Wilson, S. M., D'Esposito, M., Kayser, A. S., Grossman, S. N., Poorzand, P., et al. (2013). The salience network causally influences default mode network activity during moral reasoning. *Brain* 136, 1929–1941. doi: 10.1093/brain/awt066

Collop, N. A., Anderson, W. M., Boehlecke, B., Claman, D., Goldberg, R., Gottlieb, D. J., et al. (2007). Clinical guidelines for the use of unattended portable monitors in the diagnosis of obstructive sleep apnea in adult patients. Portable monitoring task force of the American academy of sleep medicine. *J. Clin. Sleep Med.* 3, 737–747.

Damaraju, E., Allen, E. A., Belger, A., Ford, J. M., McEwen, S., Mathalon, D. H., et al. (2014). Dynamic functional connectivity analysis reveals transient states of dysconnectivity in schizophrenia. *Neuroimage Clin.* 5, 298–308. doi: 10.1016/j.nicl.2014.07.003

Díez-Cirarda, M., Strafella, A. P., Kim, J., Peña, J., Ojeda, N., Cabrera-Zubizarreta, A., et al. (2018). Dynamic functional connectivity in Parkinson's disease patients with mild cognitive impairment and normal cognition. *Neuroimage Clin.* 17, 847–855. doi: 10.1016/j.nicl.2017.12.013

Elton, A., and Gao, W. (2015). Task-related modulation of functional connectivity variability and its behavioral correlations. *Hum. Brain Mapp.* 36, 3260–3272. doi: 10.1002/hbm.22847

Fiorenzato, E., Strafella, A. P., Kim, J., Schifano, R., Weis, L., Antonini, A., et al. (2019). Dynamic functional connectivity changes associated with dementia in Parkinson's disease. *Brain* 142, 2860–2872. doi: 10.1093/brain/awz192

Franklin, K. A., and Lindberg, E. (2015). Obstructive sleep apnea is a common disorder in the population-a review on the epidemiology of sleep apnea. *J. Thorac. Dis.* 7, 1311–1322. doi: 10.3978/j.issn.2072-1439.2015.06.11

Fu, Z., Tu, Y., Di, X., Du, Y., Pearlson, G. D., Turner, J. A., et al. (2018). Characterizing dynamic amplitude of low-frequency fluctuation and its relationship with dynamic functional connectivity: An application to schizophrenia. *Neuroimage* 180, 619–631. doi: 10.1016/j.neuroimage.2017.09.035

Harper, R. M., Macey, P. M., Henderson, L. A., Woo, M. A., Macey, K. E., Frysinger, R. C., et al. (1985). fMRI responses to cold pressor challenges in control and obstructive sleep apnea subjects. *J. Appl. Physiol.* 2003, 1583–1595. doi: 10.1152/japplphysiol.00881.2002

Hu, G., Zhang, Q., Waters, A. B., Li, H., Zhang, C., Wu, J., et al. (2019). Tensor clustering on outer-product of coefficient and component matrices of independent component analysis for reliable functional magnetic resonance imaging data decomposition. *J. Neurosci. Methods* 325:108359. doi: 10.1016/j.jneumeth.2019.108359

Huang, X., Tang, S., Lyu, X., Yang, C., and Chen, X. (2019). Structural and functional brain alterations in obstructive sleep apnea: A multimodal meta-analysis. *Sleep Med.* 54, 195–204. doi: 10.1016/j.sleep.2018.09.025

Jiang, S. F., Shi, J. Y., Yang, Z. T., Zhang, L., and Chen, H. J. (2020). Aberrant dynamic functional network connectivity in cirrhotic patients without overt hepatic encephalopathy. *Eur. J. Radiol.* 132:109324. doi: 10.1016/j.ejrad.2020.109324

Johns, M. W. (1991). A new method for measuring daytime sleepiness: The epworth sleepiness scale. *Sleep* 14, 540–545. doi: 10.1093/sleep/14.6.540

Kerns, J. G., Cohen, J. D., MacDonald, A. R., Cho, R. Y., Stenger, V. A., and Carter, C. S. (2004). Anterior cingulate conflict monitoring and adjustments in control. *Science* 303, 1023–1026. doi: 10.1126/science.1089910

Kim, J., Criaud, M., Cho, S. S., Díez-Cirarda, M., Mihaescu, A., Coakeley, S., et al. (2017). Abnormal intrinsic brain functional network dynamics in Parkinson's disease. *Brain* 140, 2955–2967. doi: 10.1093/brain/awx233

Kong, L., Li, H., Shu, Y., Liu, X., Li, P., Li, K., et al. (2022). Aberrant resting-state functional brain connectivity of insular subregions in obstructive sleep apnea. *Front. Neurosci.* 15:765775. doi: 10.3389/fnins.2021.765775

Lee, M. H., Yun, C. H., Min, A., Hwang, Y. H., Lee, S. K., Kim, D. Y., et al. (2019). Altered structural brain network resulting from white matter injury in obstructive sleep apnea. *Sleep* 42:z120. doi: 10.1093/sleep/zsz120

Li, C., Fronczek-Poncelet, J., Lange, D., Hennecke, E., Kroll, T., Matusch, A., et al. (2020). Impact of acute sleep deprivation on dynamic functional connectivity states. *Hum. Brain Mapp.* 41, 994–1005. doi: 10.1002/hbm.24855

Li, H. J., Dai, X. J., Gong, H. H., Nie, X., Zhang, W., and Peng, D. C. (2015). Aberrant spontaneous low-frequency brain activity in male patients with severe obstructive sleep apnea revealed by resting-state functional MRI. *Neuropsychiatr. Dis. Treat.* 11, 207–214. doi: 10.2147/NDT.S73730

Li, H., Li, L., Shao, Y., Gong, H., Zhang, W., Zeng, X., et al. (2016). Abnormal intrinsic functional hubs in severe male obstructive sleep apnea: Evidence from a voxel-wise degree centrality analysis. *PLoS One* 11:e164031. doi: 10.1371/journal.pone.0164031

Li, H. J., Nie, X., Gong, H. H., Zhang, W., Nie, S., and Peng, D. C. (2016). Abnormal resting-state functional connectivity within the default mode network subregions in male patients with obstructive sleep apnea. *Neuropsychiatr. Dis. Treat.* 12, 203–212. doi: 10.2147/NDT.S97449

Li, H., Li, L., Kong, L., Li, P., Zeng, Y., Li, K., et al. (2021). Frequency specific regional homogeneity alterations and cognitive function in obstructive sleep apnea before and after short-term continuous positive airway pressure treatment. *Nat. Sci. Sleep* 13, 2221–2238. doi: 10.2147/NSS.S344842

Li, P., Shu, Y., Liu, X., Kong, L., Li, K., Xie, W., et al. (2022). The effects of CPAP treatment on resting-state network centrality in obstructive sleep apnea patients. *Front. Neurol.* 13:801121. doi: 10.3389/fneur.2022.801121

Liguori, C., Maestri, M., Spanetta, M., Placidi, F., Bonanni, E., Mercuri, N. B., et al. (2021). Sleep-disordered breathing and the risk of Alzheimer's disease. *Sleep Med. Rev.* 55:101375. doi: 10.1016/j.smrv.2020.101375

Lin, W. C., Hsu, T. W., Lu, C. H., and Chen, H. L. (2020). Alterations in sympathetic and parasympathetic brain networks in obstructive sleep apnea. *Sleep Med.* 73, 135–142. doi: 10.1016/j.sleep.2020.05.038

Liu, F., Wang, Y., Li, M., Wang, W., Li, R., Zhang, Z., et al. (2017). Dynamic functional network connectivity in idiopathic generalized epilepsy with generalized tonic-clonic seizure. *Hum. Brain Mapp.* 38, 957–973. doi: 10.1002/hbm.23430

Liu, X., Chen, L., Duan, W., Li, H., Kong, L., Shu, Y., et al. (2022). Abnormal functional connectivity of hippocampal subdivisions in obstructive sleep apnea: A resting-state functional magnetic resonance imaging study. *Front. Neurosci.* 16:850940. doi: 10.3389/fnins.2022.850940

Lottman, K. K., Kraguljac, N. V., White, D. M., Morgan, C. J., Calhoun, V. D., Butt, A., et al. (2017). Risperidone effects on brain dynamic connectivity-a prospective resting-state fMRI study in schizophrenia. *Front. Psychiatry* 8:14. doi: 10.3389/fpsyt.2017.00014

Luo, Y., Qiao, M., Liang, Y., Chen, C., Zeng, L., Wang, L., et al. (2022). Functional brain connectivity in mild cognitive impairment with sleep disorders: A study based on resting-state functional magnetic resonance imaging. *Front. Aging Neurosci.* 14:812664. doi: 10.3389/fnagi.2022.812664

Malhi, G. S., Das, P., Outhred, T., Bryant, R. A., and Calhoun, V. (2019). Resting-state neural network disturbances that underpin the emergence of emotional symptoms in adolescent girls: Resting-state fMRI study. *Br. J. Psychiatry* 215, 545–551. doi: 10.1192/bjp.2019.10

Nasreddine, Z. S., Phillips, N. A., Bedirian, V., Charbonneau, S., Whitehead, V., Collin, I., et al. (2005). The montreal cognitive assessment, MoCA: A brief screening tool for mild cognitive impairment. *J. Am. Geriatr. Soc.* 53, 695–699. doi: 10.1111/j.1532-5415.2005.53221.x

Olaithe, M., Bucks, R. S., Hillman, D. R., and Eastwood, P. R. (2018). Cognitive deficits in obstructive sleep apnea: Insights from a meta-review and comparison with deficits observed in COPD, insomnia, and sleep deprivation. *Sleep Med. Rev.* 38, 39–49. doi: 10.1016/j.smrv.2017.03.005

Park, B., Palomares, J. A., Woo, M. A., Kang, D. W., Macey, P. M., Yan-Go, F. L., et al. (2016). Disrupted functional brain network organization in patients with obstructive sleep apnea. *Brain Behav.* 6:e441. doi: 10.1002/brb3.441

Park, H. R., Cha, J., Joo, E. Y., and Kim, H. (2022). Altered cerebrocerebellar functional connectivity in patients with obstructive sleep apnea and its association with cognitive function. *Sleep* 45:zsab209. doi: 10.1093/sleep/zsab209

Prilipko, O., Huynh, N., Schwartz, S., Tantrakul, V., Kim, J. H., Peralta, A. R., et al. (2011). Task positive and default mode networks during a parametric working

memory task in obstructive sleep apnea patients and healthy controls. *Sleep* 34, 293–301. doi: 10.1093/sleep/34.3.293

Seeley, W. W., Menon, V., Schatzberg, A. F., Keller, J., Glover, G. H., Kenna, H., et al. (2007). Dissociable intrinsic connectivity networks for salience processing and executive control. *J. Neurosci.* 27, 2349–2356. doi: 10.1523/JNEUROSCI.5587-06.2007

Senaratna, C. V., Perret, J. L., Lodge, C. J., Lowe, A. J., Campbell, B. E., Matheson, M. C., et al. (2017). Prevalence of obstructive sleep apnea in the general population: A systematic review. *Sleep Med. Rev.* 34, 70–81. doi: 10.1016/j.smrv.2016.07.002

Shang, J., Lui, S., Meng, Y., Zhu, H., Qiu, C., Gong, Q., et al. (2014). Alterations in low-level perceptual networks related to clinical severity in PTSD after an earthquake: A resting-state fMRI study. *PLoS One* 9:e96834. doi: 10.1371/journal.pone.0096834

Soheili-Nezhad, S., Jahanshad, N., Guelfi, S., Khosrowabadi, R., Saykin, A. J., Thompson, P. M., et al. (2020). Imaging genomics discovery of a new risk variant for Alzheimer's disease in the postsynaptic SHARPIN gene. *Hum. Brain Mapp.* 41, 3737–3748. doi: 10.1002/hbm.25083

Song, X., Roy, B., Vacas, S., Woo, M. A., Kang, D. W., Aysola, R. S., et al. (2022). Brain regional homogeneity changes after short-term positive airway pressure treatment in patients with obstructive sleep apnea. *Sleep Med.* 91, 12–20. doi: 10.1016/j.sleep.2022.02.005

Sridharan, D., Levitin, D. J., and Menon, V. (2008). A critical role for the right fronto-insular cortex in switching between central-executive and default-mode networks. *Proc. Natl. Acad. Sci. U.S.A.* 105, 12569–12574. doi: 10.1073/pnas.0800005105

Vanek, J., Prasko, J., Genzor, S., Ociskova, M., Kantor, K., Holubova, M., et al. (2020). Obstructive sleep apnea, depression and cognitive impairment. *Sleep Med.* 72, 50–58. doi: 10.1016/j.sleep.2020.03.017

Wang, C., Cai, H., Sun, X., Si, L., Zhang, M., Xu, Y., et al. (2020). Large-scale internetwork functional connectivity mediates the relationship between serum triglyceride and working memory in young adulthood. *Neural Plast.* 2020:8894868. doi: 10.1155/2020/8894868

Wang, P., Wang, J., Michael, A., Wang, Z., Klugah-Brown, B., Meng, C., et al. (2022). White matter functional connectivity in resting-state fMRI: Robustness, reliability, and relationships to gray matter. *Cereb. Cortex* 32, 1547–1559. doi: 10.1093/cercor/bhab181

Xue, K., Liang, S., Yang, B., Zhu, D., Xie, Y., Qin, W., et al. (2020). Local dynamic spontaneous brain activity changes in first-episode, treatment-naive patients with major depressive disorder and their associated gene expression profiles. *Psychol. Med.* 30, 1–10. doi: 10.1017/S0033291720003876

Yan, L., Park, H. R., Kezirian, E. J., Yook, S., Kim, J. H., Joo, E. Y., et al. (2021). Altered regional cerebral blood flow in obstructive sleep apnea is associated with sleep fragmentation and oxygen desaturation. *J. Cereb. Blood Flow Metab.* 41, 2712–2724. doi: 10.1177/0271678X211012109

Yao, Z., Shi, J., Zhang, Z., Zheng, W., Hu, T., Li, Y., et al. (2019). Altered dynamic functional connectivity in weakly-connected state in major depressive disorder. *Clin. Neurophysiol.* 130, 2096–2104. doi: 10.1016/j.clinph.2019.08.009

Zhang, Q., Qin, W., He, X., Li, Q., Chen, B., Zhang, Y., et al. (2015). Functional disconnection of the right anterior insula in obstructive sleep apnea. *Sleep Med.* 16, 1062–1070. doi: 10.1016/j.sleep.2015.04.018

Zhang, Q., Wang, D., Qin, W., Li, Q., Chen, B., Zhang, Y., et al. (2013). Altered resting-state brain activity in obstructive sleep apnea. *Sleep* 36, 651–659. doi: 10.5665/sleep.2620

Zhao, C., Huang, W. J., Feng, F., Zhou, B., Yao, H. X., Guo, Y. E., et al. (2022). Abnormal characterization of dynamic functional connectivity in Alzheimer's disease. *Neural Regen. Res.* 17, 2014–2021. doi: 10.4103/1673-5374.332161

Zhou, C., Gao, T., Guo, T., Wu, J., Guan, X., Zhou, W., et al. (2020). Structural covariance network disruption and functional compensation in Parkinson's disease. *Front. Aging Neurosci.* 12:199. doi: 10.3389/fnagi.2020.00199

frontiers | Frontiers in Aging Neuroscience

TYPE Original Research
PUBLISHED 03 November 2022
DOI 10.3389/fnagi.2022.1005298

OPEN ACCESS

EDITED BY
Fermín Segovia,
University of Granada, Spain

REVIEWED BY
Mojtaba Barzegar,
Society for Brain Mapping and Therapeutics, United States
Jon Andoni Dunabeitia,
Nebrija University, Spain

*CORRESPONDENCE
J. Wesson Ashford
ashford@stanford.edu

SPECIALTY SECTION
This article was submitted to Neurocognitive Aging and Behavior, a section of the journal Frontiers in Aging Neuroscience

RECEIVED 28 July 2022
ACCEPTED 17 October 2022
PUBLISHED 03 November 2022

CITATION
Ashford JW, Clifford JO, Anand S, Bergeron MF, Ashford CB and Bayley PJ (2022) Correctness and response time distributions in the MemTrax continuous recognition task: Analysis of strategies and a reverse-exponential model. *Front. Aging Neurosci.* 14:1005298. doi: 10.3389/fnagi.2022.1005298

Correctness and response time distributions in the MemTrax continuous recognition task: Analysis of strategies and a reverse-exponential model

J. Wesson Ashford[1,2]*, James O. Clifford[3], Sulekha Anand[4], Michael F. Bergeron[5], Curtis B. Ashford[6] and Peter J. Bayley[1,2]

[1]War Related Illness and Injury Study Center, VA Palo Alto Health Care System, Palo Alto, CA, United States, [2]Department of Psychiatry and Behavioral Science, Stanford University, Palo Alto, CA, United States, [3]Department of Psychology, College of San Mateo, San Mateo, CA, United States, [4]Department of Biological Sciences, San José State University, San Jose, CA, United States, [5]Department of Health Sciences, University of Hartford, West Hartford, CT, United States, [6]MemTrax, LLC, Redwood City, CA, United States

A critical issue in addressing medical conditions is measurement. Memory measurement is difficult, especially episodic memory, which is disrupted by many conditions. On-line computer testing can precisely measure and assess several memory functions. This study analyzed memory performances from a large group of anonymous, on-line participants using a continuous recognition task (CRT) implemented at https://memtrax.com. These analyses estimated ranges of acceptable performance and average response time (RT). For 344,165 presumed unique individuals completing the CRT a total of 602,272 times, data were stored on a server, including each correct response (HIT), Correct Rejection, and RT to the thousandth of a second. Responses were analyzed, distributions and relationships of these parameters were ascertained, and mean RTs were determined for each participant across the population. From 322,996 valid first tests, analysis of correctness showed that 63% of these tests achieved at least 45 correct (90%), 92% scored at or above 40 correct (80%), and 3% scored 35 correct (70%) or less. The distribution of RTs was skewed with 1% faster than 0.62 s, a median at 0.890 s, and 1% slower than 1.57 s. The RT distribution was best explained by a novel model, the reverse-exponential (RevEx) function. Increased RT speed was most closely associated with increased HIT accuracy. The MemTrax on-line memory test readily provides valid and reliable metrics for assessing

individual episodic memory function that could have practical clinical utility for precise assessment of memory dysfunction in many conditions, including improvement or deterioration over time.

KEYWORDS

Alzheimer's disease, cognition, cognitive impairment, dementia, episodic memory, memory, response time, recognition

Introduction

Need for screening tools for cognitive and memory impairment

Cognitive impairment often includes dysfunction of episodic memory and is currently recognized as one of the most widespread and challenging public health problems of our times. Episodic memory impairment is a hallmark of Alzheimer's disease (AD), and the rates of dementia and AD are rapidly increasing with aging populations. Traumatic brain injuries, drug side-effects, anesthesia, and many other untoward events often disrupt brain function with consequent cognitive and memory dysfunction. Accordingly, to develop early detection and monitoring change over time as key strategies in managing this escalating burden on society, assessment of cognitive function, particularly episodic memory, is critically important.

Currently, there is a significant and recognized lack of adequate instruments for brief cognitive screening and early detection of the dementia caused by AD (Ashford, 2008; De Roeck et al., 2019; Ashford et al., 2022). Most tools for assessing cognitive function require face-to-face administration using paper-and-pencil instruments, which are complex, labor-intensive, and subject to intra-rater and inter-rater variability. In the current era, computerized assessments for measuring cognition, including episodic memory, are a viable alternative, though, at this time, no test has distinguished itself as generally useful (Zygouris and Tsolaki, 2015; Sternin et al., 2019). With computerized testing, several aspects of cognitive performance can be quantified much more precisely, including correctness (accuracy) of performance and response time (RT). This study focused on a continuous recognition task (CRT), which can be efficiently implemented for memory screening for a broad range of cognitive problems including AD.

The CRT should be clearly distinguished from a similar task paradigm, the "n-back" test, which traditionally uses a limited number of stimuli (e.g., numbers or letters) and asks the subject to recall if a stimulus is a repeat from a stimulus 2, 3, or 4 back. This latter test (n-back) is useful for examining working memory (WM) and executive function, and there are several n-back tests in use, including one that is computerized (Pelegrina et al., 2015). However, in the CRT examined here, few repeated images occurred less than four images later and thus require an absolute recognition for detection, given there were five categories and five images from each category, exceeding the brains usual capacity to rely on WM. Accordingly, the CRT is substantially different than the usual n-back test.

Continuous recognition task history and signal detection theory

The present study analyzed the distribution of behavioral data produced when individuals performed an online modification of a traditional Signal Detection Task (SDT), the MemTrax CRT (Ashford et al., 2019b), to test learning, memory, and cognition. Prior in-person, not-computerized CRTs, the Continuous Visual Memory Test (Larrabee et al., 1992) and the Continuous Recognition Memory test (Fuchs et al., 1999), have used a similar format with different types of stimuli and have shown that the CRT format has construct validity. Related studies have examined the retrieval processes involved in continuous recognition (Hockley, 1982) and provided information on memory trace strength and the memory theories (Hockley, 1984b, 2022). Further, similar continuous recognition tests have shown the involvement of the frontal, parietal, and temporal cortical regions and the hippocampus in the performance of this type of memory task (Yonelinas et al., 2005; Suzuki et al., 2011), brain regions affected in AD and most types of dementia and cognitive and memory impairment. Accordingly, the MemTrax CRT was expected to provide valid data for several aspects of memory, learning, and cognition, though many other aspects, such as free recall, verbal, semantic, and remote memory would not be assessed.

Whereas most SDTs direct participants to attend to and detect a designated "target" stimulus (single or previously defined item or items), the MemTrax CRT instructs participants to consider all presented stimuli and detect a repetition of any stimulus in the randomized sequence and indicate that detection with a response (a space-bar press, a screen tap, or a mouse click referred to commonly as a "HIT"). Failure to recognize a repeated stimulus is a "Miss." The consideration

of an initial stimulus being shown without responding, for 3 s to "learn" the new information, is referred to as a "Correct Rejection," while responding to the first presentation of an image in this case would be considered a "false alarm." The primary hypothesis in this study was that SDT analytic methodology (Stanislaw and Todorov, 1999), distinguishing repeated images (signals) from initial presentations (non-signals), applied to the MemTrax output data would provide two specific metrics, the degree of correctness of performance (percent correct, reflecting the *d*' – *d*-prime - component) and the tendency to over or under respond (response balance or bias of HITs and Correct Rejections, reflecting the "beta" component), and these metrics were anticipated to differentiate cognitive function and thus explain individual performance on this CRT. The secondary hypothesis was that RT would correlate most directly with correctness of performance (related to d'), rather than the response balance, a speed-accuracy trade-off (related to beta), or percent HITs or Correct Rejections. In a prior version of MemTrax, using a PowerPoint presentation to audiences, *d*' correlated with age ($r = -0.37$), more than HIT rate ($r = -0.24$) or false alarm rate ($r^2 = -0.25$), though RT was not available (Ashford et al., 2011). However, in another study of MemTrax on-line, the correlation of percent correct with age was much less ($R^2 < 0.02$), while the correlation of RT with age was about ($R^2 = 0.08$) (Ashford et al., 2019b); percent HITs and Correct Rejections were not analyzed in that study.

A predecessor of the MemTrax CRT was used in a primate laboratory (Ashford and Fuster, 1985; Coburn et al., 1990), where visual cortical neuron response latencies to information-laden stimuli were found to occur simultaneously across recruited cortical regions, suggesting a coordinated massive reciprocal capacity for item analysis (Ashford et al., 1998a). It was further shown that the Rhesus monkeys could recognize letters in a serial visual learning and recognition task (Ashford et al., 1998a). This serial visual recognition task was later modified for clinical use with a slide projector using complex visual stimuli and then piloted as a PowerPoint presentation to large community-based audiences of elderly individuals concerned about their memory (Ashford et al., 2011). Because of the engaging nature and positive user experience reported, this task paradigm was implemented online to assess memory problems in the general population (Ashford et al., 2019b). This sophisticated but simple paradigm can be quickly administered with measurement precision far beyond that possible with paper-and-pencil tests (van der Hoek et al., 2019; Liu et al., 2021).

Episodic memory and response time to recognize visual stimuli

Episodic memory contains the 'what,' 'where,' and 'when' information that interacts and binds with information in semantic memory to form time-based concepts of those events. The organization of these defining declarative features into progressively more complex concepts optimizes capacity limitations imposed on short-term memory (STM). Recall of information from non-declarative, or implicit memory requires no conscious or intentional involvement and is referred to as perceptual memory. Thus, in contrast to content-based storage in the episodic, semantic, and declarative systems, implicit memory includes processes and procedures that reduce effort to learn, store, think about, and convert information in STM into long-term memory (LTM). An important concept is the efficiency with which information can be integrated across such processes (Weigard and Sripada, 2021).

Response time to stimuli presented in tasks has been studied extensively in evaluating episodic memory. Recognition memory is an area of notable interest. Whereas paired-associates learning provided an early method to study memory (Shepard, 1958), recognition testing provides a method for estimating the quantity of information retained in memory (Shepard, 1961). Recognition memory paradigms have been studied to determine memory capacity and limitations, particularly using SDT and speed-accuracy trade-offs, and comparing memory theories such as the recruitment model and scanning model, with important implications for decision latency, including correct responses which are shorter than incorrect responses (Pike et al., 1977). An important advance was the development of a continuous recognition approach in which new and old items were interspersed (Shepard and Teghtsoonian, 1961). Since the early studies of recognition performance, demonstrations of the utility of complex pictures in the CRT paradigm to study memory have been extensive.

Surprisingly, the first scientific study conclusively demonstrating that the human could remember large amounts of information utilized numerous complex color pictures presented to individuals who showed high levels of recognition after both short and very long delays (Shepard, 1967). In a cross-species study, pigeons and monkeys are able to recall complex pictures moderately well; however, humans remember pictures so well that to test the limits of normal human capacity, it is necessary to utilize highly complex stimuli, such as kaleidoscope images (Wright et al., 1985). With such recognition memory paradigms, RT to stimuli can be analyzed to determine the time which the individual takes to recognize and respond to a previously shown item (Hockley, 1982).

A prominent interest has been the decay of memory traces coincident with increasing intensity of intervening distractions (Hintzman, 2016), including the lag from a first to a second presentation of an image (Hockley, 1982). Complex picture recognition has been particularly useful for studying medial temporal lobe function (Suzuki et al., 2011; Koen et al., 2017). And recognition memory and CRT paradigms have been used effectively in studying neural responses in the human hippocampus to assess episodic memory (Wixted et al., 2018),

regardless of variations in the method of test administration (Bayley et al., 2008). However, behavioral pattern separation in memory progressively and distinctively declines from healthy individuals to those with mild cognitive impairment (Stark et al., 2013).

The MemTrax CRT requires complex picture information processing into STM and access and recognition of content from LTM for use in responding to the future stimuli presented in the task, because each stimulus, in addition to being a potential current target, is also potentially a new stimulus and thus a potential later target. CRTs like MemTrax are applied to examine these events in the brains of subjects instructed to attend to stimuli and indicate repetition. In this case, detection of repetition of the "target" stimulus produces an overt behavior (response, either a space-bar press, a screen touch, or a mouse click) that signals "yes, a repetition was detected" or a covert behavior (no response) indicating "no, a repetition was not detected" on a particular trial.

Response accuracy, time, and factors modifying signal detection

Signal detection task suggests that there are two factors which affect the accuracy of information processing and the time to accurately respond to a stimulus (RT) as instructed. The first factor is the internal state of the subject related to their health and prior knowledge stored in LTM. This factor relates to the motivation to participate in the testing, the ability to sense the stimulus and maintain the instructional set, and issues not related to the task. Internal state in this context alters the ability of the subject's information processing sequence to engage with the task and execute a correct behavior (HIT: target present and participant responds as instructed; and Correct Rejection: target not present and participant does not respond) or an incorrect behavior (False Alarm: target not present and participant responds in spite of instruction not to respond; and Miss: target is present, and participant does not respond as instructed) on each trail. This ability factor is referred to as *d'* (*d*-prime) and reflects the sensitivity or degree of discrimination between the targets and non-targets. Accordingly, in a CRT, the SDT models a single factor controlling recognition correctness but does not account for different internal or external issues which may differentially affect the HIT versus Miss recognition or the Correct Rejection versus False Alarm decision.

The second factor is the knowledge acquired by the subject performing the task about environmental factors, like the *a priori* probability of a particular occurrence and the payoff matrix describing the consequence for a correct versus incorrect behavior on a trial (Liu et al., 2019). Such knowledge can be used by cognitive processes directed by those operations in WM to establish a criterion for response performance on subsequent trials during the task. This second factor is referred to as "beta," reflecting the tendency to under-respond or over-respond. The predilection to miss targets (recognition failure) or wrongly identify new stimuli (incorrectly guess, False Alarm) is of great importance for interpreting performance and understanding disorders of a subject's information processing system and is related to the RT (Gordon and Carson, 1990). However, there may be many factors involved in the processing of information and cognitive impairment. So, the process of recognition may be impaired and slow responsiveness, while a separate, unrelated executive process may change the response bias and affect RT in a different manner.

Instructions provided to the participant prior to testing describe the processing required to meet task demands for a CRT (Craik, 2002). These instructions direct the required operations in WM on how to execute processes to meet task demands. In the MemTrax CRT, the neurocognitive processes are: (1) specifically compare and detect representation(s) that match prior occurrences during the test, e.g., "recognize"; (2) if a recognition occurs, manifest a response as quickly as possible; and (3) direct processes to use information on a trial to update expectations so this information is adequately encoded to be available for "recognition" for subsequent trials (Walley and Weiden, 1973; Fabiani et al., 1986; Clifford and Williston, 1992, 1993). As described for attention (Posner, 1994), instructions may alter the effects which the internal state of the subject has on processing during and between trials. Complex visual information, as shown to participants during a MemTrax trial, activates visual cortical regions, including the occipital and inferotemporal cortex (Ashford and Fuster, 1985). However, the MemTrax test instructions require attention to the stimuli for recognition and possible encoding, which will also activate the prefrontal cortex (Kapur et al., 1994; Ashford et al., 1998a).

Response time distribution skewing

The present study examined RT means and their relationship to the universal observation that the averaged distribution of RTs during CRTs differs from the normal Gaussian distribution and is skewed, with absolute lower limits and less bounded upper limits. The explanation for the skewed distribution of RTs has been difficult, though numerous models have been suggested (Burbeck and Luce, 1982; Hockley, 1982, 1984a; Moret-Tatay et al., 2018, 2021; Liu et al., 2019). An exponentially modified Gaussian probability density function (ex-Gaussian) (Ratcliff and Murdock, 1976), which provides parameters related to performance across different tests (Hockley, 1984a), has been widely used to model individual RTs. The ex-Gaussian model is based on a theory that RT reflects two underlying psychological mechanisms (processes): the decision component for sensory processes that obeys an exponential distribution (decay curve), and the transduction component related to the initiation and completion of the physical response

to the stimuli that follows a normal Gaussian distribution (Dawson, 1988; Marmolejo-Ramos et al., 2014). Following this theoretical construct, RT during these tasks has been modeled as the convolution of an exponential function and a Gaussian function to form an exponentially modified Gaussian curve (the ex-Gaussian function) sensitive to both mechanisms. The ex-Gaussian function has been invoked to explain recognition processing based on RTs (Moret-Tatay et al., 2021) and reaction time slowing in AD (Gordon and Carson, 1990; Ratcliff et al., 2021). This distribution requires three parameters to model RT, the mean and standard deviation of the Gaussian distribution and the decay constant of the exponential component.

Due to issues related to the complexity of RT measurement and explanations of the underlying neural mechanisms subserving decision making, significant effort has been expended to develop other approaches to model the skewed distribution of RTs to obtain a deeper understanding of experimental effects on the underlying neural and psychological processes supporting these data (Ratcliff et al., 2016; Weindel et al., 2021). These approaches have been divided into two groups, measurement models and process models (Anders et al., 2016; Tejo et al., 2019). The measurement models include Weibull and lognormal (Anders et al., 2016) models. The process models, which address the internal information analysis by the individual, include the diffusion model (Ratcliff and Murdock, 1976; Ratcliff and McKoon, 2008; Ratcliff et al., 2016; Liu et al., 2022) and the leaky-competing accumulator model (Usher and McClelland, 2001; Tsetsos et al., 2012). In reality, there are many mathematical models that can produce similar distributions to explain various complexities of cognitive tasks (Liu et al., 2019), and many theoretical models have attempted to provide explanations (Cousineau et al., 2016; Osmon et al., 2018; Hasshim et al., 2019), though the actual neural processing may not conform to such models.

MemTrax continuous recognition task analysis

In the present study the distributions of correct and incorrect behaviors were examined with respect to overall performance. Then, the distribution of mean RTs executed during the MemTrax CRT was evaluated. The objective of the present analyses was to determine the extent to which the cumulative distribution of performance metrics during this test, number of responses, correctness of responses, and the RT for correct responses, can be modeled, with determinations of types of performance limitations and interactions. Of particular interest were response performance levels, response biases (strategies, value-based decision-making), and the relationship of RTs to an exponential regression, which only requires two parameters. There was an earlier expectation that there would be a speed-accuracy trade-off, but prior studies showed that correctness of performance has a slight positive correlation with RT in various populations. Also, previous research examined percent correct and presumed that there would be a close relationship between HITs and False Alarms. Further, it was expected that both types of behavioral responses and RTs would be balanced, reflecting the central processing of information, consistent with an information processing model (IPMs) using SDT. While these expectations were not correct, these analyses in a large group of subjects provided new behavior models and solid bases for using the MemTrax CRT for more extensive assessments and reliable interpretation of behavioral performance. The data, though from anonymous individuals, clearly showed a distribution of several behavioral metrics and provided a guide to determine normal ranges. Metrics from such a large population can lead to the establishment of valid and reliable assessments of episodic memory function in clinical settings.

Materials and methods

Population

This study examined results from individuals who completed the MemTrax automated CRT program: https://memtrax.com on the internet between May 27, 2014, and May 7, 2022. During this time, over 2 million hits were recorded on the MemTrax website. Of these, the test was started and completed 602,272 times by 344,165 distinct users. The test was programmed to save data on the server before the test results were returned to the user. First-time users were offered an option to sign-up on the website and have their data associated with their password protected email account so that they may see their own performance over time. Of these users, 256,949 took the test only once, while 87,214 (25%) signed up for and took repeat tests. Of those who signed up, 271 of these users took the test more than 75 times and 18 took it more than 1,000 times (**Figure 1**). For this analysis, data were examined for only the first test for first-time users who took and completed the test, presumably 344,165 unique individuals.

At sign-up, subjects were asked to provide year and month of birth, sex, and education level, though there was no method for verification of this information. This demographic information was only provided by 26,834 users; however, not being verifiable, these data were discarded. Data from all tests, including RT for each individual stimulus (50), were available for analysis, though only average RT was examined in this study. The Stanford University Internal Review Board approved this test for anonymous collection and analysis of these data.

Design

The MemTrax test program was designed in WORD-PRESS so that it would perform essentially the same on any platform.

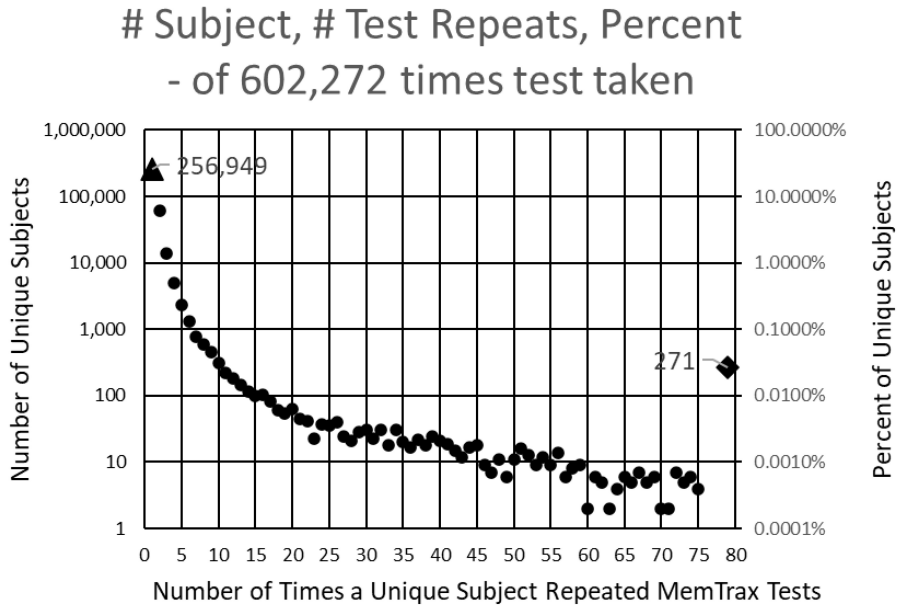

FIGURE 1
Number of subjects **(left log scale)** and percentage **(right log scale)** taking each number of tests. 344,165 presumably unique individuals took the test. Of these, 256,949 took the test only one time, and 60,642 took the test only two times. Two hundred and seventy-one took the test more than 75 times and 18 took the test more than 1,000 times.

The on-line implementation presents 50 images, 25 new and 25 repeated, with the instruction to respond to repeated images as quickly as possible. Users are allowed up to 3 s after stimulus presentation to respond to an image. The exact time for each response (1–3,000 ms) was recorded, with 200–2,999 ms considered a "response" and less than 200 ms or exactly 3,000 ms considered a "non-response." (The 200 ms lower limit was chosen as a typical RT for a fast-reaction to a stimulus change – a value well below any observed decision time, hence not a legitimate response.) Each test had five unique images from each of five categories, which were selected from 3,000 images curated into 60 categories. These images were presented in a pseudo-random order with no more than four new images or repeated images occurring in a sequence (similar to the rules of the Gellerman series, Gellerman, 1993). For the five items in each of the five categories (25 unique images), three images were repeated once, while one was repeated twice, and one was not repeated. This study did not analyze the effects of lag or number of repeats.

Basic analyses for every individual examined "Responses" either indicated by the press of a space bar, the tap of a screen, or click of a mouse, depending on platform used, for each stimulus and mean RT across all HITs. The number of "Correct Trials" was tabulated (0–50; ideally 25 HITs and 25 Correct Rejections). From these measures, other metrics were calculated, including: number of incorrect responses ("False Alarms" = "25 – Correct Rejections," optimally zero), number of failures to respond to a repeated image ("Misses" = "25 – Hits," optimally zero), "Total Number of Responses" ("HITs" plus "False Alarms"), and mean RT to "HITs" ("RT"). A more complete description of the task has been previously published (Ashford et al., 2019b).

Data analysis

For first-time tests for the 344,165 unique users, 59,499 tests with performance of chance or poorer, i.e., less than 30 correct out of 50 possible choices (random likelihood of getting 30 or more correct is less than 1/1000), which included tests with fewer than five HITs or fewer than five Correct Rejections, were removed (17% of the initial uses), leaving 284,644 tests. Also, of these tests, those with average RTs to HITs less than 0.5 s (2,350 had less than 0.5 s with very few of these having more than 30 correct responses, 0.8%) or more than 2 s (n = 156) were removed. Another 18 were removed due to a programming error. Thus, 282,140 tests were considered valid and used for this study and analyses (82% of the first-time users).

Data from these tests were analyzed with an EXCEL spreadsheet (Microsoft, Inc., Redmond, Washington, IL, USA). Main functions used included sorting, scatter plots with trend lines and Pearson correlations, COUNTIF, and AVERAGEIF. Analyses were made according to total overt responses (sum of HITs and False Alarms, based on platform, either space-bar presses, screen taps, or mouse clicks, the dependent variables), in response to the picture stimuli (initial or repeated, the independent variables) and total correct trials (sum of HITs

and Correct Rejections). Specific analyses of the numbers of types of responses (HITs, Correct Rejections, Misses, and False Alarms) across subjects were performed. The distribution of RTs was analyzed by examining the cumulative distribution and the negative natural log of the cumulative distribution which was tested for its relationship to an exponential regression. RT was analyzed for its relationship with the performance metrics.

Results

Number of responses and response correctness

About 17% of participants had exactly 25 responses (optimal number), with about 32% having less than 25 responses and about 51% having more than 25 responses, which would therefore include correct and incorrect overt responses (**Figure 2A**). There were approximately equal proportions of correctness for tests with less than 25 total responses and more than 25 responses, with a monotonic decline of correctness with progressively less and more than 25 responses (**Figure 2B**). This decline was clearly related to a progressive decrease of HITs for tests with less than 25 total responses, with a stable, high number of Correct Rejections. Symmetrically, above 25 total responses, there was a progressive decrease of Correct Rejections, with a stable, high number of HITs, indicating that the proportion of HITs and Correct Rejections was dominantly influenced by a strategy to have either fewer or more responses across all the stimuli, a pattern clearly different from a random interaction (**Figure 2C**). Though exactly 25 HITs were needed for a perfect score, for subjects with 38–49 correct trials (1–12 errors) there was a slight but clear tendency to respond to more than 25 of the repeated images (more False Alarms than Misses), with the maximum at 44 correct trials, averaging 25.8 responses (**Figure 2D**). By contrast, subjects executing 35–37 correct trials had active responses to about 25 of the repeated images (an average balance of False Alarms and Misses). Subjects with less than 35 correct trials (more than 15 errors) tended to substantially over-respond (even more False Alarms than Misses) up to an average of 26.6, an over-response rate of 7%. The pattern in **Figure 2D** indicates a complex relationship between the number of correct trials and responses.

Among these tests, only about 5% of participants had perfect performance (25 correct responses and 25 correct rejections), and 10% of the participants had 49 correct responses and correct rejections (one False Alarm or one Miss; **Figure 3A**). When the correct components, HITs and Correct Rejections, were plotted separately, they had a similar distribution to the overall correct response plot (**Figure 3B**). However, the maximum number of HITs for tests occurred at 24, for 24.5% of the tests, while the maximum number of Correct Rejections, also occurred at 24, with 21.1% of the tests. **Figure 2C** shows the discordance of HITs and Correct Rejections, showing symmetrical variation, but they have a different peak than the correct response total.

Of all tests, 63% of participants had at least 45 (90%) Correct Responses (HITs and Correct Rejections) on trials with no more than five incorrect responses (False Alarms and/or Misses) (**Figure 4A**). Of these unique subjects, 85% had at least 42 (84%) correct trials (HITs and Correct Rejections; no more than 10 errors), 92% had at least 40 (80%) correct, while less than 3% had 35 or fewer (70%) correct responses (at least 15 errors) (**Figure 4B**).

In the examination of the relationship between HITs and Correct Rejections, there was essentially no correlation (*R*-squared less than 0.001) (**Figure 5A**). When plotting the average number of Correct Rejections versus the number of HITs (**Figure 5B**), or the average number of HITs versus the Correct Rejections (**Figure 5C**), the performance above or below 25 responses noted in **Figure 2C** is clearly explained. The implication of these analyses is that subject strategies have a complex relationship with the manifest performance, including the tendency to respond to more or less than 25 images, which reflects a consistent bias across responses to new and repeated images. Accordingly, the responses of these participants are far from random, and the patterns of their responses presumably represent specific intents, biases, predispositions, or strategies.

Response time distribution

A major issue was the distribution of mean RTs for HITs during the MemTrax CRT paradigm. Only mean RTs for HITs between 0.5 and 2 s were considered for this analysis. The distribution of those RTs shows a clear inverted-U-shaped pattern skewed to the right, and the median RT was 0.89 s (**Figure 6**). Only 63 subjects had RTs for HITs between 0.500 and 0.510 s, six individuals at each millisecond interval, while more than 600 subjects had RTs at each millisecond interval between 0.8 and 0.9 s, a total of 68,550 (24%). The RT cumulative distribution (RTCD) also shows the relationship between RTs and number of tests (**Figure 7A**). For 2 standard deviation limits, 2.2% of the population had RTs faster than 0.647 s while another 2.2% of the population was slower than 1.4 s. Only 1% of the participants had RTs faster than 0.62 s, and the increase of false alarms for subjects responding in this range (see below) suggests that they were sacrificing accuracy for speed. Only 1% of subjects responded slower than 1.57 s (**Figure 7B**), and these subjects also generally had lower correct response percentages and fewer HITs (see below). The fast responders were the only participants who appeared to manifest a speed-accuracy trade-off.

The sharp rising slope of fast RTs between 0.5 and 0.7 s, the rounded peak between 0.7 and 1 s, and the prolonged tail of slow RTs beyond 1.2 s (**Figure 6**) showed the skew of the RTCD in this data. Therefore, the basis of this RTCD

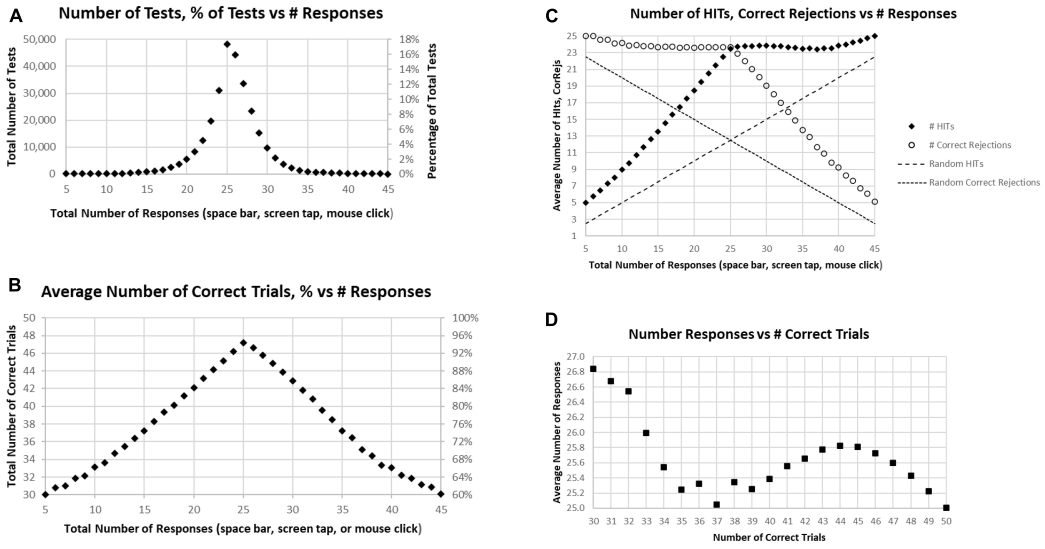

FIGURE 2
(A) Number of tests (left scale) and percentage of tests (right scale) having the specific number of responses. The optimal number is 25, consistent with the peak. **(B)** Average number correct (HITs plus Correct Rejections) of tests (left scale) and percentage of correct responses (right scale). While the number of correct responses ranged from 5 to 45, the optimal number, 25, has only an average number correct equal to 47.2. **(C)** Separated average number of HITs and Correct Rejections plotted for total responses. The pattern is clearly not random (dashed lines); so, when the number of responses is less than 25, the number of HITs declines progressively with a relatively stable number of Correct Rejections, and when the number of responses is more than 25, the number of HITs is relatively stable, with the number of Correct Rejections progressively declining. **(D)** Average number of responses for each number correct, from 30 (60% correct) to 50 (100% correct). Note 25 is optimal, but all averages are above 25 except for 100% correct. Less than 37 correct is associated with an increasing number of responses associated with fewer correct trials.

skew was considered for development of an explanatory mathematical model. Most equations have difficulty accounting for the sharp drop of the fast RTs and the prolongation of the slowed RTs. Consistent with the limited capacity of the activated neurophysiological mechanisms required for efficient engagement of the information processing sequence (Broadbent, 1965), the RTCD must reflect the time needed for information processing to occur in the neural substrates supporting resources in the visual modality. Certain elements relate to STM, and others involve processes in WM, while the slow decline reflects the lack of such resources for processes directed by operations in WM. A variety of mathematical models have been invoked to explain the skewed distribution seen in RTs. However, these models use at least three parameters to describe the skew distribution. For example, the ex-Gaussian distribution uses two Gaussian parameters and an exponential parameter (Dawson, 1988).

To better understand the skewed RTCD, a new perspective was taken to describe this RTCD. Examination of the RTCD (**Figure 7A**) demonstrated a curve similar, but in reverse, to a survival curve, also known as a Gompertz Law exponential hazard function (Hirsch, 1997; Gavrilov and Gavrilova, 2001; Raber et al., 2004). To test the applicability of this mathematical model, a negative normal log of the CD was calculated (**Figure 8A**). This exponential curve explained nearly all the variance: $R^2 = 0.9999$:

Ln(CD) = 263.94 × EXP(−6.682 × RT) (Cumulative Distribution; Response Time)

Percentile = 1-EXP(−263.94*EXP(−6.682*RT))

for RTs for HITs between 0.6 and 1.6 s, with 0.5% of the data above and the same number below these limits. Only 0.2% of the responses during these tests were above 1.8 s, and those RTs were chaotic (**Figure 9A**). Backward calculating this curve to create a reverse exponential distribution (RevEx) and superimposing this curve on the distribution of RTs for HITs shows essentially a perfect fit, considering some statistical noise and a deterioration of performance for RTs greater than 1.6 s (**Figure 8B**). Note that the Rev-Ex model requires two parameters while the ex-Gaussian requires three parameters.

Relationship between correctness of responses and response time

In general, faster RTs were associated with individual tests having above the optimal number of responses (25), with a sharp increase of number of responses for those in the fastest 2% (below 2 standard deviations, 0.64 s), and a progressive decrease of responses with higher RTs, down to an average of 22 responses at 1.5 s. There was a scattering of RTs among the slowest 2% (above 2 standard deviations, 1.4 s) (**Figure 9A**). Of note, apropos to the variation of performance/strategy for

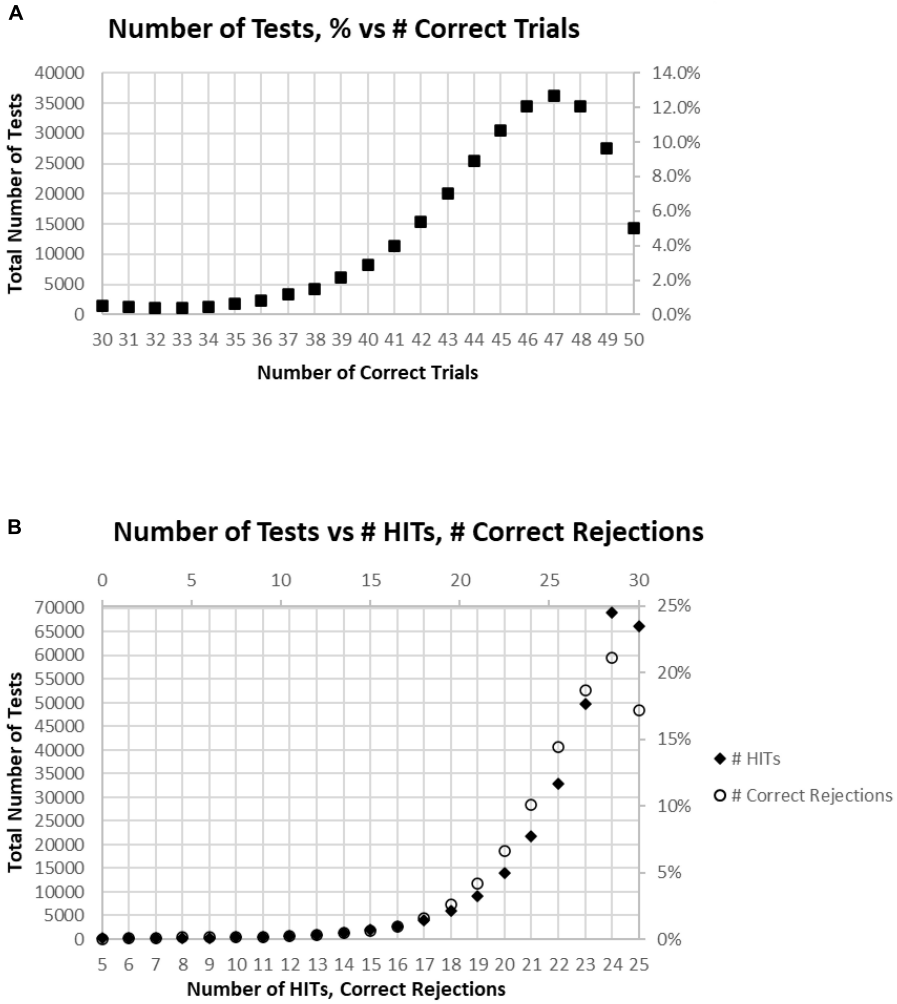

FIGURE 3
(A) Number of tests performed for each number of correct responses. **(B)** Total number of tests broken down to show as HITS and Correct Rejections.

those having more or less than 25 responses, those tests with more than 25 responses were associated with progressively faster RTs from 0.9 s for 25 responses and 0.8 s for 45 responses (Figure 9B). Alternatively, fewer than 25 responses were associated with a progressive slowing of responses to 1.278 s for 11 responses. For the 969 subjects with 5–10 responses, RTs decreased progressively to 1.05 s for only five responses (average of 127 tests).

The most correct performances were associated with RTs of 0.6–1.0 s, with the average number of correct trials for this range being 44–46 (HITs plus Correct Rejections, trials with 2–6 errors) (Figure 10A). Progressively faster RTs from 0.6 to 0.5 s were associated with a rapid deterioration of correct performance to chance, while RTs from 1.0 to 1.5 s were associated with a more gradual deterioration of correct responses to 40 (10 errors). Less than 1% of participants had RTs over 1.5 s, and these subjects had a broad range of correct responses, 30–48 (2–20 errors) (Figure 10A). Importantly, those subjects with perfect scores (0 errors) averaged 0.84 s, with increasing errors associated with progressively slower RTs for HITs, so that the average RT for those subjects having 35 correct trials (with 15 errors) was 1.07 s (Figure 10B). Below this level of performance, those having 30–35 correct trials (with 15–20 errors) had slightly faster RTs, which was associated with the increased variability of performance in this lower 3% of the group.

As noted above, there is a considerable division in behavior for HITs and Correct Rejections. As the data for correct performance is a sum of HITs and Correction Rejections, there is a substantial question of how these measures relate to RT. When RT to HITs was compared only to the number of HITs, there was a closer relationship than with number of responses or total correct trials (Figure 11A). The average number of HITs was consistently at least 20 out of 25 for RTs between 0.5 and

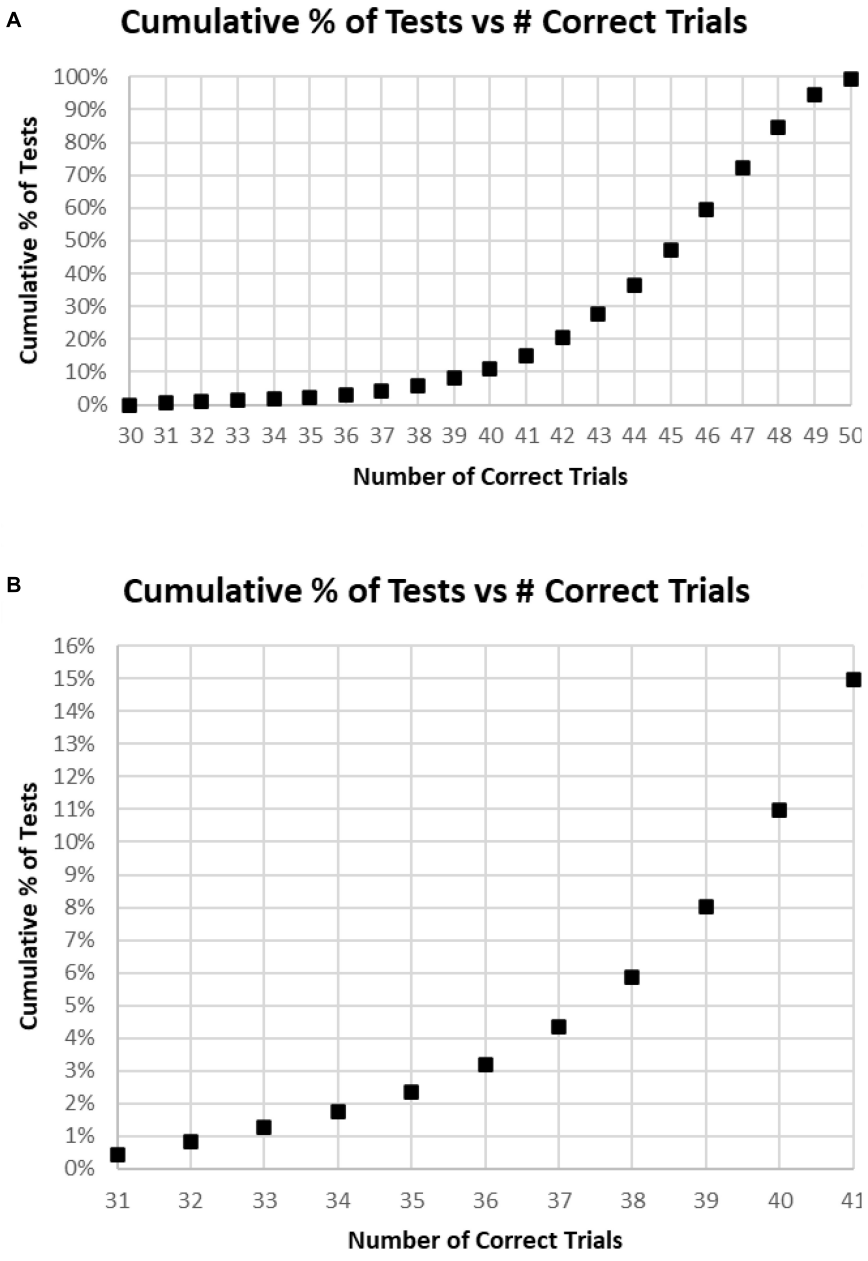

FIGURE 4
(A) Cumulative percentage of tests from 30 correct (60%) to 50 correct (100%). **(B)** Higher resolution of **(A)** to show the percent of tests more precisely for number correct 31–41.

1.4 s. The relationship between HITs and RTs showed that the optimal number of HITs, 25, was associated with a RT of 0.837 s, with a smooth slowing, decreasing HITs to 10 at a response time of 1.3 s (Figure 11B). For the 1,083 tests with only 5–9 HITs, RT was then progressively faster to 1.069 s.

A major factor associated with RT was response bias, the tendency to make fewer than or more than 25 responses (the ideal number being 25). This tendency is most clearly seen when examining the Correct Rejections. The RT had relatively little relationship with Correct Rejection count (Figure 12A). For the 95% of tests with RTs between 0.64 and 1.4 s, the number of Correct Rejections was very stably close to 22. However, for RTs less than 0.640 s, there was a clear, sharp drop in the number of Correct Rejections. Above 1.4 s, there was again a scattered pattern of Correct Rejections with no consistent relationship with RT. When the averages of RT were compared for numbers of Correct Rejections, there was only a slight slowing from the optimal number of 25 at 0.910 s

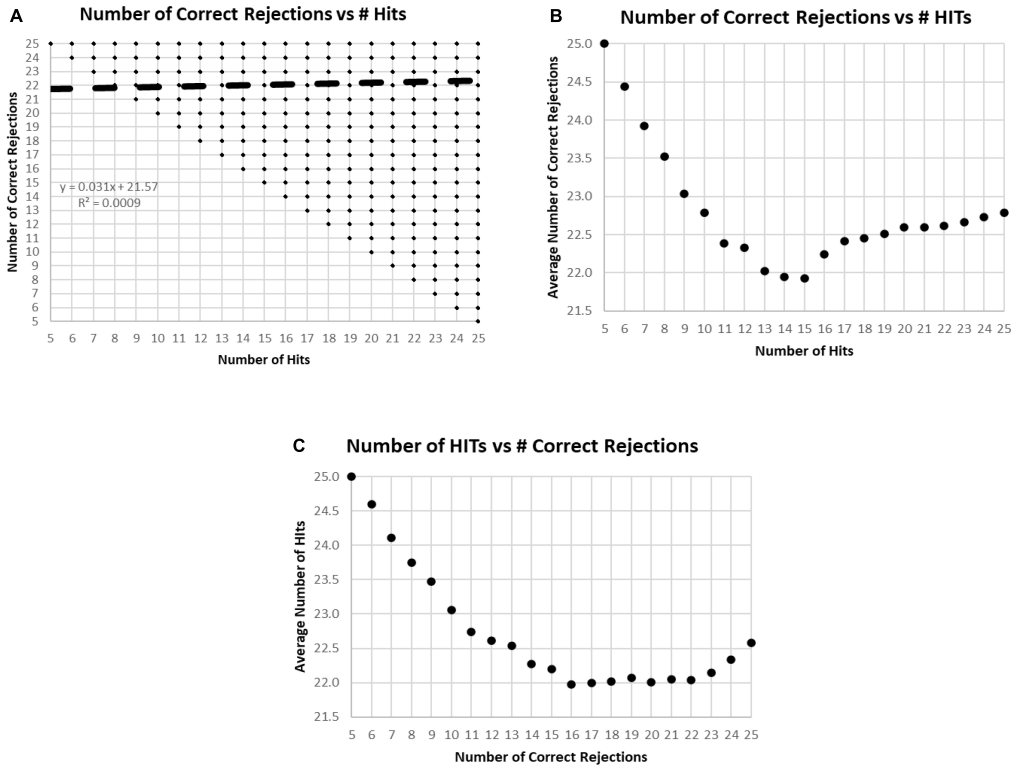

FIGURE 5
(A) Plot of number of Correct Rejections versus number of HITs. The correlation showed essentially no relationship. Among the 282,140 tests, all 231 possible variations of responses were represented. The limitation of five HITs and five Correct Rejections was due to the limitation of the data set to those subjects with at least 60% correct, 30 correct responses. **(B)** Plot of average number of Correct Rejections versus number of HITs. Note the slow decrement of correct rejections with a decrease of HITs from 25 down to 17, at which point, there is a drop of correct rejections, but then below 15 HITs there appears to be a strategy to be more careful have more correct rejections. **(C)** Plot of average number of HITs versus number of Correct Rejections. Note the decrement of HITs from 25 to 22 Correct Rejection, then below 16 Correct Rejections, there is a sharp tendency to have more HITs, which appears to be a strategy to respond more, indiscriminately.

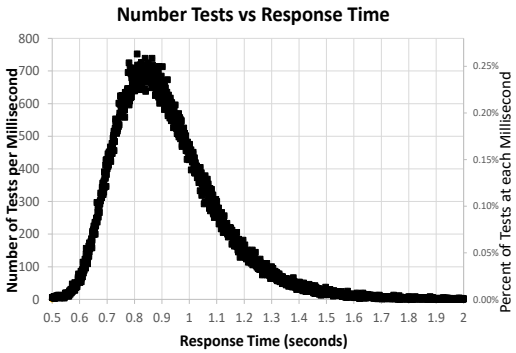

FIGURE 6
Number of tests for each millisecond RT, from 0.500 to 2.00 s, for 282,140 user tests. Note that the number of tests has a skewed distribution.

to around 930 ms for only 15 correct, showing the minimal relationship between RT and Correct Rejections for tests with better performance (Figure 12B). However, for tests with only 5–14 Correct Rejections, there was the progressive shortening of RTs with fewer Correct Rejections again seen. Clearly, the pattern of the relationship between Correct Rejections and RT was very different than the one between HITs and RT (and shown on the same axis to highlight the difference, Figure 13).

Figures 9–12 show the complex relationship between correctness of responses and response tendency to RT. To determine the Pearson correlation between correct responses and RT, the major outliers were removed. Tests with fewer than 10 HITs (1,083), fewer than 15 Correct Rejections (5,400), RT less than 600 ms (1,538), or more than 1.4 s (5,856), and trials with less than 35 correct responses (1,277) were eliminated (total removed = 15,565 = 5%), leaving 266,584 tests. This removal (had minimal effect on the correlations) produced a correlation between RTs and Correct Responses: R^2 = 0.081, while the correlation between RTs and HITs: R^2 = 0.14, was significantly higher. When averaging across RTs for each number of correct responses (35–50) or HITs, 10–25, there was a clear linear progression seen, which is like the curves of Figures 10B, 11B, with a linear regression explaining

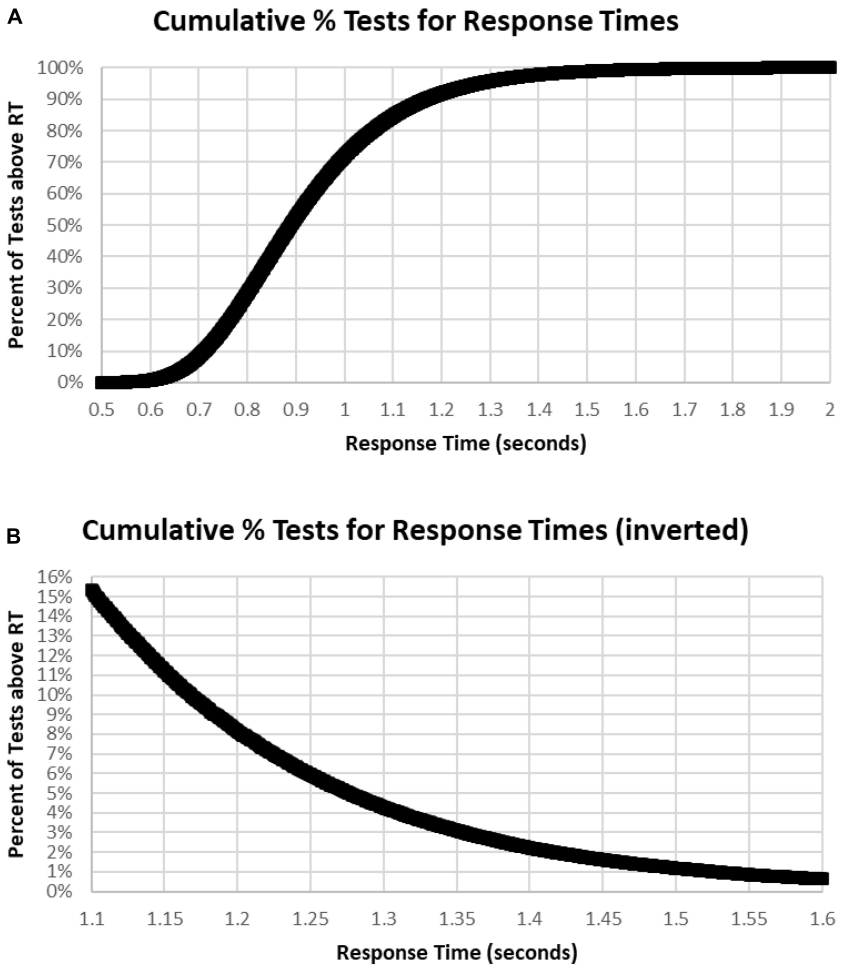

FIGURE 7
(A) Cumulative percentage of tests with respect to RT. Note that level is below 1% until over 0.620 s and 99% had RTs less than 1.570 s. Median RT was 0.900 s, at 50%. **(B)** Inverse of **(A)** at higher resolution to show the slower 15%, more than 1.1 s, and the slower 1%, more than 1.6 s.

essentially all of the variance for 35–50 correct responses and 10–25 HITs, respectively. The clear emergence of this high explanation of the variance indicates that the MemTrax test is measuring important neurophysiological phenomena in visual information processing, but there was a substantial amount of noise when assessing individual subject performances.

Discussion

The present study demonstrated that the MemTrax CRT – an inexpensive and scalable platform – can be efficiently used to obtain a large amount of reliable behavioral data describing learning, memory, and cognition in populations, with important implications for cognitive performance metrics for individuals. By selecting performances meeting non-random criteria and appropriate response characteristics, population distributions of data could be analyzed and compared. The MemTrax CRT data contained measures of correctness, Total Number Correct, HITs, Correct Rejections, False Alarms, and RTs. The first principal finding was that HITs and Correct Rejections did not correlate with each other, meaning that Signal Detection Theory analysis would not apply, and HITs and Correct Rejection accuracy had very different implications for explaining a subject's performance. The second principal finding was that the average RTs corresponded more closely with HITs than overall correctness or Correct Rejections. The third principal finding was that the RT distribution followed a reverse-exponential (RevEx) model requiring only two parameters.

Previous studies have shown effects of age and education on these MemTrax metrics (Ashford et al., 2011, Ashford et al., 2019b). Further, two comparisons with the popular cognitive screening test, the Montreal Cognitive Assessment (MoCA), have shown MemTrax to perform at least as well for distinguishing cognitive impairment from normal function using a more efficient system (Liu et al., 2021), and MemTrax RT

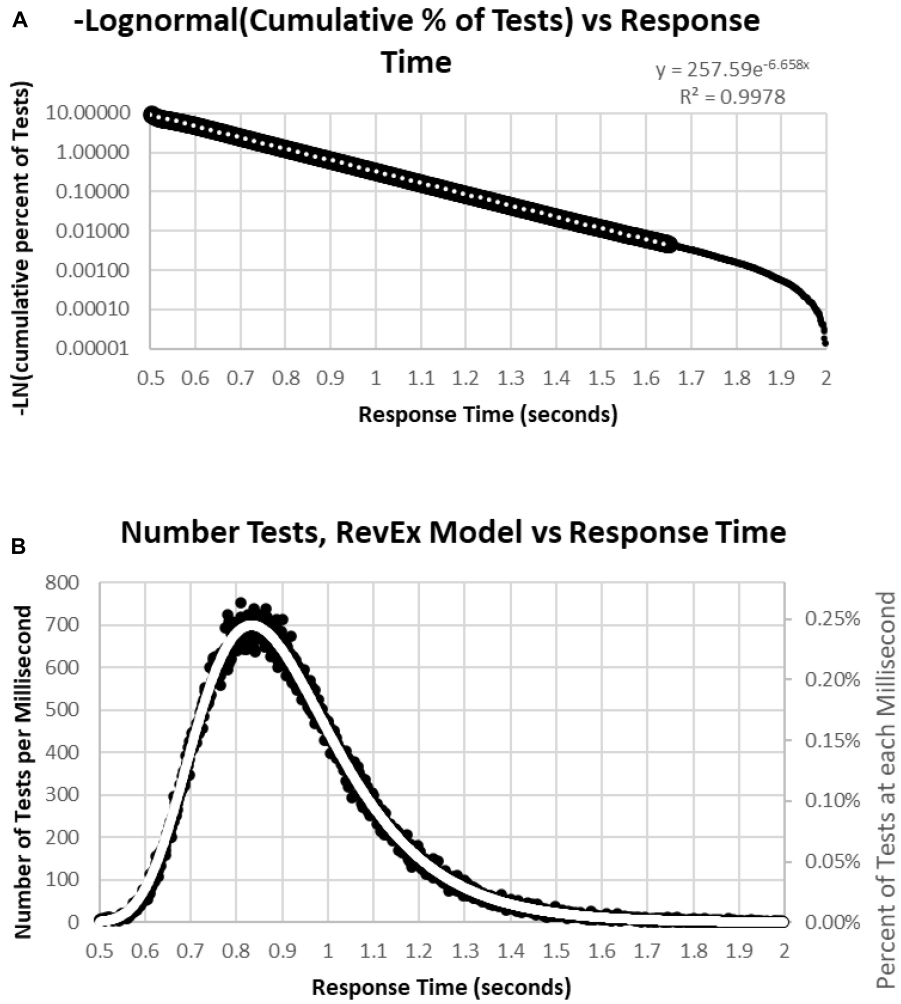

FIGURE 8
(A) Negative natural logarithm of the cumulative percentage of RTs plotted against the RT. The Pearson regression exponential curve explained nearly all the variance between 0.5 and 1.65 s. **(B)** Calculation of exponential curve back to number of RTs. The curve clearly fits the distribution of the RTs. The most responses were at 0.810 s followed by 0.839 and 0.864 s, while the peak of the RevEx model was at 0.833 s.

significantly correlated with six of the eight domains measured by the MoCA, visuospatial, naming, attention, language, and abstraction (van der Hoek et al., 2019). The MemTrax test has also been evaluated using machine learning showing relationships with other health measures (Bergeron et al., 2019). This study extends the findings of these and other prior studies using a very large population. The large population, with data selected from 344,165 presumed-unique, anonymous users, provides performances of nearly every possible variety, and reflects the behavioral diversity of the online population, which is becoming more and more representative of the whole population. And the large number of users and repeat uses reflects the degree to which this test is highly engaging. These analyses showed that both HIT responses, Correct Rejections, and RTs for those HITs to stimuli repeated can be measured and used in large projects.

Response accuracy

Of specific interest were the analyses of correct responses (HITs and Correct Rejections) and incorrect responses (False Alarms and Misses) from 282,140 users who performed this CRT paradigm within acceptable levels. The tests selected for analysis were from first-time users in which at least 30 out of 50 trials were correct, which indicated non-random performance. Further, tests were selected from which mean RTs for HITs on the correct trials were between 0.5 and 2.0 s, indicating reasonable efforts by the users. The requirement for at least 30 correct trials assured that there would be at least five HITs or five Correct Rejections on a test.

An important finding was the lack of a correspondence between HITs and Correct Rejections. Obviously, overall correct performance is an addition of HITs and Correct Rejections, so

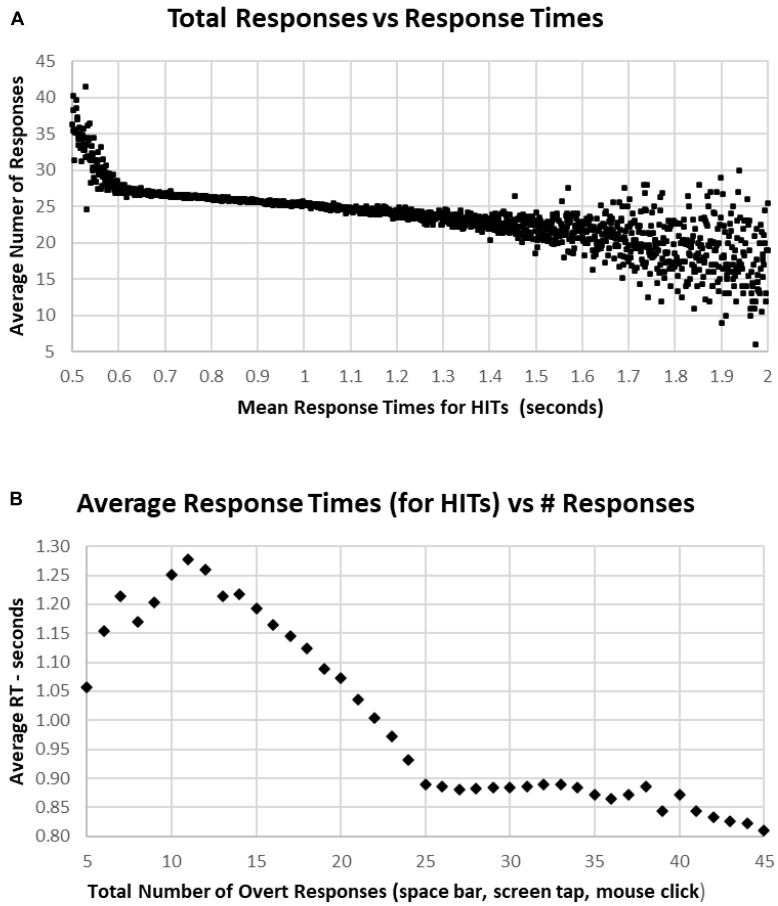

FIGURE 9
(A) Average number of responses for each HIT RT, showing that there is an increase in the average under 0.600 s, while there is an increase of variability for RTs longer than 1.5 s. The discordance between number of responses and decreased RT below 0.6 s is associated with a strategy to respond more quickly, but with less discrimination. **(B)** Same data, averaging RTs by number of responses. Note sharp change of slope below the 25-response mark, with progressive slowing until 10 or fewer responses. But there is a stable level of RTs with an increased number of responses, suggesting that by increasing the number of false alarms, that this component of accuracy was sacrificed for speed.

each will correlate with total correct. But when looking across the whole population, these two metrics had no correlation with each other (Figure 5A). Accordingly, these two independent metrics appear to represent distinct phenomena, reflecting the information processing challenges of the test and the strategy for optimizing the balance between accuracy and speed. The performance of a HIT requires recognition of a prior image, successful access of STM, and the decision to respond affirmatively. However, if there is uncertainty about the recognition or confusion with a similar image which is new, a blurring of episodic memory, a response will be a False Alarm. Because of the constant variation of stimuli and categories, HITs will reflect the level of certainty about a repeated image. Alternatively, a False Alarm will reflect a bias to respond with a lower level of certainly. Thus, the number of correct responses does not reflect a "signal detection," a degree of differentiation and a response bias. Instead, HITs reflect a recognition threshold, and False Alarms represent an error threshold. The response strategy can then reflect an effort to respond only when there is a high level of certainly or to respond to avoid missing any targets.

With respect to interpreting MemTrax performance, the occurrence of Miss errors and False Alarm errors provides information which must be managed when interpreting the MemTrax performance metrics. Understanding precise relationships between correct and incorrect responses within the MemTrax test provides information to improve its applicability to screening and assessment of learning, memory, and cognitive functions in clinical settings.

Response time distribution

Of particular interest was the skewed distribution of RTs for HITs. Analysis of the MemTrax data, at least for this population, showed a distribution with a skewed slope for

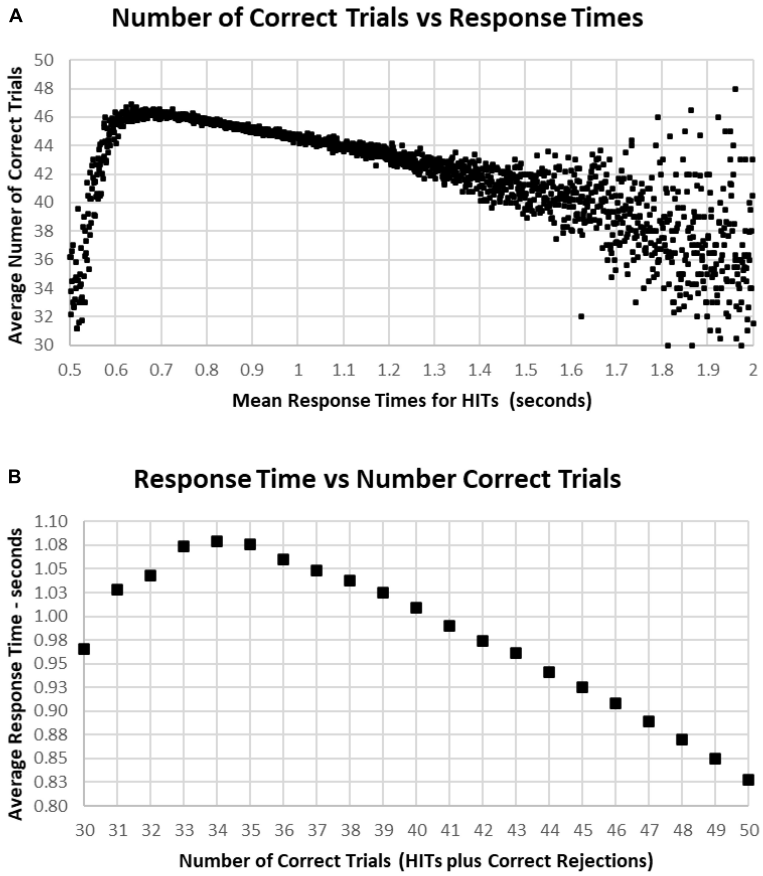

FIGURE 10
(A) Average number of correct responses for each RT. The most correct responses occurred at an RT of about 0.650 s with about 46 correct (90%). The average number correct fell sharply with faster RTs and more slowly with slower RTs, until an increased variability is seen, largely due to the smaller number of subjects with RTs slower than 1.4 s. **(B)** Again, same data averaging RT by number of correct responses. Note that 100% correct (50 correct responses) is associated with an RT of 0.828 s. With a decreased number of correct responses, there is a progressive slowing of RT until an RT of 1.079 s at 34 correct (68%), but lower numbers of correct responses again show the discordance of RTs and performance with poorer levels of performance.

averaged RTs for HITs, which was very steep for rapid RTs and particularly long for slower RTs. The analysis of the data from the present study showed an exponential function, the reverse of a survival curve, RevEx, could fully explain the variance of the RT distribution skew. This exponential function can be interpreted as a requirement for doubling the processing power for every 100 ms of decrease in RT. This pattern suggests that the nervous system must double the resources expended to analyze and respond to the complex information in the presented stimulus for each 100 ms unit of time faster, or conversely, halving the neuronal resources would slow the RT by 100 ms. This exponential increase of resources required for shortening RT explains why it is essentially impossible to respond faster than 0.5 s and maintain correct responses.

A variety of theoretical explanations have been invoked to explain this skewed distribution for RTs across many paradigms (Ratcliff et al., 2016; Moret-Tatay et al., 2021). However, the RevEx model provides a different and direct reflection of the massive, reciprocal processing capability of the brain, without reliance on concepts of a series of processing stages. This insight is consistent with neurophysiological analyses of neuron responses showing simultaneous neuronal processing across broad reciprocally connected cortical and brainstem regions (Ashford and Fuster, 1985; Coburn et al., 1990; Ashford et al., 1998a) and cannot be deduced from IPMs proposing a series of processing steps. This perspective of RTs may have important applications for identifying contributors to normal and abnormal processing. Further, the slowing of RT with neurodegeneration can be linked to the loss of neural network resources, as occurs in AD (Gordon and Carson, 1990; Ratcliff et al., 2021).

This skewed pattern of these RTs has a mathematical relationship to the survival curve of essentially all living things discovered by Benjamin Gompertz in 1825, referred to as the Gompertz Law of Aging (Hirsch, 1997; Gavrilov and Gavrilova, 2001; Ashford, 2004; Raber et al., 2004; Ashford et al., 2005),

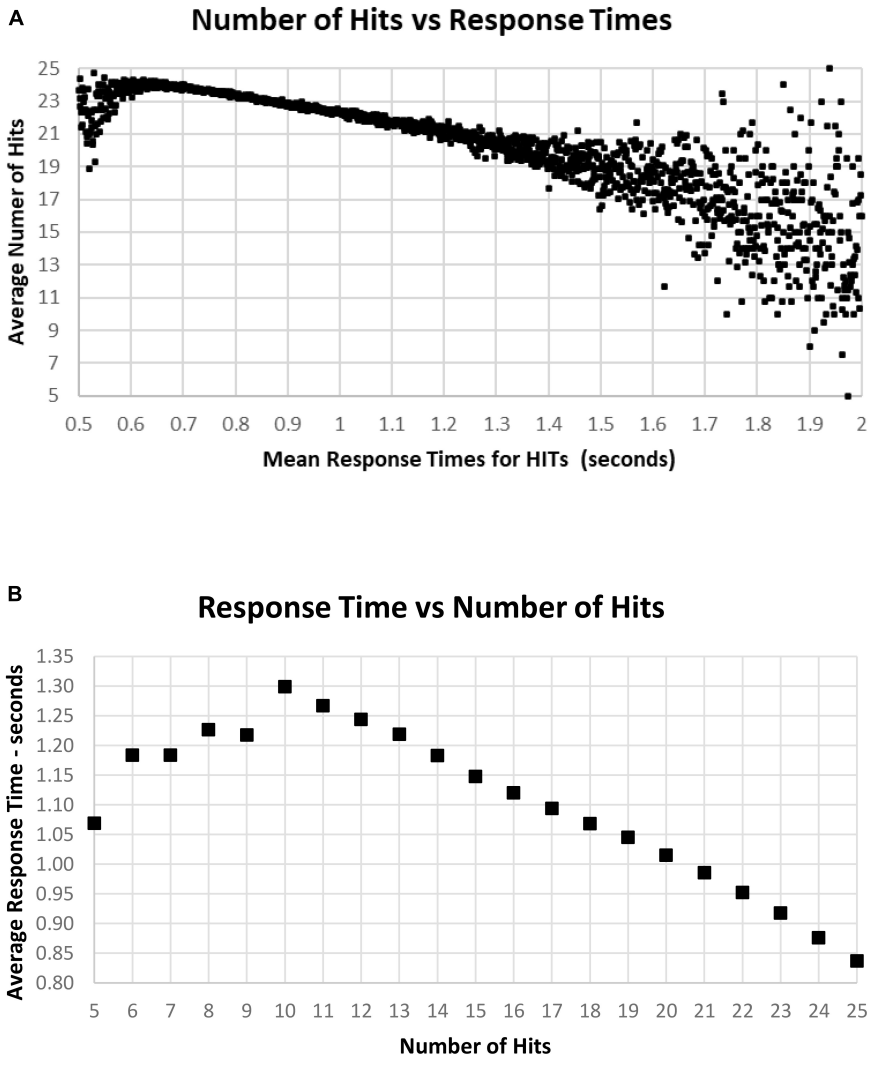

FIGURE 11
(A) Average number of HITs for each RT, showing the HIT component of correct responses. Note that the most rapid average RT is about 0.650 with an average of 24 HITs. There is a relatively small number of faster responses, most with over 21 HITs. Beyond 1.4 s, there is again a smaller number of tests, and the wide distribution of responses reflects that smaller number. **(B)** Same data as **(A)**, showing the optimal number of HITs, 25, is associated with an average RT of 0.837 s, with a progressive slowing associated with fewer HITs to an RT of 1.299 s at 10 HITs. With a smaller number of HITs, there is a faster RT, reflecting a lower level of discrimination.

just in reverse. The survival curve of all living beings is related to an exponentially increasing rate of mortality with age. This "fact of life" has been interpreted as describing an exponentially increasing rate of failures across massively redundant systems; but by contrast, the Weibull curve applies to mechanical systems, not living systems (Gavrilov and Gavrilova, 2001). The exponential increase of failures occurs in a progressively more rapidly dwindling population that leads to the appearance of a sharp rate of population decline in extreme age. These MemTrax data showed that the skewed RT distribution curve is most efficiently explained by an exponential increase of demand for information processing resources to shorten RT, a reverse-exponential (RevEx) function. The RevEx interpretation accurately describes how reducing resources in a working, learning, memory, and cognitive neurophysiological system, or information processing failures, slows RT, while implicit or explicit recruiting of additional resources to analyze and respond to the incoming information leads to a more rapid RT (Kahneman, 1973). Critically, exponentially increasing recruitment of resources initially shortens RT but finally exhausts the neural resources available for processing, so accurate RTs are nearly impossible to achieve for less than about 0.6 sec in the MemTrax CRT. The RevEx model provides a skewed RT distribution with two easily derived parameters. This curve can be used as a reference continuum describing the scale of severity against which individual responses can be compared

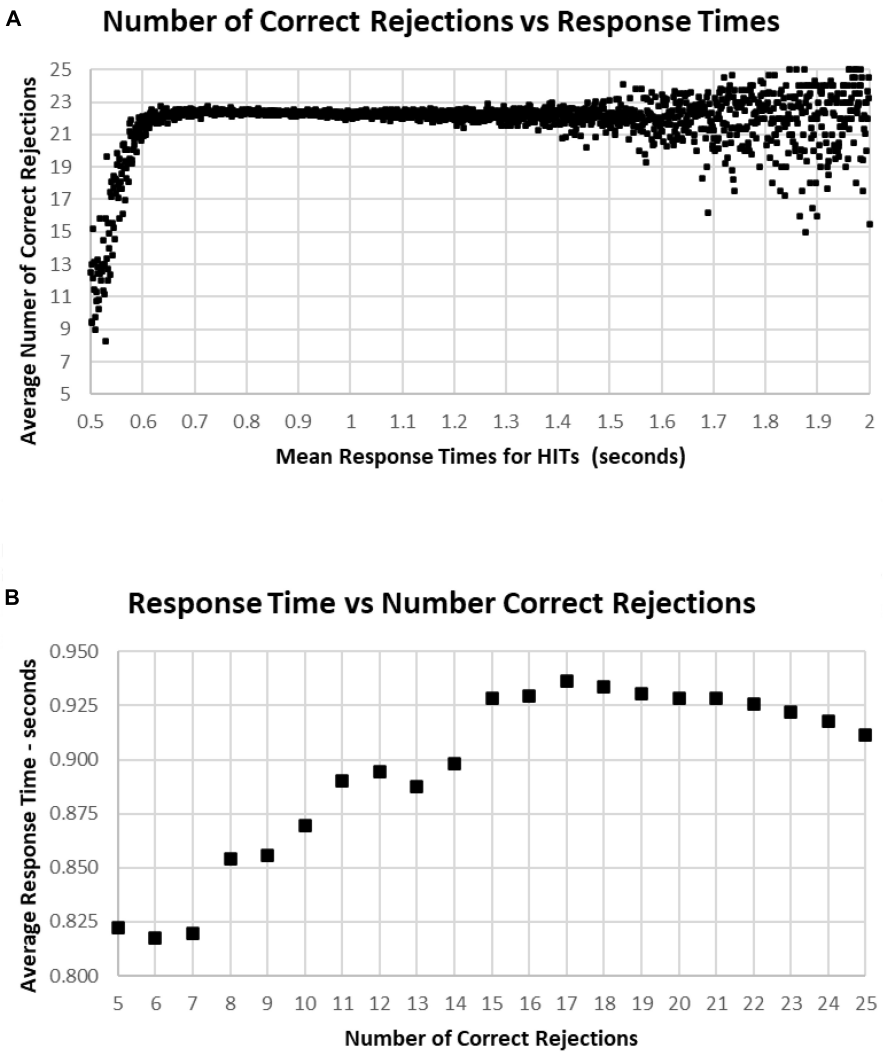

FIGURE 12
(A) Average number of Correct Rejections for each RT, showing the Correct Rejection of component of correct responses. Note that that over an RT of 0.650 s, there is essentially no relationship of Correct Rejections and RT, with about 22 Correct Rejections occurring on the average. By contrast, for faster RTs, there is a steep speed/accuracy trade-off between speed and accuracy of Correct Rejections. Again, the small number of tests above 1.4 s show the dispersion with fewer tests, but there is no indication of a different slope. **(B)** Again, same data as **(A)**, showing an RT of 0.911 s for 25 Correct Rejections and a slight increase of RT down to 15 Correct Rejection, but there are faster RTs with lower numbers of Correct Rejections, which reflects the alteration of strategy (less inhibition) associated with this aspect of poor performance on the MemTrax test.

and is likely applicable in all such information processing studies examining RT.

Relationship between performance correctness and response time

Examining various response correctness patterns in relationship to the distribution of RTs, suggests that part of the processing reflected variations in error-inducing strategies. The early part of the RT distribution appears to reflect a bias to respond (more False Alarms) that reduces time to process information and leads to more errors thus shortening the RTs for HITs. As the strategy becomes less about distinguishing between new and repeated images and more about rapid response, showing a speed/accuracy trade-off in this narrow range, with the average number of Correct Rejections dropping to 9. However, with slower RTs there is a clear relationship to decrease of HITs, reflecting the failure to either encode or recognize repeated images and taking exponentially longer to process the visual information. This analysis is particularly relevant for identifying progressive loss of synaptic connections, as seen in aging and AD (Gordon and Carson, 1990; Ratcliff et al., 2021), which are accompanied by a retrogenesis of the

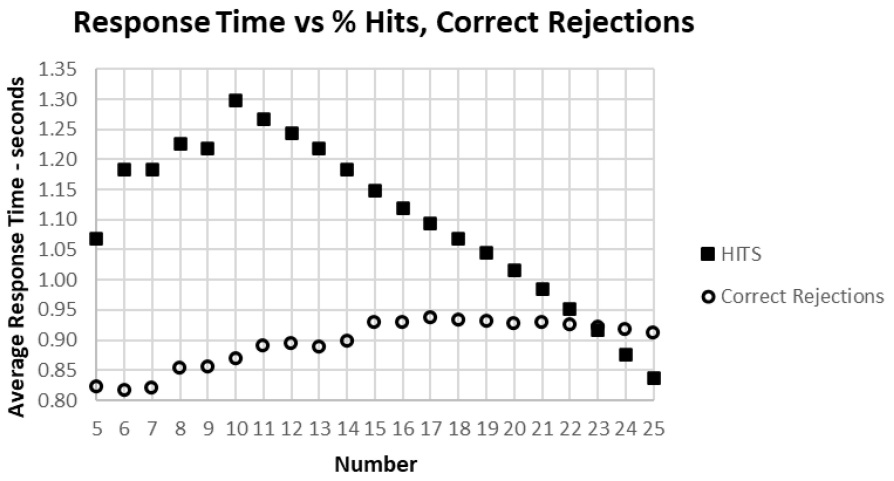

FIGURE 13
The average correct response times broken down into True Positive and True Negative groups. Note that the number of True Positive responses has a clear linear relationship with the average response time. The True Negative choices have very little effect when there are more than 15 (less than 10 false positive responses), but they have a negative relationship with RT below 15, suggesting that the increased number of false responses is related to making faster incorrect responses.

neurons (Ashford et al., 1998b; Ashford and Bayley, 2013) and changes in control of executive function (Yesavage et al., 2011). These effects likely alter neuroplasticity and the efficiency of the information processing sequence and the resources available for encoding and recognizing item information over the duration of the task (Ashford and Jarvik, 1985; Coleman and Yao, 2003; Ashford, 2019). Accordingly, each 50% loss of neural processing capacity would slow RT by about 100 ms.

The overall balance of HITS and Correct Rejections and the interaction with RT play critical roles in strategy and analytic ability. The False Alarms metrics were not associated with RT, except at the shortest 1% of RTs, where increasing False Alarms were associated with a speed/accuracy trade-off. At the fastest RTs, there is a likelihood that the participant was utilizing a strategy that made decisions so rapidly that adequate analysis of the image was not occurring. However, at more usual and slower RTs, False Alarms, which are unrelated to RT, likely represent the failure of response inhibition, responding to a new stimulus falsely processing it as a repeated stimulus. Consequently, False Alarms without a speed/accuracy trade-off likely represent failure of frontal lobe inhibitory function, as has been seen clinically in patients with diagnoses of fronto-temporal dementia (JWA, clinical observation). Alternatively, an increased number of Misses was related to a progressive slowing of RT, which likely represents a slowing of the occipital-temporal-hippocampal visual system to process information, with increasing difficulty recognizing repeated visual information and generating a recognition response. The latter condition explains the impairment of patients with mild cognitive impairment, such as AD (JWA, clinical observation), and other conditions affecting the temporal lobe.

An additional finding was the low correlation between HITs and RTs across the population, explaining 14% of the variance (the opposite of a speed/accuracy trade-off – more HITs was related to faster RTs); but when RTs were averaged for specific HIT-rates, there was a nearly perfect relationship between decreasing HITs and increasing RT, with a loss of about 30 ms per additional miss from 25 HITs to 10 HITs. The relationship between RT and average HIT-rates explained nearly 100% of the variance of the averages, suggesting a significant phenomenon. Accordingly, about 85% of the variance in the relationship between HITs and RTs was related to variables aligned with the state of the individuals at the time of testing. In principle, this individual variance could be reduced by repetitions of the MemTrax test, which can be done essentially without limit, and frequent administrations of the MemTrax test over time. Monitoring the relationship between HITs and RTs could accurately assess changes in the function of patients, related either to disease progression or treatment benefits.

The present analysis indicates that HITs, the instances in which a repeated stimulus is recognized, has a relationship with the response speed – not the tendency to under- or over-respond. Thus, False Alarms alter the relationship between RTs and HITs. The relationship between total number of responses and more subjects with faster RTs in **Figure 10A**, descending from 1.5 to 0.6 s, an improvement of speed with more responses, is not due to a speed/accuracy trade-off; but this relationship is complex and related to a portion of participants over-responding to new stimuli. However, the increased correlation after accounting for the over-response tendency indicates that there is a significant positive relationship between RTs and correct responses, not a speed/accuracy trade-off.

The time to respond (RT) to stimuli has been used as a dependent variable to study effects of non-clinical and clinical phenomena on learning, memory, and cognitive functions. Complex picture recognition has been particularly useful for studying medial temporal lobe function (Koen et al., 2017) and neural responses in the human hippocampus are related to episodic memory (Suzuki et al., 2011; Wixted et al., 2018). A cross-species study using this strategy showed that pigeons and monkeys were able to recall complex pictures moderately well, but that humans remembered pictures so well that it was necessary to utilize kaleidoscope images to test the limits of human memory and recall and recognition (Wright et al., 1985).

Information processing models provide a neurological and psychological structure to conceptualize distributions of behavioral indices which occur during a subject's performance of a task (Broadbent, 1965). A stimulus presented on a trial interacts with and engages numerous processes in the brain that sense and provide a rapid, modality-dependent analysis of the physical parameters of that stimulus. This initial sensory analysis engages attention and temporarily represents this stimulus in limited capacity STM, for determination of whether that information has been presented previously. If the stimulus is analyzed as being novel, then the information about that stimulus is transduced, integrated, associated, and consolidated with other items previously consolidated into the massive capacity memory storage system, LTM (Atkinson and Shiffrin, 1971) for later use. And it is the initial presentation in which these processes are occurring, with activation of the hippocampus, not during the later recognition (Suzuki et al., 2011). Occurrences in STM can interact with processes directed by operations in WM, a space where these events can be manipulated (Baddeley et al., 2019).

Instructions provided to the individual before the task began directed the information processing operations to execute cognitive mechanisms addressing those events in STM that satisfied task demands on a trial. Occurrences in STM also engage processes that consolidate this information and associate and integrate it with information previously stored in LTM. LTM consists of an associative neural network that inter-relates all items in LTM. This information in LTM is continuously recalled and integrated with that in STM to support perceptual stability.

Long-term memory is divided into declarative and non-declarative subcomponents. Declarative, also referred to as explicit memory, refers to information stored in LTM which can be intentionally recalled into STM, where that memory trace can be retained for seconds or minutes, but STM capacity is severely limited by exposure to additional information. A person can intentionally direct those operations in WM to execute processes that maintain the quality and distinctiveness of this occurrence in STM, but only for a limited duration. Information must be transferred into LTM systems for recognition or recall beyond the STM capacity.

TABLE 1 Tabulated data for 282,140 on-line MemTrax users, with percentiles (%iles).

%C	#C	%ile	# HITs	%ile	#CRs	%ile	RT	%ile
60	30	0.30%	9	0.30%	9	0.30%	0.5	100.00%
62	31	0.50%	10	0.40%	10	0.50%	0.6	99.20%
64	32	1.00%	11	0.50%	11	0.70%	0.7	91.40%
66	33	1.40%	12	0.70%	12	0.90%	0.8	71.60%
68	34	1.80%	13	0.90%	13	1.10%	0.9	47.50%
70	35	2.30%	14	1.20%	14	1.50%	1	28.20%
72	36	2.90%	15	1.70%	15	1.90%	1.1	15.60%
74	37	3.70%	16	2.30%	16	2.60%	1.2	8.30%
76	38	4.90%	17	3.30%	17	3.50%	1.3	4.40%
78	39	6.40%	18	4.80%	18	5.10%	1.4	2.30%
80	40	8.60%	19	6.90%	19	7.70%	1.5	1.20%
82	41	11.50%	20	10.10%	20	11.90%	1.6	0.60%
84	42	15.50%	21	15.10%	21	18.60%	1.7	0.30%
86	43	20.90%	22	22.80%	22	28.60%	1.8	0.20%
88	44	28.00%	23	34.50%	23	43.10%	1.9	0.10%
90	45	37.10%	24	52.10%	24	61.70%	2	0.00%
92	46	47.90%	25	76.60%	25	82.80%		
94	47	60.10%						
96	48	72.90%						
98	49	85.10%						
100	50	94.90%						

Behavioral patterns during these tests may separate healthy individuals from those with memory declines produced by mild cognitive impairment (Stark et al., 2013) and AD (Ashford et al., 1989; Ashford, 2008). This memory loss occurs 5–10 years before dementia diagnosis associated with AD (Tierney et al., 2005). AD impairs recognition of complex pictures after even a brief delay. This rapid loss of perceived information may reflect effects that AD has on neurological structures subserving memory, specifically, impairment of neuroplasticity (Ashford and Jarvik, 1985; Ashford, 2019). Distinguishing different modes of processing may produce data that improves clinical classification of various aspects of dementia and AD.

Response time during performance of a CRT has been used to study effects of AD on learning, memory, and cognition. Simple reaction time to stimuli is relatively preserved in AD patients with mild impairment, while choice reaction time to difference between stimuli is adversely affected (Pirozzolo et al., 1981). AD patients show substantial slowing of RT in cognitive tasks (Mahurin and Pirozzolo, 1993) requiring this maintenance of information in STM during testing. Extensive study of RTs to different types of stimuli in the elderly has shown a general proportional linear increase in RT toward those stimuli, with a disproportionate deterioration of those RTs related to memory function (Poon and Fozard, 1980; Bowles and Poon, 1982; Hines et al., 1982; Myerson et al., 1990; Yesavage et al., 1999; Ishihara et al., 2002). Consequently, these MemTrax modifications of the CRT paradigm could be of considerable utility for addressing within- and between-trial and test-retest variation that enables tracking effects that pathology has on learning, memory, and cognitive function. Evaluating such functions with computer testing can add considerable precision for early detection of clinical phenomena when the impairment is still mild along the continuum to later and more severe states.

Similar tests administered in-person, the Continuous Visual Memory Test (Larrabee et al., 1992) and the Continuous Recognition Memory test (Fuchs et al., 1999), have already been shown to have construct validity. Of note, the Continuous Recognition Memory test shows the same dissociation of HITs and Correct Rejections shown for these MemTrax data. Substantial enhancement of the applicability of MemTrax can be achieved by analyzing the several MemTrax variables and establishing their precise relationships with respect to externally obtained data and integration with other systems such as is being conducted by the Brain Health Registry (Mackin et al., 2018; Weiner et al., 2018; Cholerton et al., 2019) and factor analysis with respect to the presence and severity of organic brain dysfunction and dementia (Larrabee, 2015; Ratcliff et al., 2021). This study has shown the potential utility of the MemTrax on-line CRT for gathering information about learning, memory, and cognitive status of users. Preliminary analyses of data from the French company HAPPYneuron and the Brain Health Registry have shown similar results, indicating the generalizability of these data.

Limitations

The MemTrax data analysis presented here is from anonymous users in a convenience sample, and therefore cannot be considered validation for any specific purpose. However, the data do clearly show a distribution of responses consistent with prior studies which have included verified data. Therefore, the data and analysis provided here is likely an acceptable approximation of what would be expected in a representative sample of the general population. **Table 1** provides the tabulated data and percentiles from this anonymous group and provides precision measures to support the published studies showing the validity of MemTrax.

Further analyses are needed to determine how numerous factors, including age, sex, education, apolipoprotein-E and other relevant genetic factors, and clinical conditions relate specifically to the MemTrax parameters across numerous populations (Bergeron et al., 2019; Zhou and Ashford, 2019). MemTrax analysis with "machine learning" can further and more definitively classify cognitive function (Bergeron et al., 2020).

MemTrax data sets particularly include all the RTs for each subject's response and analysis of intraindividual variability in RT may also represent an important indicator of performance (Tse et al., 2010; Kennedy et al., 2013; Cousineau et al., 2016). While individual RTs can be easily and simply analyzed for each subject and then related to the RevEx model, additional analyses are needed to determine an individual's level of cognitive function or dysfunction more precisely.

In the MemTrax CRT, there is a variable lag between initial and repeated presentations, which can affect memory encoding (Hockley, 1982; Ashford et al., 2011). The degree of that effect, including the number of intervening items between initial and repeat presentations as well as the position of the repeat in the 50-item continuum, was not analyzed here, but this metric can be assessed as was previously shown (Ashford et al., 2011). Further, there are five items, one from each of the five categories, repeated a second time, and the degree of strengthening of the encoding of the doubly repeated items can be assessed (Hintzman, 2016). Advancing the analytic development of this CRT paradigm may lead to even more powerful assessments.

Given the global accessibility to the internet, there is essentially no verifiable information about the subjects with this isolated web-based testing that can be used as additional independent variables. For example, when asked to provide year of birth, of 344,165 presumed unique individuals who completed a test only 26,834 provided year of birth and even this information could not be independently verified in this study, though this factor was available from other studies of MemTrax and did show an age effect (Ashford et al., 2019b). Accordingly, select demographic and clinical data must be obtained through other means to further examine epidemiological effects on

data during CRTs and establish clinical utility. Data from the Brain Healthy Registry, which provides MemTrax as one of its assessment tools (Cholerton et al., 2019; Nosheny et al., 2020), has demographic and cognitive function information for comparison, and such analyses are planned. As noted above, MemTrax variables percent correct on RT significantly correlated with six of eight MoCA domains (van der Hoek et al., 2019), and adding HITs and correct rejections and with different images and different performance instruction, numerous other cognitive and cortical domains could be assessed with this platform.

The data presented here cannot be construed as representing a properly sampled population. With no clinical information, there was no clinical validation; thus, there was only a suggestion of what likely clinical indices would be. For example, 2.2% of the population (consider 2 standard-deviations) had less than 70% correct, 15 HITs, 15 Correct Rejections and RT slower than 1.4 s. For a cut-point for less impairment, 6.7% of the population (consider 1.5 standard-deviations) had less than 78% correct, 18 HITs, 18 Correct Rejections, and RTs slower than 1.23 s. For a cut-point for less impairment, 15.7% of the population (consider 1 standard-deviation) had less than 84% correct, 20 HITs, 20 Correct Rejections, and RTs slower than 1.1 s. Data from **Table 1** could be used to estimate performance levels below 1 or 1.5 deviations below the mean. Tests with fewer than 15 Correct Rejections (more than 10 False Alarms) can be considered invalid and may represent frontal-lobe dysfunction.

Conclusion

Prior studies on mild cognitive impairment (Koppara et al., 2015; Ratcliff et al., 2021) and AD (Gordon and Carson, 1990; Schumacher et al., 2019) have already shown the potential of the CRT approach for assessing disorders of learning, memory, and cognition. However, the analysis of the MemTrax data provided a different perspective on cognitive function than has been based on SDT methods alone and provided a novel perspective for understanding cognition and memory, revealing levels of complexity beyond the traditional paradigms. Moreover, MemTrax has been shown to provide at least as much information as the Montreal Cognitive Assessment (MoCA) (van der Hoek et al., 2019; Liu et al., 2021). The precision provided by MemTrax also suggests that MemTrax could improve the specification of the severity of cognitive impairment in early phases of AD (Ashford et al., 1995, Ashford et al., 2019a; Ashford and Schmitt, 2001; Ashford, 2008), as well as the pace of change over time with repeat testing. By assessing performance metrics and RT, MemTrax also has the capability to screen for many varieties of cognitive impairment and would be an ideal tool for use in the elderly US population for the Medicare Annual Wellness Visit (Ashford et al., 2022). However, more testing in clinical populations is needed to implement on-line testing for broad clinical applicability and widespread screening.

Data availability statement

The raw data supporting the conclusions of this article will be made available by the authors, without undue reservation.

Ethics statement

The studies involving human participants were reviewed and approved by Internal Review Board (IRB), Stanford University. Written informed consent from the participants' legal guardian/next of kin was not required to participate in this study in accordance with the national legislation and the institutional requirements.

Author contributions

JA did the analyses, produced the figures, and wrote the first draft of the manuscript. JC worked extensively on developing the presented concepts. SA worked with JC on the concepts. MB provided guidance, writing, and extensive editing. PB provided expert consultation on the psychological test theories, including writing and editing. CA implemented the CRT at https://memtrax.com, managed the website, and recruited all the users who took the test. All authors contributed to the article and approved the submitted version.

Conflict of interest

Author CA is the sole owner of MemTrax, LLC, which manages the MemTrax program, and a fee is charged for its use. Other authors (including CA's father, JA) are unpaid consultants to MemTrax and have no more than that potential conflict of interest pertaining to the manuscript.

The remaining authors declare that the research was conducted in the absence of any commercial or financial relationships that could be construed as a potential conflict of interest.

Publisher's note

References

Anders, R., Alario, F. X., and Van Maanen, L. (2016). The shifted Wald distribution for response time data analysis. *Psychol. Methods* 21, 309–327. doi: 10.1037/met0000066

Ashford, J. W. (2004). APOE genotype effects on Alzheimer's disease onset and epidemiology. *J. Mol. Neurosci.* 23, 157–165.

Ashford, J. W. (2008). Screening for memory disorders, dementia, and Alzheimer's disease. *Aging Health* 4, 399–432.

Ashford, J. W. (2019). The dichotomy of Alzheimer's disease pathology: Amyloid-beta and tau. *J. Alzheimers Dis.* 68, 77–83. doi: 10.3233/JAD-181198

Ashford, J. W., Atwood, C. S., Blass, J. P., Bowen, R. L., Finch, C. E., Iqbal, K., et al. (2005). What is aging? What is its role in Alzheimer's disease? What can we do about it? *J. Alzheimers Dis.* 7, 247–253.

Ashford, J. W., and Bayley, P. J. (2013). Retrogenesis: A model of dementia progression in Alzheimer's disease related to neuroplasticity. *J. Alzheimers Dis.* 33, 1191–1193. doi: 10.3233/JAD-2012-121124

Ashford, J. W., Coburn, K. L., and Fuster, J. M. (1998a). "Functional cognitive networks in primates," in *Fundamentals of neural networks: Neuropsychology and cognitive neuroscience*, eds R. W. Parks and D. S. Levine (Cambridge, MA: The MIT Press).

Ashford, J. W. (1998b). "Neurobiological," in *Advances in the diagnosis and treatment of alzheimer's join to disease*, eds V. Kumar and C. Eisdorfer (New York, NY: Springer Publishing Company).

Ashford, J. W., and Fuster, J. M. (1985). Occipital and inferotemporal responses to visual signals in the monkey. *Exp. Neurol.* 90, 444–466.

Ashford, J. W., Gere, E., and Bayley, P. J. (2011). Measuring memory in large group settings using a continuous recognition test. *J. Alzheimers Dis.* 27, 885–895.

Ashford, J. W., and Jarvik, L. (1985). Alzheimer's disease: Does neuron plasticity predispose to axonal neurofibrillary degeneration? *N Engl. J. Med.* 313, 388–389.

Ashford, J. W., Kolm, P., Colliver, J. A., Bekian, C., and Hsu, L. N. (1989). Alzheimer patient evaluation and the mini-mental state: Item characteristic curve analysis. *J. Gerontol.* 44, 139–146.

Ashford, J. W., and Schmitt, F. A. (2001). Modeling the time-course of Alzheimer dementia. *Curr. Psychiatry Rep.* 3, 20–28.

Ashford, J. W., Schmitt, F. A., Bergeron, M. F., Bayley, P. J., Clifford, J. O., Xu, Q., et al. (2022). Now is the Time to improve cognitive screening and assessment for clinical and research advancement. *J. Alzheimers Dis.* 87, 305–315. doi: 10.3233/JAD-220211

Ashford, J. W., Schmitt, F. A., Smith, C. J., Kumar, V., and Askari, N. (2019a). "Assessment of cognitive impairment, Alzheimer's disease, and other forms of dementia," in *Ethnicity and the dementias*, eds L. A. G. Gwen Yeo and D. Gallagher-Thompson (London: Routledge, Taylor & Francis Group).

Ashford, J. W., Tarpin-Bernard, F., Ashford, C. B., and Ashford, M. T. (2019b). A computerized continuous-recognition task for measurement of episodic memory. *J. Alzheimers Dis.* 69, 385–399. doi: 10.3233/JAD-190167

Ashford, J. W., Shan, M., Butler, S., Rajasekar, A., and Schmitt, F. A. (1995). Temporal quantification of Alzheimer's disease severity: 'Time index' model. *Dementia* 6, 269–280.

Atkinson, R. C., and Shiffrin, R. M. (1971). The control of short-term memory. *Sci. Am.* 225, 82–90. doi: 10.1038/scientificamerican0871-82

Baddeley, A. D., Hitch, G. J., and Allen, R. J. (2019). From short-term store to multicomponent working memory: The role of the modal model. *Mem. Cogn.* 47, 575–588. doi: 10.3758/s13421-018-0878-5

Bayley, P. J., Wixted, J. T., Hopkins, R. O., and Squire, L. R. (2008). Yes/no recognition, forced-choice recognition, and the human hippocampus. *J. Cogn. Neurosci.* 20, 505–512. doi: 10.1162/jocn.2008.20038

Bergeron, M. F., Landset, S., Tarpin-Bernard, F., Ashford, C. B., Khoshgoftaar, T. M., and Ashford, J. W. (2019). Episodic-memory performance in machine learning modeling for predicting cognitive health status classification. *J. Alzheimers Dis.* 70, 277–286. doi: 10.3233/JAD-190165

Bergeron, M. F., Landset, S., Zhou, X., Ding, T., Khoshgoftaar, T. M., Zhao, F., et al. (2020). Utility of memtrax and machine learning modeling in classification of mild cognitive impairment. *J. Alzheimers Dis.* 77, 1545–1558. doi: 10.3233/JAD-191340

Bowles, N. L., and Poon, L. W. (1982). An analysis of the effect of aging on recognition memory. *J. Gerontol.* 37, 212–219. doi: 10.1093/geronj/37.2.212

Broadbent, D. E. (1965). Information processing in the nervous system. *Science* 150, 457–462. doi: 10.1126/science.150.3695.457

Burbeck, S. L., and Luce, R. D. (1982). Evidence from auditory simple reaction times for both change and level detectors. *Percept Psychophys* 32, 117–133. doi: 10.3758/bf03204271

Cholerton, B., Weiner, M. W., Nosheny, R. L., Poston, K. L., Mackin, R. S., Tian, L., et al. (2019). Cognitive performance in Parkinson's disease in the brain health registry. *J. Alzheimers Dis.* 68, 1029–1038. doi: 10.3233/JAD-181009

Clifford, J. O. Jr., and Williston, J. S. (1992). Three dimensional vector analysis of the spatial components and voltage magnitudes of the P300 response during different attentional states and stimulus modalities. *Int. J. Psychophysiol.* 12, 1–10. doi: 10.1016/0167-8760(92)90037-c

Clifford, J. O. Jr., and Williston, J. S. (1993). The effects of attention and context on the spatial and magnitude components of the early responses of the event-related potential elicited by a rare stimulus. *Int. J. Psychophysiol.* 14, 209–226. doi: 10.1016/0167-8760(93)90035-n

Coburn, K. L., Ashford, J. W., and Fuster, J. M. (1990). Visual response latencies in temporal lobe structures as a function of stimulus information load. *Behav. Neurosci.* 104, 62–73. doi: 10.1037//0735-7044.104.1.62

Coleman, P. D., and Yao, P. J. (2003). Synaptic slaughter in Alzheimer's disease. *Neurobiol. Aging* 24, 1023–1027. doi: 10.1016/j.neurobiolaging.2003.09.001

Cousineau, D., Thivierge, J. P., Harding, B., and Lacouture, Y. (2016). Constructing a group distribution from individual distributions. *Can. J. Exp. Psychol.* 70, 253–277. doi: 10.1037/cep0000069

Craik, F. I. (2002). Levels of processing: Past, present. and future? *Memory* 10, 305–318. doi: 10.1080/09658210244000135

Dawson, M. R. W. (1988). Fitting the ex-gaussian equation to reaction time distributions. *Behav. Res. Methods Instrum Comput.* 20, 54–57.

De Roeck, E. E., De Deyn, P. P., Dierckx, E., and Engelborghs, S. (2019). Brief cognitive screening instruments for early detection of Alzheimer's disease: A systematic review. *Alzheimers Res. Ther.* 11:21. doi: 10.1186/s13195-019-0474-3

Fabiani, M., Karis, D., and Donchin, E. (1986). P300 and recall in an incidental memory paradigm. *Psychophysiology* 23, 298–308. doi: 10.1111/j.1469-8986.1986.tb00636.x

Fuchs, K. L., Hannay, H. J., Huckeba, W. M., and Espy, K. A. (1999). Construct validity of the continuous recognition memory test. *Clin. Neuropsychol.* 13, 54–65. doi: 10.1076/clin.13.1.54.1977

Gavrilov, L. A., and Gavrilova, N. S. (2001). The reliability theory of aging and longevity. *J. Theor. Biol.* 213, 527–545. doi: 10.1006/jtbi.2001.2430

Gellerman, L. W. (1933). Chance orders of alternating stimuli in visual discrimination experiments. *J. Genet. Psychol.* 42, 206–208.

Gordon, B., and Carson, K. (1990). The basis for choice reaction time slowing in Alzheimer's disease. *Brain Cogn.* 13, 148–166. doi: 10.1016/0278-2626(90)90047-r

Hasshim, N., Downes, M., Bate, S., and Parris, B. A. (2019). Response time distribution analysis of semantic and response interference in a manual response stroop task. *Exp. Psychol.* 66, 231–238. doi: 10.1027/1618-3169/a000445

Hines, T., Poon, L. W., Cerella, J., and Fozard, J. L. (1982). Age-related differences in the time course of encoding. *Exp. Aging Res.* 8, 175–178. doi: 10.1080/03610738208260361

Hintzman, D. L. (2016). Is memory organized by temporal contiguity? *Mem. Cogn.* 44, 365–375. doi: 10.3758/s13421-015-0573-8

Hirsch, H. R. (1997). Intersections of mortality-rate and survival functions: Model-independent considerations. *Exp. Gerontol.* 32, 287–296. doi: 10.1016/s0531-5565(96)00126-x

Hockley, W. E. (1982). Retrieval processes in continuous recognition. *J. Exp. Psychol. Learn. Mem. Cogn.* 8, 497–512.

Hockley, W. E. (1984a). Aanalysis of response time distributions in the study of cognitive processes. *J. Exp. Psychol.* 10, 598–615.

Hockley, W. E. (1984b). Retrieval of item frequency information in a continuous memory task. *Mem. Cogn.* 12, 229–242. doi: 10.3758/bf03197670

Hockley, W. E. (2022). Two dichotomies of recognition memory. *Can. J. Exp. Psychol.* 76, 161–177. doi: 10.1037/cep0000289

Ishihara, O., Gondo, Y., and Poon, L. W. (2002). [The influence of aging on short-term and long-term memory in the continuous recognition paradigm]. *Shinrigaku Kenkyu* 72, 516–521. doi: 10.4992/jjpsy.72.516

Kahneman, D. (1973). *Attention and effort*. Hoboken, NJ: Prentice-Hall.

Kapur, S., Craik, F. I., Tulving, E., Wilson, A. A., Houle, S., and Brown, G. M. (1994). Neuroanatomical correlates of encoding in episodic memory: Levels of processing effect. *Proc. Natl. Acad. Sci. U.S.A.* 91, 2008–2011. doi: 10.1073/pnas.91.6.2008

Kennedy, Q., Taylor, J., Heraldez, D., Noda, A., Lazzeroni, L. C., and Yesavage, J. (2013). Intraindividual variability in basic reaction time predicts middle-aged and older pilots' flight simulator performance. *J. Gerontol. B Psychol. Sci. Soc. Sci.* 68, 487–494. doi: 10.1093/geronb/gbs090

Koen, J. D., Borders, A. A., Petzold, M. T., and Yonelinas, A. P. (2017). Visual short-term memory for high resolution associations is impaired in patients with medial temporal lobe damage. *Hippocampus* 27, 184–193. doi: 10.1002/hipo.22682

Koppara, A., Frommann, I., Polcher, A., Parra, M. A., Maier, W., Jessen, F., et al. (2015). Feature binding deficits in subjective cognitive decline and in mild cognitive impairment. *J. Alzheimers Dis.* 48, S161–S170. doi: 10.3233/JAD-150105

Larrabee, G. J. (2015). The multiple validities of neuropsychological assessment. *Am. Psychol.* 70, 779–788. doi: 10.1037/a0039835

Larrabee, G. J., Trahan, D. E., and Curtiss, G. (1992). Construct validity of the continuous visual memory test. *Arch. Clin. Neuropsychol.* 7, 395–405.

Liu, X., Chen, X., Zhou, X., Shang, Y., Xu, F., Zhang, J., et al. (2021). Validity of the memtrax memory test compared to the montreal cognitive assessment in the detection of mild cognitive impairment and dementia due to Alzheimer's disease in a chinese cohort. *J. Alzheimers Dis.* 80, 1257–1267. doi: 10.3233/JAD-200936

Liu, Z., Holden, J. G., Moghaddam, M. D., and Serota, R. A. (2019). Modeling response time with power law distributions. *Nonlinear Dyn. Psychol. Life Sci.* 23, 433–464.

Liu, Z., Liu, S., Li, S., Li, L., Zheng, L., Weng, X., et al. (2022). Dissociating value-based neurocomputation from subsequent selection-related activations in human decision-making. *Cereb Cortex* 32, 4141–4155. doi: 10.1093/cercor/bhab471

Mackin, R. S., Insel, P. S., Truran, D., Finley, S., Flenniken, D., Nosheny, R., et al. (2018). Unsupervised online neuropsychological test performance for individuals with mild cognitive impairment and dementia: Results from the brain health registry. *Alzheimers Dement* 10, 573–582. doi: 10.1016/j.dadm.2018.05.005

Mahurin, R. K., and Pirozzolo, F. J. (1993). Application of Hick's law of response speed in Alzheimer and parkinson diseases. *Percept Mot Skills* 77, 107–113. doi: 10.2466/pms.1993.77.1.107

Marmolejo-Ramos, F., Cousineau, D., Benites, L., and Maehara, R. (2014). On the efficacy of procedures to normalize ex-gaussian distributions. *Front. Psychol.* 5:1548. doi: 10.3389/fpsyg.2014.01548

Moret-Tatay, C., Gamermann, D., Navarro-Pardo, E., and Fernandez de Cordoba Castella, P. (2018). ExGUtils: A python package for statistical analysis with the ex-gaussian probability density. *Front. Psychol.* 9:612. doi: 10.3389/fpsyg.2018.00612

Moret-Tatay, C., Garcia-Ramos, D., Saiz-Mauleon, B., Gamermann, D., Bertheaux, C., and Borg, C. (2021). Word and face recognition processing based on response times and ex-gaussian components. *Entropy* 23:580. doi: 10.3390/e23050580

Myerson, J., Hale, S., Wagstaff, D., Poon, L. W., and Smith, G. A. (1990). The information-loss model: A mathematical theory of age-related cognitive slowing. *Psychol. Rev.* 97, 475–487. doi: 10.1037/0033-295x.97.4.475

Nosheny, R. L., Camacho, M. R., Jin, C., Neuhaus, J., Truran, D., Flenniken, D., et al. (2020). Validation of online functional measures in cognitively impaired older adults. *Alzheimers Dement* 16, 1426–1437. doi: 10.1002/alz.12138

Osmon, D. C., Kazakov, D., Santos, O., and Kassel, M. T. (2018). Non-gaussian distributional analyses of reaction times (RT): Improvements that increase efficacy of RT tasks for describing cognitive processes. *Neuropsychol. Rev.* 28, 359–376. doi: 10.1007/s11065-018-9382-8

Pelegrina, S., Lechuga, M. T., Garcia-Madruga, J. A., Elosua, M. R., Macizo, P., Carreiras, M., et al. (2015). Normative data on the n-back task for children and young adolescents. *Front. Psychol.* 6:1544. doi: 10.3389/fpsyg.2015.01544

Pike, R., Dalgleish, L., and Wright, J. (1977). A multiple-observations model for response latency and the latencies of correct and incorrect responses in recognition memory. *Mem Cogn.* 5, 580–589. doi: 10.3758/BF03197403

Pirozzolo, F. J., Christensen, K. J., Ogle, K. M., Hansch, E. C., and Thompson, W. G. (1981). Simple and choice reaction time in dementia: Clinical implications. *Neurobiol. Aging* 2, 113–117. doi: 10.1016/0197-4580(81)90008-7

Poon, L. W., and Fozard, J. L. (1980). Age and word frequency effects in continuous recognition memory. *J. Gerontol.* 35, 77–86. doi: 10.1093/geronj/35.1.77

Posner, M. I. (1994). Attention: The mechanisms of consciousness. *Proc. Natl. Acad. Sci. U.S.A.* 91, 7398–7403. doi: 10.1073/pnas.91.16.7398

Raber, J., Huang, Y., and Ashford, J. W. (2004). ApoE genotype accounts for the vast majority of AD risk and AD pathology. *Neurobiol. Aging* 25, 641–650. doi: 10.1016/j.neurobiolaging.2003.12.023

Ratcliff, R., and McKoon, G. (2008). The diffusion decision model: Theory and data for two-choice decision tasks. *Neural Comput* 20, 873–922. doi: 10.1162/neco.2008.12-06-420

Ratcliff, R., and Murdock, B. B. (1976). Retrieval processes in recognition memory. *Psychol. Rev.* 83, 190–214.

Ratcliff, R., Scharre, D. W., and McKoon, G. (2021). Discriminating memory disordered patients from controls using diffusion model parameters from recognition memory. *J. Exp. Psychol. Gen.* 151, 1377–1393. doi: 10.1037/xge0001133

Ratcliff, R., Smith, P. L., Brown, S. D., and McKoon, G. (2016). Diffusion decision model: Current issues and history. *Trends Cogn. Sci.* 20, 260–281. doi: 10.1016/j.tics.2016.01.007

Schumacher, J., Cromarty, R., Gallagher, P., Firbank, M. J., Thomas, A. J., Kaiser, M., et al. (2019). Structural correlates of attention dysfunction in lewy body dementia and Alzheimer's disease: An ex-gaussian analysis. *J. Neurol.* 266, 1716–1726. doi: 10.1007/s00415-019-09323-y

Shepard, R. N. (1958). Stimulus and response generalization: Deduction of the generalization gradient from a trace model. *Psychol. Rev.* 65, 242–256. doi: 10.1037/h0043083

Shepard, R. N. (1961). Application of a trace model to the retention of information in a recognition task. *Psychometrika* 26, 185–203.

Shepard, R. N. (1967). Recognition memory for words, sentences, and pictures. *J. Verbal Learn. Verbal Behav.* 6, 156–163.

Shepard, R. N., and Teghtsoonian, M. (1961). Retention of information under conditions approaching a steady state. *J. Exp. Psychol.* 62, 302–309.

Stanislaw, H., and Todorov, N. (1999). Calculation of signal detection theory measures. *Behav. Res. Methods Instrum. Comput.* 31, 137–149. doi: 10.3758/bf03207704

Stark, S. M., Yassa, M. A., Lacy, J. W., and Stark, C. E. (2013). A task to assess behavioral pattern separation (BPS) in humans: Data from healthy aging and mild cognitive impairment. *Neuropsychologia* 51, 2442–2449.

Sternin, A., Burns, A., and Owen, A. M. (2019). Thirty-five years of computerized cognitive assessment of aging-where are we now? *Diagnostics* 9:114. doi: 10.3390/diagnostics9030114

Suzuki, M., Johnson, J. D., and Rugg, M. D. (2011). Decrements in hippocampal activity with item repetition during continuous recognition: An fMRI study. *J. Cogn. Neurosci.* 23, 1522–1532. doi: 10.1162/jocn.2010.21535

Tejo, M., Araya, H., Niklitschek-Soto, S., and Marmolejo-Ramos, F. (2019). Theoretical models of reaction times arising from simple-choice tasks. *Cogn. Neur.* 13, 409–416. doi: 10.1007/s11571-019-09532-1

Tierney, M. C., Yao, C., Kiss, A., and McDowell, I. (2005). Neuropsychological tests accurately predict incident Alzheimer disease after 5 and 10 years. *Neurology* 64, 1853–1859. doi: 10.1212/01.WNL.0000163773.21794.0B

Tse, C. S., Balota, D. A., Yap, M. J., Duchek, J. M., and McCabe, D. P. (2010). Effects of healthy aging and early stage dementia of the Alzheimer's type on components of response time distributions in three attention tasks. *Neuropsychology* 24, 300–315. doi: 10.1037/a0018274

Tsetsos, K., Gao, J., McClelland, J. L., and Usher, M. (2012). Using time-varying evidence to test models of decision dynamics: Bounded diffusion vs. the leaky competing accumulator model. *Front. Neurosci.* 6:79. doi: 10.3389/fnins.2012.00079

Usher, M., and McClelland, J. L. (2001). The time course of perceptual choice: The leaky, competing accumulator model. *Psychol. Rev.* 108, 550–592. doi: 10.1037/0033-295x.108.3.550

van der Hoek, M. D., Nieuwenhuizen, A., Keijer, J., and Ashford, J. W. (2019). The memtrax test compared to the montreal cognitive assessment estimation of mild cognitive impairment. *J. Alzheimers Dis.* 67, 1045–1054. doi: 10.3233/JAD-181003

Walley, R. E., and Weiden, T. D. (1973). Lateral inhibition and cognitive masking: A neuropsychological theory of attention. *Psychol. Rev.* 80, 284–302. doi: 10.1037/h0035007

Weigard, A., and Sripada, C. (2021). Task-general efficiency of evidence accumulation as a computationally-defined neurocognitive trait: Implications for clinical neuroscience. *Biol. Psychiatry Glob Open. Sci.* 1, 5–15. doi: 10.1016/j.bpsgos.2021.02.001

Weindel, G., Anders, R., Alario, F. X., and Burle, B. (2021). Assessing model-based inferences in decision making with single-trial response time decomposition. *J. Exp. Psychol. Gen.* 150, 1528–1555. doi: 10.1037/xge0001010

Weiner, M. W., Nosheny, R., Camacho, M., Truran-Sacrey, D., Mackin, R. S., Flenniken, D., et al. (2018). The brain health registry: An internet-based platform for recruitment, assessment, and longitudinal monitoring of participants for neuroscience studies. *Alzheimers Dement* 14, 1063–1076. doi: 10.1016/j.jalz.2018.02.021

Wixted, J. T., Goldinger, S. D., Squire, L. R., Kuhn, J. R., Papesh, M. H., Smith, K. A., et al. (2018). Coding of episodic memory in the human hippocampus. *Proc. Natl. Acad. Sci. U.S.A.* 115, 1093–1098. doi: 10.1073/pnas.1716443115

Wright, A. A., Santiago, H. C., Sands, S. F., Kendrick, D. F., and Cook, R. G. (1985). Memory processing of serial lists by pigeons, monkeys, and people. *Science* 229, 287–289. doi: 10.1126/science.9304205

Yesavage, J. A., Jo, B., Adamson, M. M., Kennedy, Q., Noda, A., Hernandez, B., et al. (2011). Initial cognitive performance predicts longitudinal aviator performance. *J Gerontol B Psychol Sci Soc Sci.* 66, 444–453. doi: 10.1093/geronb/gbr031

Yesavage, J. A., Taylor, J. L., Mumenthaler, M. S., Noda, A., and O'Hara, R. (1999). Relationship of age and simulated flight performance. *J. Am. Geriatr. Soc.* 47, 819–823. doi: 10.1111/j.1532-5415.1999.tb03838.x

Yonelinas, A. P., Otten, L. J., Shaw, K. N., and Rugg, M. D. (2005). Separating the brain regions involved in recollection and familiarity in recognition memory. *J. Neurosci.* 25, 3002–3008. doi: 10.1523/JNEUROSCI.5295-04.2005

Zhou, X., and Ashford, J. W. (2019). Advances in screening instruments for Alzheimer's disease. *Aging Med.* 2, 88–93. doi: 10.1002/agm2.12069

Zygouris, S., and Tsolaki, M. (2015). Computerized cognitive testing for older adults: A review. *Am. J. Alzheimers Dis. Other Demen.* 30, 13–28. doi: 10.1177/1533317514522852

frontiers | Frontiers in Aging Neuroscience

TYPE Original Research
PUBLISHED 16 November 2022
DOI 10.3389/fnagi.2022.1011510

OPEN ACCESS

EDITED BY
Cosimo Urgesi,
University of Udine, Italy

REVIEWED BY
Giorgio Arcara,
San Camillo Hospital (IRCCS), Italy
Jeevitha Mariapun,
Monash University Malaysia, Malaysia
Yibin Fang,
Shanghai Fourth People's Hospital, China

*CORRESPONDENCE
Juan Li
lijuanjr@126.com
Bei Wu
beiwu@nyu.edu
Yanpei Cao
yanpeicao@fudan.edu.cn

†These authors have contributed equally to this work

SPECIALTY SECTION
This article was submitted to Neurocognitive Aging and Behavior, a section of the journal Frontiers in Aging Neuroscience

RECEIVED 04 August 2022
ACCEPTED 31 October 2022
PUBLISHED 16 November 2022

CITATION
Li F, Kong X, Zhu H, Xu H, Wu B, Cao Y and Li J (2022) The moderating effect of cognitive reserve on cognitive function in patients with Acute Ischemic Stroke.
Front. Aging Neurosci. 14:1011510.
doi: 10.3389/fnagi.2022.1011510

The moderating effect of cognitive reserve on cognitive function in patients with Acute Ischemic Stroke

Fanfan Li[1†], Xiangjing Kong[2†], Huanzhi Zhu[1†], Hanzhang Xu[3,4†], Bei Wu[5*], Yanpei Cao[6*] and Juan Li[6,7,1*]

[1]School of Nursing, Naval Medical University, Shanghai, China, [2]Air Force Hospital of Eastern Theater Command, Nanjing, China, [3]School of Nursing, Duke University, Durham, NC, United States, [4]School of Medicine, Duke University, Durham, NC, United States, [5]Rory Meyers College of Nursing, New York University, New York, NY, United States, [6]Department of Nursing, Huashan Hospital, Fudan University, Shanghai, China, [7]National Center for Neurological Disorders, Shanghai, China

Background: Recovery of cognitive function after stroke has inter-individual variability. The theory of cognitive reserve offers a potential explanation of the variability in cognitive function after stroke.

Objective: This study aimed to investigate the moderating effect of cognitive reserve on the relationship between the stroke severity and cognitive function after stroke.

Materials and methods: A total of 220 patients with Acute Ischemic Stroke (AIS) were recruited in 2021 from two stroke centers in Nanjing, China. The National Institutes of Health Stroke Scale (NIHSS) was used to assess stroke severity upon admission. Cognitive Reserve Index questionnaire (CRIq) and validated Montreal Cognitive Assessment, Changsha Version (MoCA-CS) were used to assess cognitive reserve and cognitive function within 7 days after stroke onset, respectively. A series of multivariate linear regression models were applied to test the moderating effect of cognitive reserve.

Results: Patients with a higher level of cognitive reserve had better cognitive function after stroke compared with those with a lower level of cognitive reserve ($\beta = 0.074$, $p = 0.003$). The interaction of NIHSS and cognitive reserve was statistically significant ($\beta = -0.010$, $p = 0.045$) after adjusting for some key covariates [e.g., age, marital status, Oxfordshire Community Stroke Project (OCSP) classification, Trial of ORG 10172 in Acute Stroke Treatment (TOAST) classification, cerebral vascular stenosis, diabetes and atrial fibrillation].

Conclusion: Cognitive reserve may help to buffer the effect of stroke-related pathology on cognitive decline in Chinese acute stroke patients. Enhancing cognitive reserve in stroke patients may be one of the potential strategies for preventing vascular dementia.

KEYWORDS

Acute Ischemic Stroke, cognitive reserve, moderate effect, cognitive function, cognitive impairment, Cognitive Reserve Index questionnaire

Introduction

Stroke is the second leading cause of death in the world (Stark et al., 2021). The incidence of stroke in China was 246.8 per 100,000 person-years and death rate for cerebrovascular diseases was 149.49 per 100,000 (Wang et al., 2020). Therefore, stroke is characterized as having high morbidity, high mortality, and high recurrence rate, and has significant economic burden (Wang et al., 2020). Acute Ischemic Stroke (AIS) is the most common type of stroke, accounting for 69.6–70.8% of all stroke cases in China (Wang D. et al., 2017; Wang W. et al., 2017).About 53–81% of stroke survivors in China suffer from post-stroke cognitive impairment (PSCI) (Qu et al., 2015; Ding et al., 2019), which is characterized as experiencing impairment in at least one cognitive domains including executive function, attention, memory, language, and/or visuospatial function (Mok et al., 2017). PSCI affects the quality of life and survival time of stroke patients, and increases the subsequent incidence of dementia (Claesson et al., 2005; Melkas et al., 2009; Savva and Stephan, 2010). Therefore, it is critical to identify strategies to prevent PSCI in patients with AIS.

Cognitive reserve refers to the ability of the brain to maintain optimal cognitive functions by mobilizing pre-existing neural networks or reconstructing alternative neural networks to resist pathological damage (Stern, 2002; Barulli and Stern, 2013). A few studies have showed that cognitive reserve may explain the mismatch between the degree of pathological brain damage and clinical outcomes among some patients (e.g., cognition/motor function) (Katzman et al., 1988; Stern, 2002). Specifically, cognitive reserve shapes the brain's capacity to compensate for pathological damage through neural compensation (e.g., recruiting uninjured brain functional areas), which moderates the impact of pathological damage on clinical manifestations (Stern, 2002), and varies among different individuals (Duda et al., 2014; Stenberg et al., 2020).

Prior studies on cognitive reserve mostly focused on Alzheimer's disease and mild cognitive impairment among older adults (Yaffe et al., 2011; Liu et al., 2013; Ko et al., 2022). Findings from previous studies suggest that higher cognitive reserve can tolerate a more severe pathological burden or age-related changes and maintain a better cognitive function when there are pathophysiological changes in the brain. Emerging research has suggested a simplified methodological model of cognitive reserve in stroke patients, and claims that the cognitive reserve theory is also suitable for patients with stroke (Steffener et al., 2011; Steffener and Stern, 2012; Rosenich et al., 2020). In brief, this model includes three components: cognitive reserve, stroke-related pathological burden, and clinical outcomes, and the model demonstrates that cognitive reserve moderates the relationship between pathology of stroke and clinical outcomes after adjusting for confounding factors (e.g., age, sex, and SES) (Cizginer et al., 2017).

Several studies have assessed cognitive reserve in stroke patients and found lower levels of cognitive reserve was associated with more severe PSCI and a slower rate of post-stroke recovery (Ojala-Oksala et al., 2012; Shin et al., 2020). However, these two studies only used static and gross proxies (i.e., years of education and/or occupation) to measure cognitive reserve, which could not reflect the dynamic feature of cognitive reserve. Prior studies define cognitive reserve as a dynamic process over the lifespan that is influenced by both early life static factors (e.g., intelligence, level or years of education, occupational attainment, and socioeconomic status) as well as dynamic lifestyle activities (e.g., social activities, physical activity, and recreational activities) (Barulli and Stern, 2013). Therefore, cognitive reserve measured by more comprehensive instruments, such as the Cognitive Reserve Index questionnaire (CRIq), that capture both the static and dynamic aspects of cognitive reserve, can provide a comprehensive assessment of cognitive reserve (Gil-Pagés et al., 2019). To date, only one study used the CRIq to measure cognitive reserve in convalescent stroke patients and found that patients with higher levels of cognitive reserve had a lower prevalence of cognitive impairment after stroke (Abdullah et al., 2021). However, this study did not investigate whether the impact of cognitive reserve on cognitive function is the same across different stroke severity.

To address this knowledge gap, we aimed to investigate whether cognitive reserve moderates the relationship between stroke severity and cognitive function in Chinese stroke patients at an acute stage. We hypothesize that higher cognitive reserve in the stroke patients in a acute stroke phase is associated

with better cognitive function after stroke, and cognitive reserve moderates the impact of stroke severity on cognitive function.

Materials and methods

Participants

This cross-sectional study was conducted by using convenience sampling. We recruited patients with AIS between July and November 2021 from two large stroke centers in Nanjing, China. Patients were eligible if they were: (1) diagnosed with AIS by a neurologist or a neurosurgeon based on a focal neurologic deficit and a corresponding infarct on magnetic resonance imaging (MRI); (2) aged ≥ 18 years at stroke onset; and (3) admitted to a stroke center within 7 days after onset. Exclusion criteria were: (1) having a transient ischemic attack (TIA); (2) having mental health diseases or dementia prior to stroke onset; and (3) having dysphasia or severe visual or hearing impairment. A total of 220 eligible patients with AIS were recruited in this study.

Procedures

Two trained research assistants recruited patients for this study. Two trained neurologists assessed patients' stroke severity and cognitive function. The research assistants interviewed patients or their primary family caregivers (Nucci et al., 2012)to assess cognitive reserve of patients. All patients and their primary family caregivers provided written informed consent. Clinical characteristics of patients were obtained from the medical records.

Materials

Cognitive Reserve Index questionnaire

Cognitive Reserve Index questionnaire was used to assess cognitive reserve in AIS patients (Nucci et al., 2012). It includes three domains: (1) education, measured by years of formal and informal education; (2) occupation, classified into five levels depending on the cognitive load required for the job and the number of years spent in each occupation; and (3) leisure activity engagement, measured by the value of different activities regarding their frequency and periodicity. The total score of CRIq was then categorized into five levels: low (≤ 70), moderate low (70–84), moderate (85–114), moderate high (115–130), and high (≥ 130) (Nucci et al., 2012). CRIq had been translated into different languages and used in populations of Alzheimer's disease, stroke, acquired brain injury (Bertoni et al., 2022), multiple sclerosis (Ozakbas et al., 2021), Parkinson's disease (Guzzetti et al., 2019), and healthy adults (Maiovis et al., 2016). CRIq is a semi-structured interview questionnaire. If a patient is suspected to have cognitive deficits, a primary family member who knows the patient's past and present living habits can be asked (Nucci et al., 2012). The Chinese version of the CRIq was translated and back-translated by our research team with three Ph.D.-prepared researchers in nursing and neuroscience who were fluent in both English and Chinese. There was no substantial change in the content of each item. Team members discussed each item and reached a consensus about the translation in order to ensure the accuracy of the translation and the culturally relevance of the Chinese version. The Cronbach's α of CRIq in present study was 0.827 and the test-retest reliability was 0.995 (Li and Li, 2022).

Montreal Cognitive Assessment-Changsha version

Montreal Cognitive Assessment-Changsha Version (MoCA-CS) was used to assess cognitive function. The Montreal Cognitive Assessment (MoCA) has been widely used to screen for cognitive impairment in stroke or TIA patients (Nasreddine et al., 2005), and shown to have good sensitivity and specificity in detecting cognitive impairment (Schlegel et al., 2003; Tan et al., 2017). MoCA-CS was a Chinese version of MoCA (Tu et al., 2013)and it had been used to evaluate cognitive function in ischemic stroke patients (Ozdemir et al., 2001; Patel et al., 2002; Li et al., 2020). The Cronbach's α for MOCA-CS is 0.884 (Tu et al., 2013). Same as the MoCA, the score of MoCA-CS ranged from 0 to 30, with higher score indicating better cognitive function. Patients who had no more than 6 years of education was added one additional point to the total score. A total score ≥ 27 indicates normal cognitive function, and < 27 indicates impaired cognitive function (Tu et al., 2013).

Stroke severity

The National Institutes of Health Stroke Scale (NIHSS) was used to evaluate baseline stroke severity at admission by neurologists. Higher scores of NIHSS indicate more severe levels of stroke (Adams et al., 1999; Kasner et al., 1999).

Covariates

Covariates included sociodemographic characteristics (i.e., age, gender, rural/urban residency, and marital status), classification of stroke [the Oxfordshire Community Stroke Project (OCSP) classification and the Trial of ORG 10172 in Acute Stroke Treatment (TOAST) classification] (Adams et al., 1993; Lindley et al., 1993), comorbidities (hypertension, diabetes, dyslipidemia, and atrial fibrillation) and stroke risk factors (smoking, drinking, cerebral vascular stenosis degree, and prior history of stroke). Smoking was operationalized as smoking more than 4 times per week for more than half a year (Yes/No) (GBD 2019 Stroke Collaborators, 2021). Alcohol consumption was measured by drinking alcohol at least once per week for more than half a year (Yes/No)

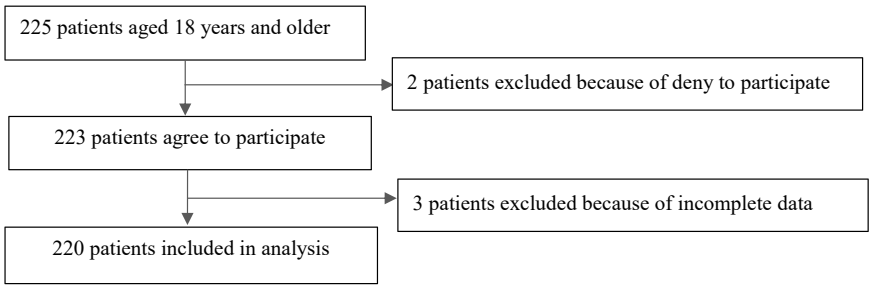

FIGURE 1
Flow chart of participants.

(GBD 2019 Stroke Collaborators, 2021). The radiologists assessed the severity of intracranial/external artery stenosis on angiography. It was divided into three grades: mild (stenosis rate of < 30%), moderate (30∼69%), and severe (70∼99%) (Kernan et al., 2014; Vascular Surgery Group, Surgery Society of Chinese Medical Association, 2017). Covariates coding is provided in the **Supplementary Table 1**.

Statistical analysis

Sociodemographic, clinical characteristics, stroke severity, cognitive reserve and cognitive function were described using mean and standard deviation or median and interquartile range for continuous variables and frequency and proportion for categorical variables. First, we conducted univariate linear regression analysis to explore the relationships among stroke severity (NIHSS), cognitive reserve, covariates and cognitive function. Then we performed Pearson/Spearman correlation analysis for those covariates which were significant ($p < 0.1$) in univariate linear regression. Only those covariates which were significant in univariate linear regression and had weak correlation with each other ($r < 0.5$, **Supplementary Tables 3**, **4**) were allowed to enter into the multivariate linear regressions. The average years of education was 9 years (SD = 4.4). Because years of education was highly correlated with cognitive reserve ($r = 0.832$, $p < 0.001$), it was not included in the analysis. To assess the moderating effects of the cognitive reserve on the relationships between stroke severity and cognitive function, we performed a series of multivariate linear regression models as following (1) Model I was the base model adjusting for baseline NIHSS; (2) Model II: model I plus CRIq; (3) Model III: model II plus interaction between NIHSS and CRIq; (4) Model IV: model III plus covariates adjustment (i.e., age, marital status, OCSP classification, TOAST classification, cerebral vascular stenosis, diabetes, and atrial fibrillation). Variance inflation factor (VIF) values of all variables are provided to ensure that there is no collinearity among variables. Given previous reports of three-way interaction of age, years of education and lesion size on the stroke outcomes (Umarova et al., 2021), we had examined the three-way interaction of age, cognitive reserve and stroke severity on cognitive function. Sensitivity analysis was conducted by using categorical variables of cognitive reserve (CRIq ≤ 84, low; CRIq 85–114, moderate; and CRIq ≥ 115, high) and stroke severity (NIHSS < 5, mild stroke; NIHSS 5–15, moderate stroke; NIHSS > 15, severe stroke) (Kasner et al., 1999; Nucci et al., 2012). However, the three-way interaction of age, cognitive reserve and stroke severity was not significant. All analyses were conducted using the SPSS version 21.0. Statistical significance was set at $p < 0.05$.

Results

Figure 1 demonstrates the flowchart of patients. The characteristics of the participants are presented in **Table 1**. A total of 220 participants enrolled in this study. The average age of the participants was 67 years (SD: 9.9). Sixty five percent were male and 82.3% were married. The median score of NIHSS was 7 (IQR: 3–11). The mean score of CRIq was 99 (SD: 16.6). One hundred thirty-four participants (60.9%) had a moderate level of cognitive reserve. The median score of MoCA was 22 (IQR: 16–26) and 79.5% of the participants were cognitively impairment (MoCA < 27).

Supplementary Table 2 presents the results from univariate linear regression analyses. Higher levels of cognitive reserve were associated with better performance in MoCA. Participants who were younger and married had higher scores in MoCA. More severe carotid artery stenosis, having comorbidities of diabetes and atrial fibrillation, and more severe stroke measured by NIHSS were significantly associated with lower scores in MoCA. Compared with participants who had Lacunar circulation infarcts (LACI) type of stroke, those with other Oxfordshire Community Stroke Project (OCSP) classifications exhibited significantly worse cognitive function. Participants with Small-artery occlusion (SAO) subtype had significant better cognitive performance on MoCA than those with Large-artery atherothrombotic (LAA) subtype.

TABLE 1 Characteristics of patients with Acute Ischemic Stroke (N = 220).

	Variables	M (SD)/N (%)
Sociodemographic characteristics	Age(years)	67 (9.9)
	Gender(male)	143 (65.0%)
	Married	181 (82.3%)
	Years of education	9 (4.4)
	Rural residency	28 (12.7%)
Classification of stroke	OCSP classification	
	TACI	22 (10.0%)
	PACI	58 (26.4%)
	POCI	63 (28.6%)
	LACI	77 (35.0%)
	TOAST classification	
	LAA	70 (31.8%)
	CE	33 (15.0%)
	SAO	73 (33.2%)
	ODE	39 (17.7%)
	UDE	5 (2.3%)
Stroke risk factors	Smoking	94 (42.7%)
	Drinking	98 (44.5%)
	Previous history of stroke	48 (21.8%)
	Stenosis degree	
	Mild	107 (48.6%)
	Moderate	94 (42.7%)
	Severe	19 (8.6%)
Comorbidities	Hypertension	167 (75.9%)
	Diabetes	95 (43.2%)
	Dyslipidemia	45 (20.5%)
	Atrial fibrillation	32 (14.5%)
Severity of stroke	NIHSS, median (IQR)	7 (3–11)
	NIHSS < 5	77 (35.0%)
	NIHSS(5–15)	123 (55.9%)
	NIHSS > 15	20 (9.1%)
Cognitive reserve	CRIq	99 (16.6)
	CRI-education	103 (18.7)
	CRI-occupation	103 (14.1)
	CRI-leisure activity engagement	91 (9.3)
	Low (≤ 70)	7 (3.2%)
	Moderate low (70–84)	40 (18.2%)
	Moderate (85–114)	134 (60.9%)
	Moderate high (115–130)	34 (15.4%)
	High (≥ 130)	5 (2.3%)
Cognitive function	MoCA-CS, median (IQR)	22 (16–26)
	Cognitive impairment(MoCA < 27)	175 (79.5%)
	Normal cognition(MoCA ≥ 27)	45 (20.5%)

OCSP, Oxfordshire Community Stroke Project; TACI, total anterior circulation infarct; PACI, partial anterior circulation infarct; POCI, Posterior circulation infarct; LACI, Lacunar circulation infarcts; TOAST, Trial of ORG 10172 in Acute Stroke Treatment; LAA, Large-artery atherothrombotic; CE, Cardioembolic; SAO, Small-artery occlusion; ODE, Other determined etiology; UDE, Undetermined etiology; NIHSS, National Institutes of Health Stroke Scale; CRIq, Cognitive Reserve Index questionnaire; MoCA-CS, Montreal Cognitive Assessment-Changsha Version; M(SD) = Mean ± Standard Deviation; IQR, Interquartile.

Table 2 presents the results from a series of linear regression models of stroke severity and cognitive reserve on cognitive function. After controlling for the covariates, higher level of stroke severity was associated with poorer cognitive function among AIS patients (β = −0.762, p < 0.001), higher level of cognitive reserve was related to better cognitive function (β = 0.074, p = 0.003). The interaction between NIHSS and CRIq was significant (β = −0.010, p = 0.045), which suggests that patients with higher level of cognitive reserve showed significant better cognitive function than those with lower level of cognitive reserve when stroke severity was mild (Figure 2). In addition, a control analysis including all variables at once in a multivariate regression confirmed the results, highlighting that the results are not bound the specific model selection procedure (Supplementary Table 5). Similar findings were observed in the sensitivity analyses (Supplementary Table 6 and Supplementary Figure 1). Patients with younger age (β = −0.116, p = 0.007) and those married had better cognitive function (β = 2.207, p = 0.040), whereas whose with diabetes had poorer cognitive function (β = −1.848, p = 0.031).

Discussion

To the best of our knowledge, the present study was the first to explore the moderating effect of cognitive reserve on the relationship between stroke severity and cognitive function among Chinese patients with AIS. Stroke severity was negatively associated with cognitive function of AIS patients. Cognitive reserve plays a moderating effect on the relationship between stroke severity and cognitive function. After adjusting for covariates, patients with higher level of cognitive reserve had better cognitive function, especially among patients with mild stroke.

There was little relevant research about cognitive reserve conducted in China. The cognitive reserve theory has been widely tested in western population, but not in Chinese population (Du and Qiu, 2019). The findings of our study were consistent with results from previous studies that cognitive reserve could buffer the cognitive impairment after stroke (Shin et al., 2020; Umarova et al., 2021). Unlike prior research that used education and/or occupation as the proxy for cognitive research, our study assessed cognitive reserve using a comprehensive and validated instrument that consists of education, occupation and leisure activities engagement (Gil-Pagés et al., 2019; Kartschmit et al., 2019), which further confirm the buffering effect of cognitive reserve on cognitive impairment in AIS patients. In addition, we found that older age, higher score of stroke severity and diabetes were associated with poor post-stroke cognition, which were in line with previous findings (Pendlebury and Rothwell, 2009; Ravona-Springer et al., 2010; Ramsey et al., 2017).

TABLE 2 Moderating effect of cognitive reserve on the relationship between stroke severity and cognitive function in patients with AIS.

	Variables	B	*p*	95% CI		VIF	Adjusted R^2	*F*
				Lower	Upper			
Model I	NIHSS	−0.893	<0.001	−1.053	−0.734	1.000	0.356	122.047
Model II	NIHSS	−0.894	<0.001	−1.051	−0.737	1.000	0.375	66.585
	CRIq	0.067	0.007	0.019	0.116	1.000		
Model III	NIHSS	−0.902	<0.001	−1.058	−0.746	1.003	0.384	46.465
	CRIq	0.067	0.006	0.019	0.115	1.000		
	NIHSS × CRIq	−0.010	0.041	−0.020	0.000	1.003		
Model IV	NIHSS	−0.762	<0.001	−0.943	−0.581	1.454	0.427	11.214
	CRIq	0.074	0.003	0.026	0.121	1.049		
	NIHSS × CRIq	−0.010	0.045	−0.020	0.000	1.070		
	Age	−0.116	0.007	−0.199	−0.033	1.149		
	Married	2.207	0.040	0.104	4.309	1.095		
	OCSP classification							
	LACI (reference)							
	TACI	−0.922	0.577	−4.175	2.331	1.617		
	PACI	−1.170	0.356	−3.665	1.325	2.005		
	POCI	0.115	0.931	−2.484	2.714	2.344		
	TOAST classification							
	LAA (reference)							
	CE	−0.684	0.607	−3.299	1.932	1.481		
	SAO	−0.446	0.744	−3.135	2.244	2.723		
	ODE	0.396	0.742	−1.971	2.763	1.387		
	UDE	−5.476	0.114	−12.324	1.372	1.131		
	Cerebral vascular stenosis							
	Mild (reference)							
	Moderate	−0.417	0.665	−2.310	1.476	1.442		
	Severe	−2.775	0.112	−6.204	0.653	1.346		
	Diabetes	−1.848	0.031	−3.525	−0.171	1.172		
	Atrial fibrillation	−0.468	0.702	−2.877	1.940	1.224		

NIHSS, National Institutes of Health Stroke Scale; CRIq, Cognitive Reserve Index questionnaire; OCSP, Oxfordshire Community Stroke Project; TACI, Total anterior circulation infarct; PACI, Partial anterior circulation infarct; POCI, Posterior circulation infarct; LACI, Lacunar circulation infarcts; TOAST, Trial of ORG 10172 in Acute Stroke Treatment; LAA, Large-artery atherothrombotic; CE, Cardioembolic; SAO, Small-artery occlusion; ODE, Other determined etiology; UDE, Undetermined etiology; CI, Confidence Interval; VIF, Variance inflation factor; B, unstandardized coefficient; $p < 0.05$.

The cognitive reserve theory may provide explanations on the moderating effects of cognitive reserve on cognitive function. Cognitive reserve has an additive effect (Stern, 2012)—patients with higher cognitive reserve generally have better premorbid cognitive performance and could tolerate more severe brain pathological damage, and therefore present a better cognitive function after stroke. On the other hand, individuals with higher levels of cognitive reserve may have more effective cognitive processing strategies and exhibit increased neuroplasticity (Barulli and Stern, 2013). As a result, when individuals with high cognitive reserve suffer from a stroke, they are able to leverage alternative neural networks that are unimpaired to maintain a relative high level of cognitive functioning (Steffener et al., 2011). However, among patients with severe stroke (NIHSS > 15), AIS patients with higher levels of cognitive reserve had worse cognitive function. It may be explained that the moderating effect of cognitive reserve was weakened in patients with severe brain pathological damage (Stern, 2009).

The incidence and disease burden of stroke are increasing in low and middle-income countries due to substantial population aging (Mijajlović et al., 2017). Cognitive reserve shows great potential in reducing the burden of stroke-induced cognitive impairment and/or vascular dementia. Prior research has suggested that cognitive reserve is dynamic and can be accumulated across the lifespan (Stern, 2012)through engaging in educational, occupational, and leisure activities (Wang H. X. et al., 2017). Participating in multiple social activities at different life stages may have different effects on the development and accumulation cognitive reserve. Prior research has suggested

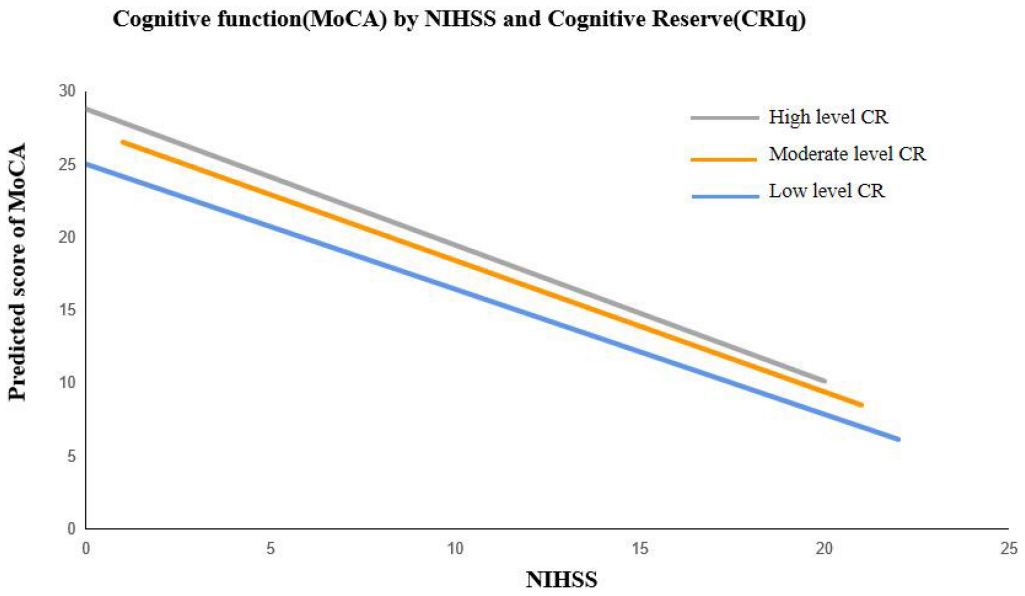

FIGURE 2
Cognitive function (MoCA) of AIS patients by stroke severity (NIHSS) and cognitive reserve. (CRIq) Cognitive reserve was stratified into low (CRIq ≤ 84), moderate (85 ≤ CRIq ≤ 114), and high (CRIq ≥ 115).

that cognitive activities in childhood (including educational, reading and other intelligent recreations) have a positive impact on cognition and cognitive reserve in adulthood (Richards and Sacker, 2003), occupational attainment in midlife protect the structural brain integrity and health and cognitive ability in older ages (Chan et al., 2018), and physical exercise and social activities in later life delay the onset of dementia (Fratiglioni et al., 2004). Even after the onset of cognitive impairment, enhancement of cognitive reserve still has the effect of delaying further cognitive decline (Dekhtyar et al., 2015; Wang H. X. et al., 2017), due to the additive effect of cognitive reserve. For AIS patients, engagement in evidence-based physical and social activities after stroke is critical to increase cognitive reserve and to reduce cognitive impairment or remain cognitive function.

This study also had several limitations: (1) Due to the difficulty in obtaining neuropathological data, we adopted the NIHSS score as severity of stroke pathological damage. However, NIHSS is an indicator of pathological damage for stroke patients and it has been widely used in stroke studies (Adams et al., 1999; Umarova, 2017). (2) We did not collect information on the infarct locations and psychiatric factors (such as depression, anxiety, sleep disorders, and fatigue, etc.) in this study although they may be associated with cognitive function after stroke (Ismail et al., 2018; Weaver et al., 2021). We will address these issues in future studies. (3) This study was a cross-sectional study using the convenience sampling method, and the sample may not be representative enough for the whole Chinese AIS population. Future studies with larger sample sizes are needed to further assess the role of cognitive reserve in severe stroke patients. (4) The cross-sectional study design prohibited us from examining the effects of cognitive reserve on the trajectory of cognitive decline over time. Longitudinal studies are needed to investigate the protective effect of cognitive reserve on cognitive function after stroke in future.

Conclusion

Our findings suggest that cognitive reserve plays a moderating role in the relationship between brain pathological damage caused by stroke and cognitive function in AIS patients. Higher level of cognitive reserve is associated with better cognitive function especially in mild stroke patients. Interventions that are designed to improve social activities would be beneficial for cognitive reserve, and in turn, may have the potential to delay post-stroke cognitive decline.

Data availability statement

The original contributions presented in this study are included in the article/**Supplementary material**, further inquiries can be directed to the corresponding authors.

Ethics statement

The studies involving human participants were reviewed and approved by the Institutional Review Board (IRB)

of Naval Medical University (NMUMREC-2021-001). The patients/participants provided their written informed consent to participate in this study.

Author contributions

FL suggested the analytical strategy, performed data analysis, and wrote the manuscript. XK and HZ collected the data and interpreted the data. HX interpreted the study findings and drafted the manuscript. JL contributed to concept formation and design of the study protocol, interpretation of data, and preparation of the manuscript. BW provided input on the conceptualization of the study, interpreted the study findings, and reviewed the manuscript. YC provided input on the study design and reviewed the manuscript. All authors contributed to the article and approved the submitted version.

Funding

This study was supported by National Natural Science Foundation of China (72104243).

Conflict of interest

The authors declare that the research was conducted in the absence of any commercial or financial relationships that could be construed as a potential conflict of interest.

Publisher's note

All claims expressed in this article are solely those of the authors and do not necessarily represent those of their affiliated organizations, or those of the publisher, the editors and the reviewers. Any product that may be evaluated in this article, or claim that may be made by its manufacturer, is not guaranteed or endorsed by the publisher.

Supplementary material

The Supplementary Material for this article can be found online at: https://www.frontiersin.org/articles/10.3389/fnagi.2022.1011510/full#supplementary-material

References

Abdullah, A. H., Sharip, S., Rahman, A., and Bakar, L. (2021). Cognitive reserve in stroke patients. *Psych. J.* 10, 444–452. doi: 10.1002/pchj.423

Adams, H. J., Bendixen, B. H., Kappelle, L. J., Biller, J., Love, B. B., Gordon, D. L., et al. (1993). Classification of subtype of acute ischemic stroke. Definitions for use in a multicenter clinical trial. TOAST. Trial of Org 10172 in acute stroke treatment. *Stroke* 24, 35–41. doi: 10.1161/01.str.24.1.35

Adams, H. J., Davis, P. H., Leira, E. C., Chang, K. C., Bendixen, B. H., Clarke, W. R., et al. (1999). Baseline NIH Stroke Scale score strongly predicts outcome after stroke: A report of the Trial of Org 10172 in Acute Stroke Treatment (TOAST). *Neurology* 53, 126–131. doi: 10.1212/wnl.53.1.126

Barulli, D., and Stern, Y. (2013). Efficiency, capacity, compensation, maintenance, plasticity: Emerging concepts in cognitive reserve. *Trends Cogn. Sci.* 17, 502–509. doi: 10.1016/j.tics.2013.08.012

Bertoni, D., Petraglia, F., Basagni, B., Pedrazzi, G., De Gaetano, K., Costantino, C., et al. (2022). Cognitive reserve index and functional and cognitive outcomes in severe acquired brain injury: A pilot study. *Appl. Neuropsychol. Adult* 29, 684–694. doi: 10.1080/23279095.2020.1804910

Chan, D., Shafto, M., Kievit, R., Matthews, F., Spink, M., Valenzuela, M., et al. (2018). Lifestyle activities in mid-life contribute to cognitive reserve in late-life, independent of education, occupation, and late-life activities. *Neurobiol. Aging* 70, 180–183. doi: 10.1016/j.neurobiolaging.2018.06.012

Cizginer, S., Marcantonio, E., Vasunilashorn, S., Pascual-Leone, A., Shafi, M., Schmitt, E. M., et al. (2017). The cognitive reserve model in the development of delirium: The successful aging after elective surgery study. *Geriatr. Psychiatry Neurol.* 30, 337–345. doi: 10.1177/0891988717732152

Claesson, L., Lindén, T., Skoog, I., and Blomstrand, C. (2005). Cognitive impairment after stroke - impact on activities of daily living and costs of care for elderly people. The Göteborg 70+ Stroke Study. *Cerebrovasc. Dis.* 19, 102–109. doi: 10.1159/000082787

Dekhtyar, S., Wang, H. X., Scott, K., Goodman, A., Koupil, I., and Herlitz, A. A. (2015). Life-course study of cognitive reserve in dementia–from childhood to old age. *Am. J. Geriatr. Psychiatry* 23, 885–896. doi: 10.1016/j.jagp.2015.02.002

Ding, M. Y., Xu, Y., Wang, Y. Z., Li, P. X., Mao, Y. T., Yu, J. T., et al. (2019). Predictors of cognitive impairment after stroke: A prospective stroke cohort study. *J. Alzheimers Dis.* 71, 1139–1151. doi: 10.3233/JAD-190382

Du, Y., and Qiu, C. (2019). Strengthening multidisciplinary research on cognitive reserve in Alzheimer's disease. *Chin. J. Neurol.* 52, 521–524. doi: 10.3760/cma.j.issn.1006-7876.2019.07.001

Duda, B., Puente, A. N., and Miller, L. S. (2014). Cognitive reserve moderates relation between global cognition and functional status in older adults. *J. Clin. Exp. Neuropsychol.* 36, 368–378. doi: 10.1080/13803395.2014.892916

Fratiglioni, L., Paillard-Borg, S., and Winblad, B. (2004). An active and socially integrated lifestyle in late life might protect against dementia. *Lancet Neurol.* 3, 343–353. doi: 10.1016/S1474-4422(04)00767-7

GBD 2019 Stroke Collaborators (2021). Global, regional, and national burden of stroke and its risk factors, 1990-2019: A systematic analysis for the Global Burden of Disease Study 2019. *Lancet Neurol.* 20, 795–820. doi: 10.1016/S1474-4422(21)00252-0

Gil-Pagés, M., Sánchez-Carrión, R., Tormos, J. M., Enseñat-Cantallops, A., and García-Molina, A. A. (2019). Positive relationship between cognitive reserve and cognitive function after stroke: Dynamic proxies correlate better than static proxies. *Int. Neuropsychol. Soc.* 25, 910–921. doi: 10.1017/S1355617719000638

Guzzetti, S., Mancini, F., Caporali, A., Manfredi, L., and Daini, R. (2019). The association of cognitive reserve with motor and cognitive functions for different stages of Parkinson's disease. *Exp. Gerontol.* 115, 79–87. doi: 10.1016/j.exger.2018.11.020

Ismail, Z., Gatchel, J., Bateman, D. R., Barcelos-Ferreira, R., Cantillon, M., Jaeger, J., et al. (2018). Affective and emotional dysregulation as pre-dementia risk markers: Exploring the mild behavioral impairment symptoms of depression, anxiety, irritability, and euphoria. *Int. Psychogeriatr.* 30, 185–196. doi: 10.1017/S1041610217001880

Kartschmit, N., Mikolajczyk, R., Schubert, T., and Lacruz, M. E. (2019). Measuring Cognitive Reserve (CR) - A systematic review of measurement properties of CR questionnaires for the adult population. *PLoS One* 14:e219851. doi: 10.1371/journal.pone.0219851

Kasner, S. E., Chalela, J. A., Luciano, J. M., Cucchiara, B. L., Raps, E. C., Mcgarvey, M. L., et al. (1999). Reliability and validity of estimating the NIH stroke scale score from medical records. *Stroke* 30, 1534–1537. doi: 10.1161/01.str.30.8.1534

Katzman, R., Terry, R., Deteresa, R., Brown, T., Davies, P., Fuld, P., et al. (1988). Clinical, pathological, and neurochemical changes in dementia: A subgroup with preserved mental status and numerous neocortical plaques. *Ann. Neurol.* 23, 138–144. doi: 10.1002/ana.410230206

Kernan, W. N., Ovbiagele, B., Black, H. R., Bravata, D. M., Chimowitz, M. I., Ezekowitz, M. D., et al. (2014). Guidelines for the prevention of stroke in patients with stroke and transient ischemic attack: A guideline for healthcare professionals from the American Heart Association/American Stroke Association. *Stroke* 45, 2160–2236. doi: 10.1161/STR.0000000000000024

Ko, K., Yi, D., Byun, M. S., Lee, J. H., Jeon, S. Y., Kim, W. J., et al. (2022). Cognitive reserve proxies, Alzheimer pathologies, and cognition. *Neurobiol. Aging* 110, 88–95. doi: 10.1016/j.neurobiolaging.2021.10.005

Li, F., and Li, J. (2022). "Reliability and validity of the Chinese version of Cognitive Reserve Index Questionnaire (CRIq) and its application in patients with Acute Ischemic Stroke[C]," in *Proceedings of the Shanghai International Nursing Conference*, (Shanghai: Shanghai International Convention Center).

Li, J., Wang, J., Wu, B., Xu, H., Wu, X., Zhou, L., et al. (2020). Association between early cognitive impairment and midterm functional outcomes among chinese acute ischemic stroke patients: A Longitudinal Study. *Front. Neurol.* 11:20. doi: 10.3389/fneur.2020.00020

Lindley, R. I., Warlow, C. P., Wardlaw, J. M., Dennis, M. S., Slattery, J., and Sandercock, P. A. (1993). Interobserver reliability of a clinical classification of acute cerebral infarction. *Stroke* 24, 1801–1804. doi: 10.1161/01.str.24.12.1801

Liu, Y., Cai, Z. L., Xue, S., Zhou, X., and Wu, F. (2013). Proxies of cognitive reserve and their effects on neuropsychological performance in patients with mild cognitive impairment. *Clin. Neurosci.* 20, 548–553. doi: 10.1016/j.jocn.2012.04.020

Maiovis, P., Ioannidis, P., Nucci, M., Gotzamani-Psarrakou, A., and Karacostas, D. (2016). Adaptation of the Cognitive Reserve Index Questionnaire (CRIq) for the Greek population. *Neurol. Sci.* 37, 633–636. doi: 10.1007/s10072-015-2457-x

Melkas, S., Oksala, N. K., Jokinen, H., Pohjasvaara, T., Vataja, R., Oksala, A., et al. (2009). Poststroke dementia predicts poor survival in long-term follow-up: Influence of prestroke cognitive decline and previous stroke. *J. Neurol. Neurosurg. Psychiatry* 80, 865–870. doi: 10.1136/jnnp.2008.166603

Mijajlović, M. D., Pavlović, A., Brainin, M., Heiss, W. D., Quinn, T. J., Ihle-Hansen, H. B., et al. (2017). Post-stroke dementia - a comprehensive review. *BMC Med.* 15:11. doi: 10.1186/s12916-017-0779-7

Mok, V. C., Lam, B. Y., Wong, A., Ko, H., Markus, H. S., and Wong, L. K. (2017). Early-onset and delayed-onset poststroke dementia - revisiting the mechanisms. *Nat. Rev. Neurol.* 13, 148–159. doi: 10.1038/nrneurol.2017.16

Nasreddine, Z. S., Phillips, N. A., Bédirian, V., Charbonneau, S., Whitehead, V., Collin, I., et al. (2005). The Montreal Cognitive Assessment, MoCA: A brief screening tool for mild cognitive impairment. *Am. Geriatr. Soc.* 53, 695–699. doi: 10.1111/j.1532-5415.2005.53221.x

Nucci, M., Mapelli, D., and Mondini, S. (2012). Cognitive Reserve Index questionnaire (CRIq): A new instrument for measuring cognitive reserve. *Aging Clin. Exp. Res.* 24, 218–226. doi: 10.3275/7800

Ojala-Oksala, J., Jokinen, H., Kopsi, V., Lehtonen, K., Luukkonen, L., Paukkunen, A., et al. (2012). Educational history is an independent predictor of cognitive deficits and long-term survival in postacute patients with mild to moderate ischemic stroke. *Stroke* 43, 2931–2935. doi: 10.1161/STROKEAHA.112.667618

Ozakbas, S., Yigit, P., Akyuz, Z., Sagici, O., Abasiyanik, Z., Ozdogar, A. T., et al. (2021). Validity and reliability of "Cognitive Reserve Index Questionnaire" for the Turkish Population. *Mult. Scler. Relat. Disord.* 50:102817. doi: 10.1016/j.msard.2021.102817

Ozdemir, F., Birtane, M., Tabatabaei, R., Ekuklu, G., and Kokino, S. (2001). Cognitive evaluation and functional outcome after stroke. *Am. J. Phys. Med. Rehabil.* 80, 410–415. doi: 10.1097/00002060-200106000-00003

Patel, M. D., Coshall, C., Rudd, A. G., and Wolfe, C. D. (2002). Cognitive impairment after stroke: Clinical determinants and its associations with long-term stroke outcomes. *Am. Geriatr. Soc.* 50, 700–706. doi: 10.1046/j.1532-5415.2002.50165.x

Pendlebury, S. T., and Rothwell, P. M. (2009). Prevalence, incidence, and factors associated with pre-stroke and post-stroke dementia: A systematic review and meta-analysis. *Lancet Neurol.* 8, 1006–1018. doi: 10.1016/S1474-4422(09)70236-4

Qu, Y., Zhuo, L., Li, N., Hu, Y., Chen, W., Zhou, Y., et al. (2015). Prevalence of post-stroke cognitive impairment in china: A community-based, cross-sectional study. *PLoS One* 10:e122864. doi: 10.1371/journal.pone.0122864

Ramsey, L. E., Siegel, J. S., Lang, C. E., Strube, M., Shulman, G. L., and Corbetta, M. (2017). Behavioural clusters and predictors of performance during recovery from stroke. *Nat. Hum. Behav.* 1:0038. doi: 10.1038/s41562-016-0038

Ravona-Springer, R., Luo, X., Schmeidler, J., Wysocki, M., Lesser, G., Rapp, M., et al. (2010). Diabetes is associated with increased rate of cognitive decline in questionably demented elderly. *Dement Geriatr. Cogn. Disord.* 29, 68–74. doi: 10.1159/000265552

Richards, M., and Sacker, A. (2003). Lifetime antecedents of cognitive reserve. *Clin. Exp. Neuropsychol.* 25, 614–624. doi: 10.1076/jcen.25.5.614.14581

Rosenich, E., Hordacre, B., Paquet, C., Koblar, S. A., and Hillier, S. L. (2020). Cognitive reserve as an emerging concept in stroke recovery. *Neurorehabil. Neural. Repair* 34, 187–199. doi: 10.1177/1545968320907071

Savva, G. M., and Stephan, B. C. (2010). Epidemiological studies of the effect of stroke on incident dementia: A systematic review. *Stroke* 41, e41–e46. doi: 10.1161/STROKEAHA.109.559880

Schlegel, D., Kolb, S. J., Luciano, J. M., Tovar, J. M., Cucchiara, B. L., Liebeskind, D. S., et al. (2003). Utility of the NIH Stroke Scale as a predictor of hospital disposition. *Stroke* 34, 134–137. doi: 10.1161/01.str.0000048217.44714.02

Shin, M., Sohn, M. K., Lee, J., Kim, D. Y., Lee, S. G., Shin, Y. I., et al. (2020). Effect of cognitive reserve on risk of cognitive impairment and recovery after stroke: The KOSCO Study. *Stroke* 51, 99–107. doi: 10.1161/STROKEAHA.119.026829

Stark, B. A., Roth, G. A., Adebayo, O. M., Akbarpour, S., Aljunid, S. M., Alvis-Guzman, N., et al. (2021). Global, regional, and national burden of stroke and its risk factors, 1990–2019: A systematic analysis for the Global Burden of Disease Study 2019. *Lancet Neurol.* 20, 795–820.

Steffener, J., and Stern, Y. (2012). Exploring the neural basis of cognitive reserve in aging. *Biochim. Biophys. Acta* 1822, 467–473. doi: 10.1016/j.bbadis.2011.09.012

Steffener, J., Reuben, A., Rakitin, B. C., and Stern, Y. (2011). Supporting performance in the face of age-related neural changes: Testing mechanistic roles of cognitive reserve. *Brain Imaging Behav.* 5, 212–221. doi: 10.1007/s11682-011-9125-4

Stenberg, J., Håberg, A. K., Follestad, T., Olsen, A., Iverson, G. L., Terry, D. P., et al. (2020). Cognitive reserve moderates cognitive outcome after mild traumatic brain injury. *Arch. Phys. Med. Rehabil.* 101, 72–80. doi: 10.1016/j.apmr.2019.08.477

Stern, Y. (2002). What is cognitive reserve? Theory and research application of the reserve concept. *J. Int. Neuropsychol. Soc.* 8, 448–460.

Stern, Y. (2009). Cognitive reserve. *Neuropsychologia* 47, 2015–2028. doi: 10.1016/j.neuropsychologia.2009.03.004

Stern, Y. (2012). Cognitive reserve in ageing and Alzheimer's disease. *Lancet Neurol.* 11, 1006–1012. doi: 10.1016/S1474-4422(12)70191-6

Tan, Y., Pan, Y., Liu, L., Wang, Y., Zhao, X., and Wang, Y. (2017). One-year outcomes and secondary prevention in patients after acute minor stroke: Results from the China National Stroke Registry. *Neurol. Res.* 39, 484–491. doi: 10.1080/01616412.2017.1322804

Tu, Q. Y., Jin, H., Ding, B. R., Yang, X., Lei, Z. H., Bai, S., et al. (2013). Reliability, validity, and optimal cutoff score of the montreal cognitive assessment (changsha version) in ischemic cerebrovascular disease patients of hunan province, china. *Dement Geriatr. Cogn. Dis. Extra* 3, 25–36. doi: 10.1159/000346845

Umarova, R. M. (2017). Adapting the concepts of brain and cognitive reserve to post-stroke cognitive deficits: Implications for understanding neglect. *Cortex* 97, 327–338. doi: 10.1016/j.cortex.2016.12.006

Umarova, R. M., Schumacher, L. V., Schmidt, C., Martin, M., Egger, K., Urbach, H., et al. (2021). Interaction between cognitive reserve and age moderates effect of lesion load on stroke outcome. *Sci. Rep.* 11:4478. doi: 10.1038/s41598-021-83927-1

Vascular Surgery Group, Surgery Society of Chinese Medical Association (2017). Guidelines for diagnosis and treatment of carotid artery stenosis. *Chin. J. Vasc. Surg.* 2, 78–84.

Wang, D., Liu, J., Liu, M., Lu, C., Brainin, M., and Zhang, J. (2017). Patterns of stroke between university hospitals and nonuniversity hospitals in mainland china: Prospective multicenter hospital-based registry study. *World Neurosurg.* 98, 258–265. doi: 10.1016/j.wneu.2016.11.006

Wang, H. X., Macdonald, S. W., Dekhtyar, S., and Fratiglioni, L. (2017). Association of lifelong exposure to cognitive reserve-enhancing factors with

dementia risk: A community-based cohort study. *PLoS Med.* 14:e1002251. doi: 10.1371/journal.pmed.1002251

Wang, W., Jiang, B., Sun, H., Ru, X., Sun, D., Wang, L., et al. (2017). Prevalence, incidence, and mortality of stroke in China: Results from a nationwide population-based survey of 480 687 Adults. *Circulation* 135, 759–771. doi: 10.1161/CIRCULATIONAHA.116.025250

Wang, Y. J., Li, Z. X., Gu, H. Q., Zhai, Y., Jiang, Y., Zhao, X. Q., et al. (2020). China Stroke Statistics 2019: A Report From the National Center for Healthcare Quality Management in Neurological Diseases, China National Clinical Research Center for Neurological Diseases, the Chinese Stroke Association, National Center for Chronic and Non-communicable Disease Control and Prevention, Chinese Center for Disease Control and Prevention and Institute for Global Neuroscience and Stroke Collaborations. *Stroke Vasc. Neurol.* 5, 211–239. doi: 10.1136/svn-2020-000457

Weaver, N. A., Kuijf, H. J., Aben, H. P., Abrigo, J., Bae, H. J., Barbay, M., et al. (2021). Strategic infarct locations for post-stroke cognitive impairment: A pooled analysis of individual patient data from 12 acute ischaemic stroke cohorts. *Lancet Neurol.* 20, 448–459. doi: 10.1016/S1474-4422(21)00060-0

Yaffe, K., Weston, A., Graff-Radford, N. R., Satterfield, S., Simonsick, E. M., Younkin, S. G., et al. (2011). Association of plasma beta-amyloid level and cognitive reserve with subsequent cognitive decline. *JAMA* 305, 261–266. doi: 10.1001/jama.2010.1995

frontiers | Frontiers in Aging Neuroscience

TYPE Systematic Review
PUBLISHED 22 November 2022
DOI 10.3389/fnagi.2022.1019088

OPEN ACCESS

EDITED BY
Cosimo Urgesi,
University of Udine, Italy

REVIEWED BY
Aleksandra Pavlovic,
University of Belgrade, Serbia
Yucheng Gu,
Nanjing Medical University, China

*CORRESPONDENCE
Dahua Wu
wdh838692@sina.com

SPECIALTY SECTION
This article was submitted to Neurocognitive Aging and Behavior, a section of the journal Frontiers in Aging Neuroscience

RECEIVED 14 August 2022
ACCEPTED 25 October 2022
PUBLISHED 22 November 2022

CITATION
Xie Y, Xie L, Kang F, Jiang J, Yao T, Mao G, Fang R, Fan J and Wu D (2022) Association between white matter alterations and domain-specific cognitive impairment in cerebral small vessel disease: A meta-analysis of diffusion tensor imaging. *Front. Aging Neurosci.* 14:1019088. doi: 10.3389/fnagi.2022.1019088

Association between white matter alterations and domain-specific cognitive impairment in cerebral small vessel disease: A meta-analysis of diffusion tensor imaging

Yao Xie[1], Le Xie[1], Fuliang Kang[2], Junlin Jiang[1], Ting Yao[1], Guo Mao[3], Rui Fang[4], Jianhu Fan[1] and Dahua Wu[1]*

[1]Department of Neurology, Hunan Academy of Traditional Chinese Medicine Affiliated Hospital, Changsha, China, [2]Department of Imaging, Hunan Academy of Traditional Chinese Medicine Affiliated Hospital, Changsha, China, [3]Office of Academic Research, Hunan Academy of Traditional Chinese Medicine Affiliated Hospital, Changsha, China, [4]College of Integrated Chinese and Western Medicine, Hunan University of Chinese Medicine, Changsha, China

Objective: To investigate the association between diffusion tensor imaging (DTI) findings and domain-specific cognitive impairment in cerebral small vessel disease (CSVD).

Methods: Databases such as PubMed, Excerpta Medical Database (EMBASE), Web of Science, Cochrane Library, Chinese National Knowledge Infrastructure Databases (CNKI), Wanfang, Chinese Biomedical Literature Database (SinoMed), and Chongqing Chinese Science and Technology Periodical Database (VIP) were comprehensively retrieved for studies that reported correlation coefficients between cognition and DTI values. Random effects models and meta-regression were applied to account for heterogeneity among study results. Subgroup and publication bias analyses were performed using Stata software.

Results: Seventy-seven studies involving 6,558 participants were included in our meta-analysis. The diagnosis classification included CSVD, white matter hyperintensities (WMH), subcortical ischemic vascular disease, cerebral microbleeding, cerebral amyloid angiopathy (CAA), cerebral autosomal dominant arteriopathy with subcortical infarcts and leukoencephalopathy (CADASIL), and Fabry disease. The pooled estimates showed that the fractional anisotropy (FA)-overall exhibited a moderate correlation with general cognition, executive function, attention, construction, and motor performance (r = 0.451, 0.339, 0.410, and 0.319), and the mean diffusitivity/apparent diffusion coefficient (MD/ADC)-overall was moderately associated with general cognition, executive function, and memory (r = −0.388, −0.332, and −0.303, respectively; $p_S < 0.05$). Moreover, FA in cingulate gyrus (CG), cerebral peduncle (CP), corona radiata (CR), external capsule (EC), frontal lobe (FL), fornix (FOR), internal capsule (IC), and thalamic radiation (TR) was strongly correlated with general cognition (r = 0.591, 0.584, 0.543, 0.662, 0.614, 0.543, 0.597, and 0.571), and a strong correlation was found

between MD/ADC and CG ($r = -0.526$), normal-appearing white matter (NAWM; $r = -0.546$), and whole brain white matter (WBWM; $r = -0.505$). FA in fronto-occipital fasciculus (FOF) ($r = 0.523$) and FL ($r = 0.509$) was strongly associated with executive function. Only MD/ADC of the corpus callosum (CC) was strongly associated with memory ($r = -0.730$). Besides, FA in CG ($r = 0.532$), CC ($r = 0.538$), and FL ($r = 0.732$) was strongly related to the attention domain. Finally, we found that the sample size, etiology, magnetic resonance imaging (MRI) magnet strength, study type, and study quality contributed to interstudy heterogeneity.

Conclusion: Lower FA or higher MD/ADC values were related to more severe cognitive impairment. General cognition and executive function domains attracted the greatest interest. The FL was commonly examined and strongly associated with general cognition, executive function, and attention. The CC was strongly associated with memory and attention. The CG was strongly related to general cognition and attention. The CR, IC, and TR were also strongly related to general cognition. Indeed, these results should be validated in high-quality prospective studies with larger sample sizes.

Systematic review registration: http://www.crd.york.ac.uk/PROSPERO, identifier: CRD42021226133.

KEYWORDS

small vessel disease (SVD), cognitive impairment, diffusion tensor imaging (DTI), neuroimage, meta-analysis

Introduction

Cerebral small vessel disease (CSVD) is a chronic, progressive disorder of small arteries, arterioles, capillaries, and venules in the brain resulting from various causes (Peng, 2019). CSVD is the most common cause of vascular cognitive impairment and accounts for 45% of dementia cases (Gorelick et al., 2011). At present, the diagnosis of CSVD mainly depends on computed tomography (CT) or magnetic resonance imaging (MRI). Given that CT has poor sensitivity for detecting brain lesions, MRI is the mainstay of the diagnosis of CSVD. Features observed on MRI include small subcortical infarcts, lacunes, white matter hyperintensities (WMH), perivascular spaces, microbleeds, and brain atrophy (Wardlaw et al., 2013). However, no biomarker is currently available to diagnose cognitive impairment in CSVD.

It is widely acknowledged that CSVD mainly leads to white matter (WM) damage. Growing evidence suggests that WM plays an important role in cognitive decline and dementia (Prins and Scheltens, 2015). Diffusion tensor imaging (DTI) is a newly developed MRI technique used to detect microscopic structural changes in WM and evaluate the integrity of WM fibers by quantifying the asymmetry (fractional anisotropy; FA) and amount of water diffusion (mean diffusivity/apparent diffusion coefficient; MD/ADC). It is widely considered a candidate imaging marker for evaluating cognitive impairment (Pasi et al., 2016). Over the years, many studies have explored cognitive impairment of CSVD by using DTI. However, the relationship between DTI and cognitive disorder in CSVD remains unclear. Indeed, different studies have examined different cognitive domains and brain regions separately. To our knowledge, no meta-analysis has hitherto summarized the association between DTI findings and cognitive outcomes following CSVD. To address this gap, our study explored the association between DTI findings and domain-specific cognitive impairment in CSVD.

Methods

The meta-analysis was conducted according to the Preferred Reporting Items for Systematic Reviews and Meta-Analyses (PRISMA) guidelines (Moher et al., 2009). This research was registered in PROSPERO (International prospective register of systematic reviews; registration number: CRD42021226133), and the meta-analysis protocol was published online after peer review (Xie et al., 2021).

Literature search and study eligibility

Databases such as PubMed, Excerpta Medical Database (EMBASE), Web of Science, Cochrane Library, Chinese National Knowledge Infrastructure Databases (CNKI), Wanfang, Chinese Biomedical Literature Database (SinoMed), and Chongqing Chinese Science and Technology Periodical Database (VIP) were retrieved for relevant studies published

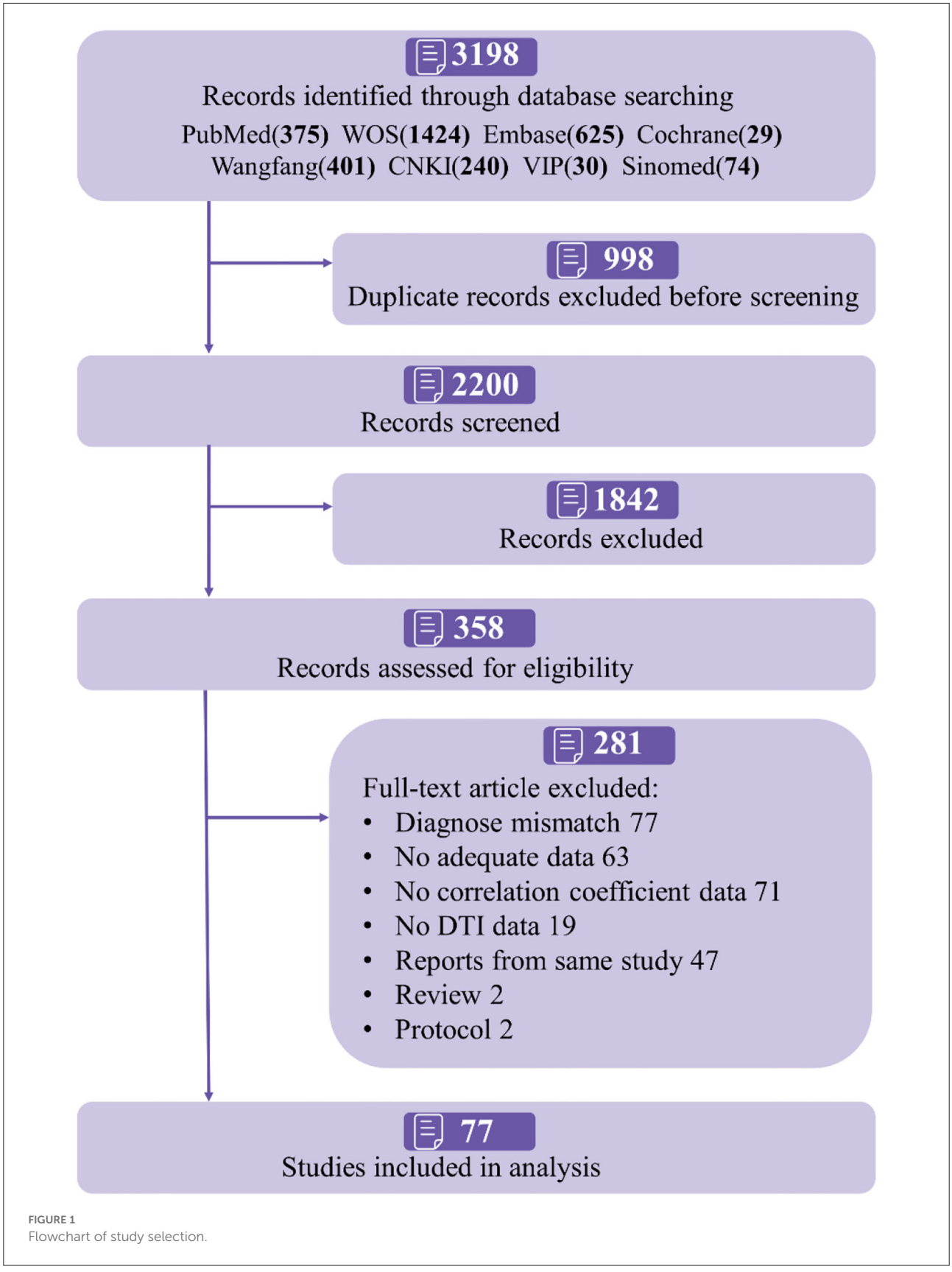

FIGURE 1
Flowchart of study selection.

TABLE 1 Summarized characteristics of the included study.

Researches	Number of studies (%) ($n = 77$)	
Diagnosis and classification		
CSVD	12 (15.6%)	
White matter hyperintensity	28 (36.4%)	
Subcortical ischemic vascular disease	24 (31.2%)	
Cerebral microbleeds	2 (2.6%)	
CADASIL	7 (9.1%)	
Cerebral amyloid angiopathy	3 (3.9%)	
Fabry	1 (1.3%)	
Study sites		
Asian	58 (75.3%)	
Europe and America	19 (24.7%)	
Study type		
Cross-sectional	68 (88.3%)	
Cohort	7 (9.1%)	
Case–control	2 (2.6%)	
Quality of research		
High quality	6 (7.8%)	
Moderate quality	50 (64.9%)	
Low quality	21 (27.3%)	
Centers		
Single center	71 (92.2%)	
Multiple centers	6 (7.8%)	
Participants	$N_{studies}$ **(%)**	**Mean or percentage**
Age	75 (97.4%)	64.8 (years)
Male	72 (93.5%)	57%
MMSE	21 (27.3%)	25.8 (scores)
MoCA	32 (41.6%)	23.1 (scores)
Hypertension	37 (48.1%)	53.8%
Smoking	25 (32.5%)	31.3%
Education	46 (59.7%)	10.3 (years)
MRI	$N_{studies}$ **(%)**	
DTI metrics		
FA	63 (81.8%)	
MD/ADC	59 (76.6%)	
$b = 1000$ (DWI)	55 (71.4%)	
Brand of scanner		
General electric	36 (46.8%)	
Philips	13 (16.9%)	
Siemens	24 (31.2%)	
MRI magnet strength		
1.5 Tesla	20 (26%)	
3 Tesla	55 (71.4%)	
Method(s) of analysis		
ROI	52 (67.5%)	
Multivariate analysis	20 (26.0%)	

from 1 January 1994, to 1 August 2021. The detailed search strategy can be found in the published protocol (Xie et al., 2021).

We included studies according to the following criteria: (1) MRI or CT was used to determine CSVD in adults (≥18 years). (2) Participants had mild cognitive impairment or dementia and suffered at least one cognitive domain disorder. (3) FA and/or MD/ADC data were reported for one or more brain regions during DTI analysis. (4) Cognitive testing scores were reported in the studies. (5) Correlations between cognitive testing scores and DTI values were reported (Pearson's *r*, Spearman's rho, or other correlation coefficients). (6) Cohort, case-control, or cross-sectional studies. Exclusion criteria were: (1) Comorbidities such as immune-mediated conditions or other severe diseases (e.g., multiple sclerosis, sarcoidosis, or radiation-induced-encephalopathy). (2) Cognitive disorder was mainly caused by neurodegenerative disorders or other diseases (e.g., Alzheimer's disease, frontotemporal dementia, Lewy body dementia, Parkinson's disease, massive cerebral infarction, trauma, toxic). (3) Reviews, case studies, and studies with very small samples ($N \leq 5$). (4) DTI data or cognitive testing scores could not be extracted, calculated, or provided by the study authors. (5) Studies that used research data from different articles.

Study selection and data extraction

Literature search results were imported into NoteExpress software (V3.0). Data extraction was performed independently by three reviewers (YX, LX, and FK). If multiple reports were published from the same study, we included the study with the most up-to-date or comprehensive information. The following data were extracted: publication, general information, study design, participant characteristics, control, comorbidities, type of CSVD, the severity of cognitive impairment, DTI metrics, cognitive testing, the brand of scanner, MRI magnet strength, method of analysis, duration of follow-up, etc. Cognitive outcomes were categorized into eight cognitive domains according to previous studies (Lezak et al., 2012): general cognition, memory, attention, processing speed and working memory, executive function, verbal skills, concept formation and reasoning, construction and motor performance.

Quality control and bias assessment

The Newcastle–Ottawa Scale (NOS) was used to evaluate the quality of the included cohort or case-control studies (Wells, 2004). It contains eight items, including selection, comparability, exposure, and outcome and the maximum score is 9. The quality of studies was graded as good (≥7), fair (4–6), or poor (<4). The quality of cross-sectional studies was assessed by the Agency for Healthcare Research and Quality (AHRQ) scale (Rostom et al., 2004), which contains 11 items. The studies were assessed

as low, moderate, and high quality for scores of 0–3, 4–7, and 8–11, respectively.

Statistical analysis

Pearson's correlation analysis was applied to assess the relationship between the DTI metrics of each brain region and individual cognitive domain. Spearman's rho was transformed with the equation ($r = 2\sin[r_s\ \pi/6]$) (Rupinski and Dunlap, 1996). Then, summary r was calculated with Fisher's Z, which was transformed with Pearson's r (Borenstein et al., 2009). Effect sizes (summary r) of 0.1, 0.3, 0.5, and 0.7 correspond to small, moderate, strong, and very strong effects (Rosenthal, 1996). The beta coefficients were also transformed into Pearson's correlation coefficient (Peterson and Brown, 2005).

The following variables were calculated in meta-regression and subgroup analysis: etiology (arteriosclerosis versus genetic), study type (cohort versus case-control versus cross-sectional studies), magnet strength (1.5T vs. 3.0T), sample size ($\leq$50 vs. $>$50), and quality of the study (low quality versus moderate quality versus high quality). The random effects model (Der Simonian and Laird method), which is more conservative, was applied in all meta-analyses, since the clinical and methodological conditions differed to some extent in included studies (DerSimonian and Laird, 1986). It has been established that the Q-test has poor power to analyze heterogeneity when few studies are included (Higgins and Thompson, 2002). In the present study, heterogeneity among the included studies was assessed by I^2. According to the Cochrane Handbook for Systematic Reviews of Interventions (version 5.1.0), the degree of heterogeneity was defined by the I^2 value. I^2 values of 0%−40% might not be important, and 30–60, 50–90, and 75%−100% represented moderate, substantial, and considerable heterogeneity.

Publication bias was assessed by the funnel plot and Egger's test. A p-value of < 0.05 was statistically significant. All analyses were performed with Stata version 15.1.

Results

Participant and study characteristics

Figure 1 shows the selection of studies to be included in the present study. Finally, 77 studies were included for systematic review (Table 1 and Supplementary Table S1 for summary information). The sample size of individual studies ranged from 23 to 801, with a total of 6,558 participants. Among those, 58 studies (75.3%) were conducted in Asia, and the rest were conducted in Europe or America. The included studies enrolled patients with CSVD, WMH, subcortical ischemic vascular disease (SIVD), cerebral microbleeds (CMB), cerebral amyloid angiopathy (CAA), cerebral autosomal dominant arteriopathy with subcortical infarcts and leukoencephalopathy (CADASIL), and Fabry disease. Patients with WMH (36.4%) and SIVD (31.2%) were the most commonly analyzed. In most cases, DTI was performed with 3 Tesla MRI (71.4%), and region of analysis (ROI) analysis was conducted in 52 studies (67.5%). Overall, eight cognitive domains and 38 brain regions were reported, with mild or moderate cognition in most studies (62.3%), while 24 studies did not report participant cognitive status. The average education degree in 37.7% of studies was 10.2 years, and 29 studies did not describe education information.

Relationship between FA, MD/ADC, and cognition

General cognition

As shown in Figures 2, 3, a moderate correlation was found between FA and general cognition [$r = 0.451$, 95% confidence interval (CI) 0.407 to 0.492, $I^2 = 80.2\%$]. Moreover, a strong correlation was found with cingulate gyrus (CG), corona radiata (CR), frontal lobe (FL), internal capsule (IC), and thalamic radiation (TR) reported in at least three studies, yielding correlation coefficients of 0.591 (0.348, 0.759), 0.543 (0.209, 0.764), 0.614 (0.500, 0.707), 0.597 (0.353, 0.764), and 0.571 (0.384, 0.713), respectively; however, considerable heterogeneity was observed. Other brain regions also showed a strong correlation effect only in one or two studies, such as the cerebellum (CER), cerebral peduncle (CP), external capsule (EC), fornix (FOR), globus pallidus (GP), hemispheric deep white matter (HDWM), inferior longitudinal fasciculus (ILF), and medial lemniscus (ML). These cross-sectional studies were not of high quality, with a relatively small sample size (smaller than 40).

As shown in Figures 4, 5, a moderate correlation was found between MD/ADC and general cognition [$r = -0.388$ (-0.435, -0.339), $I^2 = 82\%$]. Strong correlations were found with CG, normal-appearing white matter (NAWM), and whole brain white matter [WBWM; $r = -0.526$ (-0.706, -0.282); $r = -0.546$ (-0.737, -0.275); $r = -0.505$ (-0.711, -0.219)], which were supported by more than three studies, but marked heterogeneity was observed. Similarly, CP, EC, forceps minor (FMI), FOR, HDWM, and ML presented a strong correlation in low-quality studies and small sample sizes.

Executive function

The pooled correlation between FA and executive function was 0.339 (0.296, 0.381), $I^2 = 67\%$ (Supplementary Figure S1). FL was reported in five studies and the pooled estimates showed a strong correlation [$r = 0.523$ (0.382, 0.640), $I^2 = 40.60\%$]. Although the FA of CER, corticospinal tract (CT), fronto-occipital fasciculus (FOF), and hippocampus (HIP) was reported in less than three studies, a strong correlation was found with the executive function. Among these, FOF was reported by two

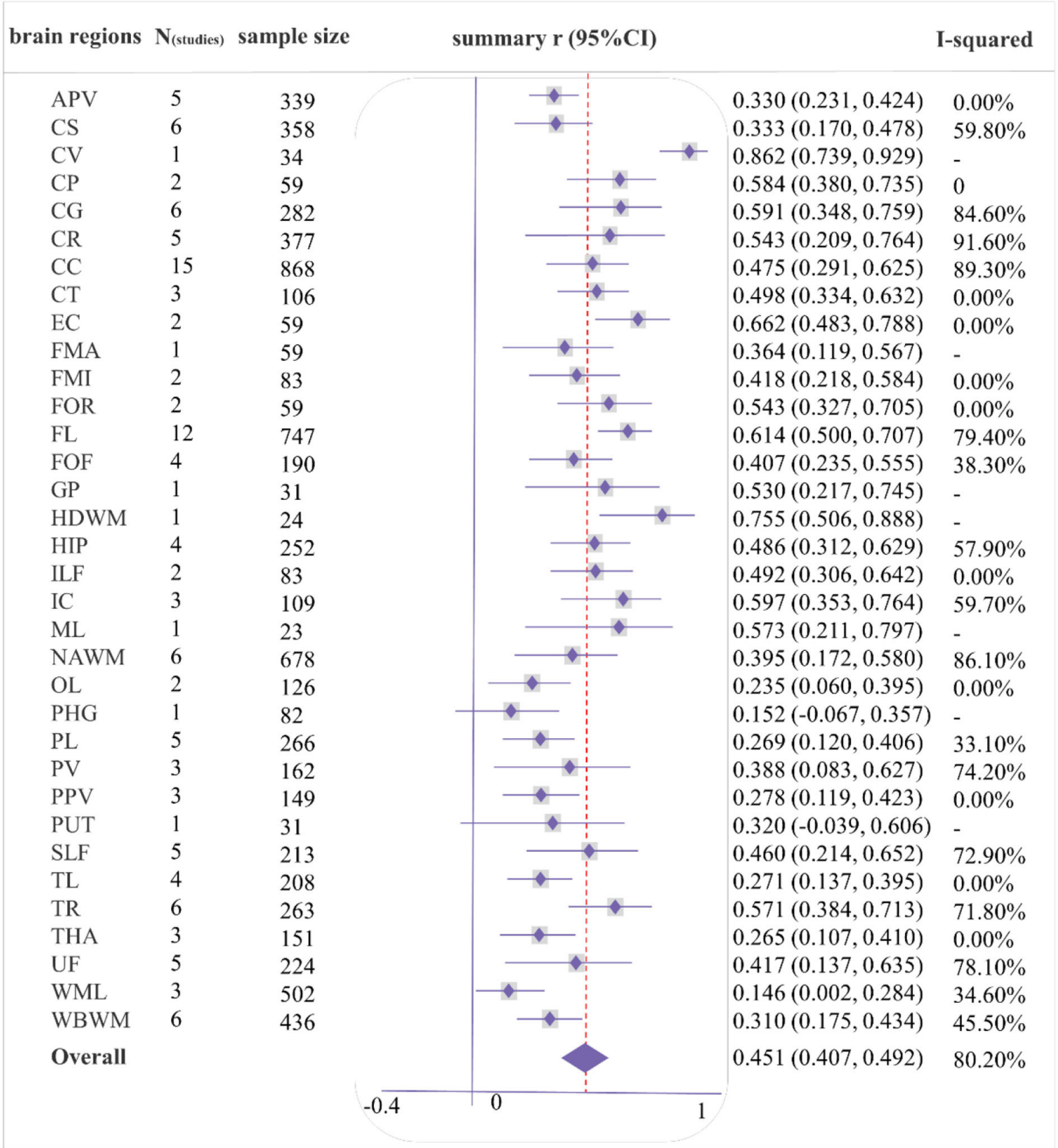

FIGURE 2
Forest plot of correlations between fractional anisotropy (FA) and general cognition by different brain regions. Summary of abbreviated words in Supplementary Table S5, the following figures are the same as above.

studies, with a total sample size of 155, and only one high-quality study was included.

The pooled correlation between MD/ADC and executive function was −0.332 (−0.382, −0.280), I^2 = 71.6% (Supplementary Figure S2). Although GP and putamen (PUT) indicated a strong correlation with executive function in one study, this study was low-quality, including less than 40 participants.

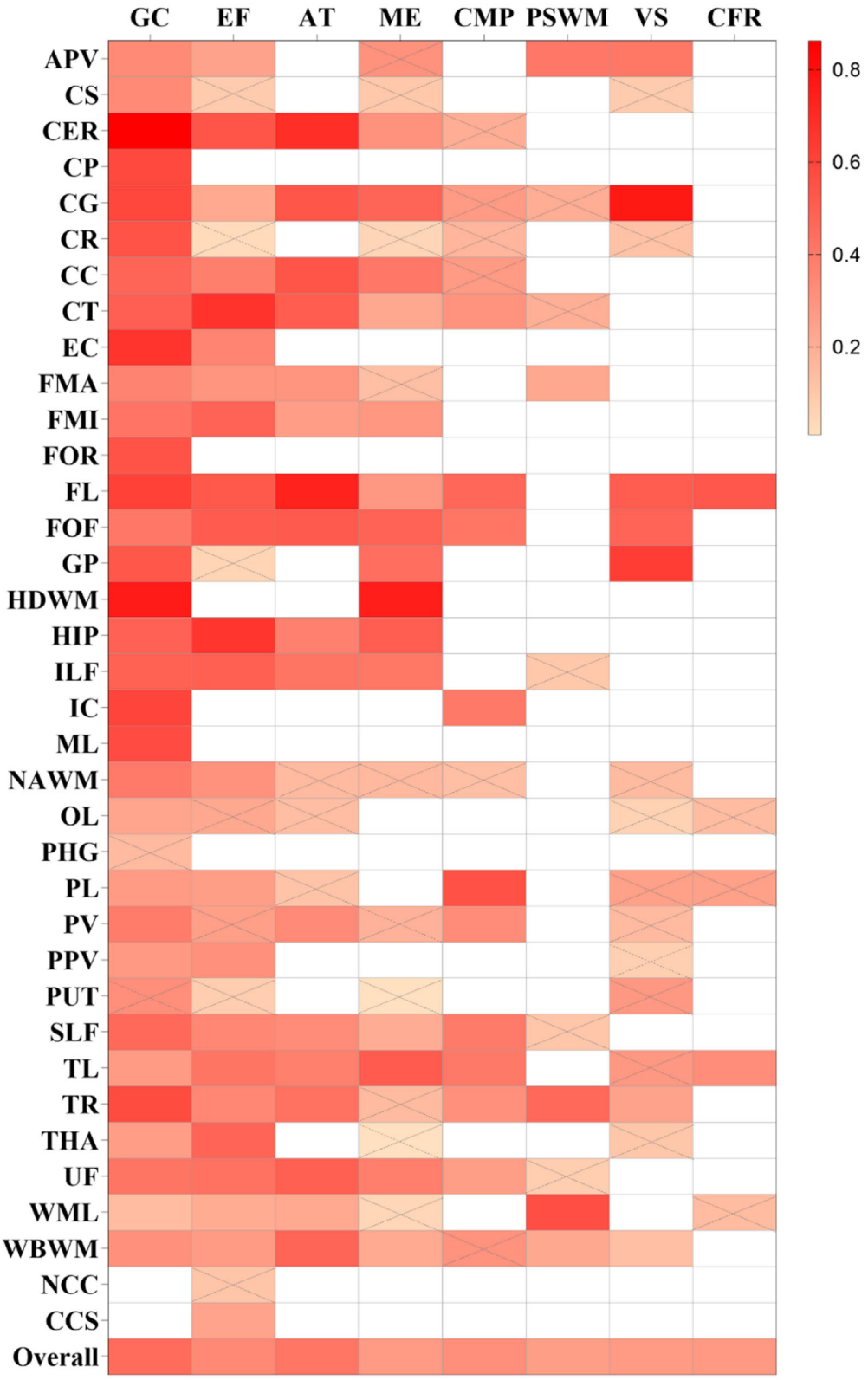

FIGURE 3
Summary correlation coefficients between different cognitive domains and fractional anisotropy (FA) in varying regions with color scales. Correlation matrix for the *r*-value of meta-analytic tests, the larger *r*-values of squares are with a brighter color. Squares with a white color represent no studies that report the relationship. Squares with gray slashes denote insignificant correlation ($p > 0.05$).

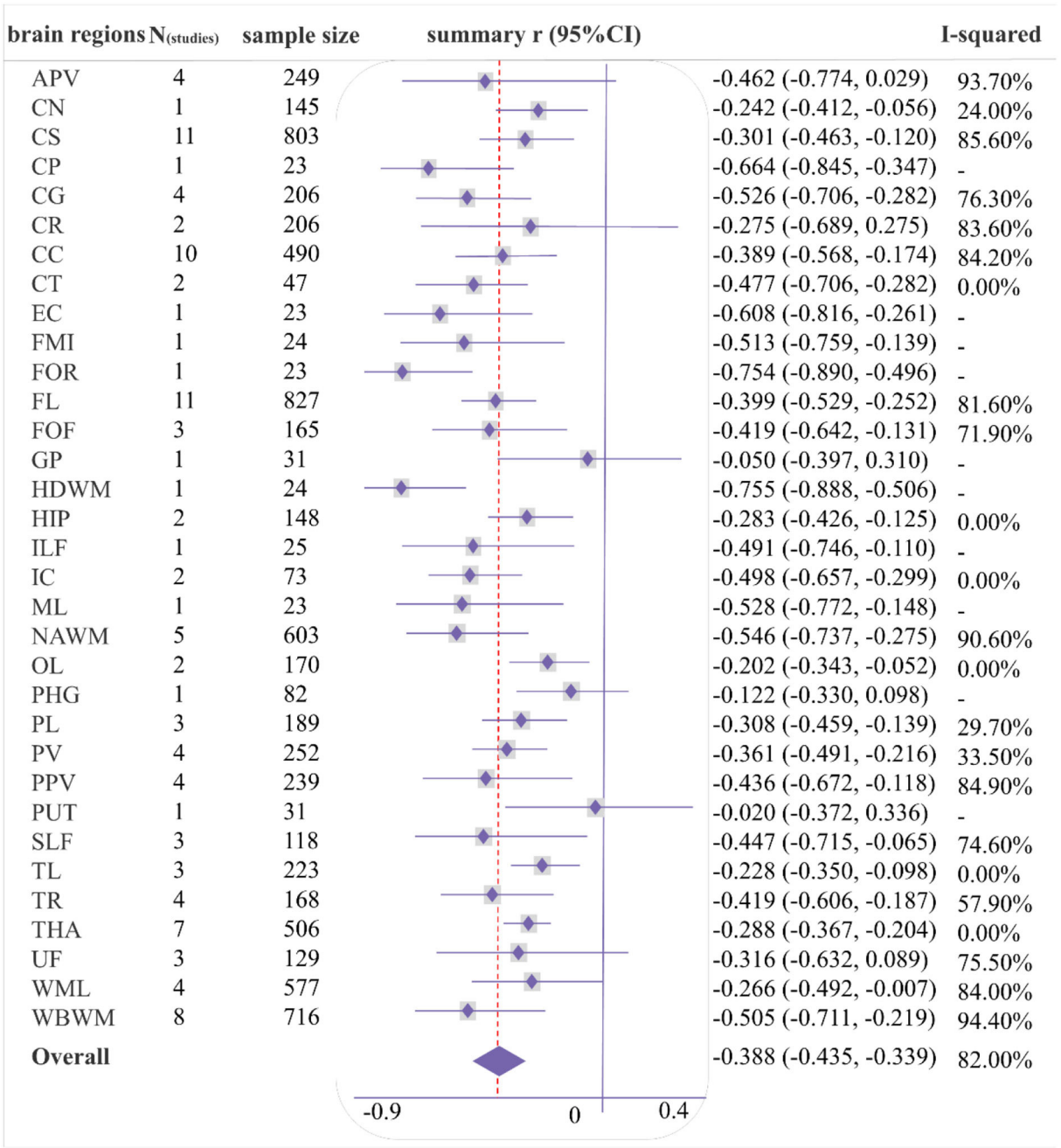

FIGURE 4
Forest plot of correlations between mean diffusivity/apparent diffusion coefficient (MD/ADC) and general cognition by different brain regions.

Memory

A weak correlation was observed between memory and FA [r = 0.276 (0.221, 0.328), I^2 = 64.8%], and a moderate association between MD/ADC and memory [r = −0.303 (−0.364, −0.241), I^2 = 64.8%; Supplementary Figures S3, S4]. Several brain regions showed a strong correlation between DTI and memory in one or two studies, including the HDWM, HIP, temporal lobe (TL) for FA, and corpus callosum (CC), HDWM, and ILF for MD/ADC. Among these, the sample size for TL or CC was more than 50, and all studies were of moderate quality. The correlation coefficients for TL and CC were 0.510 (0.289, 0.679) and −0.730 (−0.922, −0.247).

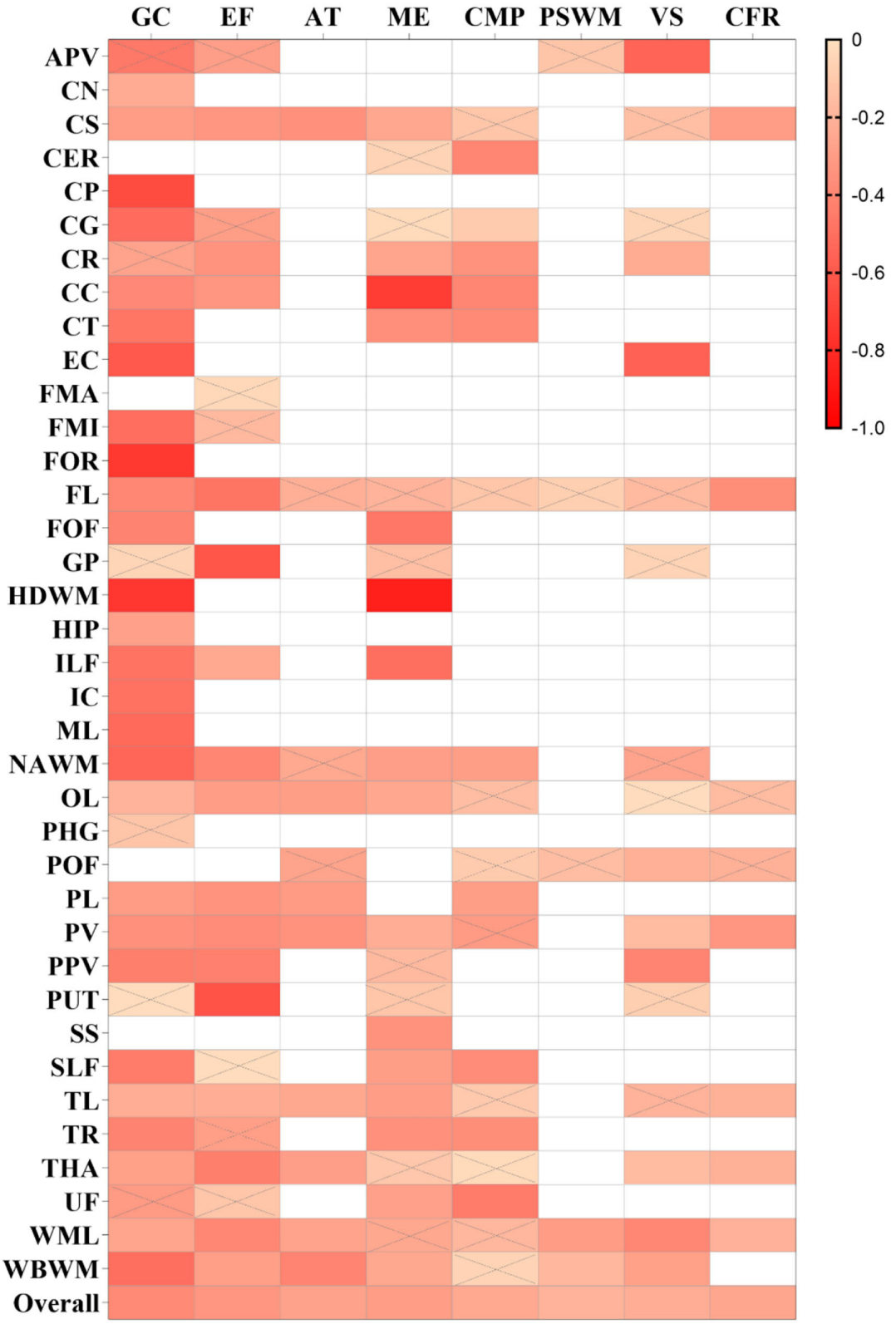

FIGURE 5
Summary correlation coefficients between different cognitive domains and mean diffusivity/apparent diffusion coefficient (MD/ADC) in varying regions with color scales. The smaller *r* values of squares are displayed in a brighter color. The others are the same as above.

Attention

A weak correlation was found between MD/ADC and attention [$r = -0.278$ (-0.357, -0.194), $I^2 = 62.9\%$; Supplementary Figure S5], while no brain regions with a strong correlation between MD/ADC and attention were observed. However, FA exhibited a moderate correlation with attention [$r = 0.410$ (0.327, 0.488), $I^2 = 75.8\%$; Supplementary Figure S6]. FA in CER, CG, CC, CT, FL, and FOF strongly correlated with attention. Two moderate-quality studies with more than 80 participants were available for CG, CC, and FL. The pooled analysis yielded correlation values of 0.532 (0.365, 0.666), 0.538 (0.141, 0.787), and 0.732 (0.608, 0.822).

Processing speed and working memory

Fractional anisotropy and MD/ADC yielded a weak correlation in processing speed and working memory [PSWM; $r = 0.259$ (0.176, 0.338), $I^2 = 64.4\%$; -0.202 (-0.310, -0.090), $I^2 = 69.6\%$; Supplementary Figures S7, S8]. Moreover, only FA in WML was strongly correlated with PSWM [$r = 0.558$ (0.331, 0.724)], which was reported by a moderate-quality study involving 50 participants.

Verbal skills

FA and MD/ADC also exhibited a weak correlation with verbal skills [$r = 0.276$ (0.177, 0.369), $I^2 = 67.6\%$; $r = -0.226$ (-0.286, -0.164), $I^2 = 30\%$; Supplementary Figures S9, S10]. However, in one study, some brain regions exhibited a strong correlation with verbal skills, including CG, FL, and GP for FA, and anterior periventricular (APV) and EC for MD/ADC. A moderate-quality study reported a correlation coefficient of 0.766 (0.625, 0.859) for CG, while other studies for Fl and GP were low-quality. Compared with APV, the study results for EC were obtained after adjusting for covariates and yielded a correlation coefficient of -0.564 (-0.743, -0.310).

Concept formation and reasoning

Overall, the strength of the correlation between FA and concept formation and reasoning (CFR) and between MD and CFR was weak [$r = 0.277$ (0.125, 0.415), $I^2 = 36\%$; $r = -0.260$ (-0.328, -0.188), $I^2 = 0\%$; Supplementary Figures S11, S12). A low-quality study indicated that FA in FL was strongly correlated with CFR [$r = 0.528$ (0.280, 0.709)].

Construction and motor performance

The overall strength of correlation between FA and construction and motor performance (CMP) was moderate [$r = 0.319$ (0.243, 0.391), $I^2 = 60.3\%$], while a weak overall correlation was found between MD and CMP [$r = -0.248$ (-0.311, -0.182), $I^2 = 49\%$; Supplementary Figures S13, S14]. The FA in the parietal lobe (PL) was strongly correlated with CMP [$r = 0.553$ (0.327, 0.719)], which was only reported by a moderate-quality study.

Meta-regression analysis and subgroup analysis

The meta-regression analysis was performed on the whole brain and a few brain regions ($N_{studies} \geq 10$; Supplementary Table S2) (Schmid et al., 2004). During meta-regression analysis between FA and the whole brain, sample size, etiology, magnet strength, study type, and study quality contributed to the heterogeneity. However, none of these covariates were associated with the heterogeneity of general cognition-related correlations in the CC, FL, and centrum semiovale (CS). Based on the results of the meta-regression analysis, a subgroup analysis was also performed to identify sources of heterogeneity (Supplementary Table S3). We found that the large sample size, 3 Tesla, and genetic etiology accounted for the close relationship between DTI metrics and cognition. However, high-quality prospective studies indicated a weaker correlation.

Bias and quality assessment

Sixty-eight cross-sectional studies, seven cohort studies, and two case-control studies were included in the meta-analysis (Table 1), including high ($n = 6$), moderate ($= 50$), and low ($n = 21$) quality. Moreover, 20 studies adjusted their baseline data during statistical analysis. Details of individual studies are provided in Supplementary Table S1. Publication bias was assessed in studies with sufficient sample size and strong correlation. Egger's test detected a significant bias only for analysis of the correlation between the MD (NAMW) and general cognition ($p = 0.01$; Supplementary Figure S15).

Discussion

In this systematic review and meta-analysis of 77 studies, eight cognitive domains were impacted by CSVD. General cognition ($N_{studies} = 57$) and executive function ($N_{studies} = 34$) were the domains of greatest interest in selected studies (Supplementary Figure S16). It is well established that executive function is the main damaged cognitive domain of CSVD (Peng, 2019; Litak et al., 2020). In the present study, FA and MD/ADC were significantly associated with these eight cognitive domains (all $p < 0.05$). During DTI analysis, low fractional anisotropy and high mean diffusivity generally reflect lower microstructural connectivity. Our meta-analysis showed that lower FA or higher MD values were related to more severe cognitive impairment.

According to the Vascular Behavioral and Cognitive Disorders (VASCOG) statement, it is recommended to evaluate multiple cognitive domains for CSVD (Sachdev et al., 2014). Different cognitive domains exhibited different correlations with DTI metrics in our study. For instance, FA-overall exhibited a moderate correlation with general cognition, executive function, attention, construction, and motor performance (r = 0.451, 0.339, 0.410, and 0.319, respectively). Moreover, MD/ADC-overall exhibited a moderate correlation with general cognition, executive function, and memory (r = −0.388, −0.332, and −0.303) and a weak correlation with the remaining domains. This finding provided the rationale for applying DTI to evaluate cognition in CSVD.

According to the Journal of the American College of Cardiology (JACC) scientific expert panel, it is very difficult to improve cognitive disorder during the late stages (Iadecola et al., 2019), emphasizing the importance of early diagnosis and treatment of cognitive impairment. Over the years, significant emphasis has been placed on biological markers for early identification and intervention in white matter damage. DTI can detect early tissue alterations, even in white matter appearing normal on conventional imaging (van den Brink et al., 2022). Some cognitive domains are affected during early cognitive impairment of CSVD, including executive function and attention (van der Flier et al., 2018; Peng, 2019). In this meta-analysis, executive function and attention were closely associated with DTI metrics.

Progressive cognitive impairment, gait disorders, and depression are the main clinical features of CSVD. Accordingly, emphasis should be placed on the specific microscopic structure changes associated with different impaired cognitive domains. Among the 77 included studies, 37 brain regions were explored. We found that white matter damage in specific areas was strongly associated with several cognitive domains (Supplementary Table S4). For instance, FL was strongly associated with the executive function and attention domains (r = 0.523, 0.732), and CC was strongly associated with the memory domain (r = −0.730). The mechanism underlying frontal lobe (FL) damage may involve dysregulation in the frontal–subcortical loop. Damage to the frontal–subcortical network can occur in the form of white matter lesions or microbleeds affecting pathways that connect cortical and subcortical regions, which result in cognitive impairments in executive function and attention (Ye and Bai, 2018). It is widely thought that white matter tracts in the CC harbor commissural fibers connecting the frontal lobe (FL) and other cortical areas, which can be damaged at the early stage of CSVD (Qiu et al., 2021). Overwhelming evidence indicates that brain network disorders lead to cognitive impairment of CSVD, and damaged network structure accounts for the association between CSVD neuroimaging lesions and cognitive deficits (Vasquez and Zakzanis, 2015). DTI technology may provide new opportunities to deepen our understanding of disconnection syndromes. Moreover, connectomics developed by DTI can be used to more specifically analyze the regions and functional connections in the cognitive impairment of CSVD.

Significant heterogeneity in participant characteristics and methodology was observed in the included studies. Random effects models and meta-regression models were applied to decrease heterogeneity. The higher quality and prospective design of studies led to more conservative and relatively lower correlation results, which yielded more reasonable conclusions. However, a larger sample size led to a more significant correlation. Current evidence suggests that genetic causes, like CADASIL, may damage white matter more severely, suggesting that DTI findings in hereditary CSVD exhibit a more obvious relationship with cognitive impairment (Cannistraro et al., 2019). In selected studies, differences in parameters, method of analysis, the brand of scanner, and MRI magnet strength led to significant interstudy heterogeneity. In this respect, 3.0 Tesla provided a larger effect size than 1.5 Tesla during meta-regression analysis which may be attributed to the better accuracy of 3.0 Tesla (Soares et al., 2013).

A comprehensive search and methodological effort were performed to summarize reliable correlation coefficients and all related brain regions. The protocol of meta-analysis had been published by peer review. In addition, different patient populations were investigated in our meta-analysis, including CSVD, WMH, SIVD, CMB, CAA, CADASIL, and Fabry disease. However, there were several limitations. First, minimizing heterogeneity attributed to clinical or methodological sources of bias was challenging, and subgroup analyses could not be performed for age, education level, and disease severity. Besides, most included studies were cross-sectional, mostly low-quality, and based on small sample sizes, which decreased the strength of our findings. Moreover, findings for some brain regions were roughly summarized and not comprehensively analyzed. For example, the splenium, body, and genu of CC were all described as CC. Moreover, the clinical assessment scales applied for cognitive tests varied in different studies.

Our findings suggest that DTI technology exhibits significant clinical value for the assessment of white matter alternations due to CSVD. High-quality prospective studies based on large sample sizes are warranted to explore the key regions and brain networks of cognitive disorders using DTI and to establish clinical value for domain-specific cognitive impairment.

Conclusion

In conclusion, the damaged regional white matter detected by DTI is associated with domain-specific cognitive deficits in CSVD. Lower FA or higher MD values are related to more severe cognitive impairment. General cognition and executive function domains are of greatest interest in

the current literature. The frontal lobe (FL) was strongly associated with general cognition, executive function, and attention. The corpus callosum (CC) was strongly associated with memory and attention. The cingulate gyrus (CG) was strongly related to general cognition and attention. The CR, IC, and TR were also strongly related to general cognition. However, sample size, etiology, MRI magnet strength, study type, and study quality contributed to heterogeneity in our study. Accordingly, our results should be further validated in prospective studies with high-quality and larger sample sizes. Future research should aim to make uniform the standard specification, analysis method, and reference value of DTI to increase the diagnostic value of DTI for cognitive impairment in CSVD.

Data availability statement

The original contributions presented in the study are included in the article/Supplementary material, further inquiries can be directed to the corresponding author.

Author contributions

The concept of this research was proposed by YX. The literature search, article screen, data extraction, and analysis were contributed by YX, LX, and FK. The protocol was drafted by YX, JJ, TY, RF, GM, and JF. The intellectual content was revised by YX and DW. All authors approved the final version of the manuscript.

Funding

This research was supported by the General project of the Hunan Provincial Health Commission (No. 202218014505), the General project of Hunan Administration of Traditional Chinese Medicine (D2022060), the Open Fund for First-class Disciplines of Integrated Traditional Chinese and Western Medicine (No. 2020ZXYJH10), the Hunan Academy of Traditional Chinese Medicine Foundation (No. 201920), the Foundation of China Center for Evidence-Based Traditional Chinese Medicine (No. 2019XZZX-NB004), the National Key Research and Development Project (No. 2018YFC1704904), and Natural Science Foundation of Hunan Province (No. 2022JJ40241).

Conflict of interest

The authors declare that the research was conducted in the absence of any commercial or financial relationships that could be construed as a potential conflict of interest.

Publisher's note

All claims expressed in this article are solely those of the authors and do not necessarily represent those of their affiliated organizations, or those of the publisher, the editors and the reviewers. Any product that may be evaluated in this article, or claim that may be made by its manufacturer, is not guaranteed or endorsed by the publisher.

Supplementary material

The Supplementary Material for this article can be found online at: https://www.frontiersin.org/articles/10.3389/fnagi.2022.1019088/full#supplementary-material

References

Borenstein, M., Hedges, L., Higgins, J., and Rothstein, H. (2009). *Introduction to Meta-analysis*. Chichester: John Wiley & Sons, Ltd. doi: 10.1002/9780470743386

Cannistraro, R. J., Badi, M., Eidelman, B. H., Dickson, D. W., Middlebrooks, E. H., Meschia, J. F., et al. (2019). CNS small vessel disease: a clinical review. *Neurology* 92, 1146–1156. doi: 10.1212/WNL.0000000000007654

DerSimonian, R., and Laird, N. (1986). Meta-analysis in clinical trials. *Control. Clin. Trials* 7, 177–188. doi: 10.1016/0197-2456(86)90046-2

Gorelick, P. B., Scuteri, A., Black, S. E., Decarli, C., Greenberg, S. M., Iadecola, C., et al. (2011). Vascular contributions to cognitive impairment and dementia: a statement for healthcare professionals from the american heart association/american stroke association. *Stroke.* 42, 2672–2713. doi: 10.1161/STR.0b013e3182299496

Higgins, J. P., and Thompson, S. G. (2002). Quantifying heterogeneity in a meta-analysis. *Stat. Med.* 21, 1539–1558. doi: 10.1002/sim.1186

Iadecola, C., Duering, M., Hachinski, V., Joutel, A., Pendlebury, S. T., Schneider, J. A., et al. (2019). Vascular cognitive impairment and dementia: JACC scientific expert panel. *J. Am. Coll. Cardiol.* 73, 3326–3344. doi: 10.1016/j.jacc.2019.04.034

Lezak, M. D., Howieson, D. B., Bigler, E. D., and Tranel, D. (2012). *Neuropsychological Assessment, 5th ed.* New York, NY: Oxford University Press.

Litak, J., Mazurek, M., Kulesza, B., Szmygin, P., Litak, J., Kamieniak, P., et al. (2020). Cerebral small vessel disease. *Int. J. Mol. Sci.* 21, 9729. doi: 10.3390/ijms21249729

Moher, D., Liberati, A., Tetzlaff, J., and Altman, D. G. (2009). Preferred reporting items for systematic reviews and meta-analyses: the PRISMA statement. *PLoS Med.* 6, e1000097. doi: 10.1371/journal.pmed.1000097

Pasi, M., van Uden, I. W., Tuladhar, A. M., de Leeuw, F. E., and Pantoni, L. (2016). White matter microstructural damage on diffusion tensor imaging in cerebral small vessel disease: clinical consequences. *Stroke.* 47, 1679–1684. doi: 10.1161/STROKEAHA.115.012065

Peng, D. (2019). Clinical practice guideline for cognitive impairment of cerebral small vessel disease. *Aging Med.* 2, 64–73. doi: 10.1002/agm2.12073

Peterson, R. A., and Brown, S. P. (2005). On the use of beta coefficients in meta-analysis. *J. Appl. Psychol.* 90, 175–181. doi: 10.1037/0021-9010.90.1.175

Prins, N. D., and Scheltens, P. (2015). White matter hyperintensities, cognitive impairment and dementia: an update. *Nat. Rev. Neurol.* 11, 157–165. doi: 10.1038/nrneurol.2015.10

Qiu, Y., Yu, L., Ge, X., Sun, Y., Wang, Y., Wu, X., et al. (2021). Loss of integrity of corpus callosum white matter hyperintensity penumbra predicts cognitive decline in patients with subcortical vascular mild cognitive impairment. *Front. Aging Neurosci.* 13, 605900. doi: 10.3389/fnagi.2021.605900

Rosenthal, J. A. (1996). Qualitative descriptors of strength of association and effect size. *J. Soc. Serv. Res.* 21, 37–59. doi: 10.1300/J079v21n04_02

Rostom, A., Dubé, C., and Cranney, A. (2004). *Celiac Disease*. Rockville, MD: Agency for Healthcare Research and Quality.

Rupinski, M. T., and Dunlap, W. P. (1996). Approximating pearson product-moment correlations from Kendall's Tau and Spearman's Rho. *Educ. Psychol. Meas.* 56, 419–429. doi: 10.1177/0013164496056003004

Sachdev, P., Kalaria, R., O'Brien, J., Skoog, I., Alladi, S., Black, S. E., et al. (2014). Diagnostic criteria for vascular cognitive disorders: a VASCOG statement. *Alzheimer Dis. Assoc. Disord.* 28, 206–218. doi: 10.1097/WAD.0000000000000034

Schmid, C. H., Stark, P. C., Berlin, J. A., Landais, P., and Lau, J. (2004). Meta-regression detected associations between heterogeneous treatment effects and study-level, but not patient-level, factors. *J. Clin. Epidemiol.* 57, 683–697. doi: 10.1016/j.jclinepi.2003.12.001

Soares, J. M., Marques, P., Alves, V., and Sousa, N. (2013). A hitchhiker's guide to diffusion tensor imaging. *Front. Neurosci.* 7, 31. doi: 10.3389/fnins.2013.00031

van den Brink, H., Doubal, F. N., and Duering, M. (2022). Advanced MRI in cerebral small vessel disease. *Int. J. Stroke*. 1078823975. doi: 10.1177/17474930221091879

van der Flier, W. M., Skoog, I., Schneider, J. A., Pantoni, L., Mok, V., Chen, C., et al. (2018). Vascular cognitive impairment. *Nat. Rev. Dis. Primers* 4, 18003. doi: 10.1038/nrdp.2018.3

Vasquez, B. P., and Zakzanis, K. K. (2015). The neuropsychological profile of vascular cognitive impairment not demented: a meta-analysis. *J. Neuropsychol.* 9, 109–136. doi: 10.1111/jnp.12039

Wardlaw, J. M., Smith, E. E., Biessels, G. J., Cordonnier, C., Fazekas, F., Frayne, R., et al. (2013). Neuroimaging standards for research into small vessel disease and its contribution to ageing and neurodegeneration. *Lancet Neurol.* 12, 822–838. doi: 10.1016/S1474-4422(13)70124-8

Wells, G. (2004). *The Newcastle-Ottawa Scale (NOS) for Assessing the Quality of Non Randomised Studies in Meta-analysis*. Available online at: www.ohri.ca//programs/clinical_epidemiology/oxford.asp (accessed October 01, 2022).

Xie, Y., Xie, L., Kang, F., Jiang, J., Yao, T., Li, Y., et al. (2021). Association between diffusion tensor imaging findings and domain-specific cognitive impairment in cerebral small vessel disease: a protocol for systematic review and meta-analysis. *BMJ Open* 11, e49203. doi: 10.1136/bmjopen-2021-049203

Ye, Q., and Bai, F. (2018). Contribution of diffusion, perfusion and functional MRI to the disconnection hypothesis in subcortical vascular cognitive impairment. *Stroke Vasc. Neurol.* 3, 131–139. doi: 10.1136/svn-2017-000080

frontiers | Frontiers in Aging Neuroscience

TYPE Original Research
PUBLISHED 20 December 2022
DOI 10.3389/fnagi.2022.958656

OPEN ACCESS

EDITED BY
Fermín Segovia,
University of Granada, Spain

REVIEWED BY
Emad Al-Yahya,
University of Nottingham,
United Kingdom
Deborah Talamonti,
Centre ÉPIC de l'Institut de Cardiologie de Montréal, Université de Montréal, Canada

*CORRESPONDENCE
Cristina Udina
cudina@perevirgili.cat

SPECIALTY SECTION
This article was submitted to Neurocognitive Aging and Behavior, a section of the journal Frontiers in Aging Neuroscience

RECEIVED 31 May 2022
ACCEPTED 23 November 2022
PUBLISHED 20 December 2022

CITATION
Udina C, Avtzi S, Mota-Foix M, Rosso AL, Ars J, Kobayashi Frisk L, Gregori-Pla C, Durduran T and Inzitari M (2022) Dual-task related frontal cerebral blood flow changes in older adults with mild cognitive impairment: A functional diffuse correlation spectroscopy study. *Front. Aging Neurosci.* 14:958656. doi: 10.3389/fnagi.2022.958656

Dual-task related frontal cerebral blood flow changes in older adults with mild cognitive impairment: A functional diffuse correlation spectroscopy study

Cristina Udina[1,2]*, Stella Avtzi[3], Miriam Mota-Foix[4], Andrea L. Rosso[5], Joan Ars[1,2], Lisa Kobayashi Frisk[3], Clara Gregori-Pla[3], Turgut Durduran[3,6] and Marco Inzitari[1,7]

[1]REFiT Barcelona Research Group, Parc Sanitari Pere Virgili and Vall d'Hebron Research Institute (VHIR), Barcelona, Spain, [2]Medicine Department, Universitat Autònoma de Barcelona, Barcelona, Spain, [3]ICFO – Institut de Ciències Fotòniques, The Barcelona Institute of Science and Technology, Barcelona, Spain, [4]Statistics and Bioinformatics Unit, Vall d'Hebron Institut de Recerca (VHIR), Barcelona, Spain, [5]Department of Epidemiology, School of Public Health, University of Pittsburgh, Pittsburgh, PA, United States, [6]Institució Catalana de Recerca i Estudis Avançats (ICREA), Barcelona, Spain, [7]Faculty of Health Sciences, Universitat Oberta de Catalunya (UOC), Barcelona, Spain

Introduction: In a worldwide aging population with a high prevalence of motor and cognitive impairment, it is paramount to improve knowledge about underlying mechanisms of motor and cognitive function and their interplay in the aging processes.

Methods: We measured prefrontal cerebral blood flow (CBF) using functional diffuse correlation spectroscopy during motor and dual-task. We aimed to compare CBF changes among 49 older adults with and without mild cognitive impairment (MCI) during a dual-task paradigm (normal walk, 2- forward count walk, 3-backward count walk, obstacle negotiation, and heel tapping). Participants with MCI walked slower during the normal walk and obstacle negotiation compared to participants with normal cognition (NC), while gait speed during counting conditions was not different between the groups, therefore the dual-task cost was higher for participants with NC. We built a linear mixed effects model with CBF measures from the right and left prefrontal cortex.

Results: MCI (n = 34) showed a higher increase in CBF from the normal walk to the 2-forward count walk (estimate = 0.34, 95% CI [0.02, 0.66], p = 0.03) compared to participants with NC, related to a right- sided activation. Both groups showed a higher CBF during the 3-backward count walk compared to the normal walk, while only among MCI, CFB was higher during the 2-forward count walk.

10.3389/fnagi.2022.958656

Discussion: Our findings suggest a differential prefrontal hemodynamic pattern in older adults with MCI compared to their NC counterparts during the dual-task performance, possibly as a response to increasing attentional demand.

KEYWORDS

mild cognitive impairment, dual-task (DT), prefrontal cortex, cerebral blood flow, spectroscopy, aging

1 Introduction

The aging of the worldwide population and the consequent increase in dementia and disability makes it crucial to improve knowledge about the pathophysiology underlying cognitive and motor impairments to establish preventive and treatment strategies to minimize related negative outcomes. Cognitive and motor impairments, both independently and concomitantly, are prevalent among older adults and have a negative impact on health-related outcomes, including increased healthcare costs and worsening quality of life (Verghese et al., 2006; Callisaya et al., 2011; Gaugler et al., 2016; Barbe et al., 2018). Pre-dementia states, such as mild cognitive impairment (MCI) or motoric cognitive risk syndrome, have been linked to a higher risk of falls and disability besides dementia (Verghese et al., 2008; Farias et al., 2009; Callisaya et al., 2016; Doi et al., 2017). In this context, there is growing evidence that supports the notion of a motor-cognitive interplay. For example, slowing gait speed predicted cognitive impairment in a longitudinal study of cognitively healthy subjects at the study's baseline (Rosso et al., 2017), and cognitive function, in particular executive function, has been associated with gait speed (Martin et al., 2013; Callisaya et al., 2014). This interplay is further supported by a common neural substrate since the prefrontal cortex (PFC) is involved in the neural control of gait and cognitive function. In particular, executive function (Alvarez and Emory, 2006; Lezak, 2012; Mirelman et al., 2018) is involved in gait control (Holtzer et al., 2006; Yogev-Seligmann et al., 2008). Furthermore, when a cognitive task is performed during a motor task, the dual-task performance declines relative to performance in each individual task, which is known as dual-task interference (Allali et al., 2007; Hausdorff et al., 2008; Montero-Odasso et al., 2012). The decrement in dual-task performance compared to the single task is larger with increasing cognitive demand (Allali et al., 2007), as well as in people with impaired mobility (Bloem et al., 2006) or cognition, especially executive dysfunction (Hausdorff et al., 2008). It seems that both tasks may compete for the same neural resources including, but not exclusively, the PFC (Collette et al., 2005; Leone et al., 2017), but the underlying neural mechanisms remain unclear. Prior studies have demonstrated that dual-task paradigms with a higher cognitive load may help differentiate individuals with MCI from their healthy counterparts (Bahureksa et al., 2017; Bishnoi and Hernandez, 2021), which may be due to competition for neural resources and reduced availability of resources in those with MCI.

Neuroimaging is an essential tool to further understand these factors, and functional neuroimaging studies have traditionally used functional magnetic resonance imaging (fMRI) and positron emission tomography, among other methods, to assess changes in brain activity related to different cognitive stimuli (Gourovitch et al., 2000; Jurado and Rosselli, 2007; Cui et al., 2011). As an attempt to study gait neural pathways, some studies have applied these techniques during the imagined walk (Blumen et al., 2014). Recently, the introduction of diffuse optical techniques, such as functional near-infrared spectroscopy (fNIRS), has allowed the study of brain activation during the execution of motor tasks, including dual-task walking (Holtzer et al., 2014). Other advantages of diffuse optics include its non-invasiveness, relatively low cost, portability, and, contrary to fMRI, suitability for patients with pacemakers, metallic implants, or those suffering from claustrophobia. Notably, an increasing body of literature from fNIRS studies supports its role in this area (Agbangla et al., 2017; Gramigna et al., 2017). Evidence from fNIRS studies suggests a different pattern in PFC oxygenation among older adults with MCI during walking under challenging circumstances compared to cognitively healthy counterparts (Udina et al., 2020).

A relatively more recent method, diffuse correlation spectroscopy (DCS) also uses near-infrared light to measure microvascular cerebral blood flow (CBF). Both fNIRS and DCS techniques use near-infrared light to obtain information about cerebral hemodynamics in a very similar manner. By using optical fibers placed on the forehead, light is emitted on the tissue and later the diffused light is collected by detector fibers as well. However, the principles and methodological analysis are different. fNIRS modality provides information about tissue oxygen metabolism through measures of oxygenated and deoxygenated hemoglobin concentrations. On the other hand, DCS techniques can provide information about the local microvascular blood flow of the measured area by assessing red blood cell movement based on laser speckle statistics (Boas et al., 1995; Boas and Yodh, 1997;

Durduran et al., 2010; Mesquita et al., 2011). According to the neurovascular coupling phenomenon, an increase in oxygen consumption to meet energy demands in activated cerebral areas would cause an increase in local blood flow, resulting in an increase in oxyhemoglobin and a decrease in deoxyhemoglobin. Underlying mechanisms consist of complex regulatory pathways that need further research (Phillips et al., 2016). The use of functional DCS (fDCS) might provide relevant information about this phenomenon since measures of CBF might complement information regarding oxygen metabolism provided by fNIRS, and hence provide insight into brain metabolism and neurovascular coupling. In addition, a great advantage of fDCS lies in the fact that the technique is more sensitive to the intracranial signal compared to extracerebral noise, as reported by Selb et al. (2014). Previous studies have validated DCS modality against standard techniques in humans and animals such as arterial-spin labeled (Yu et al., 2007; Milej et al., 2020), magnetic resonance imaging, transcranial doppler ultrasound (Buckley et al., 2009; Busch et al., 2016), positron emission tomography (Giovannella et al., 2020), and others. In addition, DCS has been used to study both inpatient and outpatient populations ranging from pediatric patients to adult neurocritical care patients (Durduran et al., 2004; Jaillon et al., 2007; Jain et al., 2014; Roche-Labarbe et al., 2014; Li et al., 2018). fDCS shares the same features as fNIRS and, therefore, could be used during motion. However, to our knowledge, the study of brain activity during gait and the dual-task with fDCS has never been reported. Assessing CBF changes during gait may complement evidence of changes in oxygenation from fNIRS studies, hence contributing to the understanding of neural mechanisms of gait provided by fNIRS studies.

The global aim of the study was to assess CBF changes in the PFC with fDCS among high-functioning, community-dwelling older adults with and without MCI during dual-task walking under various degrees of attention-demanding load. In particular, we sought to investigate whether (1) CBF changes were higher during various dual-task conditions compared to normal walk (NW); (2) CBF changes from NW to a dual-task differ between the cognitive status group [MCI vs. normal cognition (NC)], and (3) various clinical covariates affect CBF patterns. For the dual-task paradigm, we chose three dual-task (forward counting, backward counting, and obstacle negotiation) to assess the impact of different kinds of secondary tasks (Al-Yahya et al., 2011; Bishnoi and Hernandez, 2021) and increased attentional demand with two counting tasks, i.e., backward being more challenging than forward counting (Schwenk et al., 2010). We also included a heel tapping task as a rhythmic motor task that did not involve gait as we speculated it could be linked to different PFC hemodynamic changes than gait. Due to neurovascular coupling, one could speculate that the higher activation related to oxygenation changes shown in fNIRS studies during the dual-task (Doi et al., 2013; Holtzer et al., 2015; Chaparro et al., 2017) should be linked to a higher CBF (Phillips et al., 2016). Hence, we hypothesized that CBF would be higher during the dual-task compared to NW and that the CBF change from NW to the dual-task would be higher among MCI compared to persons with NC.

2 Materials and methods

2.1 Study design

A cross-sectional observational study was conducted among community-dwelling older adults with MCI and their counterparts with NC (the MEDPHOTAGE study).

2.2 Setting and participants

A convenience sample of patients from the outpatient memory clinic of Parc Sanitary Pere Virgili (Barcelona, Spain) was enrolled if they met the following criteria: $\geq$65 years old, having preserved function for activities of daily living, and being able to walk at least 50 m without assistance (walking aid devices, including cane or crutch, were accepted), according to self-reported information provided by the candidate and corroborated by relatives, when appropriate. The exclusion criteria included illiteracy, uncorrected significant visual or auditory impairment, dementia, overt psychiatric or neurological disease despite appropriate drug therapy (depression, delirium, stroke, and Parkinson's disease), cardiopulmonary disease that is not well controlled with medication, functional classification III-IV of the New York Heart Association (Dolgin, 1994) and/or the need for oxygen therapy, being terminally ill with a life expectancy less than 6 months, and current use of neuroleptics or anticonvulsants.

Demographical and clinical variables as well as neuropsychological assessment were collected at inclusion in the outpatient clinic. Then, the participants were scheduled for two separate assessments. Due to the long CBF measurement protocol that lasted around 2 h, we decided to separate the CBF measurements from the physical performance assessment (Section "2.5 Physical performance assessment").

2.3 Cognitive impairment diagnosis

A MCI diagnosis was determined in the outpatient clinic's case conference after an expert assessment by a geriatrician and a neuropsychologist following well-established criteria (Petersen, 2004). Briefly, MCI was identified if cognitive complaints were corroborated by scores in neuropsychological tests below the normal range (adjusted for age and years of education) and if the person maintained preserved activities of daily living or with functional impairment not due to cognitive

complaints. Cognitive domains assessed included global cognition (MMSE), memory (Rey auditory verbal learning test), working memory (digit span), phonemic and semantic verbal fluency, symbol digit modalities test, language (Boston Naming Test), constructive apraxia (Wechsler Adult Intelligence Scale 4th edition), ideomotor and ideational apraxia (Luria test), visual perception (Poppelreuter overlapping figures), and visuospatial recognition (Luria test). A classification into four clinical subtypes has been proposed depending on whether memory is impaired and whether there is impairment in one (single-domain) or several cognitive domains (multi-domain), such as executive functions, language, visuospatial skills, etc. In our study, MCI was classified into two groups: single-domain and multi-domain MCI following those criteria.

Patients from the outpatient clinic without cognitive impairment after clinical assessment and relatives of participants without cognitive complaints were assessed for inclusion. Participants had to score 27 or higher in the mini-mental state exam (MMSE) to be included in the NC group.

Dementia was ruled out of the outpatient memory clinic's case conference. Information regarding the performance of the activities of daily living was extracted during the interview from the participant and caregiver.

The research protocol's procedures were according to the Declaration of Helsinki and were approved by the local ethics committee (Universitat Autònoma de Barcelona, Spain). All participants provided written informed consent.

2.4 Assessment of cerebral blood flow

2.4.1 Dual-task paradigm

The measurements were performed in a quiet, well-lit room with an 8-m walkway. The researchers explained the whole protocol before the start of the first resting period, and a short instruction for each task was given after the rest period and immediately before the start of the corresponding task. The participants were asked to walk back and forth five loops, i.e., 16 m each, over the walkway for each of the four walking tasks that are described below. The total walking distance was 80 m (5 m × 16 m). A single trial of each task was performed. Importantly, the participants were instructed to walk at a self-selected pace and not to prioritize either of the tasks while performing the dual-task (Verghese et al., 2007). The researchers did not interact with the participants except to provide instructions or to assist the participant if necessary.

Instructions were provided as follows:

- Normal walk: Participants were instructed to walk five loops over the 8-m walkway.
- Walk while 2-forward counting (FWC): Participants were asked to perform serial 2-forward calculations (e.g., 2, 4, 6,. . .) while walking five loops over the walkway.
- Walk while 3-backward counting (BWC): Participants were asked to perform serial 3-backward calculations (e.g., 53, 50, 47,. . .) while walking five loops over the walkway.
- Walk while negotiating obstacles (WWO): Participants were instructed to walk over two small obstacles placed on the walkway. The first obstacle (15 cm of height) was placed at a 4-m distance from the start of the walking course and the second (10 cm of height) at a 6-m distance. See **Figure 1**.
- Heel tapping (TAP) task: Participants were instructed to alternatively elevate each heel while seated for 1 min.

Baseline CBF was assessed during resting periods before and after each task, where participants were instructed to avoid moving and talking. To avoid orthostatic changes right before the tasks, rest periods before and after walking tasks were performed standing, and resting periods before and after TAP were performed sitting on a chair. The first rest period lasted 2 min while the remaining rest periods lasted 1.5 min. The order of walking tasks was randomized; however, TAP was consistently the third test to minimize the possible effect of sitting rest in the following tasks. See **Figure 2**.

For the behavioral results, we recorded the time required to walk five loops over the 8-m walkway using a stopwatch. We report gait speed (m/sec) during each walking task [80 m/duration (s)] and dual-task cost for each task as previously described [((dual-task−single task)/single task) × 100] (Beurskens and Bock, 2012). It is worth noting that the gait assessment included turns to perform loops over the walkway, so the gait speed reported here is not limited to a steady-state walk. For the cognitive output, research assistants identified counting errors as a categorical variable. When the participant miscalculated more than three calculations, "counting errors" were identified as "Yes." Participants who were not able to perform the backward calculations while walking were instructed to stop the BWC trial.

2.4.2 Functional diffuse correlation spectroscopy system and physiological data acquisition

The optical data collection was performed with a custom-made DCS system (Durduran et al., 2010; Durduran and Yodh, 2014) with a temporal resolution of 9 s. Due to an early technical issue with the device, 6 s of the acquisition was discarded. In other words, 3 s of DCS data was acquired with a 6-s off-period in-between. This issue was identified after several subjects were measured, and to be able to keep all data comparable, we opted not to resolve it.

The device utilized probes suitable for placement over the prefrontal lobes for independent measurements of the CBF from

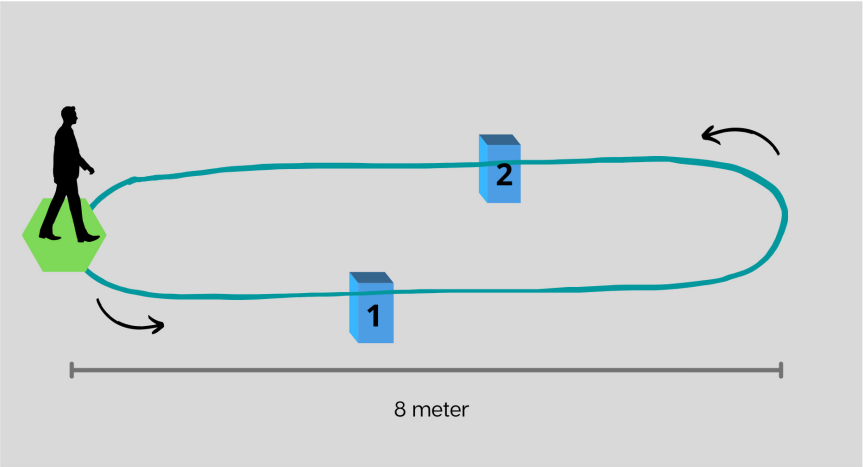

FIGURE 1
Representation of the walkway and placement of obstacles for walk while negotiating obstacles. The first obstacle (1), 15 cm in height, and placed at a 4-m distance from the start of the walking course, and the second (2), 10 cm in height, and placed at a 6-m distance.

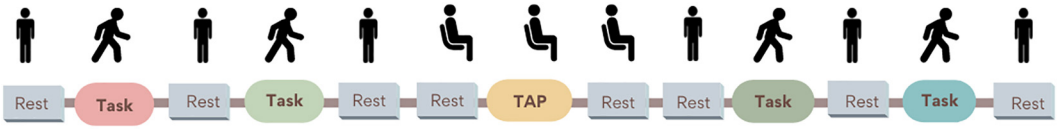

FIGURE 2
Dual-task paradigm during cerebral blood flow (CBF) measures. Rest periods: participants were instructed to remain silent and refrain from moving while standing. Only before and after the heel tapping task *(TAP)*, participants rested in a sitting position to avoid CBF changes related to orthostatic changes. Walking tasks (normal walk, walk while 2-forward count, walk while 3-backward count, and walk while negotiating obstacles) order was randomized to minimize the fatigue effect.

the two hemispheres. DCS derives a blood flow index (BFI) corresponding to microvascular CBF in the probe region that extends to the top of the cerebral cortex. The details of the technique and the instrumentation were previously published (Durduran et al., 2010; Durduran and Yodh, 2014; Gregori Pla, 2019). The device was further customized for this study. An uninterruptible power supply (K-LCD 1200, Protec-Sai, Barcelona, Spain) allowed the device to be unplugged for the motor tasks to follow each participant without disturbing their performance during the instructed tasks.

In addition to DCS, a capnography (Capnostream^{TM} 20p, Medtronic, United States) was used to record the respiratory and systemic parameters since they are known to influence diffuse optical signals. In particular, we synchronized the capnography to the DCS and obtained end-tidal carbon dioxide (CO_2) concentration, peripheral arterial oxygen saturation, and heart rate continuously. Finally, an accelerometer was also placed on the head of each participant to record the motion and to regress out potential motion artifacts during the tasks.

Prior to the probe placement, an elastic electroencephalography cap with the traditional "10–20 system" electrode positions marked was placed on the head of each participant to locate the Fp1 and Fp2 areas (Klem et al., 1999). Afterward, the DCS fiber probes with a 2.5 cm source–detector separation were placed on the forehead of the participants over Fp1 and Fp2 positions, thus assessing superficial cerebral cortex areas bilaterally (**Figure 3**). To ensure probe stability during measurement, an extra fabric layer was applied as tight as possible, considering the participant's comfort.

Signal quality checks were performed prior, during, and after each session. Initially, to check the device status, the laser power of each probe was measured with a power meter to ensure that laser power complies with the safety standards (<30 mW). After that, an ∼20-min measurement was performed on a stable tissue-mimicking phantom (INO, Biomimic^{TM} Optical Phantoms, Canada) to verify device stability. Once the probes were placed on the participant's forehead, lasers were switched off and a quick measurement was acquired. The count rate under dark conditions (without laser or external light) should stay below 1 kHz. This step was necessary to ensure probe placement and to scan whether external light was detected. If not, probes were replaced and extra tape and fabric layers were placed on top or made tighter to achieve the desired result.

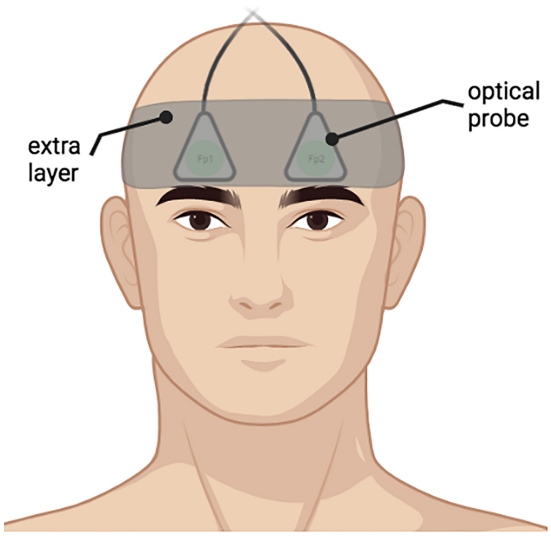

FIGURE 3
An example of placement of the optical probes on a participant bilaterally on Fp1, Fp2 positions according to "10–20 system". An extra fabric layer was applied on top of the probes to ensure data quality during measurements.

2.4.2.1 Data pre-processing, motion, and systemic signal regression

In a similar manner to fNIRS, the DCS signal contains physiological and non-physiological noise that could contaminate the data (Tachtsidis and Scholkmann, 2016). Physiological noise includes systemic physiological changes that affect both brain and extra-cerebral tissues, as well as those that do not affect the brain but are included under the probe volume which the DCS cannot separate. These not only include both the potent drivers of CBF, such as the arterial CO_2 concentration changes, but also "nuisance" parameters such as changes in heart rate, respiratory rate, etc. (Monti, 2011). Non-physiological noise refers mainly to motion artifacts that arise during walking tasks. These need to be regressed out of the signals as is routinely done in fNIRS and fMRI literature. Here, we used a relatively straightforward approach that has been utilized in both fNIRS and fMRI literature (Bowman et al., 2007; Tachtsidis et al., 2010; Gagnon et al., 2011; Kirilina et al., 2012) to de-contaminate the BFI time traces based on secondary measurements using a general linear model (GLM). An abundance of other methods have been proposed to tackle this problem in the fNIRS literature (Patel et al., 2011; Kirlilna et al., 2013; Kiguchi and Funane, 2014; Zhang et al., 2016; von Lühmann et al., 2020), but they have not been yet validated in the context of fDCS and are complex to adapt to our study due to low temporal resolution.

The first pre-processing step was to use the photon count rate to identify periods where the total number of recorded photons would be too low for a reliable analysis. During individual data processing, we reviewed that light intensity was sufficient for good data fitting. The exclusion criteria were: (a) light intensity (I) $<$ 10 kHz; (b) coefficient of variation CV(I) $>$ 5%. The signal was inspected visually for large motion artifacts, e.g., probe misplacement. In that case, data were discarded. The second step used the features of the derived DCS signal to mark periods affected by artifacts such as motion, external light, and simply poor data quality. Then, the standard DCS data analysis methods were used to obtain time traces of BFI (Durduran and Yodh, 2014).

To prepare the data for the GLM model, systemic physiological parameters, i.e., heart rate, respiration rate, end-tidal CO_2 ($EtCO_2$), oxygen saturation (SpO_2) as well as the accelerometer data were down-sampled through binning to match the timing of the BFI time traces (von Lühmann et al., 2019). All signals were temporally aligned and z-scored. For the z-score normalization, we took into account the mean and standard deviation of each regressor during the whole protocol (Monti, 2011).

For the GLM analysis, the z-scored BFI time trace was used as the dependent variable, while the z-scored systemic and accelerometer data were used as nuisance regressors. The obtained residuals of the single-subject GLM fitting were considered as the regressed BFI vector during the whole protocol period. We assumed that this is a time trace of the cortical CBF that is mainly affected by changes due to the tasks.

To obtain the changes in CBF during each task performed, the regressed BFI vector (BFI_{reg}) was segmented into blocks. Each block included a baseline period ($BFI_{reg}(t_{baseline})^{block}$), 1 min prior to instruction start, the instruction period, data during the task duration, and a recovery period of 1 min after the end of the task. From the whole time trace of each block ($BFI_{reg}(t)^{block}$) was segmented by the mean value of the data from the baseline period. Finally, the average ΔCBF (Eq. 1) during the whole task period was calculated, where the instruction period was not taken into account.

$$\Delta CBF(t) = BFI_{reg}(t)^{block} - BFI_{reg}(t_{baseline})^{block} \quad (1)$$

This process was repeated individually for each subject. We consider the units of the ΔCBF arbitrary since it refers to the result of the residuals of the GLM model, where all vectors were prior z-scored.

2.5 Physical performance assessment

We used the short physical performance battery (SPPB) with balance, gait, and chair stand as sub-items to assess physical function (Guralnik et al., 1994). Gait speed (GS) was calculated from SPPB's gait item (time required to walk 4 m) as follows: GS = 4/time (m/s). The figure-of-eight (F8T) was used as a

more complex gait assessment since it involves a curved pathway as opposed to the straight walkway usually used to calculate gait speed. For the purpose of our study, we only recorded the time and the number of steps needed to walk around the figure-of-eight path around two cones placed 1.5 m apart (Hess et al., 2010).

To further assess the dual-task interference, we performed a 4-m dual-task paradigm separate from the CBF assessments since we anticipated that the long walking distances and instrumentalization during the CBF measures could influence the participants' usual gait and overestimate the DT impact. To avoid potential learning effects with the counting DT, we chose phonemic verbal fluency (triplets S-A-R and C-P-I) as the cognitive task. The participants were instructed to perform three tasks as follows: (1) verbal fluency single-task, where the participants had to say as many words as possible starting with a predetermined letter for 20 s; (2) walking single-task, where participants had to walk over a 4-m walkway; and (3) dual-task, where participants had to walk 4 m while saying as many words as possible. The order of the tasks and triplets of letters were randomized. Three trials were performed for each task and the mean values of gait speed and the number of words were used for the analysis. For the cognitive component, we calculated word rate (words/s) as follows: number of words/20 s for the single task and number of words/ambulation time for the dual-task. Dual-task costs were calculated as follows: [((dual-task−single task)/single task) × 100].

2.6 Cognitive function assessment

We assessed global cognitive function with the MMSE (Folstein, 1975) and frontal function with the symbol digit modalities test (SDMT) (Smith, 1982) and verbal fluency tests (VF) (Patterson, 2011). For the SDMT, which assesses attention, processing speed, scanning, visual speed, and visuomotor coordination (Lezak, 2012), participants wrote down the number corresponding to each symbol according to a displayed key (the score was calculated as the number of correct responses for 90 s). For the Phonemic VF, participants were instructed to say aloud as many words as possible in 1 min starting with a given letter from the triplet P-M-R avoiding proper nouns and words with the same suffix (Lezak, 2012). For the categorical VF, participants had to say as many words as possible belonging to the categories (animals, fruits, . . .). We provide the adjusted values from the raw scores following regional normative data (Peña-Casanova et al., 2009a,b). We used the Yesavage geriatric depression scale (GDS) as a screening for depressive symptoms (Yesavage et al., 1986).

From the complete neuropsychological evaluation at the outpatient clinic, we collected scores of MMSE, VF, and GDS. Participants in the NC group who did not undergo assessment in the outpatient clinic were assessed by a research assistant (neuropsychologist) under similar conditions. The tests were performed in a quiet room without the fDCS device to provide baseline cognitive function. Only SDMT was performed during CBF measures.

2.7 Demographical and clinical characteristics

We collected demographic variables such as age, sex, education, and marital status. As part of a comprehensive clinical evaluation, we recorded the drugs prescribed at the time of enrolment to calculate polypharmacy (5 or more drugs). We collected comorbidities such as hypertension, diabetes, dyslipidemia, arrhythmia, myocardial infarction, heart failure, asthma/chronic obstructive pulmonary disease, epilepsy, stroke, Parkinson's disease, depression, history of traumatic brain injury, arthrosis, thyroid disease, and sensory impairment. We used the Charlson comorbidity index (Charlson et al., 1994). Data were extracted through an interview with the participant and relatives as well as from medical records.

The ankle-brachial index (ABI) is defined as the ratio of the systolic blood pressure measured at the leg to that measured at the brachial artery (Aboyans et al., 2012). Measurements were performed with the Minidop ES-100VX (Hadeco, Japan) Doppler ultrasound device following previously published recommendations (Aboyans et al., 2012). This measurement was included as a proxy for cardiovascular risk (Criqui et al., 1992).

We assessed functional status with the Barthel index for basic activities of daily living (Mahoney and Barthel, 1965), the Lawton index for instrumental activities of daily living (Lawton and Brody, 1969), and the clinical frailty scale (CFS) (Rockwood, 2005).

2.8 Statistical analysis

We performed a descriptive analysis of the global sample. Qualitative variables were described as numbers and percentages. Quantitative variables were described as the median and interquartile range (IQR). Confidence intervals for all analyses were considered at 95%. We performed a bivariate analysis to assess between-group differences relative to cognitive status (NC vs. MCI) with Mann–Whitney *U* test for continuous variables and the chi-square test with Yates' correction for categorical variables.

The main analysis can be explained in three sections:

1. As the optical measures were repeated within individuals and in the right/left PFC, we performed a linear mixed effects (LME) model to study the changes of CBF

across the tests in the dual-task paradigm (NW, FWC, BWC, WWO, and TAP). CBF changes measured from both sides were included in the same LME model to assess the hemodynamic changes in PFC globally and to detect potential modifications in the lateralization of brain activity. In the model, the effects from measures of each test against NW (reference) are presented as fixed effects. The cerebral PFC was measured (left/right) and the participant's identifiers were treated as random effects. NW was set as the reference, so the estimates from each task were used to assess differences in CBF during FWC, BWC, WWO, and TAP compared to NW within each cognitive status group (objective 1).

2. To assess between-group differences in the CBF pattern (objective 2), an interaction term between task and cognitive status (NC/MCI) was added to the model.
3. Next, we performed separate LME models to assess the effect of several clinical covariates: age, hypertension, diabetes, arthrosis, ABI index, SPPB's gait speed, and F8T time. These variables were chosen according to clinical relevance or due to differences observed in the bivariate analysis. To avoid the over-adjustment of the model due to the small sample size, we performed a separate model for each variable.

All statistical analyses were performed with the statistical "R" software (*R* version 4.1.3 (2022-03-10), Copyright 2015 The R Foundation for Statistical Computing.

3 Results

3.1 Sample description

From the initial sample of fifty-four, two subjects were excluded due to low-quality fDCS data, one participant was excluded due to relevant clinical data missing, one participant was excluded due to possible dementia after reviewing clinical records, and one participant could not complete the fDCS evaluation due to technical problems related to the fDCS device. Hence, we included 49 older adults (median age = 78 years, 51% women) who were high functioning in both basic and instrumental activities of daily living, with a low degree of frailty and comorbidity. Gait speed and physical function (SPPB) were slightly above the usual frailty thresholds, with 0.98 m/s and 11 points, respectively. The median MMSE score was 27, with 69.4% (n = 34) participants classified as MCI, of whom 38.8% (n = 19) had multi-domain and 30.6% (n = 15) had single-domain MCI. Table 1 shows the clinical, cognitive, functional, and dual-task performance variables of the sample.

Compared to NC (Table 1), participants with MCI were older, showed higher frailty, polypharmacy and comorbidity levels, and a higher prevalence of hypertension and diabetes. There was no significant difference in other specific comorbidities or the ABI. As expected, participants with MCI showed worse cognitive performance across all the neuropsychological tests, while the Yesavage GDS score was similar between groups. Functional status according to the Barthel and Lawton indices was similar between groups. Participants with MCI had worse physical performance (lower total SPPB score and higher time and number of steps in the F8T), while GS was similar between groups. Regarding the behavioral data during the verbal fluency dual-task paradigm, there was no significant between-group difference in GS during single-task and dual-task walks. Participants with MCI did produce a lower rate of words during single-task and dual-task verbal fluency. The dual-task cost for GS and the number of words were similar across the cognitive status.

3.2 Cerebral blood flow changes

3.2.1 Behavioral results during cerebral blood flow monitoring

Regarding the behavioral data obtained during the CBF measurements, participants with MCI showed lower GS during NW and WWO compared to NC (Table 2 and Figure 4). On the other hand, GS during FWC and BWC was not different between groups. The gait dual-task cost for FWC and BWC was higher among NC, compared to MCI, but showed no differences for WWO.

Counting errors prevalent during FWC were not statistically different between the two groups.

Twelve participants were not able to perform the BWC task because they could not perform the 3-backward calculation. Those participants did not complete the 5 loops, and hence we did not include BWC-related data in the analysis. Compared to the rest of the sample, participants who were unable to perform BWC all belonged to the MCI group and had higher comorbidity and frailty levels and worse cognitive and physical function (data not shown).

3.2.2 Functional diffuse correlation data

3.2.2.1 Comparison between motor tasks

Among participants with NC, CBF was significantly higher than NW only during BWC (estimate = 0.48, 95% CI [0.21, 0.74], $p < 0.001$) and TAP (estimate = 0.36, 95% CI [0.10, 0.63], $p = 0.008$), but not during FWC and WWO (Table 3 shows LME results).

Among participants with MCI, CBF was significantly higher than NW during FWC (estimate = 0.33, 95% CI [0.16, 0.51], $p < 0.001$), BWC (estimate = 0.44, 95% CI [0.23, 0.64], $p < 0.001$), and TAP (estimate = 0.44, 95% CI [0.26, 0.61], $p < 0.001$), but not during WWO.

3.2.2.2 Between-group comparison

3.2.2.2.1 Normal walk to dual-task change

The change in CBF from NW to FWC was significantly higher in MCI compared to NC (estimate = 0.34, 95% CI

10.3389/fnagi.2022.958656

TABLE 1 Descriptive of global sample and between-group comparison.

	Study sample $n = 49$	NC $n = 15$	MCI $n = 34$	P-value*
Sociodemographic and clinical variables				
Age	78 [72, 83]	72 [67.5, 76]	80.5 [73.2, 84]	< 0.001*
Sex (female)	51.02% (25)	46.7% (7)	52.9% (18)	0.92
Marital status (married)	55.12% (27)	80.00% (12)	44.12% (15)	0.04*
Elementary school complete	81.63% (40)	93.33% (14)	76.47% (26)	0.31
CFS score	2 [1.5, 3]	2 [1, 2]	3 [2, 3]	0.002*
Charlson index	0 [0, 1]	0 [0, 0]	1 [0, 1]	0.002*
Hypertension	72.92% (35)	28.57% (4)	91.18% (31)	< 0.001*
Diabetes	20.83% (10)	0.00% (0)	29.41% (10)	0.02*
Dyslipidemia	43.75% (21)	35.71% (5)	47.06% (16)	0.69
Arrhythmia	18.75% (9)	14.29% (2)	20.59% (7)	0.92
Myocardial infarction	12.50% (6)	7.14% (1)	14.71% (5)	0.81
Heart failure	2.13% (1)	0.00% (0)	2.94% (1)	1
Asthma/COPD	12.50% (6)	14.29% (2)	11.76% (4)	1
Thyroid disease	10.42% (5)	14.29% (2)	8.82% (3)	0.96
Traumatic brain injury	14.58% (7)	28.57% (4)	8.82% (3)	0.19
Epilepsy	0% (0)	0% (0)	0% (0)	
Stroke	12.77% (6)	0.00% (0)	18.18% (6)	0.22
Parkinson's disease	0% (0)	0.00% (0)	0.00% (0)	
Depression	29.17 % (14)	14.29% (2)	35.29% (12)	0.18
Arthrosis	25.94% (18)	33.33% (3)	60.00% (15)	0.32
Number of drugs	4.5 [2.75, 7.0]	2.5 [1.25, 3.75]	6 [4, 7]	< 0.001*
Polypharmacy (5 or more)	50.00% (24)	14.28% (2)	64.71% (22)	0.004*
Ankle-Brachial index	1.16 [1.07, 1.27]	1.18 [1.08, 1.26]	1.14 [1.06, 1.28]	0.6
Cognitive function				
MMSE score (0–30)	27 [25, 28]	28 [28, 30]	25 [24.2, 27]	< 0.001*
SDMT PE	10 [5, 11]	11 [11, 13.5]	7 [4, 10]	< 0.001*
Verbal Fluency categorical PE	8 [6, 10]	10 [9, 12]	6 [5, 9]	< 0.001*
Verbal Fluency phonemic PE	9 [7.25, 11.00]	11 [11, 12]	8 [6, 10]	< 0.001*
Yesavage GDS score (0–15)	1 [1, 2]	1 [0, 1.75]	1 [1, 2]	0.09
Physical performance				
Barthel index score (0–100)	100 [100, 100]	100 [100, 100]	100 [100, 100]	0.5
Lawton index score (0–8)	8 [7.75, 8]	8 [7.5, 8]	8 [7.25, 8]	0.8
Gait speed (m/s)	0.98 [0.86, 1.09]	1.03 [0.9, 1.17]	0.9 [0.8, 1.1]	0.09
SPPB total score (0–12)	11 [8.25, 12.00]	12 [11, 12]	10 [8, 11]	0.005*
SPPB balance score (0–4)	4 [3, 4]	4 [4, 4]	4 [2.5, 4]	0.038*
SPPB gait score (0–4)	4 [4, 4]	4 [4, 4]	4 [4, 4]	0.4
SPPB chair stand score (0–4)	3 [3, 4]	4 [3, 4]	3 [2.5, 3.5]	0.008*
Figure of eight test time	8.88 [8.03, 11.8]	8.37 [7.60, 8.58]	9.75 [8.12, 12.20]	0.005*
Figure of eight test steps	14.5 [13.0, 17.75]	13 [12, 14]	15 [13, 19]	0.015*
Dual-task performance				
Normal walk GS (m/s)	0.97 [0.84, 1.08]	0.99 [0.96, 1.11]	0.91 [0.81, 1.07]	0.1
DT verbal fluency GS (m/s)	0.54 [0.42, 0.62]	0.55 [0.46, 0.64]	0.52 [0.38, 0.59]	0.4
DT cost VF GS (%)	−44 [−50, −35]	−44 [−51, −36]	−44 [−49, −34]	1
ST verbal fluency word rate (word/s)	0.33 [0.27, 0.40]	0.38 [0.34, 0.45]	0.28 [0.25, 0.34]	0.002*
DT verbal fluency word rate (word/s)	0.48 [0.28, 0.64]	0.57 [0.53, 0.69]	0.38 [0.25, 0.56]	0.009*
DT cost word rate (%)	48 [16, 79]	47 [37, 76]	48 [5, 79]	0.7

Values reported are median [Q1, Q3] for quantitative variables and frequencies [% (n)] for categorical variables. *Indicates p-value < 0.05 assessed with the Mann–Whitney U test and the chi-square test with Yates correction to assess NC vs. MCI between-group differences. NC, participants with normal cognition; MCI, mild cognitive impairment; CFS, clinical frailty scale; COPD, chronic obstructive pulmonary disease; MMSE, mini-mental state exam; SDMT, symbol digit modalities test; BNT, Boston Naming Test; GDS, geriatric depression scale; PE, adjusted scores; SPPB, short physical performance battery; GS, gait speed; DT, dual-task; ST, single-task.

TABLE 2 Behavioral data during CBF monitoring.

	NC $n = 15$	MCI $n = 34$	P-value*
NW gait speed (m/s)	0.90 [0.86, 0.99]	0.67 [0.59, 0.84]	< 0.001*
FWC gait speed (m/s)	0.65 [0.59, 0.87]	0.62 [0.46, 0.70]	0.1
BWC gait speed (m/s)**	0.63 [0.52, 0.80]	0.61 [0.46, 0.66]	0.2
WWO gait speed (m/s)	0.86 [0.71, 0.95]	0.67 [0.59, 0.82]	0.007*
DTC FWC (%)	−20 [−3 0, −13]	−10 [−26, −4]	0.03*
DTC BWC (%)	−29 [−34, −18]	−14 [−26, −8]	0.03*
DTC WWO (%)	−4 [−9, −3]	−1 [−6, 2]	0.1
FWC counting errors	0% (0)	20.59% (7)	0.15
BWC counting errors**	26.67% (4/15)	42.86% (9/21)	0.52

Values reported are median [Q1, Q3] for quantitative variables and frequencies [% (n)] for categorical variables. *Indicates p-value < 0.05 assessed with the Mann–Whitney U test and the chi-square test with Yates correction. **Behavioral data from BWC refers to a sample of 37 (see explanation in Section "3.2.1 Behavioral results during cerebral blood flow monitoring"). NC, participants with normal cognition; MCI, mild cognitive impairment; NW, normal walk; FWC, walk while 2-forward count; BWC, walk while 3-backward count; WWO, walk while negotiating obstacles; DTC, dual-task cost.

[0.02, 0.66], p = 0.03). CBF change from NW to BWC (estimate = −0.04, 95% CI [−0.38, 0.29], p = 0.8) and WWO (estimate = 0.10, 95% CI [−0.22, 0.42], p = 0.5) was not significantly different between groups. CBF change from NW to TAP (estimate = 0.08, 95% CI [−0.24, 0.40], p = 0.6) was not different either. The PFC measured seems to affect the model with a higher CBF driven by the right PFC (estimate = 0.12, 95% CI [0.02, 0.22], p = 0.018). Figure 5 depicts CBF values during each task stratified by cognitive status. See Table 3 for LME results.

3.2.2.2.2 Effect of covariates

The previous model was repeated (one model for each covariate) adjusting for age, hypertension, diabetes, arthrosis, ABI, GS, and F8T time. No significant effect of any of the covariates on CBF was found. See Table 4.

4 Discussion

In our sample of high-functioning older adults, participants with MCI were older and showed higher levels of frailty and comorbidity and worse cognitive and physical performance, while gait performance in a 4-m verbal fluency dual-task paradigm was not different compared to the NC counterparts.

To sum up, both groups had significantly increased CBF during BWC compared to NW, along with a negative impact on gait, while only participants with MCI, the CBF also increased during FWC compared to NW, so the FWC is the dual-task in which we observed a statistically significant difference compared to participants with NC, in particular in the right PFC.

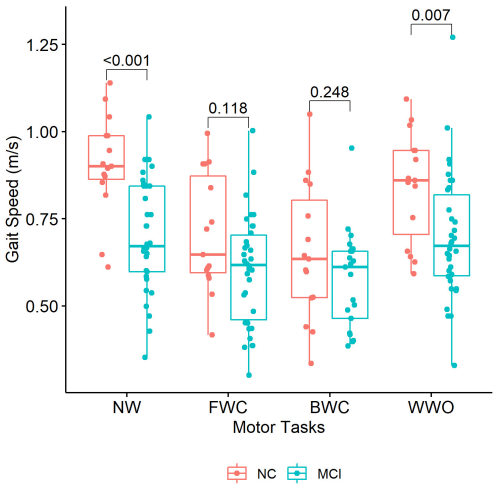

FIGURE 4
Gait speed across the dual-task paradigm during CBF monitoring. The boxplots depict gait speed during each task stratified by group (NC vs. MCI). P-values of between-group differences are indicated with brackets above the boxplots. NW, normal walk; FWC, walk while 2-forward count; BWC, walk while 3-backward count; WWO, walk while negotiating obstacles; NC, participants with normal cognition; MCI, mild cognitive impairment.

TABLE 3 Linear mixed effects model of CBF changes across the tests in the dual-task paradigm (NW, FWC, BWC, WWO, and TAP).

	Estimate	95% IC	p-value
Intercept	−0.08	−0.31, 0.14	0.47
FWC	−0.01	−0.28, 0.25	0.94
BWC	0.48	0.21, 0.74	< 0.001
WWO	0.02	−0.24, 0.29	0.88
TAP	0.36	0.10, 0.63	< 0.01
Cognitive status [MCI] × FWC	0.34	0.02, 0.66	0.03
Cognitive status [MCI] × BWC	−0.04	−0.38, 0.29	0.81
Cognitive status [MCI] × WWO	0.10	−0.22, 0.42	0.54
Cognitive status [MCI] × TAP	0.08	−0.24, 0.40	0.63
Cognitive status [MCI]	−0.02	-0.29, 0.25	0.94
PFC (Right)	0.12	0.02, 0.22	0.02

CBF from both PFCs was included in the model. Normal walk was set as a reference task and an interaction term "cognitive status × task" was added to assess between-group differences. N = 49 included in the model. NW, normal walk; FWC, walk while 2-forward count; BWC, walk while 3-backward count; WWO, walk while negotiating obstacles; TAP, heel tapping; MCI, mild cognitive impairment; PFC, prefrontal cortex.

4.1 Baseline and clinical characteristics NC vs. MCI

Compared to NC, participants with MCI showed worse physical performance in the total SPPB score and the F8T. We speculate that the curved pathway might be more challenging (Belluscio et al., 2021) for participants with worse motor and cognitive function, as seen in our MCI group. Notably, there

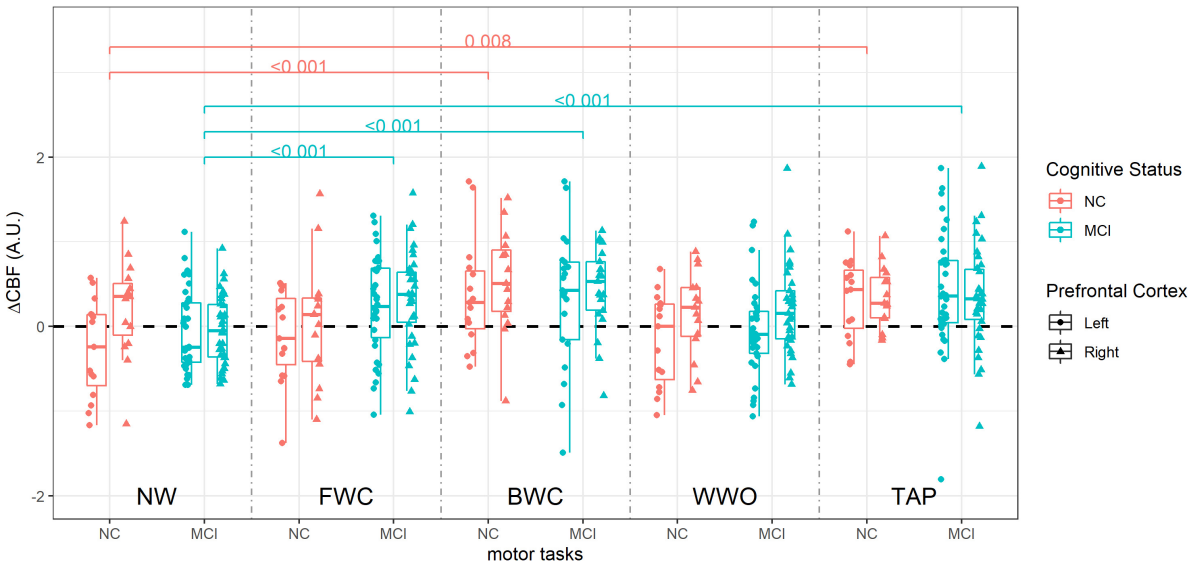

FIGURE 5
Cerebral blood flow during dual-task paradigm, stratified by group (NC vs. MCI). CBF values from each side are included (right and left prefrontal cortex). *P*-values on brackets indicate between-task CBF comparison within the cognitive status group from the linear mixed effect model. ΔCBF, cerebral blood flow change; A.U., arbitrary units; NW, normal walk; FWC, walk while 2-forward count; BWC, walk while 3-backward count; WWO, walk while negotiating obstacles; TAP, heel tapping; NC, participants with normal cognition; MCI, mild cognitive impairment.

TABLE 4 Linear mixed effects models of changes of CBF across the tests in the dual-task paradigm adjusted for clinical covariates.

	Estimate	95% CI	*P*-value model	*P*-value (LRT)*
Age	−0.01	−0.03, 0.007	0.23	0.78
Hypertension	−0.06	−0.39, 0.26	0.69	0.96
Diabetes	0.09	−0.17, 0.35	0.49	0.97
Arthrosis	0.16	−0.056, 0.38	0.14	0.84
ABI	−0.01	−0.34, 0.32	0.95	0.97
GS	−0.23	−0.79, 0.33	0.4	0.8
F8T time	0.04	−0.01, 0.09	0.09	0.9
DTC	0.27	−0.39, 0,9	0.4	0.76

Each row represents one LME model adjusted for each covariate. **P*-value (LRT) indicates the comparison of the adjusted model to the original non-adjusted model. ABI, ankle-brachial index; GS, gait speed; F8T, figure of eight; DTC, dual-task cost during verbal fluency.

was no between-group difference in GS during the single- and dual-task walk. With a quite high GS in both groups during the single task, both groups showed a relevant impact of the phonemic VF dual-task, as shown by a similar GS dual-task cost. Consistent with their worse cognitive function, participants with MCI did produce a lower rate of words during single- and dual-task verbal fluency. Previous studies have reported slower GS during single- and dual-task in MCI compared to controls (Verghese et al., 2008; Montero-Odasso et al., 2012; Pieruccini-Faria et al., 2019); however, dual-task paradigms in the included studies used animal VF and arithmetic tasks (Bahureksa et al., 2017), which limits comparability. The lack of between-group differences in dual-task cost might be due to the similar GS in the single-task and due to the VF dual-task impact seen in the NC group. Our small sample size might have contributed to the findings.

4.2 Behavioral data during cerebral blood flow monitoring

Regarding the behavioral data obtained during the CBF measurements, participants with MCI showed lower GS during NW, while GS during FWC and BWC was not different between the groups, so the dual-task cost was higher for NC. In other words, the impact of the arithmetic dual-task seems higher for participants with NC, which could be somewhat surprising. We speculate that participants with NC are better able to perform serial counting, so they allocate more attentional resources prioritizing the cognitive component during the dual-task and thus show a higher impact of the dual-task on gait. Furthermore, a higher GS during NW in participants with NC might give them more room to show a GS decrease. Regarding BWC's dual-task impact, the twelve participants who were unable to perform the calculation in BWC belonged to the MCI group and showed worse cognitive and physical performance. We cannot rule out that the exclusion of their BWC behavioral results from the analysis might affect the results. These participants might have shown an even slower GS during BWC and could have contributed to a between-group difference in BWC GS.

Notably, in this dual-task paradigm, GS in a single task was significantly lower in MCI compared to NC, while we did not find this difference in the verbal fluency dual-task paradigm, as mentioned earlier. This could be due to a fatigue contribution since the measures required longer walking distances or even due to a more challenging walking path since it included turns and instrumentalization due to DCS probes attached to the forehead. Due to the already low GS in NW, a floor effect of GS for the MCI group could contribute to the no difference in GS during the dual-task. Previous studies have reported slower GS in MCI in an arithmetic DT paradigm (Montero-Odasso et al., 2012) and higher dual-task cost in MCI vs. controls (Muir et al., 2012; Pieruccini-Faria et al., 2019). Regarding the cognitive output in the arithmetic dual-task, our study design did not include reporting accuracy rates, so we acknowledge that this limits an appropriate between-group comparison of the counting output during FWC and BWC. The lack of difference in our categorical variable (counting errors) may be also influenced by a low-demanding FWC and the exclusion of twelve participants with MCI who were unable to perform the BWC. Contrary to the findings in the arithmetic dual-task, WWO GS was significantly lower in MCI, and the gait dual-task cost related to WWO was similar between the groups. Our obstacle negotiation protocol might have not been cognitively challenging enough to impact NC's gait, so the GS during WWO remained slower in MCI compared to NC. Clark et al. (2014) found a slower GS compared to a single-task walk among older adults without cognitive impairment; however, they used 6 obstacles over a 90-m walkway. Coppin et al. (2006) reported slower gait speed in fast-paced obstacle negotiation in participants with poorer executive function.

4.3 Functional diffuse correlation data

4.3.1 Summary of comparison of CBF between motor tasks and integration with behavioral results

Cerebral blood flow during BWC and TAP was higher than during NW in both groups, while CBF during FWC was higher than NW only among participants with MCI. We found no differences in WWO-related CBF compared to CBF during NW in both groups.

Among participants with NC, the impact of the arithmetic dual-task on gait seems relevant as seen by a dual-task cost of 20% for FWC and 29% for BWC, but only BWC seems to generate a higher CBF than NW among these participants. On the other hand, among participants with MCI, with a gait dual-task cost of 10% for FWC and 14% for BWC, both FWC and BWC elicited higher CBF than NW. This might be explained by the cognitive component of the arithmetic dual-task. Thus, participants with NC were able to meet the attention load of FWC without increasing the CBF, showing, however, a decrease in GS. On the other hand, participants with MCI required an increased CBF to meet the cognitive load. The fact that CBF during BWC is higher than during NW in both groups goes in line with this explanation. This is further supported by fNIRS studies (Doi et al., 2013; Holtzer et al., 2015), where dual-task broadly show an increase in oxyhemoglobin compared to single tasks, and it is usually interpreted as a response to increasing attention demand.

Our WWO protocol with low small obstacles in fixed positions might have been not challenging enough to elicit an increase in CBF. Evidence from fNIRS studies suggests that a dual-task with obstacle negotiation causes an increase in prefrontal oxygenation compared to a single-task walk in different populations (Clark et al., 2014; Maidan et al., 2016; Chen et al., 2017).

To our knowledge, no previous studies have investigated differences in brain activation between foot tapping vs. overground walking, while foot tapping has been used in fMRI studies (Al-Yahya et al., 2016; Vinehout et al., 2019) or in comparison to motor imaginary (Batula et al., 2017). The study by Al-Yahya et al. did assess fNIRS data during a treadmill walk and fNIRS+fMRI during foot tapping. However, they do not report a comparison of the activation during walk vs. tapping. In our study, TAP caused a higher CBF than NW. This may be due to a higher attention demand of sequential tapping relative to single-task walking or due to a systemic increase in blood flow during TAP (i.e., calves contraction).

4.3.2 Summary CBF change comparison NC vs. MCI and integration with behavioral results

Participants with MCI showed an increased CBF change from NW to FWC relative to NC. We found no between-group differences in CBF change from NW to either BWC, WWO, or TAP. The PFC side had an effect in the model, where differences between MCI and NC in CBF change from NW to FWC were driven by CBF measures from the right PFC.

The CBF change from NW to FWC was significantly higher in MCI compared to participants with NC, even though the FWC's impact on gait was smaller as seen in the dual-task cost. Hence, the higher CBF change seems due to the cognitive load of FWC in participants with MCI. This is further supported by the fact that a higher CBF was related to the right PFC measures. Functional neuroimaging studies have shown that arithmetic tasks mainly require the activation of frontal and parietal cortical regions, with left-hemisphere lateralization (Burbaud et al., 1995; Kazui et al., 2000; Ueda et al., 2015). Hence, we believe that a higher right activation in MCI compared to healthier counterparts could be explained by the neural compensation theories. According to these theories, older adults with lower brain resources might show an increase in activation as an attempt to maintain performance and even require activation of additional brain regions that can lead

to a reduction in hemispheric asymmetry (Reuter-Lorenz and Cappell, 2008; Stern, 2009).

The lack of between-group differences in CBF change from NW to BWC is most possibly influenced by the 12 participants with MCI who were unable to perform the BWC test. These might have shown either higher CBF due to the higher attention load of BWC as a compensation mechanism or lower CBF that would be explained by the capacity limitation theory. Additionally, BWC might be challenging for the NC group too, so the CBF change from NW to BWC required is not different from the MCI group. We believe that WWO and TAP lacked sufficient cognitive load to cause CBF differences between cognitive status groups. Notably, we found no effect of age or any of the clinical covariates on our prefrontal CBF findings. Here, the small sample size may limit the interpretation of the results since it did not allow us to adjust for several covariates and their interactions in the same LME model.

4.4 Strengths and limitations

The main strengths of our study consist of a broad measuring protocol with different types of dual-task and a novel approach to study brain activation during motion with fDCS. We provide results from a well-characterized sample, however, of small size, which might have limited our findings. Specifically, the small sample size limited the linear mixed effects model since we were unable to adjust it for several clinical covariates and their interactions to avoid over-adjustment. We acknowledge some methodological issues in our study design: (a) the lack of CBF data during BWC of the participants who were unable to perform the task limits the interpretation of our findings and the comparison of brain activation elicited by the different dual-task; and (b) the lack of an accurate measure of cognitive behavioral results during CBF monitoring, i.e., counting accuracy rate may limit our interpretation of results of the DT interference during the walk while counting paradigm. We provide cognitive output from a separate DT paradigm to assess DT interference in a 4-m usual gait (without the fDCS device), however, with a verbal fluency task to avoid learning effects. The use of a different type of secondary task might limit the extrapolation of results to the counting DT. The low temporal resolution of fDCS is a limitation of our study since not very detailed information can be obtained about the blood flow response during task performance. For the same reason, classic signal regression techniques (e.g., filtering) could not be followed, which led us to use a GLM approach without temporal correlation analysis. We also acknowledge that the eligibility criteria of our study might limit the generalizability of the results.

Overall, to our knowledge, our study is the first to report CBF directly measured during motor tasks with diffuse optics; however, further research is needed to confirm our findings. In the future, fDCS could be combined with fNIRS (Durduran and Yodh, 2014) to elucidate changes in oxygen metabolism.

4.5 Conclusion

To sum up, our findings suggest a differential prefrontal hemodynamic pattern in older adults with MCI compared to NC counterparts during our dual-task paradigm. Participants with MCI showed higher CBF related to the dual-task cognitive demand in the easier arithmetic dual-task (2-forward count) compared to older adults with NC. Thus, our results are mainly in line with fNIRS studies, where higher cognitive demands, as in the dual-task, have been related to higher activation (i.e., higher oxyhemoglobin concentrations).

Furthermore, the higher CBF increase from NW to FWC in MCI compared to NC was specifically linked to a right-PFC activation, which we interpret as a compensatory mechanism. Further research is needed to confirm our findings and increase the knowledge about the role of fDCS in neuroimaging to study the efficacy of neural processes in aging.

Data availability statement

The raw data supporting the conclusions of this article will be made available upon request to the authors, without undue reservation.

Ethics statement

The studies involving human participants were reviewed and approved by Universitat Autònoma de Barcelona (Barcelona, Spain). The patients/participants provided their written informed consent to participate in this study.

Author contributions

CU and SA contributed to the conceptualization, data collection, statistical analysis, investigation, methodology, project administration, resources, writing the original draft, and writing, reviewing, and editing. MM-F contributed to the methodology, statistical analysis, writing the original draft, and writing, reviewing, and editing. AR contributed to the writing the original draft and writing, reviewing, and editing. JA and CG-P contributed to writing, reviewing, and editing. LK contributed to the investigation, methodology, and writing, reviewing, and editing. TD and MI the contributed to conceptualization, funding acquisition, methodology, project administration, supervision, writing the original draft, and writing, reviewing, and editing. All authors contributed to the article and approved the submitted version.

Funding

This work was supported by the Instituto de Salud Carlos III (MEDPHOTAGE, DTS 16/00099 and DTS 16/00087, 2017, and FRONT STAGE, PI 19/00734, 2020) and co-funded by European Regional Development Fund/European Social Fund "Investing in your future," the European Union's Horizon 2020 Research and Innovation Program under the Marie Skłodowska-Curie (Grant No. 713729), Fundació CELLEX Barcelona, Fundació Mir-Puig, Agencia Estatal de Investigación (PHOTOMETABO, PID2019-106481RB-C31/10.13039/501100011033), FEDER EC and LASERLAB-EUROPE V (EC H2020 number 871124) and "Severo Ochoa" Programme for Centres of Excellence in R&D (CEX2019-000910-S).

Acknowledgments

We would like to acknowledge Luis Soto-Bagaria and Julia Vázquez for their contribution to data collection, and Carmina Castellano-Tejedor and Noelia Ruzafa for their administrative support. We also thank all the participants in the study.

Conflict of interest

The authors declare that the research was conducted in the absence of any commercial or financial relationships that could be construed as a potential conflict of interest.

Publisher's note

All claims expressed in this article are solely those of the authors and do not necessarily represent those of their affiliated organizations, or those of the publisher, the editors and the reviewers. Any product that may be evaluated in this article, or claim that may be made by its manufacturer, is not guaranteed or endorsed by the publisher.

References

Aboyans, V., Criqui, M. H., Abraham, P., Allison, M. A., Creager, M. A., Diehm, C., et al. (2012). Measurement and interpretation of the ankle-brachial index: a scientific statement from the american heart association. *Circulation* 126, 2890–2909. doi: 10.1161/CIR.0b013e318276fbcb

Agbangla, N. F., Audiffren, M., and Albinet, C. T. (2017). Use of near-infrared spectroscopy in the investigation of brain activation during cognitive aging: a systematic review of an emerging area of research. *Ageing Res. Rev.* 38, 52–66. doi: 10.1016/j.arr.2017.07.003

Allali, G., Kressig, R. W., Assal, F., Herrmann, F. R., Dubost, V., and Beauchet, O. (2007). Changes in gait while backward counting in demented older adults with frontal lobe dysfunction. *Gait Posture* 26, 572–576. doi: 10.1016/j.gaitpost.2006.12.011

Alvarez, J. A., and Emory, E. (2006). Executive function and the frontal lobes: a meta-analytic review. *Neuropsychol. Rev.* 16, 17–42. doi: 10.1007/s11065-006-9002-x

Al-Yahya, E., Dawes, H., Smith, L., Dennis, A., Howells, K., and Cockburn, J. (2011). Cognitive motor interference while walking: a systematic review and meta-analysis. *Neurosci. Biobehav. Rev.* 35, 715–728. doi: 10.1016/j.neubiorev.2010.08.008

Al-Yahya, E., Johansen-Berg, H., Kischka, U., Zarei, M., Cockburn, J., and Dawes, H. (2016). Prefrontal cortex activation while walking under dual-task conditions in stroke. *Neurorehabil. Neural Repair.* 30, 591–599. doi: 10.1177/1545968315613864

Bahureksa, L., Najafi, B., Saleh, A., Sabbagh, M., Coon, D., Mohler, M. J., et al. (2017). The impact of mild cognitive impairment on gait and balance: a systematic review and meta-analysis of studies using instrumented assessment. *Gerontology* 63, 67–83. doi: 10.1159/000445831

Barbe, C., Jolly, D., Morrone, I., Wolak-Thierry, A., Dramé, M., Novella, J. L., et al. (2018). Factors associated with quality of life in patients with Alzheimer's disease. *BMC Geriatr.* 18, 1–9. doi: 10.1186/s12877-018-0855-7

Batula, A. M., Mark, J. A., Kim, Y. E., and Ayaz, H. (2017). Comparison of brain activation during motor imagery and motor movement using fNIRS. *Comput. Intell. Neurosci.* 2017:5491296. doi: 10.1155/2017/5491296

Belluscio, V., Casti, G., Ferrari, M., Quaresima, V., Sappia, M. S., Horschig, J. M., et al. (2021). Modifications in prefrontal cortex oxygenation in linear and curvilinear dual task walking: a combined fnirs and imus study. *Sensors* 21:6159. doi: 10.3390/s21186159

Beurskens, R., and Bock, O. (2012). Age-related deficits of dual-task walking: a review. *Neural Plast* 2012:131608. doi: 10.1155/2012/131608

Bishnoi, A., and Hernandez, M. E. (2021). Dual task walking costs in older adults with mild cognitive impairment: a systematic review and meta-analysis. *Aging Ment. Health* 25, 1618–1629. doi: 10.1080/13607863.2020.1802576

Bloem, B. R., Grimbergen, Y. A. M., van Dijk, J. G., and Munneke, M. (2006). The "posture second" strategy: a review of wrong priorities in Parkinson's disease. *J. Neurol. Sci.* 248, 196–204. doi: 10.1016/j.jns.2006.05.010

Blumen, H. M., Holtzer, R., Brown, L. L., Gazes, Y., and Verghese, J. (2014). Behavioral and neural correlates of imagined walking and walking-while-talking in the elderly. *Hum. Brain Mapp.* 35, 4090–4104. doi: 10.1002/hbm.22461

Boas, D. A., Campbell, L. E., and Yodh, A. G. (1995). Scattering and imaging with diffusing temporal field correlations. *Phys. Rev. Lett.* 75, 1855–1858. doi: 10.1103/PhysRevLett.75.1855

Boas, D. A., and Yodh, A. G. (1997). Spatially varying dynamical properties of turbid media probed with diffusing temporal light correlation. *J. Opt. Soc. Am. A* 14:192. doi: 10.1364/JOSAA.14.000192

Bowman, F. D., Guo, Y., and Derado, G. (2007). Statistical approaches to functional neuroimaging data. *Neuroimaging Clin. N. Am.* 17, 441–458. doi: 10.1016/j.nic.2007.09.002

Buckley, E. M., Cook, N. M., Durduran, T., Kim, M. N., Zhou, C., Choe, R., et al. (2009). Cerebral hemodynamics in preterm infants during positional intervention measured with diffuse correlation spectroscopy and transcranial Doppler ultrasound. *Opt. Exp.* 17:12571. doi: 10.1364/OE.17.012571

Burbaud, P., Degreze, P., Lafon, P., Franconi, J. M., Bouligand, B., Bioulac, B., et al. (1995). Lateralization of prefrontal activation during internal mental calculation: a functional magnetic resonance imaging study. *J. Neurophysiol.* 74, 2194–2200. doi: 10.1152/jn.1995.74.5.2194

Busch, D. R., Rusin, C. G., Miller-Hance, W., Kibler, K., Baker, W. B., Heinle, J. S., et al. (2016). Continuous cerebral hemodynamic measurement during deep hypothermic circulatory arrest. *Biomed. Opt. Exp.* 7:3461. doi: 10.1364/BOE.7.003461

Callisaya, M. L., Ayers, E., Barzilai, N., Ferrucci, L., Guralnik, J. M., Lipton, R. B., et al. (2016). Motoric cognitive risk syndrome and falls risk: a multi-center study. *J. Alzheimer's Dis.* 53, 1043–1052. doi: 10.3233/JAD-160230

Callisaya, M. L., Blizzard, C. L., Wood, A. G., Thrift, A. G., Wardill, T., and Srikanth, V. K. (2014). Longitudinal relationships between cognitive decline and gait slowing: the tasmanian study of cognition and gait. *J. Gerontol. Series A Biol. Sci. Med. Sci.* 70, 1226–1232. doi: 10.1093/gerona/glv066

Callisaya, M. L., Blizzard, L., Schmidt, M. D., Martin, K. L., Mcginley, J. L., Sanders, L. M., et al. (2011). Gait, gait variability and the risk of multiple incident falls in older people: a population-based study. *Age Ageing* 40, 481–487. doi: 10.1093/ageing/afr055

Chaparro, G., Balto, J. M., Sandroff, B. M., Holtzer, R., Izzetoglu, M., Motl, R. W., et al. (2017). Frontal brain activation changes due to dual-tasking under partial body weight support conditions in older adults with multiple sclerosis. *J. Neuroeng. Rehabil.* 14:65. doi: 10.1186/s12984-017-0280-8

Charlson, M., Szatrowski, T. P., Peterson, J., and Gold, J. (1994). Validation of a combined comorbidity index. *J. Clin. Epidemiol.* 47, 1245–1251. doi: 10.1016/0895-4356(94)90129-5

Chen, M., Pillemer, S., England, S., Izzetoglu, M., Mahoney, J. R., and Holtzer, R. (2017). Neural correlates of obstacle negotiation in older adults: an fNIRS study. *Gait Posture* 58, 130–135. doi: 10.1016/j.gaitpost.2017.07.043

Clark, D. J., Rose, D. K., Ring, S. A., and Porges, E. C. (2014). Utilization of central nervous system resources for preparation and performance of complex walking tasks in older adults. *Front. Aging Neurosci.* 6:217. doi: 10.3389/fnagi.2014.00217

Collette, F., Olivier, L., van der Linden, M., Laureys, S., Delfiore, G., Luxen, A., et al. (2005). Involvement of both prefrontal and inferior parietal cortex in dual-task performance. *Cogn. Brain Res.* 24, 237–251. doi: 10.1016/j.cogbrainres.2005.01.023

Coppin, A. K., Shumway-Cook, A., Saczynski, J. S., Patel, K. V., Ble, A., Ferrucci, L., et al. (2006). Association of executive function and performance of dual-task physical tests among older adults: analyses from the InChianti study. *Age Ageing* 35, 619–624. doi: 10.1093/ageing/afl107

Criqui, M. H., Langer, R. D., Fronek, A., Feigelson, H. S., Klauber, M. R., McCann, T. J., et al. (1992). Mortality over a period of 10 years in patients with peripheral arterial disease. *New England J. Med.* 326, 381–386. doi: 10.1056/NEJM199202063260605

Cui, X., Bray, S., Bryant, D. M., Glover, G. H., and Reiss, A. L. (2011). A quantitative comparison of NIRS and fMRI across multiple cognitive tasks. *Neuroimage* 54, 2808–2821. doi: 10.1016/j.neuroimage.2010.10.069

Doi, T., Makizako, H., Shimada, H., Park, H., Tsutsumimoto, K., Uemura, K., et al. (2013). Brain activation during dual-task walking and executive function among older adults with mild cognitive impairment: a fNIRS study. *Aging Clin. Exp. Res.* 25, 539–544. doi: 10.1007/s40520-013-0119-5

Doi, T., Shimada, H., Makizako, H., Tsutsumimoto, K., Verghese, J., and Suzuki, T. (2017). Motoric cognitive risk syndrome: association with incident dementia and disability. *J. Alzheimer's Dis.* 59, 77–84. doi: 10.3233/JAD-170195

Dolgin, M. (1994). *The Criteria Committee of the New York Heart Association. Nomenclature and Criteria for Diagnosis of Diseases of the Heart and Great Vessels*. Boston, MA: Little Brown and Co, 253–256.

Durduran, T., Choe, R., Baker, W. B., and Yodh, A. G. (2010). Diffuse optics for tissue monitoring and tomography. *Rep. Prog. Phys.* 73:076701. doi: 10.1088/0034-4885/73/7/076701

Durduran, T., and Yodh, A. G. (2014). Diffuse correlation spectroscopy for non-invasive, micro-vascular cerebral blood flow measurement. *Neuroimage* 85, 51–63. doi: 10.1016/j.neuroimage.2013.06.017

Durduran, T., Yu, G., Burnett, M. G., Detre, J. A., Greenberg, J. H., Wang, J., et al. (2004). Diffuse optical measurement of blood flow, blood oxygenation, and metabolism in a human brain during sensorimotor cortex activation. *Opt. Lett.* 29:1766. doi: 10.1364/OL.29.001766

Farias, S. T., Mungas, D., Reed, B. R., Harvey, D., and DeCarli, C. (2009). Progression of mild cognitive impairment to dementia in clinic- vs community-based cohorts. *Arch. Neurol.* 66, 1151–1157. doi: 10.1001/archneurol.2009.106

Folstein, M. F. (1975). 'Mini-mental state". a practical method for grading the cognitive state of patients for the clinician.'. *J. Psychiatr. Res.* 12, 189–198. doi: 10.1016/0022-3956(75)90026-6

Gagnon, L., Perdue, K., Greve, D. N., Goldenholz, D., Kaskhedikar, G., and Boas, D. A. (2011). Improved recovery of the hemodynamic response in diffuse optical imaging using short optode separations and state-space modeling. *Neuroimage* 56, 1362–1371. doi: 10.1016/j.neuroimage.2011.03.001

Gaugler, J., James, B., Johnson, T., Scholz, K., and Weuve, J. (2016). 2016 Alzheimer's disease facts and figures. *Alzheimer's Dement.* 12, 459–509. doi: 10.1016/j.jalz.2016.03.001

Giovannella, M., Andresen, B., Andersen, J. B., El-Mahdaoui, S., Contini, D., Spinelli, L., et al. (2020). Validation of diffuse correlation spectroscopy against 15 O-water PET for regional cerebral blood flow measurement in neonatal piglets. *J. Cereb. Blood Flow Metab.* 40, 2055–2065. doi: 10.1177/0271678X19883751

Gourovitch, M. L., Kirkby, B. S., Goldberg, T. E., Weinberger, D. R., Gold, J. M., Esposito, G., et al. (2000). A comparison of rCBF patterns during letter and semantic fluency. *Neuropsychology* 14, 353–360. doi: 10.1037/0894-4105.14.3.353

Gramigna, V., Pellegrino, G., Cerasa, A., Cutini, S., Vasta, R., Olivadese, G., et al. (2017). Near-Infrared spectroscopy in gait disorders: is it time to begin? *Neurorehabil. Neural Repair.* 31, 402–412. doi: 10.1177/1545968317693304

Gregori Pla, C. (2019). *Correlates of Cerebral Vasoreactivity Measured by Non-invasive Diffuse Optical Measurements as Biomarkers of Brain Injury Risk*. Spain: Universitat Politècnica de Catalunya.

Guralnik, J. M., Simonsick, E. M., Ferrucci, L., Glynn, R. J., Berkman, L. F., Blazer, D. G., et al. (1994). A short physical performance battery assessing lower extremity function: association with self-reported disability and prediction of mortality and nursing home admission. *J. Gerontol.* 49, M85–M94. doi: 10.1093/geronj/49.2.M85

Hausdorff, J. M., Schweiger, A., Herman, T., Yogev-Seligmann, G., and Giladi, N. (2008). Dual-Task decrements in gait: contributing factors among healthy older adults. *J. Gerontol. A Biol. Sci. Med. Sci.* 63, 1335–1343. doi: 10.1093/gerona/63.12.1335

Hess, R. J., Brach, J. S., Piva, S. R., and VanSwearingen, J. M. (2010). Walking skill can be assessed in older adults: validity of the figure-of-8 walk test. *Phys. Ther.* 90, 89–99. doi: 10.2522/ptj.20080121

Holtzer, R., Epstein, N., Mahoney, J. R., Izzetoglu, M., and Blumen, H. M. (2014). Neuroimaging of mobility in aging: a targeted review. *J. Gerontol. Series Biol. Sci. Med. Sci.* 69, 1375–1388. doi: 10.1093/gerona/glu052

Holtzer, R., Mahoney, J. R., Izzetoglu, M., Wang, C., England, S., and Verghese, J. (2015). Online fronto-cortical control of simple and attention-demanding locomotion in humans. *Neuroimage* 112, 152–159. doi: 10.1016/j.neuroimage.2015.03.002

Holtzer, R., Verghese, J., Xue, X., and Lipton, R. B. (2006). Cognitive processes related to gait velocity: results from the einstein aging study. *Neuropsychology* 20, 215–223. doi: 10.1037/0894-4105.20.2.215

Jaillon, F., Li, J., Dietsche, G., Elbert, T., and Gisler, T. (2007). Activity of the human visual cortex measured non-invasively by diffusing-wave spectroscopy. *Opt. Express* 15:6643. doi: 10.1364/OE.15.006643

Jain, V., Buckley, E. M., Licht, D. J., Lynch, J. M., Schwab, P. J., Naim, M. Y., et al. (2014). Cerebral oxygen metabolism in neonates with congenital heart disease quantified by MRI and optics. *J. Cereb. Blood Flow Metab.* 34, 380–388. doi: 10.1038/jcbfm.2013.214

Jurado, M. B., and Rosselli, M. (2007). The elusive nature of executive functions: a review of our current understanding. *Neuropsychol. Rev.* 17, 213–233. doi: 10.1007/s11065-007-9040-z

Kazui, H., Kitagaki, H., and Mori, E. (2000). Cortical activation during retrieval of arithmetical facts and actual calculation: a functional magnetic resonance imaging study. *Psychiatry Clin. Neurosci.* 54, 479–485. doi: 10.1046/j.1440-1819.2000.00739.x

Kiguchi, M., and Funane, T. (2014). Algorithm for removing scalp signals from functional near-infrared spectroscopy signals in real time using multidistance optodes. *J. Biomed. Opt.* 19:110505. doi: 10.1117/1.JBO.19.11.110505

Kirilina, E., Jelzow, A., Heine, A., Niessing, M., Wabnitz, H., Brühl, R., et al. (2012). The physiological origin of task-evoked systemic artefacts in functional near infrared spectroscopy. *Neuroimage* 61, 70–81. doi: 10.1016/j.neuroimage.2012.02.074

Kirlilna, E., Yu, N., Jelzow, A., Wabnitz, H., Jacobs, A. M., and Tachtsidis, L. (2013). Identifying and quantifying main components of physiological noise in functional near infrared spectroscopy on the prefrontal cortex. *Front. Hum. Neurosci.* 7:864. doi: 10.3389/fnhum.2013.00864

Klem, G. H., Lüders, H. O., Jasper, H. H., and Elger, C. (1999). The ten-twenty electrode system of the international federation. the international federation of clinical neurophysiology. *Electroencephalogr. Clin. Neurophysiol. Suppl.* 52, 3–6.

Lawton, M. P., and Brody, E. M. (1969). Assessment of older people: self-maintaining and instrumental activities of daily living. *Gerontologist* 9, 179–186.

Leone, C., Feys, P., Moumdjian, L., D'Amico, E., Zappia, M., and Patti, F. (2017). Cognitive-motor dual-task interference: a systematic review of neural correlates. *Neurosci. Biobehav. Rev.* 75, 348–360. doi: 10.1016/j.neubiorev.2017.01.010

Lezak, M. (2012). *Neuropsychological Assessment*, 5th Edn. New York, NY: Oxford University Press.

Li, J., Poon, C.-S., Kress, J., Rohrbach, D. J., and Sunar, U. (2018). Resting-state functional connectivity measured by diffuse correlation spectroscopy. *J. Biophoton.* 11:e201700165. doi: 10.1002/jbio.201700165

Mahoney, F. I., and Barthel, D. W. (1965). Functional evaluation: the barthel index. *Md State Med. J.* 14, 61–65.

Maidan, I., Nieuwhof, F., Bernad-Elazari, H., Reelick, M. F., Bloem, B. R., Giladi, N., et al. (2016). The role of the frontal lobe in complex walking among patients with Parkinson's disease and healthy older adults: an fNIRS study. *Neurorehabil. Neural Repair* 30, 963–971. doi: 10.1177/1545968316650426

Martin, K. L., Blizzard, L., Wood, A. G., Srikanth, V., Thomson, R., Sanders, L. M., et al. (2013). Cognitive function, gait, and gait variability in older people: a population-based study. *J. Gerontol. Series A Biol. Sci. Med. Sci.* 68, 726–732. doi: 10.1093/gerona/gls224

Mesquita, R. C., Durduran, T., Yu, G., Buckley, E. M., Kim, M. N., Zhou, C., et al. (2011). Direct measurement of tissue blood flow and metabolism with diffuse optics. *Philos. Trans. R. Soc. Mathematical Phys. Eng. Sci.* 369, 4390–4406. doi: 10.1098/rsta.2011.0232

Milej, D., He, L., Abdalmalak, A., Baker, W. B., Anazodo, U. C., Diop, M., et al. (2020). Quantification of cerebral blood flow in adults by contrast-enhanced near-infrared spectroscopy: validation against MRI. *J. Cereb. Blood Flow Metab.* 40, 1672–1684. doi: 10.1177/0271678X19872564

Mirelman, A., Shema, S., Maidan, I., and Hausdorff, J. M. (2018). "Gait,". *Handb. Clin. Neurol.* 159, 119–134. doi: 10.1016/B978-0-444-63916-5.00007-0

Montero-Odasso, M., Muir, S. W., and Speechley, M. (2012). Dual-task complexity affects gait in people with mild cognitive impairment: the interplay between gait variability, dual tasking, and risk of falls. *Arch. Phys. Med. Rehabil.* 93, 293–299. doi: 10.1016/j.apmr.2011.08.026

Monti, M. M. (2011). Statistical analysis of fMRI time-series: a critical review of the GLM approach. *Front. Hum. Neurosci.* 5:28. doi: 10.3389/fnhum.2011.00028

Muir, S. W., Speechley, M., Wells, J., Borrie, M., Gopaul, K., and Montero-Odasso, M. (2012). Gait assessment in mild cognitive impairment and Alzheimer's disease: the effect of dual-task challenges across the cognitive spectrum. *Gait Posture* 35, 96–100. doi: 10.1016/j.gaitpost.2011.08.014

Patel, S., Katura, T., Maki, A., and Tachtsidis, I. (2011). Quantification of systemic interference in optical topography data during frontal lobe and motor cortex activation: an independent component analysis. *Adv. Exp. Med. Biol.* 701, 45–51. doi: 10.1007/978-1-4419-7756-4_7

Patterson, J. (2011). "Verbal fluency," in *Encyclopedia of Clinical Neuropsychology*, eds C. B. Kreutzer and J. S. DeLuca (New York, NY: Springer), 2603–2606. doi: 10.1007/978-0-387-79948-3_1423

Peña-Casanova, J., Quiñones-Úbeda, S., Gramunt-Fombuena, N., Quintana-Aparicio, M., Aguilar, M., Badenes, D., et al. (2009a). Spanish multicenter normative studies (NEURONORMA project): norms for verbal fluency tests. *Arch. Clin. Neuropsychol.* 24, 395–411. doi: 10.1093/arclin/acp042

Peña-Casanova, J., Quiñones-Úbeda, S., Quintana-Aparicio, M., Aguilar, M., Badenes, D., Molinuevo, J. L., et al. (2009b). Spanish multicenter normative studies (NEURONORMA project): norms for verbal Span, visuospatial Span, letter and number sequencing, trail making test, and symbol digit modalities test. *Arch. Clin. Neuropsychol.* 24, 321–341. doi: 10.1093/arclin/acp038

Petersen, R. C. (2004). Mild cognitive impairment as a diagnostic entity. *J. Int. Med.* 256, 183–194. doi: 10.1111/j.1365-2796.2004.01388.x

Phillips, A. A., Chan, F. H., Zheng, M. M. Z., Krassioukov, A. V., and Ainslie, P. N. (2016). Neurovascular coupling in humans: physiology, methodological advances and clinical implications. *J. Cereb. Blood Flow Metab.* 36, 647–664. doi: 10.1177/0271678X15617954

Pieruccini-Faria, F., Sarquis-Adamson, Y., and Montero-Odasso, M. (2019). Mild cognitive impairment affects obstacle negotiation in older adults: results from "gait and brain study. *Gerontology* 65, 164–173. doi: 10.1159/000492931

Reuter-Lorenz, P. A., and Cappell, K. A. (2008). Neurocognitive aging and the compensation hypothesis. *Curr. Dir. Psychol. Sci.* 17, 177–182. doi: 10.1111/j.1467-8721.2008.00570.x

Roche-Labarbe, N., Fenoglio, A., Radhakrishnan, H., Kocienski-Filip, M., Carp, S. A., Dubb, J., et al. (2014). Somatosensory evoked changes in cerebral oxygen consumption measured non-invasively in premature neonates. *Neuroimage* 85, 279–286. doi: 10.1016/j.neuroimage.2013.01.035

Rockwood, K. (2005). A global clinical measure of fitness and frailty in elderly people. *Can. Med. Assoc. J.* 173, 489–495. doi: 10.1503/cmaj.050051

Rosso, A. L., Verghese, J., Metti, A. L., Boudreau, R. M., Aizenstein, H. J., Kritchevsky, S., et al. (2017). Slowing gait and risk for cognitive impairment. *Neurology* 89, 336–342. doi: 10.1212/WNL.0000000000004153

Schwenk, M., Zieschang, T., Oster, P., and Hauer, K. (2010). Dual-task performances can be improved in patients with dementia: a randomized controlled trial. *Neurology* 74, 1961–1968. doi: 10.1212/WNL.0b013e3181e39696

Selb, J., Boas, D. A., Chan, S.-T., Evans, K. C., Buckley, E. M., and Carp, S. A. (2014). Sensitivity of near-infrared spectroscopy and diffuse correlation spectroscopy to brain hemodynamics: simulations and experimental findings during hypercapnia. *Neurophotonics* 1:015005. doi: 10.1117/1.NPh.1.1.015005

Smith, A. (1982). *Symbol Digit Modalities Test Manual*. Los Angeles CA: Western Psychological Services.

Stern, Y. (2009). Cognitive reserve. *Neuropsychologia* 47, 2015–2028. doi: 10.1016/j.neuropsychologia.2009.03.004

Tachtsidis, I., Koh, P. H., Stubbs, C., and Elwell, C. E. (2010). Functional optical topography analysis using Statistical Parametric Mapping (SPM) methodology with and without physiological confounds. *Adv. Exp. Med. Biol.* 662, 237–243. doi: 10.1007/978-1-4419-1241-1_34

Tachtsidis, I., and Scholkmann, F. (2016). False positives and false negatives in functional near-infrared spectroscopy: issues, challenges, and the way forward. *Neurophotonics* 3:031405. doi: 10.1117/1.NPh.3.3.031405

Udina, C., Avtzi, S., Durduran, T., Holtzer, R., Rosso, A. L., Castellano-Tejedor, C., et al. (2020). Functional near-infrared spectroscopy to study cerebral hemodynamics in older adults during cognitive and motor tasks: a review. *Front. Aging Neurosci.* 11:367. doi: 10.3389/fnagi.2019.00367

Ueda, K., Brown, E. C., Kojima, K., Juhász, C., and Asano, E. (2015). Mapping mental calculation systems with electrocorticography. *Clin. Neurophysiol.* 126, 39–46. doi: 10.1016/j.clinph.2014.04.015

Verghese, J., Kuslansky, G., Holtzer, R., Katz, M., Xue, X., Buschke, H., et al. (2007). Walking while talking: effect of task prioritization in the elderly. *Arch. Phys. Med. Rehabil.* 88, 50–53. doi: 10.1016/j.apmr.2006.10.007

Verghese, J., LeValley, A., Hall, C. B., Katz, M. J., Ambrose, A. F., and Lipton, R. B. (2006). Epidemiology of gait disorders in community-residing older adults. *J. Am. Geriatr. Soc.* 54, 255–261. doi: 10.1111/j.1532-5415.2005.00580.x

Verghese, J., Robbins, M., Holtzer, R., Zimmerman, M., Wang, C., Xue, X., et al. (2008). Gait dysfunction in mild cognitive impairment syndromes. *J. Am. Geriatr. Soc.* 56, 1244–1251. doi: 10.1111/j.1532-5415.2008.01758.x

Vinehout, K., Schmit, B. D., and Schindler-Ivens, S. (2019). Lower limb task-based functional connectivity is altered in stroke. *Brain Connect.* 9, 365–377. doi: 10.1089/brain.2018.0640

von Lühmann, A., Boukouvalas, Z., Müller, K.-R., and Adalı, T. (2019). A new blind source separation framework for signal analysis and artifact rejection in functional near-Infrared spectroscopy. *Neuroimage* 200, 72–88. doi: 10.1016/j.neuroimage.2019.06.021

von Lühmann, A., Ortega-Martinez, A., Boas, D. A., and Yücel, M. A. (2020). Using the general linear model to improve performance in fNIRS single trial analysis and classification: a perspective. *Front. Hum. Neurosci.* 14:30. doi: 10.3389/fnhum.2020.00030

Yesavage, J. A., Brink, T. L., Rose, T. L., Lum, O., Huang, V., Adey, M., et al. (1986). Development and validation of a geriatric depression screening scale: a preliminary report. *J. Psychiatr. Res.* 17, 37–49. doi: 10.2307/1957152

Yogev-Seligmann, G., Hausdorff, J. M., and Giladi, N. (2008). The role of executive function and attention in gait. *Movement Disord.* 23, 329–342. doi: 10.1002/mds.21720

Yu, G., Floyd, T. F., Durduran, T., Zhou, C., Wang, J., Detre, J. A., et al. (2007). Validation of diffuse correlation spectroscopy for muscle blood flow with concurrent arterial spin labeled perfusion MRI. *Opt. Exp.* 15:1064. doi: 10.1364/OE.15.001064

Zhang, X., Noah, J. A., and Hirsch, J. (2016). Separation of the global and local components in functional near-infrared spectroscopy signals using principal component spatial filtering. *Neurophotonics* 3:015004. doi: 10.1117/1.NPh.3.1.015004

frontiers | Frontiers in Aging Neuroscience

TYPE Original Research
PUBLISHED 12 January 2023
DOI 10.3389/fnagi.2022.1002811

OPEN ACCESS

EDITED BY
Fermín Segovia,
University of Granada,
Spain

REVIEWED BY
Thomas Thierry Hinault,
Institut National de la Santé et de la Recherche Médicale, France
Zai-Fu Yao,
National Tsing Hua University, Taiwan

*CORRESPONDENCE
Marc Montalà-Flaquer
✉ mmontala@ub.edu

SPECIALTY SECTION
This article was submitted to Neurocognitive Aging and Behavior, a section of the journal Frontiers in Aging Neuroscience

RECEIVED 25 July 2022
ACCEPTED 23 December 2022
PUBLISHED 12 January 2023

CITATION
Montalà-Flaquer M, Cañete-Massé C, Vaqué-Alcázar L, Bartrés-Faz D, Peró-Cebollero M and Guàrdia-Olmos J (2023) Spontaneous brain activity in healthy aging: An overview through fluctuations and regional homogeneity.
Front. Aging Neurosci. 14:1002811.
doi: 10.3389/fnagi.2022.1002811

Spontaneous brain activity in healthy aging: An overview through fluctuations and regional homogeneity

Marc Montalà-Flaquer[1,2]*, Cristina Cañete-Massé[1,2], Lídia Vaqué-Alcázar[3,4,5], David Bartrés-Faz[3,4,5], Maribel Peró-Cebollero[1,2,3] and Joan Guàrdia-Olmos[1,2,3]

[1]Department of Social Psychology and Quantitative Psychology, Faculty of Psychology, Universitat de Barcelona, Barcelona, Spain, [2]UB Institute of Complex Systems, Universitat de Barcelona, Barcelona, Spain, [3]Institute of Neurosciences, Universitat de Barcelona, Barcelona, Spain, [4]Department of Medicine, Faculty of Medicine and Health Sciences, Universitat de Barcelona, Barcelona, Spain, [5]Institut d'Investigacions Biomèdiques August Pi i Sunyer (IDIBAPS), Barcelona, Spain

Introduction: This study aims to explore whole-brain resting-state spontaneous brain activity using fractional amplitude of low-frequency fluctuation (fALFF) and regional homogeneity (ReHo) strategies to find differences among age groups within a population ranging from middle age to older adults.

Methods: The sample comprised 112 healthy persons (M=68.80, SD=7.99) aged 48–89 who were split into six age groups (<60, 60–64, 65–69, 70–74, 75–79, and≥80). Fractional amplitude of low-frequency fluctuation and ReHo analyses were performed and were compared among the six age groups, and the significant results commonly found across groups were correlated with the gray matter volume of the areas and the age variable.

Results: Increased activity was found using fALFF in the superior temporal gyrus and inferior frontal gyrus when comparing the first group and the fifth. Regarding ReHo analysis, Group 6 showed increased ReHo in the temporal lobe (hippocampus), right and left precuneus, right caudate, and right and left thalamus depending on the age group. Moreover, significant correlations between age and fALFF and ReHo clusters, as well as with their gray matter volume were found, meaning that the higher the age, the higher the regional synchronization, the lower the fALFF activation, and the lower gray matter of the right thalamus.

Conclusion: Both techniques have been shown to be valuable and usable tools for disentangling brain changes in activation in a very low interval of years in healthy aging.

KEYWORDS

spontaneous brain activity, resting-state functional magnetic resonance imaging, fractional amplitude of low-frequency fluctuation, regional homogeneity, healthy aging

1. Introduction

Life expectancy in the general population has significantly increased in the last few years thanks to an improvement in medicine and social services, among others (Sanchez-Morate et al., 2020). The percentage of older people is growing at a rate of 3% per year (United Nations, Department of Economic and Social Affairs, Population Division, 2017). Thus, there is a need to understand the underlying processes of healthy aging.

Healthy aging is the process of developing and maintaining functional ability that enables well-being in older age (World Health Organization, 2016). However, aging is also associated with deficits in areas such as executive function or in sensory functioning (Rosano et al., 2005), among others (Park and Reuter-Lorenz, 2009). Recent longitudinal studies have shown that these deficits linked with healthy aging predict functional disability, future falls, or the onset of dementia among nondemented older adults (Johnson et al., 2009; Ewers et al., 2014; Veldsman et al., 2020). Therefore, understanding age-related changes in brain functioning could provide insights into the mechanisms underlying age-related functional declines and contribute to the actual interventions for cognitive improvements in the elderly population.

In the last few years, interest in neuroimaging studies has grown substantially. Several methods in this field, such as structural and functional connectivity (FC), have shown promising results in healthy aging (Oschmann et al., 2020; Yamashita et al., 2021; Abellaneda-Pérez et al., 2022). It is important to note that even for healthy individuals, the aging process implies changes in functional and structural connectivity (Farras-Permanyer et al., 2019; Oschwald et al., 2020; Vaqué-Alcázar et al., 2020). Regarding functional findings, aging has been associated with a decrease in FC in the default mode network (DMN) (Mowinckel et al., 2012), among other abnormalities (Chen, 2019; West et al., 2019). Aging has also been associated with decreased gray matter volume in frontal and parietal lobes (Hu et al., 2014), and these regions have also been highlighted as the most vulnerable to aging (Marchitelli et al., 2018). However, Yang et al. (2019) performing a multimodal neuroimaging analysis suggested that effect of age difference is not limited to only the frontal lobe region but in more widespread range, involving nonfrontal regions such as parietal, occipital, cuneus, and parahippocampal, among others.

The spontaneous blood-oxygen-level-dependent (BOLD) signal provides an indirect measure of the brain's hemodynamics (Gorges et al., 2014), and its FC can be extracted (Ystad et al., 2011). However, FC usually depicts the relationship between two or more areas but does not provide detailed information on which exact voxels are abnormal within networks. Moreover, as the brain ages, several brain regions and connectivity networks could be altered in terms of dynamics and location, decreasing the accuracy of regions of interest (ROIs) and seed-based analyses (Lee and Hsieh, 2017). In contrast, regional spontaneous brain activity analysis may provide this helpful information (Zou et al., 2008) and thus could help disentangle differences in regional activities (Zang et al., 2015). The functional coordination between brain areas can be assessed through the BOLD signal by analyzing the amplitude of low-frequency fluctuations (ALFF) and its regional homogeneity (ReHo).

Amplitude of low-frequency fluctuations and ReHo are data-driven analyses of the brain signal that reveal different regional characteristics of resting-state functional magnetic resonance imaging (rs-fMRI) data; hence, they require no hypotheses or a priori selection of brain (ROI) (Lee and Hsieh, 2017). Amplitude of low-frequency fluctuation measures the correlation of local amplitude of spontaneous low-frequency fluctuations in the BOLD time series (frequency-domain analysis) (An et al., 2013), whereas ReHo computes Kendall's coefficient of concordance (KCC) to assess the temporal synchronization (time-domain analysis) given a cluster of neighboring voxels (Zang et al., 2004). As ALFF appears to be sensitive to physiological noise, Zou et al. (2008) proposed the fractional amplitude of low-frequency fluctuations (fALFF), a low-pass filter of ALFF that enhances its sensitivity and specificity.

Both approaches may be complementary (Lee and Hsieh, 2017). They have been recently used in many psychiatric diseases (Lai et al., 2020; Gao et al., 2021; Wang et al., 2022), dementias (Liu et al., 2014; Yue et al., 2020), and healthy populations (Hu et al., 2014; Deng et al., 2022). Cha et al. (2015) performed an interesting meta-analysis studying functional abnormalities in amnestic mild cognitive impairment and Alzheimer's disease (AD) patients using ReHo and fALFF, among other techniques, and they found decreased functional characteristics with all approaches. The results showed that the functional characteristics in the left parahippocampal gyrus were decreased in AD patients compared with healthy subjects. Hu et al. (2014) studied fALFF during a stop signal task in a healthy aging sample and found a negative correlation with age in some areas of the frontal and prefrontal regions, among others, indicating that spontaneous neural activities in these areas decrease with age while performing a task. Hsu et al. (2020) used a graph theoretic perspective similar to fALFF and ReHo to examine the relationship between properties of topological organization in functional brain networks and motor inhibition and found the implication of frontoparietal regions among others.

Farras-Permanyer et al. (2019), in a study with the same population as the one used in this study, found a progressive decrease in FC between six groups of healthy aged individuals and was particularly pronounced concerning the group aged between 75 and 79 years old. Furthermore, the oldest group showed a slight

Abbreviations: AD, Alzheimer's disease; BNT, Boston naming test; BOLD, blood-oxygen-level-dependent; DMN, default mode network; fALFF, fractional Amplitude of Low-Frequency Fluctuations; FC, functional connectivity; FD, framewise displacement; MMSE, mini-mental state examination; MNI, Montreal Neurological Institute; NART, national adult reading test; RAVLT, Rey auditory verbal learning test; ReHo, regional homogeneity; ROI, regions of interest; Rs-fmri, resting state functional Magnetic Resonance Imaging; VBM, voxel based morphometry; WAIS, Weschsler adult intelligence scale.

increase in FC and was interpreted as a compensatory mechanism in brain functioning.

Although age is markedly related to changes in functional and anatomical connectivity when analyzing the whole-brain BOLD signal some results from different investigations are still inconsistent. Additional studies that expand upon data-driven analyses could provide supplementary information about the different regional characteristics of the brain in healthy older adults. Moreover, the spontaneous activity of age-related brain networks can be an effective indicator of individual differences and age-group differences in elderly people (Lee and Hsieh, 2017). fALFF and ReHo show remarkably high temporal stability and long-term test–retest reliability (Zuo and Xing, 2014). Consequently, both techniques have been suggested to be potential biomarkers (Küblböck et al., 2014; Zuo and Xing, 2014).

The present paper aims to study the whole-brain resting state using fALFF and ReHo strategies to find differences in spontaneous brain activity among healthy participants of different age groups from middle to advanced age. Despite the incongruencies between the studies, we predict differences in fALFF and ReHo in the frontal lobe and in the DMN. Farras-Permanyer et al. (2019) already demonstrated differences between these age groups in FC whereas spontaneous brain activity remained unexplored. Therefore, we also hypothesize to find differences between these age groups in fALFF and ReHo in the same line as Farras-Permanyer et al. (2019).

2. Materials and methods

2.1. Participants

The original data used in this study are the same as those used in Farras-Permanyer et al. (2019) comprised by rs-fMRI sequences of 121 healthy individuals merged from three different studies conducted at the Department of Medicine, School of Medicine and Health Sciences, University of Barcelona. However, two subjects were discarded because the T1-weighted acquisition was noisy, four subjects were excluded due to excessive movement during the registration (Jenkinson et al., 2002) and four subjects were excluded due to incomplete recordings, leaving a total sample of 112 participants. The three protocols were approved by the ethics committee from the Comissió de Bioètica of the Universitat de Barcelona (Approval No. PSI2012-38257) and the ethics committee from Barcelona's Hospital Clínic (Approval No. 2009-5306 and Approval No. 2011-6604).

The exclusion criteria included illiteracy or an inability to understand the protocol or undergo neuropsychological tests mentioned in the next section, prior cerebrovascular accident, any relevant psychiatric illness, advanced cognitive deterioration, dementia, or other neurodegenerative diseases (e.g., Parkinson's disease), any chronic illness expected to shorten survival (grave diseases such as heart failure, chronic liver disease, kidney failure, blood disease or cancer) and any MRI-related incompatibility (the presence of metallic objects within the body, pacemaker or claustrophobia).

The final participant sample comprised 112 healthy individuals aged 48–89 years (68.80 ± 7.99) years (50% females). The participants were split into 6 age groups (< 60, 60–64, 65–69, 70–74, 75–79, and ≥ 80) with the following group sizes: ($n_1 = 12$; $n_2 = 21$; $n_3 = 30$; $n_4 = 21$; $n_5 = 18$; and $n_6 = 10$). The age intervals were chosen to detect slight differences in relatively short aging intervals. This categorization had been used in previous studies and is coherent with the suggestion made by Sala-Llonch et al. (2015). Only two participants were younger than 55 years in the first group, and only four participants were older than 85 years.

2.2. Instruments

The three protocols contained a neuropsychological assessment of major cognitive domains, including the vocabulary scale in the Wechsler Adult Intelligence Scale (WAIS) (Lezak et al., 2004), the mini-mental state examination (MMSE) (Folstein et al., 1975; Tombaugh and McIntyre, 1992), the National Adult Reading Test (NART; Nelson and Willison, 1991) and the Boston Naming Test (BNT) (Kaplan et al., 2001).

However, specifically, the participants of the first and third protocols were also assessed with the Rey Auditory Verbal Learning Test (n = 80; Rey, 1964), and the participants of the second protocol were also assessed with the Grober and Buschke Test ($n = 32$; Grober and Buschke, 1987).

2.3. Magnetic resonance imaging acquisition and preprocessing

The three protocols used a Siemens Magnetom Trio Tim syngo 3-T system scanner at the Unitat d'Imatge per Ressonància Magnètica IDIBAPS (Hospital Clínic), Barcelona. First, a high-resolution T1-weighted structural image was obtained with a magnetization-prepared rapid acquisition gradient echo (MPRAGE) three-dimensional protocol with repetition time (TR) = 2,300 ms, echo time (TE) = 2.98 ms, 240 slices, slice thickness = 1 mm, and field of view (FOV) = 256 mm. For the resting-state acquisition, participants were instructed to lie down with their eyes closed and not fall asleep. Notably, the BOLD signal acquisition was slightly different for each protocol:

- Protocol 1: $n = 32$ participants, TR = 2,000 ms, TE = 16 ms, slice thickness = 3 mm, interslice gap = 25%, FOV = 220 mm, total: 5 min. Ethics committee of the Comisión de Bioética de la Universidad de Barcelona, approval number: PSI2012-38257.
- Protocol 2: $n = 57$ participants, TR = 2,000 ms, TE = 16 ms, slice thickness = 3 mm, interslice gap = 25%, FOV = 220 mm, total: 10 min. Ethics committee of the Barcelona's Hospital Clínic, approval number: 2009-5306.

- Protocol 3: $n = 23$ participants, TR = 2,000 ms, TE = 19 ms, slice thickness = 3 mm, interslice gap = 25%, FOV = 220 mm, total: 5 min. Ethics committee of the Barcelona's Hospital Clínic, approval number: 2011-6604.

While Protocols 1 and 3 recorded 150 dynamic points, Protocol 2 recorded a total of 300 dynamics. This difference between protocols can complicate the statistical processing of the data, so the temporal registries of Protocol 2 were truncated, and only the first 150 dynamical points were used. Additionally, a difference in the echo time (TE) on Protocol 3 was reported, but it was so slight that no further effect was seen on the sample data between protocols.

The structural T2 images of every participant were revised to identify any possible abnormality before including it in the statistical analysis. No structural abnormalities or alterations were found in any participant.

2.4. Voxel-based morphometry

The T1w-structural images were automatically processed with DPABI (Yan et al., 2016). The images were reoriented and individually checked for quality control. Afterwards, reoriented T1 images were segmented into gray matter (GM), white matter (WM) and cerebrospinal fluid (CSF; Ashburner and Friston, 2005). Finally, the DPABI module uses the Diffeomorphic Anatomical Registration Through Exponentiated Lie algebra (DARTEL) tool (Ashburner, 2007) to compute transformations from individual native space to MNI space. Finally, gray matter segmentations where resliced and smoothed to match the parameters with the functional images. Additionally, total gray matter volumes and parcellation volumes were calculated using SPM12[1] and SPM12 based scripts (Maldjian et al., 2003, 2004).

2.5. Data preprocessing

Image preprocessing was performed using the Data Processing Assistant for Resting-State fMRI (DPARSF; Yan and Zang, 2010).[2] Essentially, the pipeline is based on MATLAB, SPM12 and DPABI.

Primarily, the first ten functional images were discarded to avoid possible effects from participants adapting to the scanner and to let the magnetization equilibrate properly. Then, the remaining functional images were corrected for slice time by means of their timing acquisition, and head motion was assessed. Nuisance signals were regressed out considering white matter and cerebrospinal fluid signals, linear trends and, finally, signals associated with the 24 Friston head-motion parameters (Friston et al., 1996). The derived functional images were coregistered with their corresponding structural images, which were segmented and normalized to MNI space using DARTEL tool. The functional images were also normalized to MNI space with warped parameters and resampled to 3 mm cubic voxels. With regard to the ReHo analysis, the normalized functional images were then bandpass filtered (0.01–0.1 Hz). To assess excessive movement from the functional recording, participants exceeding the group mean plus two standard deviations (Yan et al., 2013) were excluded from the study. The mean movement group value was estimated with Jenkinson's framewise displacement (FD; Jenkinson et al., 2002), and the mean FD is shown in Table 1 for each group. As mentioned in the participants section, 10 participants were discarded, and the final sample was 112 healthy people. Therefore, further statistical analyses were performed with the covariate of mean Jenkinson's FD for every subject.

2.6. Estimation of fALFF and ReHo

The estimation of fALFF and ReHo values was performed using DPABI. To estimate ALFF, additional spatial smoothing of the voxels was performed with a 4 mm full width at half maximum Gaussian kernel. After that, the time series of each voxel was transformed to the frequency domain with a fast Fourier transform to compute the power spectrum. To compute ALFF, this power spectrum, with an initial frequency range of 0–0.25 Hz, was square-rooted at each frequency and then averaged across 0.01–0.08 Hz at each voxel. Finally, to obtain fALFF, the latter ALFF values were divided by the whole frequency range observed in the signal (0–0.25 Hz, Zou et al., 2008).

Regarding the ReHo estimation, KCC of the time series of all voxels and their neighbors (n = 27) was calculated (Zang et al., 2004). All ReHo maps were smoothed with a Gaussian Kernel of 4 mm full width at half maximum. Finally, individual fALFF and ReHo maps were standardized into z score maps by subtracting the mean and dividing by the standard deviation.

2.7. Statistical analysis

To assess differences within the neuropsychological measures between the six age groups, IBM SPSS (v26) was used to perform ANOVA tests with Tukey's multiple comparison correction, and $p < 0.05$ was set as significant.

For statistical analysis of the six groups in fALFF and ReHo, DPABI was used with a voxel-wise ANOVA test with Tukey's multiple comparison correction. As a precautionary measure and to avoid confusion effects head motion, Jenkinson's FD (Jenkinson et al., 2002), time echo and total gray matter volume were included as covariates in all analyses In addition, the criteria used to assess multiple comparisons was the Gaussian random field (Eklund et al., 2016), with a

1 http://www.fil.ion.ucl.ac.uk/spm

2 http://rfmri.org/DPARSF

TABLE 1 Description of movement and neuropsychological measures between age groups.

Age groups ($\bar{x} \pm SD$) (years)	Size	FD Jenkinson ($\bar{x} \pm SD$) (mm)	BNT ($\bar{x} \pm SD$)	NART ($\bar{x} \pm SD$)	WAIS-Voc ($\bar{x} \pm SD$)	MMSE ($\bar{x} \pm SD$)
<60 (54.67 ± 3.91)	12	0.24 ± 0.12	55.50 ± 5.22	25.17 ± 3.81	40.22 ± 12.70	*29.33 ± 0.89*
60–64 (62.29 ± 1.35)	21	0.22 ± 0.12	54.81 ± 2.94	24.86 ± 3.45	47.62 ± 16.11	28.76 ± 1.09
65–69 (67.13 ± 1.28)	30	0.23 ± 0.14	57.07 ± 8.77	28.93 ± 3.58	46.36 ± 10.75	29.31 ± 0.97
70–74 (72.33 ± 1.20)	21	0.24 ± 0.13	54.90 ± 3.70	28.71 ± 16.50	41.40 ± 9.04	28.90 ± 1.45
75–79 (76.72 ± 1.36)	18	0.25 ± 0.14	54.29 ± 3.42	25.00 ± 5.21	41.18 ± 6.39	*28.06 ± 1.75*
≥80 (82.80 ± 2.74)	10	0.21 ± 0.13	49.20 ± 4.02	23.00 ± 5.77	41.90 ± 9.68	28.20 ± 1.23

$\bar{x}$: mean; SD: standard deviation; FD: framewise displacement; WAIS-Voc: WAIS Vocabulary. The bold indication is $\bar{x}$ and SD represent the mean value and standard deviation of the different measures. BNT, Boston Naming Test; NART, National Adult Reading Test; MMSE, Mini-Mental State Examination.

TABLE 2 Description of level of education between age groups.

Age groups (years)	Primary (%)	Secondary (%)	University (%)
<60	42	33	25
60–64	38	19	43
65–69	12	44	44
70–74	43	48	9
75–79	33	22	45
≥80	40	20	40

voxel p value of.001 and a cluster threshold of $p = 0.05$. Additional thresholding, $n = 30$ voxels for ReHo and $n = 10$ voxels for fALFF, was set to exclude very small clusters, although they appeared to be significant after the strict Gaussian random field correction.

Moreover, the significant clusters found in the ANOVA test in fALFF and ReHo were extracted using DPABI and were correlated with age and gray matter volume. As the correlations were high a step-wise regression model was adjusted including as predictor variables the gray matter volume and the most common clusters through age groups found in the ANOVA analysis. Moreover, R Studio (R 4.1.2) was used for the correlations, regression analysis, and visualization matrices. In addition, complementary analyses considering age as a quantitative variable were performed to avoid a possible loss of information since age was previously considered a qualitative variable. Therefore, both whole-brain fALFF and ReHo values were correlated with age using the criteria of multiple comparisons with the threshold-free cluster enhancement (TFCE), which reaches the best balance between familywise error and test–retest reliability (Winkler et al., 2016; Chen et al., 2018). A total of 10,000 permutations were performed, and the cluster p value was set to $p < 0.05$. As in the previous analyses, there was an additional threshold with a minimum extent threshold of 30 voxels for ReHo and 10 voxels for fALFF.

For the correlation and regression analysis, only the areas which were common for the six groups were chosen in ReHo analysis. Regarding the right caudate and thalamus, as there were both regions regarding these clusters, they were both included in the correlation analysis.

3. Results

3.1. Participant characteristics analysis

In Table 1, the participants' movement and neuropsychological measures between age groups are shown.

All of the individuals in our sample had scores higher than 24 on the Mini-Mental State Examination. In addition, no significant differences were observed between the groups as determined by one-way ANOVA in either the National Adult Reading Test [$F(5, 106) = 0.925$, $p = 0.468$], the WAIS-Voc [$F(5, 99) = 1.095$, $p = 0.368$] or the MMSE [$F(5, 106) = 0.887$, $p = 0.492$] or head movement estimated by Jenkinson's FD [$F(5,106) = 0.196$, $p = 0.964$]. Significantly lower scores in the BNT were detected in the oldest group compared with all of the others [$F(5, 105) = 3.089$, $p = 0.012$, Tukey's HSD adjusted $p < 0.001$] (Table 1).

Regarding level of education, Table 2 shows the participants characteristics. Group 4 presents 43% of participants with primary studies whereas group 5 presents a 45% of participants with university studies.

3.2. Fractional amplitude of low-frequency fluctuation results between groups

Table 3 shows the significant differences between age groups in fALFF localized within the coordinates of the MNI localized in MNI coordinates and the corresponding brain region defined by the Automatic Anatomical Labeling Atlas (AAL; Tzourio-Mazoyer et al., 2002). Figure 1 shows the graphical representation of the results in fALFF visualized with DPARSF (Yan and Zang, 2010; see footnote 2).

No significant differences were found between Groups 2, 3, 4, and 6. Nevertheless, Group 1 showed increased fALFF in a cluster of voxels comprehending the superior temporal gyrus and inferior frontal gyrus compared with Group 5.

TABLE 3 Significant between-group differences in fractional amplitude of low-frequency fluctuation (fALFF) with their peak localization in MNI coordinates and the corresponding AAL ROI.

Contrast	Area	Number of voxels	*t*(peak)	Peak MNI coordinates (mm)			AAL peak region
Group 1 > Group 5	Superior temporal gyrus and Inferior frontal gyrus	13	4.69	−54	15	−6	Frontal_Inf_Opper_L

MNI: Montreal Neurological Institute; AAL: automatic anatomical labeling.

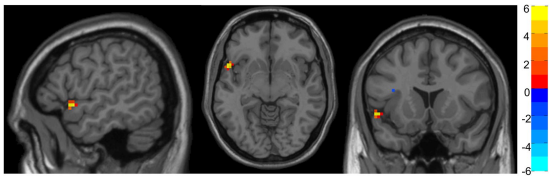

FIGURE 1
Representation of significant differences between Group 1 and Group 5 in fALFF analysis. The color bar indicates the intensity of the difference, with 6 (yellow) representing positive differences and −6 (light blue) representing negative differences.

3.3. Regional homogeneity results between groups

Table 4 shows the significant differences between groups in ReHo localized in MNI coordinates and the corresponding brain region defined by AAL. Figure 2 shows the graphical representation of the ReHo results visualized with DPARSF (Yan and Zang, 2010; see footnote 2).

All groups showed significant differences with Group 6, where increased ReHo was always found in Group 6 compared with the other groups. More concretely, Group 6 showed increased ReHo in the temporal lobe (hippocampus) compared with Group 1, and they also showed increased activity in the right hippocampus when compared with Group 2. Increased ReHo activation in two separate clusters was found when comparing Group 6 to Group 3: the first showed an increase involving the right caudate, and the other showed an increase in the right thalamus and right hippocampus. Interestingly, Group 6 again showed increased ReHo in the right caudate when compared with Groups 4 and 5.

Moreover, complementary correlation analyses were performed using age as a quantitative variable and whole-brain fALFF and ReHo values. No significant correlations were found between whole-brain fALFF and ReHo values and age.

3.4. Correlations and regressions

Figure 3 shows the correlations between the significant clusters of fALFF and ReHo and the gray matter volume of these specific regions and age. All of them are significant, but it is important to highlight those surviving to the Bonferroni correction. Interestingly, high correlations were found between age and the ReHo signal of both right thalamus clusters, ReHo signal of both right caudate clusters, and their corresponding gray matter volume. Moreover, age is also highly correlated with the fALFF signal of the frontal cluster, as well as their corresponding GM volume. All of them survive to Bonferroni correction, except the GM of the right caudate. In Table 5, the regression model predicting age is presented. The multiple regression meets the conditions (no error autocorrelation, linearity, normality, and homoscedasticity of errors tested). It had high R^2 values, meaning that a high level of prediction was achieved. Only some variables were included as predictors, including fALFF signal of the frontal lobe, ReHo signal of the right thalamus and the right thalamus gray matter volume (Figure 4).

4. Discussion

In the last few years, the importance of healthy aging has increased substantially due to the higher levels of life expectancy in the population and due also to the appearance of dementia in the general population, which dramatically increases societal costs. Therefore, disentangling the brain mechanisms of healthy aging has been a subject of interest for researchers. The aims of the present study were to study the whole-brain resting state using fALFF and ReHo strategies to explore differences in spontaneous brain activity among healthy participants of different age groups from middle to advanced age.

Regarding the whole-brain fALFF analysis, the results showed significant differences in low-frequency fluctuations between Groups 1 and 6 in the superior temporal gyrus and inferior frontal gyrus (Table 3). More concretely, group one (the youngest one) shows increased fALFF in this area.

These results are in line with those reported by other authors. The superior temporal gyrus appeared to show a volume decrease (atrophy) in healthy aging, revealing a relationship between age and the rate of atrophy (Fjell et al., 2009). This atrophy could also explain the decrease in fALFF values among this population. Moreover, Galiano et al. (2020) also found higher intrinsic connectivity contrast and higher cerebral blood flow between young and elderly groups. Oschmann et al. (2020) also reported significantly decreased FC in this area in a longitudinal study (4-year follow-up) when using the right inferior parietal sulcus as a seed. The inferior frontal gyrus, which is an area involved in language functions, has also been found to have decreased gray matter density in older adults (Pistono et al., 2021).

TABLE 4 Significant between-group differences in ReHo with their peak localization in MNI coordinates and the corresponding AAL region of interest (ROI).

Contrast	Area	Number of voxels	*t* (peak)	Peak MNI coordinates (mm)			AAL peak region
Group 6 > Group 1	Temporal lobe (hippocampus)	318	5.42	9	−24	15	Thalamus_R
	Right caudate	44	5.31	9	15	3	Caudate_R
	Left precuneus	30	3.96	−24	−48	6	Precuneus_L
Group 6 > Group 2	Temporal lobe (hippocampus)	151	4.98	12	−27	15	Thalamus_R
Group 6 > Group 3	Right caudate	80	5.39	15	18	6	Caudate_R
	Right thalamus and right hippocampus	116	5.11	12	−36	9	Hippocampus_R
Group 6 > Group 4	Right caudate	39	4.94	12	18	3	Caudate_R
	Right precuneus	34	3.87	18	−42	9	Precuneus_R
Group 6 > Group 5	Right caudate	53	5.32	12	15	3	Caudate_R
	Left thalamus	30	4.15	0	−18	15	Thalamus_L

MNI: Montreal Neurological Institute; AAL: automatic anatomical labeling.

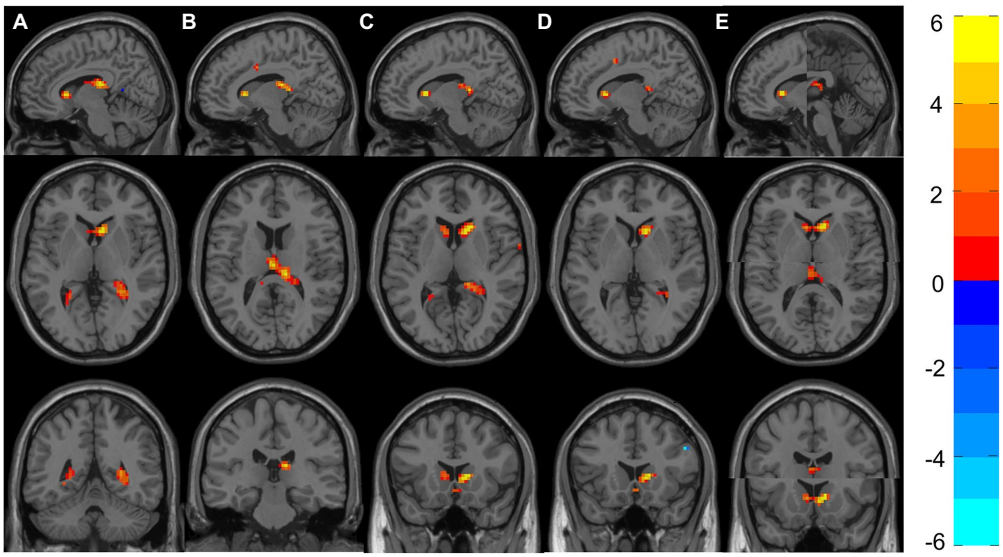

FIGURE 2
Representation of significant differences between Group 6 and Groups 1–5 in the ReHo analyses. **(A)** Shows the sagittal, axial and coronal planes with the differences between Group 6 and Group 1. Likewise, **(B–E)** Represent the differences between Group 6 against Groups 2–5. **(E)** The two clusters (Right Caudate and Left Thalamus) that appeared to be significant; therefore, two images are shown in each plane. The color bar indicates the intensity of the difference, with 6 (yellow) representing positive differences and −6 (light blue) negative differences.

Moreover, the detected cluster appears to be disrupted by aging, and the significant differences would be expected to involve the oldest group. However, the differences found in this study involve the second oldest group (Group 5) and not the oldest group. This fact is consistent with Farras-Permanyer et al. (2019), who suggested that this phenomenon could be a survival mechanism, meaning that the participants of Group 6 would have a high degree of resilience.

In relation to the ReHo results, significant differences between all groups and Group 6 were found, indicating higher synchronization of rs-fMRI signals among neighboring voxels in Group 6. More specifically, Group 6 had increased ReHo values in some areas of the temporal lobe (hippocampus) compared with Groups 1, 2. However, this cluster has different volumes depending on the groups compared. It has its maximum size (318 voxels) when comparing age Groups 1 and 6, and as the age of the

10.3389/fnagi.2022.1002811

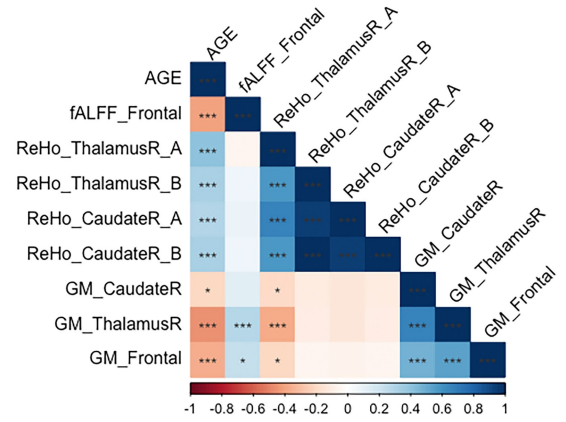

FIGURE 3
Correlation matrix regarding age, gray matter volume and significant clusters in fALFF and ReHo. *p<0.05; **p<0.01; ***p<0.00238 (corrected by Bonferroni).

TABLE 5 Parameter estimation (β) of the best stepwise linear model for age.

fALFF, ReHo and gray matter	Age
	$F = 22.52$ $R^2 = 0.39$ AIC = 738.21
Intercept	95.86
fALFF_Frontal	−6.33 ($p < 0.001$)
ReHo Thalamus Right	6.26 ($p < 0.001$)
Gray matter Thalamus right	−7.07 ($p < 0.001$)

They all have a $p < 0.001$ in the model ($df = 3;108$) and a $p > 0.05$ in Anderson's Darling test of normality, the Ramsey Regression Equation Specification Error (RESET) test, Durbin Watson's test, and the Breusch–Pagan test.

participants increases, it decreases to 151 voxels when comparing Groups 2 and 6. It is important to highlight that, even if it is smaller, the cluster is significant also in group 3 (involving the right thalamus and right hippocampus, 116 voxels). As individual effects, it is also important to remark that group 6 shows increased ReHo compared with group 1 in the left precuneus whereas group six shows increased ReHo in the right precuneus. The left thalamus is increased in ReHo values when comparing group 5 and 6. All these structures which show significant group differences among age groups include the DMN, which is one of the intrinsic resting-state networks that has been most studied with respect to aging.

Fjell et al. (2014) highlighted the hippocampus as a vulnerable region to aging. The FC of the hippocampus also decreases in Alzheimer's disease (AD; Greicius, 2008; Sheline et al., 2010). In healthy elderly individuals, Bartrés-Faz et al. (2008) examined the FC of the hippocampus during an encoding memory task and found increased connectivity with the anterior cingulate, inferior parietal lobe, and caudate in APOE-ε4 carriers. Oschmann et al. (2020) points out the importance of other networks, as the frontoparietal network, apart from the DMN. Despite these unclear conclusions (Hu et al., 2014), the hippocampus appears to be a key structure that changes with age. It is clear that a broad individual heterogeneity emerges in this population; Abellaneda-Pérez et al. (2022) proposes a combination of noninvasive brain stimulations (NIBS) and fMRI to understand how fundamental brain plasticity mechanisms operate in advancing age.

The second cluster (right caudate) shows increased ReHo values in Group 6 compared with Groups 1, 3, 4 and 6. However, as shown in Table 4, the size of this second cluster varies through age group comparisons which is higher on Group 3. These results are also in line with those reported in other studies. Bennett et al. (2011) found age-related decreases in caudate-dorsolateral prefrontal cortex tract integrity that mediated age-related differences in late-stage sequence learning. In a task-fMRI study, Bowen et al. (2020) found that older but not younger adults exhibited enhanced subsequent memory for high-reward items, supported by greater connectivity between the caudate and bilateral inferior frontal gyrus. Tang et al. (2021) found decreased FC within the right caudate and some regions of the cerebellum in AD.

Our results show that even controlling by gray matter volume, fALFF and ReHo show significant differences in healthy aging. The correlation matrix demonstrates the clear relationship between age and neuroimaging signal, beginning with ReHo signal in the right thalamus, which correlates positively with age. The ReHo signal of the right caudate also correlates positively with age. Nonetheless, fALFF signal in the frontal cluster is negatively linked with age, showing a decrease of fALFF in these areas. Remarkably, structural changes are also associated with age, finding a negative correlation with this variable. In this sense, gray matter volumes of the right thalamus, the right caudate and the frontal cluster are negatively associated with age, having therefore decreased volume as age advances. These structural abnormalities have also been reported in Pergher et al. (2019). They also show negative correlations with sociodemographic variables such as age. As high correlations were found between these measures and age, we performed step-wise regression to try to predict age by neuroimaging data. Results show a high variability explained by these structural and spontaneous brain activity measures, suggesting its utility as biomarkers of age. However, more studies are needed to demonstrate its potential. Other authors have suggested already the ability of fALFF and ReHo measures as potential biomarkers owing to their high test–retest reliability (Küblböck et al., 2014; Zuo and Xing, 2014).

Both techniques have been shown to be valuable and usable tools for disentangling brain changes in activation in different groups of healthy aging. fALFF and ReHo techniques measure different outcomes in the brain; therefore, differences in groups estimate two features involved in aging. On the one hand, the fALFF results indicate a significant difference in low-frequency fluctuations between Groups 1 and 5 despite not being translated into a significant change in performance in terms of the neuropsychological measures. However, interestingly, this

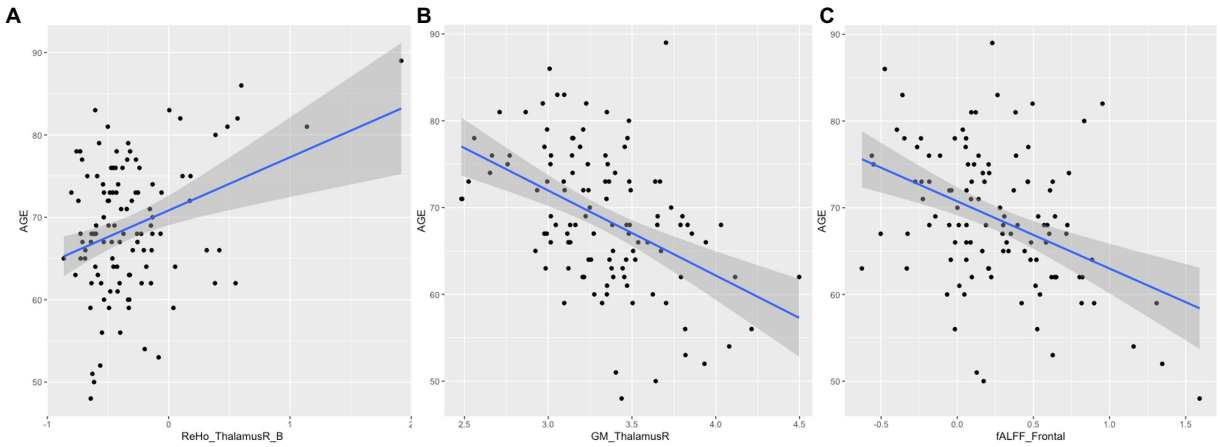

FIGURE 4
Scatter plot and regression for age. **(A)** Represents age and ReHo signal of the right thalamus; **(B)** Represents age and gray matter volume of the right thalamus. **(C)** Represents age and fALFF signal of the frontal lobe.

result is in line with the results of Farras-Permanyer et al. (2019) using the same sample concerning progressive FC decrease either in number or intensity of connections. On the other hand, the ReHo results indicate an increase in regional synchronization between Group 6 and the other age groups. Other studies have also reported increased ReHo measures and have considered it to offset functional decrease or impairment, i.e., a compensatory mechanism (Zhang et al., 2012; Song et al., 2014; Kong et al., 2015). This finding may be crucial because it directly links the increase in ReHo signal with healthy aging; furthermore, there is no evidence of impairment and no decrease in the neuropsychological performance. The differences in the findings of fALFF and ReHo, which remained in Groups 5 and 6, could be linked to the fact that both groups were healthy aging participants without any suspicion of dementia or any other cognitive decline. Meanwhile, Group 6 included more elderly individuals who therefore have higher resilience. These results demonstrate that increased ReHo values could be directly linked with compensatory mechanisms due to brain aging.

This study has some limitations. First, an important limitation is found in the sample size. Although the study cohort contains 112 participants, the size of each age group was not entirely homogeneous, leaving the oldest group with 10 participants. Therefore, sample size, distribution and dispersion may introduce a bias in the final results, especially concerning the older group. The lack of a replication dataset could also have limited the results. Second, low-frequency BOLD signals, especially in the brain regions that comprise the DMN (Birn et al., 2006), are affected by physiological noises (Birn et al., 2008; Chang and Glover, 2009). We cannot truly assess the impact of these physiological noises or any blood pressure-induced hemodynamic response fluctuation as we did not collect respiratory and cardiovascular data. Finally, motion, even if well controlled, might affect the results.

Some strengths of the study are also worth mentioning. As there is a fundamental need to better understand the neurobiological changes associated with healthy aging given the globally aging population, elucidating the differences in spontaneous brain activity between age groups of healthy aging is of major importance. This study demonstrates that changes in spontaneous brain activity may occur in very low intervals of years, and those changes could be targeted as specific therapeutic areas in cognitive rehabilitation. Finally, a highly restrictive correction for multiple comparisons was performed in this analysis to ensure that the strongest differences remained significant. The results have a large effect size, so we can affirm that significant differences in regional spontaneous brain activity using fALFF and ReHo were found between the six groups of an elderly population. Finally, the strong relationship between age and structural and spontaneous brain activity measures suggests the possibility of using them as potential biomarkers.

Data availability statement

The data analyzed in this study is subject to the following licenses/restrictions: The data are not publicly available due to privacy or ethical restrictions. The data that support the findings of this study are available on request from the corresponding author. Requests to access these datasets should be directed to mmontala@ub.edu.

Ethics statement

The studies involving human participants were reviewed and approved by Comisión de Bioética de la Universitat de Barcelona Servicio de Farmacia del Hospital Clínic de Barcelona Comité Ético de Investigación Clínica (CEIC) Comité Investigación del

Hospital Clínic de Barcelona. The patients/participants provided their written informed consent to participate in this study.

Author contributions

All authors contributed to the study's conception and design. LV-A and DB-F curated the data. DB-F and JG-O provided the resources for the study. MM-F and CC-M made the first conceptualizations of the paper, investigation, and methodology. Supervision of the paper was performed by MP-C and JG-O. All authors contributed to the article and approved the submitted version.

Funding

This work was supported by the Walnuts and Healthy Aging (WAHA) study (Grant number NCT01634841) funded by the California Walnut Commission, Sacramento, California, United States and the Spanish Ministry of Science, Innovation and Universities, Agencia Estatal de Investigación (Grant Number: PGC2018-095829-B-I00 and MICIU/FEDER; RTI2018-095181-B-C21). DB-F was supported by an ICREA Academia 2019 award.

Conflict of interest

The authors declare that the research was conducted in the absence of any commercial or financial relationships that could be construed as a potential conflict of interest.

Publisher's note

All claims expressed in this article are solely those of the authors and do not necessarily represent those of their affiliated organizations, or those of the publisher, the editors and the reviewers. Any product that may be evaluated in this article, or claim that may be made by its manufacturer, is not guaranteed or endorsed by the publisher.

References

Abellaneda-Pérez, K., Vaqué-Alcázar, L., Solé-Padullés, C., and Bartrés-Faz, D. (2022). Combining non-invasive brain stimulation with functional magnetic resonance imaging to investigate the neural substrates of cognitive aging. *J. Neurosci. Res.* 100, 1159–1170. doi: 10.1002/jnr.24514

An, L., Cao, Q. J., Sui, M. Q., Sun, L., Zou, Q. H., Zang, Y.-F., et al. (2013). Local synchronization and amplitude of the fluctuation of spontaneous brain activity in attention-deficit/hyperactivity disorder: a resting-state fMRI study. *Neurosci. Bull.* 29, 603–613. doi: 10.1007/s12264-013-1353-8

Ashburner, J. (2007). A fast diffeomorphic image registration algorithm. *Neuro Image* 38, 95–113. doi: 10.1016/j.neuroimage.2007.07.007

Ashburner, J., and Friston, K. J. (2005). Unified segmentation. Neuro. *Image* 26, 839–851. doi: 10.1016/j.neuroimage.2005.02.018

Bartrés-Faz, D., Serra-Grabulosa, J. M., Sun, F. T., Solé-Padullés, C., Rami, L., Molinuevo, J. L., et al. (2008). Functional connectivity of the hippocampus in elderly with mild memory dysfunction carrying the APOE ε4 allele. *Neurobiol. Aging* 29, 1644–1653. doi: 10.1016/j.neurobiolaging.2007.04.021

Bennett, I. J., Madden, D. J., Vaidya, C. J., Howard, J. H. Jr., and Howard, D. V. (2011). White matter integrity correlates of implicit sequence learning in healthy aging. *Neurobiol. Aging* 32, 2317.e1–2317.e12. doi: 10.1016/j.neurobiolaging.2010.03.017

Birn, R. M., Diamond, J. B., Smith, M. A., and Bandettini, P. A. (2006). Separating respiratory-variation-related neuronal-activity-related fluctuations in fluctuations from fMRI. *NeuroImage* 31, 1536–1548. doi: 10.1016/j.neuroimage.2006.02.048

Birn, R. M., Smith, M. A., Jones, T. B., and Bandettini, P. A. (2008). The respiration response function: the temporal dynamics of fMRI signal fluctuations related to changes in respiration. *NeuroImage* 40, 644–654. doi: 10.1016/j.neuroimage.2007.11.059

Bowen, H. J., Ford, J. H., Grady, C. L., and Spaniol, J. (2020). Frontostriatal functional connectivity supports reward-enhanced memory in older adults. *Neurobiol. Aging* 90, 1–12. doi: 10.1016/j.neurobiolaging.2020.02.013

Cha, J., Hwang, J. M., Jo, H. J., Seo, S. W., Na, D. L., and Lee, J. M. (2015). Assessment of functional characteristics of amnestic mild cognitive impairment and Alzheimer's disease using various methods of resting-state FMRI analysis. *BioMed Research International* 2015:907464. doi: 10.1155/2015/907464

Chang, C., and Glover, G. H. (2009). Relationship between respiration, end-tidal CO2, and BOLD signals in resting-state fMRI. *Neuro Image* 47, 1381–1393. doi: 10.1016/j.neuroimage.2009.04.048

Chen, J. J. (2019). Functional MRI of brain physiology in aging and neurodegenerative diseases. *NeuroImage* 187, 209–225. doi: 10.1016/j.neuroimage.2018.05.050

Chen, X., Lu, B., and Yan, C. G. (2018). Reproducibility of R-fMRI metrics on the impact of different strategies for multiple comparison correction and sample sizes. *Hum. Brain Mapp.* 39, 300–318. doi: 10.1002/hbm.23843

Deng, S., Franklin, C. G., O'Boyle, M., Zhang, W., Heyl, B. L., Jerabek, P. A., et al. (2022). Hemodynamic and metabolic correspondence of resting-state voxel-based physiological metrics in healthy adults. *Neuroimage* 250:118923. doi: 10.1016/j.neuroimage.2022.118923

Eklund, A., Nichols, T. E., and Knutsson, H. (2016). Cluster failure: why fMRI inferences for spatial extent have inflated false-positive rates. *Proc. Natl. Acad. Sci.* 113, 7900–7905. doi: 10.1073/pnas.1602413113

Ewers, M., Brendel, M., Rizk-Jackson, A., Rominger, A., Bartenstein, P., Schuff, N., et al. (2014). Reduced FDG-PET brain metabolism and executive function predict clinical progression in elderly healthy subjects. *Neuro Image: Clinical* 4, 45–52. doi: 10.1016/j.nicl.2013.10.018

Farras-Permanyer, L., Mancho-Fora, N., Montalà-Flaquer, M., Bartrés-Faz, D., Vaqué-Alcázar, L., Peró-Cebollero, M., et al. (2019). Age-related changes in resting-state functional connectivity in older adults. *Neural Regen. Res.* 14, 1544–1555. doi: 10.4103/1673-5374.255976

Fjell, A. M., McEvoy, L., Holland, D., Dale, A. M., and Walhovd, K. B. (2014). What is normal in normal aging? Effects of aging, amyloid and Alzheimer's disease on the cerebral cortex and the hippocampus. *Prog. Neurobiol.* 117, 20–40. doi: 10.1016/j.pneurobio.2014.02.004

Fjell, A. M., Walhovd, K. B., Fennema-Notestine, C., McEvoy, L. K., Hagler, D. J., Holland, D., et al. (2009). One-year brain atrophy evident in healthy aging. *J. Neurosci.* 29, 15223–15231. doi: 10.1016/j.neuroimage.2022.118923

Folstein, M. F., Folstein, S. E., and McHugh, P. R. (1975). "Mini-mental state": a practical method for grading the cognitive state of patients for the clinician. *J. Psychiatr. Res.* 12, 189–198. doi: 10.1016/0022-3956(75)90026-6

Friston, K. J., Williams, S., Howard, R., Frackowiak, R. S., and Turner, R. (1996). Movement-related effects in fMRI time-series. *Magn. Reson. Med.* 35, 346–355. doi: 10.1002/mrm.1910350312

Galiano, A., Mengual, E., García de Eulate, R., Galdeano, I., Vidorreta, M., Recio, M., et al. (2020). Coupling of cerebral blood flow and functional connectivity is decreased in healthy aging. *Brain Imaging Behav.* 14, 436–450. doi: 10.1007/s11682-019-00157-w

Gao, Y., Wang, X., Xiong, Z., Ren, H., Liu, R., Wei, Y., et al. (2021). Abnormal fractional amplitude of low-frequency fluctuation as a potential imaging biomarker for first-episode major depressive disorder: a resting-state fMRI study and support vector machine analysis. *Front. Neurol.* 12:751400. doi: 10.3389/fneur.2021.751400

Gorges, M., Müller, H. P., Ludolph, A. C., Rasche, V., and Kassubek, J. (2014). Intrinsic functional connectivity networks in healthy elderly subjects: a multiparametric approach with structural connectivity analysis. *Bio. Med. Res. Int.* 2014:947252. doi: 10.1155/2014/947252

Greicius, M. (2008). Resting-state functional connectivity in neuropsychiatric disorders. *Curr. Opin. Neurol.* 21, 424–430. doi: 10.1097/WCO.0b013e328306f2c5

Grober, E., and Buschke, H. (1987). Genuine memory deficits in dementia. *Dev. Neuropsychol.* 3, 13–36. doi: 10.1080/87565648709540361

Hsu, H. M., Yao, Z. F., Hwang, K., and Hsieh, S. (2020). Between-module functional connectivity of the salient ventral attention network and dorsal attention network is associated with motor inhibition. *PloS One* 15:e0242985. doi: 10.1371/journal.pone.0242985

Hu, S., Chao, H. H. A., Zhang, S., Ide, J. S., and Li, C. S. R. (2014). Changes in cerebral morphometry and amplitude of low-frequency fluctuations of BOLD signals during healthy aging: correlation with inhibitory control. *Brain Struct. Funct.* 219, 983–994. doi: 10.1007/s00429-013-0548-0

Jenkinson, M., Bannister, P., Brady, M., and Smith, S. (2002). Improved optimization for the robust and accurate linear registration and motion correction of brain images. *Neuroimage* 17, 825–841. doi: 10.1016/s1053-8119(02)91132-8

Johnson, D. K., Storandt, M., Morris, J. C., and Galvin, J. E. (2009). Longitudinal study of the transition from healthy aging to Alzheimer disease. *Arch. Neurol.* 66, 1254–1259. doi: 10.1001/archneurol.2009.158

Kaplan, E., Goodglass, H., and Weintraub, S. (2001). *Boston Naming Test* (*2*). Austin, TX: Pro Ed.

Kong, F., Wang, X., Hu, S., and Liu, J. (2015). Neural correlates of psychological resilience and their relation to life satisfaction in a sample of healthy young adults. *Neuroimage* 123, 165–172. doi: 10.1016/j.neuroimage.2015.08.020

Küblböck, M., Woletz, M., Höflich, A., Sladky, R., Kranz, G. S., Hoffmann, A., et al. (2014). Stability of low-frequency fluctuation amplitudes in prolonged resting-state fMRI. *Neuroimage* 103, 249–257. doi: 10.1016/j.neuroimage.2014.09.038

Lai, J., Xu, T., Zhang, H., Xi, C., Zhou, H., Du, Y., et al. (2020). Fractional amplitude of low frequency fluctuation in drug-naïve first-episode patients with anorexia nervosa: a resting-state fMRI study. *Medicine* 99:e19300. doi: 10.1097/MD.0000000000019300

Lee, H. H., and Hsieh, S. (2017). Resting-state fMRI associated with stop-signal task performance in healthy middle-aged and elderly people. *Front. Psychol.* 8:766. doi: 10.3389/fpsyg.2017.00766

Lezak, M. D., Howieson, D. B., Loring, D. W., and Fischer, J. S. (2004). *Neuropsychological Assessment*. (*4*). New York, NY: Oxford University Press.

Liu, X., Wang, S., Zhang, X., Wang, Z., Tian, X., and He, Y. (2014). Abnormal amplitude of low-frequency fluctuations of intrinsic brain activity in Alzheimer's disease. *J. Alzheimers Dis.* 40, 387–397. doi: 10.3233/JAD-131322

Maldjian, J. A., Laurienti, P. J., and Burdette, J. H. (2004). Precentral gyrus discrepancy in electronic versions of the Talairach atlas. *NeuroImage* 21, 450–455. doi: 10.1016/j.neuroimage.2003.09.032

Maldjian, J. A., Laurienti, P. J., Burdette, J. B., and Kraft, R. A. (2003). An automated method for neuroanatomic and Cytoarchitectonic atlas-based interrogation of fMRI data sets. *Neuroimage* 19, 1233–1239. doi: 10.1016/S1053-8119(03)00169-1

Marchitelli, R., Aiello, M., Cachia, A., Quarantelli, M., Cavaliere, C., Postiglione, A., et al. (2018). Simultaneous resting-state FDG-PET/fMRI in Alzheimer disease: relationship between glucose metabolism and intrinsic activity. *NeuroImage* 176, 246–258. doi: 10.1016/j.neuroimage.2018.04.048

Mowinckel, A. M., Espeseth, T., and Westlye, L. T. (2012). Network-specific effects of age and in-scanner subject motion: a resting-state fMRI study of 238 healthy adults. *NeuroImage* 63, 1364–1373. doi: 10.1016/j.neuroimage.2012.08.004

Nelson, H. E., and Willison, J. (1991). *National Adult Reading Test (NART)* (pp. 1–26). Windsor: Nfer-Nelson.

Oschmann, M., and Gawryluk, J. R.Alzheimer's Disease Neuroimaging Initiative (2020). A longitudinal study of changes in resting-state functional magnetic resonance imaging functional connectivity networks during healthy aging. *Brain Connect.* 10, 377–384. doi: 10.1089/brain.2019.0724

Oschwald, J., Guye, S., Liem, F., Rast, P., Willis, S., Röcke, C., et al. (2020). Brain structure and cognitive ability in healthy aging: a review on longitudinal correlated change. *Rev. Neurosci.* 31, 1–57. doi: 10.1515/revneuro-2018-0096

Park, D. C., and Reuter-Lorenz, P. (2009). The adaptive brain: aging and neurocognitive scaffolding. *Annu. Rev. Psychol.* 60, 173–196. doi: 10.1146/annurev.psych.59.103006.093656

Pergher, V., Demaerel, P., Soenen, O., Saarela, C., Tournoy, J., Schoenmakers, B., et al. (2019). Identifying brain changes related to cognitive aging using VBM and visual rating scales. *Neuroimage Clin.* 22:101697. doi: 10.1016/j.nicl.2019.101697

Pistono, A., Guerrier, L., Péran, P., Rafiq, M., Giméno, M., Bézy, C., et al. (2021). Increased functional connectivity supports language performance in healthy aging despite gray matter loss. *Neurobiol. Aging* 98, 52–62. doi: 10.1016/j.neurobiolaging.2020.09.015

Rey, A. (1964). *Clinical Tests in Psychology*. Paris: Presses Universitaires de France.

Rosano, C., Simonsick, E. M., Harris, T. B., Kritchevsky, S. B., Brach, J., Visser, M., et al. (2005). Association between physical and cognitive function in healthy elderly: the health, aging and body composition study. *Neuroepidemiology* 24, 8–14. doi: 10.1159/000081043

Sala-Llonch, R., Bartrés-Faz, D., and Junqué, C. (2015). Reorganization of brain networks in aging: a review of functional connectivity studies. *Front. Psychol.* 6:663. doi: 10.3389/fpsyg.2015.00663

Sanchez-Morate, E., Gimeno-Mallench, L., Stromsnes, K., Sanz-Ros, J., Román-Domínguez, A., Parejo-Pedrajas, S., et al. (2020). Relationship between diet, microbiota, and healthy aging. *Biomedicine* 8:287. doi: 10.3390/biomedicines8080287

Sheline, Y. I., Morris, J. C., Snyder, A. Z., Price, J. L., Yan, Z., D'Angelo, G., et al. (2010). APOE4 allele disrupts resting state fMRI connectivity in the absence of amyloid plaques or decreased CSF Aβ42. *J. Neurosci.* 30, 17035–17040. doi: 10.1523/JNEUROSCI.3987-10.2010

Song, Y., Mu, K., Wang, J., Lin, F., Chen, Z., Yan, X., et al. (2014). Altered spontaneous brain activity in primary open angle glaucoma: a resting-state functional magnetic resonance imaging study. *PLoS One* 9:e89493. doi: 10.1371/journal.pone.0089493

Tang, F., Zhu, D., Ma, W., Yao, Q., Li, Q., and Shi, J. (2021). Differences changes in cerebellar functional connectivity between mild cognitive impairment and Alzheimer's disease: a seed-based approach. *Front. Neurol.* 12:987. doi: 10.3389/fneur.2021.645171

Tombaugh, T. N., and McIntyre, N. J. (1992). The mini-mental state examination: a comprehensive review. *J. Am. Geriatr. Soc.* 40, 922–935. doi: 10.1111/j.1532-5415.1992.tb01992.x

Tzourio-Mazoyer, N., Landeau, B., Papathanassiou, D., Crivello, F., Etard, O., Delcroix, N., et al. (2002). Automated anatomical labeling of activations in SPM using a macroscopic anatomical parcellation of the MNI MRI single-subject brain. *NeuroImage* 15, 273–289. doi: 10.1006/nimg.2001.0978

United Nations, Department of Economic and Social Affairs, Population Division. (2017). World population ageing 2017: Highlights. Available at: https://www.un.org/en/development/desa/population/publications/pdf/ageing/WPA2017_Highlights.pdf (Accessed May, 2022).

Vaqué-Alcázar, L., Sala-Llonch, R., Abellaneda-Pérez, K., Coll-Padrós, N., Valls-Pedret, C., Bargalló, N., et al. (2020). Functional and structural correlates of working memory performance and stability in healthy older adults. *Brain Struct. Funct.* 225, 375–386. doi: 10.1007/s00429-019-02009-1

Veldsman, M., Tai, X. Y., Nichols, T., Smith, S., Peixoto, J., Manohar, S., et al. (2020). Cerebrovascular risk factors impact frontoparietal network integrity and executive function in healthy ageing. *Nat. Commun.* 11, 4340–4310. doi: 10.1038/s41467-020-18201-5

Wang, Q., Wang, C., Deng, Q., Zhan, L., Tang, Y., Li, H., et al. (2022). Alterations of regional spontaneous brain activities in anxiety disorders: a meta-analysis. *J. Affect. Disord.* 296, 233–240. doi: 10.1016/j.jad.2021.09.062

West, K. L., Zuppichini, M. D., Turner, M. P., Sivakolundu, D. K., Zhao, Y., Abdelkarim, D., et al. (2019). BOLD hemodynamic response function changes significantly with healthy aging. *Neuroimage* 188, 198–207. doi: 10.1016/j.neuroimage.2018.12.012

Winkler, A. M., Ridgway, G. R., Douaud, G., Nichols, T. E., and Smith, S. M. (2016). Faster permutation inference in brain imaging. *Neuroimage* 141, 502–516. doi: 10.1016/j.neuroimage.2016.05.068

World Health Organization. (2016). *Global Strategy and Action Plan on Ageing and Health (2016–2020)*. Geneva: WHO.

Yamashita, K., Kuwashiro, T., Ishikawa, K., Furuya, K., Harada, S., Shin, S., et al. (2021). Identification of predictors for mini-mental state examination and revised Hasegawa's dementia scale scores using MR-based brain morphometry. *Eur. J. Radiol. Open* 8:100359. doi: 10.1016/j.ejro.2021.100359

Yan, C. G., Cheung, B., Kelly, C., Colcombe, S., Craddock, R. C., Di Martino, A., et al. (2013). A comprehensive assessment of regional variation in the impact of head micromovements on functional connectomics. *Neuroimage* 76, 183–201. doi: 10.1016/j.neuroimage.2013.03.004

Yan, C. G., Wang, X. D., Zuo, X. N., and Zang, Y. F. (2016). DPABI: data processing and analysis for (resting-state) brain imaging. *Neuroinformatics* 14, 339–351. doi: 10.1007/s12021-016-9299-4

Yan, C. G., and Zang, Y. F. (2010). DPARSF: a MATLAB toolbox for "pipe-line" data analysis of resting-state fMRI. *Front. Syst. Neurosci.* 4, 1–13. doi: 10.3389/fnsys.2010.00013

Yang, M. H., Yao, Z. F., and Hsieh, S. (2019). Multimodal neuroimaging analysis reveals age-associated common and discrete cognitive control constructs. *Hum. Brain Mapp.* 40, 2639–2661. doi: 10.1002/hbm.24550

Ystad, M., Hodneland, E., Adolfsdottir, S., Haász, J., Lundervold, A. J., Eichele, T., et al. (2011). Cortico-striatal connectivity and cognition in normal aging: a combined DTI and resting state fMRI study. *Neuroimage* 55, 24–31. doi: 10.1016/j.neuroimage.2010.11.016

Yue, Y., Jiang, Y., Shen, T., Pu, J., Lai, H. Y., and Zhang, B. (2020). ALFF and ReHo mapping reveals different functional patterns in early-and late-onset Parkinson' disease. *Front. Neurosci.* 14:141. doi: 10.3389/fnins.2020.00141

Zang, Y., Jiang, T., Lu, Y., He, Y., and Tian, L. (2004). Regional homogeneity approach to fMRI data analysis. *Neuroimage* 22, 394–400. doi: 10.1016/j.neuroimage.2003.12.030

Zang, Y. F., Zuo, X. N., Milham, M., and Hallett, M. (2015). Toward a meta-analytic synthesis of the resting-state fMRI literature for clinical populations. *Bio. Med. Res. Int.* 2015:435265. doi: 10.1155/2015/435265

Zhang, Z., Liu, Y., Jiang, T., Zhou, B., An, N., Dai, H., et al. (2012). Altered spontaneous activity in Alzheimer's disease and mild cognitive impairment revealed by regional homogeneity. *Neuroimage* 59, 1429–1440. doi: 10.1016/j.neuroimage.2011.08.049

Zou, Q. H., Zhu, C. Z., Yang, Y., Zuo, X. N., Long, X. Y., Cao, Q. J., et al. (2008). An improved approach to detection of amplitude of low-frequency fluctuation (ALFF) for resting-state fMRI: fractional ALFF. *J. Neurosci. Methods* 172, 137–141. doi: 10.1016/j.jneumeth.2008.04.012

Zuo, X.-N., and Xing, X.-X. (2014). Test-retest reliabilities of resting-state FMRI measurements in human brain functional connectomics: a systems neuroscience perspective. *Neurosci. Biobehav. Rev.* 45, 100–118. doi: 10.1016/j.neubiorev.2014.05.009

Frontiers in
Aging Neuroscience

Explores the mechanisms of central nervous system aging and age-related neural disease

The third most-cited journal in the field of geriatrics and gerontology, with a focus on understanding the mechanistic processes associated with central nervous system aging.

Discover the latest Research Topics

See more →

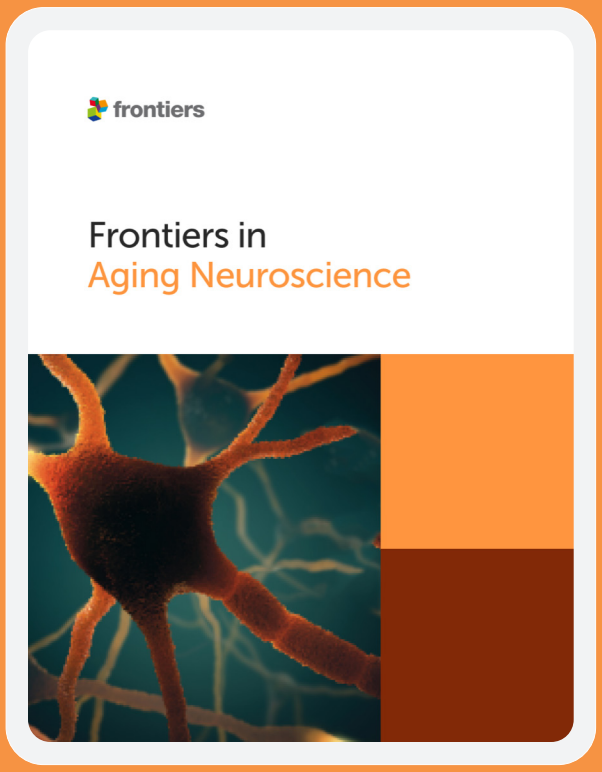

Frontiers

Avenue du Tribunal-Fédéral 34
1005 Lausanne, Switzerland
frontiersin.org

Contact us

+41 (0)21 510 17 00
frontiersin.org/about/contact